PROCEEDINGS

DEPARTMENT OF VETERINARY PATHOLOGY
WEDNESDAY SLIDE CONFERENCE
2010-2011

ARMED FORCES INSTITUTE OF PATHOLOGY
WASHINGTON, D.C. 20306-6000
2011

ML2011

Armed Forces Institute of Pathology
Department of Veterinary Pathology

WEDNESDAY SLIDE CONFERENCE
2010-2011

100 Cases
100 Histopathology Slides

PROCEEDINGS PREPARED BY:
Matthew Wegner, DVM

Chief Editor:
Edward Stevens, DVM, Diplomate ACVP

Layout & Copy Editor:
Sean Hahn

WSC Online Management and Design
Scott Shaffer,

ARMED FORCES INSTITUTE OF PATHOLOGY
Washington, D.C. 20306-6000
2011

ML2011

PREFACE

The Armed Forces Institute of Pathology, Department of Veterinary Pathology has conducted a weekly slide conference during the resident training year since 12 November 1953. This ever-changing educational endeavor has evolved into the annual Wednesday Slide Conference program in which cases are presented on 25 Wednesdays throughout the academic year and distributed to 135 contributing military and civilian institutions from around the world. Many of these institutions provide structured veterinary pathology resident training programs. During the course of the training year, histopathology slides, digital images, and histories from selected cases are distributed to the participating institutions and to the Department of Veterinary Pathology at the AFIP. Following the conferences, the case diagnoses, comments, and reference listings are posted online to all participants.

This study set has been assembled in an effort to make Wednesday Slide Conference materials available to a wider circle of interested pathologists and scientists, and to further the education of veterinary pathologists and residents-in-training. The number of histopathology slides that can be reproduced from smaller lesions requires us to limit the number of participating institutions.

This set, composed of 100 cases, 100 histopathology slides and 249 digital images, was assembled from the cases studied during the 2010-2011 conference series.

For their participation and permission to use their cases in this study set, we wish to thank each institution, and especially the individuals who prepared and submitted the selected cases. We also wish to give special thanks to the American Veterinary Medical Association and the American College of Veterinary Pathologists, who are co-sponsors of the Registry of Veterinary Pathology. The C.L. Davis Foundation also provides substantial support for the Registry.

A special note of appreciation is extended to the reviewers who helped edit and review this year's individual case summaries: Ed Stevens, Bruce Williams, Taylor Chance, and Christine Christensen. A final note of thanks goes to the moderators, who unselfishly gave of their time and expertise to help make each conference both enjoyable and educational.

Gross images and photomicrographs were submitted by contributing institutions where indicated. Additional photomicrographs were taken by CPT Lenora Dickson and MAJ Chris Schellhase.

Armed Forces Institute of Pathology, Department of Veterinary Pathology
WEDNESDAY SLIDE CONFERENCE 2010-2011
Table of Contents

WSC 2010-2011 Table of Contents

The Armed Forces Institute of Pathology
Department of Veterinary Pathology

Conference Coordinator
Matthew Wegner, DVM

WEDNESDAY SLIDE CONFERENCE 2010-2011

Conference 1

11 August 2010

Conference Moderator:
John Pletcher, MPH, DVM, Diplomate ACVP

CASE I: SPRI Case 1 (AFIP 2941205).

Signalment: 2-year-old female Sprague-Dawley rat (*Rattus norvegicus*).

History: The animal was part of the vehicle control group of a two-year gavage carcinogenicity study. A scheduled terminal necropsy was performed on day 731 of the test.

Gross Pathology: The terminal body weight was 339.1 grams. The submitted tissues correlate with two masses located in the right inguinal region. These masses were dark red to tan, lobulated, and firm. Other necropsy findings included an enlarged adrenal cortex, an enlarged pituitary compressing the ventral brain, and dark red foci throughout the liver.

Histopathologic Description: Haired skin and mammary gland: Histologically, there is an expansile, non-encapsulated but well-delineated mass within the subcutis, which compresses adjacent tissues. The mass is multilobulated with varying islands of epithelial cells separated by thick bands of dense fibrous connective tissue. Thin bands of connective tissue extend into some islands forming a trabecular pattern which separate the epithelial cells into small, single-cell lined acini and tubules while other islands have scant amounts of fibrous connective tissue and contain more dense accumulations and pilings of atypical epithelial cells which compress adjacent lobules. The epithelial cells within the trabeculae of connective tissue are well differentiated with small, dark nuclei and vacuolated cytoplasm, and lumena frequently contain basophilic secretory material. The fibrous connective tissue is also composed of well-differentiated cells with abundant streaming eosinophilic cytoplasm and small, dark nuclei. The atypical epithelial components which contain more densely cellular epithelial cells and less connective tissue also contain large ectatic pools of basophilic secretory material which are occasionally mineralized. These atypical epithelial cells exhibit mild to moderate anisocytosis with abundant basophilic to vacuolated cytoplasm and large, round, vesicular nuclei with one or two prominent magenta nucleoli. Mitotic figures are fewer than 1 per high magnification field. There is a minimal infiltrate of neutrophils scattered

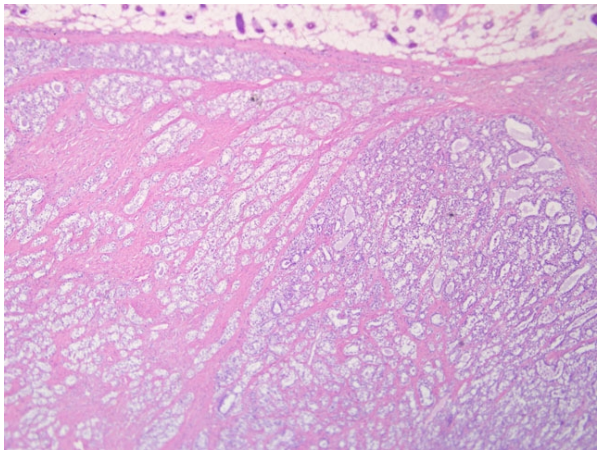

1-1. Haired skin, mammary gland, fibroadenoma, with atypia, rat. There is an expansile, well-demarcated, multilobulated, neoplasm composed of epithelial cells arranged in islands, trabeculae, and tubuloacinar structures separated by dense bands of fibrous connective tissue. (HE 20X)

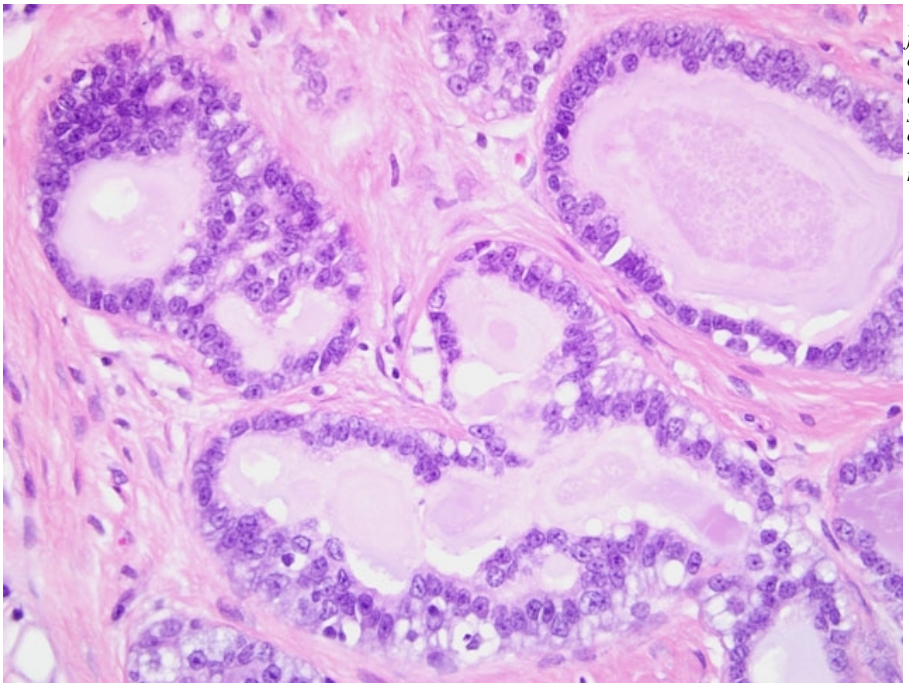

1-2. Haired skin, mammary gland, fibroadenoma, with atypia, rat. Neoplastic epithelial cells have moderate vacuolated cytoplasm and small dark nuclei; the lumina of tubuloacinar structures frequently contain secretory material. The surrounding fibrous connective tissue is composed of spindle cells with scant eosinophilic cytoplasm and small nuclei. (HE 400X)

throughout the mass. Well developed blood vessels are common throughout the mass although clear evidence of metastatic invasion is not observed.

Contributor's Morphologic Diagnosis: Mammary glands: Adenocarcinoma arising in a fibroadenoma.

Contributor's Comment: Other significant findings in this animal included: adrenal gland cortical cell adenoma; contralateral cortical atrophy, and cystic hemorrhagic degeneration; liver angiectasis and biliary ductular hyperplasia; pituitary gland pars distalis adenoma; ovarian atrophy; thymus atrophy; and uterine endometrial fibrosis. In this particular two-year study the incidence of mammary tumors in 100 control group females included 28 fibroadenomas, 3 adenomas, 25 adenocarcinomas, and 7 adenocarcinomas arising in fibroadenomas.

Mammary tumors are extremely common spontaneous lesions in aging rats although the incidence and type of tumor varies considerably from one rat strain to the next. Within the F344 strain, fibroadenomas are reported in up to 60% of females surviving the length of a two-year study.[2] The incidence of this same tumor in Wistar rats is 45% and in Sprague-Dawley rats ranges from 24-68% in females at the end of a two-year study.[4,5] In most of the common rat strains, adenocarcinomas are considerably less common than fibroadenomas. In toxicologic studies, this variation in tumor incidences between strains demonstrates the importance of relevant controls when assessing whether a tumor is test-article related or an incidental finding. Furthermore, this variation also suggests that there are important pathogenic distinctions between the strains to consider when using data from laboratory animals to evaluate human health risks. It has long been established that the quantity and ratio of estrogen to prolactin have a profound influence on the biological behavior of these tumors in rats.[5] In addition to xenobiotics, there are numerous environmental factors such as diet, pregnancy status, and housing conditions which can further influence these tumor incidences.

The criteria for classification of mammary tumors in the rat have been well described.[1] Additional clarification and refinement of diagnostic criteria have been accomplished to enhance uniformity of terminology among pathologists.[3] This harmonization is an important and ongoing process that is essential for accurate risk assessment by the various regulatory agencies throughout the world. In conjunction with this harmonization, continued monitoring of the incidence of spontaneous tumors in these various strains provides the opportunity for recognition of important biological shifts in tumor behavior over time.

AFIP Diagnosis: Haired skin, mammary gland: Mammary fibroadenoma, with atypia.

Conference Comment: Conference participants carefully considered the contributor's diagnosis of adenocarcinoma arising in fibroadenoma, which was included in the differential diagnosis, along with lobular hyperplasia, fibroadenoma, and fibroadenoma with atypia. Consistent with the contributor's description, the microscopic sections consist of haired skin and mammary gland containing an unencapsulated, well-demarcated, expansile mass composed of epithelial cells arranged in well-differentiated acini and tubules and separated by variable amounts of dense fibrous connective tissue stroma. Acini and tubules are generally lined by a single layer of neoplastic epithelial cells.

Epithelial cells are cuboidal and have moderate amounts of vacuolated cytoplasm and round to oval, finely stippled nuclei and indistinct nucleoli. There are few mitotic figures. The fibrocollagenous stroma is composed of well-differentiated spindled cells with eosinophilic fibrillar cytoplasm and small, elongate nuclei. While some participants identified scattered mitoses and areas of epithelial atypia in the neoplasm, including piling up of epithelial cells in clusters of acini, based on the sections available for evaluation participants did not observe features indicative of adenocarcinoma, such as invasion through the basement membrane, desmoplasia, necrosis, high mitotic rate, clumped chromatin, bizarre mitoses, squamous metaplasia, or the histologic patterns associated with mammary adenocarcinoma in the rat (i.e. comedo, cribriform, or papillary).[3] That said, this lesion represents the difficulty in examination of numerous sections of a neoplasm, and the initial tissue sections evaluated by the contributor may well have contained areas demonstrating convincing adenocarcinoma within mammary fibroadenoma. The adjacent chart summarizes key histologic features of the differentials as indicated in the Standardized System of Nomenclature and Diagnostic Criteria (SSNDC) Guide.[3]

Lobular hyperplasia	Lobular enlargement by histologically normal, hyperplastic alveoli Single layer of alveolar epithelium
Atypical hyperplasia	Focal irregular epithelial proliferation with cellular atypia and/or pleomorphism Formation of epithelial papillae, arches, nests or plaques projecting into the lumen
Adenoma	Well-circumscribed proliferation of clusters of tubuloacinar structures on a scanty collagenous stroma Alveoli lined by a single layer of epithelium with a small nucleus, one nucleolus and cytoplasm that is often vacuolated Papillary or cystic papillary patterns
Fibro-adenoma	Two morphologically distinct cell populations ± areas of atypia/cellular pleomorphism 1. Epithelium – single layer, uniform, with or without lipid vacuoles forming tubuloacinar structures or cysts 2. Fibrous connective tissue of variable density coursing within and between lobules with few fibrocytes
Adeno-carcinoma	Uniform epithelial cells varying from one to many cells thick; have a central round nucleus; clumped chromatin; one nucleolus and many mitoses May or may not be invasive Patterns include papillary, tubular, cribriform, or comedo
Adeno-carcinoma arising in a fibro-adenoma	Histologic pattern of adenocarcinoma Variable histologic pattern of fibroadenoma component

Contributor: Schering Plough Research Institute, 144 Route 94 PO Box 32, Lafayette, NJ 07848 www.schering-plough.com

References:

1. Boorman GA, Wilson JT, van Zwieten MJ, Eustis SL. Mammary gland. In: Boorman GA, Eustis SL, Elwell MR, Montgomery CA, MacKenzie WF, eds. *Pathology of the Fischer Rat*. San Diego, CA: San Diego Academic Press; 1990:298-305.

2. Haseman JK, Hailey JR, Morris RW. Spontaneous neoplasm incidences in Fischer344 rats and B6C3F1 mice in two-year carcinogenicity studies: A national toxicology program update. *Toxicol Pathol*. 1998;26(3): 428-41.

3. Mann PC, Boorman GA, Lollini LO, McMartin DN, Goodman DG. Proliferative lesions of the mammary gland in rats. In: *Guides for Toxicologic Pathology*; accessed at http://www.toxpath.org/nomen/index.htm, 11 August 2010. Washington D.C.: Society of Toxicologic Pathologists/ American Registry of Pathology/The Armed Forces Institute of Pathology; 1996.

4. Poteracki J, Wash KM. Spontaneous neoplasms in control Wistar rats: A comparison review. *Toxicol Sci*. 1998;45(1): 1-8.

5. Van Zwieten MJ, Hogenesch H, Majka JA, Boorman GA. Non-neoplastic and neoplastic lesions of the mammary glands. In: Mohr U, Dungworth DL, Capen CC eds. *Pathobiology of the Aging Rat* Volume 2. Washington D.C.: ILSI Press; 1994:459-475.

CASE II: PFIZER SDN CASE 2 (AFIP3135367).

Signalment: 6 to 8-week-old male Sprague-Dawley rat (*Rattus norvegicus*).

History: The rat was part of the high dose group in a gentamicin nephrotoxicity study. Subcutaneous administration of gentamicin once daily at dose of 75 mg/kg/day for 7 days was performed. The rat was euthanized at day 8. No clinical abnormalities were detected. This study was conducted in accordance with the current guidelines for animal welfare (Animals [Scientific Procedures] Act, 1986 and ILAR Guide for the Care and Use of Laboratory Animals, 1996).

Gross Pathology: Both kidneys were pale and mildly enlarged with increased absolute weights (+22% relative to control) and relative weights (+23% relative to body weight).

Laboratory Results: A slightly increased creatinine concentration (17% above mean control values) at ≥ 75 mg/kg/day on day 8 was observed. There were no significant changes in blood urea nitrogen (BUN) concentrations.

Histopathologic Description: Kidney: Histologically, the section of kidney showed degeneration and necrosis of the epithelium of predominantly cortical tubules (most likely proximal convoluted tubules) characterized by presence of varying degrees of tubular epithelial vacuolar degeneration, attenuation, loss of epithelial cellular detail with abundant pyknotic nuclei and karyorrhectic debris (necrosis), and detachment from intact basement membranes. Multifocally, in association with these changes, were basophilic tubules characterized by epithelial cells with basophilic cytoplasm, vesiculate nuclei, and infrequent mitoses (regeneration) and low to moderate numbers of mononuclear cells (lymphocytes and plasma cells) in the interstitium. There were occasional apoptotic epithelial cells and tubular casts (not observed in all submitted sections).

Contributor's Morphologic Diagnosis: Kidney: Moderate multifocal tubular epithelium degeneration and necrosis with mild regeneration.

Contributor's Comment: Gentamicin (GM) is a broad-spectrum aminoglycoside antibiotic used against life threatening bacterial infections. Its mechanism of action occurs by inhibition of bacterial protein synthesis mainly through binding with the 30S ribosomal subunit. It is well known as an inducer of acute nephrotoxicity which occurs in about 15-30% of treated animals.[1] The present case represents a classical GM-induced nephrotoxicity characterized predominantly by tubular degeneration/necrosis at the end of the dosing period on day 8.

The key histopathological features of GM-treated animals are vacuolar degeneration and necrosis of renal proximal convoluted tubular epithelium in the cortex.[4,6] Ultrastructural changes of proximal tubule epithelial cells include damage and loss of brush borders, and formation of cytosegrosomes and myeloid bodies.[4,6] Gentamicin nephrotoxicity is reversible and regeneration of tubular epithelium may occur even during continued therapy.[4,6]

The underlying mechanism by which GM causes nephrotoxicity is not fully understood. However, one of the most important mechanisms for GM induced nephrotoxicity is reactive oxygen species-mediated.[2,5] It has been shown that GM generates reactive oxygen species which produce cellular injury and necrosis via peroxidation of membrane lipids, protein denaturation, and DNA damage in the kidney.[1,2] It has also been reported that GM suppresses antioxidant defense enzymes (e.g. superoxide dismutase, catalase and glutathione peroxidase) and increases lipid peroxidation in the renal cortex and medulla.[2,5]

A recent interesting development is the attempt to use extracts from medicinal plants with antioxidant properties to

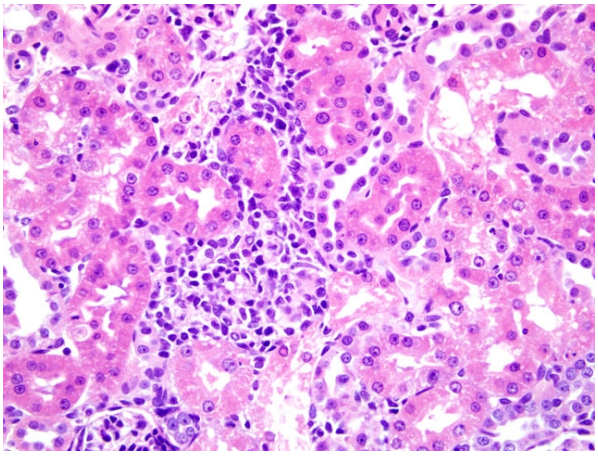

2-1. Kidney, rat. Multifocally in the cortical interstitium, there are low to moderate numbers of lymphocytes, macrophages, and plasma cells that surround degenerate and necrotic tubules. (HE 400X)

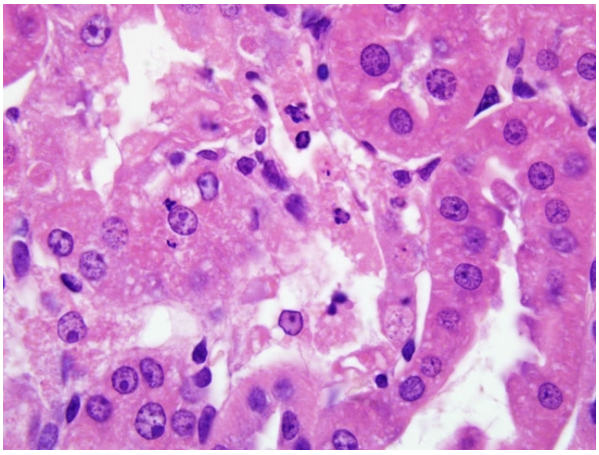

2-2. Kidney, rat. Multifocally in the renal cortex there is tubular epithelial degeneration, attenuation, and necrosis. (HE 1000X)

ameliorate/protect against GM-induced nephrotoxicity in rats. Such medicinal plants include garlic, as well as diallyl sulfide, a compound isolated from garlic, *Nigella sativa* oil, Maidenhair tree extract (*Ginkgo biloba*), *Rhazya stricta* and green tea extract.[1,5,8]

AFIP Diagnosis: Kidney, cortex: Tubular degeneration and necrosis, multifocal, mild to moderate with regeneration and lymphoplasmacytic interstitial nephritis.

Conference Comment: Renal lesions attributable to toxins vary in severity based on dose, time, strain, sex, age, route of administration and degree of hydration. Animals with poor hydration often have higher drug concentrations in renal tubular epithelium than well-hydrated animals, resulting in increased toxicity. Pale, enlarged kidneys, which bulge on cut surface and may have a white stripe in the outer stripe of the outer medulla, are indicative of acute tubular necrosis; chronically affected kidneys are often shrunken, irregular and pitted.

A focal point of discussion for conference participants was the histology of the rat kidney in relation to lesion distribution. Histologically, the rat kidney can be divided into five zones. Beginning with the capsular surface, these are: the cortex; the outer stripe of the outer medulla; the inner stripe of the outer medulla; the inner medulla; and the papilla. The proximal tubule is often subdivided into three segments: P1 and P2 contain the proximal convoluted tubule (PCT); and P3 represents the pars recta. While P1 and P2 are located in the cortex, the P3 segment is found in the outer stripe of the outer medulla. Accurate classification of renal lesions with respect to the structures affected and anatomic location can aid in determination of potential causes of renal tubular damage and associated mechanisms of action. The proximal tubule is often the site of toxic injury, with P3 most commonly affected. The histologic lesion patterns of acute renal tubular necrosis include: multifocal distribution, affecting individual cells or groups of tubules, such as with *N*-(4'-fluoro-4-biphenyl) acetamide; segmental distribution, such as when affecting only P3 (aminoglycosides, furans, thiophenes, acetaminophen, ochratoxin A and mercuric chloride); and multiple proximal tubule segments, such as that which occurs with uranyl nitrate and cisplatin.[7]

The moderator commented on the sexual dimorphism exhibited in rat kidneys. Cells within segments P1 and P2 in the male rat exhibit higher endocytic activity and have larger, more numerous lysosomes. Within the PCT of sexually mature males, cells frequently have eosinophilic cytoplasmic granules composed of alpha$_{2U}$-globulins; visualization of these granules is enhanced by staining with the Mallory-Heidenhain stain.[3] Abnormal accumulation of these granules is referred to as "hyaline droplet nephropathy" and can be seen in male rats as a result of toxic changes, or in both sexes in association with disseminated histiocytic sarcoma.[3] Female rats have more extensive smooth endoplasmic reticulum in segments P1 and P2, which suggests higher mixed-function oxidase activity and enhanced metabolism of drugs.[7]

Contributor: Pfizer Limited, Drug Safety Research and Development (DSRD), Department of Toxicological Pathology, Sandwich, Kent CT13 9NJ, United Kingdom
http://www.pfizer.co.uk/Pages/Home.aspx

References:

1. Ali BH. Agents ameliorating or augmenting experimental gentamicin nephrotoxicity: Some recent research. *Food Chem Toxicol*. 2003;41:1447-1452.
2. Banday AA, Farooq N, Priyamvada S, Yusufi, ANK, Khan F. Time dependent effects of gentamicin on the enzymes of carbohydrate metabolism, brush border membrane and oxidative stress in rat kidney tissues. *Life Sci*. 2008;82**:**450-459.
3. Hard GC, Alden CL, Bruner RH, et al. Non-proliferative lesions of the kidney and lower urinary tract in rats. In: *Guides for Toxicologic Pathology*, accessed at http://www.toxpath.org/nomen/index.htm, 11 August 2010. Washington D.C.: Society of Toxicologic Pathologists/ American Registry of Pathology/The Armed Forces Institute of Pathology; 1999.
4. Houghton DC, Harnett M, Campbell-Boswell M, Porter G, Bennett WM. A light and electron microscopic analysis of gentamicin nephrotoxicity in rats. *Am J Pathol*. 1976;82:589–612.
5. Khan SA, Priyamvada S, Farooq N, Khan S, Khan MW, Yusufi ANK. Protective effect of green tea extract on gentamicin-induced nephrotoxicity and oxidative damage in rat kidney. *Pharmacol Res*. 2009;59:254-262.
6. Mingeot-Leclerq M, Tulkens PM. Aminoglycosides: Nephrotoxicity. *Antimicrob Agents Chemother*. 1999;43(5): 1003–1012.
7. Montgomery CA Jr., Seely JC. Kidney. In: Boorman GA, Eustis SL, Elwell MR, Montgomery CA, MacKenzie WF, eds. *Pathology of the Fischer Rat*. San Diego, CA: San Diego Academic Press; 1990:127-153.

CASE III: 08/006 (AFIP 3136051).

Signalment: 82-week-old female Wistar Rat, rat (*Rattus norvegicus*).

History: This specific-pathogen-free rat was part of a carcinogenicity study as a sentinel. The rat was euthanised because of wasting, rectal prolapse and a palpable caudal abdominal mass.

Gross Pathology: At necropsy, a well-demarcated, round mass of five centimetres in diameter was present in the distal part of the uterus and the anterior part of the vagina and adherent to the rectum. It was polycystic, soft, dark to brown with multiple foci of necrosis. No other significant gross lesion was noted.

Histopathologic Description: Vagina: The mass is an ill-demarcated, non-encapsulated, infiltrating cellular proliferation involving diffusely the serosa, the tunica muscularis, the lamina propria and the epithelium which was ulcerated. The mass is moderately cellular, made of sheets of loosely packed ovoid to spindled cells separated by large amounts of pale, eosinophilic, finely fibrillar matrix with numerous blood vessels. There are numerous, disseminated, variable-sized (0.1 mm to 1 cm) cavities containing eosinophilic, reticulate, amorphous material admixed with foamy macrophages or erythrocytes and lined by closely packed neoplastic cells resembling epithelium (pseudocysts). The cells have indistinct cell borders, moderate amount of pale, eosinophilic cytoplasm, oval to fusiform, centrally-located nucleus with reticulate to hyperchromatic chromatin and one small nucleolus; the neoplastic cells surrounding the pseudocysts appear polarized with a basal nucleus. The cells have mild poikilocaryosis and anisokaryosis. Mitotic figures are rare: mean 1 per HPF (40X) with a maximum of 2. There are multifocal areas of coagulation necrosis. Few lymphocytes, plasma cells and siderophages are scattered within the mass. The lumen is filled with cellular debris, purulent exudate and bacterial colonies.

Uterine horn: The same neoplasm extends from the serosa to the lamina propria. The lumen is filled with pus.

Rectum and urethra: The same neoplasm invades the serosa and the tunica muscularis of the rectum.

Immunochemistry: Specific antibodies applied to sections of the tumor revealed positive staining for vimentin, GFAP and S-100 in the cytoplasm of tumor cells. The intensity was stronger for vimentin and GFAP than for S-100.

Contributor's Morphologic Diagnosis: Vagina, uterus and rectum: Malignant schwannoma, Wistar rat, *Rattus norevegicus*.

Contributor's Comment: Classification of peripheral nerve sheath tumors is complex and various entities are recognized in human pathology: schwannoma, neurofibroma, plexiform neurofibroma, neurofibrosarcoma,

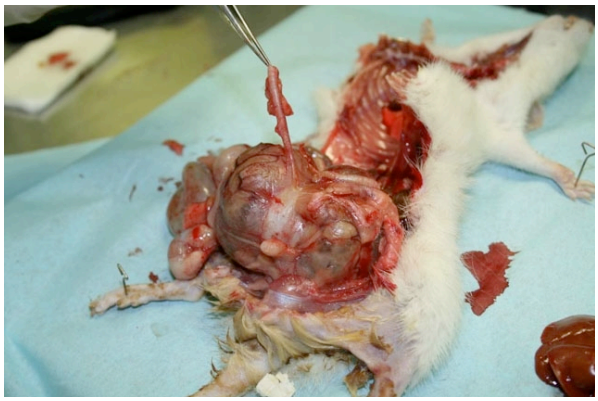

3-1. Vagina; uterus; and rectum, Malignant schwannoma, rat. There is a well demarcated, round mass in the distal part of the uterus and the anterior part of the vagina adherent to the rectum. Photograph courtesy of Ecole Nationale Veterinaire D'Alfort, Unite d'histologie et d'Anatomie Pathologique, 7, Avenue du General de Gaulle, 94704 Maisons-Alfort Cedex, France, www.vet-alfort.fr

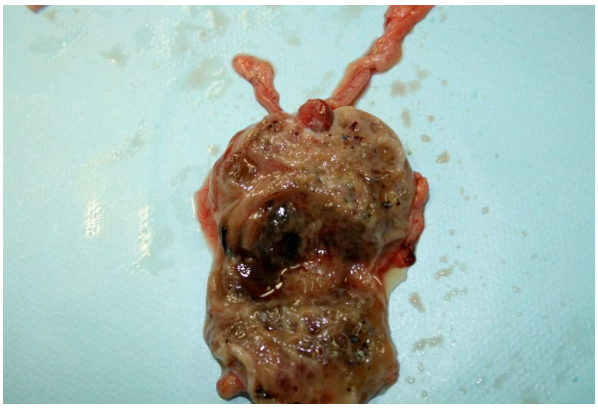

3-2. Vagina; uterus; and rectum, Malignant schwannoma, rat. There is a polycystic, soft, dark brown mass with multiple foci of necrosis. Photograph courtesy of Ecole Nationale Veterinaire D'Alfort, Unite d'histologie et d'Anatomie Pathologique, 7, Avenue du General de Gaulle, 94704 Maisons-Alfort Cedex, France, www.vet-alfort.fr

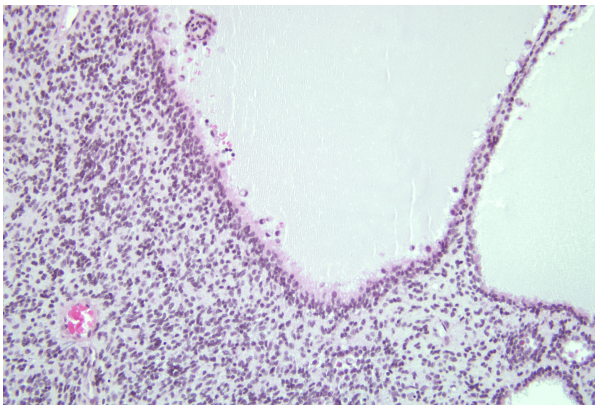

3-3. Vagina; uterus; and rectum, Malignant schwannoma, rat. Neoplastic cells have indistinct borders, small to moderate amounts of pale eosinophilic cytoplasm, oval to fusiform nuclei with dense chromatin and one small nucleolus. Neoplastic cells line variably-sized pseudocystic cavities that contain eosinophilic material admixed with few foamy macrophages and erythrocytes. (HE 200X)

malignant peripheral nerve sheath tumors, etc.[1] Because the cell of origin is often difficult to determine, and because consistent criteria are lacking, veterinary pathologists usually only classify them as benign peripheral nerve sheath tumors or malignant peripheral nerve sheath tumors.[6] However, in toxicologic pathology, the terms "benign and malignant schwannomas" are still classically used, especially in the rat.

The tumor in this case fulfills the typical morphological and immunohistochemical diagnostic criteria for uterine malignant schwannoma of the rat. The histologic appearance and demonstration of S-100 protein and GFAP by immunohistochemical procedures allow us to distinguish malignant schwannoma from the other mesenchymal neoplasms of the lower reproductive tract. Another criterion of distinction is the demonstration of basement membrane by electron microscopy.[1,7] In human pathology, two patterns are often apparent in peripheral nerve sheath tumors: Antoni A and Antoni B patterns. Antoni A pattern is composed of compact spindle cells that usually have twisted nuclei, indistinct cytoplasmic borders, and occasionally clear intranuclear vacuole. They are arranged in short bundles or interlacing fascicles. In highly differentiated Antoni A pattern areas there may be nuclear palisading, whorling of the cells and Verocay bodies (two compact rows of well-aligned nuclei separated by fibrillar cell processes). Antoni B areas are less orderly and less cellular: they are composed of spindled or oval cells arranged haphazardly within the loosely textured matrix, which is punctuated by microcystic change, inflammatory cells, and delicate collagen fibers. As in Antoni B pattern areas the schwann cells possess increased number of lysosomes and myelin figures and the basal lamina is fragmented; the Antoni B pattern could be a degenerated Antoni A pattern.[5] Rat malignant schwannomas can have areas resembling these Antoni A and Antoni B patterns.[7] The tumor in this case is characterized by numerous pseudocysts and loosely packed cells reminiscent of Antoni B pattern. The differential diagnosis of malignant schwannoma of lower reproductive tract is detailed on charts 1 and 2.[9] Spontaneous peripheral nerve sheath tumors are rare in rats.[1] Malignant schwannomas can arise in the subcutis, stomach, heart, vagina and uterus.[1,7] In the endocardium, the differential diagnosis includes benign endocardial schwannomas, which occur more frequently.

Chart 1.

Malignant Schwannoma →	Cellular atypia Invasion Positive S-100 protein, vimentin immunoreactivity Negative immunostaining for desmin
Benign Schwannoma →	No cellular atypia No invasion or distant metastasis
Fibrosarcoma →	No basal lamina Negative S-100 protein immunoreactivit
Leiomyosarcoma →	Eosinophilic blunt-ended nuclei Positive immunostaining for desmin

Chart 2.

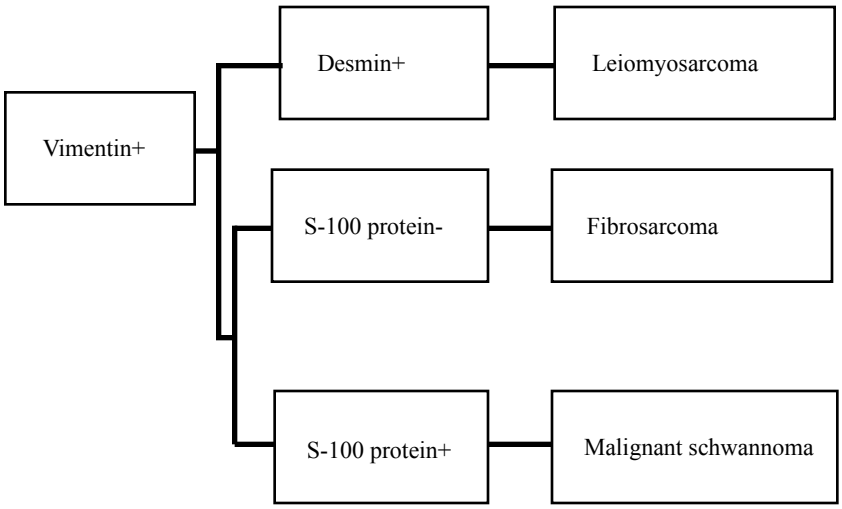

They are characterized by parallel arrays of cells, sometimes Antoni A-like pattern, and absence of prominent myocardial infiltration.[9] Endocardial schwann cell hyperplasia (neurofibromatosis) also occurs in the heart. It forms a thin layer beneath the endocardium and is well-demarcated from the myocardium; it is composed of less than 20 layers of cells.[9] In both dogs and cats, malignant peripheral nerve sheath tumors are locally invasive and may have pulmonary metastases.[6] The primary sites of benign and malignant schwannomas are the brachial plexus, the lumbosacral plexus and the subcutis in the dog whereas in the cat the neoplasms arise in the nerve roots of the lower thoracic and upper lumbar cord segments.[6] In cattle, multifocal schwannomas are common in older animals and have a predilection for the autonomic nervous system, including the epicardial plexus, thoracic and cervical sympathetic ganglia, mediastinal nerve plexus, hepatic plexus, tongue, intercostal nerves, and brachial plexus.[6]

AFIP Diagnosis: Vagina; uterus; and rectum: Malignant schwannoma (malignant peripheral nerve sheath tumor).

Conference Comment: There is marked slide variation, with some slides containing vagina and uterine horn while other sections have rectum and uterus. Conference participants commented on the abundance and prominence of the cystic structures in the tumor, and some favored the histologic diagnosis of endometriosis based on the interpretation of cystic glands within an endometrial stroma. In differentiating true cysts from pseudocysts, the conference moderator emphasized that cysts are lined by epithelial cells residing on a basement membrane. Additionally, the cells lining the cystic structures in this case are immunohistochemically positive for vimentin and negative for cytokeratin, and therefore not epithelial in origin. Additionally, while there are few reports of experimentally induced endometriosis in the rat[3], spontaneous endometriosis is typically a condition that occurs only in animals that menstruate, such as non-human primates.[4]

Another differential diagnosis considered by few conference participants included endometrial stromal sarcoma. This uterine tumor often invades the myometrium, cervix and nearby abdominal organs. The neoplastic cells are spindled and arranged in streams, intersecting fascicles, or whorls on a fibrillar matrix. Although areas of necrosis, inflammation and hemorrhage may be seen, cysts or pseudocysts are not typically associated with endometrial stromal sarcomas. This tumor is typically immunohistochemically positive for S-100 protein and vimentin, and negative for desmin and actin. The spindle cell neoplasm in the case of this rat is immunopositive for glial fibrillary acidic protein (GFAP), which is most consistent with a tumor of peripheral nerve origin.[2]

The contributor provides an excellent synopsis of the comparative pathology of peripheral nerve sheath tumors.

Contributor: Ecole Nationale Veterinaire D'Alfort, Unité d'Histologie et d'Anatomie Pathologique, 7 avenue du Général de Gaulle, 94704 Maisons-Alfort Cedex, France
www.vet-alfort.fr

References:

1. Cardesa A, Ribalta T, Vogeley KT, Reifenberger G, Wechsler W, Turusov VS. Tumors of the peripheral nervous system. In: Turusov V, Mohr U, eds. *Pathology of Tumours in Laboratory Animals*. 2nd ed., Vol. 1. Lyon, France: IARC Scientific Publications; 1990:699-723.
2. Dixon D, Leininger JR, Valerio MG, Johnson AN, Stabinski LG, Frith CH. Proliferative lesions of the ovary, uterus, vagina, cervix and oviduct in rats. In: Guides for toxicologic pathology; accessed at http://www.toxpath.org/nomen/index.htm, 11 August 2010. Washington D.C.: Society of Toxicologic Pathologists/American Registry of Pathology/The Armed Forces Institute of Pathology; 1999.
3. do Amaral VF, Dal Lago EA, Kondo W, Souza LC, Francisco JC. Development of an experimental model of endometriosis in rats. *Rev Col Bras Cir*. 2009; 36(3): 250-255.
4. Ellenson LH, Pirog EC. The female genital tract. In: Kumar V, Abbas AK, Fausto N, Aster JC, eds. *Robbins and Cotran Pathologic Basis of Disease*. 8th ed. Philadelphia, PA: Saunders Elsevier; 2010:1028-1029.
5. Enzinger FM, Weiss SW. *Soft tissue tumors*. St. Louis, MO: Mosby Press; 1995:829-837.
6. Koestner A, Higgins RJ. Tumors of the nervous system. In: Meuten DJ, ed. *Tumors in Domestic Animals*. 4th ed. Ames, IA: Iowa State Press; 2002:731-735.
7. Leininger JR, Jokinen MP. Oviduct, uterus and vagina. In: Boorman GA, Eustis SL, Elwell MR, Montgomery CA, MacKenzie WF, eds. *Pathology of the Fischer Rat*. San Diego, CA: San Diego Academic Press; 1990:455.
8. Mohr U. Soft tissue and musculoskeletal system. In: *International Classification of Rodent Tumours, Part I - The Rat*. Lyon, France: IARC Scientific Publications; 1992:34-36.
9. Mohr U. Central nervous system; Heart; Eye; Mesothelium. In: *International Classification of Rodent Tumours, Part I - The Rat*. Lyon, France: IARC Scientific Publications; 1992:34-37.

CASE IV: P99A (AFIP 3164426).

Signalment: 3.5-month-old female CB6 mouse (*Mus musculus*).

History: This mouse was a double transgene for 2 leukemogenic genes reported to be involved in acute myeloid and megakaryoblastic leukemia. During routine examination by the animal caretaker, the mouse looked sick and was sent to necropsy. It died in its cage about 2 hours after it was taken out of the animal room.

Gross Pathology: A 22.5 g female albino mouse is in rigor. The hair coat is scruffy. The tissues are pale. The gastrointestinal tract is nearly completely empty. The liver and spleen are markedly enlarged, weighing 5.2 g and 0.8 g, respectively, and 23% and 3.5% of body weight (finding age and strain-matched normal values is not easy, but in general the relative weight of the liver and spleen is approximately 4 - 5.5% and 0.2 - 0.35%, respectively). There is moderate to marked enlargement of all peripheral and visceral lymph nodes. Acute locally extensive hemorrhage is present in the mesenteric and the left axillary lymph nodes.

Histopathologic Description: Lung: A monomorphic population of round cells expands the peribronchiolar and perivascular interstitial tissue and is widely present in alveolar capillaries and in the lumen of blood vessels (leukemia). The neoplastic cells (blasts) are of intermediate size, approximately 1.5 – 2 fold larger than red blood cells, have a small amount of cytoplasm and round to slightly irregular coarsely granular nuclei, some with 1, or less commonly, several small nucleoli. There is mild anisocytosis and anisokaryosis. The mitotic rate is variable (0-2/HPF). Cellular debris is common. Also present in vascular lumena are numerous homogenous, acellular and deeply basophilic emboli of variable size and shape. Round to irregular emboli are especially prominent in larger blood vessels, but they are also widely distributed in alveolar capillaries. Some basophilic emboli contain a small amount of granular eosinophilic material. Non-aggregated intravascular dead cells and basophilic and eosinophilic cellular debris are also observed.

Liver: There is severe infiltration of neoplastic cells as described above. Diffusely, the cells fill and markedly expand the sinusoids and compress the hepatic plates. They form confluent aggregates, especially around large blood vessels. Cellular debris is common. Vascular lumena contain a large number of neoplastic cells and occasional basophilic emboli as described above.

Contributor's Morphologic Diagnosis: Lung and liver: Leukemia, undetermined type with widespread basophilic emboli (acute tumor lysis syndrome).

Contributor's Comment: This case of a hemopoietic malignancy, still awaiting full characterization, was submitted because of the presence of multiple variably sized intravascular clumps of basophilic material. The emboli showed positive fluorescent staining with Hoechst 33342, a specific stain for AT-rich regions of double stranded DNA.[1] In this mouse, other than the liver and lung, infiltration of blasts was observed in the adrenal glands, bone marrow, connective tissue, kidney, multiple lymph nodes, ovaries, salivary glands, spleen, probable thymus and uterus. Heavy neoplastic load in conjunction with emboli of this nature is typical of acute tumor lysis syndrome (ATLS).

In humans, ATLS is caused by rapid lysis of malignant cells leading to a massive release of cellular contents. The large amount of cellular debris overwhelms homeostatic mechanisms and causes an acute metabolic crisis.[1,2,3] Spontaneous ATLS, as in this case, is rare.[1] Most cases are reported in association with aggressive chemotherapy or

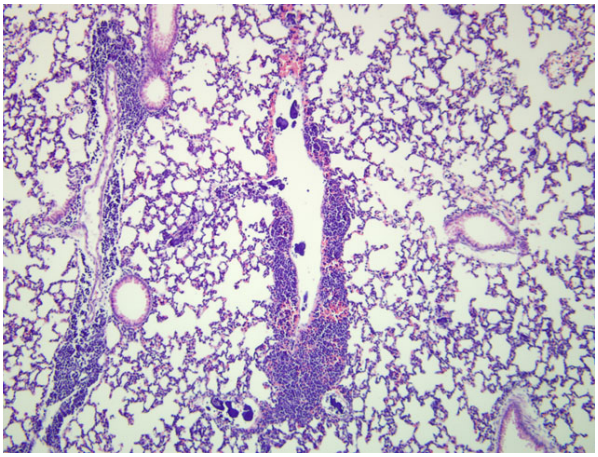

4-1. Lung, Malignant lymphoma, leukemic (Acute tumor lysis syndrome), mouse. Multifocally expanding the peribronchiolar and perivascular interstium and filling alveolar capillaries and small vessels is a monomorphic population of neoplastic lymphoid cells. Neoplastic lymphoid cells are intermediate size and have scant cytoplasm and round nuclei with coarsely stippled to clumped chromatin. Multifocally within vascular lumens are globular accumulations of homogenous, acellular deeply basophilic material (chromatin). (HE 40X)

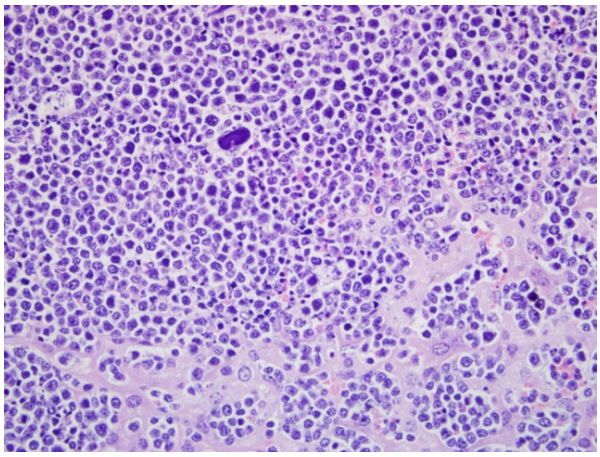

4-2. Liver, Malignant lymphoma, leukemic (Acute tumor lysis syndrome), mouse. Neoplastic lymphoid cells fill and expand sinusoids and compress hepatocytes. (HE 400X)

radiotherapy.[1,3] Acute tumor lysis syndrome is more common with hematologic malignancies than with solid tumors.[1,3] Clinically, the disorder is characterized by severe metabolic abnormalities, including hyperuricemia, hyperphosphatemia and hyperkalemia, due to substantial breakdown of nucleic acids and their release from dead tumor cells along with phosphate and potassium.[1,2,3] These abnormalities may lead to acute renal failure (the most commonly reported cause of death in human ATLS patients), bradyarrhythmias and cardiac arrest.[1,3]

In the veterinary literature, there are several case reports of chemotherapy-associated ATLS in dogs, a cat, and in a 129/SvEv mouse with PML/RARα-induced acute myeloid leukemia.[3] Spontaneous ATLS was reported in a DBA/1J mouse with leukemic lymphoma.[1] The current case is another example of spontaneous ATLS. As postulated by others, it is possible that transfer of this mouse out of the animal house led to a stress-induced surge of endogenous glucocorticoids which precipitated fatal ATLS.[1] In common with the two other murine cases, the emboli in this case were most prominent in the pulmonary vasculature.[1,3] In the case from 2003, other than the lung, emboli were identified in virtually all tissues, but were especially common in the kidney and brain.[1] In the case from 2009, emboli were observed in multiple organs, but other than the lung, were especially prominent in the liver, as in the submitted case.[3] In the submitted case, a low number of emboli in the kidney and rare emboli in lymph nodes were also observed.

In the current case, quantification of cellular death was not undertaken. Cellular debris was common, but in our slides, the number of viable cells far exceeded that of dead cells. In the other murine report of spontaneous ATLS, necrosis affected up to 90% of tumor cells.[1] In the report from 2009, caspase-3 labeled cells are described as "plentiful."[3]

Electron microscopy was done on one of the murine cases.[1] The basophilic emboli had uniform electron dense appearance similar to that of nuclear chromatin in apoptotic lymphocytes. In mixed emboli, which at the light microscopic level had a variegated basophilic and eosinophilic appearance, the eosinophilic component was composed of aggregated cytoplasmic fragments of necrotic tumor cells.[1]

Interestingly, the authors of the 2003 report in a mouse claim to be the first to describe widely disseminated DNA and cellular debris in ATLS in humans or any other species. They ascribe this to the fact that most reports of ATLS in humans are focused on clinical management and that the few reports which describe the pathologic features of this condition are based on lesions found at death, which typically occurs several days to weeks after the onset of ATLS.[1] At that point, most reported lesions are renal and attributed to urate crystal deposition in the medulla.[1]

As noted above, in the 2003 report, emboli were identified in virtually all tissues. The authors propose that mechanical obstruction of capillary beds by these emboli plays an important role in the pathogenesis of ATLS.[1] In the more recent report of ATLS, the cause of death was postulated to be respiratory failure following massive embolization of chromatin clumps and necrotic debris in pulmonary vasculature.[3]

AFIP Diagnosis: Liver; and lung: Malignant lymphoma, leukemic, with basophilic proteinaceous emboli.

Conference Comment: Conference participants briefly discussed the pathogenesis and pathophysiologic changes of acute tumor lysis syndrome (ATLS). The syndrome is typically associated with tumors displaying rapid cell proliferation, which are typically more susceptible to chemotherapeutic agents. A recent paper cites prior studies in which 5% of humans with hematologic malignancies and 25% of high-risk patients (e.g. those with T-cell acute lymphoblastic leukemia and Burkitt's lymphoma) developed clinically apparent ATLS.[4] This finding is consistent with observations in one study in which all ATLS animals had lymphoblastic lymphoma (primarily T-cell with a few B-cell types).[4] The contributor for this case further classified the malignant cell type after case submission. They classified lymphoid neoplasm as T-cell lymphoblastic lymphoma with leukemia based on neoplastic cells demonstrating strong immunopositivity for CD3, and negative immunostaining for CD45.

The underlying cause of lysis of neoplastic cells is, as of yet, undetermined. One hypothesis is that the release of an endogenous substance may cause lysis of neoplastic cells; a suspected agent is corticosteroids, which are commonly administered for the treatment of lymphoma. Once lysed, neoplastic cells release nucleic acids, potassium, and phosphorus, resulting in the observed clinicopathologic abnormalities outlined by the contributor. The nucleic acids are broken down into their respective purine and pyrimidine components. Purines are further metabolized to uric acid, which is then converted to allantoin via urate oxidase and subsequently excreted in the urine. Interestingly, humans and non-human primates lack urate oxidase and may develop hyperuricemia and uric acid crystals within renal tubules.[4,5]

The hallmark histologic finding of ATLS is that of widely disseminated microemboli of nuclear and cytoplasmic debris.[5] Microemboli are most commonly observed in the lung, kidneys, and brain. In one study, lesions of ATLS were more common in animals found dead as opposed to those that appeared sick at the time of necropsy.[4]

Contributor: Department of Veterinary Resources, Weizmann Institute of Science, Rehovot 76100, Israel
http://www.weizmann.ac.il/vet/

References:

1. Lovelace K, Van Gessel Y, Asher LV, Vogel P. Spontaneous acute tumor lysis syndrome in a DBA/1J mouse: a case report and review. *Toxicol Pathol*. 2003;31:486-90.

2. Mylonakis ME, Koutinas AF, Papaioannou N, Lekkas S. Acute tumour lysis syndrome in a dog with B-Cell multicentric lymphoma. *Aust Vet J*. 2007;85:206-208.

3. Radaelli E, Marchesi F, Patton V, Scanziani E. Diagnostic exercise: Sudden death in a mouse with experimentally induced acute myeloid leukemia. *Vet Pathol*. 2009:46:1301-1305.

4. Treuting PM, Albertson TM, Preston BD. Case series: acute tumor lysis syndrome in mutator mice with disseminated lymphoblastic lymphoma. *Toxicol Pathol*. 2010;38:476-485.

5. Vogel P, Pletcher JM, Liang Y. Spontaneous acute tumor lysis syndrome as a cause of early deaths in short-term carcinogenicity studies using *p53*$^{+/-}$ mice. *Vet Pathol*. 2010;47:719-724.

The Armed Forces Institute of Pathology
Department of Veterinary Pathology

Conference Coordinator
Matthew Wegner, DVM

WEDNESDAY SLIDE CONFERENCE 2010-2011

Conference 2

18 August 2010

Conference Moderator:
Michael J. Topper, DVM, PhD, Diplomate ACVP

CASE I: UW-N09-295 (AFIP 3 134360).

Signalment: 6-year-old male neutered domestic short hair cat (*Felis catus*).

History: 6-year-old, male neutered domestic shorthair who presented to the University of Wisconsin emergency room (ER) service 2/21/09 for severe anemia- PCV 12%. Anemia was non-regenerative, but had signs of autoagglutination, mild elevation in bilirubin, rubriblasts in peripheral blood smear, and a left shift. Mycoplasma PCR positive. Started treatment with steroids and doxycycline during visit. Came back through the ER 3/12/09 for pale white gums, murmur, collapse. Current physical exam findings: Temperature=96.1°F; Pulse=150; Respiratory rate=30; Mucous membranes=pale/white; murmur auscultated; abdomen soft.

Gross Pathology:

1. General body condition
   i. Moderate, diffuse icterus of the subcutaneous fat
2. Abdominal cavity
   i. Moderate diffuse icterus of the abdominal fat
   ii. Mild abdominal effusion
   iii. Moderate, diffuse hepatic fibrosis (presumptive)
   iv. Moderate splenomegaly
   v. Moderate, diffuse renal icterus

Laboratory Results:

Test	Results	REF INT	Units	Test	Results	REF INT	Units
RBC	2.67	5.8-10.7	x10^6/µL	WBC	23.2	5-19.5	x10^3/µL
PCV	12	-	%	Segments	17.8	-	x10^3/µL
MCV	47.4	39-55	fL	Monos	2.3	0-0.85	x10^3/µL
MCH	16	13-17	pg	Lymp	2.6	0-0.75	x10^3/µL
MCHC	34.4	30-36	g/dL	Atypical nuclear cells	1.07	-	x10^3/µL
Platelet	260	175-600	x10^6/µL				
Platelet	Clumped,> than reported value						

3. Thoracic cavity
   i. Moderate, diffuse lung collapse
   ii. Moderate, focal, right cranial lung lobe emphysema

Histopathologic Description: Bone marrow: The bone marrow is highly cellular with more than 85% of the cells being nucleated cells of the erythroid type. More than 50% of the cells have high nuclear:cytoplasmic ratios with basophilic cytoplasm, round, sometimes irregular, nuclei, finely stippled chromatin and one to two nucleoli. Mitotic figures are rare and atypical cells are also present. Based on the morphology, these cells resemble rubriblasts. Occasionally, the nuclei have moderately large magenta nucleoli. More mature cells of the erythroid type, including metarubricytes and rubricytes, are found in clusters and distributed throughout the section. The granulocytic lines are severely decreased in number. Moderate numbers of megakaryocytes are diffusely distributed throughout the bone marrow. A few, rare scattered iron stores are observed in the sections examined. Small islands of red blood cells are also seen.

The neoplastic cells are also observed in the sinusoids of liver, alveolar septae of lungs and in the vascular lumen in brain, kidney, heart and urinary bladder (sections not provided).

Contributor's Morphologic Diagnosis: Bone marrow – Erythremic myelosis, feline.

Contributor's Comment: Myeloproliferative disorders are defined as medullary and extramedullary proliferation involving marrow myeloid cell lines.[1,4] Erythremic myelosis (EM) is a proliferative disorder of early erythrocyte precursors (Di Guglielmo's disease).[4] The disease is categorized as an acute myeloid leukemia (M6b) containing only erythroid cells, with malignant erythroblasts being the predominant cell type. Erythroblasts along with prorubricytes constitute as much as 80% of all nucleated marrow cells. This is different from erythroleukemia (M6a), which constitutes proliferation of both erythroid and myeloid cells. Under veterinary adapted guidelines of French-American-British (FAB), EM is currently categorized as either a myelodysplastic syndrome with erythroid predominance (MDS-Er) or an acute myelogenous leukemia (M6-Er erythroleukemia with erythroid predominance). There are several reports of transition from M6-Er to M6 or M6a (erythroleukemia) in cats, which is described as lineage switching. M6 or M6a is rare in animals and more so in humans. M6b/M6-Er/EM are also rare in animals, but are more commonly seen in cats.[4]

Erythremic myelosis is characterized by severe non-regenerative anemia with peripheral blood smears revealing variable numbers of metarubricytes, rubricytes, and rubriblasts with markedly decreased mature erythrocytes. In a healthy animal that is not anemic, metarubricytes are a rare

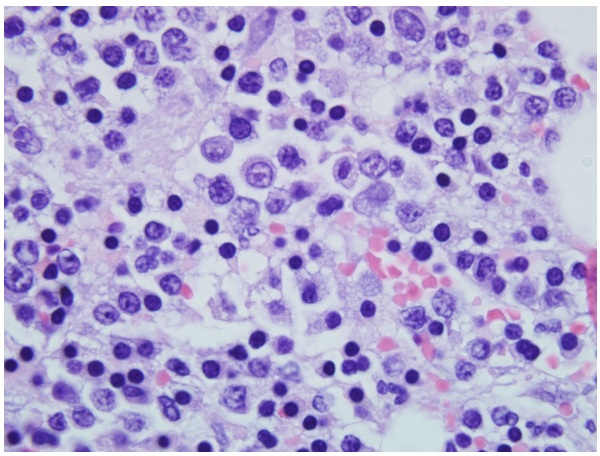

1-1. Bone marrow, cat. The highly cellular bone marrow is composed primarily of nucleated erythroid cells (greater than 85%). Over 50% of the cells are rubriblasts; metarubricytes and rubricytes are found in clusters within the field. (HE 1000X)

occurrence; further, in response to hypoxia or regenerative anemia, increase in metarubricytosis is usually transient. However, lack of significant numbers of circulating polychromatophilic erythrocytes (in Romanowsky- stained blood smears) or reticulocytes (in new methylene blue-stained blood smears) classifies the anemia as nonregenerative. In regenerative anemia, metarubricytosis may be present in acute splenic trauma, post splenectomy, bone fracture or following blood loss.

The pathogenesis of EM has not been completely elucidated, but a positive association is present with infection by Feline leukemia virus (FeLV) type C retrovirus. FeLV is a transmissible retrovirus responsible for or associated with a variety of disease processes. Three subgroups are present, A, B and C. Subgroup A is the infective, horizontally transmissible form of the virus, and subgroup B and C result from viral recombination within individual cats. Subgroup B is primarily responsible for the development of lymphoma and subgroup C is responsible for severe anemia and erythremic myelosis. Though the pathogenesis has not been identified, the prominent finding in EM is a maturation arrest of erythrocytes.[2] The erythrocyte arrest, a key component of EM and other disease, occurs before the reticulocyte stage (Diagram 1) resulting in severe anemia.

As indicated above, absence of reticulocytes in the blood in anemic animals is indicative of a disease process at the bone marrow level. A consensus exists that the site of action of the disease in the marrow is at the level of the burst-forming and colony-forming units of the erythroid line (Diagram 2).[2]

Clinically, the cats with EM present with depression of days to months, anorexia and mild icterus. The most consistent finding in cats with EM is a low hematocrit value of 12 to 15%. In addition to the severe anemia, the reticulocytes are either in the low-normal range or are not present. As EM is associated with FeLV infection, which is shown to have

Diagram 1.

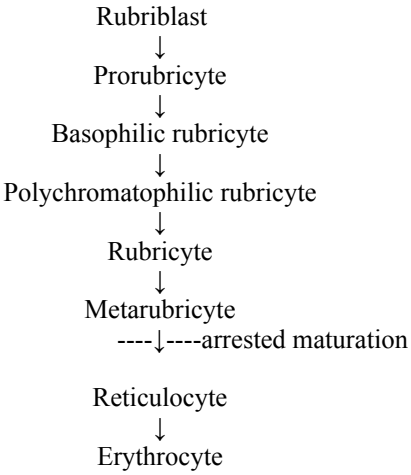

Diagram 2.

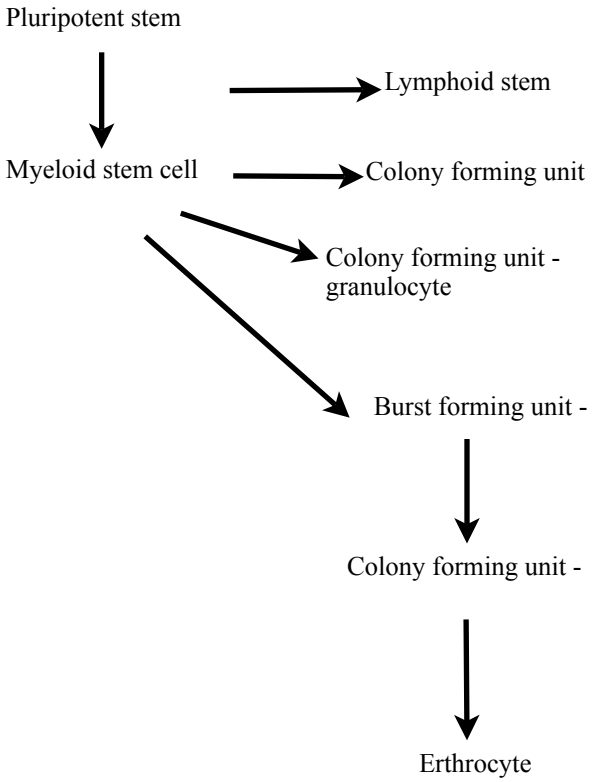

effects of all three bone marrow cell lines to varying degrees, a complete blood count along with evaluation of peripheral blood smear are indicated.

The numerous circulating nucleated red cells in M6-Er/EM/M6b can superficially mimic the finding in acute hemolytic anemia. In hemolytic anemia, the absence of rubriblasts or very immature erythroid cells in the peripheral blood and an increased reticulocyte count are characteristic of acute hemolysis with regeneration and can aid in differentiation from EM. Also the marked anemia seen with erythremic myelosis is nonregenerative and rubricytes are in maturation arrest. Feline infectious anemia caused by *Mycoplasma haemofelis* (previously *Haemobartonella felis*) is often suspected and may be present but should be recognized as an incidental finding because of the lack of polychromasia and presence of blasts in the blood of cats with EM.[4]

AFIP Diagnosis: Bone marrow: Myelodysplasia, diffuse with erythroblastosis and maturational arrest.

Conference Comment: Tissue identification was one of the diagnostic challenges experienced by some conference participants for this case, but most correctly identified the tissue as bone marrow despite the absence of bone spicules. Many conference participants also identified and described a proliferative lesion of erythroid cell lineage in the examined sections of bone marrow; but in the absence of the comprehensive clinical history and extensive laboratory data provided by the contributor, most favored a more general histologic diagnosis of myelodysplasia with erythroblastosis, and hence the diagnosis indicated above. Once the specific clinicopathologic data were revealed during conference by the moderator, participants concurred with the contributor's more specific diagnosis.

The moderator and conference participants also discussed the variety of classification schemes for proliferative bone marrow lesions in the published literature, including the WHO classification system and the French-American-British system. The differential diagnosis for hypercellular bone marrow with erythroblastosis and reduced/absent myeloid elements discussed by participants included: 1) myelodysplastic syndromes; 2) myelodysplastic/myeloproliferative diseases; 3) acute myeloid leukemia (e.g. erythremic myelosis, erythroleukemia); and 4) chronic myeloproliferative diseases.[3] Some overlap exists with specific disease entities within each group of disorders among the various current classification systems.

Myelodysplastic syndromes (MDS) are characterized by maturation defects in clonal stem cells associated with ineffective hematopoiesis and qualitative and quantitative marrow cell dysplasia, and can evolve into acute leukemias.[3,4] Clinically, animals with MDS present with poor body condition, lethargy, pale mucous membranes, and a history of recurring infections, often involving the respiratory tract. Histologically, the marrow is hypercellular

with morphologic change(s) in one or more cell lineages (i.e. erythrocytic, leukocytic, and megakaryocytic).[4] In addition to the contributor's concise discussion of erythremic myelosis in the cat, more information concerning myelodysplastic and myeloproliferative disorders of domestic animals is available within the references cited below.

Contributor: Department of Pathobiological Sciences, School of Veterinary Medicine, University of Wisconsin-Madison, 2015 Linden Drive, Madison, WI 53706-1102
http://www.vetmed.wisc.edu/Pathobiological_Sciences.15.6.html

References:

1. Comazzi S, Paltrinieri S, Caniatti M, De Dominici S. Erythremic myelosis (AML6er) in a cat. *Fel Med and Surg*. 2000;2:213-215.
2. Morrison, JA. Erythremic myelosis. *Compen Contin Edu Pract Vet*. 2001;23:880-886.
3. Stockham SL, Scott MA. Bone marrow and lymph node. In: *Fundamentals of Veterinary Clinical Pathology*. 2nd ed. Ames, IA: Blackwell Publishing; 2008:324-358.
4. Valli VEO. Hematopoietic system. In: Maxie MG, ed. *Jubb, Kennedy and Palmer's Pathology of Domestic Animals*. 5th ed., Vol. 3. Philadelphia, PA: Elsevier Ltd.; 2007:125-147.

CASE II: E18091 (AFIP 3135176).

Signalment: 8-year-old male neutered domestic-mixed breed cat (*Felis silvestris*).

History: The animal presented with anorexia and in poor general condition. Blood biochemical examination revealed increased enzyme activities of aspartate aminotransferase (AST) and alkaline phosphatase (ALP). One month later, exploratory laparotomy was performed because of further worsening of body condition. The surface of the liver was irregular, and multiple small nodules were observed on the small intestine. Wedge biopsy of the liver and small intestine was performed.

Gross Pathology: The surface of the biopsied liver tissue was irregular and multiple small nodules were scattered in the small intestine.

Laboratory Results: On day of first presentation: ALT 300 IU/L; ALP 130 IU/L; and Total bile acids 12.5µmol/L. One month later: ALT 600 IU/L; ALP 300 IU/L; and Total-bilirubin 2.8 mg/dL.

Histopathologic Description: Liver: Neoplastic lymphocytes were observed in the cytoplasm of hepatocytes, sinusoids, interlobular veins, and the interstitium of Glisson's sheath. The number of neoplastic cells in the hepatocytes was one to several. Mitotic figures were often observed among the engulfed neoplastic cells. Neoplastic cells invaded the epithelial layer and lumen of the bile duct. Some hepatocytes engulfing the neoplastic cells had lipofuscin pigments or clear vacuoles in the cytoplasm. However, apparent morphological changes suggesting cell death were not detected in these hepatocytes.

A large number of neoplastic lymphocytes had round or ovoid nuclei which were elongated or cleaved in some cells. The nuclei of neoplastic cells had darkly-stained coarse chromatin and were easily distinguishable from those of hepatocytes. The neoplastic cells had a scant amount of eosinophilic cytoplasm.

In addition, varying amounts of yellow pigment were engulfed in Kupffer cells. Neutrophils and other segmented nuclear granulocytes were increased in the sinusoids and emigrated into some hepatocytes and bile ducts.

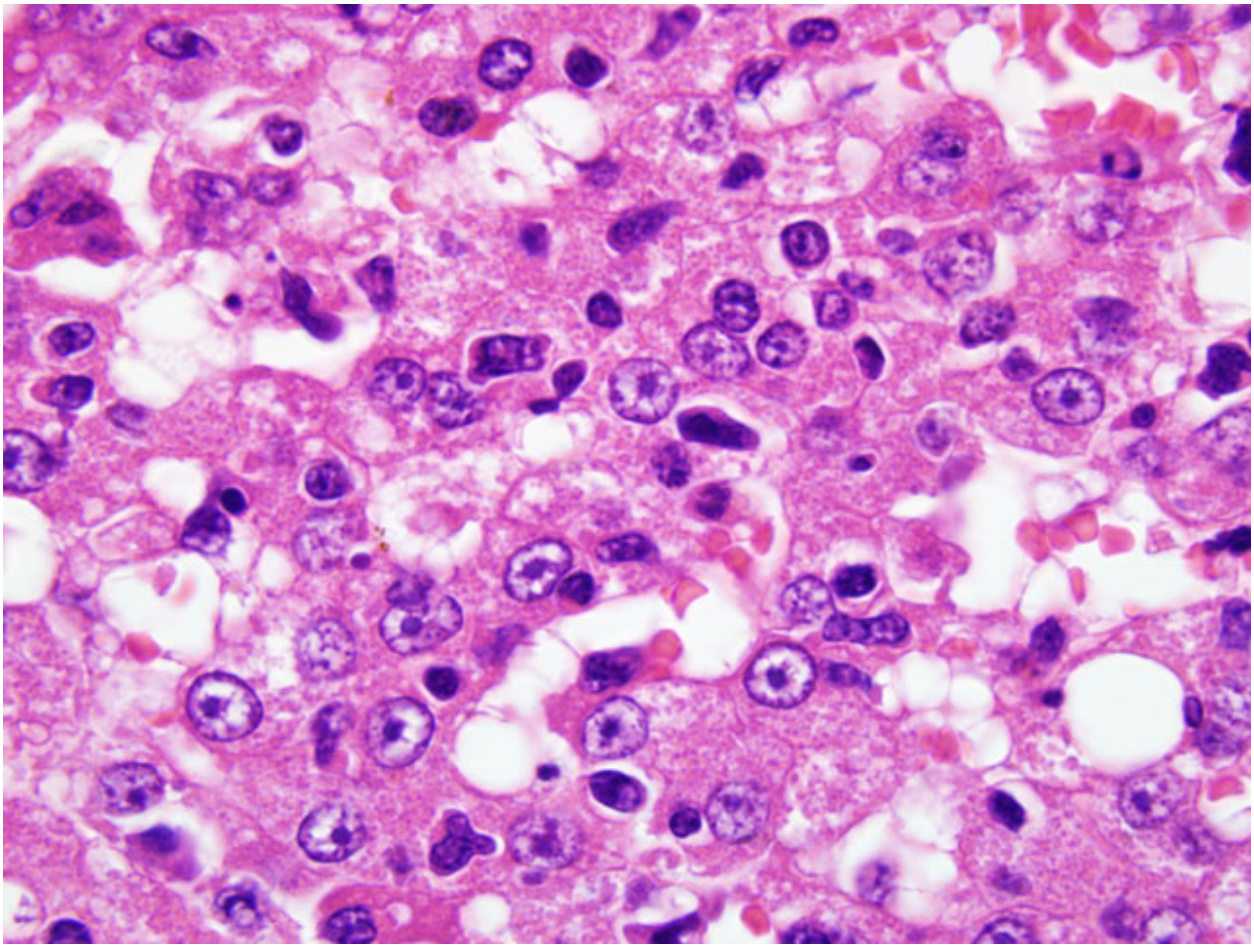

2-1. Liver, malignant lymphoma, T-cell, large granular lymphocyte type, cat. Neoplastic lymphocytes occur within sinusoids and within the cytoplasm of hepatocytes (emperipolesis). (HE 1000X)

Immunohistochemically, large number of neoplastic cells showed positive reaction for CD3. Positive reaction for CD20, CD56, and CD79 was not observed. Immunopositive reaction for cleaved-caspase 3 was not observed in the hepatocytes with or without infiltrated neoplastic cells. Immunohistochemical examination for proliferating cell markers, such as Ki-67 and PCNA, brought equivocal results due to the intense positive reaction of infiltrating neoplastic cells in these hepatocytes.

Contributor's Morphologic Diagnosis: Liver: T-cell chronic lymphocytic leukemia.

Contributor's Comment: Malignant lymphoma, including the leukemic type, is the most common neoplasm of cats and accounts for more than half of all feline hemolymphatic tumors. Among the liver tumors of hematopoietic cell origin, malignant lymphoma/leukemia is also most common in the cat; however, infiltration of tumor cells into hepatocytes is rare.[2] Epithelial invasion by neoplastic cells is a characteristic feature of some special types of malignant lymphoma, such as epitheliotropic cutaneous lymphoma and primary intestinal lymphoma in dogs and cats. In addition to epithelial invasion by neoplastic cells in these types of malignant lymphomas, emperipolesis may also occur. Emperipolesis is a phenomenon in which some kind of viable cell, for example a lymphocyte, is engulfed by a large host cell without damage to either cell. This phenomenon is usually observed among cells in tissue cultures or isolated human cell smears. The phenomenon of emperipolesis has been reported to occur under various physiological and pathologic conditions. Host cells recorded to engulf lymphocytes, granulocytes, or other blood cells include mesenchymal cells, fibroblasts, thyroid epithelial cells, endothelial cells of high endothelial venule, megakaryocytes, monocytes, macrophages, and cancer cells. Normal lymphocytes, neoplastic cells obtained from leukemias, or lymphomas were also reported to be involved in emperipolesis when cultured with macrophages. The occurrence of *in vivo* emperipolesis in humans is very rare. In animals, reports of emperipolesis *in vivo* are also very rare. The present case of feline malignant lymphoma involving the liver is considered to be the leukemic type due to the appearance of neoplastic cells in the sinusoids. Immunohistochemical findings suggest that the neoplastic lymphocytes are T-cell origin. According to the histologic criteria established by the World Health Organization (WHO), this case is T-cell chronic lymphocytic leukemia judging from the small cells with a dense chromatin distribution.

As stated above, neoplastic lymphocytes of T-cell origin occasionally have a character of infiltrating into the epidermis, the epithelium in adnexal tissues, or mucosal epithelium. In addition, as in the present case, the fact that CD3 positive neoplastic T-cell lymphocytes invaded the epithelium of a relatively large bile duct along withhepatocytes suggests that infiltration into hepatocytes reflects a common mechanism of neoplastic cells of T-cell origin.

In the present case hepatocellular damage due to intracellular invasion by neoplastic lymphocytes was considered possible; however, necrotic and apoptotic changes of hepatocytes were not detected morphologically and hepatocytes had a negative reaction for one of the enzymes concerning apoptosis, cleaved-caspase 3, by immunohistochemical examination. From these results, cytotoxic effect of infiltrating lymphocytes on hepatocytes was not evident.

AFIP Diagnosis: Liver: Malignant lymphoma, T-cell, favor mature large granular lymphocyte lymphoma with emperipolesis.

Conference Comment: This very intriguing and diagnostically challenging case stimulated a vibrant discussion during the conference, and participants were evenly divided as to whether the lesion represented an inflammatory process or malignant lymphoid neoplasia. All participants identified an infiltrate of small lymphoid cells in the liver, with frequent occurrence of the cells in the cytoplasm of hepatocytes (emperipolesis), as described by

the contributor. Close visualization of the lymphoid infiltrate under oil immersion reveals that the cells have irregularly round to ovoid, often indented nuclei with coarse chromatin and inapparent nucleoli. In some areas, eosinophilic granules are present in the cytoplasm, often within an indentation in the nucleus. Occasional mitoses are present. Hepatocytes are swollen and occasionally contain lipid vacuoles. Based on the interpretation of morphologically abnormal lymphocytes, participants ultimately favored a neoplastic process and preferred the diagnosis of malignant lymphoma. While the infiltration of malignant lymphocytes into the liver may well represent an underlying leukemic condition, bone marrow and peripheral blood evaluation are required to document the definitive diagnosis of leukemia, and hence the diagnosis indicated above. For participants favoring an inflammatory process, an autoimmune condition was suspected as the underlying cause of the lesion.

Humans have a distinct form of hepatic lymphoma termed sinusoidal T-cell lymphoma, and its histopathologic features share similarities with the case of this cat. The primary histologic finding in the human disease is diffuse infiltration of malignant T-cells into the hepatic sinusoids in the absence of a mass effect. The histologic observation of low to moderate numbers of sinusoidal lymphocytes in the liver biopsies and the clinical presentation of affected human patients often lead to the misdiagnosis of acute or chronic inflammatory liver disease.[1] The sinusoidal form of hepatic malignant lymphoma in humans demonstrates the difficulty sometimes encountered when attempting to differentiate an inflammatory process from neoplasia by histopathology.

Among the various lymphoid neoplasms affecting cats, several features in this case are suggestive for large granular

lymphocytic (LGL) lymphoma, including the contributor's gross report of nodular lesions in the small intestine, cytomorphology of neoplastic cells containing eosinophilic cytoplasmic granules, and prominent emperipolesis. The most common primary site for LGL lymphoma in the cat is the small intestine;[3] additional information concerning the gross lesions found in the small intestine, including histopathologic findings, might have been useful in this case.

This case was studied in consultation with Dr. Peter Moore, a recognized expert in the field of veterinary hematopoietic neoplasia. Dr. Moore has observed a number of similar cases in which the neoplastic lymphoid cells in feline LGL lymphoma express CD3; based on this finding and other evidence, he suspects LGL type tumors arise from intestinal epithelial lymphocytes (IEL). Dr. Moore also has observed a similar hepatic infiltration pattern for LGL lymphoma in dogs, albeit without the intestinal association; publication of the canine form of the disease is forthcoming. An IEL origin for the malignant lymphoid cells might well explain the unique histologic infiltration pattern observed in the liver of this cat, as most cases of LGL lymphoma in cats have intestinal involvement with frequent involvement of the liver, and disseminating lymphomas frequently metastasize to the liver along hepatic sinusoids.[1,3]

We thank Dr. Moore for his informative consultation with this case.

Contributor: Department of Pathology, Faculty of Pharmaceutical Science, Setsunan University,45-1 Nagaotohge-cho, Hirakata, Osaka 573-0101, Japan
http://www.setsunan.ac.jp/~p-byori/

References:

1. Ishak KG, Goodman ZD, Stocker JT. Primary hepatic lymphomas and suspected lymphomas. In: *Atlas of tumor pathology: Tumors of the liver and intrahepatic bile ducts 3rd series, fascicle 31*. Washington, DC: Armed Forces Institute of Pathology; 2001:335-338, 2001.
2. Ossent P, Stockli RM, Pospischil A. Emperipolesis of lymphoid neoplastic cells in feline hepatocytes. *Vet Pathol*. 1989;26:279-280, 1989.
3. Valli VE. T-cell and NK-cell neoplasms. In: *Veterinary Comparative Hematopathology*. Ames, IA: Blackwell Publishing; 2007:304-306.

CASE III: AP07-3021 (AFIP 3142118).

Signalment: 27-year-old male Buckskin gelding, equine (*Equus caballus*).

History: This horse presented to the North Carolina State University-Veterinary Teaching Hospital's Equine Emergency Service on 12/16/07 for evaluation of choke. He had been choking for approximately 24 hours. The referring veterinarian had attempted to relieve the choke, but was only able to extract a few leaves out of the trachea. The initial physical examination revealed a heart rate of 96 beats per minute, respiratory rate of 48 beats per minute, severe dyspnea and depression. Thoracic radiographs revealed evidence of aspiration pneumonia. The owner elected euthanasia due to poor prognosis and on humane grounds to relieve suffering. The final clinical diagnosis was aspiration pneumonia.

Gross Pathology: The necropsy findings are consistent with aspiration pneumonia. The dentition of this horse is severely worn. The esophagus is dilated and contains a 20 cm long clump of solid feed.

The right thyroid gland is markedly enlarged, measuring 12x 7x5 cm. Its capsule is intact and the gland is freely moveable. On cut surface, almost all of the parenchyma is replaced by several tan, fleshy, expansile, multi-lobulated masses, the largest measuring 5 cm in diameter. One mass is very soft, friable and is mottled yellow and black. The left thyroid gland is moderately enlarged, freely movable, and measures 5x2x1.5 cm. On cut sections there are greater than twenty 0.2-1.0 cm soft, white, well-circumscribed spherical foci scattered throughout its parenchyma.

Bilaterally, affecting 80% of the left and 50% of the right adrenal gland, the medulla is replaced and expanded by red, fleshy, shiny, multifocal to coalescing, spherical masses that vary in size from 0.5-3.5 cm in diameter. The cortices, although slightly compressed, are intact.

Histopathologic Description: Adrenal glands, bilateral: Replacing much of the adrenal medulla and multifocally compressing the cortical parenchyma are multiple densely cellular, well circumscribed, and partially encapsulated masses composed of neoplastic polygonal cells arranged in nests and cords supported by a fine fibrovascular stroma. The neoplastic cells have oval nuclei, often with a single, dark, basophilic nucleolus, amphophillic, granular cytoplasm, and variably distinct cell borders. The mitotic rate averages 1 per high power field. Multifocally throughout the neoplastic masses, there are prominent blood filled sinuses.

Right Thyroid Lobe (top tissue section): This section includes a portion of the 5 cm diameter mass described

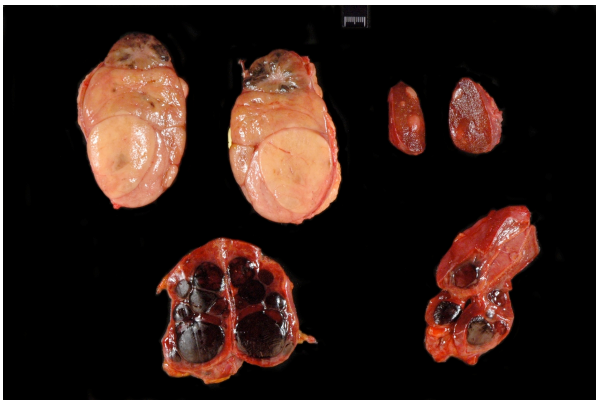

3-1. Adrenal gland and thyroid gland, horse. Both adrenal medullas (bottom) are expanded and replaced by red, fleshy, multifocal to coalescing, spherical masses that vary in size. The right thyroid gland is markedly enlarged, measuring 12x7x5 cm; the cut surface is replaced by several tan, fleshy, expansile, multilobulated masses, the largest measuring 5 cm in diameter. The left thyroid gland is enlarged measuring up to 5x2x1.5 cm; on cut section there are more than twenty (0.2-1.0 cm) white, well circumscribed spherical foci scattered throughout the parenchyma. Photograph courtesy of Mark Simpson , 37 Convent Drive Building 37 Bethesda, Maryland 20892, websterjd@mail.nih.gov

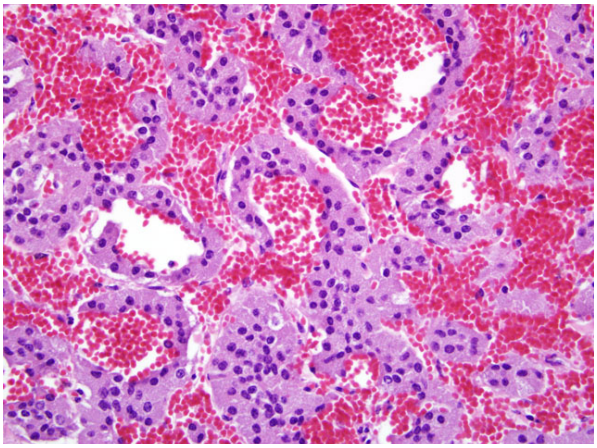

3-2. Adrenal gland, pheochromocytoma, horse. Neoplastic adrenal medullary cells are arranged in nests, packets, and trabeculae supported by a fine fibrovascular stroma. Neoplastic cells have variably distinct borders, moderate amphophilic granular cytoplasm, and an oval nucleus. (HE 400X)

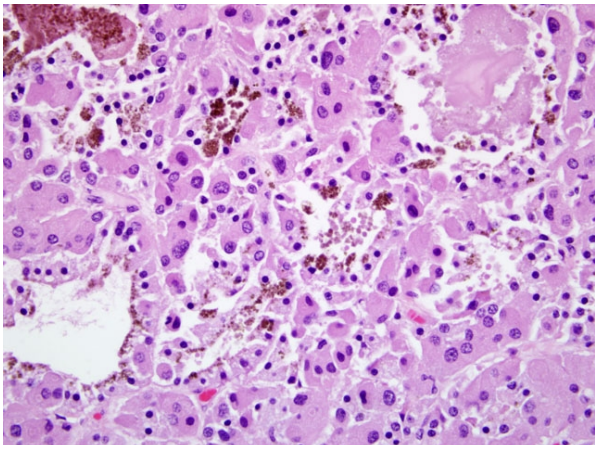

3-3. Thyroid gland, C-cell carcinoma, horse. Neoplastic thyroid parafollicular cells are arranged in nests and packets along a fine fibrovascular stroma. Neoplastic cells have moderate to abundant eosinophilic granular cytoplasm and irregularly round to oval nuclei. Cells demonstrate anisocytosis, anisokaryosis, and atypia. (HE 400X)

grossly and an adjacent, smaller multilobulated mass. The larger mass is a partially encapsulated, well circumscribed, expansile neoplasm composed of polygonal cells arranged in nests and cords. The neoplastic cells have moderate amounts of eosinophilic granular cytoplasm, round to oval nuclei that have vesicular to hyperchromatic chromatin, occasional eosinophilic intranuclear pseudoinclusions, and variably distinct cell borders. These cells demonstrate moderate to marked anisokaryosis and anisocytosis. The mitoses are less than 1 per high power field. Scattered randomly throughout the mass, accounting for approximately 40% of its composition, are entrapped and frequently compressed thyroid follicles, which are lined by low cuboidal cells with vacuolated cytoplasm and often pyknotic nuclei. A thin strip of thyroid parenchyma is compressed between the previously described mass and the smaller adjacent mass which is composed of disorganized aggregates of more uniform yet similarly shaped polygonal cells to those described in the larger mass. These cells demonstrate minimal anisocytosis and anisokaryosis. Entrapped follicles are also visible, accounting for 60-70% of this mass.

Left Thyroid Lobe (central tissue section): This section includes three of the masses seen grossly. These masses are partially encapsulated and compress the thyroid parenchyma. Otherwise these foci are similar to the smaller mass described in the right thyroid gland. Throughout the remainder of this tissue, there are aggregates of uniform yet similarly shaped polygonal cells to those already described that separate the thyroid follicles but lack any larger mass effect, encapsulation or compression affect of adjacent tissue. These aggregates of cells are interpreted to be hyperplastic foci.

Contributor's Morphologic Diagnoses: 1. Adrenal gland, bilateral: Pheochromocytoma, multifocal to coalescing.
2. Right thyroid lobe: C cell carcinoma and C cell adenomas.
3. Left thyroid lobe: C cell adenomas and multifocal C cell hyperplasia.

Contributor's Comment: The changes in the adrenals are consistent with pheochromocytomas. No evidence of vascular invasion is seen at necropsy or during histological examination of tissue sections. If these tumors were functionally active, this horse may have had hypertension.

The masses in the thyroid are consistent with a transition from C cell hyperplasia to malignant neoplasia. The determination of carcinoma for the one mass is based on degree of cellular atypia rather than any overt evidence of invasion or metastasis. Initially, our top differential for these tumors was thyroid follicular cell carcinoma. However, immunohistochemical analysis of the tissue revealed that the neoplastic cells that form aggregates and sheets stain variably positive for calcitonin indicating that the tumor is of thyroid C (parafollicular) cell origin. The cells lining the follicles that are scattered multifocally within the masses are calcitonin negative. The foci of hyperplastic cells are positive for calcitonin as are the medullary cells within the remnants of normal thyroid tissue. The latter are interpreted as normal C-cells.

Multiple endocrine neoplastic (MEN) syndrome is extensively described in humans and has multiple subtypes, many with defined genetic bases. This horse has both pheochromocytomas and C cell tumors and is therefore most consistent with MEN 2A wherein there is medullary thyroid carcinoma (C-cell neoplasia) and/or C-cell hyperplasia in nearly all cases as well as pheochromocytoma in approximately 50% of cases.[4] The cell of origin for medullary thyroid carcinoma in humans is derived from neural crest cells and is part of the amine precursor uptake and decarboxylation system (APUD). It is capable of calcitonin secretion, which is a marker for this tumor. Calcitonin levels were not measured in this horse. More common in bulls, C-cell tumors are also called ultimobranchial gland tumors due to their suggested origin from remnants of the ultimobranchial body, which is composed of cells that can differentiate into both C cells and follicular cells. The etiology of these tumors in bulls is unknown but there is a possible link with excessive long term dietary intake of calcium.[5] As in humans, bulls with C cell tumors often have pheochromocytomas and pituitary adenomas. This equine had multiple pheochromocytomas but no histologic evidence of a pituitary adenoma. De Cock et al. reported a case as well as retrospective data supporting the existence of MEN in horses. In their study, 4/72 horses had C-cell tumors only and 6/72 horses had both C-cell tumors and pheochromocytomas.[2] However, there is no mention that any of these C-cell tumors are carcinoma and their specific case is defined as a C-cell adenoma. Ueki et al. surveyed thyroid glands of aged horses and through use of immunohistochemistry found that the discrete white nodules found in 12/38 thyroid glands were consistent with thyroid C-cell adenomas. These nodules were only apparent when the thyroid was sectioned and involved only a small portion of the parenchyma. Histologically, the cells are described as mature with minimal atypia, unlike the neoplastic thyroid cells in our submission.[6]

AFIP Diagnoses: 1. Adrenal gland: Pheochromocytoma; and multifocal medullary hyperplasia.
2. Thyroid gland, right lobe (per contributor): Parafollicular (C-cell) carcinoma; and parafollicular (C-cell) adenoma.
3. Thyroid gland, left lobe (per contributor): Parafollicular (C-cell) adenoma; and multifocal parafollicular (C-cell) hyperplasia.

Conference Comment: Some conference discussion centered on the histologic distinctions among proliferative thyroid parafollicular (C-cell) lesions, and the following summarizes the general histologic features for each:[1]

- Nodular hyperplasia – multiple small foci of well-demarcated, unencapsulated cells with similar histologic appearance to normal cells

- Adenoma – solitary, well-demarcated, encapsulated, expansile mass which compresses adjacent tissue
- Carcinoma – typically larger than adenomas, with evidence of capsular invasion, secondary foci of growth within the fibroadipose tissue surrounding the gland, intravascular tumor cells, metastasis, and cellular atypia

Thyroid parafollicular neoplasms are most common in aged bulls, rats and adult horses; these tumors are often functional in older bulls, though serum calcium may be within normal limits to mildly decreased owing to the relatively slow metabolic turn-over of bone and compensatory parathyroid gland hyperplasia.[1] It has been proposed that since calcitonin is released in response to hypercalcemia, the lesion in bulls could be due to prolonged ingestion of high calcium diets. Occasionally amyloid, which is believed to be derived from calcitonin, can be found within C-cell tumors in bulls. The typical immunohistochemical staining pattern for C-cell hyperplasia, adenoma and carcinoma is as follows:[3]

- C-cell hyperplasia – consistently positive for calcitonin; variably positive for chromogranin A +B, synaptophysin, and neuron specific enolase (NSE); may be focally positive for somatostatin and bombesin
- C-cell adenoma – consistently positive for calcitonin; variably positive for chromogranin A +B, synaptophysin, NSE and protein gene product 9.5 (PGP9.5); may be focally positive for somatostatin and bombesin
- C-cell carcinoma – consistently positive for calcitonin; variably positive for chromogranin A +B, synaptophysin, and protein gene product 9.5 (PGP9.5); may be immunopositive for thyroid transcription factor 1 (TTF-1)

Among domestic animals pheochromocytomas occur most frequently in the ox and dog. Metastasis occurs in approximately half of all canine pheochromocytomas, with spread to the liver, regional lymph nodes, spleen and lungs. These malignant adrenal gland tumors are generally non-functional; when functional, clinical signs attributed to catecholamine excess include tachycardia, edema, cardiac hypertrophy, hyperthermia, arteriolar sclerosis and arteriolar medial hyperplasia.[1]

Contributor: 37 Convent Dr., Building 37/Room 2002, Bethesda, MD 20892 http://ccr.ncifcrf.gov/resources/molecular_pathology/

References:

1. Capen CC. Endocrine glands. In: Maxie MG, ed. *Jubb, Kennedy and Palmer's Pathology of Domestic Animals.* 5th ed. Vol. 3. Philadelphia, PA: Elsevier Ltd.;2007:327-328, 402-405, 419-422.

2. De Cock HEV, MacLachlan NJ. Simultaneous occurrence of multiple neoplasms and hyperplasias in the adrenal and thyroid gland of the horse resembling multiple endocrine neoplasia syndrome: case report and retrospective identification of additional cases. *Vet Pathol*. 1999;36:633-636.

3. Kiupel M, Capen C, Miller M, Smedley R. *Histological classification of tumors of the endocrine system of domestic animals*, 2nd series, Vol. XII, pp. 37-39, 46-47. Armed Forces Institute of Pathology, Washington, DC, 2008.

4. Peczkowska M, Januszewwicz A. Multiple endocrine neoplasia type 2. *Familial Cancer*. 2005;4:25-36.

5. Seimiya YM, Takahashi M, Furukawa T, Mizutani K, Kimura K, Haritani M. An aged bull with concurrent thyroid C cell carcinoma, adrenal pheochromocytoma and pituitary chromophobe adenoma. *J Vet Med Sci.* 2009;71:225-228.

6. Ueki H, Koatari T, Oyamanda T, Oikawa M, Yoshikawa H. Non-functional C-cell adenoma in aged horses. *J Comp Pathol*. 2004;131:157-165.

CASE IV: 09-129 (AFIP 3162470).

Signalment: 3-month-old male castrated Finn x Dorset lamb (*Ovis aries*).

History: On October 6, the animal was sedated with ketamine and dexmedetomidine and maintained with isoflurane anesthesia to debride a preputial laceration (presumed shearing injury). The animal was treated with intramuscular enrofloxacin once daily and flunixin meglumine twice daily until October 9, when the animal was noted to be passing pink urine (positive for blood and protein by dipstick). Diminished body condition was noted at this time. Flunixin was discontinued, and animal was started on parenteral ceftiofur and daily subcutaneous fluids. Pink urine was again noted on October 11. Due to declining clinical course, the animal was euthanatized on October 12.

Gross Pathology: There was mild muscle wasting, although visceral fat reserves were adequate. In both the left and right kidneys there were focally extensive and severe hemorrhages in the renal medulla and crest with pallor of the medulla. The renal cortices were grossly normal.

Laboratory Results (clinical pathology, microbiology, PCR, ELISA, etc.)**:**

WBC 17,100 x 10^3/µL (4,000-12,000)
Neutrophils 10,431 x 10^3/µL (61%; 400-6000)
Lymphocytes 6156 x 10^3/µL (36%; 1,600-9,000)
Monocytes 171 x 10^3/µL (1%; 0-750)
Eosinophils 342 x 10^3/µL (2%; 0-1200)
HCT 34% (27-45)
Hb 10.8 g/dL (9-15)
Adequate platelets
Fibrinogen 640 mg/dL
Serum Chemistry:
Na 146 mmol/L (139-152)
K 5.3 mmol/L (3.9-5.4)
Cl 87 mmol/L (95-103)
Tbili 0.4 mg/dL (0.14-0.32)
Creatinine 3.8 mg/dL (1.0-2.7)
BUN 86 mg/dL (8-20)
Protein 5.2 g/dL (6.0-7.9)
Albumin 3.1 g/dL (2.4-3.0)
CPK 273 U/L (42-62)
LDH 481 U/L (83.1-475.6)

Urinalysis: Clear, straw colored, SG 1.008, pH 8.5, protein 3+, glucose negative, ketones negative, small blood, WBC 0-1/HPF, RBC 10-20/HPF.

Aerobic blood cultures obtained from the jugular vein were negative for bacterial growth.

Histopathologic Description: Kidney: Sections submitted include renal medulla, crest and pelvis with variable amounts of cortex (taken from both kidneys). Within the deep medulla and crest there is focally extensive and severe subacute coagulative necrosis of tubules and interstitium with edema. Surrounding this is a zone of tubular epithelial degeneration and necrosis. Epithelial regeneration in this zone is intense, with intact basement membranes and interstitium. Numerous tubules contain luminal casts of erythrocytes or necrotic cellular debris. Low to moderate numbers of viable and occasionally degenerate neutrophils are present within small vessels as well as the interstitial matrix. The cortex is largely unaffected, although in a few sections there are remote, non-occlusive, adherent fibrin thromboemboli in cortical radial veins. A small amount of proteinaceous exudate is present within the uriniferous space of some glomeruli.

Contributor's Morphologic Diagnosis: Kidneys, bilateral, medulla and crest, necrosis, focally extensive, subacute,

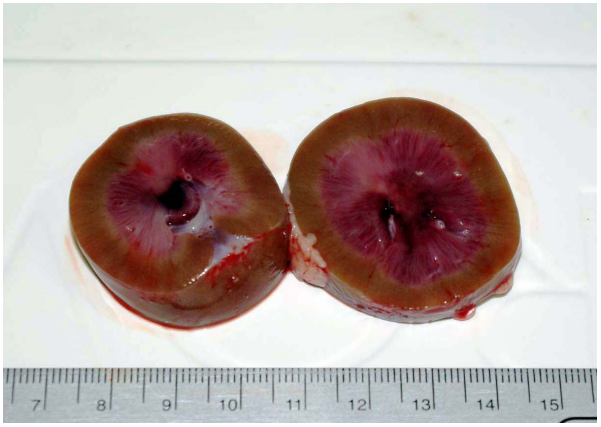

4-1. Kidney, lamb: In both the left and right kidneys there were focally extensive and severe hemorrhages in the renal medulla and crest with pallor of the medulla. The renal cortices were grossly normal. Photograph courtesy of Department of Comparative Medicine, Penn State Milton S Hershey Medical Center, Penn State College of Medicine, 500 University Dr, Hershey, PA 17033-0850, tcooper@hmc.psu.edu

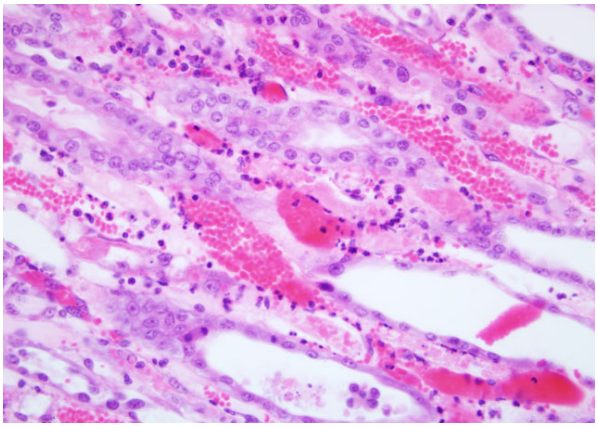

4-2. Kidney, lamb: Multifocally within the deep medulla and renal crest, there is extensive tubular degeneration, necrosis, and regeneration; in the adjacent interstitium there is hemorrhage, congestion, and mild acute inflammation. (HE 400X)

severe, with tubular erythrocyte casts and epithelial regeneration.

Contributor's Comment: Clinical signs and gross and histologic lesions are consistent with ischemic necrosis of the renal medulla and crest due to non-steroidal anti-inflammatory drugs (NSAIDs).[3,6] Anatomically, this lesion is appropriately termed renal medullary crest necrosis in sheep and horses, and renal papillary necrosis in rodents, man, and dogs.[7] Prostanoids are produced by cyclooxygenase-1 (COX-1) and COX-2 in the kidneys and exert a number of autocrine and paracrine effects. Most significantly, the prostanoids prostaglandin E_2 and PgI_2 modulate renal blood flow and glomerular filtration rate.[6] Additional COX products play roles in renal handling of sodium and release of renin. Renal distribution of the COX-1 and particularly COX-2 isoforms and susceptibility to NSAID nephrotoxicity is species-dependent.[2] The medulla and papilla/crest predominantly express the COX-1 isoform in most species, where prostanoids products modulate urine concentrating ability, antagonize vasopressin-mediated water and solute reabsorption, alter distal tubule potassium secretion, and promote dilation of the vasa recta to maintain medullary blood flow. Rats and dogs also express COX-2 in the papillary interstitial cells and are relatively sensitive to developing renal papillary necrosis,[2] suggesting that NSAIDs may also be directly toxic to the interstitial cells.[3] Humans are relatively resistant to NSAID nephropathy, and there is typically intercurrent disease or overdose (analgesic abuse).[2] Flunixin meglumine is a potent and non-specific COX inhibitor. Recently, the NSAID diclofenac has been associated with vulture population declines in southern Asia as a result of relay toxicosis and acute renal failure.[4]

In addition to NSAIDs, renal papillary necrosis can be induced by tyrosine kinase inhibitors and can be observed spontaneously in diabetes mellitus, sickle cell disease, and pyelonephritis.[5] Papillary necrosis has also been documented in dehydrated racing greyhounds and with amyloidosis in cats.[3] Renal papillary antigen-1 has been proposed as a urinary biomarker of papillary necrosis.[5]

Although fluoroquinolones and cephalosporins can be associated with renal toxicity, this classically presents as an acute interstitial nephritis (AIN) with mononuclear and occasionally eosinophilic infiltrates suggestive of a hypersensitivity reaction.[1] Certain members of both classes of drugs have also been associated with tubular crystal development.

AFIP Diagnosis: 1. Kidney, medulla: Tubular degeneration, necrosis and regeneration, diffuse, moderate to severe, with few cellular casts.
2. Kidney, medulla: Coagulative necrosis, acute, focally extensive (infarct).

Conference Comment: As indicated by the contributor, based on the clinical history the tubular changes are most likely due to NSAID administration. Participants reviewed the mechanisms of toxicity elegantly outlined by the contributor. Conference participants interpreted the acute renal crest infarct as most likely a perimortem event resulting from thrombosis of vessels.

In general, the differential diagnosis for renal papillary/crest necrosis across species includes hypoxic and toxic insults (which may occur in concert), dehydration, and urinary obstruction with or without pyelonephritis.[3] The contributor provides an excellent explanation of the pathogenesis of toxic insults. Dehydration contributes to papillary necrosis in dogs (primarily racing greyhounds) and lambs and kids treated with phenothiazines.[3] Urinary obstruction and pyelonephritis was high on the differential list for some participants due to the observation of moderate numbers of neutrophils within the renal crest. However, in this case most of the neutrophils occur in the medullary interstitium, and not in the tubules. The moderator emphasized that ascending pyelonephritis from the lower urinary tract typically produces a neutrophilic tubulitis, which is not evident in the case of this animal.

Contributor: Department of Comparative Medicine, H054, Penn State Milton S Hershey Medical Center, Penn State College of Medicine, 500 University Dr, Hershey, PA, 17033-0850
http://www.hmc.psu.edu/comparativemedicine/

References:
1. John R, Herzenberg AM. Renal toxicity of therapeutic drugs. *J Clin Pathol.* 2009;62:505-515.
2. Khan KN, Venturini CM, Bunch RT, et al. Interspecies differences in renal localization of cyclooxygenase isoforms: Implications in nonsteroidal antiinflammatory drug-related nephrotoxicity. *Toxicol Pathol.* 1998;26:612-620.
3. Maxie MG, Newman SJ. Urinary system. In: Maxie MG, ed. *Jubb, Kennedy, and Palmer's Pathology of Domestic Animals*. 5th ed., Vol 3. Philadelphia, PA; Saunders Elsevier; 2007:425-522.
4. Oaks JL, Gilbert M, Virani MZ, et al. Diclofenac residues as the cause of vulture population decline in Pakistan. *Nature.* 2004;427:630-633.
5. Price SA, Davies D, Rowlinson R, et al. Characterization of renal papillary antigen 1 (RPA-1), a biomarker of renal papillary necrosis. *Toxicol Pathol.* 2010;38:346-358.
6. Radi ZA. Pathophysiology of cyclooxygenase inhibition in animal models. *Toxicol Pathol.* 2009;37:34-46, 2009.
7. Read WK. Renal medullary crest necrosis associated with phenylbutazone therapy in horses. *Vet Pathol.* 1983;20:662-669.

The Armed Forces Institute of Pathology
Department of Veterinary Pathology

Conference Coordinator
Matthew Wegner, DVM

WEDNESDAY SLIDE CONFERENCE 2010-2011

Conference 3

25 August 2010

Conference Moderator:
Bruce Williams, DVM, Diplomate ACVP

CASE I: 05-8848 (AFIP 2986919).

Signalment: 10-week-old female Yorkshire x Landrace, pig (*Sus scrofa domesticus*).

History: This feeder operation with 1200 pigs experienced repeated episodes of scouring and high rates of weight loss in younger pigs. The farm had changed production to "natural" approximately 12 months previously. Diseased pigs had not been treated. The ration was a corn/soybean mix supplemented with vitamins and mineral concentrate. Six, 10-week old pigs were submitted alive. The vaccination status of the submitted animals was unknown.

Gross Pathology: All six pigs were runted, dehydrated and had fecal stains around the anus. The tissues on the conference slide were taken from a single pig (pig #1) and all subsequent descriptions focus on this animal. The soles of the feet and the right hind food had up to 0.5 cm in diameter, sharply demarcated depressions that lacked epithelial covering. Both palatine tonsils each had a single, sharply demarcated, red -green, 0.5 to 1.0 cm in diameter, deep depression that lacked epithelial covering. The mucosa of the caudal ileum was diffusely thickened to 2 mm and slightly granular. The contents of all intestinal segments were watery. The colonic and cecal contents also had thick aggregates of yellow, rubbery material that was multifocally slightly adherent to the mucosa. A few other piglets had cranioventral consolidation of the lungs and rare, small, renal cortical cysts.

Laboratory Results: Coronavirus was detected on electron microscopic examination of ileal mucosal scrapings. *Lawsonia intracellularis* was detected by immunohistochemistry in sections of ileum. A specific pathogen was not isolated from cecal mucosal scrapings. Endoparasites were not identified on fecal flotation. PCR was positive for porcine circovirus type 2 (PCV). PCR was negative for swine influenza virus and porcine respiratory and reproductive syndrome virus (PRRSV).

Histopathologic Description: Sections were cut from two blocks resulting in slight variation between slides. Nonetheless, all slides should show the three main lesions to some degree.

Diffusely, small intestinal villi are moderately to severely blunted and many are fused. Ileal segments have a thickened lamina epithelialis mucosae with long, branching crypts. The lamina propria mucosae has multifocal, mild, neutrophilic infiltrates. Peyer's patches are moderately depleted and rarely have individual multinucleate giant cells. The colon has multifocal crypt necrosis and dilation and segmental ulceration with massive bacterial colonization. On Warthin-Starry silver impregnated re-cuts, large numbers of short, comma-shaped bacteria colonize the apical aspect of affected ileal enterocytes.

Contributor's Morphologic Diagnosis: 1. Ileum: Severe diffuse proliferative ileitis (with intraepithelial, comma-shaped bacteria as per special stain).
2. Small intestine: Moderate to severe diffuse vill us atrophy.

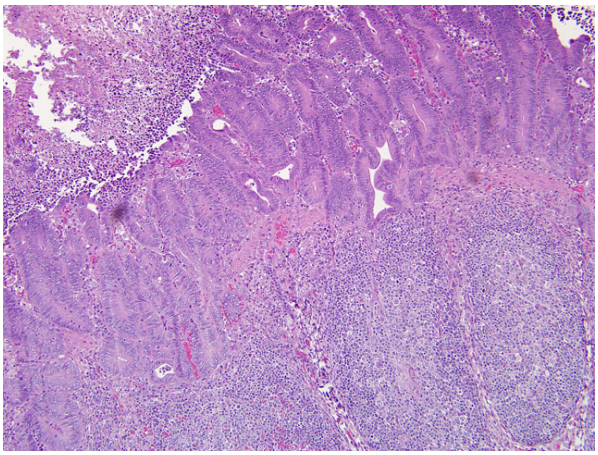

1-1. Ileum, pig. Diffusely in the mucosa there is blunting and fusion of villi, and intestinal crypts are elongated and branching (epithelial proliferation). (HE 100X)

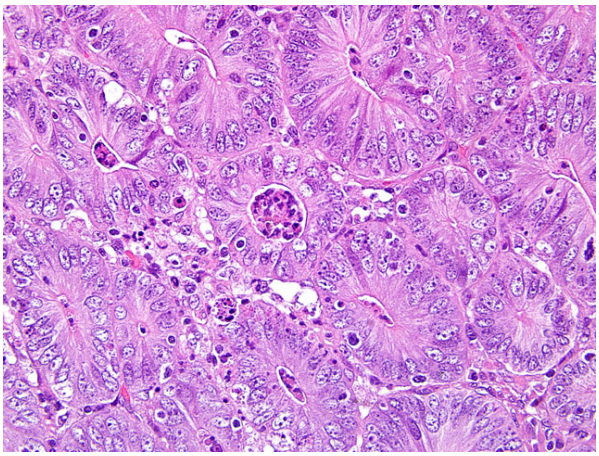

1-2. Colon, pig. In the mucosa, there are multifocal crypt abscesses. Crypts are lined by closely packed, tall columnar epithelial cells with amphophilic to basophilic cytoplasm (hyperplasia). (HE 200X)

3. Colon: Moderate multifocal, acute, fibrino-necrotizing colitis with intralesional colonies of mixed bacteria.

Contributor's Comment: This case is a good example for the complexity of enteric disease in pigs. Clearly there are (at least) three disease processes.

1. The diffuse villus atrophy of the small intestine is characteristic of a viral infection. It is a bit surprising that a coronavirus was still detectable in this 10-week-old pig.

2. The proliferative ileitis and the morphology of the intraepithelial bacteria on silver impregnation are suggestive of an infection with either *Lawsonia intracellularis* or *Campylobacter* spp. The presence of *L. intracellularis* was confirmed by immunohistochemistry.

The nomenclature of this bacterial pathogen has been changed numerous times in the past decades, most recently from "ileal symbiont intracellularis" to *Lawsonia intracellularis*.[9] Proliferative enteropathy (PE) with intraenterocytic *L. intracellularis* has been described in a wide range of hosts. The distribution of lesions varies with the host ranging from ileum (white tailed deer, horse, guinea pig, and rhesus macaques), to caudal ileum and colon (pig and hamster), cecum and colon (rabbit, blue fox, and ferret), to rectum (emu). Four forms of enteric lesions have been associated with *L. intracellularis* infection in pigs.[7] Weaners or young growing pigs are most commonly affected by a persistent uncomplicated proliferation sometimes described as porcine intestinal adenomatosis (PlA). The lower ileum and – less commonly – colon have small, raised, opaque islands to an irregular nodular or folded surface. Histologically, proliferating crowded immature enterocytes form branched and elongate crypts replacing the normal villous epithelium. Villus loss and the lack of a brush border on affected cells clearly interfere with intestinal physiology. Affected enterocytes are colonized by apical, comma-shaped bacteria that reside free in the cytoplasm. In mature animals (>4 months of age), infection results in proliferative hemorrhagic enteropathy (PHE), an acute clinical disease in which major intestinal hemorrhage arises from a proliferative ileal lesion. Proliferation may not be as severe as in PAI and bacteria may be seen also extracellular and in macrophages. Necrotic enteritis (NE) and regional ileitis (RI) represent a proliferative lesion that has been subject to further insult. Necrotic enteritis is an extensive coagulative necrosis of the epithelium that often results in rapid death. Regional ileitis is thought to be the outcome of NE with replacement of the damaged mucosa by granulation tissue associated with hypertrophy of the tunica muscularis ("hosepipe gut"). In a recent study on the infection dynamics of *L. intracellularis* under field conditions, shedding was detected by PCR in 75% of 100 pigs at 10-12 weeks of age (22-29 kg) and had ceased by 18 weeks of age. Seroconversion was detected after the expected lag time at 12-14 weeks of age and 92% of the pigs remained seropositive until slaughter.[11] A negative effect on growth rate was documented shortly before and during early infection followed by a compensatory impact. In another study, pigs from *L. intracellularis* seronegative and seropositive gilts were challenged intragastrically with *L. intracellularis*; seroconversion and seroprevalencewere compared.[2] Piglets from seronegative gilts had highest seroprevalence at 5 weeks (84%) that declined gradually from week 11 to week 26 (10%). Offspring of seropositive gilts had only a seroprevalence of 23% at 5 weeks that decayed much faster to 0% at week 17. Cellular immune response *to L. intracellularis* infection has been documented in piglets challenged intragastrically with wild type and attenuated live vaccine by ELISPOT assay for IFN-gamma.[4]

Very little is known about the pathogenesis of *L. intracellularis* infection. This is largely due to the obligate intracellular nature of the pathogen, which does not allow application of standard molecular techniques.[8] An outer membrane protein LsaA (Lawsonia surface antigen) has recently been identified and partially characterized. It is a member of the TlyA family, which are proteins present in a wide range of bacteria that in a few cases cause hemolysis. LsaA does not mediate hemolysis, but is expressed during

infection and monoclonal antibodies to LsaA significantly inhibit in vitro infectivity of *L. intracellularis*. This suggests a role of LsaA in attachment and/or entry of *L. intracellularis*. The site of attachment and entry in vivo are immature enterocytes at the base of crypts. How the proliferative character of the lesion comes about has yet to be determined. Some data suggests that bacterial replication and dissemination is tied to replication of the host cell. (data reviewed in[7])

L. intracellularis is difficult to culture (requires co-culture with mammalian cells). Histopathology in conjunction with demonstration of bacteria in tissues by silver impregnation can only suggest an infection with *L. intracellularis* as *Campylobacter* spp. share morphologic characteristics and can be encountered in enterocytes of proliferative enteritis cases in pigs. *L intracellularis* can be identified by PCR on feces or diseased intestine; immunohistochemistry; or immunofluorescence on sections of affected intestine.[5,6]

The fibrino-necrotizing colitis is interpreted as a sequel of the proliferative enteropathy. The colonization with bacteria is thought to be a tertiary problem as a specific pathogen was not isolated. The differential diagnosis for fibrinonecrotic colitis should include salmonellosis and European [classical] and African swine fever.

The significance of the detection of porcine circovirus type 2 (PCV) is uncertain, as it can be detected in clinically healthy pigs. The only lesion present that could be associated with a PCV2 infection in this piglet was the rare multinucleate giant cells in Peyer's patches, yet they lacked cytoplasmic inclusion bodies.

AFIP Diagnosis: 1. Ileum: Enteritis, proliferative, diffuse, moderate, with crypt necrosis and abscesses, and villar atrophy, blunting, and fusion.
2. Colon: Colitis, proliferative and necrotizing, diffuse, moderate, with crypt herniation.
3. Jejunum: Enteritis, lymphoplasmacytic, diffuse, moderate, with villar blunting and fusion.

Conference Comment: Conference participants appreciated this real-world case with overlapping lesions containing more than one etiology. Since the submission of this case in 2005, there have been several advances concerning the pathogenesis of *L. intracellularis* infection in pigs; for example, it has been shown that bacterial entry into host cells requires host cell activity and actin polymerization. Additionally, there is speculation that a type III bacterial secretion system may be involved, similar to that used by *Salmonella* spp.[1] Briefly, this is a process by which bacterial proteins are transferred into enterocytes which then activate host cell Rho GTPases triggering actin rearrangement and bacterial uptake.[12] The method by which the *L. intracellularis* bacterium stimulates host cell replication remains unknown.

Lawsonia intracellularis shares many features with other obligate intracellular pathogens in the orders *Chlamydiales* and *Rickettsiales*. Obligate intracellular bacterial pathogens often obtain a portion of their energy needs from the host cell; acquiring all of their metabolic demands from the host cell would be disadvantageous as this would reduce host cell proliferative potential. While both rickettsial and chlamyidal organisms are capable of generating their own energy, they also use the host cell as a supplementary source of energy, as well as a source of nucleotides. Based on genomic analysis, there is speculation that *L. intracellularis* can generate its own energy; however, the bacterium still requires supplementation from the host cell, and this is accomplished through the use of an ATP/ADP translocase whereby bacterial ADP is exchanged for host cell ATP. The ATP/ ADP translocase enzyme belongs to a broad class of translocases termed nucleotide transport (NTT) proteins which import nucleotides or ATP from the host cell into the bacterium.[10]

In the past decade, *L. intracellularis* has been seen with increasing frequency in foals and weanlings. A retrospective study of infections in Kentucky between 2005 and 2007 found infection to be most common in two to eight-month-old thoroughbreds between the months of August and January. The most common clinical findings were ventral edema and hypoalbuminemia.[3]

Contributor: Veterinary Diagnostic Laboratory, Oregon State University, 105 Magruder Hall, Corvallis, OR 97331
http: //www.vet.orst.edu /

References:

1. Alberdi MP, Watson E, McAllister GE, et al. Expression by *Lawsonia intracellularis* of type III secretion system components during infection. *Vet Microbiol*. 2009;139:298-303.
2. Barna P, Bilkei G. Effect of gilt seropositivity to *Lawsonia intracellularis* (LI) on their offspring's seropositivity to LI and on diarrhoea after a pure-culture challenge. *Prev Vet Med*. 2003;61:71-78.
3. Frazer ML. *Lawsonia intracellularis* infection in horses: 2005-2007. *J Vet Intern Med*. 2008;22:1243-1248.
4. Guedes RM, Gebhart CJ. Onset and duration of fecal shedding, cell-mediated and humoral immune responses in pigs after challenge with a pathogenic isolate or attenuated vaccine strain of *Lawsonia intracellularis*. *Vet Microbiol*. 2003;91:135-145.
5. Guedes RM, Gebhart CJ, Winkelman NL, Mackie-Nuss RA, Marsteller TA, Deen J. Comparison of different methods for diagnosis of porcine proliferative enteropathy. *Can J Vet Res*. 2002;66:99-107.
6. Huerta F, Arenas A, Carrasco L, et al. Comparison of diagnostic techniques for porcine proliferative enteropathy *(Lawsonia intracellularis* infection). *J Comp Pathol*. 2003;129:179-185.
7. Lawson GH, Gebhart CJ. Proliferative enteropathy. *J Comp Pathol*. 2000;122:77-100.

8. McCluskey J, Hannigan J, Harris JD, Wren B, Smith DG. LsaA, an antigen involved in cell attachment and invasion, is expressed by *Lawsonia intracellularis* during infection in vitro and in viva. *Infect Immun*. 2002;70:2899-2907.
9. McOrist S, Gebhart CJ, Boid R, Barns SM. Characterization of *Lawsonia intracellularis* gen. nov., sp. nov., the obligately intracellular bacterium of porcine proliferative enteropathy. *Int J Syst Bacteriol*. 1995;45:820-825.
10. Schmitz-Esser S, Haferkamp I, Knab S, et al. *Lawsonia intracellularis* contains a gene encoding a functional rickettsia-like ATP/ADP translocase for host exploitation. *J Bacteriol*. 2008;190:5746-5752.
11. Stege H, Jensen TK, Moller K, Vestergaard K, Baekbo P, Jorsal SE. Infection dynamics of *Lawsonia intracellularis* in pig herds. *Vet Microbiol* 2004;104:197-206.
12. Turner JR. The gastrointestinal tract. In: Kumar V, Abbas AK, Fausto N, Aster JC, eds. *Robbins and Cotran Pathologic Basis of Disease*. 8th ed. Philadelphia, PA: Elsevier Saunders; 2009:801.

CASE II: 9759624 (AFIP 3162239).

Signalment: 6-year-old male neutered domestic short hair cat (*Felis silvestris catus*).

History: Chronic history of respiratory disease. Chest radiographs showed pneumonia or possible pulmonary mass.

Gross Pathology: The postmortem was performed by the referring veterinarian. There were multifocal firm regions in the right middle lung lobe and a mass compressing the right medial bronchus. Lung and mediastinal lymph nodes were submitted for histopathological examination.

Laboratory Results: Not available.

Histopathologic Description: Lung: There are multifocal to coalescing inflammatory areas effacing the normal lung parenchyma. These areas are characterized by large numbers of neutrophils and macrophages with abundant foamy cytoplasm that occasionally form multinucleated cells. Within the inflammatory foci there are many round large, 30-60 µm in diameter spherules with a thick double wall (up to 2µm) (fungal yeast). Some of these organisms represent the variable morphology typical of *Coccidioides immitis*, such as mature spherules with round sporangia with thick birefringent capsule containing endospores or immature spherules containing blue flocculent material.

Contributor's Morphologic Diagnosis: Lung: Severe multifocal to coalescing necrotizing and granulomatous pneumonia with intralesional yeast organisms consistent with *Coccidioides* spp.

Contributor's Comment: Coccidioidomycosis is non-contagious fungal disease caused by a dimorphic soil-borne fungus called *Coccidioides immitis* or *C. posadassi*. The disease is also known as San Joaquin Valley Fever (in California), Desert fever, and Valley Fever. It is an endemic disease in specific ecological regions that include the southern United States, northern parts of Mexico and some countries in South America. Coccidioidomycosis is a dimorphic fungus; in soil it presents as a mycelium or arthrospore form that behaves as a saprophytic organism, and when the fungus gains access to tissues and body fluids it becomes the spherule form where it behaves as a parasitic organism. The pathogenesis starts with inhalation of the infective arthrospores (common in dry environment especially after a long dry weather season followed by heavy rain) or direct inoculation to the skin.

Even though the disease affects humans it is not considered a zoonosis. This disease is not transmitted through animal-animal contact. The only mode of transmission is through contaminated soil or dust with mature arthrospores. Coccidioidomycosis could develop infective arthrospores during fungal culture, and laboratory workers should be cautioned for possible source of infection.

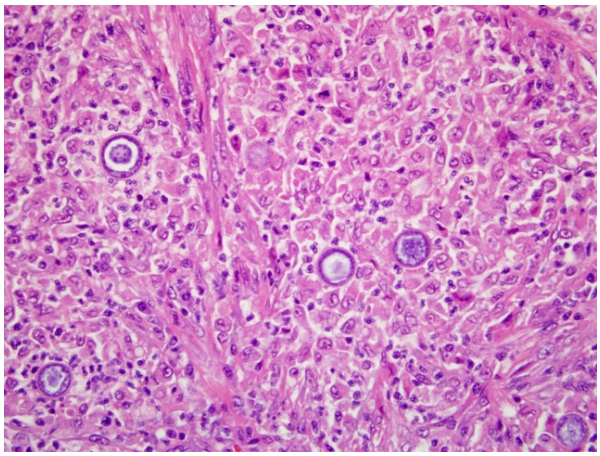

2-1. Lung, cat. Many viable and degenerate neutrophils and macrophages efface the lung and surround large (30-60 µm), round fungal yeasts that have thick double contoured walls. Fungal sporangia contain endospores or immature spherules containing blue flocculent material. (HE 400X)

Cats are not particularly susceptible to coccidioidomycosis compared to dogs. The most common presentation in cats is skin and pulmonary. Clinical signs are not very specific, as this organism can affect different tissues including skin, lung, eyes, nervous tissue.

Diagnostic tests available include:

1. Cytology smears/ FNA with identification of spherules (definitive diagnosis)
2. Histopathology with identification of spherules (definitive diagnosis). The variable morphology of *C immitis* is diagnostic: Sporangia 30-200 µm in diameter containing 2-4 µm endospores (mature spherules); immature spherules
3. Agar gel immunodeficiency (AGID) assay for IgG and IgM- specific test but not sensitive enough
4. ELISA to detect IgG and IgM- sensitive test but false positive results are common. Serological tests appear to be poor in cats

Greene described 48 feline coccidioicomycosis cases with skin (56%), respiratory (25%) musculoskeletal (19%), and CNS and ophthalmic (19%) involvement. There is no current effective treatment available. Fungal culture is not a useful diagnostic tool since definitive identification depends on spherule formation which is the only form in tissues during the parasitic phase of the life cycle of this peculiar fungus. Species affected by this fungus include many mammalian species such as dogs, cats, horses, sheep, cattle, pigs, non-human primates and South American camelids.

The OIE reports this disease as a differential for tuberculosis since the granulomatous, multifocal to coalescing inflammatory process will efface the normal architecture in lymph nodes and lung similar to the pattern encountered in tuberculosis.

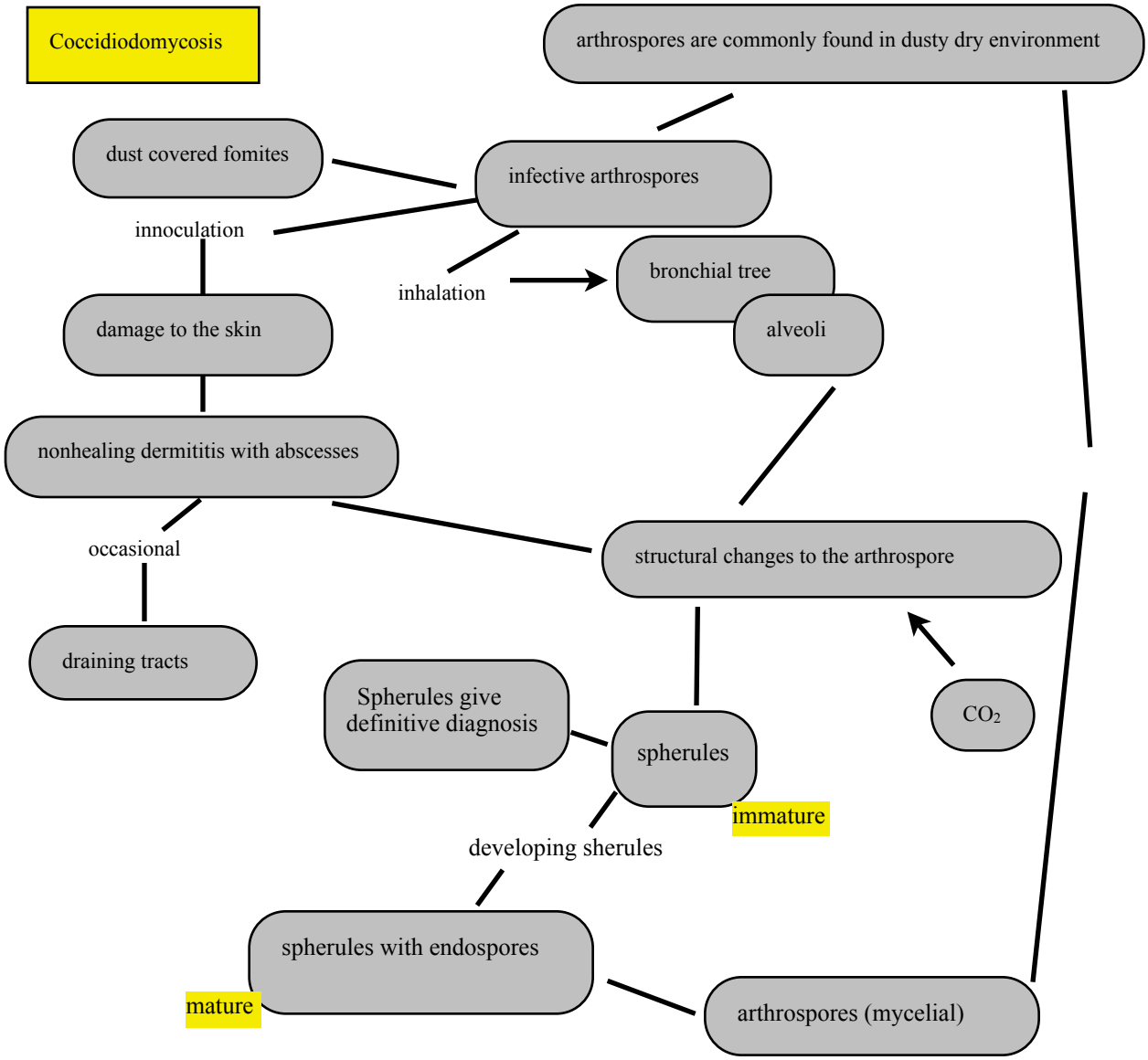
Coccidiodomycosis
arthrospores are commonly found in dusty dry environment
dust covered fomites
infective arthrospores
innoculation
inhalation
bronchial tree
alveoli
damage to the skin
nonhealing dermititis with abscesses
occasional
structural changes to the arthrospore
draining tracts
Spherules give definitive diagnosis
spherules
CO_2
immature
developing sherules
spherules with endospores
mature
arthrospores (mycelial)

AFIP Diagnosis: Lung: Pneumonia, pyogranulomatous, diffuse, severe with numerous endosporulating yeast, etiology consistent with *Coccidioides* spp.

Conference Comment: Nearly all conference participants diagnosed pyogranulomatous pneumonia, though a few participants interpreted some of the histologic lesions as granulomas. The moderator discussed the distinguishing histologic features between granulomas versus granulomatous/pyogranulomatous inflammation; the former are histologically well-organized and characterized by a central aggregate of epithelioid macrophages surrounded by a collar of mononuclear leukocytes, principally lymphocytes and occasionally plasma cells; older granulomas may be bounded by an outer rim of reactive fibroblasts and connective tissue.[8] Granulomatous and pyogranulomatous inflammation are not characterized by the same level of histologic organization.

Conference participants discussed the typical clinical presentation of *Coccidioides immitis* infection in the dog and cat. Most infections in the dog are pulmonary, with occasional systemic dissemination to multiple organs including bones and the skin. Bone infections tend to occur in long bones, and result in both lytic and productive lesions; thus, radiographically, coccidioidal osteomyelitis is included in the differential diagnosis for osteosarcoma. In contrast to dogs, the lesions in cats are primarily cutaneous and clinically characterized by multiple draining nodules without underlying bone involvement.

The moderator shared some experiential histopathologic features of pulmonary blastomycosis, coccidioidomycosis, and cryptococcosis. In general, pulmonary blastomycosis tends to be fibrosing; coccidioidomycosis is necrotizing; and cryptococcosis incites very little inflammatory response.

Conference participants also briefly reviewed some of the microorganisms which reproduce via endosporulation, including :

- *Coccidioides immitis*
- *Rhinosporidium seeberi*
- *Prototheca wickerhamii, P. zopfi*
- *Chlorella* spp.
- *Batrachochytrium dendrobatidis* (chytridiomycosis)

Contributor: Section of Pathology, College of Veterinary Medicine, Western University of Health Sciences, Pomona, CA 91766
http://www.westernu.edu/xp/edu/veterinary/about.xml

References:

1. Caswell, JL, Williams K. Respiratory system. In: Maxie MG, ed. *Jubb, Kennedy and Palmer's Pathology of Domestic Animals*. 5th ed., Vol. 2. Philadelphia, PA: Elsevier; 2007:644-645.

2. Chandler FW, Watts JC. Coccidioidomycosis. In: *Pathologic Diagnosis of Fungal Infections*. Chicago, IL: ASCP Press; 1987:13-15.

3. Chiller TM, Galgiani JN, Stevens DA. Coccidioidomycosis. *Infect Dis Clin N Am*. 2003;17:41-57.

4. Graupmann-Kuzma A, Valentine BA, Shubitz LF, Dial SM, Watrous B, Tornquist SJ. Coccidioidomycosis in dogs and cats: a review. *J Am Anim Hosp Assoc*. 2008;44:226-235.

5. Greene RT, Troy GC. Coccidioidomycosis in 48 cats: a retrospective study (1984-1993). *J Vet Intern Med*. 1995;9:86-91.

6. Greene RT. Coccidioidomycosis. In: Greene CE, ed. *Infectious Diseases of Dogs and Cats*. 2nd ed. Philadelphia, PA: WB Saunders Co.; 2002:391-398.

7. Kerl ME. Update on canine and feline fungal diseases. *Vet Clin North Am*. 2003;33:721-747.

8. Kumar V, Abbas AK, Fausto N, Aster JC. Acute and chronic inflammation. In: Kumar V, Abbas AK, Fausto N, Aster JC, eds. *Robbins and Cotran Pathologic Basis of Disease*. 8th ed. Philadelphia, PA: Elsevier Saunders; 2009:73-74.

9. OIE, Center for food Security and Public Health: Coccidioidomycosis. http://www.cfsph.iastate.edu/Factsheets/pdfs/coccidioidomycosis.pdf CVM, Iowa State University, Ames, IA, 2004

CASE III: BK1 (AFIP 3166500).

Signalment: 1-year-old male pit bull terrier/boxer mix, dog (*Canis familiaris*).

History: This mixed breed dog was rescued and adopted at one year of age, and was initially energetic and in good health. The patient developed and was treated for diarrhea and a wheezing cough shortly after adoption. At this time, he developed a cyst-like nodule on his left front paw at the first digit nail bed. He was treated with Epsom salt bath soaks and Benadryl®. This lesion progressed multifocally to the other paws, forming papillary, exophytic growths that spread proximally up the legs to the elbows. At the time of biopsy submission, the patient was having difficulty ambulating. Concurrently, the patient developed a hive-like rash around the face with red welts. Fine needle aspirates, cultures, and biopsies of the affected areas were submitted.

Gross Pathology: Multifocal to coalescing, well demarcated, papillary, proliferative, nodular masses expand the plantar surfaces of the feet, expanding from the foot pads, nail beds, and proximal haired skin of the lower leg. Many of the masses are reddened, ulcerated, and hyperkeratotic.

Histopathologic Description: Haired skin: In this section of haired skin, there is a circumscribed, unencapsulated, shallow, bowl-shaped endophytic, neoplastic proliferation of the surface epithelium compressing and displacing adnexal structures in the underlying dermis. Neoplastic cells are arranged in broad infolds and papillary projections supported on thin fibrovascular cores. There is hyperplasia of the basal cells with differentiation to large polygonal, hyperplastic epithelial cells with distinct borders, abundant basophilic cytoplasm, and round to oval central nuclei with finely stippled chromatin. Frequent cells have amorphous eosinophilic intranuclear inclusions that measure 10-15 µm in diameter peripherally marginating chromatin (papillomavirus inclusions). Many other nuclei have a glassy appearance with intranuclear cytoplasmic invagination. Mitoses are 1-2 per hpf. Rare epithelial cells, especially in the stratum spinosum, have clear to pale cytoplasm with eccentric nuclei (koilocytes, viral cytopathic effect). Inverted epithelial papillary fronds are covered with a variably thick band of parakeratotic cells and some keratin material continous with acanthosis, parakeratotic and orthokeratotic hyperkeratosis of the adjacent epithelium. Inflammation infiltrating the stroma is comprised of macrophages, neutrophils, and fewer lymphocytes. In some sections, associated superficial epithelium has an overlying thick serocellular crust composed of degenerate keratinocytes, keratin material, red blood cells, degenerate neutrophils and eosinophilic cellular and pyknotic material. Neoplastic cells approach lateral surgical margins in many sections.

Contributor's Morphologic Diagnosis: Haired skin: inverted papilloma, viral

Contributor's Comment: The papillary nature of this tumor with prominent intranuclear papillomavirus inclusions suggests that this inverted papilloma is caused by papillomavirus (PV) infection. Immunohistochemistry using monoclonal antibody against human papillomaviruses (HPV-1, 6, 11, 16, 18, and 31) using SDS-disrupted bovine papillomavirus type 1 immunogen (Millipore Billerica, MA) was positive with multifocal intense intranuclear staining.[1]

At least four different PVs are believed to infect dogs.[2] Classification of PVs is often based on the L1 gene, which encodes the viral capsid and packages viral DNA with L2, because it is the most conserved region of the PV genome.[11] Oral papillomatosis in dogs, characterized by multifocal cauliflower growths affecting the tongue, gingiva, buccal mucosa, lips, and pharynx, is believed to be caused by the lambda papillomavirus COPV.[2] Dogs that clinically manifest oral papillomas are generally less than 3 years old, but papillomas can appear in immunosuppressed and older dogs. Papillomatosis in dogs is considered to be a self-limiting disease with spontaneous regression of tumors, so treatment is generally not recommended.[2] Occasionally, these tumors persist and undergo malignant transformation. PVs are associated with cutaneous neoplastic transformation in several species, including sarcoids in cats and horses, and squamous cell carcinoma in dogs, cats, rabbits, bandicoots, and rodents.[7]

It has been proposed that cutaneous papillomatosis is caused by a different PV. A novel, epidermotropic PV has been recently described, termed CfPV-2.[10] Unlike COPV, lesions associated with CfPV-2 appear to be restricted to the footpads, with more chronic lesions lasting greater than 6 months. Experimentally, CfPV-2 is unable to induce oral papillomas in immunocompetent dogs, and vaccination against COPV is not effective against CfPV-2.[10] In addition, chronic infection with CfPV-2 is associated with highly malignant squamous cell carcinoma with distal metastases, although the exact pathogenesis of CfPV-2-associated neoplastic transformation is not known. The link between different PVs and specific tumor manifestations is also unclear. Recently, genotyping of PVs associated with canine inverted papillomas discovered the presence of either CfPV-2, COPV, or unknown canine PVs, suggesting that more than one type of PV may cause inverted papillomas.[6]

Canine papillomatosis can provide a model for studying regression of warts in human PV-associated cervical papillomatosis, because the predictable nature of lesion regression in canine papillomas closely mimics regression in cervical warts. In canines, papilloma regression is associated with leukocyte influx, with an abundance of CD4+ and CD8+ lymphocytes.[8]

Differentials for this case include nail bed inverted squamous papilloma. These masses arise from nail bed epithelium, and histologically contain laminated, compact keratin within a

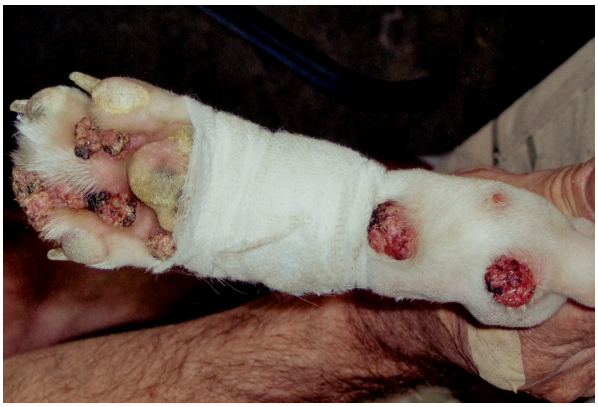

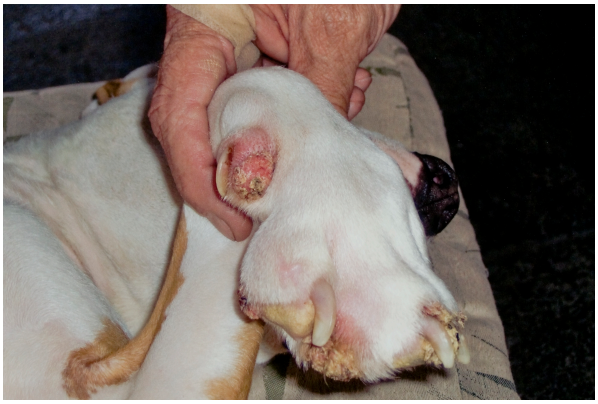

3-1, 3-2. Haired skin, Inverted viral papilloma, dog. Multifocal to coalescing, well demarcated, papillary, proliferative, nodular masses expand the plantar surfaces of the feet, extending from the foot pads, nail beds, and proximal haired skin of the lower leg. Many of the masses are reddened, ulcerated and hyperkeratotic. Photographs courtesy of Johns Hopkins School of Medicine, Department of Molecular and Comparative Pathobiology, 733 N. Broadway St., Baltimore, Maryland 21205, nnath2@jhmi.edu

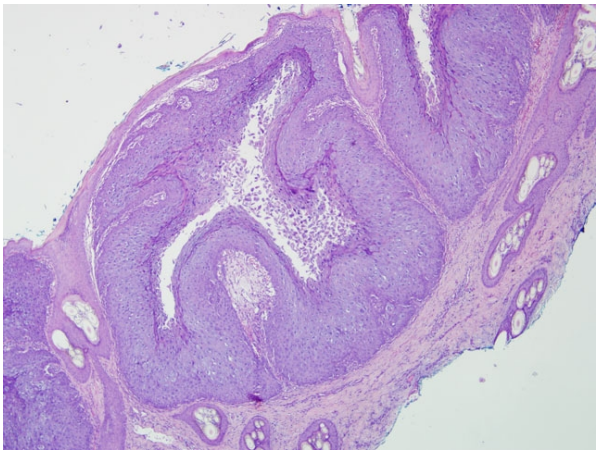

3-3. Haired skin, Inverted viral papilloma, dog. Expanding the dermis is a well circumscribed, unencapsulated, endophytic (bowl-shaped), epithelial neoplasm that compresses and displaces adnexal structures. Neoplastic cells are arranged in broad infolds and papillary projections supported by a thin fibrovascular core. (HE 40X)

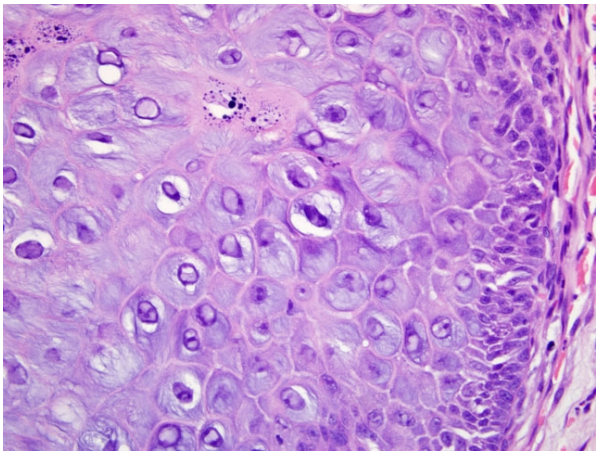

3-4. Haired skin, Inverted viral papilloma, dog. Neoplastic basal cells differentiate into larger epithelial cells that have distinct borders, abundant amphophilic cytoplasm, and round to oval nuclei with finely stippled chromatin. Occasionally, there are eosinophilic intranuclear inclusion bodies that marginate the chromatin. Few epithelial cells in the stratum spinosum have abundant clear to pale cytoplasm with an eccentric nucleus (koilocytes, viral cytopathic effect). (HE 400X)

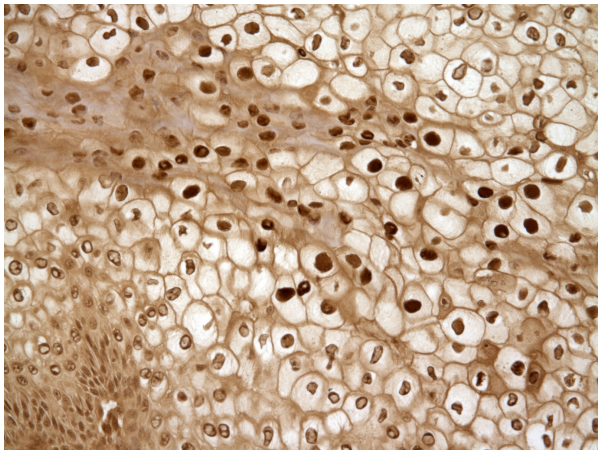

3-5. Haired skin, Inverted papilloma, dog. Neoplastic epithelial cells are immunopositive for papillomavirus. Photographs courtesy of Johns Hopkins School of Medicine, Department of Molecular and Comparative Pathobiology, 733 N. Broadway St., Baltimore, Maryland 21205, nnath2@jhmi.edu

hollow mass.[9] The nails are also grossly broken or missing; however, viral inclusions, lack of involvement of the nails, and lack of cyst formation rule out nail bed inverted papilloma. In this case, the papilloma likely originated from the skin adjacent to the nail bed, consistent with previous reports.[2] In the absence of viral inclusions, other differentials include cutaneous squamous papilloma of non-viral origin.

AFIP Diagnosis: Haired skin: Inverted papilloma, viral.

Conference Comment: Two prominent histologic characteristics of viral papillomas are koilocytes and intranuclear inclusion bodies. Koilocytes, seen primarily in the spinous layer, are enlarged epithelial cells that have eccentric pyknotic nuclei surrounded by a clear "halo"; their ghosts may be seen in the more superficial stratum corneum.[4] In the stratum spinosum, the normal eosinophilic cytoplasm is replaced by more basophilic cytoplasm; the nuclei of the

Species*	Virus	Tissue(s) affected	Disease(s)
Ox	Bovine papilloma virus (BPV) 1, 2 & 5	Udder, teats, head, neck, shoulders, omasum, vagina, vulva, penis and anus; BHV-2 also affects the urinary bladder	"Teat frond" warts; cutaneous warts; "rice grain" fibropapillomas; transmissible fibropapilloma in bulls
Ox	BPV-3	Skin	Papillomas of the skin
Ox	BPV-4	Alimentary tract e.g. mouth, pharynx and upper alimentary tract	"Bovine alimentary papillomata;" associated with squamous cell carcinoma and squamous papilloma of the alimentary tract and urinary bladder
Equine	BPV-1 & -2	Skin	Sarcoid
Sheep	OvPV-1	Skin	Fibropapillomas
Feline	FdPV-1 & -2	Skin	Viral plaque progressing to Bowenoid carcinoma in-situ; FdPV-2 linked to squamous cell carcinoma
Feline	FdPV-2	Skin	Squamous cell carcinoma (SCC)
Canine	CfPV-3 & -4	Skin; mucous membranes of the eye, skin and genitals	Papillomas; viral plaque progressing to Bowenoid carcinoma in-situ and SCC
Canine	CfPV-2	Skin	Inverted papilloma; SCC
Rabbit	CRPV	Tongue; skin	Lingual papillomas; SCC
Western barred Bandicoot	BPCV1	Skin	SCC

*Adapted from Munday and Kiupel

cells may contain pale basophilic (amphophilic) or smaller eosinophilic viral inclusions.[4] Some degenerating keratinocytes may also contain intracytoplasmic eosinophilic material resembling inclusions; these are not true viral inclusions, but rather merely aggregates of keratin thought to be a byproduct of the viral cytopathic effect.[4,7]

The precise role that papillomaviruses play in the development of cutaneous neoplasia in animals is not entirely understood. It has been proposed that ultraviolet light and papillomaviruses may act as co-carcinogens. Ultraviolet light causes damage to nuclear DNA, which increases the likelihood of oncogenic transformation.[3] Simultaneously, papillomavirus infection promotes epithelial proliferation.[4]

Many important papilloma viruses of animals exist and are beyond the scope of this discussion; those interested are invited to consult the references.[3,7] The included chart summarizes several papilloma viruses in animal species.[7]

Contributor: The Department of Molecular and Comparative Pathobiology, Johns Hopkins School of Medicine, 733 N. Broadway St., Suite 811, Baltimore, MD 21205
http://www.hopkinsmedicine.org/mcp/index.html

References:

1. Balara JM, McCarthy RJ, Kiupel M, Buote MA, Wise AG, Maes RK. Clinical, histologic, and immunohistochemical characterization of wart-like lesions on the paw pads of dogs: 24 cases (2000-2007). *J Am Vet Med Assoc*. 2009;234:1555-1558.
2. Debey BM, Bagladi-Swanson M, Kapil S, Oehme FW. Digital papillomatosis in a confined Beagle. *J Vet Diagn Invest*. 2001;13:346-348.
3. Ginn PE, Mansell EKL, Rakich PM. Skin and appendages. In: Maxie MG, ed. *Jubb, Kennedy and Palmer's Pathology of Domestic Animals*. 5th ed., Vol. 1. Philadelphia, PA: Elsevier Ltd; 2007:647-648.
4. Goldschmidt MH, Dunstan RW, Stannard AA, von Tscharne C, Walder EJ, Yager JA. Histological classification of epithelial and melanocytic tumors of the skin of domestic animals, 2nd series, Vol. III. Washington, D.C.: Armed Forces Institute of Pathology; 1998:19-20.
5. Kusewitt DF, Rush LJ. Neoplasia and tumor biology. In: McGavin MD, Zachary JF, eds. *Pathologic Basis of Veterinary Disease*. 4th ed. St. Louis, MO: Elsevier; 2007:265-267.
6. Lange CE, Tobler K, Brandes K, et al. Canine inverted papillomas associated with DNA of four different papillomaviruses. *Vet Dermatol*. 2009;21:287-291.
7. Munday JS, Kiupel M. Papillomavirus-associated cutaneous neoplasia in mammals. *Vet Pathol*. 2010;47:254-264.
8. Nicholls PK, Moore PF, Anderson DM, et al. Regression of canine oral papillomas is associated with infiltration of CD4+ and CD8+ lymphocytes. *Virology*. 2001;283:31-39.
9. Plattner BL, Hostetter JM. Cutaneous viral papilloma with local extension and subungual cyst formation in a dog. *J Vet Diagn Invest*. 2009;21:551-554.
10. Yuan H, Ghim S, Newsome J, et al. An epidermotropic canine papillomavirus with malignant potential contains an E5 gene and establishes a unique genus. *Virology*. 2007;359:28-36.
11. Yhee JY, Kwon BJ, Kim JH, et al. Characterization of canine oral papillomavirus by histopathological and genetic analysis in Korea. *J Vet Sci*. 2010;11:21-25.

CASE IV: H38407 (AFIP 3166566).

Signalment: Age unknown, sex unknown, red fox (*Vulpes vulpes*).

History: A free-ranging red fox (*Vulpes vulpes*) (age and sex not recorded) was submitted to a veterinary practice in Cheshire, England in May 2000. The animal was depressed and exhibited mild jaundice at the time of admission. It died one day later.

Gross Pathology: At necropsy, the fox was mildly jaundiced and had a congested liver, with mild accentuation of the hepatic lobular pattern. The mesenteric and hepatic lymph nodes were mildly enlarged and congested.

Histopathologic Description: Liver: Histopathologic examination of the liver reveals numerous amphophilic intranuclear inclusion bodies in hepatocytes. Hepatocytes are swollen, mildly vacuolated and dissociated. There is individual degeneration and necrosis of hepatocytes. Hepatic sinusoids are congested and contain fibrin deposits. There is expansion of the space of Dissé.

Contributor's Morphologic Diagnosis: Hepatocellular degeneration, acute, diffuse, moderate, with numerous intranuclear inclusion bodies, infectious canine hepatitis (canine adenovirus type 1).

Contributor's Comment: The presence of intranuclear inclusion bodies and degeneration of hepatocytes in this case were consistent with infectious canine hepatitis (ICH), which is caused by canine adenovirus type 1 (CAV-1). Intranuclear inclusion bodies were also observed in renal glomeruli, renal tubular epithelial cells and endothelial cells lining blood vessels. CAV-1 was isolated from a liver sample of the affected red fox.[7]

Spontaneous ICH has been reported mostly in domestic dogs, farmed foxes and other captive carnivores.[7] The disease was first identified in North America in captive silver foxes, a colour variant of the red fox (*Vulpes vulpes*), and has also has been reported in farmed Arctic (blue) foxes (*Alopex lagopus*). Red foxes and gray foxes (*Urocyon cinereoargenteus*) are susceptible to experimental infection with CAV-1. The first case of ICH in a free-ranging gray fox was identified in 2004 in Georgia, USA.[2] The present case represents one of the first recorded cases of ICH in free-ranging red foxes in Europe.[7]

Clinical signs and pathologic findings in red foxes with ICH are similar to those described in other species of foxes and in dogs.[2,7] Clinical signs in foxes appear after an incubation period of 2 to 6 days and may include anorexia, rhinitis, hemorrhagic diarrhea, hyperexcitability, seizures, paralysis, coma and death. Death may occur after a brief clinical course or may occur suddenly without prior clinical signs. Uveitis and keratitis ("blue eye") may develop in non-fatal cases of ICH in silver foxes. Gross lesions in foxes with ICH are considered to be less distinctive than in dogs, with generalized congestion and mild enlargement of the liver, spleen and adrenal glands. On histopathologic examination, vasculitis is considered to be a prominent feature of ICH in foxes, but was not a major finding in three red foxes with ICH examined in the United Kingdom.[7] Necrosis of hepatocytes and renal tubular epithelial cells are evident in foxes with ICH, but hepatic necrosis may be less severe than in dogs.

There is serologic evidence of exposure to CAV-1 in free-ranging red and gray foxes in North America, Germany, Australia and the United Kingdom.[1,3,4,7,8] Antibodies against CAV-1 have been detected in serum from 2/57 (3%) free-ranging North American red foxes in Wisconsin, USA, 17/485 (3.5%) free-ranging red foxes in Germany and

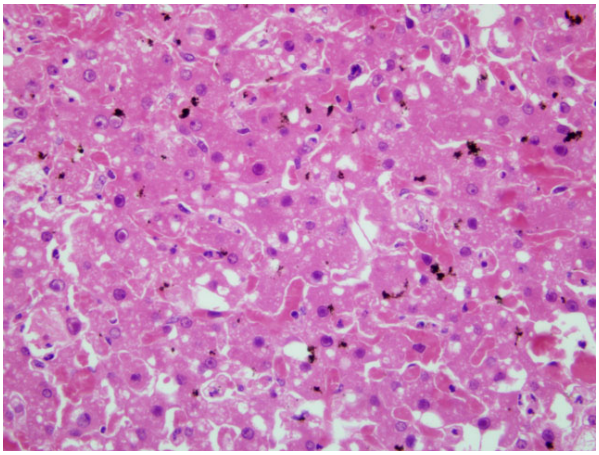

4-1. Liver, fox. Diffusely hepatocytes are swollen and vacuolated (degeneration) or disassociated and necrotic. (HE 400X)

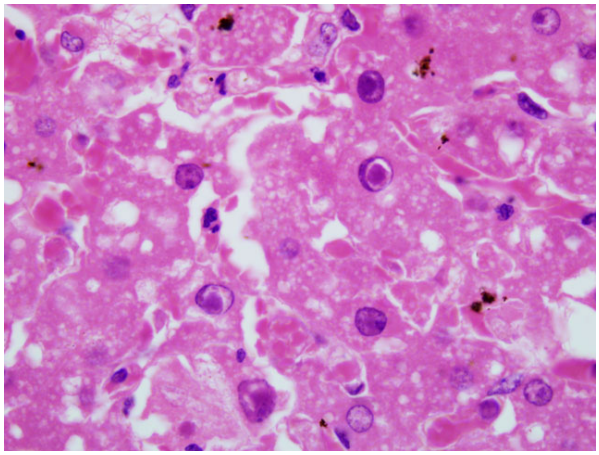

4-2. Liver, fox. Many degenerate hepatocytes contain eosinophilic intranuclear inclusion bodies that marginate the chromatin. (HE 1000X)

308/1326 (23.2%) free-ranging naturalized red foxes in Australia.[1,4,8] Antibodies against canine adenovirus type 1 were detected in postmortem fluid extracts from 11/58 (19%) frozen red fox carcasses from the United Kingdom.[7] Antibodies against CAV-1 have also been detected in 24/27 (88%) free-ranging gray foxes in the USA.[3]

The roles of red and gray foxes in the epidemiology of ICH are uncertain. It is not known if foxes are an important reservoir of infection with CAV-1 and thus a source of infection for domestic dogs, or vice versa.

AFIP Diagnosis: Liver: Hepatocellular degeneration and necrosis, diffuse, moderate, with numerous hepatocellular viral intranuclear inclusions and sinusoidal fibrin thrombi.

Conference Comment: The structural unit of the liver is classically referred to as the hepatic lobule; however, when viewed with respect to its functionality and proximity to the blood supply, it is commonly referred to in the literature as a hepatic acinus. Both the hepatic lobule and acinus are further subdivided anatomically and physiologically into areas or zones. Hepatocytes in zone 1of the acinus are closest to the incoming supply of oxygenated blood; in terms of lobular structure, this is the periportal area. Zone 2 corresponds to mid-zonal hepatocytes. Zone 3 (periacinar) hepatocytes are furthest from the oxygenated blood, and surround the portal vein; from an anatomic standpoint, this area is referred to as centrilobular. A single layer of hepatocytes at the periphery of the lobule forms a histologically distinct zone referred to as the limiting plate.[5]

When examining the liver, the pattern and extent of necrosis, can provide insight into potential etiologies. Necrosis is often classified based on the part(s) of the lobule affected. Centrilobular necrosis is common with viral infection and many toxins. As cells of this region are the last in the liver to receive oxygenated blood, processes resulting in hypoxemia (anemia or circulatory failure) often result in centrilobular necrosis. Pure mid-zonal lesions are extremely rare. Periportal necrosis is indicative of direct-acting toxins that do not need to be metabolized to a toxic intermediate via the cytochrome P450 system.[6]

The World Small Animal Veterinary Association Liver Standardization group published accepted, standardized nomenclature and corresponding diagnostic criteria of hepatic disease.[5] Within sites of hepatic inflammation, there can be individual apoptotic or necrotic cells referred to as **apoptotic** or **acidophil** bodies. **Confluent** necrosis involves large areas of the liver, may have a random or zonal distribution and, when bridging vasculature structures, is more aptly termed **bridging** necrosis. When cells in all regions of the acinus/lobule are necrotic, the term **massive** necrosis is often employed, such as that observed in hepatosis dietetica, cocklebur intoxication and *Amanita* spp. intoxication. The pattern of **piecemeal necrosis** is characterized by hepatocyte death at the interface of parenchyma and connective tissue.[5,6]

Contributor: University of Glasgow, Faculty of Veterinary Medicine, Glasgow, Scotland, United Kingdom
http://www.gla.ac.uk/vet/

References:

1. Amundson TE, Yuill TM. Prevalence of selected pathogenic microbial agents in the red fox (*Vulpes fulva*) and gray fox (*Urocyon cinereoargenteus*) of southwestern Wisconsin. *J Wildl Dis*. 1981;17:17-22.
2. Gerhold RW, Allison AB, Temple DL, Chamberlain MJ, Strait KR, Keel MK. Infectious canine hepatitis in a gray fox (*Urocyon cinereoargenteus*). *J Wildl Dis*. 2007;43:734-736.
3. Riley SP, Foley J, Chomel B. Exposure to feline and canine pathogens in bobcats and gray foxes in urban and rural zones of a national park in California. *J Wildl Dis*. 2004;40:11-22.
4. Robinson AJ, Crerar SK, Waight Sharma N, Müller WJ, Bradley MP. Prevalence of serum antibodies to canine adenovirus and canine herpesvirus in the European red fox (*Vulpes vulpes*) in Australia. *Aust Vet J*. 2005;83:356-361.
5. Rothuizen J, Bunch SE, Charles JA, et al. Morphological classification of parenchymal disorders of the canine and feline liver: 1. Normal histology, reversible hepatocytic injury and hepatic amyloidosis; and 2. Hepatocellular death, hepatitis and cirrhosis. In: *WSAVA Standards for Clinical and Histological Diagnosis of Canine and Feline Liver Disease.* St. Louis, MO: Elsevier; 2006:78-79, 85-88.
6. Stalker MJ, Hayes MA. Liver and biliary system. In: Maxie MG, ed. *Jubb, Kennedy and Palmer's Pathology of Domestic Animals*. 5th ed., Vol. 2. Philadelphia, PA: Elsevier Ltd; 2007:320-322.
7. Thompson H, O'Keeffe AM, Lewis JCM, Stocker LR, Laurenson MK, Philbey AW. Infectious canine hepatitis in red foxes (*Vulpes vulpes*) in the United Kingdom. *Vet Rec*. 2010;166:111-114.
8. Truyen U, Müller T, Heidrich R, Tackmann K, Carmichael LE. Survey on viral pathogens in wild red foxes (*Vulpes vulpes*) in Germany with emphasis on parvoviruses and analysis of a DNA sequence from a red fox parvovirus. *Epidemiol Infect*. 1998;121:433-440.

The Armed Forces Institute of Pathology
Department of Veterinary Pathology

Conference Coordinator
Matthew Wegner, DVM

WEDNESDAY SLIDE CONFERENCE 2010-2011

Conference 4

1 September 2010

Conference Moderator:
Sarah L. Hale, DVM, Diplomate ACVP

CASE I: PFIZER SND CASE 1 GP (AFIP 3164302).

Signalment: Adult female transgenic β-actin luciferase mouse on an FVB strain background (*Mus musculus*).

History: Animals were supplied by a commercial vendor and held as stock animals with routine husbandry for approximately 1 month without undergoing any procedure or treatment. Animals were found during morning health checks to be non-responsive with a hunched posture, and were subsequently euthanized. Four stock animals in this batch were found moribund within a 48 hour period. Clinical signs recorded in animals included a hunched posture, piloerection, dehydration and inappetance, a reddish nasal discharge, and a wet chin and chest.

Gross Pathology: No significant abnormalities were noted at necropsy in animals submitted from this batch.

Histopathologic Description: Sections of the brain show multifocal acute neuronal necrosis in many areas. Necrotic neurons are shrunken and angular with pyknotic nuclei and red cytoplasm. Necrotic neurons can be found scattered in most nuclei; however, regions of the cerebral cortex, thalamus and hippocampus are severely affected, but the distribution varies between individuals. Half of the affected animals from this batch additionally had multifocal random areas of hepatic coagulative necrosis.

Contributor's Morphologic Diagnosis: Brain: Severe acute neuronal necrosis.

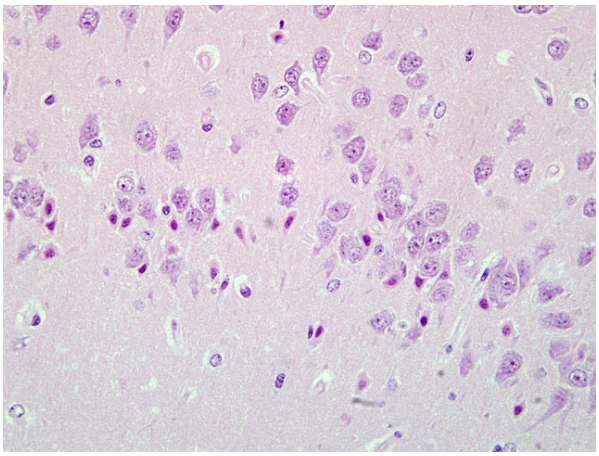

1-1. Brain, mouse. In multiple sections of brain (cerebral cortex, thalamus, hippocampus), there is multifocal neuronal necrosis characterized by neurons which are shrunken and angular with pyknosis and hypereosinophilic cytoplasm. (HE 400X)

Contributor's Comment: The presentation of these animals clinically, associated with lesions of widespread neuronal necrosis and occasional hepatic coagulative necrosis, is classic for a strain related entity in FVB mice reported as lethal epileptic syndrome or 'Space cadet' syndrome.[1,2] The FVB is an inbred mouse strain used extensively in transgenics research because of its superior reproductive performance and large pronuclei which facilitate microinjection of genomic material.[2] However, the strain is recognized as seizure prone, with both spontaneous and induced seizures (tail tattooing, fur clipping, and

audiogenic) being reported.[2] Additionally, FVB mice are more prone to neuronal death with kainate-induced seizures, compared with C57Bl/6 mice, even with seizures of equal duration and intensity scores.[8] In some colonies, spontaneous mortality rates in animals 4-12 months of age may approach 20%, with many investigators reporting that female mice are more prone to seizures than males.[1,2,6] Observed seizures include facial grimace, chewing automatism, ptyalism with matting of ventral neck and forelimbs, and clonic convulsions that may progress to tonic convulsions and death.[2] When seizures are not observed clinical signs are generally non-specific, including lethargy, moribundity, matting of fur, or being found dead.[2] Syndrome-associated histologic lesions include neuronal necrosis in the cerebral cortex, hippocampus and thalamus; astrocytosis, gliosis, and poliomalacia are reported in animals with a longer post-seizure survival interval.[1,2] Acute coagulative necrosis of hepatocytes has also been reported, which Goelz et al. interpret as resulting from terminal hypoxia in seizuring animals.[2]

The neuronal necrosis observed in these mice is reminiscent of that observed in cases of status epilepticus. Excitotoxicity is a proposed mechanism of neuronal death in status epilepticus, though hyperthermia, hypoxia, hypotension and hypoglycaemia associated with prolonged seizuring may exacerbate brain injury.[5] Excitotoxic neuronal death is caused by elevated levels of excitatory neurotransmitters, particularly glutamate, with the subsequent opening of the glutamate receptor-associated ion channels causing prolonged depolarization of neurons and increased intracellular calcium levels which lead to cell death.[7] The cause of FVB epileptic syndrome has not been determined to our knowledge, although genes involved in hippocampal excitability, hyperexcitability and glutamate release have been proposed as likely candidates.[4] Work by Schauwecker et al has determined that the susceptibility of FVB mice compared to C57Bl/6 mice to seizure-associated neuronal death is linked to the galanin receptor 1 (GalR1) gene.[8] FVB mice have increased levels of GalR1 in the hippocampus by quantitative real time PCR relative to C57Bl/6 mice, although these authors report no polymorphisms between the two mouse strains in the regions of the gene analyzed.[4] GalR1 and its ligand, the neuropeptide galanin, reduce seizure threshold by modulating the excitatory tone in the hippocampus by a hyperpolarizing action, and can inhibit the excitatory neurotransmitter glutamate.[7] GalR1 null mutation mice have spontaneous seizures and enhanced susceptibility to excitotoxin-induced neuronal injury.[4,7] The relationship of increased GalR1 to the mechanisms of seizure susceptibility and increased neuronal death FVB mice is undetermined, though it may reflect a compensatory change to increased excitatory neurotransmitter levels or increased excitatory tone in the hippocampus.

AFIP Diagnosis: Brain, cerebral cortex, hippocampus, and pyriform plexus: Neuronal necrosis, acute, multifocally extensive.

Conference Comment: The moderator and conference participants commented on the well-preserved sections of brain with minimal tissue artifact. The moderator observed that this case presents an excellent example of neuronal necrosis. A focal point of discussion was differentiation between dark neurons and necrotic neurons. Dark neurons have been reproducibly induced by exerting pressure on fresh, unfixed tissues (i.e. post-mortem manipulation) or inadequate perfusion-fixation. The histologic characteristics of dark neurons are contracted, darkly stained neurons with an indistinct nucleus and a corkscrew-shaped apical dendrite.[3] In contrast, necrotic neurons, colloquially characterized as "red and dead," are shrunken and angular with pyknosis or karyorrhexis and vacuolization of the surrounding neuropil.

Differentiation of dark neurons from necrotic neurons can be extremely difficult, especially considering some conditions causing acute neuronal necrosis, e.g hypoglycemia, status epilepticus and ischemia reperfusion can appear histologically similar.[3] Knowledge of post-mortem tissue handling, circumstances surrounding the animal's death, and expected lesions based on historical data of previous toxicologic studies provide a clearer interpretation of the lesion and corroborative evidence. The included chart outlines some of the histologic differences and corroborative evidence to help distinguish between the two:

Dark Neurons	Necrotic Neurons
1. Appear contracted, darkly stained neurons with an indistinct nucleus and a corkscrew-shaped apical dendrite	1. Appear shrunken and angular with pyknosis or karyorrhexis and vacuolization of the surrounding neuropil
2. Collapsed brain microvessels indicating poor or inadequate perfusion-fixation	2. Sequence of degradative changes indicating the changes occurred at different times
3. Consistent histomorpholgic features among all affected neurons	3. Evidence of an inflammatory response: microglial cells, reactive astrocytes, etc.
4. No reported clinical signs	4. Associated clinical signs

Contributor: Pfizer Global Research and Development, Sandwich Laboratories, Sandwich, Kent, United Kingdom.

References:

1. Donnelly TM. What's your diagnosis: 'Space cadet' syndrome in female FVB/n mice. *Lab An*. 2007;36:16.
2. Goelz MF, Mahler J, Harry J, et al. Neuropathologic findings associated with seizures in FVB Mice. *Lab An Sc*. 1998;48:34-37.
3. Jortner BS. The return of the dark neuron. A histological artifact complicating contemporary neurotoxicologic evaluation. *Neurotoxicology*. 2006;27:628-634.

4. Kong S, Lorenzana A, Deng Q, McNeill TH, Schauwecker PE. Variation in Galr1 expression determines susceptibility to excitotoxin-induced cell death in mice. *Genes Brain Behav*. 2008;7:587-598.
5. Lowenstein DH, Alldredge BK. Status epilepticus. *N Engl J Med*. 1998;338:970-976.
6. Mahler JF, Stokes W, Mann PC, Takaoka M, Maronpot RR. Spontaneous lesions in aging FVB/N mice. *Toxicol Pathol*. 1996;24:710-716.
7. Mitsukawa K, Lu X, Bartfai T. Galanin, galanin receptors and drug targets. *Cell Mol Life Sci*. 2008;65:1796-1805.
8. Schauwecker PE. Genetic basis of kainate-induced excitotoxicity in mice: phenotypic modulation of seizure-induced cell death. *Epilepsy Res*. 2003;55:201-210.

CASE II: 081090-99 (AFIP 3136041).

Signalment: 3-year-old female "French trotter" equine (*Equus caballus*).

History: For the past five months the mare showed poor condition with severe weight loss and generalized exfoliative dermatitis, easily epilated hair, and multifocal severe alopecia with pruritus. The pruritus decreased with dexamethasone treatment. In spite of treatment, the body condition of the mare remained poor. Clinically, a suspicion of an immune-mediated skin disease was made. The animal was euthanized for humane reasons.

Gross Pathology: Generalized severe amyotrophy and severe weight loss (generalized cachexia) was noted at necropsy. The examined animal presented with generalized, exfoliative dermatitis characterized by diffuse hypertrophy of skin, dry scales, serous exudates, and severe multifocal profound ulceration and alopecia involving the head, neck, flanks and hind limbs. Further, multiple deep ulcers, measuring 1 to 3 cm of diameter with fibrotic margins, were observed on the lips, upper and lower gingiva, and tongue. Two masses measuring 15 cm were observed near the duodenum and the right dorsal colon; these masses replaced the pancreas and were whitish-yellow with nodular, firm, fibrous appearance and dry cut section.

The gastric mucosa contained multifocal chronic ulcerations of the non-glandular mucosa, the fundus, and the margo plicatus and were characterized by elevated fibrous margins and a dry appearance. Moderate hyperplasia of the mucosa was noticed in the proximal duodenum and right dorsal colon.

Moderate, diffuse, lymphadenomegaly, with a wet and whitish cut surface indicating a reactive lymphadenitis, was noticed in the gastric, pancreatic and mesenteric lymph nodes.

Macroscopic diagnoses:
- Dermatitis, hyperplastic, exfoliative, and parakeratotic, diffuse, chronic, severe, with multifocal alopecia.
- Pancreatitis, sclerosing, diffuse, chronic, severe.
- Cheilitis, stomatitis and gastritis, ulcerative, multifocal, chronic, severe.

Laboratory Results (clinical pathology, microbiology, PCR, ELISA, etc.)**:** See included charts.

Histopathologic Description: Skin: The skin lesions are characterized by focal ulceration and covered by fibrinous exudate admixed with cellular debris. The adjacent epidermis presents with parakeratotic hyperkeratosis and diffuse hyperplasia characterized by proliferation of keratinocytes (acanthosis) and formation of irregular rete ridges into the superficial dermis. Moderate multifocal lymphocytic exocytosis and multifocal vacuolar degeneration of keratinocytes are observed. The superficial dermis is severely infiltrated by lymphocytes, plasma cells, less numerous eosinophils, and in the ulcerated areas by numerous degenerate neutrophils (suppuration); it shows moderate multifocal fibrosis, vascular congestion with lymphatic ectasia, and perivascular lymphoplasmacytic and eosinophilic infiltrates. There is a slight lymphocytic infiltration of hair follicles and sebaceous glands.

Pancreas: The architecture of the pancreatic parenchyma is completely distorted and characterized by severe, diffuse, fibrosis containing thick mature collagen fibers and few fibroblasts. Only a few pancreatic epithelial cells and islets of Langerhans are observed in the sections. Severe ductular hyperplasia with columnar to cubioidal monostratified epithelium and abundant intraluminal amphophilic

Biochemical Analysis:

Parameter	Value	Normal value
Total bilirubin (mg/L)	7.8	0-35
Calcium (mg/L)	117.6	107–129
Creatinine (mg/L)	11.2	8-22
GGT (Gamma glutamyl transferase) (UI/L)	23	0-40
Total protein (g/L)	66	56-79
Urea (g/L)	0.43	0.1–0.24
AST (UI/L)	193	100-600
Fibrinogen (g/L)	3.25	2-4.5

Complete Blood Count:

Parameter	Value	Normal value
Hematocrit (%)	5	32-52
Hemoglobin (g/100mL)	17.3	11-19
Leucocytes (cells/mm^3)	12,040	6,000-12,500
Neutrophils (cells/mm^3)	8,416	2,000-5,500
Eosinophils (cells/mm^3)	626	0-700
Basophils (cells/mm^3)	24	0-100
Monocytes (cells/mm^3)	253	0-600
Lymphocytes (cells/mm^3)	2,661	1,600-4,600
Thrombocytes (cells/ mm^3)	175,000	90,000-350,000

2-1. Haired skin, horse. (a) Cachexia and generalized exfoliative dermatitis with multifocal alopecia involving the head, neck, flanks, and hind legs. (b) Head, dermal lesions: dry scales, serous exudates, multifocal ulceration and alopecia. (c) Oral cavity: cheilitis, stomatitis and gingivitis, ulcerative, multifocal, chronic, severe. (d) Detail of the skin lesions, hindlimb: diffuse hypertrophy of the skin, dry scales, serous exudates and severe multifocal profound ulcerations and alopecia. Photographs courtesy of Ecole Nationale Veterinaire D'Alfort, Unite d'Histologie et d'Anatomi Pathologique, 7 avenue du General de Gaulle, 94704 Maisons-Alfort Cedex, France, www.vet-alfort.fr

amorphous material (mucus) can be noticed. Severe multifocal infiltration by numerous non-degranulated and degranulated eosinophils, as well as lymphocytes and plasma cells, is one of the main features of this lesion. Vascular fibrosis and lymphocytic eosinophilic transcytosis are further observed features.

Colon (histoslides not submitted): The colonic crypts are separated by severe infiltration by lymphocytes, plasma cells and a few eosinophils, and are multifocally atrophic and degenerate with superficial enterocyte loss. Further, the middle sized arterioles exhibit vacuolar degeneration of the medial cells with formation of multifocal intimal and intramedial calcification foci (intimal bodies).

Contributor's Morphologic Diagnosis: 1. Skin: Dermatitis, interface and perivascular, lymphoplasmacytic and eosinophilic, diffuse, chronic, severe, with focal ulceration and suppuration.
2. Pancreas: Pancreatitis, eosinophilic and sclerosing, diffuse, chronic, severe with subtotal epithelial atrophy, ductular hyperplasia and moderate multifocal lymphocytic infiltration.
3. Colon: Colitis, lymphoplasmacytic and eosinophilic, diffuse, severe, chronic with superficial epithelial erosion.

Contributor's Comment: Equine multisystemic eosinophilic epitheliotropic disease (MEED) is a rare, sporadic disease of horses characterized by eosinophilic infiltration into several organs.[10,12] The condition is characterized by exfoliative dermatitis, ulcerative stomatitis, wasting, and infiltration of epithelial tissues by eosinophils and lymphocytes. Scaling and crusting usually begin on the face or coronary bands.[3,9] Histopathologic findings in the dermis include superficial and deep perivascular to diffuse dermatitis or granulomatous dermatitis.[4,6,9,11] Similar inflammatory lesions, often associated with varying degrees of fibrosis, are seen in other epithelial organs, especially the pancreas, salivary glands, oral mucosa, gastrointestinal tract, esophagus, biliary tracts and bronchial mucosa.[1,2,10,11] There is no breed or sex predisposition.[11] Although horses can be affected at any age, most cases involve young animals (mean age of 3 to 4 years).[12] There is no specific clinical diagnostic test for this disease.[13] The etiopathogenesis of the disease is unknown; a hypersensitivity reaction to larvae of *Strongylus equinus* or food allergens is suspected, as well as an epitheliotropic cell-associated virus or a genetic basis.[3,4,7,11,12] The differential diagnosis includes dermatophilosis, dermatophytosis, pemphigus foliaceous, systemic lupus erythematosus, sarcoidosis, bullous pemphigoid, pemphigus vulgaris, vasculitis, erythema multiforme, epitheliotropic lymphoma, drug eruption and various toxicoses. The definitive diagnosis is based in the histopathologic examination.[11,12] The condition is generally associated with a poor prognosis.[7,8]

Idiopathic hypereosinophilic syndrome has been reported in humans, dogs, cats, horses, and ferrets.[2,7,13] The hypereosinophilic syndrome in man is characterized by marked peripheral eosinophilic infiltrates in various organs of which the skin is the second most common. The most frequently affected organ is the heart.[8] Immunosuppressive doses of systemic glucocorticoids (dexamethasone) may be effective in horses if administered early in the course of the disease (before wasting).[3,7,11] Hydroxyurea is an orally active antineoplastic agent whose mode of action is to inhibit

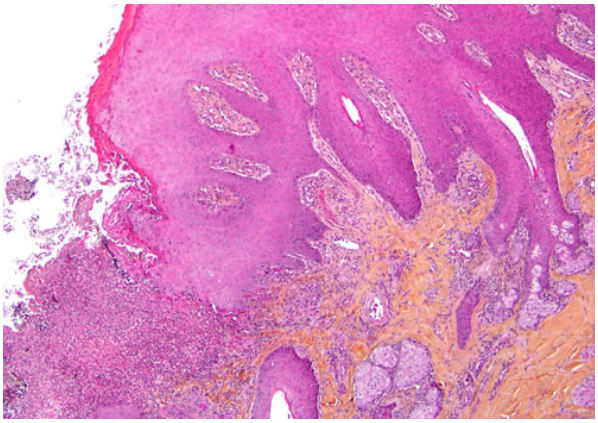

2-2. Haired skin, horse. Focally within the epidermis is an area of ulceration. Diffusely, the adjacent epidermis is hyperplastic and hyperkeratotic and there is an inflammatory cellular infiltrate in the dermis. (HE 40X)

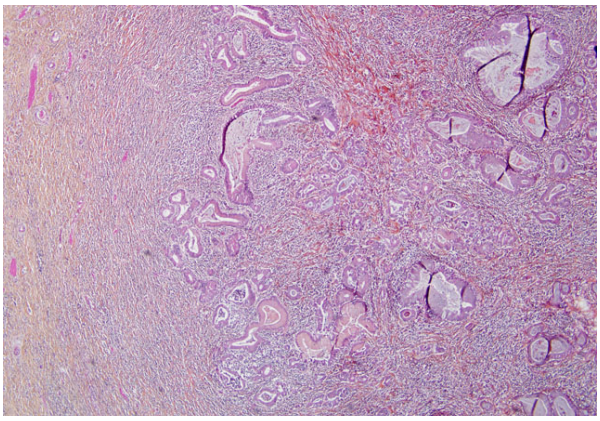

2-3. Pancreas, horse. Diffusely, the pancreatic parenchyma is distorted and replaced by extensive fibrous connective tissue and inflammatory cells; there is loss of exocrine pancreatic acini and remnant ducts are hyperplastic, ectatic and filled with mucinous material. (40X)

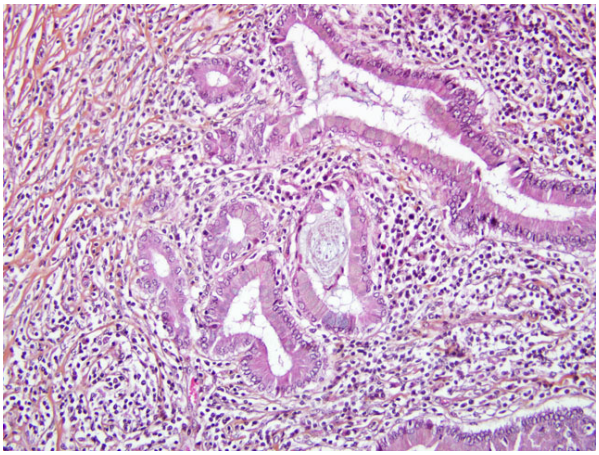

2-4. Pancreas, horse. Reactive fibrosis admixed with lymphocytes, plasma cells, macrophages, and eosinophils separate and surround ectatic hyperplastic ducts that are lined by columnar to cuboidal epithelium and filled with mucin. (HE 200X)

DNA synthesis without affecting RNA or protein synthesis; it has been used successfully for treating humans with hypereosinophilic syndrome and has been suggested for the treatment of cats. An improvement of the clinicopathological signs was noticed in a horse treated with corticosteroid and hydroxyurea and suggests that this therapy could be effective in attempts to treat this condition.[7]

AFIP Diagnosis: 1. Pancreas: Pancreatitis, sclerosing, lymphoplasmacytic and eosinophilic, diffuse, marked with ductular hyperplasia, duct ectasia, and mucinous metaplasia. 2. Haired skin and mucocutaneous junction, lip: Dermatitis and cheilitis, lymphoplasmacytic and eosinophilic, perivascular, multifocal, mild to moderate, with ulceration, epidermal hyperplasia and parakeratotic hyperkeratosis.

Conference Comment: Conference participants agreed the histopathologic findings in the submitted sections of pancreas and haired skin with lip are most consistent with the contributor's diagnosis of equine multisystemic eosinophilic epitheliotropic disease (MEED). Most conference participants characterized the inflammatory pattern in the skin and lip as perivascular, rather than interface, based on the observation that most of the inflammation centers around vessels in the superficial dermis and subepithelial connective tissue. In contrast, interface dermatitis is typified by inflammatory cells that obscure the dermal-epidermal junction and associated damage to the basal layer of keratinocytes;[5] with the exception of the areas of ulceration, participants did not observe these features.

The moderator provided several useful guidelines for approaching the histologic evaluation of the tissues submitted for this case to arrive at the most accurate diagnosis. Many conference participants struggled with tissue identification for the pancreas due to the extensive fibrosis that replaces almost all of the glandular components. To address this difficulty, the moderator suggested first evaluating the section of skin to identify the histologic features of the lesion and develop a histomorphologic diagnosis. Knowledge of the key histologic features in the skin lesion then provides insight into the underlying disease process and pathogenesis, and then leads the astute diagnostic pathologist to consider the other tissues likely to be affected in equine multisystemic eosinophilic disease, such as the pancreas. The moderator noted that lymphoplasmacytic and eosinophilic pancreatitis and exfoliative dermatitis are classic lesions of MEED.

The contributor indicates the pathogenesis of MEED is unknown, and lists some potential etiologies. In addition to the etiologies listed, it has also been suggested that clonal proliferation of epitheliotropic T-lymphocytes in affected tissues results in secretion of interleukin-5, thereby attracting eosinophils. Another potential etiology is repeated type I hypersensitivity reactions that occur in response to inhaled, ingested (dietary), or parasitic antigens.[5] The contributor provides excellent information on MEED. For additional information on other causes of eosinophilic dermatitis in

horses the reader is referred to WSC 2009-2010, Conference 4, Case I.

Contributor: Ecole Nationale Veterinarie D'Alfort, Unité d'Histologie et d'Anatomie Pathologique, 7 avenue du Général de Gaulle, 94704 Maisons-Alfort Cedex, France
www.vet-alfort.fr

References

1. Breider MA, Kiely RG, Edwards JF. Chronic eosinophilic pancreatitis and ulcerative colitis in a horse. *J Am Vet Med Assoc*. 1985;186:809-811.
2. Carmalt J. Multisystemic eosinophilic disease in a Quarter horse. *Equine Veterinary Education*. 2004;16:231-234.
3.Fadok VA. An overview of equine dermatoses characterized by scaling and crusting. *Vet Clin North Am Equine Pract*. 1995;11:43-51.
4. Gibson KT, Alders RG. Eosinophilic enterocolitis and dermatitis in two horses. *Equine Vet J*. 1987;19:247-252.
5. Ginn PE, Mansell JEKL, Rakich PM. Skin and appendages. In: Maxie MG, ed. *Jubb, Kennedy and Palmer's Pathology of Domestic Animals*. 5th ed., Vol. 1. Philadelphia, PA: Elsevier Ltd; 2007:739-741.
6. Henson FMD, Milner PÏ, Sheldon O. Multisystemic eosinophilic epitheliotropic disease in a Welsh pony. *Equine Veterinary Education*. 2002;14:176-178.
7. Hillyer MH, Mair TS. Multisystemic eosinophilic epitheliotropic disease in a horse: attempted treatment with hydroxyurea and dexamethasone. *Vet Rec*. 1992;130:392-395.
8. McCue ME, Davis EG, Rush BR, Cox JH, Wilkerson MJ. Dexamethasone for treatment of multisystemic eosinophilic epitheliotropic disease in a horse. *J Am Vet Med Assoc*. 2003;223:1320-1323.
9. Nimmo Wilkie JS, Yager JA, Nation PN, Clarck EG, Townsend HG, Baird JD. Chronic eosinophilic dermatitis: a manifestation of a multisystemic, eosinophilic, epitheliotropic disease in five horses. *Vet Pathol*. 1985;22: 297-305.
10. Sanford SE. Multisystemic eosinophilic epitheliotropic disease in a horse. *Can Vet J*. 1989;30: 253-254.
11. Scott DW. Unusual immune-mediated skin diseases in the horse. *Equine practice*. 1991;13:10-18.
12. Scott DW, Miller WH. Miscellaneous skin diseases: multisystemic eosinophilic epitheliotropic disease. In: *Equine Dermatology*. Philadelphia, PA: WB Saunders Company; 2003:661-695.
13. Singh K, Holbrook TC, Gilliam LL, Cruz RJ, Duffy J, Confer AW. Severe pulmonary disease due to multisystemic eosinophilic epitheliotropic disease in a horse. *Vet Pathol*. 2006;43:189-193.

CASE III: 4039 (AFIP 3067196).

Signalment: 10-month-old male castrated Red Angus calf (*Bos taurus*).

History: A disease characterized by loss of body weight, dehydration, deep depression, blindness and, in some cases, opisthotonos, aggressiveness and ataxia, was observed in a herd of 87 cattle with ages between ten to fourteen months during October 2003. The herd had been transferred from another paddock some days before the observation of the first cases. The clinical manifestation period of the disease was of 14 to 15 days. Four animals were affected; three died and one apparently recovered.

Gross Pathology: One calf showing emaciation, dehydration, severe depression and blindness was euthanized and necropsied. Yellowish and depressed areas were observed in the cerebral cortex. The meninges were hemorrhagic or congested.

Histopathologic Description: Brain, cerebral cortex: There were extensive areas of malacia in many regions of the cerebral cortex with infiltration of mononuclear cells mainly macrophages and gitter cells. Perivascular cuffing with many layers of mononuclear cells and multifocal hemorrhages was also observed. Blood vessels in the areas of malacia had hyperptrophied endothelial cells. Intranuclear inclusion bodies were observed within some astrocytes and neurons. Similar lesions of malacia were observed on the basal nuclei and thalamus. Discrete lesions were also observed in pons and cervical medulla (not included).

Contributor's Morphologic Diagnosis: 1. Brain, cerebral cortex: Malacia, focally extensive, and encephalitis, subacute, accentuated with intranuclear inclusion bodies in astrocytes and neurons, etiology consistent with Bovine herpesvirus type-5, red Angus, calf.
2. Brain, meninges: Meningitis, diffuse, moderate.

Contributor's Comment: Bovine herpesvirus-5 (BoHV-5) is a cause of necrotizing meningoencephalitis in young cattle. The disease is frequent in South American countries, especially Brazil and Argentina; it has been reproduced experimentally in cattle, rabbits and sheep.[1,2,3,6,7,8] BoHV-5 belongs to the family *Herpesviridae*, subfamily *Alphaherpesvirinae*, genus Varicellovirus. Previously, BoHV-5 was considered a subtype of BoHV-1, known as BoHV-1.3. Later, based on biological, molecular and epidemiological characteristics, it was identified as another virus. Both BoHV-1 and BoHV-5 are neurotropic and establish latency in the trigeminal ganglia after intranasal or conjunctival inoculation, but they differ in their ability to cause encephalitis. BoH-1 is occasionally neuroinvasive, but rarely causes encephalitis, whereas BoHV-5 has marked neurotropism.[1] During latency viral particles cannot be isolated and viral antigens cannot be demonstrated in the cells, but viral DNA can be identified by *in situ* hybridization.[4]

After acute infection, viruses of the alphaherpesvirus family establish latency in neurons of the sensorial ganglia. Experimental studies demonstrated that the latent infection can be reactivated by the administration of synthetic corticosteroids.[6] In natural outbreaks of the disease it is reported that stress, such as weaning, transportation,

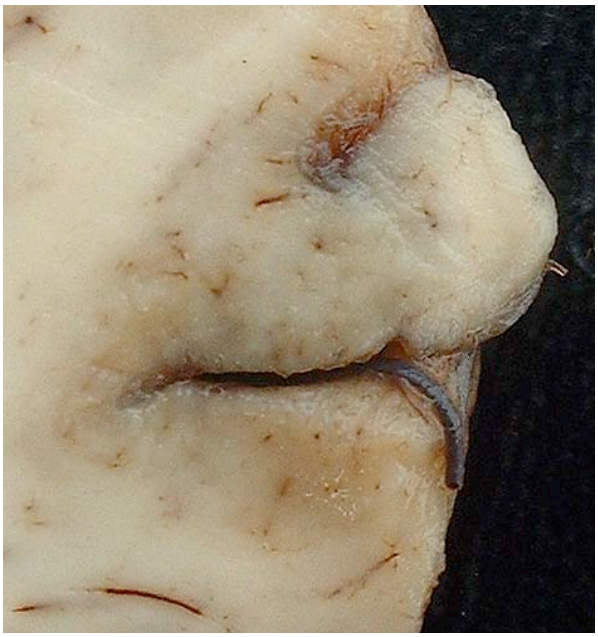

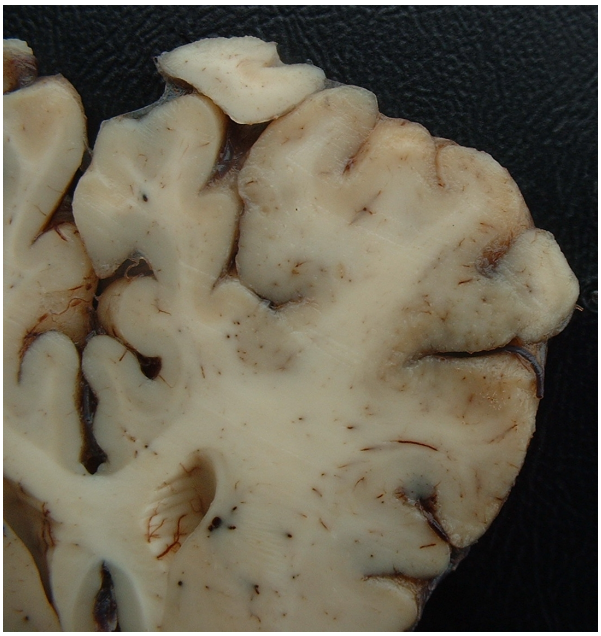

3-1, 3-2. Brain, cerebrum, calf. Yellowish and depressed areas are observed in the cerebral cortex. The meninges are hemorrhagic or congested. Gross photographs courtesy of Departmento of Patologia Animal, Faculdade de Veterinaria, UF Pel- campus Universitario, 96010-900 Pelotas-RS Brazil, crisgeyf@ufpel.edu.br

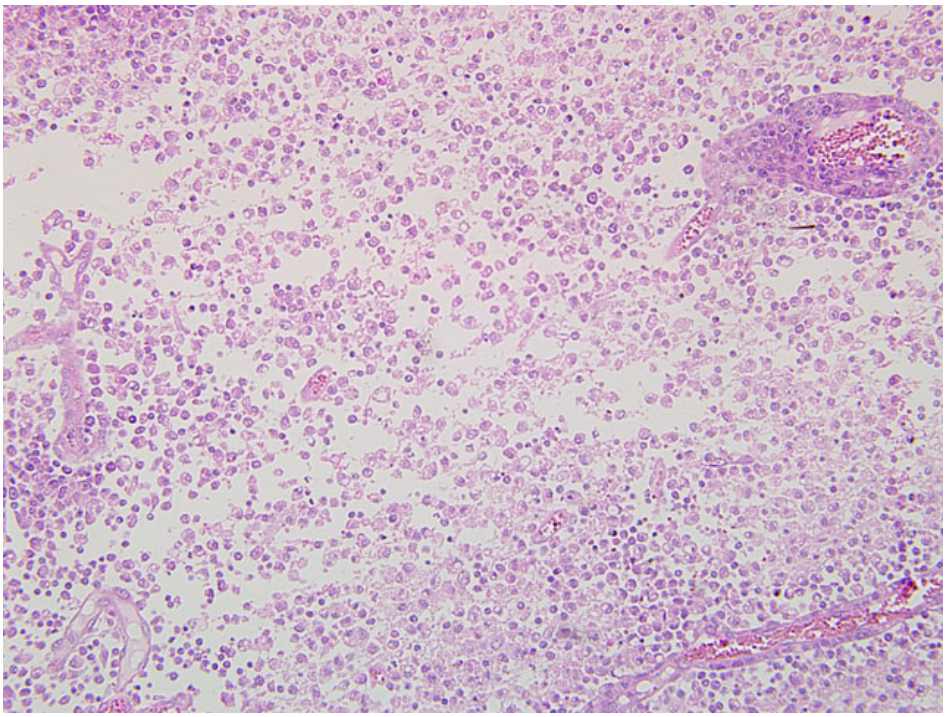

3-3. Brain, cerebrum, calf. Multifocally, there is malacia and cavitation of the neuropil and replacement with mononuclear cells, gitter cells, and cellular debris (necrosis). Additionally, there is moderate mononuclear perivascular cuffing. (HE 200X)

vaccination, confinement, and sudden variations in temperature can reactivate latent BoHV-5 infection. Rabbits and sheep had been used as models for acute disease and latency.[8] Several pathways have been proposed for the invasion of BoHV-5 in the CNS. It can occur by hematogenous route, because cattle experimentally infected present a phase of viremia. The invasion can occur also through the nervous fibers of the respiratory mucosa. Neuronal dissemination occurs by retrograde, intra-axonal transport in local neurons.[4] Experimental infections in calves[5] and rabbits[1] suggest that viral infection of the brain occurs more directly along olfactory nerves.

Necrotizing meningoencephalitis caused by BoHV-5 is frequent in Brazil and Argentina, affecting mainly cattle seven months to two years of age. Calves (14 days to 3 months) and adult cattle (up to 4-5 years) are occasionally affected.[2,3,7] Morbidity is variable; in calves it can be up to 30%, with a fatality rate of nearly 100%. In cattle after weaning morbidity is 3-8%. In most outbreaks the fatality rate is 100%, but in some instances a fatality rate of 50-75% has been reported. Sporadic cases also occur in cattle of different ages. Cattle up to 6 years old can be affected. Clinical signs are blindness, deep depression, and other signs of cerebral involvement. Opisthotonos and signs of brain stem lesions, including tongue paralysis, nystagmus, ataxia, other gait alterations, and excessive salivation are reported. Anorexia and severe weight loss can also occur. The clinical manifestation period is 1-15 days.

One common fact in cases of BoHV-5 encephalitis in Brazil is the presence of deep lesions of malacia in basal nuclei, thalamus, and mesencephalon similar to those reported in polioencephalomalacia (PEM). In Brazil, outbreaks of meningoencephalitis by BoHV-5 and outbreaks of PEM show similar epidemiological features, suggesting that meningoencephalitis may be associated with reactivation of a latent BoHV-5 infection during the development of PEM.[2] Both diseases affect grazing cattle bred extensively, and do not show any particular seasonal distribution. In addition, the age of affected cattle is similar. The hypothesis that BoHV-5 can be reactivated in cattle which develop PEM, and this reactivation results in severe encephalitis and PEM, was demonstrated, at least experimentally, in cattle infected experimentally by BoHV-5 that received ammonium sulphate from days 114 to 180 after inoculation. One out of 3 cattle developed BoHV-5 meningoencephalitis with lesions of PEM. Other animals recovered after the development of clinical signs but continued to manifest chronic signs of PEM. Histologically, chronic lesions of PEM and mild meningoencephalitis were observed.[2] In Argentina BoHV-5 infections also have the same characteristics as PEM. In a retrospective study from 1972 to 1999, of 89 cases previously diagnosed as PEM, 12 were caused by BHV-5 infections.[7]

In reports from other countries malacia of the cerebral cortex is absent or rarely reported.[2] Malacia of the cerebral cortex had also been reproduced in cattle inoculated with BoHV-5, but in most experimental reproductions of the disease this lesion is not reported. Nevertheless, some of these authors mentioned neuronal degeneration and necrosis or the presence of focal rarefaction necrosis. Deep malacia had not been reported in cases of BoHV-5 infections in other countries or in the experimental reproduction of the disease.[2]

The differential diagnosis of BoHV-5 infection in Brazil includes the different causes of PEM (sulphur intoxication, sodium chloride intoxication/water deprivation, lead intoxication, and thiamin deficiency). Other infectious diseases, like rabies, malignant catarrhal fever (MCF), and listeriosis, have to be included in the differential diagnosis list. In rabies, clinical signs and distribution of the lesions

more frequently affect the spinal cord, brain stem and cerebellum, but some animals also show signs of cerebral involvement. Inclusion bodies are found in approximately 90% of the cases, mainly in the cerebellum, but also in brain stem, spinal cord and cerebrum. Some cases of MCF have signs of cerebral disease, but most also have keratitis and corneal opacity, as well as ulcerative lesions in the oral cavity and respiratory system. Listeriosis is a sporadic disease with characteristic lesions and signs affecting the brain stem.

AFIP Diagnosis: Brain, cerebrum: Encephalitis, necrotizing and lymphohistiocytic, subacute, multifocally extensive, moderate to severe, with meningitis and eosinophilic intranuclear inclusion bodies.

Conference Comment: Conference participants commented on the variability of the lesions among the examined slides, including the absence of extensive necrosis in some sections. Additionally, the moderator noted the uneven distribution of viral inclusions, which tended to occur in small clusters. The moderator also emphasized that the most remarkable histologic lesion is the irreparable large area of necrosis in the cerebrum.

One reference text on veterinary neuropathology describes three features of inflammation within the central nervous system: 1) perivascular cuffing; 2) gliosis; and 3) neuronal satellitosis and neuronophagia.[9] Perivascular cuffing and extension of inflammatory cells into the adjacent neuropil is a significant histologic finding that should propel the pathologist to search for the underlying cause of the lesion. The leukocyte populations b surrounding the vessels may offer clues as to the type of inflammatory process and associated etiology, e.g. lymphoplasmacytic for viral infections, suppurative for bacterial infections, etc.[9]

Gliosis is characterized by the increased prominence of glial cells due to hyperplasia, hypertrophy or both. Glial cells can: undergo transformation to macrophages; surround degenerating neurons (satellitosis); and begin phagocytosis of the neuron (neuronophagia).[5] Astrocytes also undergo reactive changes in response to tissue damage characterized by cell swelling, cytoplasmic eosinophilia, large vesiculate nuclei, and, rarely, multiple nuclei. Reactive astrocytes are frequently referred to as gemistocytes or gemistocytic astrocytes. In addition to the reactive astrocytic changes, there is often hyperplasia of astrocytes. As the severity of the lesion worsens, the number of astrocytes typically increases resulting in more pronounced and dense astrocytosis; these cells frequently remain at the affected site after the lesion is resolved (glial scar).[5]

The contributor provides a thorough discussion of the epidemiology, clinical presentation, pathogenesis, lesions and differential diagnosis list for BoHV-5 infection.

Contributor: Departamento de Patologia Animal/ Laboratório Regional de Diagnóstico, Faculdade de Veterinária, UFPel. 96010-900, Pelotas- RS, Brazil
www.ufpel.edu.br/fvet/oncovet; www.ufpel.edu.br/fvet/lrd.

References:

1. Chowdhury SI, Onderci M, Bhattacharjee PS, Al-Mubarak A, Weiss ML, Zhoou Y. Bovine herpesvirus 5 (BHV-5) Us9 is essential for BHV-5 neuropathogenesis. *J Virol*. 2002;6:3839-3851.
2. David N, Hubner SO, Riet-Correa F, Halfen D, Lemos RA. Reactivation of latent bovine herpesvirus type 5 in cattle with polioencephalomalacia induced by ammonium sulphate. *Pesq Vet Bras*. 2007;27:445-441.
3. Elias F, Schild AL, Riet-Correa F. Meningoencefalite e encefalomalacia por herpes vírus bovino-5: distribuição das lesões no sistema nervoso central de bovinos naturalmente infectados. *Pesq Vet Bras*. 2004;24:123-131.
4. Engels M, Ackermann M. Pathogenesis of ruminant herpesvirus infections. *Vet Microbiol*. 1996;53:3-15.
5. Maxie MG, Youssef S. Nervous system. In: Maxie MG, ed. *Jubb, Kennedy and Palmer's Pathology of Domestic Animals*. 5th ed., Vol. 1. Philadelphia, PA: Elsevier Ltd; 2007:292-295.
6. Perez SE, Bretschneider MR, Leunda MR, Osorio FA, Flores EF, Odeón AC. Primary infection, latency, and reactivation of bovine herpesvirus type 5 in the bovine nervous system. *Vet Pathol*. 2002;39:437-444.
7. Perez SE, Vagnozzi A, Sur JH, Odriozola E, Campero CM, Odeón AC. Análisis retrospectivo de casos con diagnóstico de necrosis cerebrocortical y su relación com herpesvirus bovino tipo 5. *Rev Arg Microbiol*. 2003;35:69-73.
8. Silva AM, Weiblen R, Irigoyen LF, et al. Experimental infection of sheep with bovine herpesvirus type-5 (BHV-5): acute and latent infection. *Vet Microbiol*. 1999;66:89-99.
9. Summers BA, Cummings JF, de Lahunta A. Principles of neuropathology. In: *Veterinary Neuropathology*. St. Louis, MO: Mosby; 1995:39-42.

CASE IV: 09-2735 (AFIP 3164124).

Signalment: 15-year-old male neutered domestic shorthair feline (*Felis catus*).

History: This 15-year-old castrated male domestic shorthair cat had a history of diabetes mellitus since two years of age; it was well controlled. The cat was diagnosed with mild to moderate hypertrophic cardiomyopathy. The cat presented due to acute onset of seizures and obtundation. There was severe white matter swelling/edema of unknown etiology found on an MRI. The blood pressure was 174 mmHg. There was partial cerebellar herniation. Treatment included prednisone and mannitol that resulted in clinical improvement for a period of approximately two weeks prior to reoccurrence of the clinical signs. Despite aggressive medical management with mannitol, hypertonic saline, steroids and antibiotics the cat's condition worsened and the owner elected euthanasia.

Gross Pathology: Gross necropsy findings reported by the submitting veterinarian were confined to partial herniation of the cerebellum. There was partial herniation of the cerebellum.

Histopathologic Description: Brain: There is marked diffuse edema of the white matter. Clear space and small eosinophilic lakes of edema fluid separate nerve fibers. Astrocytes in the white matter often have increased amounts of eosinophilic cytoplasm. In the meninges, arteries exhibit changes characterized by either myointimal hyperplasia and adventitial proliferation or fibrinoid necrosis. Around vessels with fibrinoid necrosis there are perivascular and mural infiltrates of neutrophils along with a few macrophages. The tunica media contains many pyknotic nuclei. A few of the vessels have concentric layers of proliferating fibrocytes in the tunica adventitia. Mild to moderate white matter edema is also present in the pons, medulla and cerebellar white matter. There are no vascular changes in those regions.

Contributor's Morphologic Diagnosis: 1. Edema, diffuse, severe, cerebral white matter.
2. Fibrinoid necrosis and adventitial hyperplasia, multifocal, arteries, meninges.

Contributor's Comment: The white matter edema and the vascular changes are consistent with hypertensive encephalopathy. This condition has been reported in cats with chronic renal disease and following renal transplantation.[1] However, any condition that results in hypertension could theoretically cause the brain pathology.[2] These conditions include hyperthyroidism, primary hyperaldosteronism, diabetes mellitus, pheochromocytoma and erythropoietin therapy. About 20% of cases of hypertension in cats have no identifiable cause (i.e. idiopathic hypertension). The cat had a history of diabetes mellitus that could have caused the hypertension. However, a full necropsy was not performed, and the other conditions could not be entirely ruled-out.

The pathogenesis of hypertensive encephalopathy is thought to involve the development of vasogenic edema as a result of sudden increases in blood pressure that exceed the autoregulatory capacity of the vasculature in the brain resulting in endothelial injury and breakdown of the blood-brain barrier.[2] The edema is primarily in the white matter where it results in separation of axons and myelin sheaths and pallor of the tissue. There is sometimes increased perivascular space around white matter vessels. Vascular changes, usually in the pia, are consistent with hypertension and include onion-skinning of the vessels (hyperplastic arteriosclerosis) and, occasionally, fibrinoid or hyaline change (hyaline arteriosclerosis).

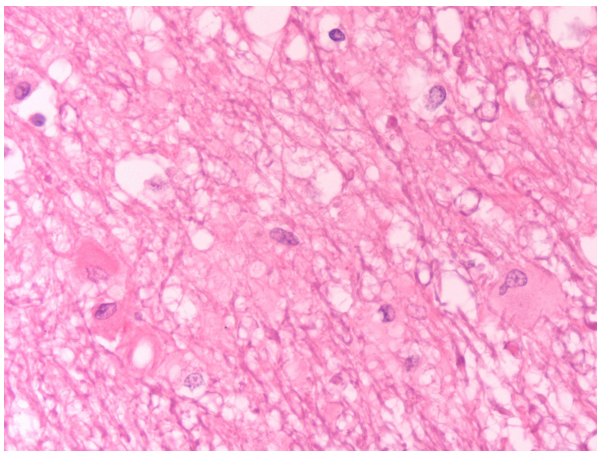

4-1. Brain, cerebrum, white matter, cat. Diffusely within the white matter there is edema. Multifocally, astrocytes contain increased amounts of eosinophilic cytoplasm. Photograph courtesy of Arizona Veterinary Diagnostic Laboratory, 2831 N. Freeway, Tuscon, Arizona 85705, gabrad@ag.arizona.edu

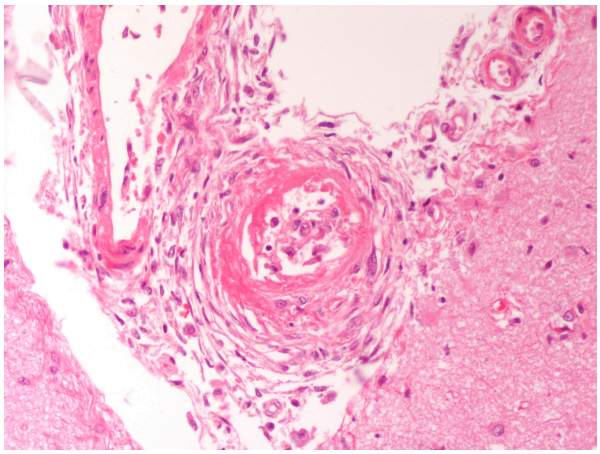

4-2. Brain, meninges, cat. In the meninges, the arteries exhibit arterial myointimal hyperplasia with adventitial proliferation or fibrinoid necrosis. Photograph courtesy of Arizona Veterinary Diagnostic Laboratory, 2831 N. Freeway, Tuscon, Arizona 85705, gabrad@ag.arizona.edu

Chart 1.

	Vasogenic Edema	Cytotoxic Edema
Pathogenesis	Damage to cerebral vasculature → fluid and proteins leave vessel under hydrostatic pressure → edema	Glial cell injury → disturbed cellular osmoregulation → acute cell swelling with maintenance of vascular integrity
Gross findings	Flattened gyri and narrowed sulci Herniation (i.e. cerebellar coning) Edematous swelling of the white matter	Similar to findings in vasogenic edema with possible displacement May be grossly normal
Distribution of the edema	White matter; may affect grey matter if severe	Grey matter White matter Both
Histologic Findings	Generalized pallor Swelling and necrosis of astrocytes Astrocyte hypertrophy Eosinophilic lakes of edema fluid	Astrocyte swelling White matter spongiosis (if oligodendrocytes affected) Intracellular fluid accumulation

AFIP Diagnosis: 1. Brain, cerebrum, white matter: Edema, diffuse, moderate, with reactive astrocytosis.
2. Brain, meninges: Hyaline vascular necrosis, multifocal, moderate with perivascular sclerosis.

Conference Comment: Almost all conference participants observed the histologic lesions confined to the white matter of the cerebrum and interpreted the findings as consistent with edema; but only a few noted and diagnosed the vascular lesions. When evaluating nervous tissue, the differentiation of edema and preparation artifact is often difficult. Rough handling and autolysis often exacerbates the degree of artifact seen in tissue sections. In the tissue sections of this case, in addition to the physical separation of nerve fibers by clear space, many astrocytes are enlarged with increased eosinophilic cytoplasm, presumably as the result of edema. Recognizing the vascular lesions and their association with feline hypertension provides an identifiable explanation for diffuse white matter edema in this cat.

In general, there are four mechanisms of edema:[4]

1. Increased microvascular permeability (*e.g.* vasculitis secondary to endotoxemia)
2. Increased intravascular hydrostatic pressure (*e.g.* pulmonary hypertension)
3. Decreased intravascular osmotic pressure (*e.g.* protein-losing nephropathy/enteropathy)
4. Decreased lymphatic drainage (*e.g.* intestinal lymphangectasia)

Because the structural qualities of the brain differ from other tissues, including the absence of a lymphatic system in the parenchyma, the mechanisms and pathogenesis of edema in the central nervous system are somewhat unique; and if not promptly treated, it is often fatal. Two mechanistic categories of edema of the brain are recognized and summarized in chart 1.[4]

McGavin and Zachary's *Pathologic Basis of Veterinary Disease* expands the mechanistic list by including hydrostatic (interstitial) and hypo-osmotic types of brain edema. Briefly, hydrostatic edema is characterized by extracellular periventricular fluid accumulation as a result of increased hydrostatic pressure within the ventricles. Hypo-osmotic edema occurs with water and salt intoxication in which the differences in osmotic pressure between the brain and the plasma results in movement of fluid from the vasculature into the brain.[5]

In this case, partial herniation of the cerebellum through the foramen magnum (colloquially referred to as "cerebellar coning") was noted at necropsy. In addition to the foramen magnum, there are two other potential locations of herniation during brain swelling. The occipital cortex may herniate caudally beneath the tentorium cerebelli or, in cases of unilateral swelling, the cingulate gyrus of the unaffected hemisphere may be forced laterally under the falx cerebri.[4]

Participants also discussed the differential diagnosis for white matter spongiosis, which can be broadly classified as either idiopathic or toxic/metabolic. A more detailed discussion of the various idiopathic spongiform myelinopathies is available within the selected references.[3,4] Toxic and metabolic causes of status spongiosis include, but are not

limited to, hepatic encephalopathy, renal encephalopathy, branched chain α-ketoacid decarboxylase deficiency (i.e. maple syrup urinary disease), hexachlorophene toxicosis, halogenated salicylanilide toxicosis, bromethalin toxicity and several plant species.[3]

Contributor: Arizona Veterinary Diagnostic Laboratory, Agricultural Experiment Station, The University of Arizona.

References:

1. Brown CA, Munday JS, Mathur S, Brown SA. Hypertensive encephalopathy in cats with reduced renal function. *Vet Pathol*. 2005;42:642-649.
2. Kent M. The cat with neurological manifestations of systemic disease; key conditions impacting on the CNS. *Journal of Feline Med Surg*. 2009;11:395-407.
3. Maxie MG, Youssef S. Nervous system. In: Maxie MG, ed. *Jubb, Kennedy and Palmer's Pathology of Domestic Animals*. 5th ed., Vol. 1. Philadelphia, PA: Elsevier Ltd; 2007:385-388.
4. Summers BA, Cummings JF, de Lahunta A. Principles of neuropathology. In: *Veterinary Neuropathology*. St. Louis, MO: Mosby; 1995:36-36.
5. Zachary JF. Nervous system. In: McGavin MD, Zachary JF, eds. *Pathologic Basis of Veterinary Disease*. 4th ed. St. Louis, MO: Elsevier; 2007:862-865.

The Armed Forces Institute of Pathology
Department of Veterinary Pathology

Conference Coordinator
Matthew Wegner, DVM

WEDNESDAY SLIDE CONFERENCE 2010-2011

Conference 5

8 September 2010

Conference Moderator:
Dale G. Dunn, DVM, Diplomate ACVP

CASE I: 396/08 (AFIP 3162240).

Signalment: 42-day-old broiler breeder chicks (*Gallus gallus domesticus*).

History: Eyes were submitted from 42-day-old broiler breeder chicks with a history of unilateral ocular disease and possible flock history of *Chlamydophila* conjunctivitis. Birds were otherwise healthy and the submitted eyes returned negative PCR for *Chlamydophila*. *Scediosporum apiospermum* was cultured from corneal tissue.

Gross Pathology: Eyes from six birds, five with macroscopic corneal changes and one grossly normal, were submitted. The damaged eyes had opaque, white cream corneas that bulged abruptly to a height of 1 to 2 mm above the limbus. All eyes were opened with temporal calottes. Corneas were thickened, and in some birds the anterior chamber was obliterated by grey-white fleshy tissue. These birds also had disruption of integrity of the iris leaflets and iridocorneal angles were obliterated. Lens changes varied from mild focal anterior opacification to severe extensive opacity with roughening of the anterior lens capsule.

Histopathologic Description: Changes in the affected eyes varied in degree but not type. There was complete loss of the epithelium over much of the cornea. The stroma was expanded by a severe superficial and midstromal infiltrate of granulocytes, lymphocytes, plasma cells and histiocytes, the latter occasionally forming prominent multinucleated giant cells. Granulocytes predominated in the superficial layers and plasma cells in deeper layers. The inflammation extended to full thickness in the central cornea in most birds but in more severely affected birds the inflammation was full thickness to penetrating across most of the cornea.

The stroma showed patchy to extensive necrosis, and activation and proliferation of keratocytes. Within the inflammation, particularly near areas of necrosis in the superficial and mid stroma there were few to moderate numbers of branched, septate fungal hyphae. Staining with both PAS and GMS highlights the fungi.

Endothelium and Descemet's membrane were missing from the central corneal region at the area of full thickness inflammation. There was a wedge of fibrous tissue bridging the gap. In the worst affected birds, Descemet's membrane, which is very thin in this age of bird, could not be detected. Where present, endothelial cell density was considered normal.

In birds with obliteration of the anterior chamber there is extensive adhesion of the iris to the posterior cornea, particularly at the areas of full thickness inflammation. In these birds the iris was only identifiable by the lines of pigment. In other birds there is moderate to severe infiltration of the iris and ciliary body with inflammatory cells of similar mixture to those in the cornea. Granulocytes predominate with few giant cells.

Lens epithelium was irregular and heaped up centrally and at one pole in more moderately affected birds. The worst affected birds had wrinkles and sometimes fragmented lens capsule outlining a pocket of proliferative epithelial cells.

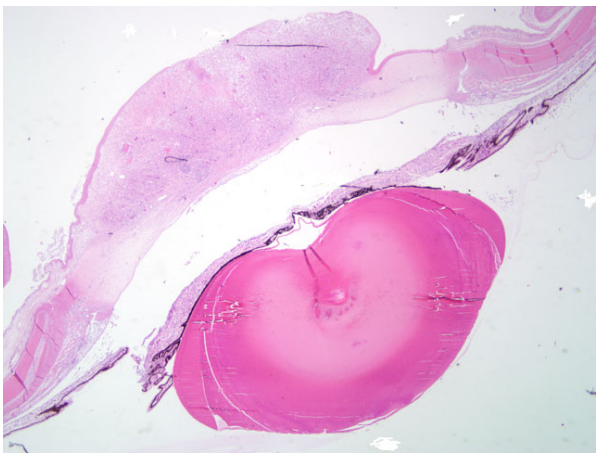

1-1. Eye, chick. The corneal stroma is focally expanded by a cellular infiltrate, and there is loss of the overlying corneal epithelium. The iris is adhered to the lens (posterior synechia). (HE 20X)

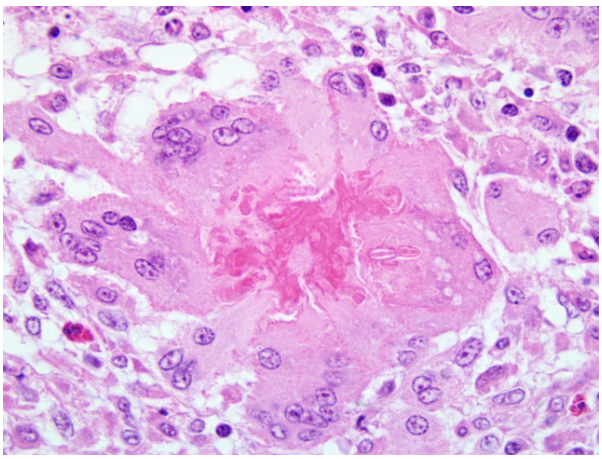

1-2. Eye, chick. The corneal stroma is expanded and replaced by many lymphocytes, plasma cells, epithelioid macrophages, few heterophils, and occasional multinucleated giant cells. (HE 1000X)

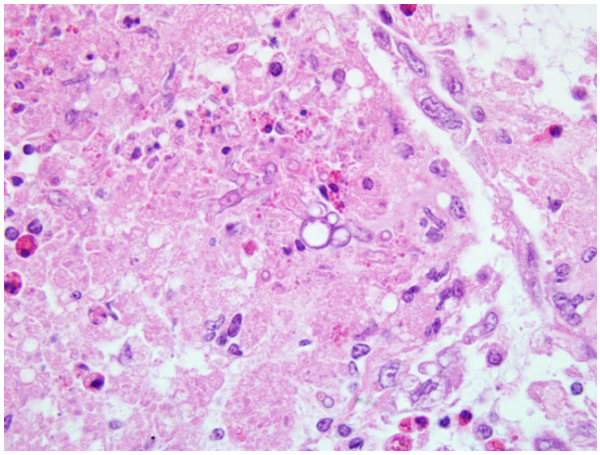

1-3. Eye, chick. Within areas of necrosis and inflammation in the corneal stroma there are few, branched septate fungal hyphae. (HE 1000X)

These birds had marked lymphocytic inflammation of the pecten but the posterior segment in all birds was otherwise unremarkable except for some retinal folding, which may be normal for this age.

There was moderate to severe lymphocytic conjunctivitis in some birds more evident ventrally, in the birds that had it, than in the dorsal lids. There was no evidence in any submitted eye of chlamydophilosis.

Contributor's Morphologic Diagnosis: Severe chronic diffuse, mixed cellular, mycotic keratitis.
Severe chronic active iritis with extensive anterior synechia.
Cataract and pectenitis secondary to intraocular inflammation.

Contributor's Comment: Reports of fungal keratitis in poultry are few. Reis (1940)[10,11] described lesions involving much of the anterior segment in birds 2 to 5 weeks of age which were reproducible by dropping a suspension of *Aspergillus fumigatus* onto a deeply scarified cornea. Subsequent reports of outbreaks of *Aspergillus* describe the development of a caseous pellet under the nictitating membrane in up to 10% of chicks in a flock, often at around a week of age. Itakura et al. (1972), reporting on natural cases, showed that infection was related to the environment of the birds; morbidity coincided with the introduction of chip litter.[10] Likewise, Beckman showed corneal lesions caused by excessive ammonia fumes may permit fungal colonization in chickens.[1] In humans, the species in which mycotic keratitis is best described, damage to the corneal surface is most commonly caused by surgery and extended contact lens wear.[16]

Fungal lesions arising in the cornea may extend to involve the anterior segment, but rarely progress into the posterior part of the eye; in contrast, endophthalmitis, associated with fungal respiratory disease, typically affects the retina and vitreous, but the cornea remains unaffected. Interestingly, corneal infections are almost always unilateral.

In all previous reported cases of fungal keratitis in chickens, the isolated agent has been *Aspergillus fumigatus* which makes this outbreak unique. *Scedosporium apiospermum* (and its teleomorph, or sexual stage, *Pseudallescheria boydii*) is a filamentous fungus of widespread distribution, recently described as "one of the clinically significant emerging mycoses."[17] It has, however, a long history, being first recognized in human otitis in the late 19th century, and in the mycetoma known as "madura foot" in the early 20th century. Taxonomy has been confused, but the present designation is *S. apiospermum* for the asexual state and *P. boydii* for the sexual.

S. apiospermum is best known for its association with near drowning events and subsequent pneumonia and disseminated disease.[5,17] Its tolerance to cold, low oxygen tension and high salinity make it a survivor in polluted environments and recovery of the species from unpolluted environments is rare.[5] Cytological and histological

distinction from *Aspergillus* spp. is difficult. The two genera are closely related and share antigenic epitopes in formalin fixed tissues.[17]

Corneal infections have been reported in humans and are associated with a guarded prognosis for sight because of the resistance of this fungus to commonly used therapeutic agents.[16] To date no other species has been reported with this infection in the cornea or ocular tissues, but the increasing rate of environmental detection of *S. apiospermum* suggests that infection may become more common in domestic species and poultry as it has in humans.

AFIP Diagnosis: 1. Eye: Keratitis, ulcerative, granulomatous and heterophilic, diffuse, severe with ulcerative conjunctivitis and fungal hyphae.
2. Eye, iris: Anterior uveitis, heterophilic and lymphoplasmacytic, diffuse, marked with synechia.

Conference Comment: Conference attendees reviewed the histologic anatomy of the avian eye, to include the 10 layers of the retina. Unlike the mammalian eye, in many species of birds the cartilaginous sclera ossifies with age and there are bony ossicles at the corneal-scleral junction. Consequently, care should be taken to decalcify avian eye specimens to prevent damage to the microtome when sectioning occurs. Another difference between the avian and mammalian eye is that the avian eye has a specialized pigmented and vascular structure that projects from the retina into the vitreous humor known as the pecten.[14] The pecten's function is thought to be to provide nutrients to the avascular retina.

Most attendees identified the fungal hyphae as *Aspergillus* species. Given the morphologic similarity between *S. apiospermum* and *Aspergillus* spp., the confusion is understandable and highlights the utility of microbial culture in arriving at a definitive diagnosis when mycotic organisms are observed during histologic examination of tissues. Because mild conjunctivitis was present in some conference attendees' slides, participants briefly reviewed several common causes of conjunctivitis in avian species, among which include: *Chlamydophila psittaci*, Newcastle disease virus, avian influenza virus, infectious bronchitis virus, infectious laryngotracheitis virus, and fowl poxvirus. Likewise, causes of cataract formation in the bird eye were discussed, two of which include vitamin E deficiency and avian encephalomyelitis virus.[14] Additionally, congenital cataracts of unknown etiology sporadically occur in commercial turkeys.[14]

The contributor provides detailed information on *S. apiospermum* as an important emerging mycotic disease. The moderator stressed that, in addition to the outbreak of *S. apiospermum* in this flock of chickens, *S. apiospermum* (*Pseudallescheria boydii*) has been noted to occur in elephant seals[8] and in the nasal passages of cattle,[13] horses,[6] and dogs.[2,3,4] In addition to the nasal passage, bones and joints appear to be other common locations for infection in dogs.[7,9] Other species of *Scedosporium* have been reported to cause osteomyelitis in animals, including *S. prolificans* in a horse[15] and *S. inflatum* in a dog.[12] In contrast to humans, *S. apiospermum* infection in animals has not yet been linked to immunosuppression.[13]

Multiple eyes from several different animals are submitted, and hence anterior or posterior synechia may be present, depending on the section evaluated. Additionally, the lens in some sections contains cataractous change.

Contributor: University of Melbourne, Faculty of Veterinary Science
www.vet.unimelb.edu.au

References:

1. Beckman BJ, Howe CW, Trampel DW, et al. *Aspergillus fumigatus* keratitis with intraocular invasion in 15-day-old chicks. *Avian Dis*. 1994;38:660-665.
2. Cabanes FJ, Roura X, Garcia F, Domingo M, Abarca ML, Pastor J. Nasal granuloma caused by *Scedosporium apiospermum* in a dog. *J Clin Microbiol*. 1998;36:2755-2758.
3. Caro-Vadillo A, Garcia-Real I, Paya-Vicens MJ, Sainz-Rodriguez A, Rodriguez-Franco F, Rodriguez-Bertos A. Fungal rhinitis caused by *Scedosporium apiospermum* in laborador retriever. *Vet Rec*. 2005;157:175-177.
4. Coleman MG, Robson MC. Nasal infection with *Scedosporium apiospermum* in a dog. *N Z Vet J*. 2005;53:81-83.
5. Cortez KJ, Roilides E, Quiroz-Telles F, et al. Infections caused by *Scedosporium* spp. *Clin Microbiol Rev*. 2008;21:157-197.
6. Davis PR, Meyer GA, Hanson RR, Stringfellow JS. *Pseudallescheria boydii* infection of the nasal cavity of a horse. *J Am Vet Med Assoc*. 2000;5:707-709.
7. Elad D, Perl S, Yamin G, Blum S, David D. Disseminated pseudallescheriosis in a dog. *Med Mycol*. 2010;48(4): 635-638.
8. Haulena M, Buckles E, Gulland FM, et al. Systemic mycosis caused by *Scedosporium apiospermum* in a stranded northern elephant seal (*Mirounga angustirostris*) undergoing rehabilitation. *J Zoo Wildl Med*. 2002;33:166-171.
9. Hugnet C, Marrou B, Dally C, Guillot J. Osteomyelitis and discospondylitis due to *Scedosporium apiospermum* in a dog. *J Vet Diagn Invest*. 2009;21:120-123.
10. Itakura C, Goto M, Fujiwara M. Pathological observation of fungal (*Aspergillus fumigatus*) ophthalmitis in chicks. *Nippon Juigaku Zasshi*. 1973;35:473-479.
11. Mustaffa-Babjee A. Specific and non specific conditions affecting avian eyes. *Vet Bull*. 1969;39:681- 687.
12. Salkin IF, Cooper CR, Bartges JW, Kemna ME, Rinaldi MG. *Scedosporium inflatum* osteomyelitis in a dog. *J Clin Microbiol*. 1992;30:2797-2800.
13. Singh K, Boileau MJ, Streeter RN, Welsh RD, Meier WA, Ritchey JW. Granulomatous and eosinophilic rhinitis in a cow caused by *Pseudallescheria boydii* species complex

(*Anamorph Scedosporium apiospermum*). *Vet Pathol*. 2007;44:917-920.
14. Swayne DE. Eye and ear. In: Riddell C, ed. *Avian Histopathology*. 2nd ed. Tallahassee, FL: American Association of Avian Pathologists, Rose Printing; 1996:204-206.
15. Sweczek TW, Donahue JM, Hunt RJ. *Scedosporium prolificans* infection associated with arthritis and osteomyelitis in a horse. *J Am Vet Med Assoc*. 2001;218:1800-1802.
16. Thomas PA. Current perspectives on ophthalmic mycoses. *Clin Microbiol Rev*. 2003;16:730-797.
17. Walts AE. Pseudallescheria: an underdiagnosed fungus? *Diagn Cytopathol*. 2001;25:153-157.

CASE II: C10-629 (AFIP 3165176).

Signalment: 13-year-old male castrated warmblooded horse (*Equus caballus*).

History: The owner noted two masses on the inside of the prepuce that have been present for two months and are rapidly growing.

Gross Pathology: There are two pieces of non-haired skin that are disrupted by a central tan, firm, nodule, measuring 2 x 1.5 x 1 cm in one piece, and 11 x 11 x 8 mm in the other.

Histopathologic Description: Prepuce: The dermis is markedly expanded by large, dense, nodular aggregates of lymphocytes and plasma cells containing multiple smaller dense aggregates of epithelioid macrophages and multinucleated giant cells, with fewer scattered eosinophils. Multifocally within the inflammatory aggregates and frequently surrounded by macrophages and giant cells are cross-sections of nematodes, ranging up to 15 µm in diameter. These have a very thin cuticle, with low, indistinct platymyarian-meromyerian musculature, a pointed tail, numerous deeply basophilic 2-3 µm internal structures, and an esophagus with a prominent corpus, isthmus, and bulb (rhabditiform esophagus). There are moderate numbers of lymphocytes and plasma cells and fewer eosinophils scattered throughout the dermis surrounding the nodule. There is marked epidermal hyperplasia with compact hyperkeratosis overlying the nodule.

Contributor's Morphologic Diagnosis: Posthitis, lymphoplasmacytic, eosinophilic, and granulomatous, severe, chronic, multifocal, with intralesional rhabditiform nematodes.

Contributor's Comment: *Halicephalobus gingivalis* (formerly known as *Micronema deletrix* or *Halicephalobus delatrix*) is a free-living rhabditiform nematode. Infections in horses are infrequently reported; when found, organisms typically infiltrate the central nervous system,[2,3] but have also been reported in the prepuce,[4,10] kidney,[1,15] eye,[11] bone,[5] and one case of systemic infection.[13] In addition to *Halicephalobus*, other free-living rhabditoid nematodes, such as the genus *Cephalobus* [6] and *Pelodera*,[12] have been reported to cause skin infections in horses, and cannot be ruled out in this case. In addition to horses, other equids, such as zebras, have also been reported to be infected.[8]

To date, only female *Halicephalobus* have been found in tissue samples.[10] While the route of infection and pathogenesis of disease are poorly understood, it is suspected that the organism gains entry via existing wounds. In some cases, viable *Halicephalobus* organisms have been detected in sperm and urine;[9] while no transmission via this route has been proven, it is another possible source of infection. Organisms access the central nervous system via blood vessels, and cause necrosis and inflammation due to migration through the tissue.

Under light microscopy, adult females are typically approximately 20 µm in diameter and 350 µm long, with a thin, smooth cuticle and tapered, pointed tail. They have platymyarian-meromyarian musculature, a rhabditiform esophagus, and an intestine lined by low cuboidal cells. Larvae are approximately 10 µm in diameter, with tapered, pointed tails. Typically, tissue sections have numerous parasites; this may be explained by the fact that females are parthenogenetic and thus can produce offspring in the absence of males.

Other rule outs for rhabditoid parasites in tissue sections include *Cephalobus* spp., *Strongyloides westeri*, and *Pelodera strongyloides*.[12] *Cephalobus* spp. can be differentiated from *Halicephalobus* spp. by examination of the tail, which is blunt in *Cephalobus*.[6] *Strongyloides westeri*

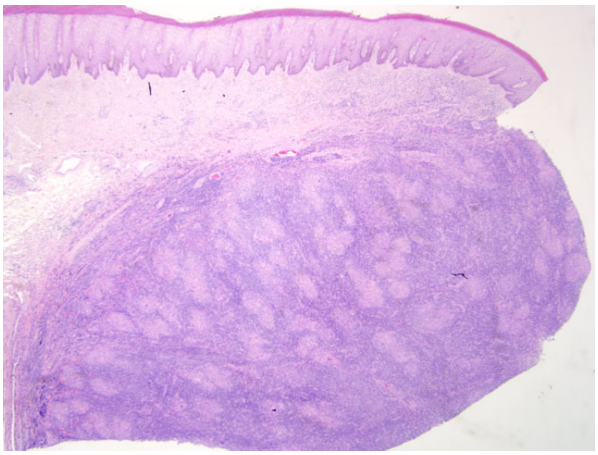

2-1. Glabrous skin, prepuce, horse. The dermis is markedly expanded by a nodular focus of granulomatous inflammation. Diffusely, the overlying epidermis is hyperplastic and hyperkeratotic. (HE 20X)

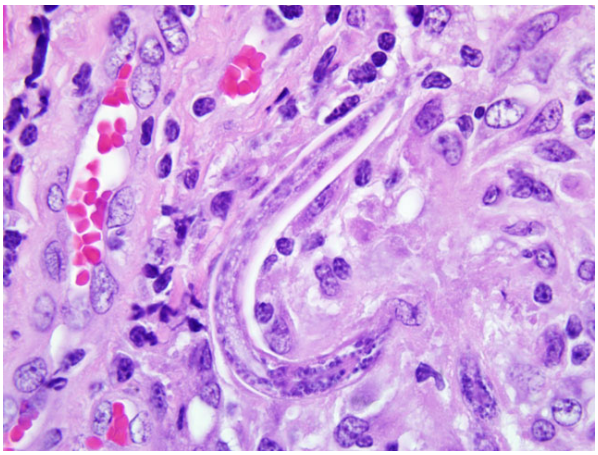

2-2. Glabrous skin, prepuce, horse. Lymphocytes, plasma cells, and epithelioid macrophages surround an adult nematode that has a thin cuticle, indistinct platymyarian-meromyerian musculature, pointed tail, and numerous deeply basophilic 2-3 µm internal structures. (HE 1000X)

have alae, which *Halicephalobus* spp. lack.[6] *Pelodera strongyloides* also have two lateral alae, as well as two lateral cords noted by two densi nuclei.[7]

AFIP Diagnosis: Glabrous skin, prepuce: Posthitis, granulomatous and eosinophilic, focally extensive, marked with rhabditiform nematode adults, larvae and eggs, etiology consistent with *Halicephalobus gingivalis*.

Conference Comment: The contributor provides an excellent overview of halicephalobiasis in the horse. Most conference participants correctly identified the nematode as *H. gingivalis*, though some participants identified the tissue as gingiva rather than skin from the prepuce. As *H. gingivalis* causes granulomatous inflammation at both anatomic locations, tissue identification is important. Upon closer examination of the tissue sample, all participants subsequently identified scattered sebaceous and apocrine glands, and some sections contain rare hair follicles, consistent with glabrous skin. Conference participants also reviewed the differential diagnosis for this lesion, which the contributor discusses in detail. In addition to the morphologic features provided by the contributor, the moderator commented that a unique anatomic feature of *H. gingivalis* is the presence of a dorsally reflexed ovary, which is often difficult to appreciate on routine histologic examination, but when present is diagnostic.

In addition to the histomorphologic differences among the various nematodes, clinicopathologic presentation may assist with differentiating them. Although *H. gingivalis* dermatitis may occur anywhere on the skin of horses, it generally localizes near or on the prepuce; lesions tend to be papules or nodules that are well circumscribed, measure 0.5 cm to 8 cm in diameter, and are often ulcerated.[14] In contrast, *Pelodera* dermatitis is characterized by papules, pustules, ulcers, crusts, alopecia, and scales on areas of the skin that typically have contact with damp soil and decaying organic matter, such as the limbs, ventral thorax, and abdomen;[14] pruritis is usually moderate to intense.

We thank Dr. Christopher Gardiner, Consulting Parasitologist for the AFIP's Department of Veterinary Pathology, for his study and diagnostic commentary for this case.

Contributor: Department of Infectious Diseases and Pathology, College of Veterinary Medicine, University of Florida, P.O. Box 110880, Gainesville, FL 32611-0880

References

1. Akagami M, Shibahara T, Yoshiga T, et al. Granulomatous nephritis and meningoencephalomyelitis caused by *Halicephalobus gingivalis* in a pony gelding. *J Vet Med Sci* 2007;69:1187-1190.
2. Bryant U, Lyons E, Bain F, Hong C. *Halicephalobus gingivalis*-associated meningoencephalitis in a Thoroughbred foal. *J Vet Diagn Invest.* 2006;18:612-615.
3. Bröjer J, Parsons D, Linder K, Peregrine A, Dobson H. *Halicephalobus gingivalis* encephalomyelitis in a horse. *Can Vet J*. 2000;41:559-561.
4. Dunn D, Gardiner C, Dralle K, Thilsted J. Nodular granulomatous posthitis caused by *Halicephalobus* (syn. *Micronema*) sp. in a horse. *Vet Pathol*. 1993;30:207-208.
5. Ferguson R, van Dreumel T, Keystone J, et al. Unsuccessful treatment of a horse with mandibular granulomatous osteomyelitis due to *Halicephalobus gingivalis*. *Can Vet J*. 2008;49:1099-1103.
6. Greiner E, Mays M, Smart GJ, Weisbrode S. Verminous mastitis in a mare caused by a free-living nematode. *J Parasitol*. 1991;77:320-322.
7. Gutierrez Y. *Diagnostic Pathology of Parasitic Infections with Clinical Correlations*. 2nd ed. New York, NY: Oxford University Press; 2000:307.
8. Isaza R, Schiller C, Stover J, Smith P, Greiner E. *Halicephalobus gingivalis* (Nematoda) infection in a Grevy's zebra (Equus grevyi). *J Zoo Wildl Med*. 2000;31:77-81.
9. Kinde H, Mathews M, Ash L, St Leger J. *Halicephalobus gingivalis* (H. deletrix) infection in two horses in southern California. *J Vet Diagn Invest*. 2000;12:162-165.
10. Muller S, Grzybowski M, Sager H, Bornand V, Brehm W. A nodular granulomatous posthitis caused by *Halicephalobus* spp. in a horse. *Vet Dermatol*. 2008;19:44-48.
11. Rames D, Miller D, Barthel R, et al. Ocular *Halicephalobus* (syn. *Micronema*) *deletrix* in a horse. *Vet Pathol*. 1995;32:540-542.
12. Rashmir-Raven A, Black S, Rickard L, Akin M. Papillomatous pastern dermatitis with spirochetes and *Pelodera strongyloides* in a Tennessee Walking Horse. *J Vet Diagn Invest*. 2000;12:287-291.
13. Ruggles A, Beech J, Gillette D, Midla L, Reef V, Freeman D. Disseminated *Halicephalobus deletrix* infection in a horse. *J Am Vet Med Assoc*. 1993;203:550-552.
14. Scott DW, Miller WH, Jr. *Equine Dermatology*. St. Louis, MO: Elsevier Ltd; 2003:366-369.
15. Shibahara T, Takai H, Shimizu C, Ishikawa Y, Kadota K. Equine renal granuloma caused by *Halicephalobus* species. *Vet Rec*. 2002;151:672-674.

CASE III: Colorado State University CSU-CVMBS 090-TK01 (AFIP 3166610)

Signalment: Young male intact commercial grower turkey (*Meleagris gallopavo*).

History: A male commercial production turkey was submitted for necropsy (donation) by a large commercial production company. The company has multiple complexes in multiple states in the United States. This bird came from a premisis in Arkansas with a flock size of 40,000 birds. All birds in this flock are males and are sent to slaughter around 20 weeks of age. This bird was found dead. The company did not report a higher than normal rate of turkey mortality.

Gross Pathology: Liver: There are multifocal to coalescing circular regions of necrosis with depressed pale tan/yellow centers surrounded by a slightly raised, often hemorrhagic rim. Lesions range in size from 0.5 to 3.0 cm in diameter and are disseminated randomly throughout the parenchyma.

Ceca: Both ceca are moderately distended and fluid filled with thickened hyperemic walls mottled tan to dark red. The mucosal surface is multifocally ulcerated with occasional partially adhered caseous debris amidst abundant luminal hemorrhagic exudate.

Histopathologic Description: Liver: Approximately 50 to 80% of the parenchyma is largely obliterated by multifocal, random, discrete and coalescing to regionally extensive areas of coagulative hepatic necrosis. Affected areas are characterized by shrunken hepatocytes with intensely eosinophilic cytoplasm and pyknotic to lytic nuclei or loss of hepatocytes, disruption of hepatic cords, and replacement with eosinophilic cellular and karyorrhectic debris. Mainly within necrotic foci and variably expanding portal triads are pleocellular infiltrates composed of moderate to large numbers of macrophages (many hemosiderin-laden), lymphocytes, heterophils, few plasma cells and variable numbers of foreign body-type multinucleate giant cells. Phagocytized by multinucleated giant cells as well as free and within the lumen of ectatic, hyperplastic bile ducts are individual to clustered 12-20 µm in diameter eosinophilic to amphophilic protozoal trophozoites. Trophozoites may contain a 2-4 µm diameter oval shaped basophilic central to slightly eccentric nucleus. Pericholangial inflammation and fibrosis is prominent around large sized bile ducts with remaining hepatic parenchyma interrupted by numerous variably sized newly formed bile ductules. Numbers of multinucleate cells and organisms vary depending on the section received.

Cecum: Diffusely expanding the lamina propria and multifocally extending transmurally with effacement of up to 50% of the muscular coat is an inflammatory infiltrate composed predominantly of lymphocytes and macrophages with fewer plasma cells and heterophils admixed with numerous 12-20 µm diameter protozoal trophozoites similar

3-1. Liver, turkey. There are multifocal to coalescing circular regions of necrosis with depressed pale tan/yellow centers surrounded by a slightly raised, often hemorrhagic rim. Lesions range in size from 0.5 to 3.0 cm in diameter and are disseminated randomly throughout the parenchyma. Photograph courtesy of Colorado State Diagnostic Medicine Center, 300 W. Drake Rd., Fort Collins, CO 80523, ej.ehrhart@colostate.edu

3-2. Cecum, turkey. Both ceca are moderately distended and fluid filled with thickened hyperemic walls mottled tan to dark red. The mucosal surface is multifocally ulcerated with occassional partially adhered caseous debris amidst abundant luminal hemorrhagic exudate. Photograph courtesy of Colorado State Diagnostic Medicine Center, 300 W. Drake Rd., Fort Collins, CO 80523, ej.ehrhart@colostate.edu

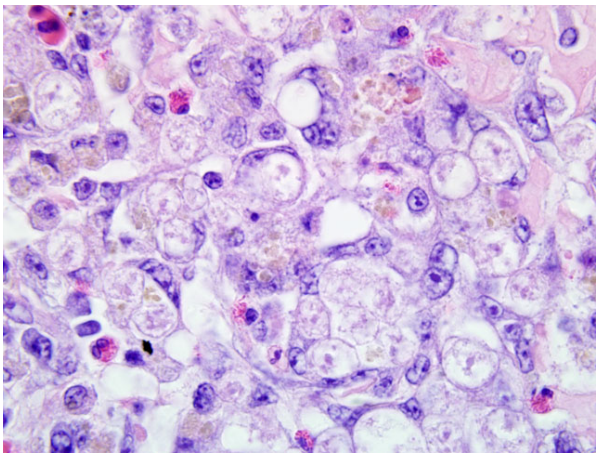

3-3. Liver, turkey. Areas of hepatic necrosis contain many hemosiderin-laden macrophages, lymphocytes, heterophils, fewer plasma cells, and numerous intrahistiocytic and extracellular, 12–20 µm trophozoites. Trophozoites may contain a 2-4 µm oval shaped basophilic central to slightly eccentric nucleus. (HE 1000X)

to those described within the liver. There is extensive loss of crypts and remnant crypts are hyperplastic, tortuous and ectatic with piling of 2-3 epithelial cells layers, and luminal aggregates of detached epithelial cells and degenerate leukocytes, mainly heterophils (crypt microabscesses). There is multifocal extensive mucosal ulceration, and in some sections the cecal lumen contains a dense core of eosinophilic cellular and karyorrhectic debris, erythrocytes, fibrin, degenerate protozoal trophozoites, macrophages and heterophils, and aggregates of rod shaped bacteria (cecal core).

Contributor's Morphologic Diagnosis: Liver: Multifocal and coalescing, random, necrotizing, sub-acute-to-chronic, lymphohistiocytic and heterophilic hepatitis with biliary hyperplasia and intralesional protozoal trophozoites, etiology consistent with *Histomonas meleagridis*.

Cecum: Transmural, marked, sub-acute-to-chronic lymphohistiocytic and heterophilic typhlitis with fibrinonecrotic core (variable) and intralesional protozoal trophozoites consistent with *H. meleagridis*.

Contibutor's Comment: Histomoniasis, also known as blackhead and infectious enterohepatitis, is a disease of gallinaceous birds caused by *Histomonas meleagridis*, a flagellated amoeboid protozoan which remains an important disease economically for the commercial poultry industry. Two aspects of this disease worthy of brief review are 1) the unique life cycle of the organism and 2) differences in transmission and extent of disease in turkeys and chickens.

The role of the cecal worm *Heterakis gallinarum* as an intermediate host has been well-described.[2,3] The exact mechanism of infection of *Heterakis* eggs with histomonads remains unknown, but it has been suggested that the protozoan may be transferred to the female worm during mating and are then incorporated into embryonated eggs.[2] Infected eggs pass in feces where they may be ingested directly by birds or by earthworms who may serve as a transport host. Ingestion of either egg-laden feces or earthworms by the bird results in transport to the cecum where flagellated trophozoites are released from the nematode egg, multiply in the cecal lumen and penetrate the cecal wall. The tissue stage loses the flagella becoming amoeboid. Eventually the histomonads gain entry into the bloodstream and are carried to the liver via the hepatic-portal system. It is important to note that the fragile trophozoite of *Histomonas*, which cannot survive long outside of any of its hosts, would be unable to survive passage through the stomach if not within a nematode egg or an earthworm. Therefore, fecal oral transmission is not thought to be an important route of transmission. Interestingly, some recent publications have shown the existence of a cyst stage in some species of *Histomonas in vitro* sparking interest in the possibility of this happening under certain conditions in the natural disease allowing for persistence in the environment and the possibility of oral transmission.[4,7]

Extension to the liver as described above occurs at a higher rate in turkeys than chickens, with a much higher associated mortality rate. Concurrent infection with *Eimeria tenella* results in increased liver lesions in chickens. Histomonad virulence also requires the presence of cecal bacteria such as *Escherichia coli*, *Clostridium perfringens*, and/or *Bacillus subtilis*, especially in turkeys.[2,3] As mentioned previously, turkeys suffer from a much higher mortality rate than chickens, with the latter being better able to control the disease but still suffering decreased productivity. A recent publication showed that chickens mount a more effective innate immune response to *H. meleagridis* in the ceca than do turkeys resulting in better control of parasite numbers in chickens.[5] Furthermore, unregulated cell-mediated immunity in the liver is more pronounced in the turkey than the chicken often leading to lymphoid depletion of the spleen.[5] Another difference of histomoniasis in turkeys is that, in addition to transmission via ingestion of *Heterakis* eggs, turkeys appear to be able to transmit histomonads directly via "cloacal drinking" where cloacal droppings from an infected bird can be pulled retrograde into the ceca of a susceptible bird if the droppings contact the vent of the uninfected bird.[2,3]

AFIP Diagnosis: 1. Liver: Hepatitis, random, necrotizing, lymphohistiocytic and heterophilic, multifocal coalescing, severe, with biliary hyperplasia and protozoal trophozoites, etiology consistent with *Histomonas meleagridis*.
2. Cecum: Typhlitis, transmural, lymphohistiocytic and heterophilic, diffuse, severe, with fibrinonecrotic core and protozoal trophozoites, etiology consistent with *Histomonas meleagridis*.

Conference Comment: The contributor provides an excellent review of the pathology and life cycle of *Histomonas meleagridis*. While attendees found this to be a relatively uncomplicated histologic diagnosis given the species and abundance of trophozoites, all were interested and engaged in the discussion that the case precipitated.

Conference participants noted that "blackhead" is an imprecise colloquialism in that cyanosis of the head is neither a constant feature nor a unique clinical sign of histomoniasis.[6] Other diseases, such as turkey enteric coronavirus (bluecomb disease), avian influenza, and various respiratory pathogens may cause a cyanotic head in turkeys and chickens. Gross digital images were shown during the conference to reinforce the point that the macroscopic lesions of histomoniasis are very distinctive, and when classical lesions are present in both the liver and cecum simultaneously, the findings are considered pathognomonic for the condition. When only cecal cores are present, other etiologic considerations would include salmonellosis for both chickens and turkeys, and *Eimeria tenella* in chickens.

In addition to histomoniasis, cecal heterakiasis was also discussed by participants. Although *H. gallinarum* can cause thickened cecal walls, nodule formation, and inflammation in

its own right in turkeys and chickens, its practical and economic importance is the nematode's ability to serve as a carrier for *H. meleagridis*.[1] In pheasants, however, *Heterakis isolonche* causes severe cecal disease with mortality rates that may exceed 50%.[2] The disease in pheasants is characterized by a marked inflammatory response, fibrosis, and coalescing cecal wall nodules.

Contributing: Colorado State University, College of Veterinary Medicine and Biomedical Sciences
www.cvmbs.colostate.edu

References:

1. Goodwin MA. Alimentary system. In: Riddell C, ed. *Avian Histopathology*. 2nd ed. Tallahassee, FL: American Association of Avian Pathologists, Rose Printing; 1996: 127-129.
2. McDougald LR. Histomoniasis (Blackhead) and other protozoan diseases of the intestinal tract. In: Saif YM, ed. *Disease of Poultry*, 12th ed. Ames, IA: Blackwell Publishing Professional; 2008:1095-1100.
3. McDougald LR. Blackhead disease (Histomoniasis) in poultry: a critical review. *Avian Dis*. 2005;49:462-476.
4. Munsch MH, Mehlhorn S, Al-Quraishy AR, Lotfi, Hafez HM. Molecular biological features of strains of *Histomonas meleagridis*. *Parasitol Res*. 2009;104:1137-1140.
5. Powell FL, Rothwell L, Clarckson MJ, Kaiser P. The turkey, compared to the chicken, fails to mount an effective early immune response to *Histomonas meleagridis* in the gut. *Parasite Immunol*. 2009;31:312-327.
6. Trees AJ. Parasitic diseases. In: McMullin PF, ed. *Poultry Diseases*, 6th ed., Edinburgh: Elsevier Limited; 2008:458-459.
7. Zaragatzki E, Hess M, Grabensteiner E, Abdel-Ghaffar F, Al-Rasheid K, Mehlhorn H. Light and transmission electron microscopic studies of the encystation of *Histomonas meleagridis*. *Parasitol Res*. 2010;106:977-983.

CASE IV: V10-02733 (AFIP 3167339).

Signalment: 3-year-old female Rambouillet ovine (*Ovis aries.)*

History: This animal was one from a herd of approximately 1200 sheep on open range in the "Four Corners" region of northwestern New Mexico. During a winter snowstorm in the area, the shepherd moved the animals from the mesa tops down into surrounding lower country (arroyos, valleys). During the day and night following the move, it had snowed approximately 8 inches. The following morning the shepherd found 50 animals dead and 5 animals that were down, debilitated, and showing "neurological" signs. The water source was snow; sheep were ranged on the country described above. Trace mineral salt was supplemented. The shepherd was with sheep at all times.

Gross Pathology: This ewe was presented alive, but down, and with neuromuscular fasciculations of the head and neck. The animal was unable to get up, and was euthanized. On gross exam, the rumen was engorged with a somewhat woody or brushy type plant material; this had a somewhat pungent odor. Both the rumen and reticulum were somewhat edematous. The kidneys were pale, swollen and bulged on cut surface.

Histopathologic Description: The kidneys had flattening and destruction of proximal convoluted tubular epithelial cells, with prodigious aggregates of birefringent crystals in these tubules. These crystals also were seen in distal convoluted tubules, but in much lower numbers. Crystals had layers or sheaves aggregated together; these were consistent with oxalates histologically.

Contributor's Morphologic Diagnosis: Nephrosis, toxic tubular, kidney, ovine due to potassium oxalate intoxication from excessive ingestion of "greasewood" (*Sarcobatus vermiculatus*).

Contributor's Comment: Brushy plants found in the rumen were identified as greasewood (*Sarcobatus vermiculatus*), a plant commonly found in the western and Southwestern range country. This is a plant browsed extensively by sheep, usually without any problems when eaten in combination with other forages. However, when eaten as an exclusive diet (and thus in excess), it is highly toxic and can cause massive die-off, such as with this case. In this particular situation, greasewood was the only browse poking thru the recent snowfall, and sheep are not prone to paw or dig for forage like cattle. Hence, in this circumstance of weather, terrain, and ready availability of a poisonous plant, coupled with grazing habits of sheep, a "perfect storm" of all the above ingredients resulted in the excessive ingestion of *Sarcobatus* spp. and subsequent intoxication and die-off of animals. The shepherd had moved the sheep into a fenced pasture and put out high grade alfalfa hay prior to bringing this animal in for necropsy, as he was suspicious of greasewood being the cause of the problem. A few more animals died, but the change in diet resolved any further problem.

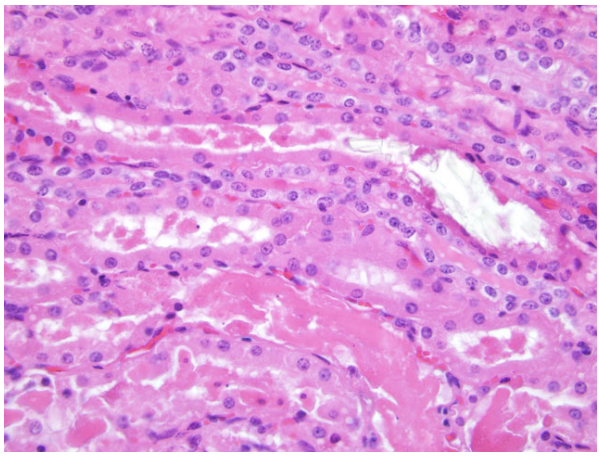

4-1. Kidney, ewe. Multifocally in the cortex, the epithelium of the proximal and distal convoluted tubules is degenerate and necrotic, and there are many intraluminal birefringent oxalate crystals. (HE 400X)

Histologic lesions are quite similar to those of antifreeze (ethylene glycol) intoxication in a number of species; however, these are potassium oxalates with the *Sarcobatus* spp. intoxication, versus calcium oxalates crystals seen with antifreeze poisoning. Histologically, the lesions and crystals are very similar.

Sarcobatus spp. contains a mixture of neutral sodium and potassium oxalates - about 10-15% d.w. in leaves and in smaller amounts in stems and fruits. Oxalate concentrations reach a peak in early fall. Aqueous extracts of the plant containing 40% oxalates, when given to sheep, produced the same signs and lesions as when the plant was eaten.[1]

Other oxalate producing plants that can cause poisoning in sheep and cattle include halogeton (*Halogeton glomeratus*), common rhubarb (*Rheum rhaponticum*), soursob (*Oxalis cernua*), and sorrel dock (*Rumex* spp).[2]

AFIP Diagnosis: Kidney: Tubular necrosis, acute, diffuse, with intratubular oxalate crystals.

Conference Comment: Case discussion focused on the pathogenesis of oxalate nephrosis in animals. Sheep are able to consume oxalate-containing plants without toxicity due to the rumen's ability to metabolize oxalates to bicarbonate and carbonate; however, changes in the microbial balance of the rumen may reduce this ability. In this case, unmetabolized oxalates are absorbed into the circulation where they chelate calcium ions, and thus forming insoluble calcium oxalate complexes. In the kidney, these complexes may crystallize in vessel walls, or within the lumens of blood vessels or renal tubules. Deposition within vessels results in renal hemorrhage and necrosis, while deposition in renal tubules results in obstruction and acute renal failure. Furthermore, intracellular chelation of calcium and magnesium ions may

interfere with oxidative phosphorylation, resulting in nephrotoxicity in addition to physical tubular obstruction.[2]

Electrolyte disturbances in affected animals include increased plasma sodium, potassium and calcium; of these changes, the cardiotoxic potential of hyperkalemia is most life-threatening. In addition, ingestion of oxalate-containing plants by sheep results in hypocalcemia due to chelation and may result in tetany. Acidosis and azotemia are other common clinicopathologic findings in acute renal failure, with acidosis in affected animals often being the most significant contributory factor in the cause of death.[2]

Contributor: NMDA – Veterinary Diagnostic Services, P.O. Box 4700, Albuquerque, NM 87196-4700
http://www.nmda.nmsu.edu/animal-and-plant-protection/veterinary-diagnostic-services

References:

1. Burrows GE, Tyrl RJ. Chenopodiaceae vent. In: *Toxic Plants of North America.* 1st ed. Ames, IA: Iowa State University Press; 2001:358-359.
2. Maxie MG, Newman SJ. Urinary system. In: Maxie MG, ed. *Jubb, Kennedy and Palmer's Pathology of Domestic Animals*. 5th ed., Vol. 3. Philadelphia, PA: Elsevier Ltd; 2007:432-433, 470-472.

The Armed Forces Institute of Pathology
Department of Veterinary Pathology

Conference Coordinator
Matthew Wegner, DVM

WEDNESDAY SLIDE CONFERENCE 2010-2011

Conference 6

22 September 2010

Conference Moderator:
Marc E. Mattix, DVM, MSS, Diplomate ACVP

CASE I: S 1120/08 (AFIP 3133964).

Signalment: 2-year-old female Guereza monkey (*Colobus guereza*).

History: The monkey was housed in an open-range recreation park together with numerous other monkeys of the same species and in close contact to other animal species and human visitors. Clinically, a poor body condition, dyspnoea and abdominal discomfort were noticed for two days prior to death.

Gross Pathology: Necropsy revealed a poor body condition and moderate hyperplasia of hepatic and gastric lymph nodes. Approximately 30% of the liver tissue was replaced by multifocal to coalescing, variably demarcated, irregularly shaped, pale yellow, occasionally slightly elevated nodules measuring 0.5 - 4.0 cm in diameter. On the cut surface, they showed a pale yellow coloration and a dry, elastic consistency. In addition, a moderate multifocal fibrino-necrotizing gastritis and mild acute diffuse catarrhal enteritis were observed.

Laboratory Results: Urinalysis revealed a pH value of 8.0; 300 mg protein/liter; a normal amount of glucose and urobilinogen; and no leukocytes, nitrites, ketones or bilirubin.

The liquid of the anterior eye chamber contained a urea concentration of 19.98 mmol/L (120 mg/dL).

Aerobic and anaerobic microbiological cultures of the liver resulted in a mild amount of α-hemolytic *Streptococcus* spp.

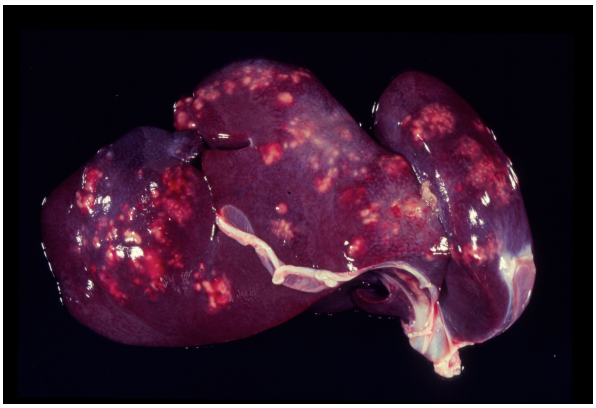

1-1. Liver, guereza monkey. Approximately 30% of the liver tissue is replaced by multifocal to coalescing, variably demarcated, irregularly shaped, pale yellow, occasionally slightly elevated nodules of 0.5-4.0 cm in diameter. Photograph courtesy of Department of Pathology, University of Veterinary Medicine, Hannover, Germany, peter.wohlsein@tiho-hannover.de

and coagulase-negative *Staphylococcus* spp. Aerobic and anaerobic microbiological cultures of the stomach revealed a mild amount of *Enterococcus* species, coagulase-negative *Staphylococcus* spp., coryneform bacteria, α-hemolytic *Streptococcus* spp., *Geotrichium* species, *Prevotella bivia* and *Prevotella intermedia*. Both organs were culturally negative for *Listeria monocytogenes* under cold enrichment.

PCR of the liver was negative for human hepatitis virus A, B, C, and *Francisella tularensis*.

Immunohistology of the liver was positive for *Entamoeba histolytica* and negative for *Toxoplasma gondii*, *Coxiella burnetti* and *Listeria monocytogenes*.

Histopathologic Description: Liver: There are randomly arranged, multifocal to coalescing, irregular to round, pale eosinophilic, hypocellular areas surrounded by a poorly demarcated hypercellular rim. The centrally located pale eosinophilic, floccular mass with an irregularly distributed scant amount of karyorrhectic debris gradually changes into a peripheral zone of dissociated hepatic cells with pale, irregularly vacuolated cytoplasm, loss of cellular detail, ruptured outer membranes, and karyorrhexis and karyolysis. This area is surrounded by a zone composed of an inner layer of macrophages, epithelioid macrophages and few neutrophilic granulocytes, gradually changing into an outer layer consisting of macrophages, lymphocytes, plasma cells and fibroblasts embedded in an extracellular matrix exhibiting a moderate to high amount of collagen fibres that irregularly extends into the neighbouring hepatic tissue. Within the center of the lesions there is a moderate amount of multifocal, oval, indistinct, unicellular structures of approximately 20-30 µm diameter with clear borders, abundant finely vacuolated, lightly eosinophilic cytoplasm, and a single, eccentrically located, small, round, pale amphophilic nucleus (interpreted as protozoan trophozoites). These protozoal organisms are labelled brightly red in periodic-acid-Schiff (PAS)-stained sections. The surrounding hepatic tissue displays a mild to moderately increased amount of periportal fibroblasts and collagen fibre-rich extracellular matrix (periportal fibrosis), a mildly increased amount of periportal bile ducts, and moderately increased amount of intravascular and intrasinusoidal erythrocytes (congestion).

Contributor's Morphologic Diagnosis: Liver: Hepatitis, granulomatous and necrotizing, multifocal to coalescing, chronic, severe with intralesional protozoal trophozoites consistent with *Entamoeba histolytica*.

Contributor's Comment: *Entamoeba (E.) histolytica* is a protozoan parasite belonging to the phylum Sarcomastigophora, subphylum Sarcodina (Rhizopoda), order Amoebida, family Entamoebidae, genus *Entamoeba*. It is the etiologic agent of human amoebiasis, with an incidence of up to 50 million clinical cases per year, including up to 100,000 fatalities.[13,19,21,23] *Entamoeba histolytica* is distributed worldwide among human beings, but is also reported to occur in a wide range of New and Old World monkeys.[5,13,20] It is rarely found in domestic animals, including dogs, cats, cattle and captive macropods.[2,14,15,20] Furthermore, guinea pigs and hamsters are susceptible to experimental infection.[2,3,17] In addition to *E. histolytica*, multiple non-pathogenic species of the genus *Entamoeba*, including *E. dispar* and *E. moshkovskii*, are frequently detected in faeces and the intestinal tract of humans and non-human primates.[13,16,20] The only other pathogenic species of the genus *Entamoeba* is *E. invadens*, which occurs in reptiles.[6] Notably, it is impossible to differentiate the cysts of the highly related species *E. histolytica, E. dispar*, and *E. moshkovskii* by light microscopic investigation of fecal smears.[13,16,19,21,23] However, morphological differences, including a slightly larger size of *E. histolytica* trophozoites (20-30 µm) as compared to *E. dispar* trophozoites (12-15 µm), have been described. Furthermore, only *E. histolytica* is erythrophagocytic and invasive and therefore can be detected within tissues upon histological examination.[19] In histological sections, *E. histolytica* trophozoites exhibit a granular and lightly stained cytoplasm and a round nucleus with chromatin plaques at the periphery and a small endosome.[6]

Infection with *E. histolytica* occurs via the fecal–oral route. In human patients, excystation takes place in the large intestine. The trophozoites are usually commensals within the intestinal lumen, reproducing by binary fission and encysting as they move further down the digestive tract. Cysts are shed for many months to years in untreated humans. The cysts remain infective for weeks to months in a moist environment.[13,19] A complete intra-intestinal life cycle,

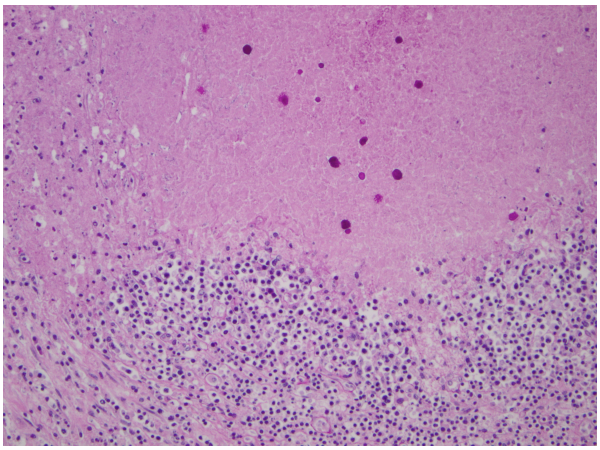

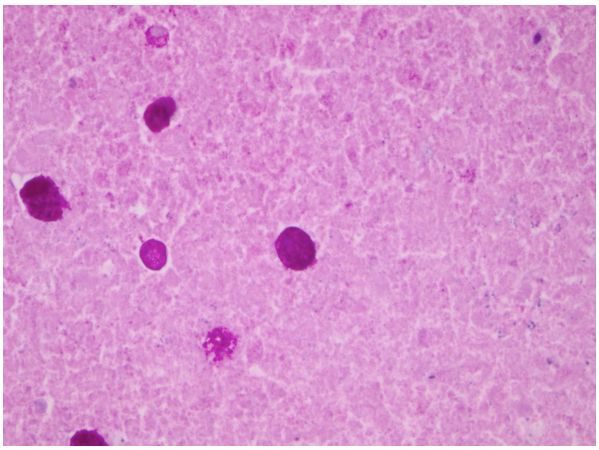

1-2, 1-3. Liver, guereza monkey. There are multifocal to coalescing, randomly arranged, irregular to round, pale eosinophilic, necrotic areas surrounded by a poorly demarcated, hypercellular rim. Within the center of the lesion are few PAS positive oval, indistinct unicellular structures of approximately 20-30 µm in diameter. Photographs courtesy of Department of Pathology, University of Veterinary Medicine, Hannover, Germany, peter.wohlsein@tiho-hannover.de

including cyst formation, is only reported to occur in humans and non-human primates; therefore, the zoonotic potential of infected non-primate mammals is thought to be limited.[18]

Pathogenicity of *E. histolytica* is affected by the strain of organism, host species infected, nutritional status, environmental factors and bacterial flora of the gastrointestinal tract.[20] Only in cases of mucosal invasion, which happens in less than 10% of human patients, does *E. histolytica* become pathogenic and lead to amoebic dysentery.[13,19] Clinical signs in affected monkeys include apathy, lethargy, weakness, dehydration, gradual weight loss, anorexia, vomiting, and severe diarrhea, which may be catarrhalic or hemorrhagic.[20] Amoebiasis commonly presents as necrotizing colitis in humans and many non-human primates.[5,13,19,20] However, fibrino-necrotizing gastritis seems to be the principal lesion in certain species of leaf-eating monkeys of the subfamily colobinae [old world monkeys (Cercopithecoidea), family cercopithecidae], including colobus monkeys (*Colobus guereza*), silvered leaf monkeys (*Presbytis cristatus*), dusky leaf monkeys (*Presbytis obscurus*), and proboscic monkeys (*Nasalis larvatus*).[4,8-11] The stomach of the colobinae is divided into four parts: presaccular, saccular, tubular, and pyloric portion, with the first two portions serving as enlarged fermentation chambers as a special adaption to the leaf-eating lifestyle. It is suggested that the normal neutral pH within these gastric compartments provides a favourable environment for excystation of ingested *E. histolytica* cysts, followed by tissue invasion.[4,8] Invasive trophozoites are regularly detected within the ulcerative gastric lesions.[4,8-11] In rare cases, and independently of whether the primary lesion is in the stomach or in the colon, some trophozoites are thought to enter the vessels of the mesenteric vasculature, thereby leading to metastatic foci of amoebic infection in distant parts of the body.[20] Fatal amoebiasis with abscess formation, particularly in the liver and more infrequently the lung and the central nervous system, is reported in man, baboons, chimpanzees, orang-utans, spider monkeys, douc langurs, and several colobus monkeys.[4,5,8,11,13,18-20] Amoebic hepatic lesions may become clinically obvious many years after the initial exposure and without concurrent intestinal lesions and fecal cyst shedding.[8,13,18] Similar to the presented case, most reported cases of amoebic hepatic lesions in non-human primates were characterized by a multifocal distribution and granulomatous and necrotizing lesions.[4,8,11,18] The central necrotic areas of the lesions are thought to represent foci of caseous necrosis due to the action of lytic substances produced by the trophozoites.[8] In human patients, however, the liver lesions are mainly situated in the right liver lobe and consist of a single abscess in most patients (65-75%).[13]

The differential diagnosis of granulomatous and necrotizing hepatic lesions in primates includes yersiniosis, salmonellosis, listeriosis, tularemia, tuberculosis, necrobacillosis, Q-fever, histoplasmosis, yellow fever, infections with lymphocytic choriomeningitis virus (callitrichid hepatitis), human hepatitis B virus, herpesvirus simiae (herpesvirus B), herpesvirus saimiri, simian varicella virus, herpesvirus tamarinus, herpes simplex virus, cytomegalovirus, ebola virus, toxoplasmosis, *Capillaria hepatica*, and schistosomiasis. Non-human primates are possible reservoir hosts of human hepatitis A virus; however, they display only slight hepatocellular degeneration, necrosis and inflammation and are most likely clinically asymptomatic. Furthermore, chimpanzees have been experimentally infected with the human hepatitis C virus; however, spontaneous infections of non-human primates have not been reported.[1] Due to the zoonotic potential of most of these diseases, increased personal protection and a thorough etiologic work-up is suggested in cases of hepatitis in non-human primates.

AFIP Diagnosis: Liver: Hepatitis, random, necrotizing and granulomatous, multifocal to coalescing, severe, with amoebic trophozoites.

Conference Comment: Conference participants discussed the virulence factors in *Entamoeba histolytica* infection. The first of three virulence factors is a multifunctional lectin (Gal/GalNAc lectin); in addition to binding to glycoprotein residues of the target cell, it also plays a role in cytolysis, invasion, resistance to complement and possibly the process of encystation. The second virulence factor is the amoebapore, a channel-forming protein analogous to T-cell perforins and NK-lysin from Natural Killer (NK) cells; once the channel is inserted into the host cell membrane, extracellular water and ions rush into the cell causing cell lysis. The final virulence factor is a family of cysteine proteases produced by *E. histolytica*. These proteins function to break down the extracellular matrix, facilitating invasion. Not only does this aid organism invasion, the breakdown of the extracellular matrix also results in loss of cellular adhesion, possibly contributing to further cellular death.[12]

These virulence factors must enable *E. histolytica* to overcome a variety of innate host defenses. The first and most extensive host barrier is the layer of mucin extending from the oral cavity to the rectum. The glycoproteins found in host mucin competitively bind to residues used in amoebic attachment; resident intestinal bacteria also bind to mucin, further reducing available binding sites to the protozoan. The complement system plays a role in the innate immune response to *E. histolytica*. The neutral cysteine proteinase elaborated by the parasite has been shown to activate complement via the classical and alternative pathways, thus activating the immune response. However, the Gal/GalNAc lectin possessed by the organism binds C8 and C9, thus preventing formation of the membrane attack complex.[12]

In addition to lectin-mediated evasion of the complement system, *E. histolytica* has several methods by which it evades the host immune system. The cysteine proteinases and hydrolytic enzymes not only degrade extracellular matrix proteins, they also degrade IgA and IgG antibodies, thereby facilitating initial invasion of the intestinal epithelium as well as aiding in systemic dissemination.[12] When immune complexes bind to the amoeba, a unique process of capping

takes place whereby the bound antibodies are quickly moved to the posterior pole of the organism, the cap is "released" and the plasma membrane is regenerated;[7] thus, immune complexes are essentially shed from the protozoal cell surface. *E. histolytica* is also able to alter the host acute-phase immune response, primarily via an unknown mechanism of T-cell-modulated macrophage function, especially Th1.[12] The amoeba also produce monocyte locomotion-inhibitory factor which inhibits the respiratory burst in macrophages. Research also has demonstrated the presence of surface perioxiredoxin which neutralizes host-generated reactive oxygen species and nitric oxide.[7] Serine proteases secreted by *E. histolytica* bind to cathepsin G secreted by neutrophils, and protozoal arginase consumes host L-arginine, a precursor for the nitric oxide production by host macrophages.[7]

Contributor: Department of Pathology, University of Veterinary Medicine Hannover, Bünteweg 17, D-30559 Hannover, Germany.
http://www.tiho-hannover.de/einricht/patho/index.htm

References:

1. Brady AG, Morton DG. Digestive system, V. Liver. In: Bennett B, Henrickson R eds. *NonhumanPrimates in Biomedical Research*. San Diego, CA: Academic Press; 1998:401-406.
2. Brown CC, Baker DC, Barker IK. Alimentary system. In: Maxie MG, ed. *Jubb, Kennedy and Palmer's Pathology of Domestic Animals*. 5th ed., Vol. 2. Philadelphia, PA: Elsevier Ltd; 2007:3-296.
3. Crisostomo-Vazquez M del P, Jimenez-Cardoso E, Arroyave-Hernandez C. *Entamoeba histolytica* sequences and their relationship with experimental liver abscesses in hamsters. *Parasitol Res*. 2006;98:94-98.
4. Frank H. Pathology of amoebiasis in leaf monkeys (colobidae). Proceedings 24th Int Symp Dis Zoo Anim 1982:321-326.
5. Fremming BD, Vogel FS, Benson RE, Young RJ. A fatal case of amebiasis with liver abscesses and ulcerative colitis in a chimpanzee. *J Am Vet Med Assoc*. 1955;126:406-407.
6. Gardiner CH, Fayer R, Dubey JP. Amoebae. In: Gardiner C, Dubey JP, eds. *An Atlas of Protozoan Parasites in Animal Tissues*. 2nd ed. Washington, DC: Armed Forces Institute of Pathology; 1998.
7. Lejune M, Rybicka J, Chadee K. Recent discoveries in the pathogenesis and immune response toward *Entamoeba histolytica*. *Future Microbiol*. 2009;4:105-118.
8. Loomis MR, Britt JO, Gendron AP, Holshuh HJ. Hepatic and gastric amebiasis in black and white colobus monkeys. *J Am Vet Med Assoc*. 1983;183:1188-1191.
9. Muller R, Ruedi D. Gastric amebiasis in a proboscic monkey (*Nasalis larvatus*). *Acta Zoolog Pathol Antverpiensia*. 1981;76:9-16.
10. Palmieri PR, Dalgard DW, Connor DH. Gastric amebiasis in a silvered leaf monkey. *J Am Vet Med Assoc*. 1984;185:1374-1375.
11. Pang VF, Chang CC, Chang WF. Concurrent gastric and hepatic amebiasis in a dusky leaf monkey (*Presbytis obscurus*). *J Zoo Wildl Med*. 1993;24:204-207.
12. Petri, WA Jr. Intestinal invasion by *Entamoeba histolytica*. *Subcell Biochem*. 2008;47:221-232.
13. Pritt BS, Clark CG. Amebiasis. *Mayo Clin Proc*. 2008;83:1154-1160.
14. Shimada A, Muraki Y, Awakura T, et al. Necrotic colitis associated with *Entamoeba histolytica* infection in a cat. *J Comp Pathol*. 1992;106:195-199.
15. Stedman NL, Munday JS, Esbeck R, Visvesvara GS. Gastric amebiasis due to *Entamoeba histolytica* in a Dama wallaby (*Macropus eugenii*). *Vet Pathol*. 2003;40:340-342.
16. Takano J, Narita T, Tachibana H, et al. *Entamoeba histolytica* and *Entamoeba dispar* infections in cynomolgus monkeys imported into Japan for research. *Parasitol Res*. 2005;97:255-257.
17. Takeuchi A, Jervis HR, Phillips BP. Electron-microscope studies of experimental *Entamoeba histolytica* infection in guinea pig. 3. Histolysis of cecum. *Virchow's Archiv B-Cell Pathology Including Molecular Pathology*. 1977;24:263-277.
18. Tammer R, Mätz-Rensing K, Rolle S, Kaup FJ. A case of hepatic amebiasis in a colobus guereza monkey. *Primate Rep*. 2002;63:21-26.
19. Tannich E. The laboratory diagnosis of *Entamoeba histolytica* infections. *J Lab Med*. 2004;28:491-497.
20. Toft JD, Eberhard ML. Protozoan parasites, B. Sarcodines: Amoeba. In: Bennett BT, Henrickson R, eds. *Nonhuman Primates in Biomedical Research*. San Diego, CA: Academic Press; 1998:116-119.
21. Walsh JA. Problems in recognition and diagnosis of amebiasis - estimation of the global magnitude of morbidity and mortality. *Rev Inf Dis*. 1986;8:228-238.
22. Wittnich C. *Entamoeba histolytica* infection in a German shepherd dog. *Can Vet J*. 1976;17:259-263.
23. World Health Organization: Amoebiasis. *Weekly Epidemiological Record* 1997;72:97-99.

CASE II: 2/10 (AFIP 3165171).

Signalment: 4-year-old female Holstein-Friesian cow (*Bos taurus*).

History: The affected animal belonged to a herd of 122 milking cows with a mean daily milk production of 23 liters. The herd experienced a sudden increase in the incidence of acute clinical mastitis, mainly after parturition. Clinically the outbreak was characterized by drastic decrease in milk production and diminished milk quality with most of the affected cows exhibiting a somatic cell count (SCC) > 1,000,000. Over a period of two months, approximately 20 cows were culled because of the sustained unresponsiveness to antibiotic therapy. No cases of pneumonia or arthritis were noted in association with the episodes of mastitis. Bacteriology performed on milk samples from several of the affected cows yielded the isolation of *Mycoplasma bovis*.

Gross Pathology: Grossly the mammary gland was severely reduced in size and increased in consistency at palpation. The parenchyma was disrupted by multiple small coalescing nodules. The scant material that could be drawn from the most severely affected quarter consisted of very thick yellowish exudate. On cut surface the normal mammary parenchyma was completely obliterated by thick bands of fibrotic tissues. Embedded within the fibrotic reaction were segmentally distended mammary ducts, and recesses of the cysterna were filled and replaced by dense purulent-like yellowish material.

Laboratory Results: Swabs from the affected portions of mammary gland were cultured using routine bacteriological procedures on BHI-agar and MacConkey-agar in a normal atmosphere and on blood agar in a microaerophilic atmosphere. Swabs were cultured also for *Mycoplasma* spp. directly on pleuropneumonia-like organism (PPLO) agar plates. Bacterial culture yielded a massive growth of *Mycoplasma* spp. colonies characterized by the typical "fried-egg" morphology. No other bacterial organisms were identified. The isolates of *Mycoplasma* spp. were confirmed to be *M. bovis* through specific PCR amplification.

Immunohistochemically, abundant *M. bovis* antigen was detected in the cytoplasm of degenerate neutrophils and foamy reactive macrophages or admixed with the necrotic debris. Necrosuppurative foci were surrounded by severe fibrosis with marked infiltration of degenerated neutrophils, CD3-positive T-cells, CD79α-positive B-cells, and CD68-positive histiocytes.

Histopathologic Description: Mammary gland: Multifocal to coalescing inflammatory lesions affect and partially efface 40% of the mammary gland parenchyma. Inflammatory foci are mainly located in the lumen of ducts with complete loss of epithelial lining (necrosis). Inflammatory foci have a multilayered appearance and are characterized by a central area of colliquative necrosis bordered by elevated numbers

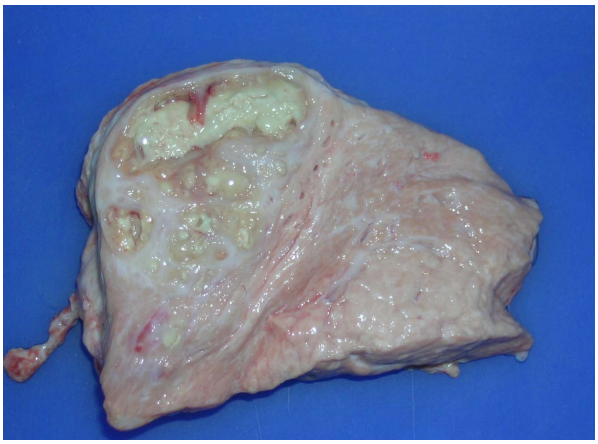

2-1. Mammary gland, cow. The mammary gland contains multiple small coalescing nodules. On cut section, normal mammary gland is obliterated by thick bands of fibrotic tissue. Embedded within the fibrotic reaction are segmentally distended mammary ducts and cysterna that are filled with dense purulent yellow material. Photograph courtesy of Dipartimento di Patologia Animale, Igiene e Sanita' Pubblica, Sezione Anatomia Patologica Aviare, Facolta' di Medicina Veterinaria, Via Celoria 10, 20133 Milano, Italy; paola.roccabianca@unimi.it

of karyorrhectic neutrophils, a more peripheral layer of inflammation composed of numerous lymphocytes and plasma cells intermixed with fewer foamy reactive macrophages, and an external fibrous capsule. The less affected lobules are characterized by a moderate number of lymphocytes and plasma cells and fewer eosinophils expanding the interstitium.

Alveoli are multifocally lined by 2-3 layers of epithelial cells (moderate hyperplasia) and occasionally contain lipid vacuoles. The interlobular septa are expanded by a moderate amount of fibrous connective tissue. In some sections moderate to severe atrophy of alveoli secondary to severe interstitial fibrosis is evident.

Contributor's Morphologic Diagnosis: Mammary gland: Severe, multifocal to coalescing, chronic, necrotizing and pyogranulomatous mastitis with diffuse and moderate fibrosis and atrophy.

Contributor's Comment: *Mycoplasma bovis* infection is associated with a variety of bovine clinical diseases including bronchopneumonia, mastitis, polyarthritis, tenosynovitis, otitis media, myocarditis, meningoencephalitis and reproductive disorders. An increasing number of epidemiological and clinicopathological data underline that *M. bovis* is emerging worldwide as one of the most pathogenic organisms involved in bovine bronchopneumonia. Especially in beef cattle, *M. bovis* infection has been associated with the so-called chronic pneumonia-polyarthritis syndrome (CPPS) and bovine respiratory disease (BRD) complex.[8]

Besides its major role as a respiratory pathogen and as a causative organism of polyarthritis in beef cattle, *M. bovis* is also considered an important agent of mastitis in dairy cows.

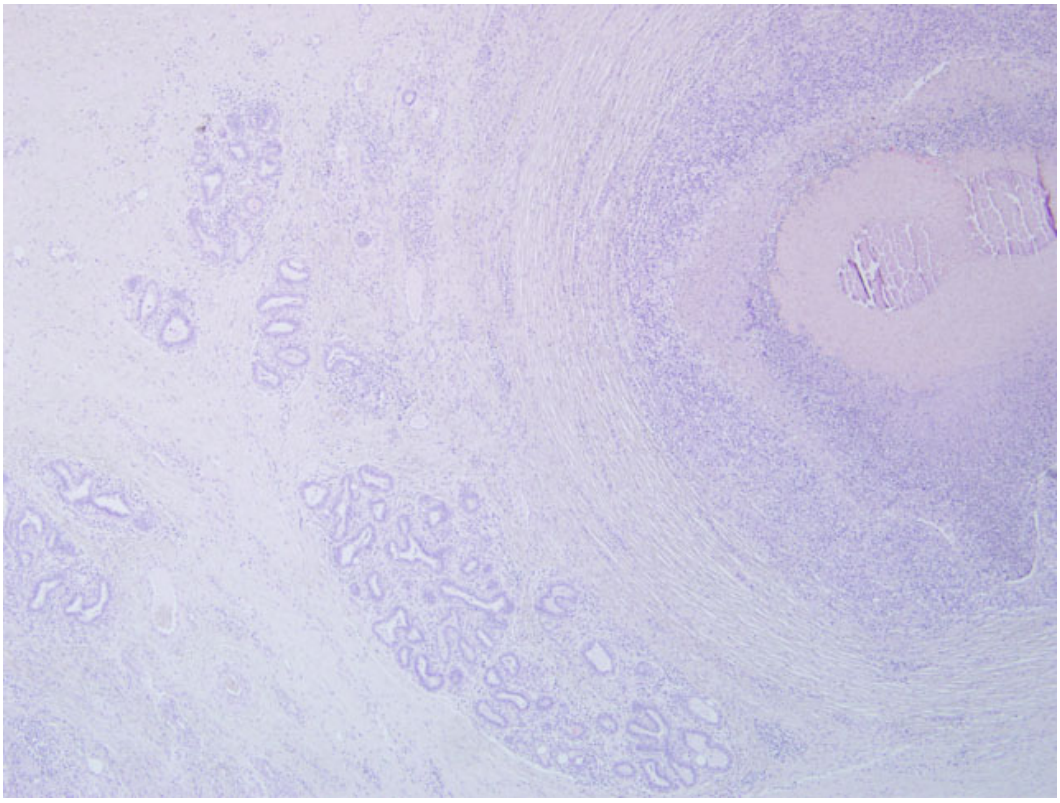

2-2. Mammary gland, cow. Multifocal to coalescing areas of inflammation and fibrosis replace glands and ducts, with adjacent large areas of lytic necrosis. (HE 40X)

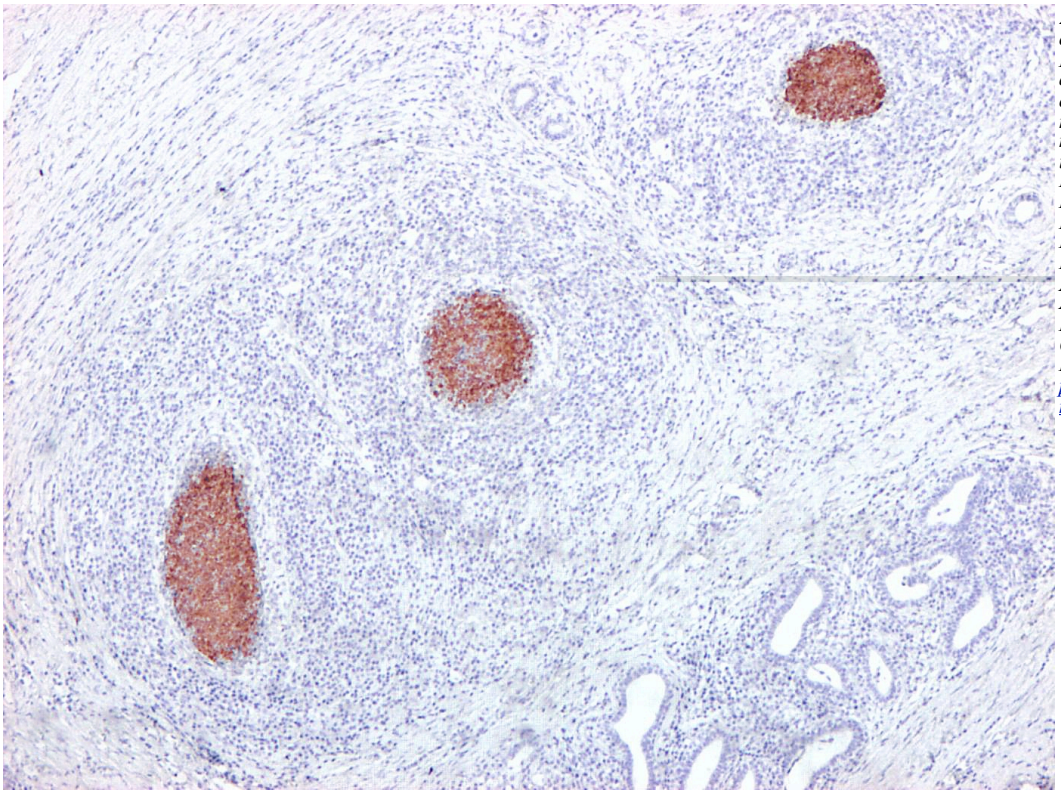

2-3. Mammary gland, cow. Abundant Mycobacterium bovis antigen is detected in the cytoplasm of degenerate neutrophils, foamy macrophages, or within the necrotic debris. Photograph courtesy of Dipartimento di Patologia Animale, Igiene e Sanita' Pubblica, Sezione Anatomia Patologica Aviare, Facolta' di Medicina Veterinaria, Via Celoria 10, 20133 Milano, Italy, paola.roccabianca@unimi.it

Mastitis caused by *M. bovis* has been estimated to cost the U.S. dairy industry over USD $100 million annually, with infection rates of up to 70% in some herds, which is even greater than the losses resulting from mycoplasmal pneumonia.[9] Over recent years, with the replacement of classical bacteriological techniques and the development of more reliable and accurate PCR and ELISA-based diagnostic tests for the identification of mycoplasmas, *M. bovis* is being increasingly recognized as a primary agent of mastitis also in Europe.[1] The substantial economic losses caused by *M. bovis* derive from the development of a chronic progressive mastitis with decreased milk production and lower milk quality. Because no efficacious antibiotics or vaccines have been approved for the treatment or prevention of *M. bovis* mastitis, culling is recommended for controlling the disease, even if this drastic measure of control results in considerable animal replacement costs.[10]

Epidemiological and pathogenetic mechanisms responsible for *M. bovis*-induced mastitis are far from being fully elucidated. Ascending and hematogenous routes of infection are both implicated in the development of disease. Fomites, such as contaminated milking equipment or solutions used for intramammary infusion, represent the most documented routes of *M. bovis* transmission among dairy cows. The existence of environmental sources for *M. bovis* and their role in transmission and clinical disease are poorly characterized, although recent investigations pointed out the role of recycled bedding sand as a potential source of *M. bovis*.[6] Secondary colonization of the mammary glands starting from primary foci of bronchopneumonia and polyarthritis or during septicemia has been also postulated as a likely event leading to mastitis. The contrary is also true where the mammary gland acts as a primary focus of infection followed by septicaemia and polyarthritis. Vertical transmission of *M. bovis* with congenital mammary gland infection in prepubertal heifers has been also hypothesized in a recent investigation. In dairy herds, direct galactogenic transmission of *M. bovis* infection from cows with mastitis represents one of the main causes of bronchopneumonia, otitis media and polyarthritis in suckling calves.[4,14]

M. bovis infection of the mammary gland elicits a persistent inflammatory response characterized by the up-regulation of several proinflammatory cytokines and chemokines, complement activation, massive local recruitment of neutrophils and eosinophils and drastic increase in vascular permeability. Despite the sustained inflammation mounted by the host in response to *M. bovis*, several lines of evidence suggest that this reaction is not sufficient to eradicate the pathogen from the mammary gland, and infection usually persists over multiple lactations.[2,7] A similar situation has been also observed in the context of respiratory infections where the ability of *M. bovis* to establish persistent infections characterized by chronic progressive bronchopneumonic lesions may result from an inadequate and ineffective Th-2-polarized immune response.[13]

Although not pathognomonic for *M. bovis* mastitis, the combination of the following clinical features in lactating cows should prompt the suspicion of mycoplasmal infection:

a. drastic rise in bulk and individual milk somatic cell counts;
b. sudden onset of agalactia, with firm swollen and painless quarters;
c. rapid separation of the milk drawn from affected quarters in a floccular precipitate and a watery supernatant;
d. rapid spread of the infection from quarter to quarter;
e. rapid spread of the infection from cow to cow within the affected herds;
f. unresponsiveness to antibiotic therapy;
g. decreased milk production with marked atrophy of affected quarters in clinically recovered cows.

Clinical signs of systemic involvement are generally rare although enlargement of supramammary lymph nodes, fever, anorexia, and concurrent polyarthritis have been reported in several outbreaks.[5,12]

Based on the few and inconsistent data reported in the current literature, the pathology of *M. bovis* mastitis generally consists of an early phase dominated by massive infiltration and/or exudation of granulocytes (both neutrophils and eosinophils) in the edematous lobular interstitium, in the wall of cistern and within the acinoductal luminal compartment. The acute phase is soon followed by chronic progressive changes mainly characterized by proliferation of the affected ductuloalveolar epithelium and gradual interstitial fibrosis accompanied by infiltration of lymphocytes, macrophages and plasma cells. Epithelial erosion/ulceration in the larger ducts and cisterns may lead to the formation of polypoid proliferations of granulation tissue protruding into and occluding the luminal compartment. The chronic phase progresses to an end stage condition where fibrosis and fibroplasia prevail on the acinoductal epithelial hyperplasia with intense atrophy and scarring of the affected parenchyma.

The few morphological studies reported so far in the literature appear largely inadequate to address the entire spectrum of pathological manifestations associated with *M. bovis* infection of the mammary gland. The unusual case of *M. bovis* mastitis provided best illustrates this concept. In contrast to the pathological features previously described for *M. bovis* mastitis, the lesional picture in this case is characterized by severe chronic necrosuppurative and fibrosing galactophoritis consisting of segmental ectasia of affected mammary ducts with collection of necrotic debris and degenerated neutrophils, formation of multinodular coalescing abscesses/pyogranulomas and intranecrotic foci of dystrophic mineralization. Interestingly, foci of necrosuppurative galactophoritis described share many pathological features with the characteristic *M. bovis*-

associated bronchocentric lesions frequently observed in the lungs of beef cattle. These peculiar inflammatory changes possibly reflect a common pathogenesis for lesions originating both from bronchi/bronchioli and mammary ducts.

Gross and microscopic findings similar to those described in our case could be elicited also by other common causes of bovine galactophoritis, including *Mycobacterium bovis*, *Nocardia asteroides*, *Arcanobacterium pyogenes*, *Prototheca zopfii*, and *Cryptococcus neoformans*. However, as confirmed by bacteriological examination, *Mycoplasma bovis* represented the sole bacterial pathogen implicated in our case. Furthermore, specific histochemical stains (Ziehl-Neelsen, PAS and Gram stains) were also applied to rule out other possible agents of bovine galactophoritis. Other less frequent causes of mycoplasmal mastitis in dairy cows include *Mycoplasma californicum, Mycoplasma bovigenitalium* and *Mycoplasma canadense.*

AFIP Diagnosis: Mammary gland: Mastitis, pyogranulomatous, multifocal to coalescing, marked, with fibrosis and glandular atrophy and loss.

Conference Comment: The contributor provides an excellent review of *Mycoplasma bovis*. Based on the chronicity of the lesion, many conference participants favored other etiologies, including *Mycobacterium bovis*; pyogenic bacteria, such as *Arcanobacterium pyogenes*; or higher order bacteria, such as *Nocardia asteroides*. Conference attendees noted that necrotizing lesions typically associated with *Staphylococcus aureus* or *Escherichia coli* were not observed; this stimulated a discussion on the various methods by which to classify pathogens of the mammary gland.

Bacterial pathogens of the mammary gland can be grouped by any one of a variety of criteria. McGavin and Zachary's *Pathologic Basis of Veterinary Disease* suggests dividing the organisms into two groups based on the source of infection to other cows. First are those in which the mammary gland itself serves as the primary source of infection, such as *S. aureus*, *Streptococcus agalactiae*, and *Mycoplasma* species, and cow-to-cow transmission occurs. Second are the coliform organisms, which are acquired from the environment; infection occurs through teat contact with contaminated material or equipment. Finally, *Streptococcus uberis* and *Streptococcus dysgalactiae* form an overlapping group in which the mammary gland and environmental contamination serve as important sources of infection. This type of epidemiologic classification system provides valuable information for the producer and veterinarian regarding disease prevention and treatment.[3]

From a pathologic and pathogenesis perspective, categorizing bacterial mastitis according to the type of lesion produced is helpful in determining an underlying etiology. Gram-negative bacilli produce such lesions as vasculitis, necrosis, hemorrhage and edema, leading to endotoxemia. Gram-positive bacteria typically result in acute necrotizing mastitis or chronic suppurative mastitis. With acute necrotizing mastitis, Gram-positive bacteria, such as *S. aureus*, secrete bacterial products which elicit a massive neutrophilic response that contributes to extensive necrosis which progresses to gangrenous mastitis. In contrast, in chronic suppurative mastitis the pus-forming Gram-positive bacteria, such as *Streptococcus dysgalactiae,* and *Arcanobacterium pyogenes*, invoke a neutrophilic response resulting in suppuration and fibrosis, which is often centered on lactiferous ducts and sinuses; *Mycoplasma bovis* elicits a similar histologic lesion.[3]

	Portion(s) affected	Gross appearance	Histologic appearance	Spread
Disseminated miliary form	Interacinar areas	1. Caseous nodules 2. Thick fibrous capsule 3. ± mineralization	1. Replacement of lobules by tubercle 2. Interlobular duct lumena expanded by cellular exudate 3. Tubercles in supramammary lymph nodes	Remain localized in affected lobule(s)
Chronic organ form	Entire lobule Intra- and inter-lobular ducts	1. Grey-red to white 2. Bulge on cut surface 3. Smoothly bumpy with a dry appearance	1. Retention of lobular outlines with sparing of interlobular septa 2. Acini obliterated by tuberculous granulation tissue 3. Intra- and inter-lobular duct walls expanded by granulation tissue	Intramammary spread via ducts; no lymph node involvement
Caseous tuberculous form	Entire gland	1. Gland markedly enlarged by irregular caseous areas 2. Hyperemic margin 3. ± areas of chronic organ tuberculosis	1. Fibrin and leukocyte exudation 2. Surrounded by hyperemic granulation tissue 3. ± hemorrhage	Readily spreads to unaffected areas; no lymph node involvement

Because many conference attendees considered tuberculous mycobacteria high on the differential diagnosis, a brief outline of the pathologic features of bovine mycobacterial mastitis is provided in the chart on the preceeding page.[11]

Contributor: Dipartimento di Patologia Animale, Igiene e Sanita' Pubblica Veterinaria, Sezione di Anatomia Patologica e Patologia Aviare, Facolta' di Medicina Veterinaria, Milano, Italy
http://www.anapatvet.unimi.it/

References:

1. Ball HJ, Nicholas RA. *Mycoplasma bovis*-associated disease: here, there and everywhere. *Vet J*. 2010; 186(3): 280-281.
2. Byrne W, Markey B, McCormack R, Egan J, Ball H, Sachse K. Persistence of *Mycoplasma bovis* infection in the mammary glands of lactating cows inoculated experimentally. *Vet Rec*. 2005;156:767-771.
3. Foster RA. Female reproductive system. In: McGavin MD, Zachary JF, eds. *Pathologic Basis of Veterinary Disease*. 4th ed. St. Louis, MO: Elsevier; 2007:1308-1314.
4. Fox LK, Muller FJ, Wedam ML, Schneider CS, Biddle MK. Clinical *Mycoplasma bovis* mastitis in prepubertal heifers on 2 dairy herds. *Can Vet J*. 2008;49:1110-1112.
5. Houlihan MG, Veenstra B, Christian MK, Nicholas R, Ayling R. Mastitis and arthritis in two dairy herds caused by *Mycoplasma bovis*. *Vet Rec*. 2007;160:126-127.
6. Justice-Allen A, Trujillo J, Corbett R, Harding R, Goodell G, Wilson D. Survival and replication of *Mycoplasma* species in recycled bedding sand and association with mastitis on dairy farms in Utah. *J Dairy Sci*. 2010;93:192-202.
7. Kauf AC, Rosenbusch RF, Paape MJ, Bannerman DD. Innate immune response to intramammary *Mycoplasma bovis* infection. *J Dairy Sci*. 2007;90:3336-3348.
8. Krysak DE. Chronic pneumonia and polyarthritis syndrome in a feedlot calf. *Can Vet J*. 2006;47:1019-1020, 1022.
9. Nicholas R, Ayling R, McAuliffe L. Mycoplasma mastitis. *Vet Rec*. 2007;160:382-383.
10. Nicholas RA, Ayling RD. *Mycoplasma bovis*: disease, diagnosis, and control. *Res Vet Sci*. 2003;74:105-112.
11. Schlafer DH, Miller RB. Female genital system. In: Maxie MG, ed. *Jubb, Kennedy and Palmer's Pathology of Domestic Animals*. 5th ed., Vol. 3. Philadelphia, PA: Elsevier Ltd; 2007:558-560.
12. van der Burgt G, Main W, Ayling R. Bovine mastitis caused by *Mycoplasma bovis*. *Vet Rec*. 2008;163:666.
13. Vanden Bush TJ, Rosenbusch RF. Characterization of the immune response to *Mycoplasma bovis* lung infection. *Vet Immunol Immunopathol*. 2003;94:23-33.
14. Walz PH, Mullaney TP, Render JA, Walker RD, Mosser T, Baker JC. Otitis media in preweaned Holstein dairy calves in Michigan due to *Mycoplasma bovis*. *J Vet Diagn Invest*. 1997;9:250-254.

CASE III: NEPRC CASE 1 (AFIP 3163068).

Signalment: 5-year-old male intact rhesus macaque (*Macaca mulatta*).

History: This macaque was inoculated with SIVmac239 and had undergone routine phlebotomies. More than a year after inoculation, the animal developed diarrhea, dehydration, and marked weight loss. A weight loss of 2.1 kg (from 8 to 5.9 kg) was recorded over a one month period.

Gross Pathology: The body of this five-year-old, SIV239-infected, male macaque had minimal amounts of body fat. The lymph nodes were enlarged, and the spleen was irregular in shape with mild follicular hyperplasia. No other significant gross lesions were present.

Laboratory Results: Immunohistochemistry (IHC) of liver and pancreas for adenovirus was positive.

Histopathologic Description: Pancreas: Replacing approximately 90% of exocrine pancreatic tissue, sparing only the main pancreatic duct, are multifocal to coalescing areas of necrosis composed of degenerate epithelial cells that are admixed by deposits of fibrin, cellular debris, and fibrosis that often encircle remnant islets of Langerhans. These areas of necrosis are characterized by large numbers of degenerate epithelial cells that have vacuolated cytoplasm and nuclear pyknosis. Scattered acinar cells bordering the regions of necrosis contain prominent, 6-10 µm magenta, round, intranuclear inclusion bodies. Similar inclusion bodies are rarely noted within the ductular epithelium, almost exclusively in small degenerate epithelial cells that are partially exfoliated into the ductular lumen. There is scattered hyperplasia of the remnant exocrine epithelial cells characterized by moderate anisocytosis and scattered mitotic figures. The fibrosis is loosely organized in many areas and is often interspersed with moderate to abundant numbers of lymphocytes and plasma cells with fewer macrophages and degenerate neutrophils. There are scattered hemosiderin-laden macrophages throughout the pancreas. In the peri-pancreatic fat and surrounding blood vessels within the adipose tissue there are small to moderate numbers of lymphocytes and plasma cells.

Immunohistochemistry for adenovirus: There are multifocal positive cells noted within the areas of necrosis and in the ductular epithelium. Immunoreactivity is strong and intranuclear. The isotype matched negative control revealed no immunoreactivity.

Contributor's Morphologic Diagnosis: Pancreas: Severe, multifocal to coalescing, chronic, necrotizing and fibrosing pancreatitis with intraepithelial intranuclear adenoviral inclusions.

Contributor's Comment: Rhesus adenovirus is a non-enveloped, hexagonal in outline with icosahedral symmetry, 80-100 nm in diameter, double-stranded DNA virus belonging to the Adenoviridae family and Mastadenovirus genus.[8,11] A sizeable number of simian adenoviruses (SAdVs) that infect Old World monkeys and chimpanzees have been characterized. Approximately 24 simian adenovirus prototypes are recognized and additional isolates are currently awaiting better characterization. The majority of simian adenoviruses have been isolated from *Macaca* spp., *Cercopithecus aethiops*, *Papio cynocephalus*, and *Saimiri sciureus*.[7] The viral genome consists of a single linear molecule of double-stranded DNA, 36 to 44 kbp in size. Viruses replicate in the nucleus and their replication is facilitated by extensive modulation of the host immune response. Virions are composed of 252 capsomers: 240 hexons that occupy the faces and edges of the 20 equilateral triangular facets of the icosahedrons and 12 pentons that occupy the vertices. From each penton projects a penton fiber 20 to 50 nm in length, with a terminal knob.[11] Roughly 40 proteins are coded for by the viral genome and are transcribed following a complex RNA splicing. The structural proteins make up the hexons, penton, penton fibers, and other associated virion structures.

Adenoviruses are capable of establishing chronic infections following an initial exposure that may or may not be clinically relevant.[13] All of the adenoviruses have narrow host ranges. Many cause acute respiratory or gastrointestinal disease but also may cause persistent infection with periods of latency that become reactivated upon immunosuppresion.[6] In dogs and other canids, canine adenovirus-1 causes infectious canine hepatitis that produces acute necrosis and inflammation in the liver often accompanied by grossly visible edema of the gallbladder.[4] Canine adenovirus-2 is one of the known causative agents of canine infectious tracheobronchitis, which is commonly referred as "kennel cough."[9] Canine adenovirus type 2 can cause pneumonia in dogs which is clinically mild unless complicated with secondary bacterial infections.[9] Acute rhinitis that is manifested as part of general respiratory disease can be caused by both adenovirus type 1 and 2.[9] Adenoviruses are pneumotropic and enterotropic in ruminants.[6,9] Equine adenovirus type 1 (EAdV1) causes upper respiratory tract disease, follicular conjunctivitis, bronchopneumonia, and infection of the gastrointestinal tract. EAdV1 is peculiarly associated as a dominant pathogen in the uniformly fatal, inherited disease syndrome known as primary severe combined immunodeficiency disease (PSCID). The foals are born devoid of B and T lymphocytes and a consistent and dominant feature of PSCID is an inexorably progressive EAdV1 bronchopneumonia.[14] Mice are host to two distinct adenoviruses: mouse adenovirus type 1 (MAV-1), causing hemorrhagic foci of necrosis in multiple organs and wasting disease (especially in nude and SCID mice); and mouse adenovirus type 2 (MAV-2), which is asymptomatic and does not exhibit clinical disease.[12]

In rhesus macaques, adenovirus infection is one of the most common opportunistic infections to accompany terminal

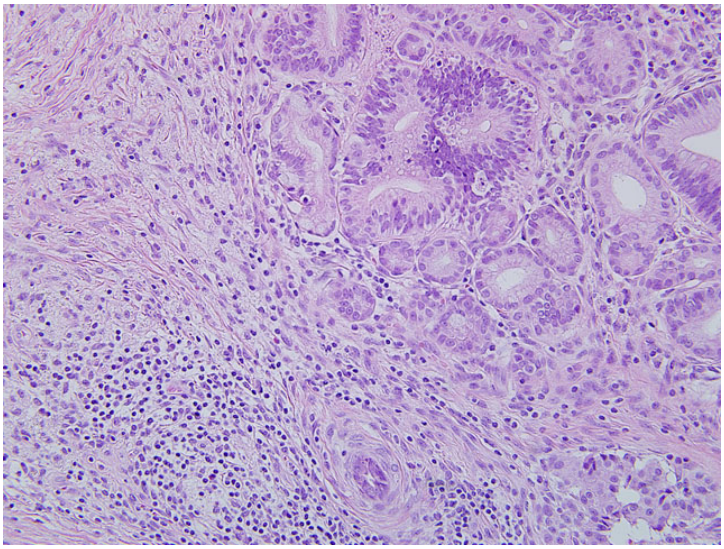

3-1. Pancreas, rhesus macaque. Surrounding pancreatic ducts is loosely arranged fibrosis admixed with moderate to abundant lymphocytes and plasma cells. (HE 200X)

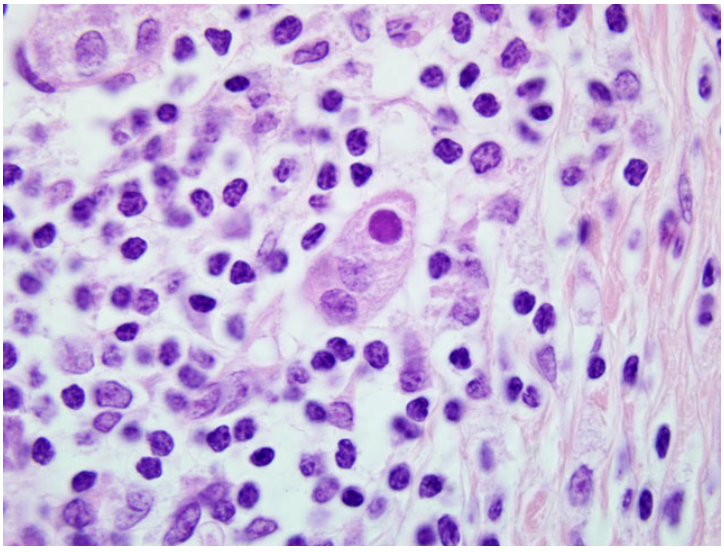

3-2. Pancreas, rhesus macaque. Within epithelial cells there are rare eosinophilic intranuclear inclusion bodies. (HE 1000X)

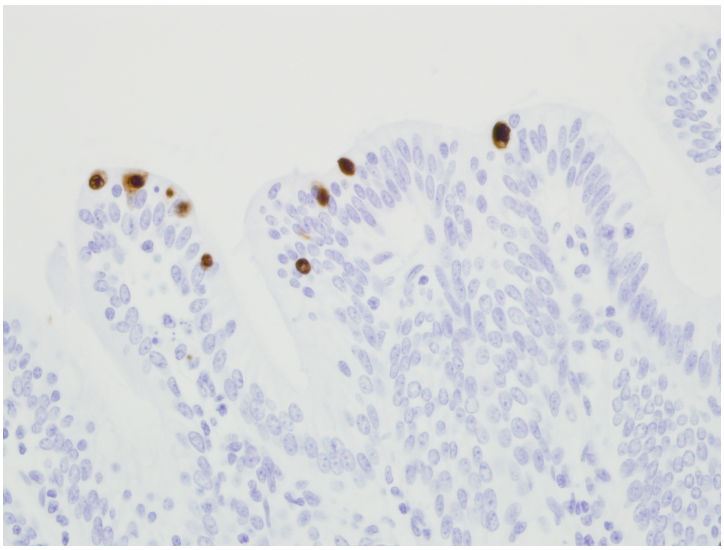

3-3. Pancreas, rhesus macaque. Pancreatic ductular epithelium shows multifocal strong nuclear immunopositivity. Photograph courtesy of New England Primate Research Center, Harvard Medical School, One Pine Hill Drive, Southborough, MA 01772, Andrew_Miller@hms.harvard.edu

cases of SIV infection. Adenoviral pancreatitis can also be seen in animals that are immunosuppressed for organ transplantation and in neonates. Adenovirus associated disease in rhesus macaques is most commonly found in the small and large intestine, the liver and gallbladder, and the pancreas. The pancreatic lesion is often fulminant with abundant necrosis making organ identification difficult. If the pancreatitis persists for long periods of time the marked epithelial hyperplasia and proliferation that occurs can be confused with a pre-neoplastic change.

Chronic pancreatitis is characterized by destruction of exocrine tissue and is typically accompanied by fibrosis, parenchymal atrophy, and in late stages with destruction of endocrine parenchyma.[3,4] Chronic pancreatitis may present as repeated bouts of acute pancreatitis, the major distinction being an irreversible impairment of pancreatic function with the former. Chronic inflammation of the pancreas with mostly lymphoplasmacytic infiltration is seen most commonly in the dog, but does occur in the cat, horse and cattle.[4]

The most frequently reported pancreatic disease in nonhuman primates is diabetes mellitus secondary to the deposition of islet amyloid polypeptide (amylin) in the Islets of Langerhans. In addition, pancreatitis and islet destruction in nonhuman primates can be induced by certain drug treatments, such as streptozotocin, and interference with the pancreatic duct and blood supply.[10] Prior to the discovery of SIV as a major immunocompromising pathogen in rhesus macaques, spontaneous pancreatitis was reported rarely in nonhuman primates, and at least two cases were reported in rhesus monkeys with adenoviral inclusions.[1,2,5,10] The spontaneous nature of these early reports of adenoviral pancreatitis is dubious, as it is highly likely that an as yet unrecognized pathogen likely caused immunosuppresion predisposing to adenoviral disease in these animals. In cases of pancreatitis in nonhuman primates, especially rhesus macaques, it is imperative to determine if adenovirus played a role and if the animal was immunocompromised.

AFIP Diagnosis: Pancreas: Pancreatitis, necrotizing, chronic, diffuse, severe, with fibrosis, exocrine acinar atrophy and loss; ductular hyperplasia; and rare epithelial intranuclear inclusion bodies.

Conference Comment: Some slide variation exists, with some sections containing areas of lytic necrosis and others characterized by extensive fibrosis with little discernible pancreatic tissue.

Participants discussed the relationship between the location of viral inclusion bodies within the cell and the properties of the viral genome. In general, DNA viruses tend to replicate in the nucleus and produce intranuclear inclusion bodies, *e.g.* herpesviruses, adenoviruses, parvoviruses, etc. One notable exception to this generality is the Poxviridae family, which induce eosinophilic intracytoplasmic inclusion bodies. In the dog, few RNA viruses produce viral inclusion bodies visible by light microscopy, the most notable of which include: rabies virus, which results in the classic intracytoplasmic Negri body within infected neurons; and canine distemper virus, a morbillivirus that can result in both intranuclear and intracytoplasmic viral inclusion bodies.

The contributor provides an excellent overview of the viral properties of the *Adenoviridae,* comparative pathology of adenoviral infection, and pancreatic disease in nonhuman primates.

Contributor: New England Primate Research Center, Harvard Medical School, One Pine Hill Dr., Southborough, MA 01772.
http://www.hms.harvard.edu/nerprc/

References:

1. Chandler FW, Callaway CS, Adams SR. Pancreatitis associated with an adenovirus in a rhesus monkey. *Vet Pathol*. 1974;11:165-171.
2. Chandler FW, McClure HM. Adenoviral pancreatitis in rhesus monkeys: current knowledge. *Vet Pathol*. 1982;19:171-180.
3. Crawford JM. Liver and biliary tract. In: Kumar V, Abbas AK, Fausto N, Aster JC, eds. *Robbins and Cotran Pathologic Basis of Disease*. 8th ed. Philadelphia, PA: Elsevier Saunders; 2009:942-946.
4. Cullen JM. Liver, biliary system, and exocrine pancreas. In: McGavin MD, Zachary JF, eds. *Pathologic Basis of Veterinary Disease*. 4th ed. St. Louis, MO: Elsevier; 2007:440-443, 458-59.
5. Doepel FM, Anver MR, Hofing GL. Pancreatitis in two new world monkeys. *Vet Pathol*. 1980;17:505-508.
6. Geldberg HB. Alimentary system. In: McGavin MD, Zachary JF, eds. *Pathologic Basis of Veterinary Disease*. 4th ed. St. Louis, MO: Elsevier; 2007:361.
7. Kalter SS. Enteric viruses of non-human primates. *Vet Pathol*. 1982;19:33-43.
8. Kovacs GM, Harrach B, Zakhartchouk AN, Davison AJ. Complete genome sequence of simian adenovirus 1: An Old World monkey adenovirus with two fiber genes. *J Gen Virol*. 2005;86:1681-1686.
9. Lopez A. Respiratory System. In: McGavin MD, Zachary JF, eds. *Pathologic Basis of Veterinary Disease*. 4th ed. St. Louis, MO: Elsevier; 2007:440-443, 522, 531.
10. McClure HM, Chandler FW. A survey of pancreatic lesions in non-human primates. *Vet Pathol*. 1982:19:193-209, 1982
11. Murphy FA, Gibbs EPJ, Horzinek MC, Studdert MJ. Viral Taxonomy and Nomenclature. In: *Veterinary Virology*. 3rd ed. vol.1. San Diego, CA: Elsevier Academic Press; 1999:32
12. Percy DH, Barthold SW. Mouse. In: *Pathology of Laboratory Rodents and Rabbits*. 2nd ed. Ames, IA: Iowa State University Press; 2001:16-17.
13. Roy S, Vandenberghe LH, Kryazhimskiy S, et al. Isolation and characterization of adenoviruses persistently

shed from the gastrointestinal tract of non-human primates. *PLoS pathogens*. 2009;5:e1000503.
14. Studdert MJ. Equine Adenoviruses. In: *Equine Respiratory Diseases*. Ithaca, NY: International Veterinary Information Service (www.ivis.org); 2003.

CASE IV: N09-1 (AFIP 3134310).

Signalment: 12-year-old male castrated mixed-breed horse (*Equus caballus*).

History: The horse was housed on pasture with five other horses. Its diet consisted of orchard and brome grass hay and 12% sweet feed. The water source was a flowing river. Vaccinations for Eastern equine encephalitis (EEE), Western equine encephalitis (WEE), and tetanus were current.

The owners noted depression and dysuria. Following three days of progressive signs to include lethargy and decreased thirst, the referring veterinarian examined the animal. A fever of 103.3°F was recorded, along with a decreased appetite, trouble prehending hay and grain, and teeth grinding. The veterinarian treated the animal with sulfa antibiotics and flunixin meglumine (Banamine™). The next day the horse was more lethargic, reluctant to move, and had a temperature of 101.5°F.

On day 4, the horse was referred to the University of Tennessee (UT) Large Animal Clinic. Upon presentation, the horse was depressed and lethargic, had a weak gait, and dragged both toes of the pelvic limbs at the walk. The neurologic exam revealed a grade III-IV weakness of all four limbs with variable ataxia. The tongue tone was weak, especially to the right, and the horse had difficulty prehending food. There were intermittent fasciculations of the facial muscles, but no other cranial nerve deficits were noted. Additionally, the mucous membranes were icteric and injected, and the horse had multiple abrasions on the tongue and lips and hemorrhages on the gums. Rectal examination, abdominocentesis, equine infectious anemia titers, and upper airway endoscopy were within normal limits. Gastroscopy revealed small ulcers along the lesser curvature of the stomach. Treatments at the UT College of Veterinary Medicine included DMSO, flunixin meglumine (Banamine™), trimethoprim sulfa, IV fluids, dexamethasone, penicillin, and gentamicin (Gentocin™). Despite therapies, the horse became more ataxic and weak, to the point of falling down. He was maintained in the sling overnight, and by the morning of the 6th day, he was head pressing and completely unaware of his surroundings.

Gross Pathology: The horse was humanely euthanized and presented for necropsy to the UT Department of Pathobiology. Thirty-six hours later, the brain was removed and half was submitted for rabies IFA testing and half was placed in formalin. The trigeminal ganglion appeared swollen. The pituitary was enlarged and had several raised tan masses (adenomatous hyperplasia) on the capsular surface.

Laboratory Results: Clotting factors and biochemistry were within normal limits. A complete blood count revealed an HCT of 27%. A lumbosacral cerebrospinal fluid (CSF) tap on day 5 failed to detect abnormalities.

Histopathologic Description: Pituitary gland, pars nervosa: There was marked lymphocytic perivascular cuffing with infiltration into the adjacent neuropil affecting the pars nervosa. The tissue was markedly expanded by edema, and the perivascular cuffing also involved the vasculature of the pars intermedia, which is generally of even thickness, although there is multifocal cystic degeneration with accumulation of a brightly eosinophilic acellular material.

Contributor's Morphologic Diagnosis: Pituitary gland, pars nervosa: Severe subacute lymphocytic neurohypophysitis (encephalitis) with neuronal necrosis and spongiosis.

Contributor's Comment: The histologic lesions in this case are consistent with the diagnosis of viral encephalitis. Negri bodies, the pathognomonic lesion of rabies virus infection, were not observed in this case. The absence of Negri bodies can occur in cases where the animal is euthanized before the disease has run its full course. Immunohistochemistry, with appropriate controls, was performed on sections of the pituitary gland and thalamus/hippocampus by the Cornell Veterinary Diagnostic Laboratory, and viral antigen/Negri bodies were not detected. The IFA assay performed on fresh brain (half submitted) was positive. IFA is the gold standard in antemortem rabies diagnoses; when used on fresh brain tissues, it consistently detected 100% of rabies-positive archival cases.[7]

Rabies is a zoonosis with one of the highest fatality rates.[3] The rabies virus belongs to the genus *Lyssavirus* of the Rhabdoviridae family and is classically spread by a bite from an infected animal.[10] The virus replicates locally before moving along peripheral nerves, where it binds to the nicotinic acetylcholine receptors at the neuromuscular junctions. The virus moves via peripheral nerves toward the central nervous system (CNS) by retrograde axoplasmic transport.[10] Once in the spinal cord, movement occurs using both anterograde and retrograde axoplasmic flow. The virus can also move along peripheral nerves so that the salivary glands become involved, allowing transmission to occur through saliva.[10] This early spread of virus allows for dissemination of infection often before severe clinical signs and immune responses develop.

There are typically no gross lesions in rabies cases. Microscopic lesions are variable and include non-suppurative leptomeningitis with perivascular cuffs, neuronal degeneration and neuronophagia, gliosis, malacia of the spinal cord grey matter, and ganglioneuritis. Infected neurons may contain intracytoplasmic acidophilic inclusions (Negri bodies), which, while pathognomonic for rabies, are not present in all cases. Negri bodies tend to occur in large neurons, particularly in the pyramidal neurons of the hippocampus, neurons of the medulla oblongata and Purkinje cells of the cerebellum. Hence, these locations are preferred for microscopic or fluorescent antibody diagnosis of rabies.

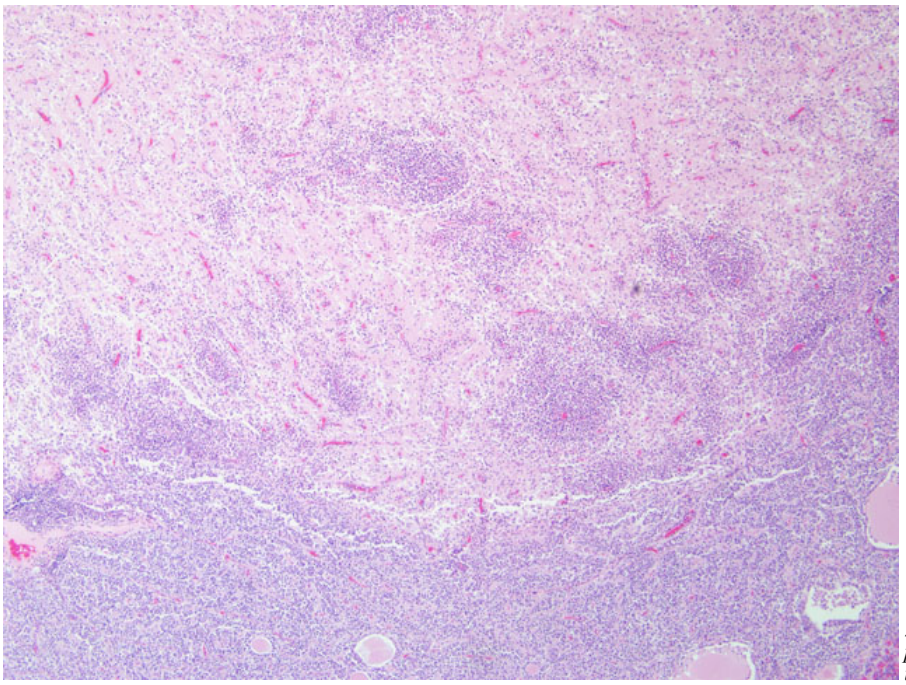

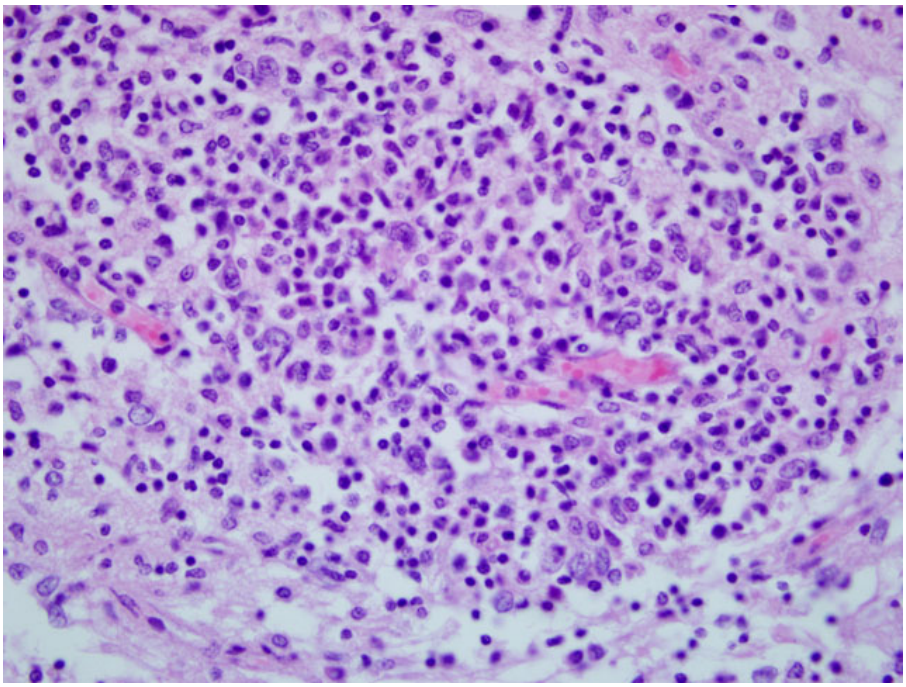

4-1, 4-2. Pituitary gland, pars nervosa and pars intermedia, horse. Surrounding vessels in the pars nervosa and extending into the neuropil and adjacent pars intermedia are moderate numbers of lymphocytes, macrophages, and plasma cells. (HE 40X, HE 400X)

Negri bodies were identified in the brain of 10/21 horses examined in one large study.[3] It was thought that they occurred more commonly in horses that survived longer than 4 days.[3] Negri body size may be affected by length of clinical disease and stage of infection when the animal was euthanized.[2] Detection of Negri bodies with hematoxylin and eosin and Sellers stain is limited, as it detected only 50-80% of positive samples, gave false positive results, and had reduced effectiveness in autolyzed samples.[1]

Dr. Adelchi Negri identified the intracytoplasmic inclusions in infected neurons that bear his name in 1903. Even today, the true significance of these structures is still mysterious. It seemed to Negri that fixed strains (passaged in the laboratory) of rabies were less likely to produce Negri bodies because neurons were destroyed early and that the street strains (natural disease) favored their formation, partly because they caused less significant neuronal damage.[6]

Rabies in horses in particular has been associated with a spectrum of clinical signs that include, but are not limited to, ataxia, recumbency, pharyngeal paralysis, fever, hyperesthesia, loss of tail and/or anal sphincter tone, progressive paresis, muscle tremors, sweating, anorexia, colic, and lameness.[3] Paresis and hind limb ataxia are the most commonly observed clinical signs.[3] In equine cases, where a CSF tap is performed, pleocytosis with lymphocyte prominence and fewer mononuclear cells, macrophages, and neutrophils is documented. The clinical signs may be related to the concentration of inoculated virus, the pathogenicity of the strain, and the proximity of CNS tissue to the site of inoculation. The spinal cord form and dumb form are much more common than the furious form in horses.[3]

Differentials for CNS disease in horses include vertebral malformation, trauma, infections, abiotrophy, and degenerative or idiopathic lesions. Viruses to consider include rabies, EEE, WEE, St. Louis encephalitis, Louisiana virus, snowshoe hare virus, Cache Valley virus, and Main Drain virus.[5] In one large study, wobbler syndrome and equine protozoal myelitis were the most common diagnoses.[5] The nicotinic acetylcholine receptors have been proposed as the rabies virus receptors.[3] The virus may influence secretion of neuro-modulators and thereby induce functional impairments at sites remote from the site of viral replication. Toll-like receptor 3 has also been implicated in the spatial arrangement of rabies virus-induced Negri bodies and overall success of viral replication.[9] Viruses can exploit cellular proteins for their own benefit.[9]

Immunoperoxidase has been determined to be a useful, accurate, and rapid method for rabies diagnosis.[1] Immunoperoxidase is thought to be more sensitive in early diagnoses of suspected cases in which conventional histology and IFA might not detect viral antigens. In a small case series of four IFA-confirmed rabies cases, IMHC on paraffin tissue detected all rabies cases. Only 2/4 cases had Negri bodies.[5] Similarly, immunoperoxidase on 40 rabies cases showed a specificity of 100% and a sensitivity of 97.6%. Additionally, in another case series, 39/40 cases were positive for rabies with immunoperoxidase, making it a reliable diagnostic technique.[4] Negri bodies were seen in only a fraction of these cases (10/17).[4] Viral antigens were detected in dendrites, axons, glial cells, granular cells in Ammon's horn, pyramidal cells and pericaryons of neurons in stratum gangliosum and stratum granulosum of cerebellar cortex.[1]

The amount of rabies antigen varies depending on location within the brain. Following testing of 252 confirmed rabies cases, the thalamus, pons, and medulla were the most reliable parts of brain for testing. Previously, the hippocampus was recommended due to the need to find large inclusion bodies, which occurred at the highest frequency at this site.[2] Current recommendations suggest that the hippocampus and brainstem be sampled.[2]

AFIP Diagnosis: Pituitary gland, pars nervosa and pars intermedia: Hypophysitis, perivascular, lymphohistiocytic and plasmacytic, multifocal, moderate, with gliosis.

Conference Comment: The contributor provides an excellent discussion of rabies infection, pathogenesis, clinical signs and diagnostics.

Several participants included rabies virus infection in their differential diagnosis list along with other causes of viral encephalitis in the horse. There are two biotypes of rabies virus: fixed virus and street virus. As mentioned by the contributor, the fixed virus is stable and used for developing vaccine strains. The street virus is the "wild-type" virus involved in disease outbreaks.

Upon inoculation of a susceptible animal, the virus initially replicates in myocytes before budding from the muscle cell and infecting nerves at the neuromuscular junction.[10] The rabies virus glycoprotein receptors for neuronal cell adhesion molecule (NCAM) and the p75 neurotrophin receptor convey the neurotropism displayed by the virus.[8] Retrograde axonal transport may involve virus phosphoprotein interaction with microtubule motor protein dynein LC8. Once the virus reaches the CNS, transmission of the virus between neurons results in ascending and descending spread of the virus and precipitating the typical clinical signs and pathologic changes.[10]

The exact mechanism by which rabies causes neuronal lesions and ultimately death is unknown. One possibility is marked viral-induced down-regulation of genes in the brain; affected genes are often involved in regulating cellular metabolism, growth and differentiation. Elevation in the nitric oxide content in rabies-infected brains suggests nitric oxide neurotoxicity. Mouse models of rabies infection demonstrate virus-induced apoptosis, another possible mechanism of neuronal injury and lesions.[10]

Contributor: Department of Pathology, College of Veterinary Medicine, University of Tennessee, 2407 River Dr., Knoxville, TN 37996-4542

References:

1. Arslan A, Saglma YS, Temur A. Detection of rabies viral antigen in non-autolysed and autolysed tissues by using an immunoperoxidase technique. *Vet Rec*. 2004;155:550-552.
2. Bingham J, van der Merwe M. Distribution of rabies antigen in infected brain material: Determining the reliability of different regions of the brain for rabies fluorescent antibody test. *J Virol Methods*. 2002;101:85-94.
3. Green SL, Smith LL, Vernau W, Beacock SM. Rabies of horses: 21 cases (1970-1990). *J Am Vet Med Assoc*. 1992;200:1133-1137.
4. Hamir AN, Moser G. Immunoperoxidase test for rabies: Utility as a diagnostic test. *J Vet Diagn Invest*. 1994;6:148-152.

5. Hamir AN, Moser G, Rupprecht CE. A five year (1985-1989) retrospective study of equine neurological disease with special reference to rabies. *J Comp Pathol*. 1992;106:411-421.
6. Kristensson K, Dastur DK, Manghani DK, Tsiang H, Bentivoglio M. Rabies: Interactions between neurons and viruses: A review of the history of Negri inclusion bodies. *Neuropathol Appl Neurobiol*. 1996;22:179-187.
7. Kulonen K, Fekadu M, Whitfield S, Warner CK. An evaluation of immunofluorescence and PCR methods for detection of rabies in archival Carnoy-fixed paraffin embedded brain tissues. *Zentralbl Veterinarmed B*. 1999;46:151-155.
8. Maxie MG, Youssef S. Nervous system. In: Maxie MG, ed. *Jubb, Kennedy and Palmer's Pathology of Domestic Animals*. 5th ed., Vol. 1. Philadelphia, PA: Elsevier Ltd; 2007:413-416.
9. Menager P, Roux P, Megret F, et al. Toll-like receptor 3 (TLR3) plays a major role in the formation of rabies virus Negri Bodies. *PLoS Pathog* 5(2):e1000315. doi:10.1371/journal.ppat.10000315
10. McGavin MD, Zachary JF, eds. In: *Pathologic Basis of Veterinary Disease*. 4th ed. St. Louis, MO: Elsevier; 2007:833-971.

The Armed Forces Institute of Pathology
Department of Veterinary Pathology

Conference Coordinator
Matthew Wegner, DVM

WEDNESDAY SLIDE CONFERENCE 2010-2011

Conference 7

29 September 2010

Conference Moderator:
Thomas Lipscomb, DVM, Diplomate ACVP

CASE I: 598-10 (AFIP 3165072).

Signalment: 14-month-old female intact Boxer dog (*Canis familiaris*).

History: Intestine and colon biopsies were submitted from a patient with chronic diarrhea.

Gross Pathology: Not reported.

Histopathologic Description: Colon: The small intestine is normal but the colonic submucosa is greatly expanded by swollen, foamy/granular histiocytes that occasionally contain a large clear vacuole. A few of these histiocyt es are in the deep mucosal lamina propria as well, between the muscularis mucosa and the crypts. Many scattered small lymphocytes with plasma cells and neutrophils are also in the submucosa, and the histiocytic inflammation is also expanding into the inner muscular wall in some areas (may not be in submitted slide). The histiocytes sometimes contain many PAS-positive granules (showing PAS positive and negative histiocytes with Goblet cells in colonic mucosa), many do not, and no fungi or acid-fast bacteria are present.

Contributor's Morphologic Diagnosis: Histiocytic ulcerative colitis of Boxer dogs.

Contributor's Comment: Boxers are prone to this condition, usually before two years of age, and an altered immunity is suspected.[1] The histiocytes sometimes contain many PAS-positive granules which are thought to be phagocytic debris and possibly phagocytized organisms that perhaps Boxers and French bulldogs are not able to process due to a genetic lysosomal defect.[1] In recent years, the condition has been successfully treated with enrofloxacin[2] and a new report indicates that this treatment correlates with eradication of intramucosal *Escherichia coli*, and the few cases that don't respond have an enrofloxacin-resistant strain of *E. coli*.[3]

The histiocytic influx is reportedly centered in the submucosa and into the deep mucosa and may expand through the muscular wall to the serosa and adjacent lymph nodes.[1] Mucosal biopsies only may miss the lesions. Mucosal ulceration progresses with chronicity from superficial erosions to patchy ulcers that stop at the submucosa to only patchy intact islands of mucosa.

This dog was euthanized for this condition. A male littermate is normal. Interestingly, the clinician reported that he had an unrelated (unconfirmed) case in a young Boxer about this time and it did respond well to three weeks of enrofloxacin treatment.

AFIP Diagnosis: 1. Colon: Colitis, histiocytic and lymphoplasmacytic, mucosal and submucosal, diffuse, severe with intrahistiocytic granular eosinophilic material.
2. Small intestine: Enteritis, histiocytic and lymphoplasmacytic, focally extensive, moderate with intrahistiocytic granular eosinophilic material.

Conference Comment: A number of studies over the years have noted bacteria within macrophages in histiocytic ulcerative colitis of Boxer dogs (HUC), but recognized

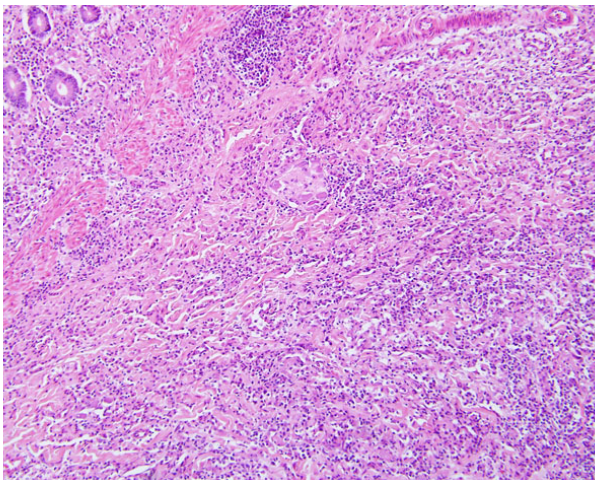

1-1. Colon, dog. The mucosa and submucosa are markedly expanded by many mixed inflammatory cells that widely separate and replace colonic crypts. (HE 100X)

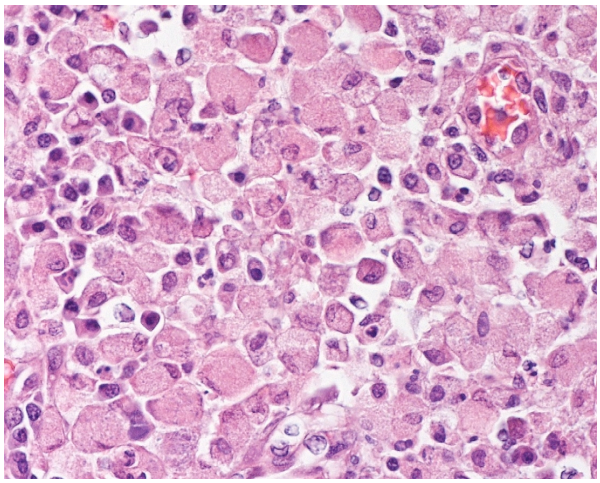

1-2. Colon, dog. The cellular infiltrate is composed of many swollen, foamy to granular histiocytes. Photograph courtesy of AR Livestock and Poultry Commission Lab, Little Rock, AR 72215, jbritt@alpc.ar.gov

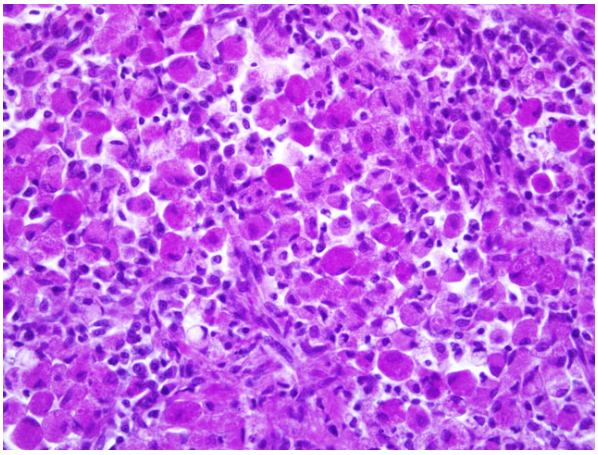

1-3. Colon, dog. Histiocytes are filled with many granules that are demonstrated by the PAS stain. (Periodic-acid Schiff 400X)

pathogens such as *Salmonella*, *Campylobacter* and *Shigella* have not been detected. The very strong breed predisposition and the absence of an identified infectious agent resulted in the conclusion that the condition is a breed specific immune-mediated disease of unknown cause. However, some affected dogs were found to respond to treatment with chloramphenicol and, more recently, to enrofloxacin (a fluoroquinolone antibiotic). It has been noted that HUC has features that are similar to human forms of inflammatory bowel disease, such as Crohn's disease. Common features include granulomatous inflammation, bacteria within macrophages and responsiveness to fluoroquinolone antibiotics. HUC also has similarities to ulcerative colitis and Whipple's disease. Recent studies have shown that certain adherent and invasive strains of *Escherichia coli* are present in the lesional tissues of affected dogs. These strains have strong similarities to *E. coli* strains associated with some cases of Crohn's disease. HUC and Crohn's disease associated strains are more similar to *E. coli* associated with extraintestinal disease than to those causing diarrhea. These findings support the emerging concept that inflammatory bowel diseases result from an overly aggressive immune response to bacterial microflora in genetically susceptible individuals.[4]

In the sections of small intestine examined during conference, predominantly histiocytic inflammation similar to that present in the colon was found.

Contributor: Arkansas Livestock and Poultry Commission Lab, P.O. Box 8505, Little Rock, AR 72215
http://www.arlpc.org

References:

1. Brown, CR, Baker, DC, Barker, IK. Alimentary System. In: Maxie MG, ed. *Jubb, Kennedy and Palmer's Pathology of Domestic Animals*. 5th ed., Vol. 2. Philadelphia, PA: Elsevier Ltd; 2007:112-113.
2. Davies DR, O'Hara, AJ, Irwin, PJ, Guilford, WG. Successful management of histiocytic ulcerative colitis with enrofloxacin in two Boxer dogs. *Australian Vet J*. 2004;82:58-61.
3. Mansfield, CS, James FE, Craven, JM, et al. Remission of histiocytic ulcerative colitis in Boxer dogs correlates with eradication of invasive intramucosal *Escherichia coli*. *J Vet Intern Med*. 2009;23:964-969.
4. Simpson, KW, Dogan, B, Rishniw, M et al. Adherent and invasive *Escherichia coli* is associated with granulomatous colitis in Boxer dogs. *Infection Immunity*. 2006;74:4778-4792.

CASE II: 9-1947 (AFIP 3164947).

Signalment: Adult female Pacific white-sided dolphin (*Lagenorhynchus obliquidens*).

History: An approximately 31-year-old and 126 k, adult female Pacific white-sided dolphin (*Lagenorhynchus obliquidens*) maintained in a semi-closed, 3.8 million litre captive display pool with a long history of intermittent gastrointestinal problems was presented with sudden anorexia, abdominal pain, and vomiting. The aging dolphin had had multiple antibiotic treatments in response to inflammatory blood profiles and inappetence at several public display institutions and was known as an "old dolphin that often goes off-feed". Although gastrointestinal disease had been suspected, the cause of the recurrent inflammatory changes in the peripheral blood was never definitively diagnosed. Starting in 2006, budding yeast and pseudohyphae were found on oral and gastric cytology in association with lethargy, inappetence and recurring inflammatory changes. Antifungal agents including oral itraconazole and nystatin were used and appeared to speed recovery and decrease the severity of the clinical signs. Repeated endoscopy of the esophagus and proximal stomach showed no significant lesions, although a thick koilin coating of the stomach occasionally hampered close examination of the gastric mucosa.

Gross Pathology: Necropsy showed an emaciated animal with moderate abdominal distension. On incision of the abdominal wall, there was approximately 2 L of serosanguineous ascites and an intestinal torsion within the craniodorsal aspect of the abdominal cavity with displacement of adjoining viscera. Extending from the duodenum caudally to the midlevel of ileum, there was multifocal to coalescing and occasional segmental yellow discoloration of the intestinal mucosa with variable amounts of submucosal edema and multifocal caseous to friable yellow white deposits. In more distal regions of the bowel, the serosa featured a fine cobblestone to granular texture, and was glistening and stippled to mottled dark red black.

Laboratory Results: Special culture on selective media identified *Candida krusei*.

Histopathologic Description: Jejunum and small intestine: Microscopically, there was marked fibrinosuppurative and lymphohistiocytic enteritis with florid intralesional yeast.

Contributor's Morphologic Diagnosis: 1) Jejunum: Torsion, severe, segmental, acute with infarction and hemorrhage (Gross diagnosis).
2) Small intestine: Enteritis, marked, nodular to diffuse, lymphohistiocytic and fibrinosuppurative, with florid intrahistiocytic yeast morphologically consistent with *Candida* spp.

Contributor's Comment: Microscopic assessment of the grossly noted submucosal nodular proliferations in the multiple segments of small intestine disclosed florid, predominantly intrahistiocytic, yeast morphologically suggestive of *Histoplasma capsulatum, Blastomyces dermatitidis, Paracoccidioides brasiliensis, Sporothrix schenckii, Torulopsis* (*Candida*) *glabrata*, and *Candida* spp. In-house culture yielded moderate growth of *Candida* spp. and submission of fresh tissue to a reference lab, the British Columbia Centre for Disease Control, for special culture on selective media identified *C. krusei*, which is considered significant.[1] This organism is the conidal state of *Issatchenkia orientalilis* and is considered a commensal of the mucus membranes and skin of animals and humans. *Candida krusei* has been occasionally associated with bovine mastitis and there is a single case report of bronchopneumonia secondary to candidemia in a Holstein heifer. Fatal colonization of a gastrostomy tube has been reported in a cat. *Candida* spp. infections in humans are

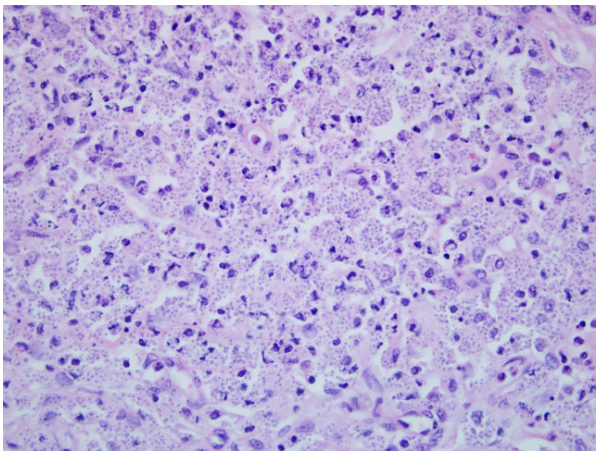

2-1. Intestine, Pacific white-sided dolphin. The inflammatory population is composed of many macrophages, lymphocytes, and neutrophils. Within histiocytes there are numerous fungal yeast. (HE 400X)

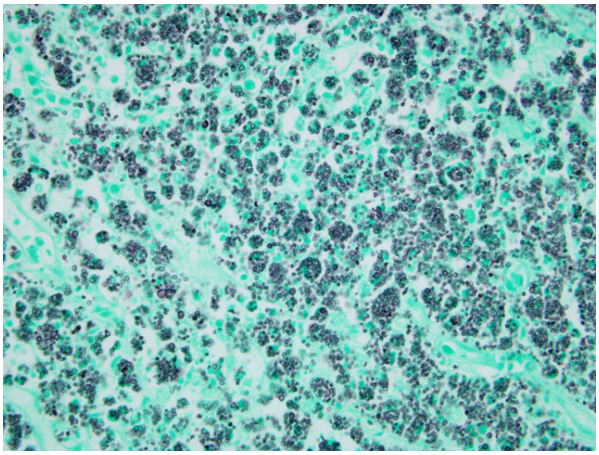

2-2. Intestine, Pacific white-sided dolphin. The intrahistiocytic yeasts are highlighted by the Gomori-Grocott methenamine silver stain. (GMS 400X)

generally localized to the gastrointestinal, urogenital and respiratory tracts and have been associated with prolonged antibiotic administration, haemodialysis, chemotherapeutic agents, cancer or other severely debilitating disease, penetrating abdominal trauma, or patients with indwelling catheters. The pathogenesis of infection is characterized by initial colonization of mucocutaneous junctions of mucosa of the gastrointestinal tract, then proliferation, and then deeper tissue invasion. Candidiasis has been documented in a number of marine mammals, including bottlenose dolphins, killer whales, false killer whales, harbour seals, northern fur seals, California sea lions and a pygmy sperm whale. Infection may present as disseminated or more localized, such as dermatitis, blowhole erosions, glossitis, pharyngitis, pneumonia, nephritis, cystitis, or esophagitis.[4] To the best of our knowledge, *C. krusei* has not previously been reported in marine mammals. In this animal, there were no apparent pre-existing conditions within the examined tissues which may have predisposed or exacerbated infection.

AFIP Diagnosis: 1. Intestine: Enteritis, histiocytic, lymphocytic and neutrophilic, multifocally extensive, severe, with extensive ulceration and myriad intrahistiocytic yeast.
2. Intestine: Enteritis, mesenteritis, and peritonitis, fibrinosuppurative, multifocally extensive, severe, with necrosis, hemorrhage and myriad bacilli.

Conference Comment: Conference participants favored *Histoplasma capsulatum* as the etiology of the fungal infection. This highlights the potential problems associated with relying on morphology alone in the diagnosis of many infections. Correlation of histomorphology with culture and other specific techniques can avoid diagnostic errors. Intrahistiocytic clusters of the yeast-like forms of *Candida* can closely resemble *Histoplasma* in histologic sections. This is particularly true of *Candida glabrata*. Additionally, bacilli, which were demonstrated to be gram-negative, were present in areas of fibrinosuppurative inflammation and necrosis in the sections examined at conference.

Participants found this case to be a good opportunity to review the clinicopathologic features of candidiasis. As noted by the contributor, candidiasis typically presents clinically as a superficial mycosis of mucous membranes most often in young, debilitated, or immunocompromised animals, or those receiving prolonged courses of antibiotic therapy. Common anatomic locations of candidiasis include the mouth, esophagus, crop, and proventriculus in birds; the oral mucosa in mammals; and the stomach in piglets.[2] Birds are affected by *Candida* species more frequently than mammals. Grossly, infection by *Candida* results in a white pseudomembrane overlying mucous membranes. Histologically, pseudohyphae, blastoconidia, hyphae, and yeast-like organisms are present, and there is often necrosis or ulceration.

Conference participants also discussed specifics of virulence and immunity in candidiasis. *Candida* species have the ability to change phenotypes in a random and reversible manner in response to changes in the host environment resulting from antibiotic treatment, immune response, or altered host physiology. The phenotypic variants can exhibit changes in colony morphology, cell shape, antigenicity, and virulence. Virulence is related to the organism's ability to adhere to cells, and adherence to host cell is mediated by several classes of adhesins. One class of adhesins is an integrin-like protein which binds to arginine-glycine-aspartic acid groups on fibrinogen, fibronectin, and laminin. A second adhesin class, resembling transglutaminase substrates, binds to epithelial cells; and a third group of agglutinins binds to endothelial cells or fibronectin. Several secreted enzymes, such as aspartyl proteinases, aid in tissue degradation, facilitating organism invasion. *Candida* species also secrete adenosine to block neutrophil degranulation, thus preventing the production of free oxygen radicals which would be damaging to the organisms.[2]

Both innate and cell-mediated immunity are necessary for clearing infections. Neutrophil and macrophage phagocytosis and subsequent oxidative destruction of the yeast are important in preventing establishment of infection. The filamentous form of this organism escapes the phagolysosome and replicates in the cytoplasm of infected cells. *Candida* yeasts stimulate dendritic cell production of IL-12 to a greater degree than the filamentous form, resulting in a protective T_H1 response; in contrast, the filamentous form induces a non-protective T_H2 response.[3] Similar to other fungi, this organism elicits a T_H17 response, resulting in recruitment of neutrophils and monocytes to the site of infection. For a thorough review of the general pathology involved in the various T-cell responses, readers are encouraged to review WSC 2008-2009, Conference 16, Case 4.

Contributor: Animal Health Center, British Columbia Ministry of Agriculture and Lands, 1767 Angus Campbell Road, Abbotsford, BC, V3G 2M3

References:

1. Hager JL, Mur MR, Hsu S. *Candida krusei* fungemia in an immunocompromised patient. *Dematol Online J*. 2010;16(4):5.
2. Jones TC, Hunt RD, King NW. Diseases caused by fungi. In: *Veterinary Pathology*. 6th ed. Baltimore, MD: Williams and Wilkins; 1996:519-522.
3. McAdam AJ, Sharpe AH. Infectious diseases. In: Kumar V, Abbas AK, Fausto N, Aster JC, eds. *Robbins and Cotran Pathologic Basis of Disease*. 8th ed. Philadelphia, PA: Elsevier Saunders; 2009:382-384.
4. Reidarson, T, McBain, J, Dalton, L, Rinaldi, M. Mycotic Diseases. In: Dierauf LA, Gulland FMD, eds. *CRC Handbook of Marine Mammal Medicine*. 2nd ed. Washington D.C.: CRC Press; 2001:337-352.

CASE III: TAMU-02 2010 (AFIP 3167479).

Signalment: 13-year-old female domestic long hair feline (*Felis catus*).

History: The cat had a 5-day history of increased respiration, with 3-4 days of rapid shallow breathing and 2 weeks of weight loss. The owners had noticed a recent change in the cat's vocalization. Thoracic radiographs revealed a diffuse bronchointerstitial pattern throughout the lungs. There was no response to treatment with bronchodilators or glucocorticoids.

Gross Pathology: All lung lobes are diffusely firm, fail to collapse, and have an irregular surface that is mottled pink and dark red. The lungs ooze red fluid on cut section (edema).

Laboratory Results: Histoplasmosis antigen detection using an enzyme immunoassay was negative.

Histopathologic Description: Lung: Throughout the section of lung, large numbers of alveoli and alveolar ducts contain densely packed, round to slightly spindle-shaped cells with variably distinct cell borders that completely fill the alveolar and ductal lumens. The cells form dense rounded clusters within alveoli and are often arranged in a lightly streaming pattern. The infiltrating cells have a histiocytic appearance, characterized by a moderate amount of lightly eosinophilic to pale basophilic cytoplasm, which is sometimes lightly vacuolated, and cell nuclei that are round to oval, often eccentrically placed and slightly indented, and which contain variably condensed basophilic chromatin. Mitotic figures are rare (<1 per 400x field). Some alveoli also contain individual or small central clusters of macrophages with abundant, highly vacuolated, foamy cytoplasm and small condensed nuclei. Many alveoli are segmentally lined by prominent, cuboidal epithelial cells (type II pneumocyte hyperplasia). The smooth muscle within alveolar septae is markedly thickened in many areas (smooth muscle hyperplasia). Peribronchiolar and peribronchial lymphocytes are prominent, and clusters of densely packed lymphocytes with lesser numbers of plasma cells are also scattered throughout the section. Many alveoli contain abundant eosinophilic proteinaceous fluid (edema). In some areas the normal alveolar architecture is replaced by thin interlacing bands of collagenous tissue (interstitial fibrosis), with moderate numbers of lymphocytes and plasma cells and multifocal areas of mild hemorrhage. Alveolar septae are lost in many areas resulting in enlarged, confluent air spaces (emphysema).

Contributor's Morphologic Diagnosis: Severe, diffuse, proliferative, alveolar histiocytosis with smooth muscle hyperplasia, interstitial fibrosis and type II pneumocyte hyperplasia.

Contributor's Comment: The marked pulmonary histiocytic disease in the lungs of this cat is representative of a recently described histiocytic proliferative disorder in cats, pulmonary Langerhans cell histiocytosis (PLCH), that targets the lungs but can variably affect other organs.[3] The severe bronchial pattern with a moderate interstitial component observed throughout the lungs in thoracic radiographs of this cat was clinically suggestive of histoplasmosis, severe asthma, or inflammatory airway disease. However, histoplasmosis antigen detection using an enzyme immunoassay to detect antigenuria was negative, and the cat did not respond to treatment with bronchodilators or glucocorticoids. Gross necropsy findings, which included impression smears showing a uniform population of what was presumed to be spindle cells, were more suggestive of pulmonary neoplasia or fibrosis. The presence of a uniform population of cohesive and streaming histiocytic cells within many alveoli and alveolar ducts throughout the lung of this cat is consistent with PLCH. The infiltrating cells were strongly positive for vimentin, CD18, and E-cadherin, which supports a Langerhans cell phenotype as previously described.[3]

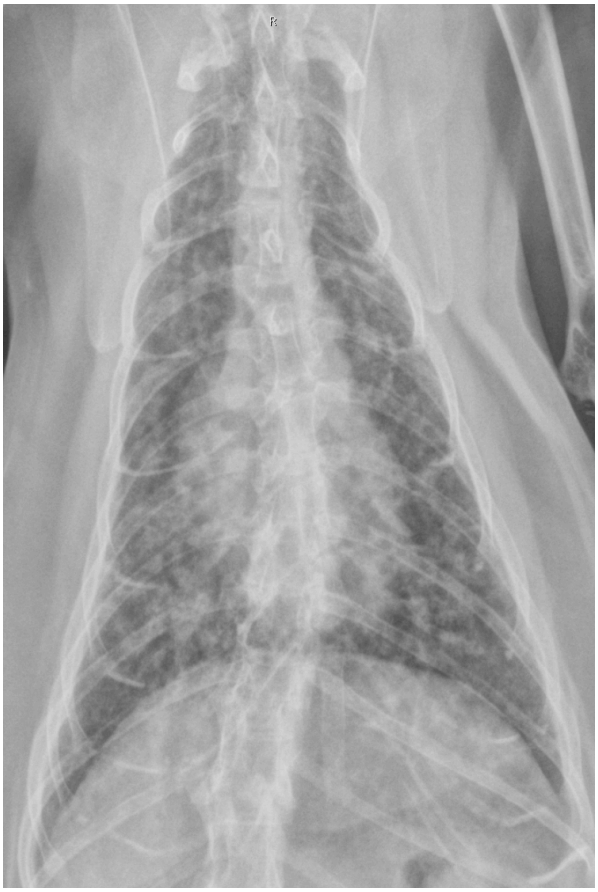

3-1. Lung, cat. Thoracic radiographs demonstrate a bronchointerstitial pattern throughout the lungs. Photograph courtesy of Department of Pathobiology, College of Veterinary Medicine and Biomedical Sciences, Texas A&M University, College Station, Texas, wcorapl@cvm.tamu.edu

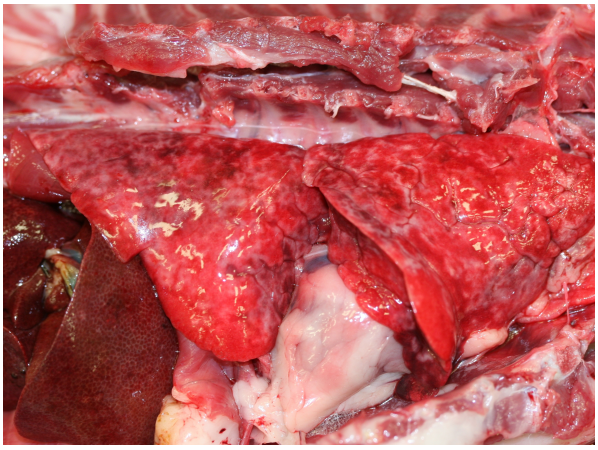

3-2. Lung, cat. Lung lobes are firm, fail to collapse, and have an irregular surface that is mottled pink to dark red. Photograph courtesy of Department of Pathobiology, College of Veterinary Medicine and Biomedical Sciences, Texas A&M University, College Station, Texas, wcorapi@cvm.tamu.edu

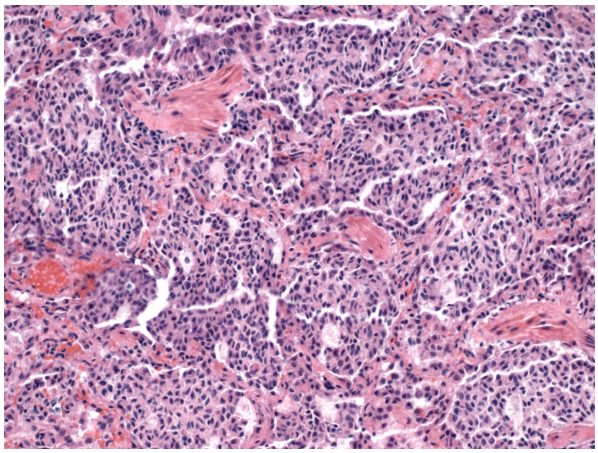

3-3. Lung, cat. Multifocally, many alveoli and alveolar ducts contain a uniform population of cohesive and streaming histiocytic cells with abundant foamy cytoplasm. Photograph courtesy of Department of Pathobiology, College of Veterinary Medicine and Biomedical Sciences, Texas A&M University, College Station, Texas, wcorapi@cvm.tamu.edu

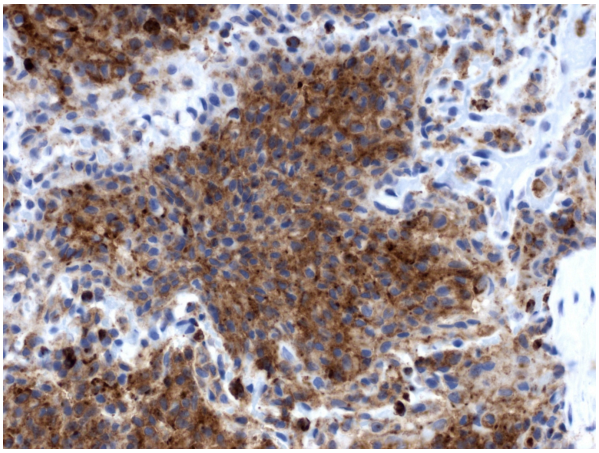

3-4. Lung, cat. Diffusely, infiltrating histiocytes are immunopositive for CD-18. Photograph courtesy of Department of Pathobiology, College of Veterinary Medicine and Biomedical Sciences, Texas A&M University, College Station, Texas, wcorapi@cvm.tamu.edu

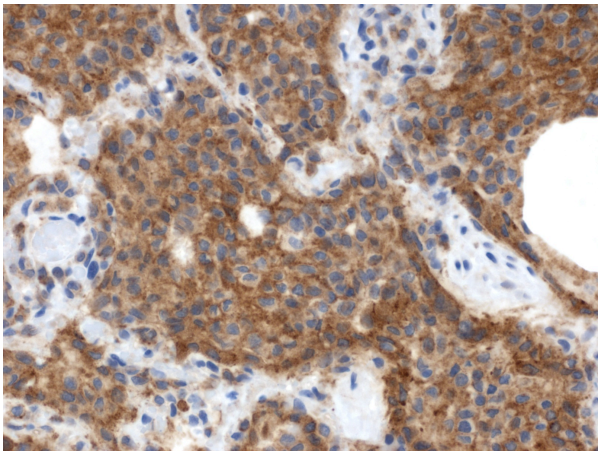

3-5. Lung, cat. Diffusely, infiltrating histiocytes are immunopositive for E-cadherin. Photograph courtesy of Department of Pathobiology, College of Veterinary Medicine and Biomedical Sciences, Texas A&M University, College Station, Texas, wcorapi@cvm.tamu.edu

In the corresponding human interstitial lung disease, which occurs primarily in young adult cigarette smokers, PLCH was found to be the result of mixed clonal and nonclonal expansion of nonmalignant Langerhans cells that arises in a setting of Langerhans cell hyperplasia.[11] This, along with the fact that it is frequently associated with clinical regression after steroid therapy and cessation of smoking, supports the view that PLCH represents a reactive disorder rather than a neoplastic process. It occurs in a slightly higher percentage in women and is frequently found only in the lungs, although multiorgan involvement may also occur.[9,10] PLCH represents one of a spectrum of Langerhans cell proliferative diseases (Langerhans cell histiocytosis), which occur more frequently in children and are marked by proliferation and infiltration of various organs by Langerhans cells.[8,10] In addition to the lung, the organs most commonly affected by Langerhans cell histiocytosis include bone and skin, although any organ can be affected. In the recent report of PLCH in 3 cats, affected organs included the lung, pancreas, kidney, liver, and various lymph nodes.[3] Extrapulmonary involvement was not observed in the present case. A characteristic feature of PLCH, in addition to the marked proliferation of alveolar histiocytes, is the presence of rod-shaped Birbeck granules, the hallmark organelle of the Langerhans cell, within the cytoplasm of lesional histiocytes when viewed with transmission electron microscopy.

AFIP Diagnosis: Lung: Histiocytosis, atypical, intrabronchiolar and intra-alveolar, multifocal, marked, with extensive alveolar edema, moderate lymphoplasmacytic and histiocytic inflammation, and hyperplasia of bronchiolar smooth muscle, consistent with pulmonary Langerhans cell histiocytosis.

Conference Comment: Conference participants readily identified the overwhelming infiltrate of histiocytic cells in the lung described by the contributor, but most experienced difficulty with histologic interpretation of the underlying pathologic process; some favored a neoplastic condition,

while others interpreted the lesion as granulomatous inflammation. The conference moderator emphasized that the infiltrative cell type consists almost exclusively of histiocytic cells with mildly atypical morphology, including mild anisokaryosis and hyperchromatic nuclei, supporting a histiocytic proliferative lesion versus granulomatous inflammation. The striking similarity to the cases reported by Busch *et al*. strongly supports pulmonary Langerhans cell histiocytosis (PLCH). The immunohistochemical findings reported by the contributor provide further confirmation.

Reports of histiocytic diseases of the cat are few and limited to feline progressive histiocytosis,[2] feline pulmonary Langerhans histiocytosis,[3] histiocytic sarcoma[7] and hemophagocytic histiocytic sarcoma;[4] the cell type in the first two conditions is of Langerhans cell lineage, dendritic cell origin for the third, while the findings in the last entity are most consistent with macrophage origin. In the feline progressive histiocytosis and feline pulmonary Langerhans histiocytosis, it remains uncertain whether the conditions represent a reactive or neoplastic process. In contrast to cats, histiocytic diseases in the dog are much more common, and the nature of the conditions as reactive or neoplastic are better characterized. The classifications and corresponding cell of origin are as follows: reactive cutaneous/systemic histiocytosis (interstitial dendritic cell); cutaneous histiocytoma (Langerhans cell); local and disseminated histiocytic sarcoma (myeloid dendritic cell); and hemophagocytic histiocytic sarcoma (macrophage).[1,5,7]

Development of dendritic cells, Langerhans cells and macrophages begins with CD34+ progenitor cells in the bone marrow, and further differentiation produces three subsets of cells: CD34+/CLA+ (cutaneous lymphocyte antigen); CD34+/CLA-; and CD34+/IL-3Rα-rich cells.[1] The CD34+/CLA+ and CD34+/CLA- cells, under the influence of stem cell factors or GM-CSF and TNF-α differentiate into CD1+/CD14- and CD1a-/CD14+ cells, respectively. Again, under the influence of GM-CSF and TNF-α, CD1a-/CD14+ cells differentiate into interstitial dendritic cells, or, if stimulated by M-CSF, undergo differentiation to macrophages. The CD1+/CD14- subtypes differentiate into Langerhans cells under the influence of GM-CSF, TNF-α, and TGF-α. The CD1a/CD14+ subtypes can also arise from CD14+ blood monocytes under the influence of GM-CSF and IL-4. Myeloid dendritic cells arise from CD34+/IL-3Rα-rich cells when stimulated by IL-3 and GM-CSF.[1]

The immunophenotyping of the cells comprising the histiocytic diseases varies based on the reference text or journal consulted, and reflects the continuous information explosion in this very active field of research. After review of the literature and the veterinary reference text of *Jubb, Kennedy and Palmer's Pathology of Domestic Animals*, the following list outlines the most consistent and commonly cited immunophenotypes:[1-7]

- Langerhans cells: MHC II; CD1a, c; CD11c; CD18; langerin; ICAM-1; and E-cadherin positive
- Interstitial dendritic cells: MHC II; CD1c; CD4; CD11b, c; CD18; CD90 (Thy-1) positive
- Myeloid dendritic cells: MHC II; CD1; CD11c; ICAM-1; ± CD90 positive
- Macrophage: MHC II; CD11d/CD18; α2-integrin; ± CD11c/CD18 and CD1c positive

Readers are encouraged to review Wednesday Slide Conference 2008-2009, Conference 24, Case 4, for a thorough review of canine histiocytic diseases.

Contributor: Department of Veterinary Pathobiology, College of Veterinary Medicine and Biomedical Sciences, Texas A&M University, College Station, TX 77845-4467
http://www.cvm.tamu.edu/vtpb/

References:

1. Affolter VK, Moore PF. Localized and disseminated histiocytic sarcoma of dendritic cell origin in dogs. *Vet Pathol*. 2002;39:74-83.
2. Affolter VK, Moore PF. Feline progressive histiocytosis. *Vet Pathol*. 2006;43:646-655.
3. Busch MDM, Reily CM, Luff JA, Moore PF. Feline pulmonary Langerhans cell histiocytosis with multiorgan involvement. Vet Pathol. 2008;45(6):816-824.
4. Friedrichs KR, Young KM. Histiocytic sarcoma of macrophage origin in a cat: Case report with a literature review of feline histiocytic malignancies and comparison with canine hemophagocytic histiocytic sarcoma. *Vet Clin Pathol*. 2008;37(1):121-128.
5. Fulmer AK, Mauldin GE. Canine histiocytic neoplasia: an overview. *Can Vet J*. 2007;48:1041-1050.
6. Ginn PE, Mansell JEKL, Rakich PM. Skin and appendages. In: Maxie MG, ed. *Jubb, Kennedy and Palmer's Pathology of Domestic Animals*. 5th ed., Vol. 1. Philadelphia, PA: Elsevier Ltd; 2007:768-770.
7. Gross TL, Ihrke PJ, Walder EJ, Affolter VK. Histiocytic Sarcoma. In: *Skin diseases of the dog and cat, clinical and histopathologic diagnosis*. 2nd ed., Ames, Iowa: Blackwell Science Ltd; 2005:848-852.
8. Moore PF, Affolter VK, Vernau W. Canine hemophagocytic histiocytic sarcoma: A proliferative disorder of CD11d+ macrophages. *Vet Pathol*. 2006:43:632-645.
9. Satter, EK. High WA. Langerhans cell histiocytosis: a review of the current recommendations of the histiocyte society. *Pediatr Dermatol*. 2008;25(3)291-295.
10. Vassalo, R, Ryu JH. Pulmonary Langerhans' cell histiocytosis. Clin Chest Med. 2004;25(3):561-571.
11. Vassalo, R, Ryu, JH, Colby TV, et al. Pulmonary Langerhans'-cell histiocytosis. N Engl J Med. 2000;342(26): 1969-1978.
12. Yousem SA, Colby TV, Chen YY, et al. Pulmonary Langerhans cell histiocytosis: molecular analysis of clonality. Am J Surg Pathol. 2001;25(5):630-636.

CASE IV: UFSM-1 (AFIP 3065818).

Signalment: 5-year-old male mongrel dog (*Canis familiaris*).

History: The dog presented with apathy, anorexia, vomiting, and diarrhea with blood, icterus, fever (40.8°C), mild dehydration, tachycardia, dyspnea and subcutaneous edema in the pelvic limbs and generalized enlargement of the lymph nodes.

Laboratory Results: A CBC performed at presentation revealed hypochromic macrocytic regenerative anemia, leucocytosis due to regenerative left shift and lymphocytosis, and regenerative thrombocytopenia (Table 1). Blood smears revealed marked anisocytosis and polychromasia, several RBC's with Howell-Jolly bodies, and large numbers of nucleated RBC's, mainly metarubricytes (23/100 leucocytes), but also lesser numbers of rubricytes (2/100 leucocytes). Marked spherocytosis and large platelets (macroplatelets) were additional findings in the blood smear. No blood parasites were found either within blood cells or free in the plasma.

The biochemistry panels showed mild increase in total plasma proteins due to increase in albumin, moderate increase in serum activity of alanine aminotransferase and marked increase in the total serum bilirubin (Table 2). Urinalysis revealed marked bilirubinuria.

Based on the laboratory results described above, a clinical diagnosis of extravascular hemolytic anemia was established. The marked spherocytosis suggested an immune mediated origin. The dog was treated with 1 mg/kg prednisone but died the following day.

Gross Pathology: There was marked yellow discoloration (icterus) of mucous membranes, skin, subcutaneous tissues and intima of large arteries. The spleen was markedly (about 5x) enlarged and had a dry (no blood oozing) fleshy texture to the cut surface. All lymph nodes were moderately enlarged, soft, light brown and wet at cut surfaces. The mucosa of the entire small intestine was dark red (hemorrhagic) and the contents were admixed with blood. The lungs were red and wet and did not collapse when the thoracic cavity was opened. Large amounts of fluid oozed from the cut surface of the lungs. A large amount of whitish-pink foam could be observed within the trachea and main bronchi (pulmonary edema). Additional findings included serous atrophy in the coronary adipose tissue of the heart, hydropericardium, petechiae and paint brush hemorrhages in the endocardium of the left ventricle. The bone marrow of the long bones was markedly red and filled the whole marrow space.

Histopathologic Description: Spleen and heart: In the spleen there is a marked inflammatory infiltrate consisting of some lymphocytes and large numbers of plasma cells. The cellular infiltrate obliterates a large part of the splenic red pulp. There are few plasmablasts and Mott cells within the inflammatory infiltrate; however, the majority of the inflammatory cells consists of mature plasma cells. Multiple aggregates of histiocytes are seen throughout the spleen and compress the adjacent splenic tissue. Oval to round, 2 µm protozoal organisms can be observed within the cytoplasm of endothelial cells of the splenic capillaries, but not in venules, arterioles, veins or arteries. There are 5-20 organisms per parasitized cell. In the liver (not submitted), there was paracentral coagulative zonal necrosis; the cholangioles and bile ductules were distended by bile pigment and there was a lymphoplasmacytic inflammatory infiltrate in the portal triads. The same inflammatory infiltrate is observed in the myocardium, renal interstitium, and pulmonary interalveolar septa. In the myocardium, the inflammatory infiltrate is associated with mild degeneration of cardiomyocytes. Large numbers of nucleated RBC's occurred within hepatic sinusoids. The protozoal organisms described in the spleen and myocardium can also be observed parasitizing endothelial cells of capillaries in the kidney, lymph nodes, liver, bone marrow and choroid plexus of the fourth ventricle. Transmission electron microscopy (TEM) of the choroid plexus (Fig. 4-9) shows zoites (z) within the cytoplasm (asterisk) of an endothelial cell. Zoites (z) can also be visualized by TEM within endothelial cells of a lymph node.

Contributor's Morphologic Diagnosis: 1) Spleen, reactive hyperplasia, lymphoplasmacytic, associated with intraendothelial zoites, morphology consistent with *Rangelia vitalii*. 2) Myocardium, myocarditis, lymphoplasmacytic, mild to moderate, with mild fiber degeneration, associated with intraendothelial zoites, morphology consistent with *Rangelia vitalii*.

Contributor's Comment: Based upon the clinicopathological findings, a diagnosis of hemolytic anemia associated with infection by *Rangelia vitalii* (rangeliosis) was made. Rangeliosis, colloquially known as nambi-uvú (in native Brazilian Indian idiom meaning literally "bleeding ear"), "peste de sangue" and "febre amarela dos cães" (Portuguese for "blood ill" and "yellow fever of dogs," respectively) is an extravascular hemolytic disorder affecting dogs from southern Brazil. For several reasons this disease remained almost forgotten for the last 50 years, and during this period it was variably mistakenly diagnosed as other canine infectious diseases (hemolytic or otherwise), such as babesiosis, erlichiosis and leishmaniasis. The true nature of the disease surfaced again in 2001 when a group of Brazilian researchers put forth an effort to elucidate its cause, pathogenesis and etiology, and thus established it as a distinct disease entity of dogs.[3,4,6] Although the precise taxonomic classification of the causative organism of rangeliosis is still uncertain, the agent was established as a protozoal organism of the phylum Apicomplexa, order Piroplasmorida based on ultrastructural, immunohistochemical and *in situ* hybridization studies.[5] Until definitive nomenclature is established, *Rangelia vitalii*

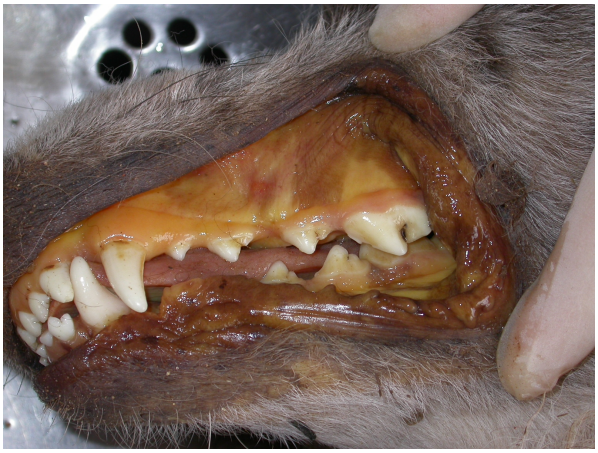

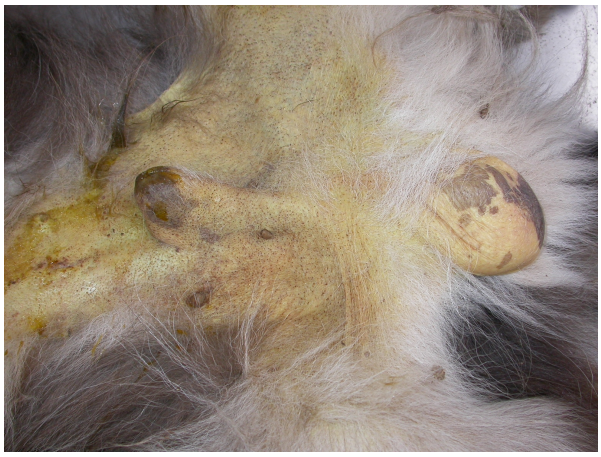

4-1, 4-2. Oral mucosa and skin, dog. Diffusely there is yellow discoloration (icterus) of mucous membranes and skin. Photographs courtesy of Departmento de Pathologia, Universidade federal de Santa Maria, Santa Maria Brazil, claudioslbarros@uol.com.br

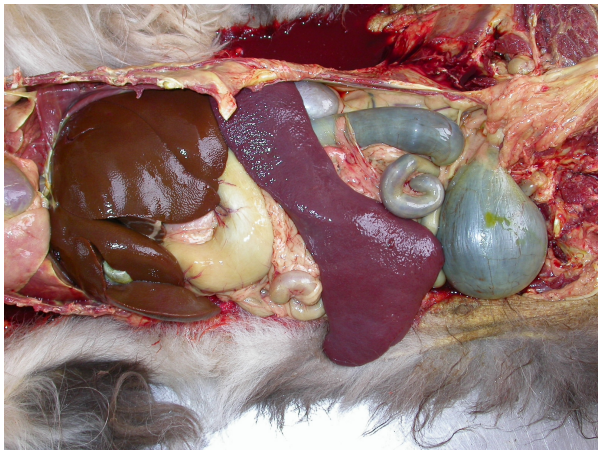

4-3, 4-4. Spleen, dog. The spleen is enlarged and has a dry, fleshy texture on cut surface. Photographs courtesy of Departmento de Pathologia, Universidade federal de Santa Maria, Santa Maria Brazil, claudioslbarros@uol.com.br

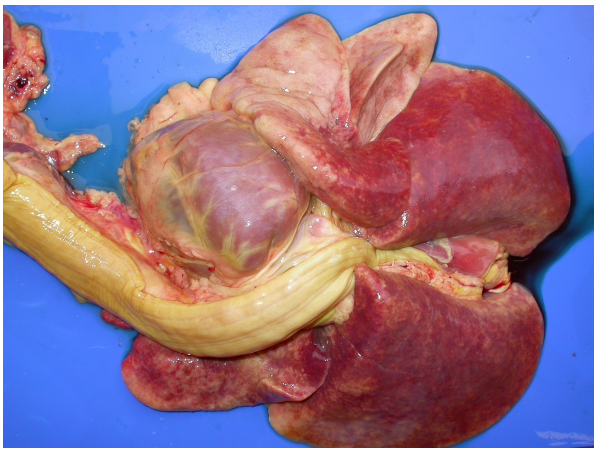

4-5. Heart and lung, dog. The lungs are red and wet and oozed large amounts of fluid from the cut surface. Photograph courtesy of Departamento de Pathologia, Universidade federal de Santa Maria, Santa Maria Brazil, claudioslbarros@uol.com.br

(named after two Brazilian researchers – from the first half of the 20th Century - Rangel and Vital) is maintained as the parasite's designation.

It is currently accepted that *R. vitalii* is transmitted by tick vectors (*Rhipicephalus sanguineus* and *Amblyomma aureolatum*) to dogs and several wild mammal species in the State of Rio Grande do Sul (RS) in southern Brazil. The life cycle of *R. vitalii* is unknown, but it has been speculated that the vectors *R. sanguineus* and *A. aureolatum* circulate the protozoan between wild mammals and domestic dogs, the latter probably being an aberrant host.[3] Experimental transmission to susceptible dogs using blood from spontaneously affected dogs was achieved recently in two independent studies.[4,5] The clinical and laboratory aspects of experimental disease differ somewhat from natural disease, suggesting that the parasite needs to replicate in the tick in order to acquire some aspects of virulence. Experimental disease is also fatal if left untreated.

The great majority of dogs with spontaneous rangeliosis develop clinical signs of extravascular hemolysis: pallor of mucous membranes; icterus; and hepatosplenomegaly.[3,4]

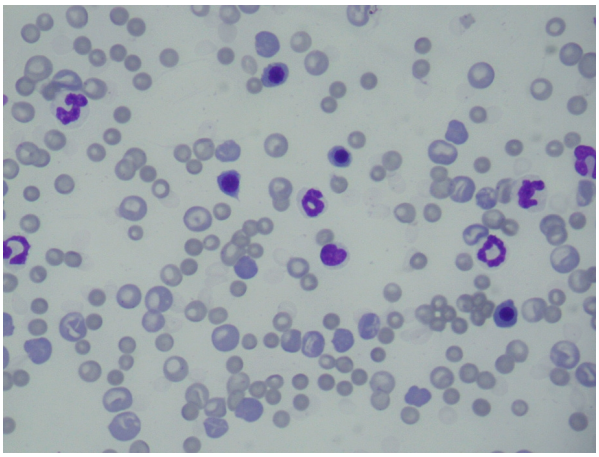

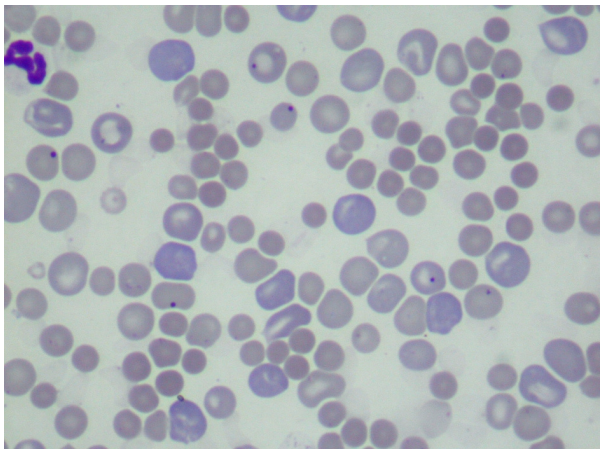

4-6, 4-7. Peripheral blood, dog. There is marked anisocytosis and polychromasia and several erythrocytes contain Howell-Jolly bodies. There are also many nucleated erythroid cells. Photographs courtesy of Departamento de Pathologia, Universidade federal de Santa Maria, Santa Maria Brazil, claudioslbarros@uol.com.br

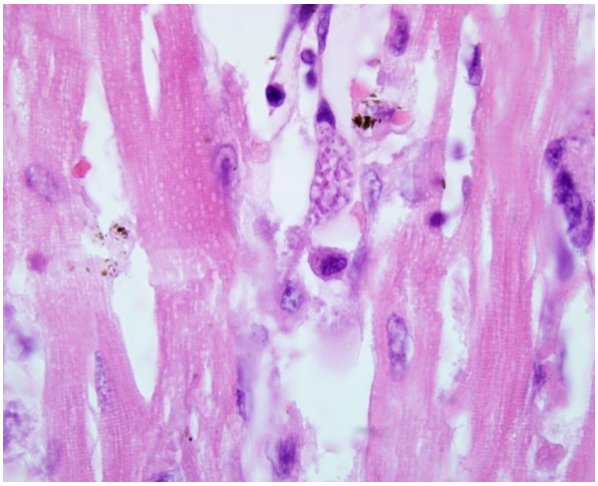

4-8. Heart, dog. Intraendothelial protozoal zoites measuring 5-20um are found vicinity areas of mild inflammation and degenerate cardiomyocytes. (HE 1000X)

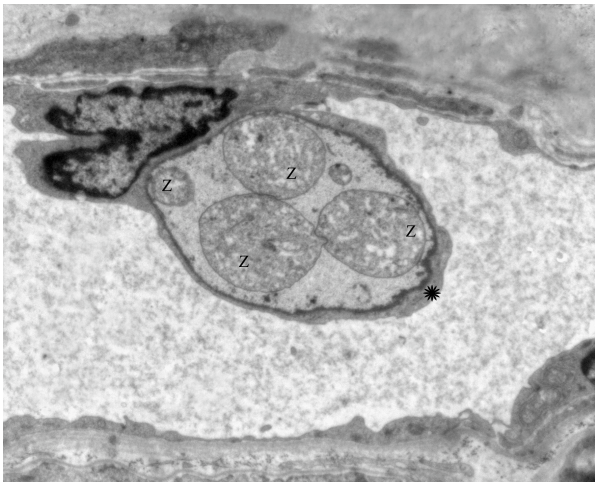

4-9. Choroid plexus, endothelial cell, dog. The cytoplasm contains several protozoal zoites (Z).(TEM) Photograph courtesy of Departamento de Pathologia, Universidade federal de Santa Maria, Santa Maria Brazil, claudioslbarros@uol.com.br

Other clinical signs include apathy, anorexia, fever, vomiting, diarrhea, mucopurulent oculonasal discharge, tachypnea, tachycardia, subcutaneous edema of the pelvic limbs, and petechiae and ecchymosis on the mucous membranes.[3]

Hematologic findings are typical of extravascular hemolysis and include hypochromic macrocytic anemia with excessive regeneration. Anisocytosis, polychromasia, Howell-Jolly bodies and several nucleated red blood cell precursors (metarubricytes and rubricytes) are observed on peripheral blood smears.[3,4] Most of the affected dogs also present with varying degrees of spherocytosis,[3,4] a hematological finding highly suggestive of immune mediated hemolytic anemia.[1] The numbers of circulating reticulocytes are high (5%-28%, average 12.5%). Erythrophagocytosis is occasionally observed, particularly in those cases in which there is marked associated spherocytosis. Normochromic normocytic anemia is observed on occasion due to the extreme contrast between the small and falsely hypochromic-appearing spherocytes and the large polychromatophils recently released from the bone marrow. Plasma from affected dogs is bright yellow. White blood cell counts frequently reveal leucocytosis due to regenerative left shift resulting from long-standing and non-specific stimulation on the bone marrow. In some of the cases the leucocytosis may present as a leukemoid reaction. Other common hematological findings include lymphocytosis and monocytosis.[3]

In a smaller percentage of the cases of spontaneous canine rangeliosis, affected dogs develop a bleeding disorder similar to disseminated intravascular coagulation (DIC) characterized by extensive hemorrhage from the tips, margins, and outer surface of the pinnae.[5] Dogs affected in this manner have a moderate decrease in platelet numbers and numerous large platelets are observed in the circulation, indicating regenerative thrombocytopenia. However, due to its moderate intensity, it is apparent that thrombocytopenia itself is insufficient to induce the hemorrhage in these dogs,

Table 1 – CBC (reference values are within parentheses)

WBCs (/mm^3)	32,200	(6,000-17.000)	RBC's (x10^6/mm^3)	1.3	(5.5-8.5)
Neutrophils (%)	72	(60%-77%)			
Neutrophils (abs.)	23,184	(3,000-11,500)			
Bands (%)	6	(0%-3%)	Hemoglobin (g/dL)	3.8	(12.0-18.0)
Bands (abs.)	1,932	(0-300)			
Metamyelocytes (%)	2	(0%)			
Metamyelocytes (abs.)	644	0	Hematocrit (%)	12	(37-55)
Myelocytes (%)	-	(0%)			
Myelocytes (abs.)	-	0			
Lymphocytes (%)	17	(12%-30%)	MCV (fl)	92.3	(60.0-77.0)
Lymphocytes (abs.)	5,474	(1,000-4,800)			
Monocytes (%)	2	(3%-10%)			
Monocytes (abs.)	644	(150-1,350)	MCHC (%)	31.7	(32.0-36.0)
Eosinophils (%)	1	(2%-10%)			
Eosinophils (abs.)	322	(100-1,250)			
Basophils (%)	-	(rare)	Platelets (x10^3/mm^3)	98	(200-500)
Basophils (abs.)	-	(rare)			

Table 2 – Biochemistry panel

Parameter	**Unit**	**Result**	**Reference values**
Alanine aminotransferase	U/L	180	4.0-24.0
Albumin	g/dL	4.4	2.6-3.3
Creatinine	mg/dL	1.2	0.5-1.5
Total bilirubin	mg/dL	6.5	0.1-0.5
Fibrinogen	mg/dL	200	200-400
Globulins	g/dL	4.2	2.7-4.4
Total plasma proteins	g/dL	8.8	6.0-8.0
BUN	mg/dL	56	21.0-60.0

and some other disorder(s) of hemostasis may be in place.[3,4] There is no specific biochemical test for the diagnosis of rangeliosis, but serum alanine aminotransferase (ALT) is increased in most cases. This elevation most likely results from anemia, hypoxia of centrolobular hepatocytes, and death of these cells. Bilirubin levels are consistently increased due to the extravascular hemolysis and the urine is darkened by the excretion of large amounts of bilirubin and urobilinogen; hemoglobinuria is never part of the clinical picture.[3]

In contrast to most infectious hemolytic anemias, the clinical diagnosis of rangeliosis is generally made on response to therapy, since the parasite is seldom found in the blood smears from affected dogs (only in approximately 4% of the cases).[3] Currently, there are no commercial or in-house tests to detect antibodies or antigens associated with *R. vitalii*. Fine needle aspiration (FNA) or excisional biopsy of lymph nodes, spleen and bone marrow with subsequent cytological evaluation can also be important aids in the clinical diagnosis. Due to the intraendothelial location of the parasite, fine needle aspiration may yield false negative results.

Necropsy findings in dogs dying from rangeliosis are consistent with those seen in other causes of extravascular hemolysis. The mucous membranes, subcutaneous tissue, muscle fascia, serosal surfaces and arterial intima are markedly icteric and peripheral blood is thin and watery. The liver is enlarged and has a red-orange hue or, in more severe cases, a greenish discoloration. Accentuation of the hepatic lobular pattern is common. The spleen is enlarged and fleshy and all lymph nodes are swollen, moist, and red,[3] and may have multifocal to coalescing white areas.[5] Hyperplastic bone marrow is markedly red and fills the entire marrow space.

Microscopic evaluation of lymph nodes reveals marked erythrophagocytosis and, depending on the stage of the disease, there is hemosiderosis and severe paracortical lymphoid hyperplasia. In the spleen, there is lymphoid hyperplasia characterized by marked plasmacytosis which, in some cases, resembles the plasma cell proliferation pattern observed in myelomas; however, in rangeliosis, most plasma cells are mature and there are few plasmablasts, Mott cells and/or "flame cells."[3]

In non-lymphoid organs, the same lymphoplasmacytic infiltrates are observed, and occasionally there is a granulomatous infiltrate which includes multinucleate giant cells that sometimes phagocytize parasitized endothelial cells.[4] In the liver, there is centrolibular coagulative necrosis and accumulation of bile pigment. In the bone marrow, there is marked erythroid and megakaryocytic hyperplasia characterized by replacement of the marrow adipose tissue by hematopoietic cells with high mitotic index, a drop in the myeloid to erythroid ratio, and increased numbers of megakaryocytes and megakaryoblasts. Foci of extramedullary hematopoiesis can be observed frequently in the spleen and liver and less frequently in the lymph nodes and adrenal glands.[3]

The parasite is found within the cytoplasm of endothelial cells in several organs and consists of 2.0-2.5 µm round to oval, basophilic organism when stained with hematoxylin and eosin; its cytoplasm is pale and inconspicuous and the nucleus is prominent, basophilic and eccentrically located.[3,5] The frequency in which the parasite was observed in several organs was reported from the study of 11 cases of canine rangeliosis as: kidneys (7/11), lymph nodes (7/11), liver (6/11), bone marrow (4/11), spleen (3/11), tonsils (2/11), lung, brain, stomach and gallbladder (1/11).[4] The authors pointed out that not all organs were histologically examined in each of the 11 cases. Other reports indicate lymph nodes, bone marrow, kidneys and choroid plexus are the organs with the highest parasite load.[4] About 20-30 organisms can be found within the cytoplasm of each parasitized endothelial cell. The organisms usually can be seen in smears from bone marrow sampled during the necropsy and stained with Giemsa and Panoptic.[4] In various reports, immunostaining for *Leishmania chagasi*, *Neospora caninum* and *Toxoplasma gondii* was consistently negative;[4,5] however, the parasite reacted positively with an anti-*Babesia microti* antibody.[5] *Rangelia vitalii* was also positive on *in situ* hybridization for *B. microti*[4] indicating that the organism belongs to the same group as *Babesia*. However, unlike babesia, *R. vitalii* is characterized by an intraendothelial stage. Parasitized cells are immunopositive for Von Willebrand factor, indicating their endothelial nature. The ultrastructural characteristics of *R. vitalii* were reported by Loretti & Barros 2005, (these authors mistakenly spelled the parasite's name as *R. vitalli*) as having an apical complex that includes a polar ring and rhoptries but no conoid; the parasite is contained within a parasitophorous vacuole that had a trilaminar membrane with villar protrusions and was located within the cytoplasm of capillary endothelial cells.[6]

Necropsy finding of dogs dying from rangeliosis, coupled with the hematological findings, suggest the diagnosis of hemolytic anemia; the finding of the causative agent in the cytoplasm of endothelial cells confirms a presumptive diagnosis.

Differentials for this case should include infection by *R. vitalii*, *Histoplasma capsulatum*, *Trypanosoma cruzi*, *Leishmania* spp., *Toxoplasma gondii*, and *Neospora caninum*. *Histoplasma* and *Leishmania* organisms are typically found in macrophages and may elicit an intense histiocytic to granulomatous response. *Histoplasma capsulatum* yeasts stain with PAS and GMS stains. *Leishmania* and *T. cruzi* have a kinetoplast, which is absent in *R. vitalii.* Additionally, the amastigotes of *T. cruzi* form pseudocysts within the sarcoplasm of cardiomyocytes and not within endothelial cells. The zoites of *T. gondii* and *N. caninum* form 2-5 µm and 4-7 µm tachyzoites, respectively, and have no kinetoplast. *N. caninum* can parasitize

	Extravascular Hemolysis	Intravascular Hemolysis
Cause (general categories)	1. Antibody and/or complement mediated 2. Decreased RBC deformability 3. Premature RBC aging (decreased glycolysis and [ATP]) 4. Increased macrophage phagocytosis	1. Complement-mediated lysis 2. Physical damage 3. Oxidative damage 4. Osmotic lysis 5. Membrane alterations
Onset	Usually chronic course with insidious onset	Peracute to acute
CBC	Neutrophilia, monocytosis, thrombocytosis	No significant findings
Biochemistry	Hyperbilirubinemia with the unconjugated form dominating early	1. Hemoglobinemia: plasma discolored red; increased MCHC and MCH; decreased serum haptoglobin 2. Hyperbilirubinemia with unconjugated form dominating early
Urinalysis	Bilirubinuria	Hemoglobinuria; hemosiderinuria; ± bilirubinuria
Erythrocyte morphology	Spherocytes, schistocytes, keratocytes; if a regenerative response, reticulocytes, Howell-Jolly bodies, polychromasia and macrocytosis	Schistocytes, keratocytes, Heinz bodies, eccentrocytes

endothelial cells but usually parasitize a large spectrum of host cells and are PAS positive. Similarly, *T. gondii* affects a large spectrum of host cells, although usually not endothelial cells, and induces a whole different set of lesions.

AFIP Diagnosis: 1. Heart: Myocarditis, lymphoplasmacytic and histiocytic, multifocal, mild to moderate with cardiomyocyte degeneration, capillary fibrin thrombi and numerous intraendothelial protozoa.
2. Spleen: Plasmacytosis, diffuse, marked with multifocal reticuloendothelial cell hyperplasia and scattered intraendothelial protozoa.

Conference Comment: The contributor provides an excellent, thorough discussion of this unique and poorly-known infection. Conference participants were unfamiliar with this condition, and many favored *T. cruzi.* The key observation necessary to reach the correct diagnosis is the intraendothelial location of the organism. Once that is recognized, literature searches could lead to articles on this fascinating disease.

While reviewing the submitted CBC, biochemistry panel and cytology, conference participants discussed the clinicopathologic differentiation between extravascular and intravascular hemolysis. The diagnostic features for each are briefly summarized in the chart above.[2]

Certain breeds of dogs and cats possess hereditary biochemical deficiencies or predispositions to extravascular hemolysis.[2] In dogs, phosphofructokinase deficiency is seen in cocker spaniels, English springer spaniels and some mixed breeds. Pyruvate kinase deficiency is noted to occur in the Basenji, beagle, Chihuahua, dachshund, pug, miniature poodle, West Highland White terrier, and Cairn terriers as well as Abyssinian, Somali and domestic short-haired cats. A hereditary predisposition to hemolytic anemia is suspected in the border collie, cocker spaniel, English springer spaniel, German shepherd dog, Irish setter, Old English sheepdog, poodle and the whippet.

Contributor: Departamento de Patologia, Universidade Federal de Santa Maria, Santa Maria, RS, Brazil. http://www.ufsm.br/lpv

References:
1. Barker RN. Anemia associated with immune responses. In: Feldman BF, Zinkl JG, Jain NC, eds. *Schalm's Veterinary Hematology*. 5th ed. Philadelphia, PA: Lippincott Williams & Wilkins; 2000:169-177.
2. Brockus CW, Andreasen CB. Erythrocytes. In: Latimer KS, Mahaffey EA, Prasse KW, eds. *Duncan and Prasse's Veterinary Laboratory Medicine: Clinical Pathology*. 4th ed. Ames, IA: Blackwell Publishing; 2003:26-38.
3. Fighera RA. Rangeliose. *Acta Scientiae Veterinariae* 2007;35(Supl2):264-266.
4. Krauspenhar C, Fighera RA, Graça DL. Anemia hemolítica em cães associada a protozoários. *MEDVEP* 2008;1:273-281.
5. Loretti A, Barros SS. Hemorrhagic disease in dogs infected with an unclassified intraendothelial piroplasm in southern Brazil. *Vet Parasitol*. 2005;134:193-213.
6. Loretti A, Barros SS: Infecção por Rangelia vitalli ("Nambiuvú, "Peste de Sangue") em caninos: revisão. *MEDVEP*. 2004;2:128-144.

The Armed Forces Institute of Pathology
Department of Veterinary Pathology

Conference Coordinator
Matthew Wegner, DVM

WEDNESDAY SLIDE CONFERENCE 2010-2011

Conference 8

6 October 2010

Conference Moderator:
Mike Garner, DVM, PhD, Diplomate ACVP

CASE I: S981/08 (AFIP 3163067).

Signalment: 1-year-old male Snowy owl (*Nyctea scandiaca*).

History: The owl lived in a farm with several other birds, including owls and different birds of prey. The animal had no history of previous illnesses and developed clinical signs one day before death in autumn 2008. The vaccination status of the owl is unknown. Predominant clinical signs were apathy and severe cyanosis, thus the private veterinarian started a therapy against shock. Because the clinical symptoms did not improve, the owl was euthanized due to poor prognosis.

Gross Pathology: The carcass was in good body condition with plenty of adipose tissue. Both the liver and spleen were dark red to reddish purple and were mild to moderately enlarged (hepato- and splenomegaly). During cut sections, a small amount of blood flowed from the organs (mild hyperaemia). Throughout the whole parenchyma of liver and spleen, numerous yellow-white partly coalescing caseous foci (approximately 1.0 to 2.0 mm size in diameter) were found. These were interpreted to be necrosis. The serous membranes of both organs were normal. Further findings during necropsy were moderate numbers of granulomas diffusely distributed among the aerosaccula, and mild to moderate uric acid scaling within the kidneys. Additionally, some bird lice (*Menacantus* sp.) were found on the feathers. All other organs, including the bone marrow, appeared normal.

Laboratory Results: Microbiological and virological examination was performed from samples of the liver, spleen and the lungs. The results are listed below.

Lungs: *Aspergillus* spp.; coagulase-negative *Streptococcus* spp.; and *Escherichia coli.*

Liver and spleen: no bacterial growth observed.

Extracts from liver and spleen were cultured on chicken-embryo-hepatocytes and chicken-embryo-fibroblasts in cell culture and the supernatant was analyzed on an electron microscope. These examinations revealed *Herpesviridae* in both organ samples.

Histopathologic Description: Liver: The parenchyma is multifocally replaced by areas of degenerate hepatocytes and acute central(ly) coagulating necrosis. Several affected areas are coalescing. Adjacent to these areas, the hepatocytes show variable stages of degeneration with pyknosis and karyorrhexis and peripheral nuclear hyperchromasia. Numerous affected hepatocytes, primarily at the edges of necrotic regions, show eosinophilic intranuclear inclusion bodies (Cowdry A-type). There is no inflammatory infiltration or demarcation of the necrotic regions. Occasionally, intravascular coagulopathy is seen in some arterial and venous vessels of the portal fields and central veins sometimes contain fibrin thrombi. Some portal vessels and central veins frequently show intravascular leucocytostasis. The capsule of the organ, as well as portal fields, bile ducts and hepatocytes of unaffected areas are normal.

Spleen: The parenchyma is replaced by multifocal to coalescing areas of acute necrosis, partly associated with acute haemorrhages resulting in complete loss of the typical architecture of the organ. Several reticuloendothelial cells of the white pulp closely adjacent to these regions contain eosinophilic intranuclear inclusion bodies (Cowdry A-type). A beginning demarcation of necrotic regions by granulocytes is seen in some areas of the spleen. The unaffected white pulp is highly depleted. Furthermore, numerous histiocytes are filled with a brown, chunky pigment (haemosiderocytes). Frequently, areas with an accumulation of dark brown pigment that appears green at the borders can be seen (formalin-pigment). The capsule of the organ is normal.

Contributor's Morphologic Diagnosis: 1. Liver: Moderate, acute, multifocal sometimes coalescing necrosis, with multifocal eosinophilic intranuclear inclusion bodies, *Herpesviridae*.
2. Spleen: Severe, acute, multifocal to coalescing necrosis, with multifocal eosinophilic intranuclear inclusion bodies, *Herpesviridae*.

Contributor's Comment: The clinical and pathological findings in this case represent the typical syndrome of *hepatosplenitis infectiosa strigum* (HSIS) in a snowy owl. This infectious disease of wildlife and captive birds usually runs fatal within a few days and is caused by a herpesvirus.

The family of avian herpesviruses comprises three subfamilies, including alpha-, beta- and gamma-Herpesviruses. Each name for the genera derives from the predominant clinical and pathological findings.[10] *Hepatosplenitis infectiosa strigum* (HSIS) is caused by the *strigid herpesvirus-1* (SHV-1) and is dedicated to the betaherpesviruses (synonym "hepatosplenitis viruses"). This disease occurred in 1915 in Austria for the first time (retrospective examination of fixed tissue samples of affected birds),[3] but was first described in the United States in 1936.[8] It is seen frequently in Germany since 1969.[4,12] The SHV-1 is a strict host-specific pathogen that reveals close similarities to the *falconid herpesvirus-1* (FHV-1) and the *columbid herpesvirus-1* (CHV-1). Due to the large genomic homology, a PCR styled to detect the CHV-1 can also be used to detect SHV-1 and FHV-1.[1] Reported susceptible species of owls for HSIS are: the Eagle Owl (*Bubo bubo*), the Great Horned Owl (*Bubo virginianus*), the Striped Owl (*Asio clamator*), the Long-eared Owl (*Asio otus*), the Snowy Owl (*Nyctea scandiaca*), the Little Owl (*Athene noctua*), and the Boreal Owl (*Aegolius funereus*), whereas the Eurasian Tawny Owl (*Strix aluco*) and the Barn Owl (*Tyto alba*) seem to be naturally resistant.[4] However, other authors have shown that American Kestrels, Budgerigars and Ring-Necked Doves are susceptible for experimental infections, as well.[12]

Additionally, evidence for latent infections was found, given the fact that antibody-positive but healthy animals could be observed.[9] As reported by Burtscher and Sibalin,[4] only owls with a yellow or orange coloured iris (of the aforementioned species) have proven to be susceptible, whereas species with dark irises (e.g. Tawny Owls and Barn Owls) were resistant, even to massive experimental infections. However, the authors considered this finding not to be significant, but remarked further investigations were needed to clarify.

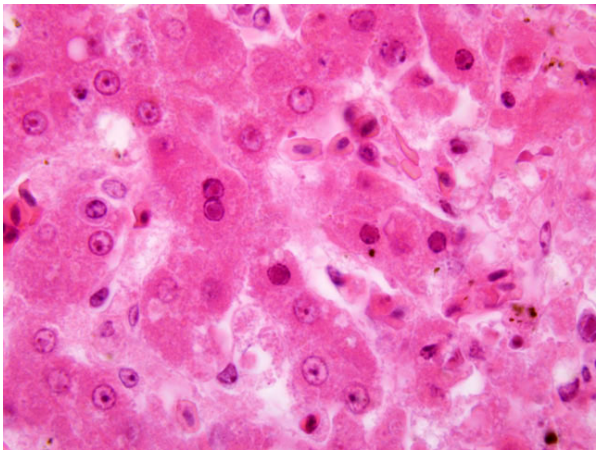

1-1. Liver, owl. Multifocally, degenerate hepatocytes occasionally contain eosinophilic intranuclear inclusion bodies that marginate the chromatin. (HE 1000X)

The virus has a tropism for mesenchymal cells and to a lesser extent epithelial cells.[2,4] An oropharyngeal route of infection is assumed. Virus-shedding takes place through the pharynx and urine. After an incubation period of 7 to 10 days, affected animals show apathy, anorexia and ruffled feathers. At later stages, they support themselves with their wings standing on the soil and fall into the prone position in which they are perishing in the following period.[2,8,11]

As in the present case, findings during necropsy are: good nutritional condition, swelling of the liver (hepatomegaly) and pale white foci of caseous necrosis in liver, spleen and bone marrow (not recorded in this case). Microscopic examinations reflect the necrotic regions to be mostly without any inflammatory reaction presumably due to the fulminant clinical progress of the disease. Viable and degenerating hepatocytes, particularly at the edges of the necrotic foci, show intranuclear eosinophilic inclusion bodies (Cowdry A-type).[2,8,11]

It was not possible to establish the source of the infection in this case. Even intense anamnestic survey could not identify potential reservoirs (no acquisition of animals, no contact to wildlife animals and no changes in the acquisition of prey animals). Regardless, no further infections were recorded in this aviary. This might be due to the strict hygienic prevention (including the prey animals) that was performed acting upon the advice of the private veterinarian and the Institute of Pathology of the University of Leipzig.

AFIP Diagnosis: 1. Liver: Hepatitis, random, necrotizing, acute, multifocal, moderate, with hepatocellular intranuclear eosinophilic inclusion bodies.

2. Spleen: Splenitis, necrotizing, acute, multifocal to coalescing, marked with intranuclear eosinophilic inclusion bodies.

Conference Comment: Most participants readily identified the intranuclear hepatocellular inclusions, which all diagnosed as consistent with herpesviral infection. A brief discussion of other causes of intranuclear inclusion bodies followed, which in addition to viral etiologies, include heavy metals, such as lead or bismuth); cytoplasmic nuclear invaginations that result in pseudoinclusions; and occasionally, neoplastic cells accumulate tubules and filaments resulting in histologically visible intranuclear inclusions.[5,6] In addition to infection by other herpesviruses, other avian viruses producing intranuclear inclusions include avian adenoviruses, psittacine circovirus, avian paramyxovirus 1 (Newcastle disease) and avian polyoma virus. Avian adenoviruses and herpesviruses are the primary agents causing intranuclear inclusions in the hepatocytes of owls.

Some discussion focused on the epidemiology of HSIS in wild birds of prey. The moderator mentioned that this disease is only seen in wild, and not captive, falcons and owls. Recent research demonstrated that the herpesviruses isolated from owls, falcons, hawks and pigeons were all identical. The authors concluded that owls, falcons and hawks are infected with the same virus, Columbid herpesvirus-1, and therefore captive birds of prey should not be fed pigeons.[7]

The moderator commented that a few avian herpesviruses are associated with neoplasia. One example, Psittacid herpesvirus-1, the etiology of Pacheco's disease, is known to cause psittacine papillomatosis; gross findings are papillomas in the choana and cloaca.[14] The herpesviral induced proliferative epithelial lesions can undergo malignant transformation to squamous cell carcinoma or adenocarcinoma. More recently, DNA from this virus was detected in a pancreatic duct carcinoma in a macaw.[13]

Contributor: Institut für Veterinär-Pathologie, An den Tierkliniken 33, 04103 Leipzig, Germany
http://pathologie.vetmed.uni-leipzig.de/

References:

1. Aini I, Shih LM, Castro AE, Zee YC. Comparison of herpesvirus isolates from falcons, pigeons and psittacines by restriction endonuclease analysis. *J Wildl Dis*. 1993;29:196-202.
2. Burki F, Burtscher H, Sibalin M. Herpesvirus strigis: a new avian herpesvirus. I. Biological properties. *Arch Gesamte Virusforsch*. 1973;43:14-24.
3. Burtscher H. Die virusbedingte Hepatosplenitis infectiosa strigum. 1. Mitteilung: Morphologische Untersuchungen. *Pathol Vet*. 1965;2:227-255.
4. Burtscher H, Sibalin M. Herpesvirus strigis: host spectrum and distribution in infected owls. *J Wildl Dis*. 1975;11:164-169.
5. Cheville NF. Response to cellular injury. In: *Ultrastructural Pathology: The Comparative Basis of Cellular Disease*. 2nd ed. Ames, IA: Wiley-Blackwell; 2009:13.
6. Cheville NF. The neoplastic cell. In: *Ultrastructural Pathology: The Comparative Basis of Cellular Disease*. 2nd ed. Ames, IA: Wiley-Blackwell; 2009:7665.
7. Gailbreath KL, Oaks JL. Herpesviral inclusion body disease in owls and falcons is caused by the pigeon herpesvirus (Columbid herpesvirus 1). *J Wildl Dis*. 2008; 44(2):427-433.
8. Green RG, Shillinger JE. A virus disease of owls. *Am J Pathol*. 1936;12:405-410.
9. Kaleta EF, Drüner K. Hepatosplenitis infectiosa strigum und andere Krankheiten der Greifvögel und Eulen. *Zentralblatt Vet Med*. 1976;25(Suppl):173-180.
10. Kaleta EF. Herpesviruses of birds: a review. *Avian Pathol*. 1990;19:193-211.
11. Lee LF, Armstrong RL, Nazerian K. Comparative studies of six avian herpesviruses. *Avian Dis*. 1972;16:799-808.
12. Mare CJ. Herpesviruses of birds of prey. *J Zoo Animal Med*. 1975;6:6-11.
13. Mundhenk L, Müller K, Lierz M, et al. Psittacid herpesvirus DNA in a pancreatic duct carcinoma in a macaw. *Vet Rec*. 2009;164:306-308.
14. Styles DK, Tomaszewski EK, Jaeger LA, Phalen DN. Psittacid herpesviruses associated with mucosal papillomas in neotropical parrots. *Virology*. 2004;325(1):24-35.

CASE II: A09-35528 (AFIP 3138059).

Signalment: Group of less than 1-year-old mixed sex African cichlid fish, Family Cichlidae, Genus and species unknown.

History: The fish were part of a large shipment of pond raised African cichlid fish that had been held in quarantine approximately two weeks prior to the onset of mortalities. Losses had reached 25% at the time of submission. Reported gross necropsy findings included abdominal distension and cloudy, gelatinous intracoelomic fluid.

Gross Pathology: None provided.

Histopathologic Description: Whole body, transverse section: Changes vary slightly between sections from individual fish. The normal architecture of the gastric wall has been transmurally effaced and replaced by broad sheets of predominantly epithelioid macrophages, interspersed with variable mixed numbers of lymphocytes, proliferating fibroblasts, and occasional discrete granulomas. However, more extensive, multifocal to coalescing granuloma formation, with central necrosis and wide mantles of epithelioid cells are more frequently encountered in some sections. Only isolated remnants of gastric mucosa and smooth muscle remain. Present throughout are small vacuolated spaces containing one to several, elongated pyriform, approximately 5 x 10 µm organisms with a distinct nucleus and dense basophilic kinetoplast located peripherally against one long body axis. Large numbers of mixed bacteria are widely distributed in most sections. The degree to which the inflammatory process extends beyond the gastric serosa also varies between individual fish. In some sections, isolated foci of granulomatous inflammation and granulomas are scattered throughout the mesenteric fat, while in others extensive sheets of inflammatory cells and fibroplasia encroach upon and infiltrate the hepatic capsule. In these sections, multiple foci of necrosis, granuloma formation, and organisms as previously described can be found in the liver and head kidney.

Contributor's Morphologic Diagnosis: 1. Stomach: Gastritis, necrotizing and granulomatous, transmural, diffuse, severe, with multifocal granulomas, adjacent granulomatous peritonitis and intralesional protozoa.
2. Liver and Kidney (variable between sections): Multifocal necrosis, granulomatous inflammation and epithelioid granulomas with intralesional protozoa.

Contributor's Comment: Consistent with the referring veterinarian's findings, follow-up necropsies performed on euthanized moribund fish revealed abdominal distension and cloudy ascites. Stomachs were extremely friable when manipulated and large numbers of bi-flagellated protozoans, with undulating motility, were observed in gastric mucosal scrapings.

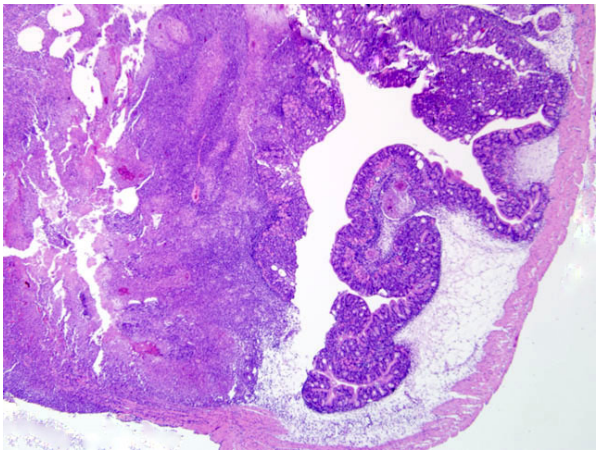

2-1, 2-2. Stomach, African cichlid fish. Transmurally, the stomach is infiltrated and effaced by many epithelioid macrophages, fewer lymphocytes, and fibroblasts. Admixed with inflammatory cells are clear vacuoles that contain one to several 5x10 µm elongated, pyriform organisms. (HE 40X, 1000X)

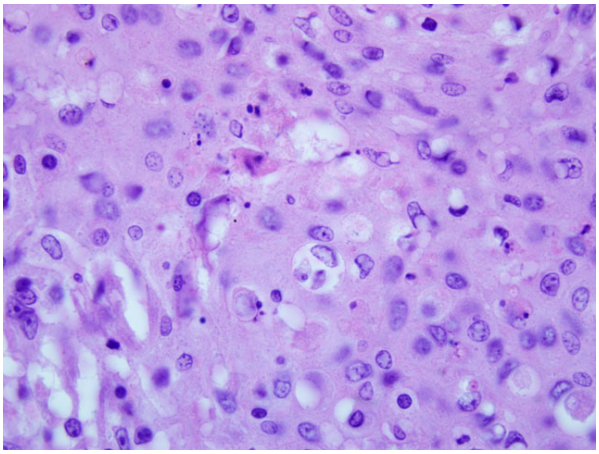

Microscopic findings of severe granulomatous gastritis are consistent with descriptions of *Cryptobia iubilans* (order Kinetoplastida, family Bodonidae) infection in other cichlid fishes.[1,4,6] The Kinetoplastidea are flagellates with long, tubulous mitochondria curved inside the cell, which contain a kinetoplast, an organized DNA "nucleoid." Easily detected by Giemsa and Feulgen stains, it is usually single and located close to the kinetosome. One or two flagella may be present and most parasitic forms are transmitted by a vector.

Although 52 *Cryptobia* spp. have been tentatively identified in fish, most are leech transmitted hemoparasites and it has been proposed they be assigned to the Trypanoplasma.[2,3] The only fish pathogenic intestinal species, *C. iubilans*, has a direct life cycle and is common in cichlid fishes. The parasite is ovoid to elongate and averages 19 x 5 µm. The anterior flagellum is 1.5 - 2 times the body length and the recurrent flagellum, attached along the ventral axis, extends 11-19 µm beyond the body. Posterior to the flagellar pocket is a slender triangular kinetoplast. A spherical nucleus lies in the anterior half of the body and the cytoplasm contains large vacuoles filled with glycogen reserves.[3] Additional electron microscopic features are available in the literature.[6]

Histopathologic lesions in light infections are confined primarily to the stomach and may range from isolated granulomas to diffuse granulomatous gastritis. In severe cases there can be multi-organ involvement associated with a similar necrotizing and granulomatous response, as seen in the livers and head kidney of some sections. The parasite may occur extracellularly or intracellularly within macrophages, where it is confined to a large parasitophorus vacuole.[2,6]

It has been suggested that *C. iubilans* may be a part of the normal gastrointestinal fauna, becoming pathogenic only under certain stressful conditions.[6] There are no effective treatments and losses can be acute and severe. Differentials for *C. iubilans* infection include other flagellates, primarily *Spironucleus vortens*. This organism is seen typically in the intestinal lumen and while it does not evoke as intense an inflammatory response, systemic spread can occur as well. On wet mounts this diplomonad is differentiated from *C. iubilans* by its linear movement and 8 flagella.[6] Although mycobacteriosis was considered, acid-fast stains and mycobacterial cultures performed on multiple fish were negative.

AFIP Diagnosis: 1. Stomach and intestines: Gastroenteritis, transmural, granulomatous and necrotizing, diffuse, severe with protozoal trophozoites and many bacilli.
2. Liver; pancreas; mesentery; and kidney: Granulomas, with coelomitis.

Conference Comment: The moderator pointed out that most cases of *Cryptobia* spp. infection in fish are not as visually appealing as in the slides of this case in which there is excellent tissue preservation and minimal autolysis. The moderator commented on the difficulty in detecting this organism during routine histologic examination within necrotic tissues, because the dead organisms appear remarkably similar to degenerate inflammatory cells. Finally, the moderator noted that cryptobiasis is the most important infectious disease of cichlids. Another species in the genus, *Cryptobia salmositica*, infects Pacific salmonids in the western United States.

The contributor provides an excellent review of this important disease of cichlids. Clincally, parasitemia results in anemia, exophthalmia, ascites, positive Coombs' test, microcytic hypochromic anemia, and anorexia. As a brief additional note, isolation of a cysteine protease and metalloprotease from the organism recently provided useful information regarding the pathogenesis of disease; current research is focused on the metalloproteinase that causes lysis of erythrocytes. Additionally, the protein degrades types I, IV and V collagen and laminin, aiding invasion and generation of the observed histologic lesions.[5]

Contributor: Department of Pathology, College of Veterinary Medicine, University of Georgia, Athens, GA 30602
http://www.vet.uga.edu/VPP/index.php

References:
1. Dykova I, Lom J. Definition of flagellates and lesions Due to various flagellates. In: *Histopathology of Protistan and Myxozoan Infections in Fishes: An Atlas*. Praha, Czech Republic: Academia; 2007:79-87.
2. Francis-Floyd R, Yanong R. Cryptobia iubilans in Cichlids. University of Florida Institute of Food and Agricultural Sciences Extension Publication VM 104.
3. Gou FC, Woo PTK. Selected parasitosis in cultured and wild fish. *Vet Parasitol*. 2009;163: 207-216.
4. Lom J, Dykova I. Flagellates (Phylum Mastigophora Diesing, 1866). In: *Protozoan Parasites of Fishes*. Amsterdam, The Netherlands: Elsevier Science Publishers; 1992:48-53.
5. Woo PTK. Immunological and therapeutic strategies against salmonid cryptobiosis. *J Biomed Biotechnol*. 2010;10(Article ID 341783):9 pages.
6. Yanong RP, Curtis E, Russo R, et al. *Cryptobia iubilans* infection in juvenile discus. *J Am Vet Med Assoc*. 2004;224:1644-1650.

CASE III: G08-049679 (AFIP 3167328).

Signalment: Male mature captive bred Timneh African Grey parrot (*Psittacus erithacus timneh*).

History: This bird was one member of a research colony that had been created to study fecal virus shedding in psittacine birds with proventricular dilatation disease (PDD). All birds in this colony had a history of exposure to other birds with PDD. This individually caged bird had not shown any signs of neurological or gastrointestinal disease over the course of the study.

Gross Pathology: No gross lesions seen at necropsy.

Laboratory Results: Histopathological lesions consistent with PDD were identified in cerebrum, cerebellum, brainstem, spinal cord, brachial nerve, vagus nerve, adrenal gland, crop, proventriculus, ventriculus and heart. Tissues positive for avian bornavirus (ABV) antigen by immunohistochemistry (IHC) include cerebellum, brainstem, spinal cord, adrenal gland and ventriculus. Tissues positive for ABV antigen by RT-PCR include cerebrum, cerebellum, brain stem, spinal cord and adrenal gland.

Histopathologic Description: Brain: Multiple cerebral and meningeal vessels are lined by mildly hypertrophied endothelial cells with partial to complete perivascular cuffs of variable thickness (1-8 cells thick) composed of predominantly lymphocytes and plasma cells with fewer macrophages.

Crop: Variable numbers of plasma cells and lymphocytes infiltrate around and within blood vessels, nerves and ganglia in the tunica muscularis. Infrequently, a few plasma cells and lymphocytes have infiltrated between smooth muscle fibers of the tunica muscularis. Occasional moderate sized lymphoid aggregates are present in the lamina propria.

Contributor's Morphologic Diagnosis: 1. Mild to moderate cerebral and meningeal lymphoplasmacytic perivascular cuffing.
2. Mild to moderate multifocal lymphoplasmacytic ganglioneuritis and mild multifocal non-suppurative leiomyositis of the crop compatible with proventricular dilatation disease (PDD).

Contributor's Comment: Plasmacytic and lymphocytic infiltrates in the myenteric ganglia of the crop, proventriculus, ventriculus and duodenum are characteristic of proventricular dilatation disease (PDD). This disease has also been called macaw wasting disease, neuropathic gastric dilatation in psittaciformes[7] and myenteric ganglioneuritis[6] and has been reported in many species of psittacine birds.

Similar pathological findings have been identified in Canada geese[2] and recently in various Passeriformes.[11] Psittacine birds affected with PDD can exhibit gastrointestinal signs including anorexia, emaciation, weight loss, regurgitation, delayed crop emptying, diarrhea and the presence of undigested seeds in the feces and/ or neurological signs such as ataxia, tremors, seizures and motor or proprioceptive defects.[3] Sudden death with the absence of clinical signs has also been reported. It is now known that the characteristic lymphoplasmacytic infiltrates can occur in many tissues of the central and peripheral nervous system and not all affected birds exhibit nervous signs clinically[1] as demonstrated by this bird. This bird did not show any signs of neurological disease for a year prior to euthanasia but histologically had widespread cerebral and meningeal perivascular lymphoplasmacytic cuffing.

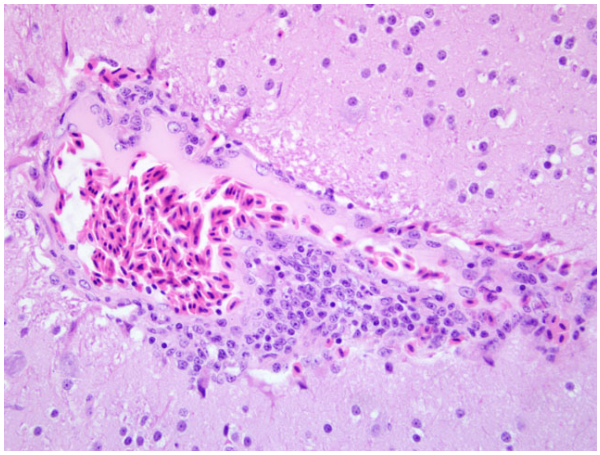

3-1. Brain, African grey parrot. Multifocally, cerebral vessels are surrounded by low to moderate numbers of lymphocytes, macrophages, and plasma cells and the endothelium is hypertrophied and reactive. (HE 400X)

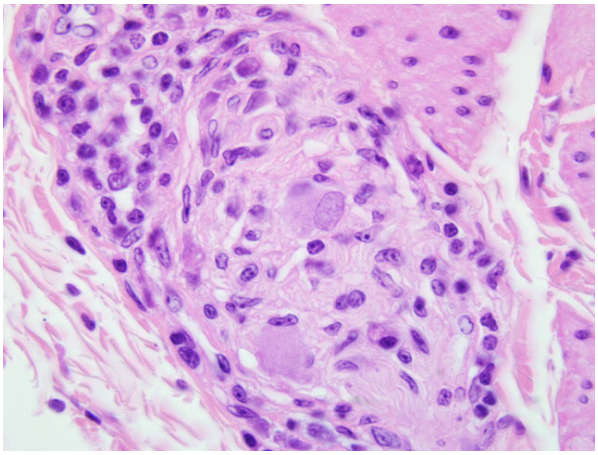

3-2. Crop, ganglia, African grey parrot. Multifocally, ganglia are infiltrated by low numbers of lymphocytes, macrophages, and plasma cells. (HE 1000X)

The characteristic cellular infiltrates of PDD are variable in size and distribution as demonstrated by the lesions in the sections of brain and crop provided for this case. In some sections of crop, numerous plasma cells and lymphocytes are present within the nerves and ganglia, while in other sections, only rare plasma cells or lymphocytes can be identified. Historically, examination of multiple sections of biopsied

tissues, such as crop, or multiple sections of gastrointestinal tract collected at necropsy was needed to improve diagnostic accuracy.

An avian bornavirus (ABV) has recently been proposed as the etiological agent of PDD, and evidence from bird inoculation studies is strongly supportive.[4,5] Through collaborative efforts of researchers from the University of California, San Francisco, the Ontario Veterinary College and the Animal Health Laboratory, University of Guelph, an ABV specific RT-PCR screening test and immunohistochemistry (IHC) that detects the ABV nucleocapsid protein have been developed and tissues from psittacine birds with and without PDD were tested. Those results were compared with the histopathologic diagnoses and the sensitivity and specificity of IHC for detection of ABV antigens on a bird by bird basis were found to be 100% and 100%, respectively. Many more tissues were positive for ABV RNA by RT-PCR than were positive histopathologically or for viral antigens by IHC. Brain tissues, but not crop tissues, from this bird were positive by RT-PCR for ABV antigen. Similar results were obtained with IHC testing. Overall, brain tissue appears to be the tissue that is most consistently positive with both PCR and IHC testing. It is suggested that IHC and or RT-PCR testing of biopsy specimens, in addition to histopathology, may help increase the sensitivity of diagnosis of PDD allowing for earlier identification of infected birds.[11]

AFIP Diagnosis: 1. Brain: Meningoencephalitis, lymphohistiocytic and plasmacytic, perivascular, multifocal, mild.
2. Crop, ganglia: Ganglioneuritis, lymphohistiocytic and plasmacytic, multifocal, mild.

Conference Comment: Borna disease virus (BDV) is the sole member of the family *Bornaviridae*, order *Mononegavirales*. The virus is spherical and enveloped with negative-sense single-stranded RNA.[8] Replication within infected cells occurs in the nucleus; viral inclusions typically are seen only in cell culture. BDV is neurotropic, resulting in persistent, non-cytolytic infection of the central nervous system.[9] The virus is known to naturally infect a wide variety of animals, including horses, sheep, cattle and rabbits.[8] The virus is implicated in human neuropsychoses, such as depression, schizophrenia, obsessive compulsive disorder and chronic fatigue syndrome.[12] The disease is best characterized in equids, where after a four week incubation period the infected horse exhibits non-specific signs of colic, fatigue, coughing and icterus followed by alternating periods of excitability and somnolence. Neurologic signs progress over the next 3-20 days, leading to the death of the animal.[8]

The pathogenesis and persistence of the virus within infected cells is complex. Once infection is established, the virus interferes with many intracellular signaling pathways involved in spread of the virus, maintenance of viral persistence, and modulation of neurotransmitter pathways.[9] Neuronal death is due to effector CD8+ T cells which kill infected cells.[12] Studies in laboratory infected mice demonstrated a positive correlation between lesion severity and increased levels of IL-6, TNF-α, IL-α and inducible nitric oxide synthase mRNA.[12]

Contributor: Animal Health Laboratory, University of Guelph, Guelph, Ontario, Canada
http://ahl.uoguelph.ca

References:
1. Berhane Y, Smith DA, Newman S, et al. Peripheral neuritis in psittacine birds with proventricular dilatation disease. *Avian Pathol*. 2001;30:563-570.
2. Daoust PY, Julian R, Yason CV, Artsob H. Proventricular impaction associated with nonsuppurative encephalomyelitis and ganglioneuritis in two Canada geese. *J Wildlife Dis*. 1991; 27:513-517.
3. Degernes LA, Flammer K, Fisher P. Proventricular dilatation syndrome in a Green-Winged Macaw. *Proceedings of the Annual Conference of the Association of Avian Veterinarians*. 1991;45-49.
4. Gancz AY, Kistler AL, Greninger AL, et al. Experimental induction of proventricular dilatation disease in cockatiels (*Nymphicus hollandicus*) inoculated with brain homogenates containing avian bornavirus 4. *Virol J*. 2009;6:100.
5. Gray P, Hoppes S, Suchodolski P, et al. Use of avian bornavirus isolates to induce proventricular dilatation disease in conures. *Emerg Infect Dis*. 2010;16:473-479.
6. Joyner KL, Kock N, Styles D. Encephalitis, proventricular and ventricular myositis, and myenteric ganglioneuritis in an Umbrella Cockatoo. *Avian Dis*. 1989;33:379-381.
7. Mannl A, Gerlach H, Leipold R. Neuropathic gastric dilatation in Psittaciformes. *Avian Dis*. 1987;31:214-221.
8. Murphy FA, Gibbs EPJ, Horzinek MC, Studdert MJ. Bornaviridae. In: *Veterinary Virology*. 3rd ed. vol.1. San Diego, CA: Elsevier Academic Press; 1999:455-458.
9. Planz O, Pleschka S, Wolff T. Borna disease virus: A unique pathogen and its interaction with intracellular signaling pathways. *Cell Microbiol*. 2009;11(6):872-879.
10. Perpiñán D, Fernández-Bellon H, López C, Ramis A. Lymphoplasmacytic myenteric, subepicardial and pulmonary ganglioneuritis in four non-psittacine birds. *J Avian Med Surg*. 2007;21:210-214.
11. Raghav R, Taylor M, Delay J, Kistler A, Smith D. Avian bornavirus is present in many tissues of psittacine birds with histopathologic evidence of proventricular dilatation disease. *J Vet Diagn Invest*. 2010 Jul;22(4):495-508
12. Thakur R, Sarma S, Sharma B. Role of Borna disease virus in neuropsychiatric illnesses: Are we inching closer? *Indian J Med Microbiol*. 2009;27(3):191-201.

CASE IV: SP-09-6422 (AFIP 31642241).

Signalment: Adult female red-footed tortoise (*Geochelone carbonaria*).

History: According to the provided history, an adult female red-footed tortoise (*Geochelone carbonaria*) from a privately-owned Midwestern zoological garden presented with progressive lethargy. As the animal was non-responsive to treatment, necropsy was performed on site following euthanasia, and tissues were submitted to the Diagnostic Center for Population and Animal Health, Lansing, MI, for histopathologic examination.

Gross Pathology: No gross description was provided with the tissue submission.

Laboratory Results: After a diagnosis was made, water from the pond where this tortoise was kept was submitted for parasitological analysis but yielded no significant results.

Histopathologic Description: Kidney: Diffusely in a section of kidney, the renal tubular epithelium is variably degenerate and necrotic. Within affected tubules, epithelial cells are often dissociated, variably swollen, with eosinophilic finely vacuolated to floccular cytoplasm, and pyknotic to karyolytic to absent nuclei (degeneration and necrosis). Few large, irregular, and mildly atypical cells with prominent vesicular nuclei are also present (regeneration). Multifocally, tubules are filled with small to moderate amounts of eosinophilic smooth to floccular material (proteinosis), sloughed-off epithelial cells, and few heterophils. Occasional tubular epithelial cells contain up to 10, 10-15 µm, intracytoplasmic, refractile, amphophilic ellipsoidal organisms obscuring the cytoplasm and nucleus. These organisms contain two apical polar capsules, approximately 2 µm in diameter, and basophilic nuclear material in between polar capsules (morphology suggestive of myxozoans). Similar organisms are also present in tubular lumina, within sloughed-off epithelial cells or individually amidst intraluminal debris. Low numbers of lymphocytes and heterophils expand the renal interstitium, together with rare pigment-laden macrophages (hemosiderin). Diffusely within the section, glomerular tufts are segmentally to globally, mildly to moderately thickened. Multifocally, there is rare segmental synechiation and mild expansion of the urinary space, which is mostly devoid of contents (clear space). Rare intratubular basophilic casts (mineral) are also identified. Degenerate sloughed-off epithelial cells, heterophils, and myxozoan organisms are present in the renal pelvic lumen. Multifocally within the subepithelial stroma of the pelvis are occasional foci of coarse deeply basophilic salt deposition (dystrophic mineralization).

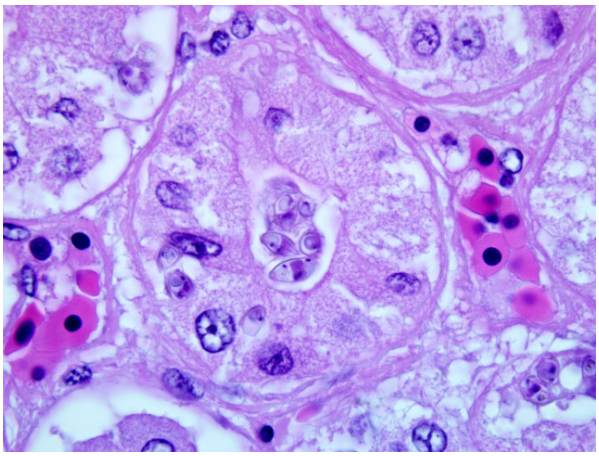

4-1. Kidney, red footed tortoise. Renal tubular epithelial cells are swollen and vacuolated (degeneration). Within the cytoplasm of epithelial cells and in tubular lumens there are refractile, amphophilic, ellipsoid myxozoans that measure up to 15µm in diameter. Occasionally, organisms contain two apical polar capsules and basophilic nuclear material between the capsules. (HE 1000X)

The above described organisms were not highlighted by PAS, acid-fast, or Giemsa histochemistries.

Additional findings in other organs (not included): multifocal myocardial mineralization and severe heterophilic hepatitis. No organisms were observed within any other examined tissues, including but not limited to liver, biliary ducts, and urinary bladder.

Contributor's Morphologic Diagnosis: 1. Kidney: Moderate diffuse tubular degeneration, and necrosis, with intralesional, intraepithelial and intratubular myxozoa-type parasites (*Myxidium* spp.).
2. Kidney: Moderate diffuse membranous glomerulonephritis, with mild tubular proteinosis.
3. Kidney: Minimal multifocal dystrophic mineralization.

Contributor's Comment: Microorganisms of the phylum *Myxozoa* are spore-forming, metazoan parasites that infect the biliary, urinary, and gastrointestinal tracts of cold-blooded aquatic vertebrates, especially fishes but rarely also reptiles, amphibians, and birds, with alternate life cycle stages in invertebrates.[2,4,5] Infection is believed to be of little clinical importance in most species, although in the recent years, life-threatening disease has been documented in a variety of species.[2] In the reported cases, the kidneys, biliary tract, and liver are the most commonly compromised organs. Affected kidneys are often grossly pale and swollen, while histologically the infection is characterized by degeneration and necrosis of the tubular epithelium infected with intralesional spores.[5] All myxozoans known to infect reptiles are in the genus *Myxidium*, and all reports involve aquatic turtles.[5]

In an attempt to elucidate the species involved in this case, additional ancillary tests such as ultrastructural analysis, phase contrast microscopy, and molecular analysis of the samples were performed.

Ultrastructural analysis on infected kidney tissue revealed 60 x 20 µm spores, with a mean polar capsule dimension of 15 x1 0 µm. Phase contrast microscopy and transmission electron microscopy demonstrated only mature spores, with two asymmetrical valve cells and a binucleated sporoplasm between two opposing polar capsules. Valve cells were longitudinally striated, with two overlapping sigmoidal capsule sutures. Polar capsules contained a single polar filament, coiled 5 to 7 times and surrounded by a double-layered wall. Based on spore morphology, these myxozoa were classified in the genus *Myxidium*.

Macerated formalin-fixed tissue yielded plentiful spores from which DNA extraction was attempted. At least two distinct extraction methods were used (using *Myxozoan* and *Myxydium* generic primers) with no success, likely as a result of formalin-fixation nucleic acid damage to the samples (additional fresh samples were not readily available).

To the best of the contributor's knowledge, renal myxozoanosis has not been documented in terrestrial chelonids.

AFIP Diagnosis: 1. Kidney: Tubular degeneration and proteinosis, multifocal, mild with rare tubular epithelial necrosis and intraepithelial and intratubular myxozoan parasites.
2. Adipose tissue, perirenal: Fat atrophy, diffuse moderate.

Conference Comment: Several participants included some form of glomerulonephritis in the histomorphologic diagnosis. The moderator pointed out that early studies and descriptions of the histomorphology of the chelonian kidney mistakenly identified aging changes as glomerulonephritis, and he assessed the glomeruli in this tortoise as essentially normal. Tortoises and other reptiles possess smaller glomeruli with reduced vascularity as compared to amphibians, birds and mammals.[3] This morphologic feature acts to conserve water for these animals that often live in an arid, dehydrating environment. The reduced glomerular size and vascularity results in an ostensibly thicker mesangium with pronounced mesangial cells, and these normal histoanatomical features may be mistaken for glomerulonephritis by pathologists lacking extensive experience in evaluating reptile tissues. Additionally, the moderator believed there was little "corroborative evidence" to support a diagnosis of glomerulonephritis, e.g., lack of interstitial inflammatory infiltrates.

A subtle, but important, histologic finding in this case is the depletion of perirenal adipose tissue. The moderator indicated this was the most striking lesion, as it indicates negative energy balance. When conducting gross and histologic examination of reptiles and amphibians, assessment of adipose tissue provides valuable insight into the metabolic state of the animal.

Participants discussed species affected by myxozoan parasites. In addition to cold-blooded vertebrates, the moderator indicated that several ducks, both native wild and captive exotic species, have been infected with *Myxidium anatidum* n. sp.[1] Myxozoan parasites which infect ducts preferentially infect biliary epithelium.

Contributor: Michigan State University, Diagnostic Center for Population and Animal Health, 4125 Beaumont Rd, Lansing, MI 48910
www.animalhealth.msu.edu

References:
1. Bartholomew JL, Atkinson SD, Hallett SL, et al. Myxozoan parasitism in waterfowl. *Int J Parasitol*. 2008;38(10):1199-1207.
2. Garner MM, Bartholomew JL, Whipps CM, Nordhausen RW, Raiti P. Renal myxozoanosis in crowned river turtles *Hardella thurjii*: description of the putative agent *Myxidium hardella* n. sp. by histopathology, electron microscopy, and DNA sequencing. *Vet Pathol*. 2005;42:589-595.
3. Jacobsen ER. Overview of reptile biology, anatomy, and histology. In: *Infectious Diseases and Pathology of Reptiles*. New York, NY: CRC; 2007:13-14.
4. Roberts JF, Whipps CM, Bartholomew JL, Schneider L, Jacobson ER. *Myxidium scripta* n. sp. identified in urinary and biliary tract of Louisiana-farmed red-eared slider turtles *Trachemys scripta elegans*. *Dis Aquat Organ*. 2008;80:199-209.
5. Zwart, P. Renal pathology in reptiles. *Vet Clin North Am Exot Anim Pract*. 2006;9:129-159.

The Armed Forces Institute of Pathology
Department of Veterinary Pathology

Conference Coordinator
Matthew Wegner, DVM

WEDNESDAY SLIDE CONFERENCE 2010-2011

Conference 9

20 October 2010

Conference Moderator:
Brett Saladino, DVM, MBA, Diplomate ACVP

CASE I: AFIP 3 (AFIP 3152405).

Signalment: 70-week-old male Wistar-Han rat (*Rattus norvegicus*).

History: Tissue from the thoracic cavity of a control group male rat on a two year carcinogenicity study.

Gross Pathology: The thoracic cavity contained a 3 x 3 x 2 cm, tan, multilobular mediastinal mass.

Laboratory Results: Immunohistochemical stain: immunolabeling for UCP-1 (uncoupling protein 1). Transmission electron microscopy: numerous mitochondria with transverse cristae.

Histopathologic Description: Fibroadipose tissue: Tissue consists of lobules of neoplastic cells separated by irregular thin to broad trabeculae of fibrous connective tissue. Neoplastic cells are polyhedral with homogeneous eosinophilic to microvacuolated cytoplasm and nuclei are round to oval with stippled chromatin and 0-2 nucleoli. Mitoses are 0-1/HPF. These cells are frequently admixed with unilocular adipocytes that have eccentric nuclei. There is marked anisocytosis and anisokaryosis, and there are scattered karyomegalic cells. There are multiple foci of coagulative necrosis sometimes surrounded by foamy macrophages, multinucleate giant cells, and occasional lakes of proteinaceous fluid containing foamy macrophages. In some sections, connective tissue trabeculae contain hemorrhage and loose aggregates of pigmented macrophages (hemosiderophages), plasma cells, and lymphocytes.

Contributor's Morphologic Diagnosis: Hibernoma, malignant.

Contributor's Comment: Hibernomas are rare, well-characterized neoplasms of brown adipose tissue (BAT) in humans and animals. Historically, the background incidence has been low in rodent carcinogenicity studies. This tissue was from a two year study, in group-housed male and female Wistar-Han rats, with an unusually high incidence of non-test article-related hibernomas (up to 12% in control animals).[3] For an unknown reason, the incidence was higher in males. For males and females, the majority of hibernomas were noted in the thoracic cavity as tan to red lobulated masses. Larger tumors had necrotic foci bordered by granulomatous inflammation. Tumor emboli were present in vascular lumina as well as in the lungs. Characteristic ultrastructural features were abundant mitochondria with parallel lamellar cristae and variably sized lipid droplets. Immunohistochemically, neoplastic cells stained positively for UCP1 (uncoupling protein 1), generally considered a specific marker of brown adipocytes. Although stimulation and regression of BAT secondary to changes in the ambient environment as well as chronic disease states is reported,[7] a high incidence of spontaneous hibernomas occurred in this study. Hibernomas were not observed in the concurrent mouse carcinogenicity study with the same test article conducted at the same laboratory.[3] Although hyperplasia and/or neoplasia of BAT have been observed with several classes of unrelated pharmaceutical compounds,[1,6,7] the historical incidence of spontaneous hibernomas in rats has

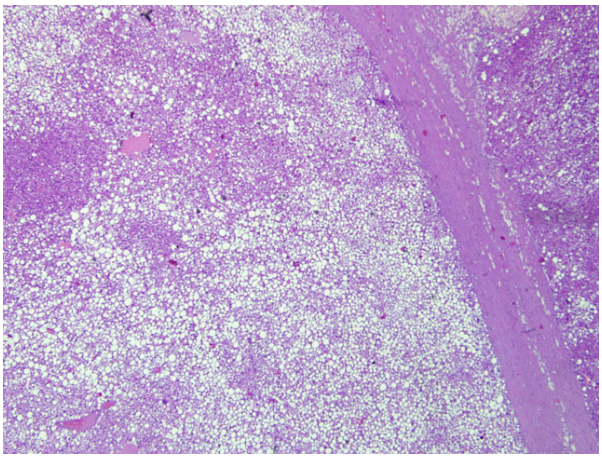

1-1. Fibroadipose tissue, Wistar-Han rat. The multilobulated neoplasm is divided by variably dense bands of fibrous connective tissue and composed of large, vacuolated polygonal cells. (HE 40X)

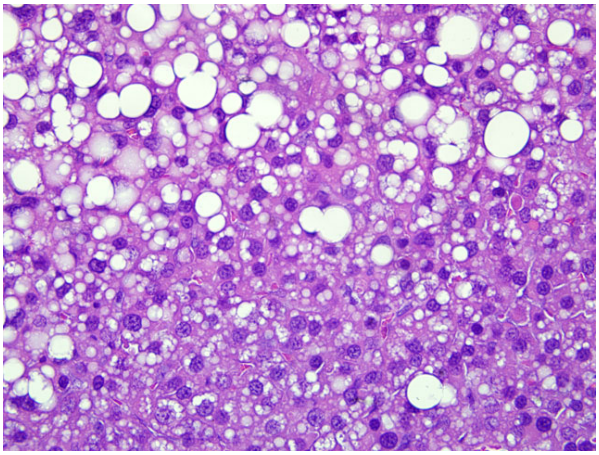

1-2. Fibroadipose tissue, Wistar-Han rat. Neoplastic cells have vacuolated cytoplasm and round to oval nuclei with finely stippled chromatin. Neoplastic cells are often admixed with unilocular adipocytes that have an eccentric nucleus. (HE 400X)

been very low. Increased incidences of spontaneous hibernomas unrelated to the administration of test articles were also observed in Sprague-Dawley rats in three different carcinogenesis bioassays conducted during approximately the same time period.[2]

The primary function of brown adipose tissue is to provide nonshivering thermogenesis during periods of cold-induced stress. Brown adipose tissue is considered especially critical in neonates, in which deposits are within abdominal and thoracic cavities as well as in subcutaneous tissue of the interscapular region. In rodents, BAT deposits normally persist in multiple locations throughout life. Brown adipose cells, packed with mitochondria, are specialized for thermogenesis.[4] Cold stress induces the release of norepinephrine, which binds to β-adrenergic receptors on brown adipocytes.[2] This binding activates lipoprotein lipase to liberate free fatty acids, and initiates the adenylcyclase-cAMP-lipase activation signal that stimulates β–oxidation of fatty acids in mitochondria.[4] Free fatty acids act as ionophore uncouplers in BAT mitochondria. UCP-1, localized to the inner mitochondrial membrane, uncouples fatty acid oxidation from ADP phosphorylation and promotes the dissipation of the energy generated by oxidation as heat.[2]

AFIP Diagnosis: Fibroadipose tissue: Hibernoma.

Conference Comment: Participants generally agreed with the diagnosis of hibernoma for the lesion. With no discernable normal tissue, features of malignancy, such as stromal invasion, evidence of metastasis or tumor emboli within lymphatics or vasculature, cannot be adequately assessed. After the moderator provided additional information from the contributor during the conference, a diagnosis of malignant hibernoma is appropriate.

Historically, the literature refers to benign tumors of brown adipose tissue as hibernomas while classifying malignant tumors of brown adipose tissue liposarcomas.[5] Utilizing immunohistochemical and ultrastructural examination, closer investigation of tumors of brown adipose tissue supports a diagnosis of malignant hibernoma rather than liposarcoma.[2,3] This raises the possibility that malignant hibernomas previously have been misdiagnosed/misclassified and are therefore more common than previous data suggest. This presents a problem from a toxicologic pathology standpoint in that historical data may be skewed. It is therefore difficult to discern whether malignant hibernomas are test-article related or are spontaneous occurrences in certain strains of rats.

The contributor provides an excellent overview of the function and physiology of brown adipose tissue.

Contributor: Covance Laboratories, Inc, Madison, Wisconsin, USA.
www.covance.com

References:

1. Brees DJ, Elwell MR, Tingley FD, et al. Pharmacological effects of nicotine on norepinephrine metabolism in rat brown adipose tissue: Relevance to nicotinic therapies for smoking cessation. *Toxicol Pathol*. 2008;36:568-575.
2. Bruner RH, Novilla MN, Picut CA, et al. Spontaneous hibernomas in Sprague-Dawley rats. *Toxicol Pathol*. 2009;37:547-552.
3. Chandra S, Dochterman W, Ploch S, et al. A carcinogenicity study with unusually high incidence of spontaneous hibernomas in Wistar-Han rats. *Toxicol Pathol*. 2009;37:127(P14).
4. Cheville NF. An introduction to interpretation In: *Ultrastructural Pathology*. Ames, IA: Iowa State University Press; 1994:14.

5. Greaves P, Faccini JM, Courtney CL. Proliferative lesions of soft tissues and skeletal muscles in rats, MST-1. In: *Guides for Toxicologic Pathology*. Washington, D.C.: STP/ARP/ AFIP; 1992:3.
6. Herman JR, Dethloff LA, McGuire EJ, et al. Rodent carcinogenicity with the thiazolidinedione antidiabetic agent troglitazone. *Toxicol Sci*. 2002;68:226-236.
7. Poulet FM, Berardi MR, Halliwell W, Hartman B, Auletta C, Bolte H. Development of hibernomas in rats dosed with phentolamine mesylate during the 24-month carcinogenicity study. *Toxicol Pathol*. 2004;32:558-566.

CASE II: PFIZER SND CASE 2 (AFIP 3164224).

Signalment: Mature male Wistar-Han rat (*Rattus norvegicus*).

History: This rat was part of an exploratory toxicity study; it was approximately eight weeks old at study initiation. The rat was administered a once weekly intravenous bolus of doxorubicin (3 mg/kg) for 6 weeks and was found dead on study day 52, a few hours before the scheduled euthanasia/ necropsy.

Gross Pathology: Macroscopic findings in these animals included small testes and epididymides which correlated with marked to severe degeneration of the seminiferous tubules and epididymal oligospermia histologically. Some animals were also observed to have a gelatinous edematous pancreas.

Histopathologic Description: Heart: Within the heart there is severe cardiomyocyte degeneration in the left atrium with marked vacuolation, and lesser myofiber disorganization, fragmentation and hypereosinophilia. Rarely, myofiber necrosis is present, with necrotic myocytes exhibiting apoptotic or karyorrhectic nuclei. Vessels within the left atrium have plump reactive endothelium and contain marginating neutrophils. A 4-6 mm diameter laminated fibrin thrombus distends the left atrium and is multifocally adherent to the endocardium. The margin of the thrombus contains numerous degenerate and viable neutrophils, and abundant apoptotic debris. Depending on the section, rare to large colonies of 1-2 µm bacterial coccobacilli are noted within the thrombus, extracellularly or phagocytosed by leukocytes. The left atrial endocardial endothelium is plump and reactive, multifocally eroded, and the endocardium is expanded by transmigrating neutrophils. Additionally, there is minimal to mild cardiac myofiber degeneration with myofiber vacuolation and myofibrillar disorganization within the septum, left ventricle and right atrium.

Additional histologic lesions in these rats referable to doxorubicin administration are present in the kidneys, testes, epididymides and lungs. Kidney lesions included tubular degeneration/ regeneration, glomerular atrophy and vacuolation and hyperplasia/ hypertrophy of Bowman's capsule. Testicular lesions consisted of germ cell loss, with only Sertoli cells remaining within seminiferous tubules in severe cases. A secondary oligospermia was present within the epididymides. Within the lung there was degeneration, with prominent vacuolation, of the muscular media in large arteries, sometimes accompanied by inflammation and fibrinoid necrosis.

Contributor's Morphologic Diagnosis: 1. Heart: Multifocal cardiac myocyte degeneration with prominent vacuolation, and rare necrosis.
2. Heart, left atrium: Atrial thrombosis and neutrophilic endocarditis, with intralesional bacteria.

Contributor's Comment: Doxorubicin (adriamycin) is an anti-cancer drug with a very wide antitumor spectrum, and efficacy against both solid tumors and haematological malignancies.[2,5] However, use of the drug is limited by the frequent occurrence of dose-dependent cardiotoxicity which produces cardiomyopathy and secondary congestive heart failure.[2] Acute doxorubicin toxicity in patients includes gastrointestinal complaints, cardiac arrhythmias, phlebitis and tissue necrosis from paravasal leakage, and hypersensitivity reactions.[5] Delayed toxicity includes myelosuppression, alopecia and cardiomyopathy, with chronic cardiotoxicity manifesting as congestive heart failure.[5] Doxorubicin has been used for nearly three decades as a chemotherapeutic, but only recently have some of the cytotoxic mechanisms of the drug been elucidated.[5] These include free radical formation, membrane lipid peroxidation, iron-dependent oxidative damage to macromolecules, direct

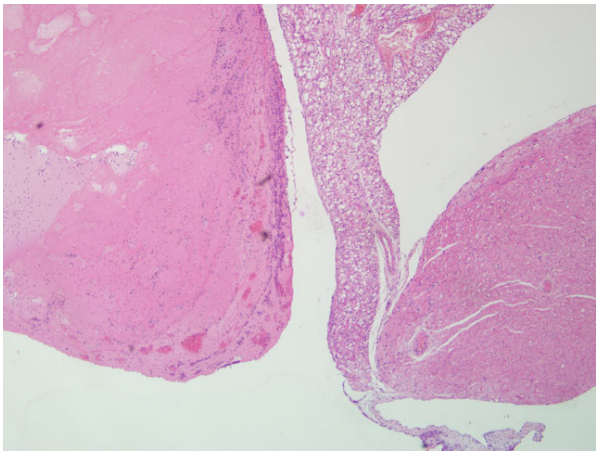

2-1. Heart, Wistar-Han rat. There is diffuse cardiomyocyte vacuolation, degeneration, necrosis, and loss in the left atrial wall. The left atrium is dilated and partially filled by a large thrombus adhered to the endocardium. (HE 40X)

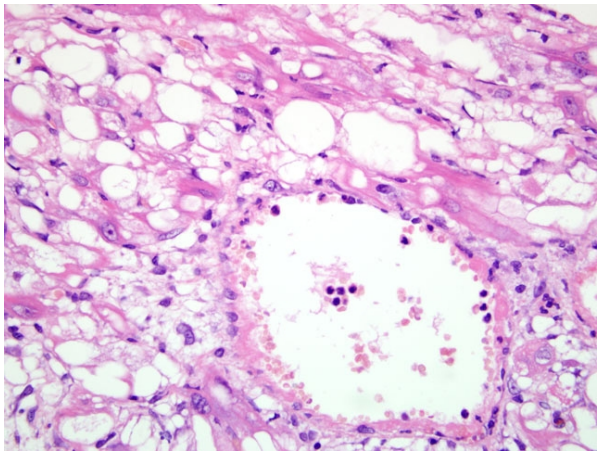

2-2. Heart, atrium, Wistar-Han rat. Endothelial cells in vessels of the left atrium are hypertrophied, reactive, and multifocally eroded and transmigrated by moderate numbers of neutrophils. (HE 400X)

DNA damage or interference with DNA repair, mitochondrial damage and induction of immune reactions involving antigen-presenting cells in the heart.[1,2] Free radical formation and redox cycling associated with doxorubicin treatment cause the generation of reactive oxygen species such as superoxide anion, hydrogen peroxide and hydroxyl radical.[2] Tissues with a less developed antioxidant defense mechanism, like the heart, are highly susceptible to anthracycline-induced oxygen radicals.[2]

The doxorubicin-induced lesions in this study increased in incidence and/or severity with increasing duration of dosing. Both the cumulative effect and the morphologic characteristics of the lesions were consistent with findings reported in the literature. The myocardial degeneration induced in the ventricles and septum in this study in rats was representative of that reported in mice in the literature; however, atrial lesions were much more severe. A similar pattern was described previously in mice treated with doxorubicin,[3] although the bulk of the literature describing heart lesions caused by doxorubicin is based on examination of transverse tissue sections taken through the mid-ventricular and septal areas, which do not include evaluation of the atria. In mice, vacuolation and degeneration of atrial myocytes are shown with electron microscopy to be dilation of the sarcoplasmic reticulum and increased numbers of normal and/or degenerate mitochondria.[3] Atrial interstitial inflammatory cell infiltrates within the myocardium and endocardium are also reported.[3] Additionally, mice treated with doxorubicin show an incidence of atrial thrombosis approaching 75%.[3] The proposed cause of the atrial thrombosis in the mice was endothelial inflammation accompanied by abnormal blood flow secondary to the myocardial damage.[3]

AFIP Diagnosis: Heart, atria: Cardiomyocyte vacuolar degeneration, necrosis and loss, diffuse, mild to severe with left atrial thrombosis and rare regeneration.

Conference Comment: The contributor provides an excellent review of doxorubicin toxicity. The moderator highlighted the point that the contributor makes above; that is, although doxorubicin toxicity is traditionally associated with ventricular, rather than atrial, cardiomyocyte vacuolization and degeneration, this is related to tissue sample sectioning rather than to a change in pathologic mechanism of doxorubicin. The atrial lesions in previous studies likely were not noted earlier because the atria were not sectioned for histopathologic examination. This underscores the complexity of toxicologic pathology and the importance of being thorough in toxicity studies. This case also represents a paradigm shift in how some participants evaluate and interpret the tissue changes, i.e. they initially speculated that doxorubicin could cause this type of lesion in the heart, but then discounted it as the etiology because the lesion is observed in the atrium rather than the ventricle. Lack of awareness that doxorubricin could induce lesions in the cardiac atria caused several participants to dismiss it as a possible etiology in favor of other toxic causes, thus illustrating the informational utility of this case.

Discussion then focused on the secondary effects of the histologic lesions in the atria. Residents concluded that the primary lesion is the myocardial change, which results in ineffective myocardial contraction, endothelial damage, release of prothrombotic substances and thrombosis. Three perturbations promoting thrombus formation, colloquially referred to as Virchow's triad, are endothelial injury, altered normal blood flow (turbulence or stasis), and hypercoagulability.[4] Endothelial cell damage is not restricted to physical damage; any damage capable of disrupting the prothrombotic-antithrombotic balance favoring thrombosis is included in this category.[4]

Normal, non-activated endothelial cells have antithrombotic activity; activation or damage resulting from bacterial endotoxin, cytokines or changes in hemodynamic properties promote thrombus formation. The included chart summarizes the mechanisms for these actions.[4]

Platelets play an equally important role in hemostasis. Once contact is made with extracellular matrix (ECM) proteins, platelets have three functions:[4]

1. Adhere to collagen with glycoprotein Ib via vWF; additional glycoprotein receptors bind other ECM components.
2. Secretion of α- and dense-granule contents promoting thrombus formation. P-selectin-coated α-granules contain fibrinogen, fibronectin, platelet factor 4, PDGF, TGF-β, and factors V and VIII. Dense (δ) granules have ionized calcium, histamine, serotonin, epinephrine, ADP and ATP.
3. Platelets aggregate and change shape, forming the primary hemostatic plug.

The severity modifier in our morphologic diagnosis is intended to indicate that the lesion in the right atrium is mild, while the lesion in the left atrium is severe. There is likely some sectioning variability as participants did not see the bacteria described by the contributor.

Contributor: Pfizer Global Research and Development, Sandwich Laboratories, Sandwich, Kent, United Kingdom.

References:

1. Arola OJ, Saraste A, Pulkki K, Kallajoki M, Parvinen M, Voipio-Pulkki LM. Acute doxorubicin cardiotoxicity involves cardiomyocyte apoptosis. *Cancer Res*. 2000;60:1789-1792.
2. Ayaz SA, Bhandari U, Pillai KK. Influence of DL α-lipoic acid and vitamin-E against doxorubicin-induced biochemical and histological changes in the cardiac tissue of rats. *Indian J Pharmacol*. 2005;37(5):294-299.

Antithrombotic Properties of Endothelial Cells		**Prothrombotic Properties of Endothelial Cells**	
Antiplatelet effects	• Covers thrombogenic subendothelial extracellular matrix (ECM) • Produce PGI_2 and nitric oxide inhibiting adhesion • Produces adenosine diphosphatase to degrade ADP	Platelet effects	• Endothelial injury exposes subendothelial ECM → platelet adherence via von Willebrand factor
Anticoagulant effects	• Heparin-like molecules enhance thrombin inactivation via antithrombin III: 1. Thrombomodulin → binds thrombin → activates protein C → inactivates factors Va and VIIIa → inhibits clotting 2. Produces protein S and tissue factor pathway inhibitor → direct inhibition of factor VIIa (tissue factor) and factor Xa	Procoagulant effects	• Cytokine (TNF or IL-1) or endotoxin → endothelial production of tissue factor → activation of the extrinsic clotting cascade • Augment the catalytic function of activated factor IXa and Xa
Fibrinolytic effects	Produce tissue plasminogen activator → cleaves plasminogen to plasmin → cleaves fibrin → thrombus dissolution	Antifibrinolytic effects	Secrete inhibitors of plasminogen activator → reduces fibrinolysis

3. Fujihira S, Yamamoto T, Matsumoto M, et al. The high incidence of atrial thrombosis in mice given doxorubicin. *Tox Pathol*. 1993;21(4):362-368.
4. Mitchell RN. Hemodynamic disorders, thromboembolic disease and shock. In: Kumar V, Abbas AK, Fausto N, Aster JC eds. *Robbins and Cotran Pathologic Basis of Disease.* 8th ed. Philadelphia, PA: Elsevier Saunders; 2009:115-123.
5. Speth PAJ, van Hoesel Q, Haanen C. Clinical pharmacokinetics of doxorubicin. *Clin Pharm*. 1988;15:15-31.

CASE III: 10-016 (AFIP 3168181).

Signalment: 11 to 12-month-old male and female Balb/c transgenic mice (HSP70, TLR2) (*Mus musculus*).

History: Three Balb/c mice weighing about 35 gm were submitted with a large submandibular swelling.

Gross Pathology: Incision of the skin in the submandibular region revealed a large, smooth, soft, round, blood-filled, multi-lobulated mass measuring about 1.5 to 2 cm in diameter.

Histopathologic Description: Salivary gland: Expanding and infiltrating the salivary gland (submandibular, parotid or sublingual gland, varying depending on mouse and section), there is a large, variably encapsulated mass with multiple large cystic spaces filled with pale eosinophilic mucinous material and blood. Multifocally, irregular, variably-sized necrotic areas may be filled with amorphous eosinophilic cellular debris intermixed with pyknotic nuclear debris, or may form pseudocysts with no lining epithelium. Adjacent to blood vessels, the neoplastic cells tend to form palisades and have a predominant epithelioid morphology. The mass consists of variably distinct foci composed of spindle cell and polygonal epithelioid cell populations. The neoplastic spindloid cells have scant to moderate amounts of pale eosinophilic fibrillar cytoplasm and vesicular nuclei with 1-2 distinct nucleoli. There is moderate to marked nuclear atypia and numerous mitoses. The epithelioid cells have abundant pale eosinophilic fibrillar cytoplasm and round to oval basophilic stippled nuclei. There are rare misshaped and attenuated ducts and tubules entrapped within the neoplastic cell population, especially at the periphery of the mass. In addition, there are multifocal lymphoid cell infiltrates near the periphery of the neoplasm. Surrounding the neoplastic tissue, there are multifocal areas of a variable amount of granulation tissue intermixed with hemorrhage and inflammatory cells (neutrophils and large foamy macrophages) that often extends into the dermis.

Contributor's Morphologic Diagnosis: Salivary gland: Myoepithelioma.

Contributor's Comment: These are very rare neoplasms seen most commonly in BALB/c, A, and C58 strains.[3,5] Clinically, the neoplasm presents as fluctuant swelling in the ventral aspect of the neck. Macroscopically, the neoplasms are dark red to yellow, solid to cystic masses filled with mucus, blood and necrotic cellular debris. They are presumed to arise from the myoepithelial cells of the salivary glands (mainly parotid and submandibular and less commonly the sublingual gland). Histologically, these neoplasms are biphasic and are comprised of varying proportions of mesenchymal (spindle) cells and large epithelioid cells; either of these cell types may be the predominant population in a given tumor. Areas of degeneration and necrosis are relatively common. A

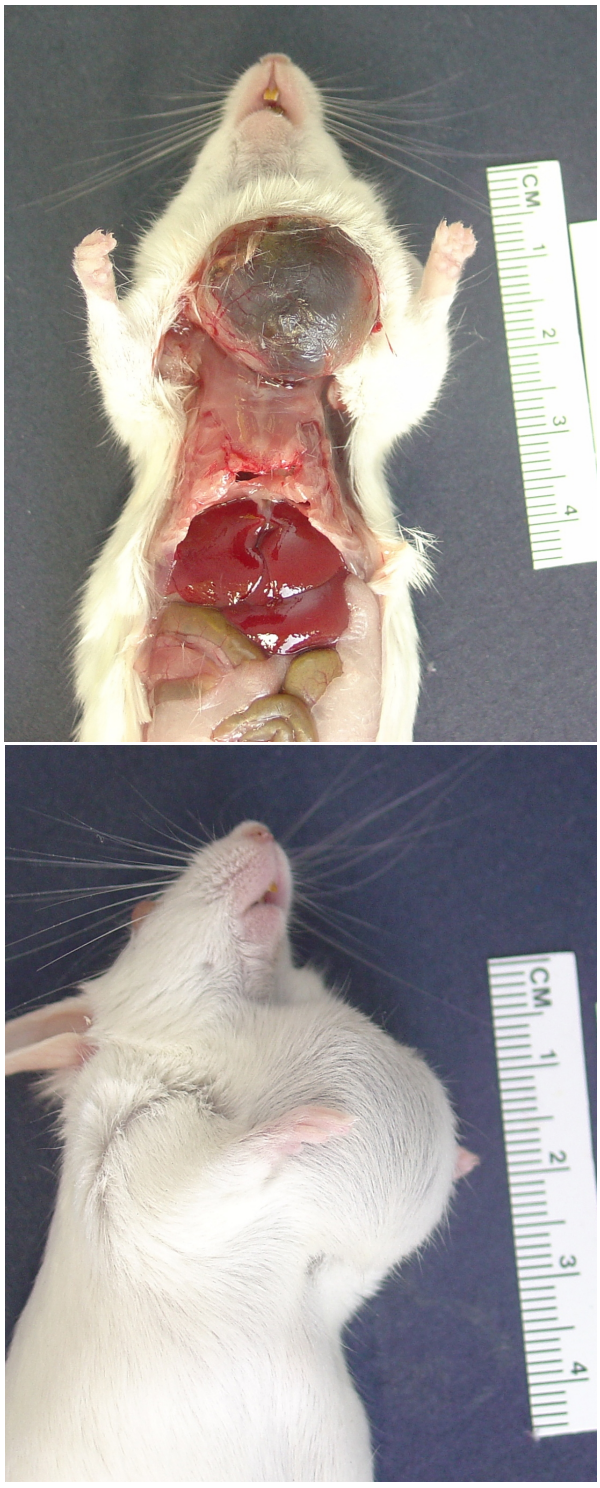

3-1, 3-2. Salivary gland, Balb/c mouse. The submandibular region contains a large, smooth, soft, round, blood-filled multilobulated mass measuring about 1.5 to 2.0 cm in diameter. Photographs courtesy of Experimental Pathology Laboratories, Inc., PO Box 13566, Research Triangle Park, NC 27709, nallison@epl-inc.com

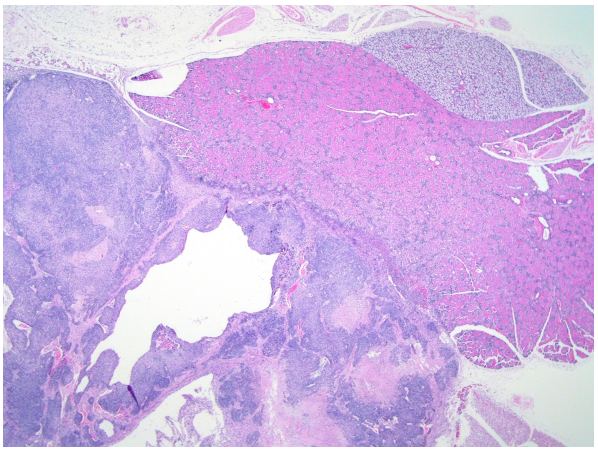

3-3. Salivary gland, Balb/c mouse. Expanding and infiltrating the salivary gland (parotid) is a large, variably encapsulated neoplasm with multiple, often blood filled cystic spaces. Photograph courtesy of Experimental Pathology Laboratories, Inc., PO Box 13566, Research Triangle Park, NC 27709, nallison@epl-inc.com

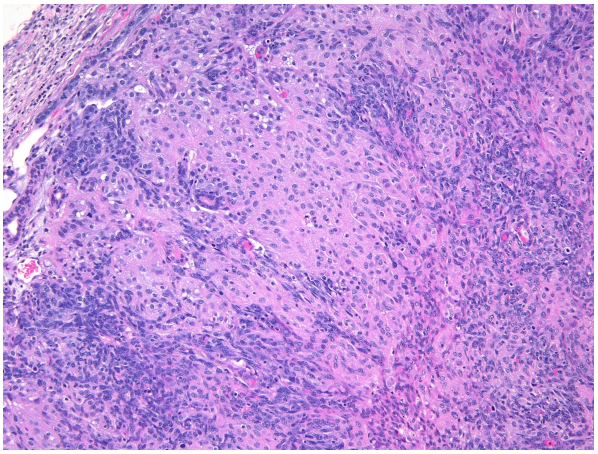

3-4, 3-5. Salivary gland, Balb/c mouse. The neoplasm is composed of both polygonal (large epithelioid) cells and spindle cells. Neoplastic spindle cells have scant to moderate amounts of pale eosinophilic cytoplasm and vesicular nuclei. The epithelioid cells have abundant pale eosinophilic fibrillar cytoplasm and round to oval basophilic stippled nuclei. Multifocally at the periphery of the neoplasm there are moderate numbers of lymphocytes. Photographs courtesy of Experimental Pathology Laboratories, Inc., PO Box 13566, Research Triangle Park, NC 27709, nallison@epl-inc.com

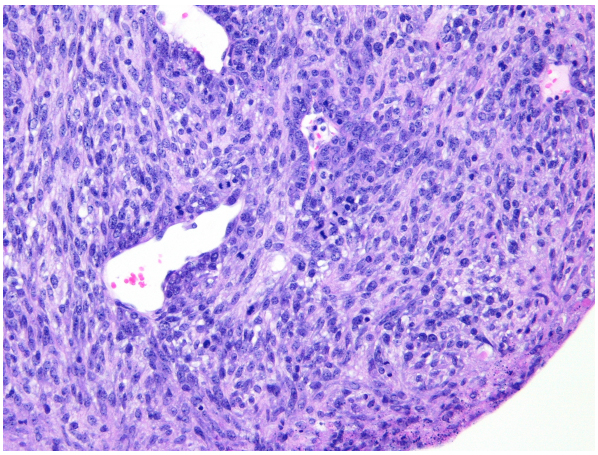

majority of myoepitheliomas are circumscribed with a thin capsule and variable degree of invasion into adjacent tissues. However, metastasis to regional lymph nodes and lungs may be seen in rare cases.

The characteristic absence of formation of acini or ducts by the neoplastic cells aids in differentiating these tumors from adenomas and carcinomas. The presence of a single solitary mass on the ventral aspect of the neck helps to differentiate these neoplasms from polyomavirus-induced pleomorphic tumors that are multicentric in origin and not limited to the salivary glands.[3] Myoepitheliomas can also occur within mammary glands, Harderian glands, clitoral glands and preputial glands.

In humans, salivary gland myoepitheliomas are classified based on morphology (plasmacytoid, spindle, stellate, clear or epithelioid) of the neoplastic cells into spindle cell myoepithelioma, clear cell myoepithelioma, etc. Due to the histologic heterogeneity, no single immunostain is diagnostic. For human salivary myoepitheliomas, a panel of markers consisting of AE1/AE3 (PAN-K), S-100, P63, GFAP, calponin and vimentin is commonly used for diagnosis.[4] A panel of markers, such as vimentin and cytokeratin (especially k5 and k14), may be used for immunohistochemical diagnosis of these tumors in mice. Also, PTAH staining will aid in confirmation of the presence of intracytoplasmic fibrils within the neoplastic epithelioid cells. Ultrastructurally, these fibrils are composed of abundant microfilaments in parallel orientation with periodic focal densities, characteristic of smooth muscle fibrils, and are arranged in dense parallel bundles around the nucleus.[3] These tumors are usually negative for smooth muscle actin and desmin.

Acknowledgements: We appreciate the help of Drs. Terry Blankenship-Paris, Mark Hoenerhoff, and Steven Kleeberger at NIEHS, RTP, NC for graciously sharing the case material.

AFIP Diagnosis: Salivary gland: Myoepithelioma, malignant.

Conference Comment: Conference participants agreed the histomorphologic features are consistent with the diagnosis of myoepithelioma. As indicated by the contributor, myoepitheliomas can have a diverse histomorphology. From personal experience, the moderator mentioned that the presence of spindle cells which palisade around the outer edge of the tumor forming a dark rim is a common histologic feature of the neoplasm. Additionally, neoplastic cells adjacent to vessels often take on an epithelial-type arrangement.[1] In addition to the features described by the contributor and the moderator, myoepithelioma also can occur histologically as a squamous form, both with keratin pearl formation or without the presence of keratinization.[1]

Participants discussed the differential diagnosis, which included poorly differentiated carcinoma/adenocarcinoma,

carcinosarcoma, and sarcoma arising or metastatic to glandular organs, such as the salivary, mammary, lacrimal, and Harderian glands. All participants interpreted the tumor as arising from the salivary gland, and thus considered a neoplasm of other regional glandular tissues less likely, including mammary, lacrimal, or Harderian origin. Based on the absence of desmoplasia and glandular or squamous differentiation, participants considered a tumor of epithelial origin less likely; the glandular or ductular profiles occasionally found in the neoplasm were interpreted as preexisting salivary structures entrapped by neoplastic cells. Participants did observe the large pseudocystic structures in the neoplasm described by the contributor, which were not interpreted as evidence of glandular differentiation.

Finally, participants discussed the difficulty in the histologic differentiation of salivary myoepithelioma from polyomavirus-induced salivary neoplasms. Polyomavirus inoculated into neonatal mice of susceptible strains induces tumors in multiple organs, in particular the parotid salivary gland.[2] Histologically, polyoma virus-induced salivary neoplasia most commonly occurs as mixed mesenchymal and epithelioid populations, although neoplasms composed of pure mesenchymal or epithelioid populations may be observed.[2] In contrast to polyomavirus-induced salivary tumors, myoepitheliomas typically are not infiltrated by lymphocytes and plasma cells.[1]

The use of tissue from multiple animals in this case contributed to slide variation, with some slides having one type of salivary gland and others having more than one type present.

Contributor: Experimental Pathology Laboratories, Inc., PO Box 13566, Research Triangle Park, NC 27709
http://www.epl-inc.com

References:

1. Betton GR, Whiteley LO, Anver MR, et al. Gastrointestinal tract. In: Moore U, ed. *International Classification of Rodent Tumors: The Mouse*. Berlin, Germany: Springer-Verlag; 2001:29.
2. Botts S, Jokinen M, Gaillard ET, Elwell MR, Mann PC: Salivary, Harderian, and lacrimal gland glands. In: Maronpot RR, ed. *Pathology of the Mouse*. Vienna, IL: Cache Valley Press; 1999:56-60.
3. Burger GT, Frith CH, Townsend JW. Myoepithelioma, Salivary glands, mouse. In: Jones TC, Popp JA, Mohr U, eds. *Digestive System. Monographs on Pathology of Laboratory Animals*. Berlin, Germany: Springer-Verlag; 1997:231-235.
4. Hunt JL, Barnes L. Immunohistology of head and neck neoplasms. In: Dabbs D, ed. *Diagnostic Immunohistochemistry*. 2nd ed. Philadelphia, PA: Churchill Livingstone (Elsevier Inc.); 2006:245-247.
5. Sundberg JP, Hanson CA, Roop DR, Brown KS, Bedigian HG. Myoepitheliomas in inbred laboratory mice. *Vet Pathol*. 1991;28:313-323.

CASE IV: 10-4230 HE (AFIP 3170127).

Signalment: 9-year-old female spayed German shepherd dog, canine (*Canis lupus familiaris*).

History: A 9-year-old female spayed German shepherd dog presented to the referring veterinarian with a history of anorexia, vomiting and diarrhea of approximately 12 hours duration. A chemistry panel revealed a severely elevated ALT and low blood glucose. No abnormalities were noted on abdominal radiographs. The dog was treated with IV fluids and anti-emetics for a brief period of time, but developed seizures, at which point the owners elected to euthanize the dog.

Gross Pathology: (per RDVM history): The liver contained generalized multifocal pinpoint raised yellow areas. The stomach contents consisted of dark ingesta with hemorrhage. Scattered petechiae were noted within the pancreas. The abdominal and subcuticular adipose was diffusely yellow (jaundice).

Histopathologic Description: Liver: Severe diffuse loss of hepatocytes characterizes the section. Remaining hepatocytes are discohesive with pyknotic or karyolytic nuclei, with either micro-vacuolated (lipidosis, probable) or condensed and hypereosinophilic cytoplasm (necrosis). Confluent areas of hemorrhage, along with hemosiderin-laden macrophages fill spaces left by hepatocyte loss. On this background of necrosis and hemorrhage there are ribbons of preserved bile ducts, scattered foci of erythroid precursors (extramedullary hematopoiesis), and focal islands of plump, basophilic, often binucleate hepatocytes (regenerative nodules). Some centrilobular hepatocytes remain and are arranged in regenerative, irregular cords. Bile ducts are mildly ectatic and contain moderate amounts of pale homogenous basophilic material (bile; cholestasis). Lymphatics in the connective tissue surrounding large vessels are dilated (portal hypertension).

Contributor's Morphologic Diagnosis: Liver: Severe multifocal to coalescing subacute massive necrosis with mild cholestasis.

Contributor's Comment: The histologic finding of massive hepatic necrosis, in combination with the history of hypoglycemia, is highly suggestive of xylitol toxicity.

Xylitol is a 5-carbon sugar alcohol that occurs in small amounts as a natural intermediary during the metabolism of L-xylulose to D-xylulose.[2] It is marketed for human consumption as a sugar substitute. Profound differences exist between species in insulin secretion after administration of xylitol. In humans, rhesus monkeys, rats, and horses, the insulin release is negligible, but in dogs, rabbits, cows, goats, and baboons, insulin levels increase significantly and rapidly.[6] Xylitol's effect in cats and ferrets is unknown. In dogs, clinical signs of xylitol ingestion include vomiting, weakness, ataxia, hypoglycemia, hypokalemia, and seizures within 30 to 60 minutes of ingestion.[3]

The pathogenesis of xylitol-induced hepatic necrosis in dogs is not known, although two mechanisms have been proposed.[2] In the first proposed scenario, cellular ATP, ADP, and inorganic phosphorus reserves are depleted by intermediates of xylitol metabolism, leading to loss of membrane integrity and cell death. In the second proposed scenario, reactive oxygen species damage cellular membranes and macromolecules, leading to cell death. These proposed mechanisms are not mutually exclusive, and both, or other as yet unknown, mechanisms may be responsible.[2]

A recent paper describing the histologic lesions in two dogs exposed to xylitol described centrilobular periacinar to midzonal necrosis (zones II and III) in one sample and centrilobular necrosis (zone III) in the other.[2] However, no zonal distribution was detected in this case.

The histologic picture of severe, massive hepatic necrosis is not pathognomonic, and can occur with a variety of hepatic insults, including chemicals (carbon tetrachloride), drugs (carprofen, potentiated sulfonamides), bacterial infections (*Clostridium piliformis*), and toxins (blue-green algae, Sago Palm seeds, *Amanita* mushrooms).[1,5,7,8] Anamnesis and clinicopathologic data are needed to prioritize the list of differential diagnoses.

AFIP Diagnosis: Liver: Hepatocellular degeneration, necrosis and loss, massive, subacute, diffuse, severe, with hepatocyte dissociation, hemorrhage and regeneration.

Conference Comment: The contributor provides an excellent review of xylitol toxicity in domestic species. During the conference, participants were interested in the regenerative hepatic nodules in the submitted slide. The reason for this regeneration is not evident histologically; attendees considered the possibility of concurrent pre-existent hepatic disease of a toxic nature.

The liver's ability to regenerate is intriguing and unique. The potential for hepatic regeneration depends on the viability of the hepatic stroma. Without stroma, there is no scaffolding for plate organization of new hepatocytes. Normal hepatocytes are in the G_0 resting stage of the cell cycle. Damage to the liver results in tumor necrosis factor alpha (TNF-α)-mediated activation of Kupffer cells, which then release IL-6. The effect of IL-6 on hepatocytes allows them to respond to growth factors, such as hepatocyte growth factor (HGF), transforming growth factor-α (TGF-α) and epidermal growth factor. Viable hepatocytes near the area of damage begin replicating. As restoration of the liver mass proceeds, there is increased responsiveness to growth inhibitors TGF-β and activin A. These compounds, which are downregulated during regeneration, suppress hepatocyte replication and induce extracellular matrix.[9]

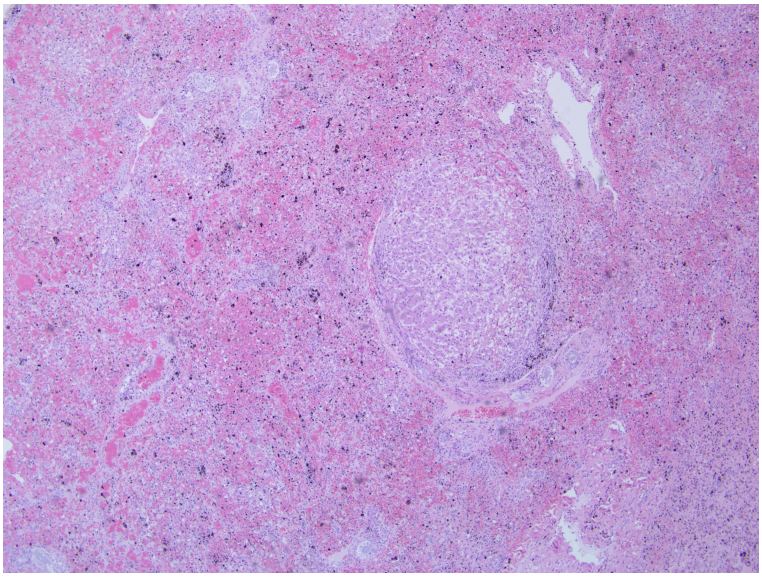

4-1. Liver, dog. Diffusely there is loss of normal hepatic parenchyma (necrosis) with multifocal islands of plump basophilic regenerative nodules. Multifocally, bile ducts and lymphatics are ectatic (HE 40X)

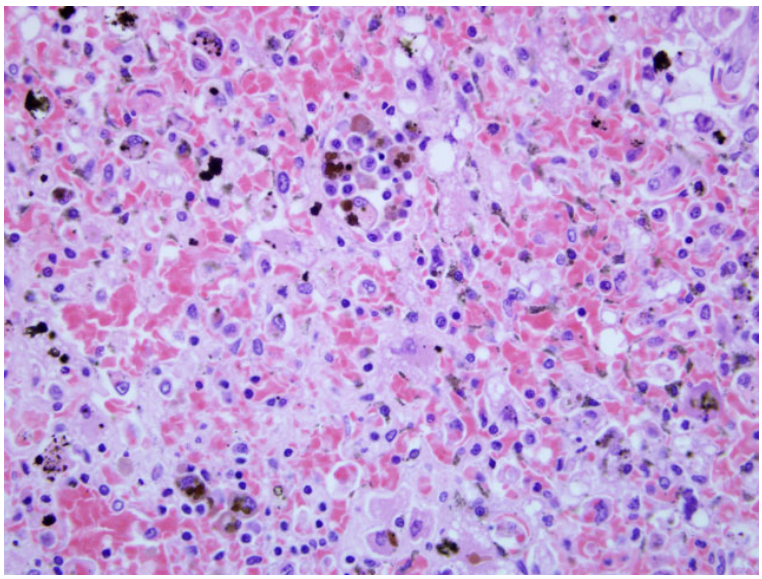

4-2. Liver, dog. Multifocally, remaining hepatocytes are discohesive with pyknosis or karyorrhexis nuclei (necrosis) or have a microvacuolated cytoplasm (lipidosis)(HE 400X)

Participants briefly discussed causes of hypoglycemia which fall into one of six broad categories:[4]

1. Excess insulin or insulin analogs
2. Reduced hormones that maintain glucose homeostasis
3. Reduced hepatic glycogen storage
4. Increased glucose usage
5. Reduced glucose intake or gluconeogenesis
6. Drugs

Based on the signalment, a reasonable differential diagnosis for hypoglycemia in this case would include gram-negative sepsis, malnutrition, paraneoplastic syndrome, insulinoma, or laboratory error. If the serum has prolonged contact with the blood clot in the collection tube, glucose will be depleted because of insulin-independent uptake of glucose by erythrocytes. In addition to marked hypoglycemia, hypophosphatemia, hypokalemia, hypercalcemia and increased levels of alanine aminotransferase (ALT) and aspartate aminotransferase (ASP) have been observed with xylitol intoxication in both experimental and clinical settings.[2,10]

Contributor: Department of Anatomic Pathology, Biomedical Sciences, College of Veterinary Medicine T4 018 Veterinary Research Tower, Cornell University, Ithaca, NY 14853
http://www.vet.cornell.edu/biosci/pathology/services.cfm

References:

1. DeVries SE, Galey FD, Namikoshi M, Woo JC. Clinical and pathologic findings of blue–green algae (*Microcystis aeruginosa*) intoxication in a dog. *J Vet Diagn Invest.* 1993;5:403-408.
2. Dunayer EK, Gwaltney-Brant SM. Acute hepatic failure and coagulopathy associated with xylitol ingestion in eight dogs. *J Am Vet Med Assoc*. 2006; 229(7):1113-1117.
3. Dunayer EK. Hypoglycemia following canine ingestion of xylitol-containing gum. *Vet Hum Toxicol*. 2004;46:87-88.
4. Evans EW, Duncan JR. Proteins, lipids and carbohydrates. In: Latimer KS, Mahaffey EA, Prasse KW, eds. *Duncan and Prasse's Veterinary Laboratory Medicine: Clinical Pathology*. 4th ed. Ames, IA: Blackwell Publishing; 2003:181-187.
5. MacPhail CM, Lappin MR, Meyer DJ, et al. Hepatocellular toxicosis associated with administration of carprofen in 21 dogs. *J Am Vet Med Assoc*. 1998;212(12):1895-1901.
6. Piscitelli CM, Dunayer EK, Aumann M. Xylitol toxicity in dogs. *Compendium* 2010. E1-E4.
7. Puschner B, Rose HH, Filigenzi MS. Diagnosis of amanita toxicosis in a dog with acute hepatic necrosis. *J Vet Diagn Invest*. 2007;19(3):312-7.
8. Senior DF, Sundlof SF, Buergelt CD, et al. Cycad intoxication in the dog. *J Am Anim Hosp Assoc*. 1985;21:103-109.
9. Stalker MJ, Hayes MA. Liver and biliary system. In: Maxie MG, ed. *Jubb, Kennedy and Palmer's Pathology of Domestic Animals*. 5th ed., vol. 2. Philadelphia, PA: Elsevier Ltd; 2007:324-325.
10. Xia Z, He Y, Yu J. Experimental acute toxicity of xylitol in dogs. *J Vet Pharmacol Ther*. 2009;32:465-469.

The Armed Forces Institute of Pathology
Department of Veterinary Pathology

Conference Coordinator
Matthew Wegner, DVM

WEDNESDAY SLIDE CONFERENCE 2010-2011

Conference 10

27 October 2010

Conference Moderators:
Edward Stevens, DVM, Diplomate ACVP

Taylor Chance, DVM, Diplomate ACVP

CASE I: 3090525001 (AFIP 3144268).

Signalment: 10-month-old intact male pony (*Equus ferus caballus*).

History: A ten-month-old male pony was submitted for necropsy with a history of poor growth and poor body condition. The submitting veterinarian suspected a congenital defect.

Gross Pathology: The animal was in poor body condition, with pale muscles and mucous membranes as well as marked subcutaneous edema. The liver was firm, tan to grey in color, and numerous cords of fibrous tissue coursed through the parenchyma. The entire left lobe and portions of the quadrate lobe were markedly atrophied (~50% of normal size). The right lobe was diffusely enlarged. Multifocally, fibrous villous proliferations were present on the serosal surface (perihepatitis villosa). Many adult trematodes, between 2-2.5 cm long, were evident within dilated and thickened bile ducts. The femoral metaphyseal bone marrow was reddened.

Laboratory Results: Clinical biochemistry: Anemia, hypoalbuminemia.

Histopathologic Description: Liver: Liver sections reveal marked multifocal, mainly portal bridging fibrosis admixed with multifocal infiltrates of moderate numbers of eosinophils and large numbers of lymphocytes and plasma cells. There is marked bile duct hyperplasia.

Large bile ducts contain an adult trematode characterized by a cuticle without spikes, a digestive tract, and vitellaria within

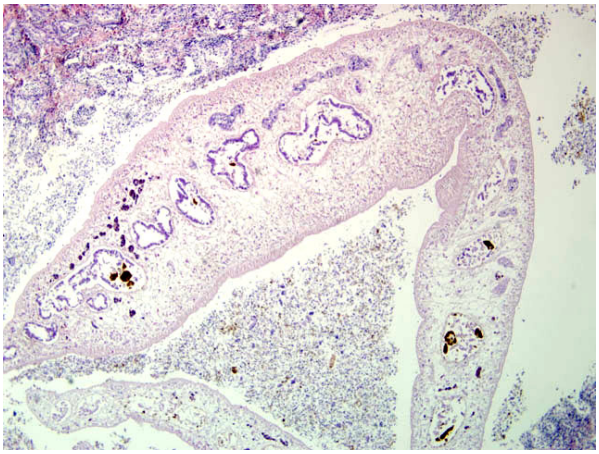

1-1. Liver, horse. Within a dilated bile duct there is an adult trematode characterized by an outer tegument, spongy parenchyma, ceca containing blood pigment, and vitellaria. (HE 40X)

a spongy parenchyma. Sections through adult trematodes show testes with mature sperm, uteri with eggs, and also occasional miracidia (morphologically consistent with *Fasciola hepatica*).

Contributor's Morphologic Diagnosis: Marked diffuse chronic lymphoplasmacytic and eosinophilic hepatitis and (peri-)cholangitis with marked portal bridging fibrosis and intralesional adult trematode (morphologically consistent with *Fasciola hepatica*).

Contributor's Comment: In our experience (4 reports over a 21 year period), trematode infection is rare in equids in The Netherlands, and there are only a few reports of its prevalence in the literature. The reported prevalence of infection of horses in Europe ranges from approximately 1% in central Europe to 77% of horses from Ireland and the United Kingdom.[4] A German study found that between 38 and 71% of horses and 11% of donkeys were positive for the presence of eggs in their feces, while a similar Turkish study reported that the feces of 4.7% of equids were positive for eggs.[2,5]

Fascioliasis is common in cattle and sheep. The life cycle of *Fasciola hepatica* includes a Lymnead snail as an intermediate host. The snail is found in damp environments, such as marshy ground, ponds, and along the banks of slow moving streams. The miracidia of *Fasciola hepatica*, which are ingested along with the feces of the final host, infect the snail by burrowing through its body wall. Once within the snail, the larvae pass through a number of developmental stages including a sporocyst, three generations of rediae, and finally a cercarial stage which leaves the snail and encysts on vegetation to become a metacercaria. The infective metacercariae are ingested by the final host and excyst within the duodenum and migrate to the liver. Adult flukes reside in the bile ducts.[3]

In comparison to cattle and sheep, equids appear to mount an, as yet poorly understood, early immunological challenge to infection, which leads to the destruction, immobilization or developmental retardation of the larval flukes, the result being that only a few trematodes reach maturity in the bile ducts of equids.[2]

AFIP Diagnosis: Liver: Cholangiohepatitis, proliferative and fibrosing, chronic and eosinophilic, diffuse, marked with hepatocellular loss, dark brown anisotropic pigment, and few trematode eggs and adults.

Conference Comment: Based on the histologic findings, a reasonable differential diagnosis list would include *Fasciola hepatica*, *Fasciola gigantica*, and *Dicrocoelium dendriticum*. All three of these trematodes reside in the bile ducts of affected animals; *Fascioloides magna* inhabits the liver parenchyma and therefore would be an unlikely etiologic agent. Speciation of trematodes in histologic samples is nearly impossible. With the exception of *F. magna*, the histologic lesions are similar, and thus identification of flukes at gross necropsy is more reliable, as the morphology can be more adequately characterized. To that end, *F. hepatica* is approximately 2.5 cm long and leaf shaped; *F. gigantic* is double or triple the size of *F. hepatica*; *D. dendriticum* is 0.5-1cm long and lancet-shaped; and *F. magna* is 8 cm in length.[3]

Given the limited clinical information and history provided to participants, most favored *D. dendriticum* as the causative agent. In addition to horses, this trematode also infects ruminants, pigs, dogs and cats. *Fasciola hepatica* and *F. gigantica* primarily affect sheep and cattle. Wild cervids are the natural host for *F. magna*, though it can infect cattle and sheep. Other trematodes infecting domestic animals include: *Eurytrema pancreaticum* and *E. coelomaticum* in ruminants; *Opisthorchis viverrini* in cats and dogs; and *Pseudamphistomum truncatum*, *Metorchis* spp., *Parametorchis complexus*, *Concinnum procyonis*, and *Platynosum fastosum* in cats and dogs.[1]

Two possible sequelae to hepatic trematodiasis are black disease in sheep and bacillary hemoglobinuria in sheep and cattle. Black disease occurs when anaerobic, necrotic foci in the liver resulting from *F. hepatica* migration allow germination of ingested *Clostridium novyi* spores in the liver. Once active, *C. novyi* elaborates a necrotizing beta toxin and hemolytic phospholipase C, and together, these toxins produce large areas of coagulative necrosis in the liver resulting in severe edema, congestion, hemorrhage and death, often with no premonitory signs. The pathogenesis of bacillary hemoglobinuria, caused by *Clostridium haemolyticum*, is similar to black disease with respect to the fluke involved, germination of spores, and toxin production. The toxins of *C. haemolyticum* produce intravascular hemolysis with associated anemia and hemoglobinuria.[1]

Contributor: Utrecht University, Faculty of Veterinary Medicine, Department of Pathobiology
http://www.uu.nl/diergeneeskunde/pathobiologie

References:

1. Cullen JM. Liver, biliary system and exocrine pancreas. In: McGavin MD, Zachary JF, eds. *Pathologic Basis of Veterinary Disease*. 4th ed. St. Louis, MO: Elsevier; 2007:435-436.
2. Eckert J. Helminthosen der Equiden. In: Rommel M, Eckert J, Kutzer E, Körting W, Schnieder T, eds. *Veterinärmedizinische Parasitologie*. 5th ed. Parey; 2000:353-354.
3. Stalker MJ, Hayes MA. Liver and biliary system. In: Maxie MG, ed. *Jubb, Kennedy and Palmer's Pathology of Domestic Animals*. 5th ed., Vol. 2. Philadelphia, PA: Elsevier Ltd; 2007:354-356, 359-362.
4. Wintzer HJ, Kraft W. Parasitäre Krankheiten des Pferdes. In: Wintzer HJ, ed. *Krankheiten des Pferdes*. 3th ed. Parey; 1999:229.

5. Uslu U, Guclu F. Prevalence of endoparasites in horses and donkeys in Turkey. *Bull Vet Inst Pulawy*. 2007;51:237-240.

CASE II: D-10-0751 (AFIP 3164918).

Signalment: 2-week-old male pig (*Sus scrofa*).

History: The young pig was submitted for necropsy with a history of sudden death.

Gross Pathology: The coronary bands of all four feet were pale and blanched, but there were no vesicles. A pale, sloughed, necrotic area measuring 1.5 cm in length and 1 cm in width was present on the dorsum of the tongue. There was severe hydropericardium, with 5-6 mL of yellowish fluid with fibrin clots present in the pericardial sac. The heart was diffusely involved, with pale streaks separated by darker areas noted on the epicardium and cut surfaces of the heart. Fibrin strands were found in the abdominal cavity.

Laboratory Results: Heart, claw, tongue and pericardial fluid samples were positive for Foot and Mouth Disease Virus type O by antigen capture ELISA.[1,2] Results were from the World Foot and Mouth Disease Reference Laboratory at Pirbright.

Heart, claw , tongue and pericardial fluid samples were positive for FMDV type O, Southeast Asia (SEA) topotype, Mya-98 lineage, by nucleotide sequencing.[10] Results were from the World Foot and Mouth Disease Reference Laboratory at Pirbright.

Histopathologic Description: Heart: Severe diffuse myocardial necrosis. Necrotic cardiomyocytes were intensely eosinophilic, fragmented, had lost their cross striations and had pyknotic nuclei. Moderate numbers of macrophages and smaller numbers of lymphocytes and neutrophils were present in the necrotic areas. Similar inflammatory cells were present on the epicardial surface.

Contributor's Morphologic Diagnosis: Heart: Myocardial necrosis, acute, severe with histiolymphocytic infiltrates, pig (*Sus scrofa*). The lesion is consistent with foot and mouth disease.

Etiologic Diagnosis: Aphthovirus myocarditis.

Contributor's Comment: Foot and mouth disease (FMD) affects cloven hoofed animals, with the most dramatic clinical infections of domestic swine and cattle.[7] It is caused by seven serologically distinct types (A, O, C, Asia 1, Southern African Territories [SAT] 1, 2, and 3) of Foot and Mouth Disease Virus (FMDV) in the genus *Aphthovirus*, family *Picornaviridae*.[1] Type O and Asia 1 viruses are the most widespread viruses and are endemic in Asia.[9] The SAT type viruses have never been reported in Asia.

FMDV is a single stranded RNA virus with a protein capsid consisting of four viral proteins enumerated as VP1, VP2, VP3 and VP4.[1] Subtype-specific neutralization epitopes have been identified among the four capsid proteins, primarily within VP1.[6,8] The serotype prevalent in Hong Kong SAR has been and continues to be serotype O.[4] However, the topotype has recently changed from Cathay to the South East Asia topotype with a subsequent increase in clinical signs and mortalities. The Southeast Asia (SEA) topotype, Mya-98 lineage, has been confirmed by the World Foot and Mouth Disease Reference Laboratory at Pirbright. Similar topotypes have been identified in the Republic of Korea and Japan recently. This recent spread of FMD in the Far East indicates the possibility of disease spread both within and outside the region, as happened during the FMD O PanAsia pandemic of 1999-2001.[4,10]

In swine, vesicles often form on the rostrum of the snout and around the nares. Foot lesions, when present, frequently extend along the coronary bands and dewclaws, and in severe cases can cause sloughing of the claw. Tongue lesions tend to coalesce and ooze a serous fluid when ruptured, leaving behind a visible raw and denuded stratum germinativum.[6]

Mortality is not commonly seen in FMD cases unless young pigs are affected. Young pigs up to 14 weeks of age, but particularly those less than 8 weeks of age, may die without developing any clinical signs of FMD due to heart failure,

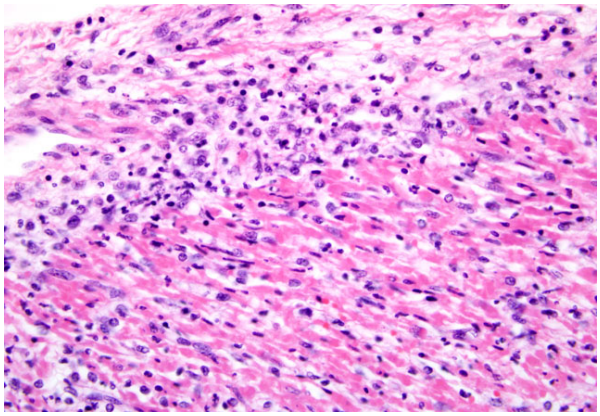

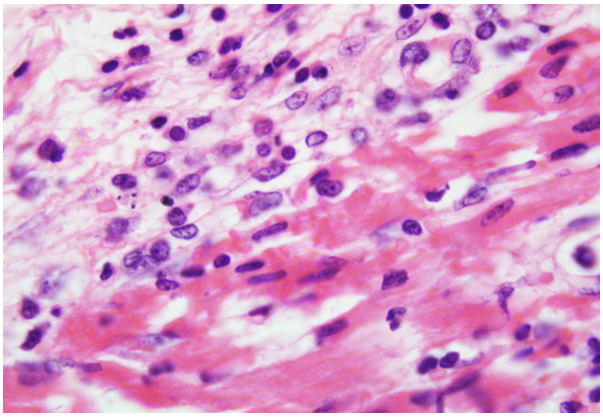

2-1, 2-2. Pig, heart. Within the myocardium and epicardium are moderate numbers of macrophages, with fewer lymphocytes and neutrophils. There is degeneration and necrosis of subjacent ventricular cardiomyocytes. (HE 400X, 1000X)

which is characterized by acute myocarditis that at times may be seen macroscopically as whisps of blanched areas on the epicardium that extend into the endocardium, a consequence of the damage caused by viral replication in the developing myocardium.[3,9,11]

AFIP Diagnosis: Heart: Myocarditis and epicarditis, necrotizing, subacute, diffuse, severe, with lymphohistiocytic and neutrophilic interstitial inflammation and perivasculitis.

Conference Comment: Conference discussion focused on the differential diagnosis for myocarditis in the pig. Encephalomyocarditis virus (EMCV), a *Cardiovirus* of the *Picornaviridae* family, was the favored etiology by most participants. Histologic findings are similar to those found in this case with diffuse myocardial necrosis, and the inflammatory infiltrate with EMCV is typically mononuclear. Other viruses associated with myocarditis in the pig include porcine parvovirus and porcine circovirus 2 which is associated with postweaning multisystemic wasting syndrome.[7] Vitamin E/selenium deficiency causes myocardial necrosis; however, inflammation is minimal. Additionally, several parasitic etiologies can cause myocarditis, including *Toxoplasma gondii*, *Sarcocystis* spp., *Taenia* spp., *Trypanosoma* spp. and *Trichinella spiralis*.[12]

The exact cause of death in myocarditis is unknown. Death could be due to the effects of the offending agent (e.g. viral damage to myocytes), the ensuing inflammatory response, or both. Infiltrating cytotoxic T lymphocytes can produce direct myocyte necrosis. Activated histiocytes and lymphocytes produce a cytokine milieu resulting in myocyte metabolic disturbances, reduced contractility, and dysrhythmia. Death during the acute phase of myocarditis is often attributed to dysrhythmias.[7] Animals surviving the acute phase begin resolution in which macrophages arrive to remove the necrotic debris. Due to the continuous contraction of cardiac myocytes, their regenerative capabilities are limited; therefore, healing most often occurs through fibrosis.[5]

Contributor: Tai Lung Veterinary Laboratory, Agriculture, Fisheries and Conservation Department, Lin Tong Mei, Sheung Shui, New Territories, Hong Kong SAR
http://www.afcd.gov.hk

References:

1. Davies G. Foot and mouth disease. *Res Vet Sci.* 2002;73:195-199.
2. Hoffmann B, Beer M, Reid S, et al. A review of RT-PCR technologies used in veterinary virology and disease control: Sensitive and specific diagnosis of five livestock diseases notifiable to the World Organization for Animal Health. *Vet Microbiol*. 2009;139:1-23.
3. Kitching RP, Alexandersen S. Clinical variation in foot and mouth disease. *Rev Sci Tech Off Int Epiz*. 2002;21(3): 513-518.
4. Knowles NJ, Samuel AR, Davies PR, Midgley RJ, Valarcher J-F. Pandemic strain of Foot-and-Mouth Disease Virus Serotype O. *Emerg Infect Dis*. 2005;11(12):1887-1893.
5. Kumar V, Abbas AK, Fausto N, Aster JC. Tissue, renewal, regeneration and repair. In: Kumar V, Abbas AK, Fausto N, Aster JC, eds. *Robbins and Cotran Pathologic Basis of Disease*. 8th ed. Philadelphia, PA: Elsevier Saunders; 2009:85-86.
6. Lubroth J. Foot and mouth disease: A review for the practitioner. *Vet Clin Food Anim*. 2002;18:475-499.
7. Maxie MG, Robinson WF. Cardiovascular system. In: Maxie MG, ed. *Jubb, Kennedy and Palmer's Pathology of Domestic Animals*. 5th ed., Vol. 3. Philadelphia, PA: Elsevier Ltd; 2007:41-43.
8. Meyer RF, Knudsen RC. Foot and mouth disease: A review of the virus and the symptoms. *J Envir Health*. 2001;64(4):21-23.
9. Oeem JK, Yeh MT, McKenna TS, et al. Pathogenic characteristics of the Korean 2002 isolate of Foot and Mouth Disease Virus serotype O in pigs and cattle. *J Comp Path*. 2008;138:204-214.
10. Paton DJ, King DP, Knowles NJ, Hammond J. Recent spread of foot-and-mouth disease in the Far East. *Vet Rec*. 2010;166:569-570.
11. Ryan E, Horsington J, Durand S, et al. Foot and mouth disease virus infection in young lambs: Pathogenesis and tissue tropism. *Vet Microbiol*. 2008;127:258-274.
12. Van Vleet JF, Ferrans VJ. Cardiovascular system. In: McGavin MD, Zachary JF, eds. *Pathologic Basis of Veterinary Disease*. 4th ed. St. Louis, MO: Elsevier; 2007:563-564, 591-593.

CASE III: HN2585 (AFIP 3167483).

Signalment: 3-year-old male Tokara (Japanese native) goat (*Capra hircus domesticus*).

History: Four goats and nine sheep were kept in a zoological garden. The present case was born at the garden in 2006; and the zoo staff noticed that the goat showed decreased appetite and weight loss from January 2009. He had intermittently excreted soft feces since May 2009, and overt diarrhea was noted in October of the year. He died in November 2009.

Gross Pathology: The carcass was in poor nutritional condition and post mortem autolysis was mild. The oral mucosa and conjunctiva were pale white. The liver diffusely showed centrilobular congestion and periportal white discoloration, such as in nutmeg liver. There was a foreign body (tight handkerchief) in the content of rumen. Numerous white small foci due to mucosal thickening, approximately 2 mm in diameter, were visible from the serosa of the small intestine. About 50% of lung lobes, mainly in both cranial lobes, were dark red, wet and consolidated.

Laboratory Results: Tissues from this goat were not examined microbiologically. After the necropsy, a monitoring study in the herd was performed for *Mycobacterium avium* spp. *paratuberculosis* (MAP) with johnin reaction, complement fixation (CF) test, and the isolation from feces five times in all for 5 months. MAP was not isolated from any animals, but 6 sheep were positive in both johnin reaction and CF test.

Histopathologic Description: Liver: The liver showed severe interlobular, periportal, and intralobular infiltration of macrophages, epithelioid cells and a small number of lymphocytes. There was atrophy, degeneration and loss of the hepatocytes adjacent to the foci due to the extensive invasion of the macrophages. Mild proliferation of bile ducts and arterioles was noted in expanded portal areas. Hemosiderin-laden macrophages (Kupffer cells) were scattered in sinusoids throughout the parenchyma. The Ziehl-Neelsen stain showed a massive presence of acid-fast rod-shaped bacteria in the epithelioid cells. Additionally, epithelioid macrophages diffusely infiltrated and proliferated in lamina propria mucosae of the ileum and colon. Epithelioid macrophages aggregates were occasionally observed around the vessels and lymphatics under the serosa. Similar foci were also noted in the mesenteric adipose tissue. These epithelioid cells also contained numerous acid-fast rod shaped bacilli in the cytoplasm. Obvious necrosis and mineralization could not be found in any granulomatous foci.

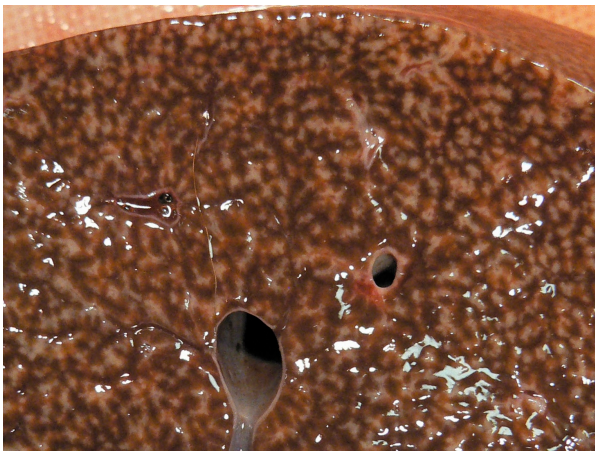

3-1. Liver, goat. Diffusely throughout the hepatic parenchyma are numerous periportal white foci. Photograph courtesy of Laboratory of Comparative Pathology, Graduate School of Veterinary Medicine, Hokkaido University, Sapporo, Japan, umemura@vetmed.hokudai.ac.jp

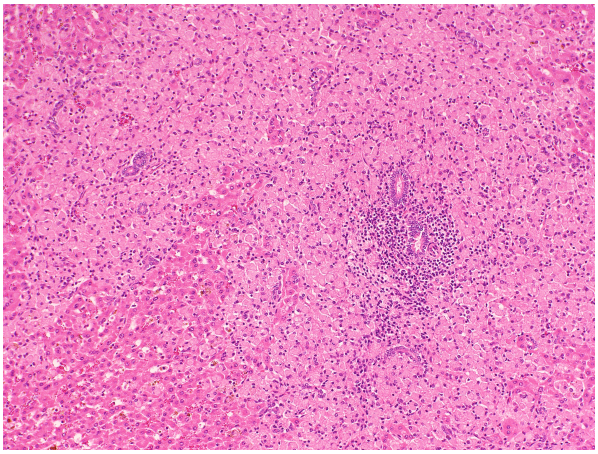

3-2. Liver, goat. Diffusely expanding periportal areas are many macrophages with abundant foamy cytoplasm and indistinct cell borders. Photograph courtesy of Laboratory of Comparative Pathology, Graduate School of Veterinary Medicine, Hokkaido University, Sapporo, Japan, umemura@vetmed.hokudai.ac.jp

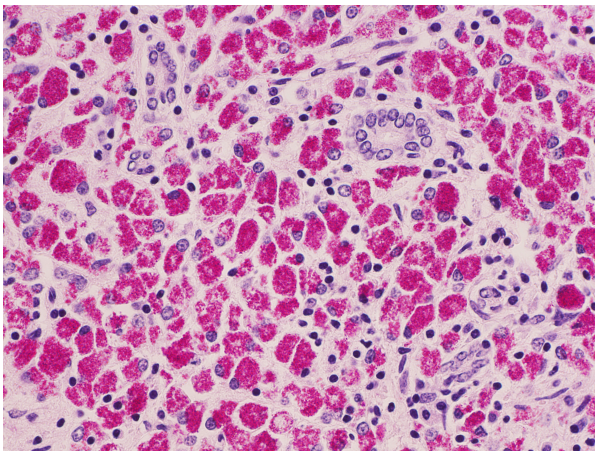

3-3. Liver, goat. The staining by the Ziehl-Neelsen method reveals numerous acid-fast bacilli within the cytoplasm of macrophages. Photograph courtesy of Laboratory of Comparative Pathology, Graduate School of Veterinary Medicine, Hokkaido University, Sapporo, Japan, umemura@vetmed.hokudai.ac.jp

Organism Factor	Cell Pathway	Mechanism	Result
Man-LAM	TLR2-MAPK-p38	IL-10 overexpression	Decreased: IL-12, IL-8, and TNF-α, MHC class II, apoptosis, phagosome acidification, and organism killing
Man-LAM	IL-10-mediated	Decreased: IL-12, IL-8, and TNF α expression	Attenuation of: 1. Inflammatory response 2. Th 1-type immune response
Man-LAM	IL-10-mediated	Decreased MHC class-II expression	Decreased antigen presentation
Unknown	IL-10-mediated; decreased TNF-α	Decreased apoptosis	Increased cell survival
Man-LAM	IL-10-mediated; TLR2-MAPK-p38 signaling	Decreased phagolysosome fusion and acidification	Increased organism survival

Contributor's Morphologic Diagnosis: Liver: Hepatitis, granulomatous, multifocal to coalescing, marked, with numerous intrahistiocytic acid-fast bacilli.

Contributor's Comment: Paratuberculosis, or Johne's disease, caused by MAP infection, mainly occurs in domestic ruminants and is responsible for considerable economic losses all over the world.[2,5] The disease has been spontaneously recognized in pigs, free-ranging and captive wild ruminants, camelids, and rarely in equids and captive primates. Speculation exists that Johne's disease is zoonotic and associated with Crohn's disease in human beings, although MAP has still not been accepted as the cause of the human disease.

MAP is very resistant to environmental stressors, particularly in regions with acid soils. The bacterium enters the M cells that cover the intestinal Peyer's patches, and ingested bacteria are subsequently phagocytized by macrophages.[2] In cattle, susceptibility to infection is greatest in the first 30 days of life, although clinical disease does not usually develop until 2-5 years of age. The progression from asymptomatic to clinical Johne's disease is associated with a decrease in peripheral cell-mediated immunity and increasing production of non-protective IgG1 antibodies.[7,8] The disease is clinically characterized by untreatable diarrhea accompanied by progressive weight loss and hypoproteinemia. The characteristic gross lesion in the symptomatic cattle is chronic segmental thickening of the ileum, mesenteric lymphadenopathy, and lymphangitis. Histologically, cattle usually have non-caseating granulomas in the affected bowel and lymphoid tissues.[2]

Although the pathogenesis of Johne's disease in small ruminants is assumed to be similar to that in cattle, there are several differences in clinical signs and pathology. Sheep and goats reveal emaciation and hypoproteinemia, but overt diarrhea is unusual.[2,5] In sheep, goats, and deer, enteric gross lesions are often mild, with little obvious thickening, and no transverse ridges.[2,4]

Two main pathological forms of the intestinal lesion have been described in symptomatic sheep.[3,9] The first form is multibacillary or lepromatous, in which macrophages filled with numerous mycobacteria are the main inflammatory cells. The second form is paucibacillary or tuberculoid, in which the inflammatory infiltrate is composed of lymphocytes and few macrophages and caseous necrosis and calcification may be observed. It is difficult to find acid-fast mycobacteria in macrophages in the latter form. It is uncertain whether the two distinct forms represent sequential or divergent stages. Asymptomatic sheep may have small granulomas in the interfollicular and basal areas of ileal Peyer's patches, usually with no visible intracellular organisms.[9]

Corpa et al.[4] characterizes the intestinal lesions of caprine tuberculosis in four categories: focal, diffuse multibacillary, diffuse lymphocytic, and diffuse mixed. Histological classification for sheep is valid for goats, and the lower frequency of focal lesions in goats compared to sheep appears to indicate that the former species has only limited ability to control the infection. In this species, granulomatous lesions are likely to be more severe in the jejunum than in the ileum, although the distribution could not be determined in this case. Currently, the similar histological classification is applicable also in bovine paratuberculosis.[6]

The ileum of the present case showed diffuse multibacillary lesions. The monitoring study in remaining sheep and goats supported the histological diagnosis. Previously, focal granulomas have been seen in lymph nodes elsewhere in the body, liver, lung, spleen, and other organs in symptomatic sheep and goats.[2-4] However, the number of histiocytic infiltrates in the liver was unusual.

AFIP Diagnosis: Liver: Hepatitis, portal and random, histiocytic, diffuse, marked with numerous intrahistiocytic acid-fast bacilli.

Conference Comment: The pathogenesis of *Mycobacterium avium* ssp. *paratuberculosis* (MAP, Johne's) is assumed to be similar in cattle and sheep. The greatest susceptibility to infection is within the first 30 days of life. Infection occurs when MAP is ingested, taken up by M cells overlying intestinal Peyer's patches, and transported to resident macrophages. The bacteria localize in the mucosa and draining lymph nodes; rarely in small ruminants, MAP-associated lesions can be found in the walls of blood vessels, meninges, liver and spleen.[2] These disseminated lesions are thought to result from irregular lymphogranulomatous foci; affected animals typically have a negative response to intradermal johnin testing.[2]

Mycobacteria species utilize a complex interplay of virulence factors and the host immune system to evade being killed. The included chart is adapted from Weiss and Souza[10] and summarizes the mechanisms by which MAP suppresses monocyte-macrophage microbicidal response.

Interleukin 10, as noted in the chart above, plays a pivotal role in the MAP-directed immune modulation; a brief review of IL-10 follows. IL-10 is produced by a variety of cells, including T regulatory lymphocytes, Th 2 lymphocytes, and dendritic cells. The primary function of IL-10 is to direct the immune system to a Th 2-type immune response by enhancing Th 2 activity and suppressing Th 1 activity; Th 1 suppression is accomplished by inhibiting macrophage IL-12 production. Antigen presentation by dendritic cells is decreased through IL-10 mediated down-regulation of MHC class-II.[1]

As commented by the contributor, the distribution and extent of the histiocytic infiltrate in the liver is striking. While most participants interpreted the lesion as consistent with *Mycobacterium avium spp. paratuberculosis* infection, they were nevertheless impressed by the number of infiltrating macrophages filled with acid- fast bacilli. A similar histopathologic presentation is reported in dogs infected with *M. avium-intracellulare* complex (MAC), as exemplified by Wednesday Slide Conference 2009-2010, Conference 5, Case 1, and in the absence of special stains may result in the histologic interpretation of histiocytic neoplasia or a sarcomatous lesion, rather than an infectious process.

Contributor: Laboratory of Comparative Pathology, Graduate School of Veterinary Medicine, Hokkaido University, Sapporo 060-0818, Japan
http://www.hokudai.ac.jp/veteri

References:

1. Ackermann MR. Acute inflammation; Chronic inflammation and wound healing. In: McGavin MD, Zachary JF, eds. *Pathologic Basis of Veterinary Disease*. 4th ed. St. Louis, MO: Elsevier; 2007:149,157-160.
2. Brown CC, Baker DC, Barker IK. Alimentary system. In: Maxie MG, ed. *Jubb, Kennedy and Palmer's Pathology of Domestic Animals*. 5th ed., Vol. 2. Philadelphia, PA: Elsevier Ltd; 2007:222-225.
3. Clark CJ. The pathology and pathogenesis of paratuberculosis in ruminants and other species. *J Comp Pathol.* 116:217-261, 1997
4. Corpa JM, Garrido J, García Marín JF, Pérez. Classification of lesions observed in natural cases of paratuberculosis in goats. *J Comp Pathol*. 2000;122:255-265.
5. Gelberg HB. Alimentary system. In: McGavin MD, Zachary JF, eds. *Pathologic Basis of Veterinary Disease*. 4th ed. St. Louis, MO: Elsevier; 2007:372-374.
6. González J, Geijo MV, García-Pariente C, et al. Histopathological classification of lesions associated with natural paratuberculosis infection in cattle. *J Comp Pathol*. 2005;133:184-196.
7. Koets A, Rutten V, Hoek A, et al. Progressive bovine paratuberculosis is associated with local loss of CD4+ T cells, increased frequency of γδ T cells, and related changes in T-cell function. *Infect Immun*. 2002;70:3856-3864.
8. Kurade NP, Tripathi BN, Rajukumar K, Parihar NS. Sequential development of histologic lesions and their relationship with bacterial isolation, fecal shedding, and immune responses during progressive stages of experimental infection of lambs with *Mycobacterium avium* subsp. *paratuberculosis*. *Vet Pathol*. 2004;41:378-387.
9. Pérez V, Gacía Marín JF, Badiola JJ. Description and classification of different types of lesions associated with natural paratuberculosis infection in sheep. *J Comp Pathol*. 1996;114:107-122.
10. Weiss DJ, Souza CD. Modulation of mononuclear phagocyte function by *Mycobacterium avium* subsp. *paratuberculosis*. *Vet Pathol*. 2008;45:829-841.

CASE IV: 518-10-1 (AFIP 3167496).

Signalment: Juvenile (18.5 kg) female pig (*Sus scrofa*).

History: In a finishing herd, there were some pigs with a decreased rate of body weight gain and a couple of pigs had died during the previous week.

Gross Pathology: This pig was one of four growing pigs submitted for necropsy at the same time. The pig was in poor nutritional condition. The main gross lesions were observed in the lungs. There were pneumonic lesions in the cranial lung lobes and the caudal part of the left diaphragmatic lobe was covered with thick fibrinous exudate and attached to the wall of the pleural cavity. The cranial part of the left diaphragmatic lobe also contained abscesses.

Laboratory Results: Bacteriology: *Actinobacillus pleuropneumoniae* and *Pasteurella multocida* were cultured from the lungs. *Salmonella* bacteria was not cultured.

Virology: Swine influenza was not detected (RT-PCR).

Immunohistochemistry: Porcine circovirus-2 antigen was demonstrated in lymph nodes.

Histopathologic Description: Lung: The lung parenchyma contains multifocal demarcated pale or basophilic areas bordered by a thick band of degenerate neutrophils and macrophages, often with elongated, "streaming" or "oat cell" nuclei, eosinophilic fibrillar material and nuclear dust, and occasionally also fibroblasts. The alveolar walls inside are pale and necrotic, congested or thickened with inflammatory cells. The alveolar space is often filled with variable numbers of degenerate macrophages and neutrophils. The lobular septae are severely dilated and contain pale edema fluid, eosinophilic fibrillar material, macrophages and few neutrophils. The pleura is severely thickened by fibroblasts and covered by a thick eosinophilic fibrillar membrane with large numbers of degenerate macrophages and neutrophils with streaming nuclei and occasional bacterial colonies. The bronchi are multifocally filled with degenenerate neutrophils, macrophages and sloughing bronchial epithelial cells. Multifocally some arteriolar walls are disrupted and infiltrated with degenerate neutrophils (vasculitis).

Contributor's Morphologic Diagnosis: Severe, subacute, multifocal and locally extensive necrotizing and fibrinosuppurative bronchopneumonia and pleuritis.

Contributor's Comment: Pleuropneumonia caused by *Actinobacillus pleuropneumoniae* is one of the most important respiratory infections of swine. The disease is common worldwide and causes severe morbidity and mortality, especially in growing pigs, but pigs of all ages can be affected. The disease can be peracute, acute, subacute or chronic.

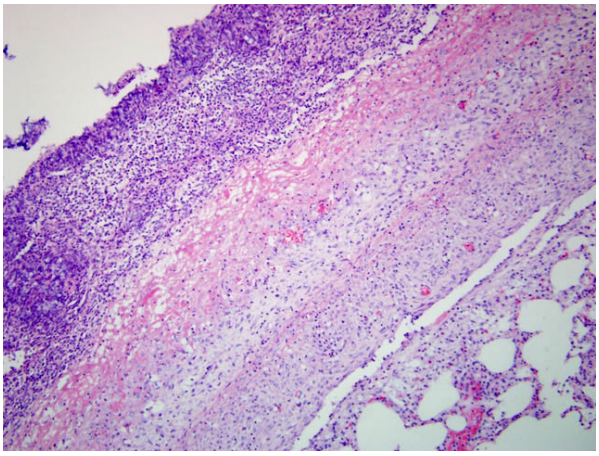

4-1. Lung, pig. The visceral pleura is covered by abundant fibrin, necrotic cellular debris, and many degenerate neutrophils and expanded by increased amounts of fibrous connective tissue and edema. (HE 20X)

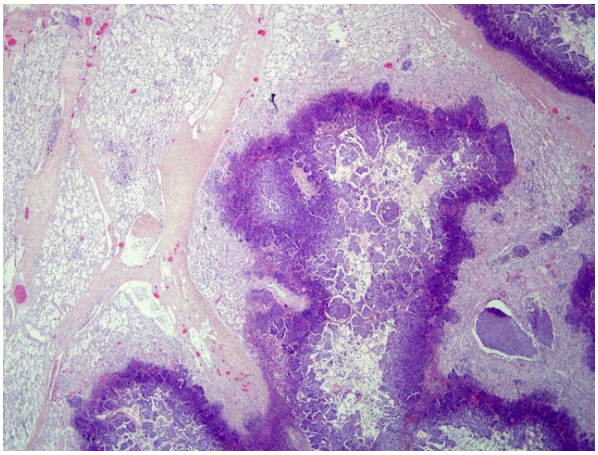

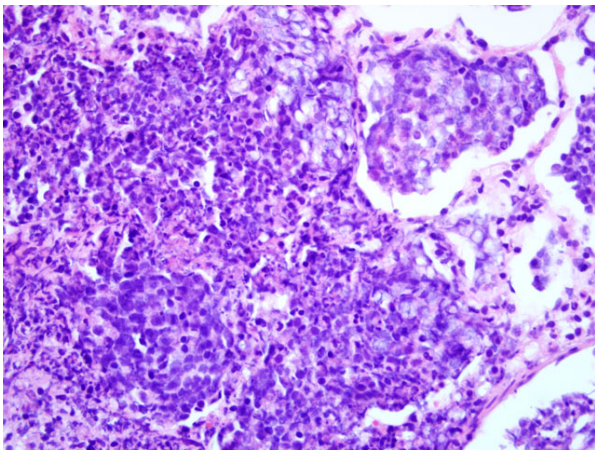

4-2, 4-3. Lung, pig. Filling and replacing bronchioles and alveoli and expanding interlobular septa are many degenerate neutrophils and macrophages admixed with abundant fibrin and necrotic cellular debris. Alveoli contain oat cells. (HE 20X, 400X)

In peracute cases, pigs can be found dead before clinical signs are observed. In acute cases pigs have high fever, apathy and anorexia, occasionally dyspnea and diarrhea or vomiting, cyanosis of skin and blood-tinged discharge from the nostrils. Gross lesions can be observed anywhere in the lungs, but often one or both of the caudal lung lobes is affected. Blood-stained froth fills the trachea. Fibrinous pleuritis and pleural adhesions are characteristic. Histologically there is a lobar fibrinosuppurative hemorrhagic and necrotizing pneumonia and fibrinous pleuritis. Vasculitis with thrombosis is often seen. Differential diagnoses in acute cases include *Salmonella choleraesuis* and *Actinobacillus suis* infections.

The disease is caused by a gram-negative encapsulated coccobacillus, *Actinobacillus pleuropneumoniae.* The bacterial agent is divided into two biovars according to the requirement of NAD (nicotinamide adenine dinucleotide). Biovar 1 strains are NAD-dependent and biovar 2 strains are NAD-independent. There are 15 serotypes based on capsular polysaccharides.

Clinical signs and pathological findings are associated with several bacterial virulence factors combined with the host reaction. In addition to capsular components and cellular lipopolysaccharides, *A. pleuropneumoniae* produces several cytotoxins and proteolytic enzymes that can resist macrophage and complement killing. Acute disease is often followed by chronic encapsulated necrotic lung lesions and local pleuritis with adhesions. Chronic pleuritis seen at slaughter is common in herds with endemic infection. Asymptomatic carrier pigs spread the disease by direct contact or by aerosols.

A. pleuropneumoniae is capable of causing severe disease without predisposing factors, but the severity of the disease is affected by the immune status of the pigs and environmental factors, such as crowding, ambient temperature or the moving and mixing of animals. There are also differences in the virulence within and between strains. Disease problems can be enhanced by other concurrent pathogens, for example *Mycoplasma hyopneumoniae*, swine influenza virus, porcine arterivirus (porcine respiratory and reproduction syndrome virus) or porcine circovirus-2.

Other uncommon lesions associated with *A. pleuropneumoniae* include endocarditis, pericarditis, arthritis, osteomyelitis, meningitis, otitis media, granulomatous hepatitis and granulomatous pneumonia.[3]

A. pleuropneumoniae was cultured from lung lesions of all four examined pigs. In this case, *Pasteurella multocida* was also isolated from the lungs. *Pasteurella multocida* can cause suppurative pneumonia in pigs, but it is often a secondary invader. The lymph nodes exhibited depletion of lymphocytes and loss of the follicular architecture. Porcine circovirus-2 antigen was also detected by immunohistochemistry in lymph nodes of this pig. These lesions were indicative of PMWS (postweaning multisystemic wasting syndrome). However, in this pig the lesions associated with PCV-2 were considered to be an additional finding.

AFIP Diagnosis: Lung: Pleuropneumonia, fibrinosuppurative and necrotizing, multifocal to coalescing, severe, with oat cells, fibrinonecrotizing vasculitis, and colonies of coccobacilli.

Pneumonia	Route of Exposure	Anatomic Distribution	Lung Texture	Anatomic Location of Injury	Example	Common Pulmonary Sequelae
Broncho-pneumonia	Aerogenous	Cranioventral	Firm, hard	Bronchiolar-alveolar junction	Enzootic pneumonia; Pneumonic mannheimiosis	Abscesses, pleural adhesions
Interstitial	Aerogenous or hematogenous	Diffuse	Elastic, rubbery	Alveolar or interlobular septae	PRRS, PCV-2	Edema, type II pneumocyte hypertrophy, alveolar fibrosis
Broncho-interstitial	Aerogenous	Multifocal	Firm to rubbery	Bronchioloar and alveolar epithelium	BRSV, swine influenza	Mix of broncho- and interstitial-pneumonias
Granuloma-tous	Aerogenous or hematogenous	Multifocal	Nodular	Non-specific	Tuberculosis, blastomycosis	Dissemination of infection
Embolic	Hematogenous	Multifocal	Nodular	Pulmonary vasculature	Vegetative endocarditis	Random abscesses

Adapted from Table 9-4, McGavin and Zachary's *Pathologic Basis of Veterinary Disease*[2]

Conference Comment: The moderator focused the discussion on recognizing patterns of pneumonia and lung injury. Participants classified patterns of pneumonia as bronchopneumonia, interstitial, bronchointerstitial, embolic and granulomatous. The authors of McGavin and Zachary's *Pathologic Basis of Veterinary Disease* provide an excellent overview of pneumonia. The table below summarizes key points of each pattern.[1,2]

The moderator discussed additional patterns of lung injury. Bronchitis and bronchiolitis result from direct damage to and subsequent necrosis of airway epithelium leading to airway inflammation. Potential etiologic agents or disease syndromes resulting in this pattern include feline asthma, viral infection, inhalation of toxic gases, toxins metabolized by P450 cytochrome oxidase of Clara cells, and inhaled irritants.[1]

As noted by the contributor, *Actinobacillus pleuropneumoniae* has several virulence factors which play a unique role in the pathogenesis of porcine pleuropneumonia. The organism produces three RTX toxins (Apx I, II, and III) which are cytolytic for neutrophils, erythrocytes, alveolar macrophages, and epithelial cells. Once lysed, the contents of neutrophils and macrophages damage host tissue. Macrophages activated by lipopolysaccharide secrete neutrophil chemoattractants, activate complement, and promote coagulation. In addition to resisting macrophage phagocytosis, the bacterial capsule prevents complement activation. In order to survive in the milieu of cytotoxins and reactive oxygen species from lysed leukocytes, *Actinobacillus pleuropneumoniae* produces a variety of antioxidant enzymes, including superoxide dismutase, catalase and hydrogen peroxide reductase.[1]

Contributor: Finnish Food Safety Authority Evira, Oulu, Finland
http://www.evira.fi

References:

1. Caswell JL, Williams KJ. Respiratory system. In: Maxie MG, ed. *Jubb, Kennedy and Palmer's Pathology of Domestic Animals*. 5th ed., Vol. 2. Philadelphia, PA: Elsevier Ltd; 2007:555-575,587-588.
2. Lopez A. Respiratory system. In: McGavin MD, Zachary JF, eds. *Pathologic Basis of Veterinary Disease*. 4th ed. St. Louis, MO: Elsevier; 2007:508-517.
3. Ohba T, Shibahara T, Kobayashi H,et al. Prevalence of granulomatous pleuropneumonia associated with *Actinobacillus pleuropneumoniae* serotype 2 in slaughter pigs. *J Vet Med Sci*. 2009;71:1089-1092.

The Armed Forces Institute of Pathology
Department of Veterinary Pathology

Conference Coordinator
Matthew Wegner, DVM

WEDNESDAY SLIDE CONFERENCE 2010-2011

Conference 11

17 November 2010

Conference Moderator:
Terrell Blanchard, DVM, Diplomate ACVP

CASE I: SP-09-2326 (AFIP 3162243).

Signalment: 12-year-old spayed female miniature schnauzer (*Canis familiaris*).

History: This dog had a recent history of inappetence and upon abdominal palpation a multinodular mass was noted in the cranial abdomen. Radiographs confirmed a multinodular mass affecting the liver. Abdominal surgery was performed, and biopsy samples were collected from the nodular masses present on the liver.

Laboratory Results: Moderate elevation in alkaline phosphatase levels were reported by the referring veterinarian.

Histopathologic Description: Slides contain representative sections of one of the liver masses. Sections consist of a poorly demarcated, non-encapsulated, pseudolobulated hepatocellular neoplasm. Multifocally, neoplastic hepatocytes are arranged in cords and trabeculae (2-6 cells thick) supported by a fine fibrovascular stroma. These regions transition into areas of architectural collapse, composed of small nests and clusters of anaplastic cells suspended within edematous fibrous stroma and separated by large, cystically dilated sinusoids and lymphatics. Neoplastic cells are polygonal and have a moderate amount of eosinophilic cytoplasm with distinct cell borders. Nuclei are round with euchromatic, stippled chromatin, and 1-2 prominent nucleoli. Mitoses range from 0 to 4 per high power field. There is marked anisocytosis and anisokaryosis, and occasional neoplastic hepatocytes contain large clear cytoplasmic vacuoles. Portal triads are absent.

Immunohistochemistry was performed. Regions of well differentiated neoplastic hepatocytes have strong stippled cytoplasmic expression of Hepatocyte Paraffin 1 (Hep Par 1) with loss of expression of this antigen along the periphery of pseudolobules as neoplastic cells become anaplastic. Anaplastic cells have strong cytoplasmic expression of Cytokeratin 7.

Contributor's Morphologic Diagnosis: Liver: Multinodular combined hepatocellular cholangiocarcinoma.

Contributor's Comment: The incidence of malignant hepatocellular neoplasms is less than 1 percent of all canine neoplasms, with fewer reported cases of biliary tumors.[3] The subset, hepatocellular cholangiocarcinoma (HCCC) or hepatocholangiocarcinoma, is extremely rare with only three cases reported in dogs[7] and one case reported in a horse.[4] Established classification systems of HCCCs describe 3 main histologic types: 1) Type I- occurrence of both histologically distinct hepatocellular carcinoma and cholangiocarcinoma that can present either as distinctly separate masses or as coalescing masses (collision tumor); 2) Type II-combined tumor with commingling and often transitional elements of both hepatocellular carcinoma and cholangiocarcinoma (transitional tumor), and 3) Type III-fibrolamellar variant, resembling fibrolamellar hepatocellular carcinomas but with pseudoglands containing mucin.[7] Based on the published criteria, this neoplasm would be classified as type II.

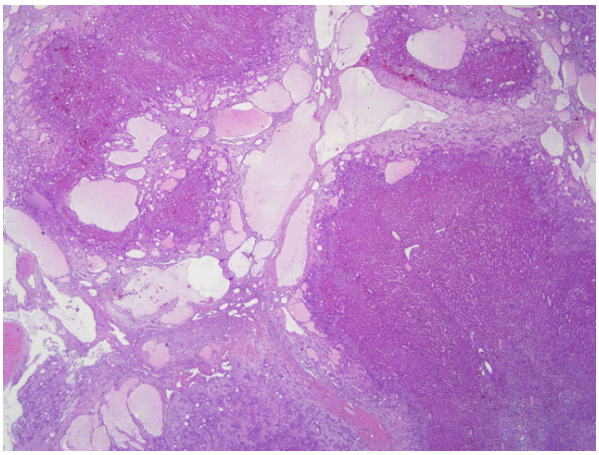

1-1. Liver, hepatocholangiocarcinoma, dog. The liver is infiltrated by a densely cellular, lobulated neoplasm composed of polygonal cells arranged in cords and trabeculae and containing variably-sized cystic structures filled with eosinophilic proteinaceous material. (HE 20X)

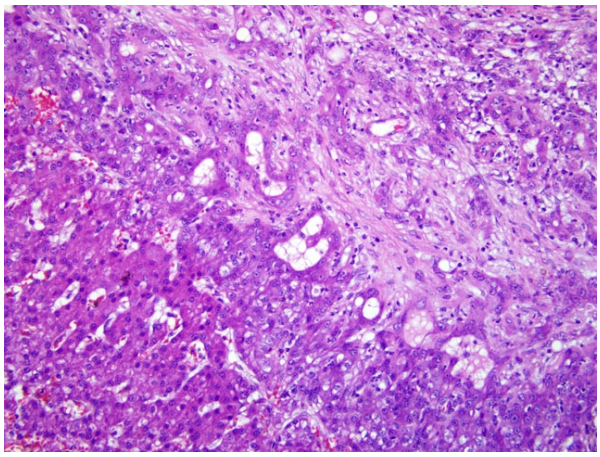

1-2. Liver, hepatocholangiocarcinoma, dog. Cords of neoplastic hepatocytes with abundant eosinophilic cytoplasm transition with neoplastic biliary epithelial cells arranged in irregular ductular structures separated by variable amounts of reactive fibrous stroma. (HE 200X)

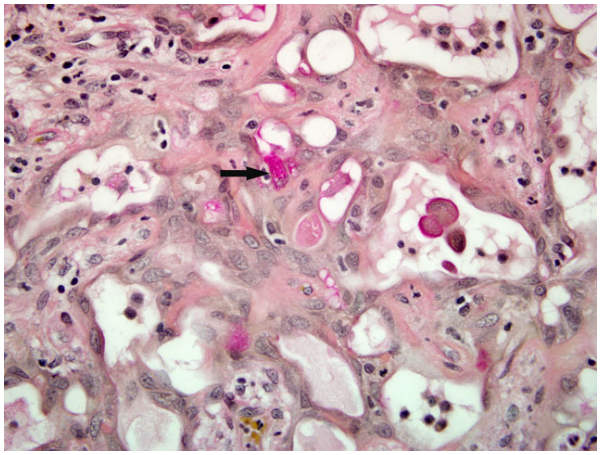

1-3 Liver, hepatocholangiocarcinoma, dog. Occasionally, the cytoplasm of neoplastic biliary epithelial cells contains carminophilic material (arrow). The lumens of ductular structures contain variable amounts of similar carminophilic material. (Mucicarmine 400X)

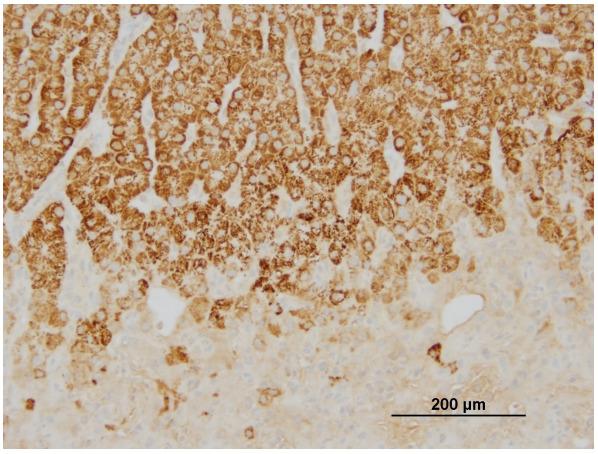

1-4. Liver, hepatocholangiocarcinoma, dog. The neoplastic hepatocellular component demonstrates strong cytoplasmic immunoreactivity for hepatocyte paraffin 1, with loss of expression of this antigen along the periphery of the pseudolobules as neoplastic cells become anaplastic. (Hep Par-1). Photograph courtesy of Diagnostic Center for Population & Animal Health, 4125 Beaumont Road, Lansing, MI 48910, Fitzgerald@dcpah.msu.edu

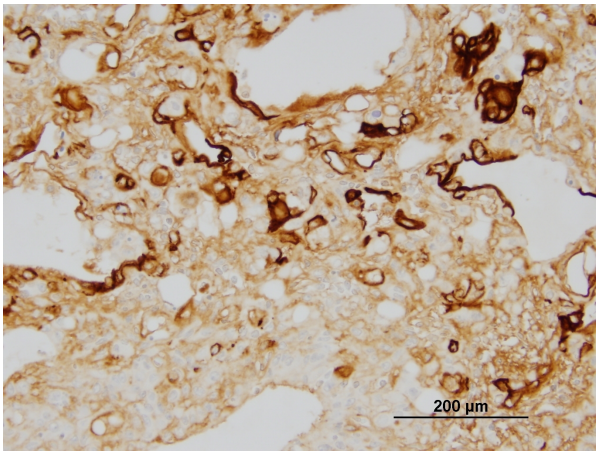

1-5. Liver, hepatocholangiocarcinoma, dog. Anaplastic cells of the biliary component demonstrate strong cytoplasmic immunopositivity for cytokeratin 7. (Cytokeratin 7). Photograph courtesy of Diagnostic Center for Population & Animal Health, 4125 Beaumont Road, Lansing, MI 48910, Fitzgerald@dcpah.msu.edu

Hep Par-1 can be used to demonstrate hepatocellular origin, whereas Cytokeratin 7 can be used to demonstrate biliary origin.[6] Other immunohistochemical markers used to differentiate primary liver neoplasms, including hepatoblastomas, are α-fetoprotein (AFP) and carcinoembryonic antigen (CEA).[6,7]

Survival or behavioral data has not been established specifically for HCCCs. Metastasis of hepatocellular carcinomas occurs earliest and most frequently to the hepatic lymph nodes and lungs.[3] However, one year after making the diagnosis we have no further information on this animal's survival or disease progression. Surgical resection of affected liver lobes can prolong the animal's life by approximately one year on average;[3] however, in this case, only portions of the neoplasm were removed, and not the entire affected lobe.

AFIP Diagnosis: Liver: Hepatocholangiocarcinoma.

Conference Comment: Based on evaluation of the hematoxylin & eosin stained sections, participants readily agreed on the presence of a biliary component to the specimen, but were divided as to the presence of a hepatocellular component. Slide variation likely contributed to this divergence in histologic interpretation, as some slides contain markedly more cystic sections with minimal parenchyma. The presence of a biliary component was confirmed by carminophilic staining of the neoplastic biliary epithelial cells with the mucicarmine histochemical stain at the AFIP. Further evidence supporting a hepatocellular cholangiocarcinoma (HCCC) is the histomorphologic appearance of gradual transition from the hepatocellular component to a biliary component, which is quite evident when comparing the immunohistochemical staining results for Hep Par-1 and cytokeratin 7 provided by the contributor.

Within the canals of Hering reside a population of bipotential progenitor cells referred to in the literature as oval cells. With proper stimulation, these cells can differentiate into hepatic cells or biliary epithelial cells. In response to chronic hepatitis, fulminant liver failure or severe, end-stage cirrhosis, oval cells begin proliferating. This is seen histologically as ductular reaction with reduplication of biliary epithelium and occurs prior to hepatocyte or cholangiocyte differentiation.[1] Several molecular pathways appear to play a role in oval cell regulation. The Wnt/β catenin and Sonic Hedgehog signaling pathways both regulate oval cell renewal; deregulation (i.e. increased signaling) allowing oval cell proliferation of these pathways is reported in hepatocellular carcinomas.[1,5] Conversely, Notch signaling results in decreased oval cell proliferation and increased apoptosis; this pathway is frequently down-regulated in HCC.[5]

There is unresolved debate regarding the histogenesis of hepatic neoplasia including HCC, cholangiocarcinoma (CC) and combined HCC-CC (i.e. HCCC). The two current, popular theories propose either de-differentation of malignant hepatocytes or cholangiocytes to a hepatic stem cell; or neoplastic transformation of oval cells resulting in neoplasia involving one or both cell types.[1,5,8,10] An interesting feature of hepatic tumorigenesis supporting the hepatic stem cell theory is the histologic observation of a ductular reaction prior to tumor development.[2] Likewise, Tang et al. induced hepatic stem cells to transform into liver cancer through IL-6 stimulation with concurrent TGF-β signaling inactivation.[8]

A thorough discussion of the stem cell theory of cancer is beyond the scope of this paper, and readers are invited to read the recent review paper by Trosko for an overview of the two theories of cancer histogenesis.[9] During the conference discussion the moderator did reference a recent symposium of the National Toxicology Program which discussed HCCC in B6C3F1mice.[2] The overall incidence of HCCC in mice, based on the NTP database, is less than 1% with a greater number of males affected than females; overall, metastasis is high at 84%.

We would like to thank the staff pathologists in the Department of Hepatic Pathology for reviewing this case.

Contributor: Michigan State University, Diagnostic Center for Population and Animal Health, 4125 Beaumont Rd, Lansing, MI 48910
www.animalhealth.msu.edu

References:

1. Alison MR, Islam S, Lim S. Stem cells in liver regeneration, fibrosis and cancer: The good, the bad and the ugly. *J Pathol*. 2009;217:282-298.
2. Bach U, Hailey JR, Hill GD, et al. Proceedings of the 2009 National Toxicology Program Satellite Symposium. *Toxicol Pathol*. 2010;38(1):9-36.
3. Cullen JM, Popp JA. Tumors of the liver and gall bladder. In: Meuten DJ, ed. *Tumors in Domestic Animals*. 4th ed. Ames, IA: Wiley-Blackwell; 2002:486-492.
4. Kato M, Higuchi T, Orita Y, Ishikawa Y, Kadota K. Combined hepatocellular carcinoma and cholangiocarcinoma in a mare. *J Comp Pathol*. 1997;116(4): 409-413.
5. Lee TKW, Castilho A, Ma S, Ng IOL. Liver cancer stem cells: Implications for a new therapeutic target. *Liver Int*. 2009;DOI:10.1111/j.1478-3231.2009.02040.x:955-965.
6. Ramos-Vara JA, Miller MA, Johnson GC. Immunohistochemical characterization of canine hyperplastic hepatic lesions and hepatocellular and biliary neoplasms with monoclonal antibody hepatocyte paraffin 1 and a monoclonal antibody to cytokeratin 7. *Vet Pathol*. 2001;38(6):636-643.
7. Shiga A, Shirota K, Enomoto M. Combined hepatocellular and cholangiocellular carcinoma in a dog. *J Vet Med Sci*. 2001;63(4):483-486.
8. Tang Y, Kitsin K, Jogunoori W, et al. Progenitor/stem cells give rise to liver cancer due to aberrant TGF-β and IL-6 signaling. *Proc Natl Acad Sci U S A*. 2008;105(7): 2445-2450.
9. Trosko JE. Cancer stem cells and cancer nonstem cells: From adult stem cells or from reprogramming of differentiated somatic cells. *Vet Pathol*. 2009;46(2):176-193.
10. Yeh MM. Pathology of combined hepatocellular-cholangiocarcinoma. *J Gastroenterol Hepatol*. 2010;25:1485-1492.

CASE II: N10-41-1 (AFIP 3165181).

Signalment: 11.5-year-old spayed female Chihuahua dog (*Canis familiaris*).

History: This dog was presented to Tufts emergency clinic for acute onset of worsening dyspnea. Pulmonary computed tomography (CT) revealed diffuse patchy interstitial, alveolar and airway changes affecting all lung lobes and mild lobar bronchi traction bronchiectasis. An echocardiogram demonstrated moderate pulmonary hypertension. Due to poor prognosis, euthanasia was elected.

Gross Pathology: At necropsy, 80 % of all lung lobes are mottled dark red to dark brown, slightly firm and wet on cut surface.

Histopathologic Description: Most terminal bronchioles are obliterated by variably sized (25-200 µm diameter) aggregates of fibrin, collagen, fibroblasts, macrophages (often containing intracytoplasmic yellow-brown pigments, hemosiderophages) and few lymphocytes and plasma cells. Moderate numbers of macrophages/hemosiderophages and erythrocytes are present within the alveoli. There is multifocal hyperplasia of type II pneumocytes. Alveolar septa are variably thickened by the previously described inflammatory cells and small amounts of fibrous tissue. Moderate amounts of fibrous tissue expand the subpleural space segmentally.

Contributor's Morphologic Diagnosis: Lung: Chronic, severe, intra-bronchiolar and intra-alveolar organizing fibrosis with chronic hemorrhage (bronchiolitis obliterans with organizing pneumonia)

Contributor's Comments: The histopathologic changes in the lungs are consistent with bronchiolitis obliterans with organizing pneumonia (BOOP), a well-documented entity in humans.[1,7] BOOP, synonymous with cryptogenic organizing pneumonia (COP), is a distinct clinicopathological entity with clinical, imaging and prognostic features different from those of obliterative bronchiolitis and usual interstitial pneumonia/idiopathic pulmonary fibrosis (UIP/IPF). The disease is an inflammatory reaction to lung injury and has been associated with a wide variety of causes, including infections, drugs, inhalants, collagen-vascular disorders, and graft-versus-host disease in heart and bone marrow transplants. A substantial percentage of cases are idiopathic. Clinically, the patients are presented with acute to subacute (weeks to a few months) onset of dyspnea, coughing, malaise, and fever (flulike signs). Thoracic radiographs reveal patchy bilateral airspace opacification that may be

2-1. Lung, dog. Multifocally, terminal bronchioles are partially to completely filled with variably sized aggregates of immature collagen, reactive fibroblasts, and hemosiderin-laden macrophages. (HE 100X)

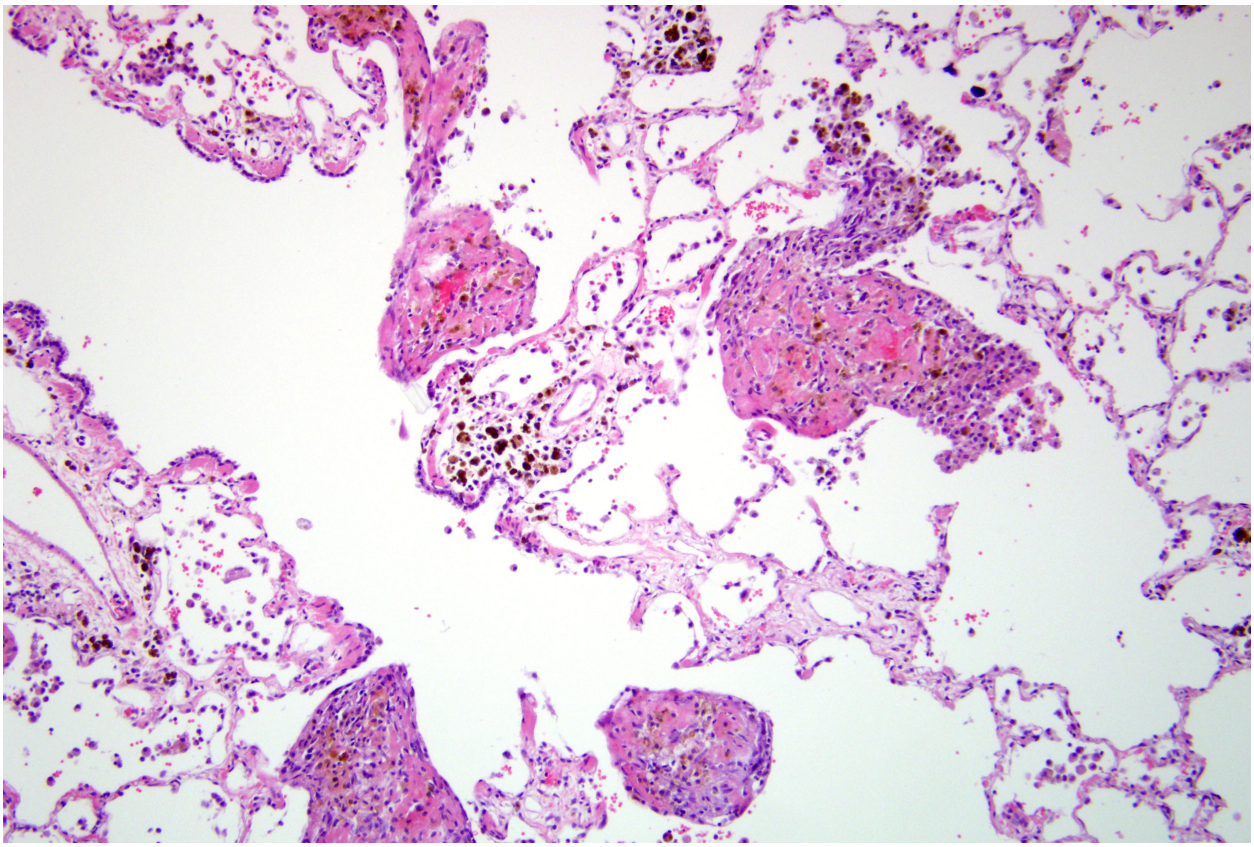

difficult to distinguish from other conditions, such as usual interstitial pneumonitis and small airway disease. Lung biopsy is the preferred method for the definitive diagnosis of this entity. In humans, the prognosis is excellent, with complete recovery occurring within weeks or months. The lesions usually respond to treatment with corticosteroids.[1,7]

Histologically, BOOP is characterized by patchy fibrosis filling the lumens of terminal and respiratory bronchioles and extending in a continuous fashion into alveolar ducts and alveoli. Typically, fibrosis is characterized by plugs of young fibroblasts embedded in a myxoid matrix and admixed with scant mononuclear inflammatory cells that adopt a polypoid appearance (granulation tissue) within the lumen of the airspaces ("Masson bodies"). Other histological features include chronic inflammation in the walls of the surrounding alveoli with reactive type II cells, increased foamy macrophages in the alveoli, and preservation of lung architecture. The fibrotic process is confined to the lumen of the airspaces and does not involve the interstitium. A unique feature of the BOOP is its temporal uniformity (i.e. all lesions seem to be in the same stage at any given time). Ultrastructurally, the cellular proliferation is composed of fibroblasts and myofibroblasts. BOOP is differentiated from organizing pneumonia, which is defined by the presence of granulation tissue in the distal air spaces, while obliterative bronchiolitis (or constrictive bronchiolitis obliterans) is characterized by narrowing of the bronchiolar lumens by concentric fibrosis and inflammation. The histologic changes in BOOP may be similar to those of diffuse alveolar damage, except that they are localized to the peribronchiolar parenchyma.[1,7]

This disease entity has been rarely reported clinically in dogs,[6] but has been produced experimentally by infecting dogs with adenovirus[1] or accidental intra-airway exposure with pure oleic acid.[5] In the present case, there is no evidence of infectious agents within the examined tissues and the etiology of the severe pulmonary changes is uncertain. Though BOOP has not been well described in animals, especially its response to corticosteroids, lung biopsy would be helpful to establish a definitive diagnosis.

AFIP Diagnosis: Lung: Bronchiolitis obliterans, multifocal, moderate, chronic with hemosiderosis.

Conference Comment: The contributor provides an excellent overview of bronchiolitis obliterans with organizing pneumonia (BOOP). Conference participants briefly discussed ascribing a human disease name to a similar condition in animals. The moderator commented that, while in some instances it is appropriate, there may be instances in which the disease process differs from that of humans; therefore use of human disease nomenclature may not be warranted. This case was reviewed by the AFIP Department of Pulmonary and Mediastinal Pathology. They offered a diagnosis of BOOP with hemosiderin most likely resulting from an infection leading to hemorrhage followed by resolution. They further speculated that the acute process occurred 3-6 weeks prior to this phase of the lesion.

Although the cause of pulmonary fibrosis is not completely understood, recent advancements indicate that an exuberant fibroblastic or myofibroblastic proliferation has a significant impact on its development. As in any wound, fibrinous exudates that are not rapidly removed are replaced by fibrosis.[2] It is currently thought that injury to type I alveolar epithelial cells results in release of transforming growth factor-β1 (TGF-β1). TGF-β1is fibrogenic and stimulates the transformation of fibroblasts into myofibroblasts with the subsequent deposition of collagen and the development of fibrosis. TGF-β1 accomplishes this by negatively regulating telomerase activity and inhibiting caveolin-1. By negatively affecting telomerase activity, epithelial cell apoptosis is facilitated which leads to cell death and repair mechanism activation. By inhibiting caveolin-1, which is an inhibitor of pulmonary fibrosis, TGF-β1 increases pro-fibrogenic mechanisms leading to the development of exuberant pulmonary fibrosis.[4]

We thank Dr. Russell Harley of the Department of Pulmonary and Mediastinal Pathology, AFIP, for reviewing this case.

Contributor: Department of Biomedical Sciences, Section of Pathology, Tufts Cummings School of Veterinary Medicine, 200 Westboro Rd, North Grafton, MA
http://www.tufts.edu/vet/

References:

1. Castleman WL. Bronchiolitis obliterans and pneumonia induced in young dogs by experimental adenovirus infection. *Am J Pathol*. 1985;119(3):495-504.
2. Caswell JL, Williams KJ. Respiratory system. In: Maxie MG, ed. *Jubb, Kennedy and Palmer's Pathology of Domestic Animals*. Vol. 2, 5th ed. Philadelphia, PA: Elsevier Ltd; 2007:559-560.
3. Epler GR. Bronchiolitis Obliterans organizing pneumonia. *Arch Intern Med*. 2001;161(2):158-164.
4. Husain AN. The lung. In: Kumar V, Abbas AK, Fausto N, Aster JC, eds. *Robbins and Cotran Pathologic Basis of Disease*. 8th ed. Philadelphia, PA: Elsevier Saunders; 2009:694-696.
5. Li X, Botts S, Morton D, Knickerbocker MJ, Adler R. Oleic acid-associated bronchiolitis obliterans-organizing pneumonia in beagle dogs. *Vet Pathol*. 2006;43(2):183-185.
6. Phillips S, Barr S, Dykes N, et al. Bronchiolitis obliterans with organizing pneumonia in a dog. *J Vet Intern Med*. 2000;14(2):204-207.
7. Weidner N, Cote R, Suster S, Weiss L, eds. *Modern Surgical Pathology*. 2nd ed. Philadelphia, PA: WB Saunders; 2002:409-411, 421.

CASE III: B10-13908 (AFIP 3167237).

Signalment: 12-year-old male castrated Bengal cat (hybrid of *Prionailurus bengalensis* and *Felis catus*).

History: This cat had a history of several cutaneous masses on the right flank present for a few weeks with a rapid growth rate. The masses were surgically excised and initially diagnosed as a possible variant of eosinophilic granuloma complex. The lesions recurred at the same site approximately 3.5 months later, and were surgically excised and submitted for a second biopsy.

Gross Pathology: The lesion was described by the referring veterinarian as a raised, erythematous, ulcerated mass measuring 2 x 2 x 1 cm.

Histopathologic Description: Haired skin, right flank: The epidermis is extensively ulcerated and covered by thick serocellular crusts consisting of fibrin, cell debris, and numerous necrotic granulocytes. The remaining epidermis is eroded in some regions, with multifocal spongiosis and acanthosis. The necrosis, spongiosis, and acanthosis extend to the adjacent hair follicles with multifocal loss and destruction of adnexal units. The superficial and deep dermis is infiltrated by numerous eosinophils with lesser numbers of macrophages, plasma cells, lymphocytes, neutrophils, and mast cells, as well as variable fibroplasia and fibrosis. Within the dermis, there are multiple foci of necrosis often centered around remaining islands of adnexal epithelial cells. In these regions, there is a similar dense inflammatory cell infiltrate consisting predominantly of eosinophils and macrophages with abundant cell debris and fibrin. Keratinocytes in these regions often have pale eosinophilic cytoplasm, and occasionally contain intranuclear inclusion bodies. The intranuclear inclusions are glassy and amphophilic with marginated chromatin measuring approximately 10-12 µm. In other areas, the intranuclear inclusions are eosinophilic surrounded by a clear halo with peripheralized chromatin measuring 4-7 µm in diameter. In some of the sections, macrophages and eosinophils surround blood vessels with occasional destruction of the vessel wall and adjacent cell debris and fibrin. Immunohistochemistry revealed multifocal predominantly cytoplasmic staining with feline herpesvirus 1 antibodies both in the epidermis and adnexal epithelium adjacent to areas of necrosis.

Contributor's Morphologic Diagnosis: Haired skin (right flank): Severe ulcerative necrotizing eosinophilic and histiocytic dermatitis with intranuclear inclusion bodies (consistent with feline herpesvirus 1).

Contributor's Comment: Feline herpesvirus 1 (FeHV-1), an alphaherpesvirus, is a double-stranded DNA enveloped virus causing primarily upper respiratory disease and conjunctivitis in cats.[1] FeHV-1 infection has also been associated with pneumonia, keratitis, ulcerative dermatitis and ulcerative stomatitis. Similar to other alphaherpesviruses, FeHV-1 causes necrosis of epithelial cells and establishes a latent infection in the trigeminal ganglion, optic nerve, olfactory bulb and cornea.[1] Clinical signs are most common in kittens, but may occur in adults following recrudescence of latent infections due to stress, corticosteroid therapy, lactation or change in housing.[1] Systemic disease is uncommon; however, it may occur in young or debilitated animals. Classic respiratory lesions of FeHV-1 include necroulcerative fibrinosuppurative rhinitis and bronchointerstitial pneumonia, often with intranuclear inclusion bodies.

Ulcerative facial and nasal dermatitis with eosinophilic infiltrates associated with FeHV-1 has been reported in cats.[4] Lesions of FeHV-1 dermatitis are predominantly seen in the face and rarely on distal extremities.[3,4] Cats with herpesviral associated dermatitis may have a history of previous or concurrent respiratory disease. Preceding glucocorticoid therapy and environmental stress were suspected triggers of disease in a report.[4] Grossly, the lesions are characterized by erosion and ulceration of the face, with the dorsal and lateral muzzle, nasal planum and periorbital regions most commonly affected.[3,4] Hallmarks of facial herpesvirus dermatitis in cats include intense eosinophilic dermatitis with ulceration and epithelial cell necrosis. Intranuclear inclusion bodies are often present within keratinocytes, both in the epidermis and hair follicles, as well as in sebaceous glands.[3,4] However, inclusion bodies may not be present in all cases or may be rare. Similar lesions associated with FeHV-1 have been described in cheetahs, characterized by dense infiltrates of eosinophils and plasma cells, and pseudoepitheliomatous hyperplasia.[6] Lesions in cheetahs were present predominantly on the face, although lesions also occurred at the top of the head, distal forelegs, flank, tail, and footpads.[6]

Grossly, the differential diagnosis for FeHV-1 facial ulcerative dermatitis includes mosquito bite hypersensitivity, food allergy, pemphigus foliaceus, and neoplasia.[3] Cases of herpesvirus dermatitis may be misdiagnosed histologically as a variant of the eosinophilic granuloma complex (EGC) or allergic dermatitis. Immunohistochemistry and PCR can serve as useful diagnostic tools to differentiate herpesvirus associated dermatitis from other causes of eosinophilic dermatitis.[4,5] Proper diagnosis is important regarding treatment, since glucocorticoid therapy used to treat other eosinophilic skin disorders may cause worsening of skin lesions caused by FeHV-1. Vaccination does not seem to prevent this cutaneous manifestation of herpesvirus infection, either in cats or cheetahs.[4,6] It is imperative to thoroughly search for intranuclear inclusion bodies within the epithelium in feline skin samples showing intense eosinophilic inflammation, especially if accompanied by ulcers and hair follicle involvement/necrosis.

The presence of this lesion in the right flank of this cat is highly unusual. Direct contact of the face and salivary gland secretions during grooming may be the cause of the lesion at this unusual location, similar to what has been previously

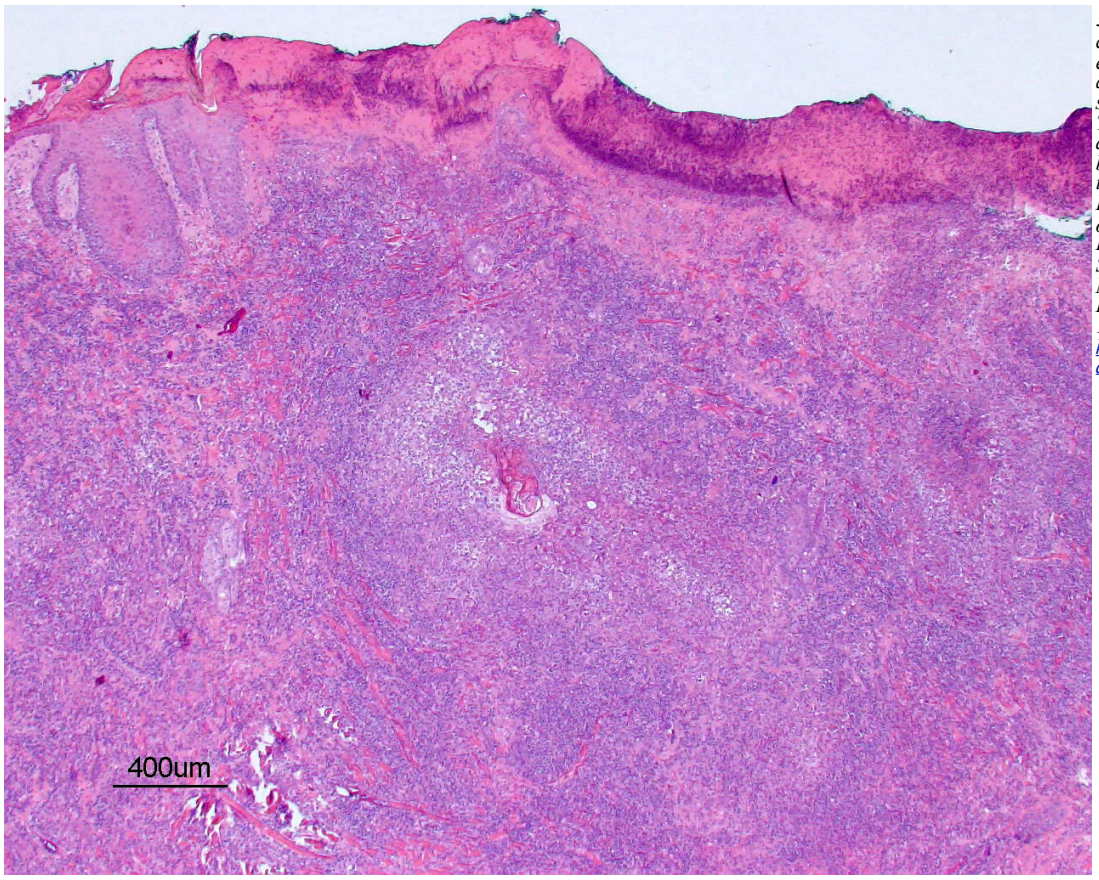

3-1. Haired skin, cat. The epidermis is extensively ulcerated and covered by a serocellular crust. The subjacent dermis is expanded by numerous inflammatory cells. Photograph courtesy of University of Pennsylvania, School of Veterinary Medicine, Philadelphia, PA 19104, kolsky@vet.upenn.edu

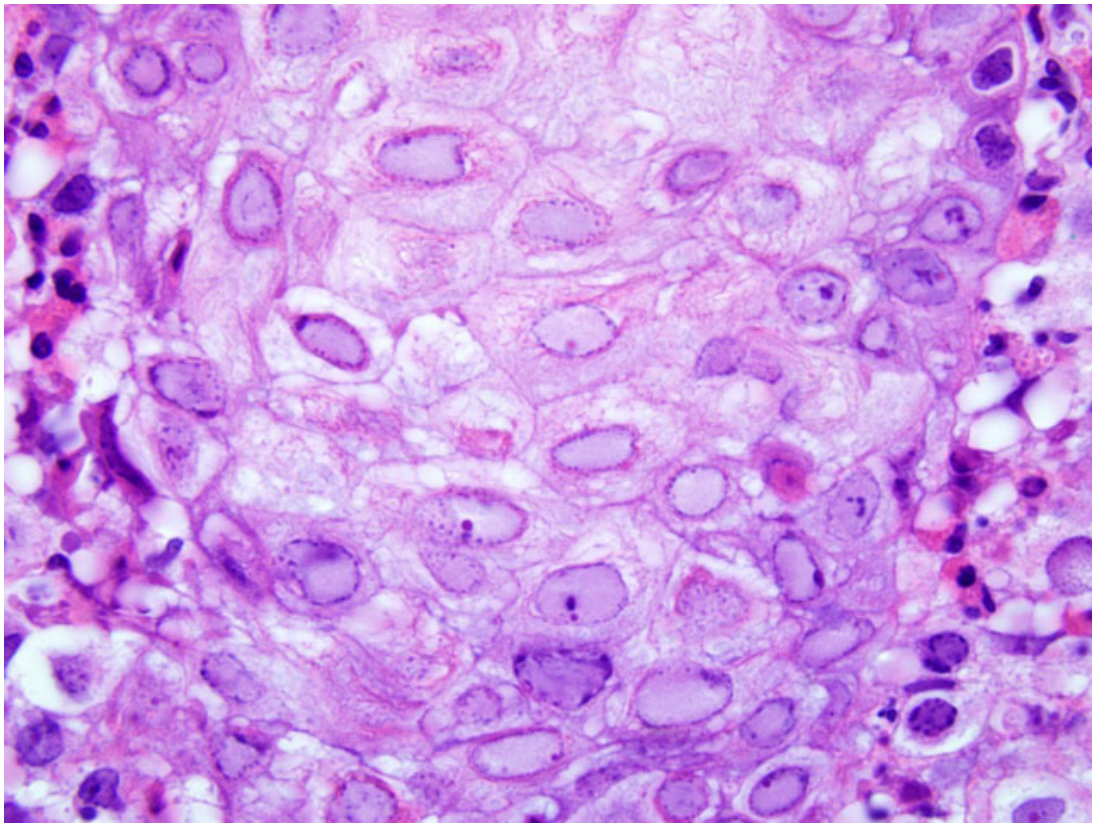

3-2. Haired skin, cat. Keratinocytes contain pale eosinophilic cytoplasm and nuclei with glassy, amphophilic intranuclear inclusion bodies which peripheralize the chromatin. (HE 1000X)

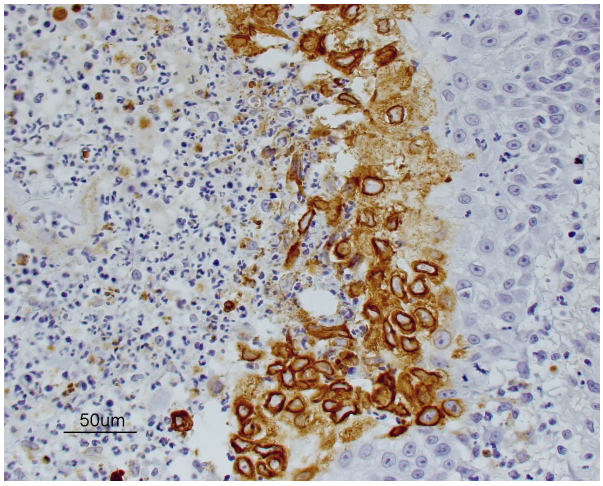

3-3. Haired skin, cat. Keratinocytes demonstrate cytoplasmic immunoreactivity for anti-feline herpesvirus 1 antibodies. Photograph courtesy of University of Pennsylvania, School of Veterinary Medicine, Philadelphia, PA 19104, kolsky@vet.upenn.edu

postulated for lesions in the distal extremities.[3,6] Therefore, FeHV-1 associated dermatitis should not be ruled out based on the location of the lesion.

AFIP Diagnosis: Haired skin: Dermatitis and folliculitis, necrotizing, eosinophilic and lymphohistiocytic, multifocal to coalescing, severe, with ulceration and epithelial intranuclear inclusion bodies.

Conference Comment: As commented by the contributor, detection of the characteristic intranuclear inclusion bodies associated with herpesviral infection is the key to identifying the underlying etiology in this case. Participants were intrigued by the unusual location of this herpesviral lesion; in the absence of the characteristic inclusions, many would not have included herpesviral infection as the primary differential diagnosis. This observation stimulated discussion concerning the differential diagnosis for eosinophilic and ulcerative dermatitis in the cat, including the various forms of feline eosinophilic granuloma complex: feline eosinophilic plaque, feline eosinophilic granuloma and indolent ulcer. The chart below summarizes the often overlapping findings of each of these entities.[2]

The moderator also stressed the importance of knowing the ultrastructural properties of viruses known to infect the skin. Some of the viruses known to infect the skin of domestic cats and their corresponding ultrastructural features include:[7]

- Felid herpesvirus-1: Enveloped, 150 nm in diameter with an icosahedral 100 nm diameter nucleocapsid
- Felis domesticus papillomaviruses 1 and 2: Non-enveloped, 50 nm diameter spherical, with icosahedral symmetry
- Feline leukemia virus and feline immunodeficiency virus: Enveloped, 80-100 nm, with a three layered structure containing an innermost genome-nucleoprotein complex, surrounded by an icosahedral capsid which is further bounded by the envelope with glycoprotein peplomeres

Contributor: Department of Pathobiology, University of Pennsylvania, School of Veterinary Medicine, Suite 4005, MJR-VHUP, 3800 Spruce Street, Philadelphia, PA 19104
http://www.vet.upenn.edu/FacultyandDepartments/Pathobiology/PathologyandToxicology/tabid/412/Default.aspx

Disease Form	Cause	Anatomic Location	Gross Appearance	Histologic Findings
Feline eosinophilic plaque	Suspected hypersensitivity to food, parasites or related to atopy	Inguinal, axillary, perineal areas or lateral thigh	Red, raised, ulcerated plaques; pruritic	• Epidermal acanthosis, spongiosis, eosinophil exocytosis • Diffuse to perivascular eosinophilic dermatitis
Feline eosinophilic granuloma	Unknown; suspect hypersensitivity or hereditary	• Linear form: caudal or medial thigh • Nodular form: lips, chin, oral cavity, face • Also footpads and mucocutaneous junctions	Raised, pink, alopecic	• Diffuse eosinophilic dermatitis • Flame figures: degranulating eosinophils surrounding collagen • Macrophages and multi-nucleated giant cells
Indolent ulcer	Unknown	Upper lip adjacent to philtrum; uni- or bi-lateral	Non-pruritic and non-painful ulcer	• Acute: diffuse infiltrates of eosinophils with neutrophils, mast cells and macrophages • Chronic: lymphocytes, plasma cells, macrophages, neutrophils, fibrosis

References:

1. Caswell JL, Williams KJ. Respiratory system. In: Maxie MG, ed. *Jubb, Kennedy and Palmer's Pathology of Domestic Animals*. Vol. 2, 5th ed. Philadelphia, PA: Elsevier Ltd; 2007:648-649.

2. Ginn PE, Mansell JEKL, Rakich PM. Skin and appendages. In: Maxie MG, ed. *Jubb, Kennedy and Palmer's Pathology of Domestic Animals*. Vol. 3, 5th ed. Philadelphia, PA: Elsevier Ltd; 2007:738-739.

3. Gross TL, Ihrke PJ, Walder EJ, Affolter VK. *Skin Diseases of the Dog and Cat: Clinical and Histopathologic Diagnosis.* 2nd ed. Ames, IA: Blackwell Science Ltd.; 2005:124-126.

4. Hargis AM, Ginn PE, Mansell JEKL, Garber RL. Ulcerative facial and nasal dermatitis and stomatitis in cats associated with feline herpesvirus-1. *Vet Dermatol*. 1999;10:267-274.

5. Lee M, Bosward KL, Norris JM. Immunohistological evaluation of feline herpesvirus-1 infection in feline eosinophilic dermatoses or stomatitis. *J Feline Med Surg*. 2010;12:72-79.

6. Munson L, Wack R, Duncan M, et al. Chronic eosinophilic dermatitis associated with persistent feline herpes virus infection in cheetahs (*Acinonyx jubatus*). *Vet Pathol*. 2004;41:170-176.

7. Murphy FA, Gibbs EPJ, Horzinek MC, Studdert MJ. In: *Veterinary Virology*. 3rd ed. San Diego, CA: Elsevier Academic Press; 1999:308,339,373.

CASE IV: HN2598 (AFIP 3167484).

Signalment: Approximately 3-year-old adult male sheep (*Ovis aries*).

History: This sheep suddenly died in the early Spring without any noticeable clinical signs. The animal was fed a hay diet and was not grazed on the pasture.

Gross Pathology: The liver showed marked atrophy (17 × 10 × 10 cm), pale brownish to yellowish color and a round shape. The gallbladder was slightly enlarged containing yellow bile. On the liver's diaphragmatic surface, thin firm whitish regions of fibrosis were noted. Thoracic and abdominal cavities contained 1,000 and 4,000 mL of clear and yellowish fluids, respectively. The carcass showed evidence of emaciation with serous atrophy of subcutaneous and bone marrow adipose tissue.

Histopathologic Description: Liver: Moderate to severe fatty degeneration of hepatocytes in centrilobular regions coalesced throughout the liver. Necrosis of hepatocytes and fatty cyst formation were also prominent. Fibrosis appeared mainly around Glisson's sheath and sometimes bridged adjacent hepatic lobules. Proliferation of bile ducts was also marked in Glisson's sheath and subcapsular area. Small regenerative nodules of hepatocytes were sometimes observed. Accumulation of ceroid-like yellow to pale brownish material occasionally appeared in the cytoplasm of macrophages and hepatocytes. Infiltrations of lymphocytes, plasma cells and neutrophils were noted in fibrotic areas and around necrotic hepatocytes.

Contributor's Morphologic Diagnosis: Fatty degeneration and necrosis of hepatocytes, severe, diffuse, with fibrosis and bile ducts hyperplasia.

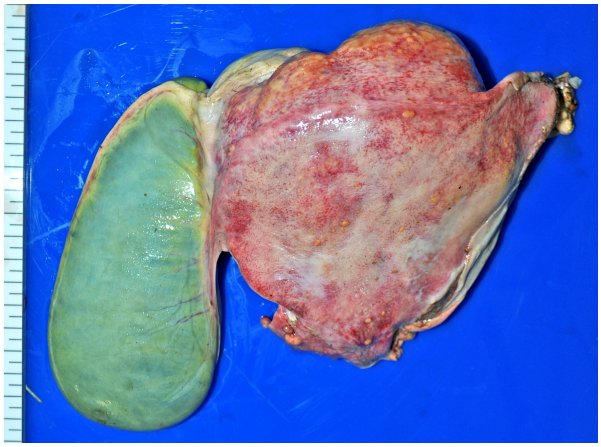

4-1. Liver, sheep. The liver is markedly atrophied, rounded, and pale brown to yellow. The gallbladder is slightly enlarged. Photograph courtesy of Graduate School of Veterinary Medicine, Hokkaido University, Department of Veterinary Clinical Sciences, Laboratory of Comparative Pathology, Sapparo, Japan, umemura@vetmed.hokudai.ac.jp

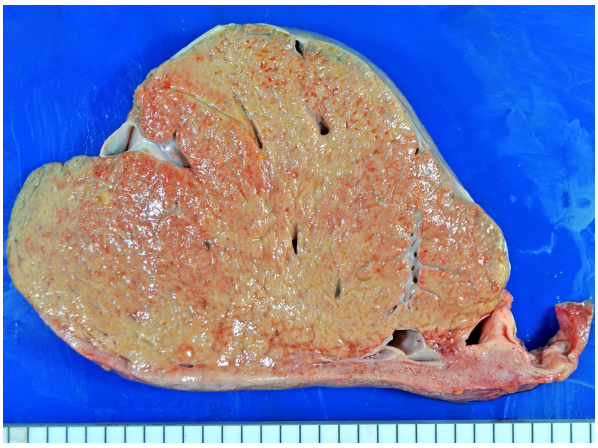

4-2. Liver, sheep. On cut surface, the liver contains thin white regions of fibrosis. Photograph courtesy of Graduate School of Veterinary Medicine, Hokkaido University, Department of Veterinary Clinical Sciences, Laboratory of Comparative Pathology, Sapparo, Japan, umemura@vetmed.hokudai.ac.jp

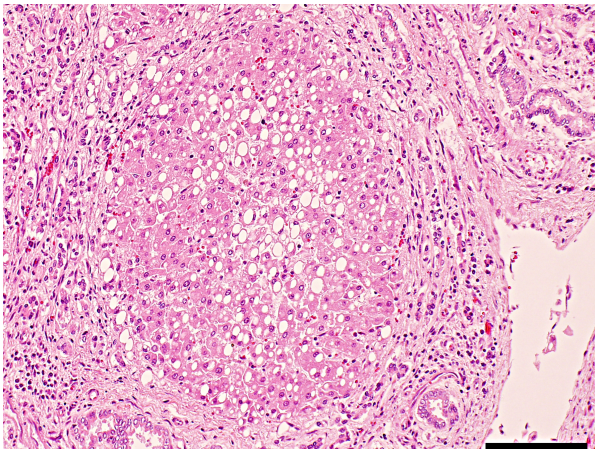

4-3. Liver, sheep. Multifocally, the liver contains regenerative hepatocellular nodules surrounded by areas of fibrosis. Photograph courtesy of Graduate School of Veterinary Medicine, Hokkaido University, Department of Veterinary Clinical Sciences, Laboratory of Comparative Pathology, Sapparo, Japan, umemura@vetmed.hokudai.ac.jp

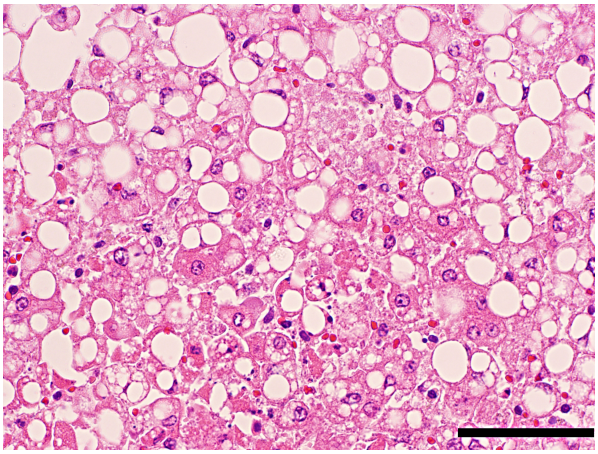

4-4. Liver, sheep. Multifocally within centrilobular regions there is moderate to severe hepatocellular lipid vacuolar degeneration. Photograph courtesy of Graduate School of Veterinary Medicine, Hokkaido University, Department of Veterinary Clinical Sciences, Laboratory of Comparative Pathology, Sapparo, Japan, umemura@vetmed.hokudai.ac.jp

Contributor's Comment: Fatty liver has been reported in animals affected with various conditions, such as hypoxia (anemia and passive venous congestion), diabetes, intoxication, and nutritional deficiencies.[6] In ruminants, pregnancy and heavy lactation also contribute to fatty liver. Hepatic lipidosis is a common and sensitive response to hepatocellular injury. This lesion occurs following interruption of the normally high throughput of fatty acids and triglycerides and secretion of lipoproteins at various points in the hepatic lipid metabolism pathway. The microscopic appearance of triglyceride globules in hepatocytes ranges from small discrete microvesicles to large coalescing macrovesicles.

Hepatic fibrosis is a complicated spectrum of reactions that increase the deposition of extracellular matrix in injured areas.[6] The distribution of fibrosis in the liver reflects the pathogenesis of the necroinflammatory response, (i.e., biliary fibrosis, post-necrotic scarring, diffuse hepatic fibrosis and periacinar fibrosis). Cirrhosis, the end stage of several pathogenic processes resulting in hepatocytic death, chronic inflammation and fibrosis, is characterized by nodular regeneration, fibrovascular bridging scars and pseudolobular formations. Veterinary pathologists have been reluctant to use the term "hepatic cirrhosis" since ongoing regeneration and organization are rarely observed in animals.

Hepatic fatty cirrhosis, or "hard yellow-liver disease", is a progressive and chronic disease of sheep, goats, cattle, deer and antelope, which shows similar hepatic lesions to nutritional hepatic injury.[2] Grossly, the liver lesions in affected sheep begin in the subcapsular hepatic parenchyma as pale yellow firm areas that spread peripherally to involve approximately 80% of the liver in the final stages of the disease. Microscopically, periacinar hepatocytic fatty degeneration involving the entire lobule, with rupture and formation of fatty cysts are observed in the later stages. Periacinar fibrosis accompanies the ruptured fatty cysts, progressing to widespread bridging periacinar fibrosis, with islands of regenerating hepatocytes. The etiology of the disease is unknown, but unidentified hepatotoxins (mycotoxins and plant toxicosis)[6] and nutritional stress (a soil cobalt deficiency and low vitamin B_{12})[7] have all been postulated.

The histopathologic changes in the submitted liver are similar to changes seen in hepatic fatty cirrhosis. The cause of the liver injury in this case was undefined, but similar mechanisms including chronic nutritional deficiency or intoxicosis might have contributed to the development of the hepatic lesion.

AFIP Diagnosis: Liver: Hepatocyte fatty degeneration and necrosis, centrilobular to midzonal, diffuse, moderate with marked bridging portal fibrosis, biliary hyperplasia, and mild lymphoplasmacytic portal hepatitis.

Conference Comment: This challenging case led to a lively discussion of the microscopic anatomy of the hepatic sinusoids. The sinusoids are lined by endothelial cells with thin fenestrations which rest on a thin network of reticulin fibers that support hepatocytes; resident macrophages, i.e. Kupffer cells, are also present within the sinusoids. A narrow space between endothelial cells and hepatocytes is known as the "space of Disse". Within this space are the hepatic stellate cells (HSC, also known as Ito cells or lipocytes); these mesenchymal cells store and release retinoids, assist in the production and turnover of extracellular matrix, and regulate sinusoidal blood flow.[6] In response to hepatic injury, Kupffer cells secrete transforming growth factor-β (TGF-β), stimulating fibrogenesis.[2] Additionally, quiescent HSC can be directly activated by lipopolysaccharide binding to Toll-like receptor-4 (TLR4),[7] resulting in chemokine release and Kupffer cell recruitment as well as down-regulation of the inhibitory TGF-β pseudoreceptor Bambi.[7] Together, these two signals result in unrestricted Kupffer cell activation of HSC. Hepatic stellate cell migration, survival, and proliferation are maintained by platelet-derived growth factor (PDGF).[2]

There is a niche at the junction of the biliary ductular system and parenchymal hepatocytes within the canals of Hering which contains a specialized microenvironment for mesenchymal, endothelial and other cell types. At this site during chronic hepatic disease, these cell types give rise to bipotential progenitor cells which in the literature are referred to as "oval cells."[2] Chronic hepatic disease results in a concurrent reduction in hepatocyte proliferation as well as the development of an "oval cell reaction."[1] Prior to differentiation of the oval cells into hepatocytes or cholangiocytes, the oval cell reaction amplifies a biliary-derived cell population resulting in "ductular reaction."[1] Oval cells generally do not play a role in hepatic regeneration unless there is fulminant hepatic failure, chronic hep atitis, advanced liver cirrhosis, or hepatic tumors.[2]

Contributor: Laboratory of Comparative Pathology, Department of Veterinary Clinical Sciences, Graduate School of Veterinary Medicine, Hokkaido University, Sapporo 060-0818, Japan.
http://www.vetmed.hokudai.ac.jp/

References:

1. Alison MR, Islam S, Lim S. Stem cells in liver regeneration, fibrosis and cancer: The good, the bad and the ugly. *J Pathol*. 2009;217:282-298.
2. Crawford JM, Liu C. Liver and biliary tract. In: Kumar V, Abbas AK, Fausto N, Aster JC, eds. *Robbins and Cotran Pathologic Basis of Disease*. 8th ed. Philadelphia, PA: Elsevier Saunders; 2009:837-838.
3. Helman RG, Adams LG, Bridges CH. The lesions of hepatic fatty cirrhosis in sheep. *Vet Pathol*. 1995;32:635-640.
4. Kierszenbaum AL. Digestive glands. In: *Histology and Cell Biology: An Introduction to Pathology*. 2nd ed. New York, NY: Mosby Inc.; 2007:504-505.

5. Pradere J-P, Troeger JS, Dapito DH, Mencin AA, Schwabe RF. Toll-like receptor 4 and hepatic fibrogenesis. *Semin Liver Dis*. 2010;30:232-244.
6. Stalker MJ, Hayes MA. Liver and biliary system. In: Maxie MG, ed. *Jubb, Kennedy and Palmer's Pathology of Domestic Animals*. Vol. 2, 5th ed. Philadelphia, PA: Elsevier Ltd; 2007:305-329, 368-382.
7. Sutherland RJ, Cordes DO, Carthew GC. Ovine white liver disease: a hepatic dysfunction associated with vitamin B12 deficiency. *NZ Vet J*. 1979;27:227-232.

The Armed Forces Institute of Pathology
Department of Veterinary Pathology

Conference Coordinator
Matthew Wegner, DVM

WEDNESDAY SLIDE CONFERENCE 2010-2011

Conference 12

1 December 2010

Conference Moderator:
Jim Raymond, DVM, Diplomate ACVP

CASE I: M08-1488 (AFIP 3138058).

Signalment: 1-year-old male Quaker parrot (*Myiopsitta monachus*).

History: The bird died suddenly with no overt clinical signs. The local veterinarian performed a gross necropsy and reported that the liver was yellow with black flecks throughout. A single piece of formalin-fixed liver was submitted.

Histopathologic Description: Liver: The architecture of the liver is disrupted by large areas of hemorrhage and coagulative necrosis, along with numerous degenerate cystic structures, interpreted to be ruptured protozoal megaloschizonts. Within both the necrotic areas and the cystic structures are scattered aggregates of approximately 3µm in diameter coccoid protozoal merozoites, some of which palisade along the remaining rim of the ruptured megaloschizonts. Scattered foci of lymphocytes and plasma cells are seen. Numerous clustered hepatocytes contain a moderate amount of brown, coarse granular, intracytoplasmic pigment.

Contributor's Morphologic Diagnosis: Liver: Multifocal hepatocellular necrosis and hemorrhage, with ruptured

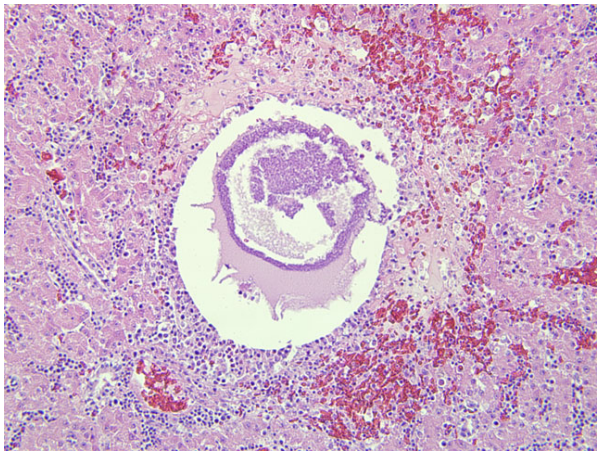

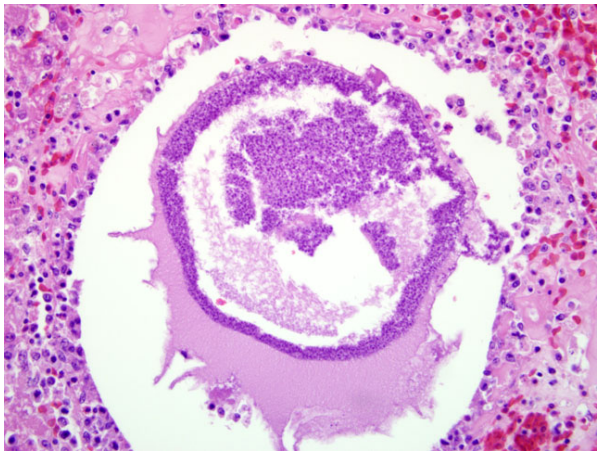

1-1, 1-2. Liver, parrot. Multifocally the architecture of the liver is disrupted by areas of hemorrhage and necrosis that surround cystic structures containing 3 µm in diameter coccoid protozoal merozoites. (HE 200X, 400X)

protozoal megaloschizonts and mild lymphoplasmacytic hepatitis.

Contributor's Comment: *Haemoproteus* spp. are hemoparasites which are typically of low pathogenicity in birds. However, infection can result in clinical disease in certain avian species, including pigeons, quail, and non-indigenous species, along with nestlings and immunocompromised hosts. Clinical signs of infection include hemolytic anemia, anorexia, and depression. Occasionally animals die suddenly with no overt clinical signs.[4]

The parasites are transmitted by blood-sucking insect vectors which ingest intraerythrocytic gametocytes when they feed. The gametocytes develop inside the insect host to become sporozoites within the salivary gland. These are injected into the new avian host when the insect feeds. The sporozoites enter the bird's vascular endothelial cells, primarily those in the lung, liver, bone marrow, and spleen, where they undergo schizogony. Megaloschizonts are occasionally found in cytologic and histologic sections of infected tissue. These appear as large round cysts which contain numerous packeted zoites called cytomeres that rupture and release merozoites into the bloodstream. These enter erythrocytes and become gametocytes which are ingested by insect hosts to complete the life cycle.[4]

In two recent studies, none of the birds in which this disease is fatal demonstrated a detectable erythrocytic parasitemia.[1,3] This is likely due to peracute death associated with the pre-erythrocytic form of the parasite, which is speculated to cause host cell destruction with rupture of megaloschizonts, interference with circulation, and/or toxin release. The exact mechanism of death in these animals is still not completely understood.

AFIP Diagnosis: Liver: Hepatitis, random, necrohemorrhagic, acute to subacute, multifocally extensive, marked with protozoal megaloschizonts.

Conference Comment: Participants pursued discussion of a differential diagnosis list for megaloschizonts in birds; they generally agreed the list should include *Haemoproteidae*, *Leukocytozoidae*, and *Plasmodiidae*. Though all three groups of protozoa are related, there are distinct differences in the life cycles that, when present, serve as useful diagnostic aids. The included chart summarizes key life cycle, morphologic and diagnostic criteria.[2,5]

The moderator and participants commented on the slide variability. Those sections with ruptured schizonts contained more pronounced hemorrhage and inflammation, as one would expect.

Contributor: Department of Pathology, College of Veterinary Medicine, University of Georgia, Athens, GA 30602
http://www.vet.uga.edu/VPP/index.php

				Gametocytes		
	Pigment	**Schizont/Oocyts**	**Merogony**	**Development**	**Morphology**	**Misc.**
Haemoproteidae	Gametocytes: variable size, shape, location and number of granules	In endothelial cells of lung, kidney, liver, spleen: elongate, twisted; megaloschiz-onts	In fixed tissue;* NOT erythrocytes or leukocytes	Erythrocytes	Elongate, horseshoe-shaped; embrace erythrocyte nucleus	Can diagnose with micro-gametes/ gamonts in blood or schizonts in tissues
Plasmodiida	Meronts and gametocytes: randomly scattered aggregates and clumps	In erythrocytes: multiple chromatin masses	In fixed tissue* and erythrocytes	Erythrocytes	Round, oval to elongate with pigment	Erythrocytic merogony is periodic i.e. every 24, 48, or 72 hours
Leukocytozoidae	NONE	In hepatocytes: megalo-schizonts	In hepatocytes;NOT in erythrocytes	Erythrocytes and/or leukocytes	Round and displace host cell nucleus or oval to elliptical, becoming bizarre and elongate	Can diagnose based on gamonts or gametes in smears; presence of megaloschi-zonts

*Fixed tissue as used here simply means tissue that is non-circulatory, with no reference to formalin-fixation.

References:

1. Donovan TA, Schrenzel M, Tucker TA, Pessier AP, Stalis IH. Hepatic hemorrhage, hemocoelom, and sudden death due to *Haemoproteus* infection in passerine birds: Eleven cases. *J Vet Diagn Invest*. 2008;20:304-313.

2. Gardiner CH, Fayer R, Dubey JP. *An Atlas of Protozoan Parasites in Animal Tissues*. 2nd ed. Washington D.C.: Armed Forces Institute of Pathology, American Registry of Pathology; 1998:65, 73.

3. Hall DG, Harmon BG, Howerth EW, Gregory CR, Clubb SL. Sudden death in psittacine and non-psittacine birds associated with hepatic infection with an unclassified haemosporozoan parasite: Eight cases (1994-1996). Proceedings of the 1st International Virtual Conference in Veterinary Medicine, Diseases of Psittacine Birds. University of Georgia, Athens, GA, 1998.

4. Thrall MA, Baker DC, Campbell TW, et al. Hematology of Birds. In: *Veterinary Hematology and Clinical Chemistry*. Ames, IA: Blackwell Publishing; 2006:245-246.

5. Valkiūnas G. *Avian Malarial Parasites and Other Haemosporidia*. New York, NY: CRC Press; 2005.

CASE II: 09-2131 (AFIP 3164851).

Signalment: Estimated 1-month-old female alpaca cria (*Vicugna pacos*).

History: This alpaca cria was found down by the owners. The animal was weak, had been losing body condition, and was found down again several days later despite supportive care and supplemental nutrition. The cria died enroute to the veterinary hospital.

Gross Pathology: The animal was emaciated and severely dehydrated. The liver was mildly enlarged with rounded edges and exhibited an accentuated lobular pattern that was overlain by myriad, random, pinpoint, occasionally coalescing white foci.

Histopathologic Description: Liver: Approximately 40% of the hepatic parenchyma is disrupted by multifocal to coalescing, randomly arranged foci of coagulative to lytic necrosis that are characterized by accumulation of eosinophilic and karyorrhectic, necrotic, cellular debris and small amounts of fibrin with variable retention of cellular architecture. These areas are infiltrated by moderate numbers of neutrophils and macrophages with rare lymphocytes. Within the cytoplasm of occasional hepatocytes located along the periphery of these foci are faintly visible, haystack arrangements of fine, filamentous bacteria. The hepatic sinusoids are diffusely congested with mild dilation of sublobular and portal lymphatics.

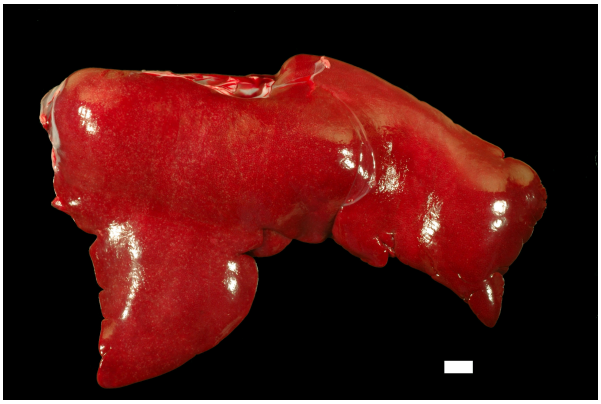

2-1. Liver, alpaca, cria. The liver is mildly enlarged with rounded edges and a bulging surface. All lobes contain randomly arranged, pin point, occasionally coalescing white foci. Photograph courtesy of Department of Population Health and Pathobiology, College of Veterinary Medicine, North Carolina State University, 4700 Hillsborough Street, Raleigh, NC 27606, sandra_horton@ncsu.edu

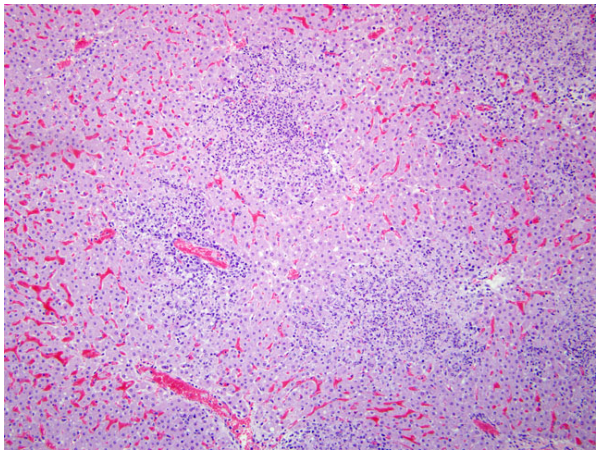

2-2. Liver, alpaca, cria. Up to 40% of the hepatic parenchyma is disrupted and replaced by multifocal to coalescing, random areas of necrosis that contain variable numbers of degenerate neutrophils and macrophages. (HE 40X)

Contributor's Morphologic Diagnosis: Liver: random necrotizing hepatitis, multifocal to coalescing, marked, with intralesional, intracellular, filamentous bacteria.

Contributor's Comment: The intracellular bacteria that are faintly visible with H&E staining are more readily apparent with Giemsa staining. These lesions are consistent with Tyzzer's Disease caused by *Clostridium piliforme*. Although not performed in this case, additional visualization of the organism and confirmation of its identity can be made through the use of silver stains, immunohistochemistry, or PCR. This organism is very difficult to culture and diagnosis is typically made by the characteristic morphologic lesions and the demonstration of the causative organism by these methods.[1,2]

Clostridium piliforme (formerly *Bacillus piliformis*) is a gram-negative, obligate intracellular bacterium that has been reported to cause disease in a wide range of animals. It is best recognized as a pathogen of rabbits, rats, guinea pigs, hamsters, gerbils, and foals, but the list of species in which it has been recognized is diverse including calves, dogs, cats, a Eurasian otter, a red panda, and even a rainbow lorikeet.[1-3,5,6]

The exact pathogenesis of Tyzzer's disease has not been fully elucidated. Affected animals are usually very young or immunosuppressed. Lesions are necrotizing in nature and most frequently involve the liver with less consistent involvement of the gastrointestinal tract and heart.[2] Infection

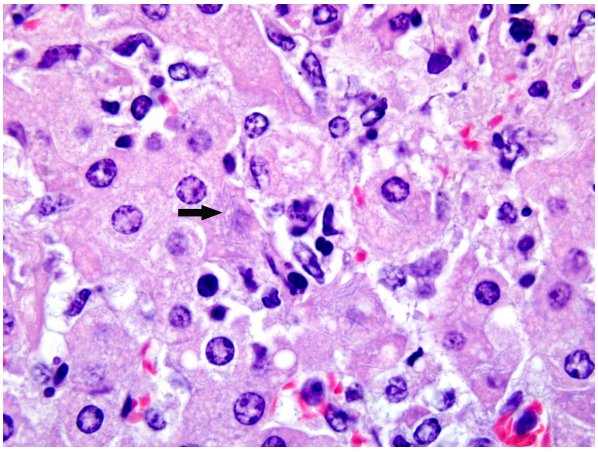

2-3. Liver, alpaca, cria. Along the periphery of necrotic areas degenerate hepatocytes contain intracytoplasmic haystack arrangements of fine, filamentous bacteria (black arrow). (HE 1000X)

follows a rapid course and is typically fatal with few exceptions.[1]

AFIP Diagnosis: Liver: Hepatitis, random, necrotizing, acute, multifocal to coalescing, marked with intrahepatocellular filamentous bacilli.

Conference Comment: Though typically a disease of foals and laboratory animals, Tyzzer's disease can affect a variety of species as described by the contributor and demonstrated in this case. In cases of multifocal random hepatic necrosis, especially in young animals, infections with *Clostridium piliforme*, *Salmonella* species, or an alphaherpesvirus are worthy etiologies to consider in most animal species.

Infections with *Clostridium piliforme* are classically characterized by a triad of enteritis (usually affecting the ileum and occasionally the cecum), hepatitis, and myocarditis, with some species and strain variations among laboratory animals. Of note in mice, those with a B6 background are considered resistant to infection, while DBA/2 strain mice are susceptible. Neutralization of IL-12, depletion of NK cells, and neutrophil depletion increase the susceptibility to disease in mice, even in those strains considered resistant. Resistance is also partially conferred by B lymphocyte function in mice.

In addition to the "Tyzzer's triad" of lesions, rats may also develop megaloileitis. Intestinal lesions in the hamster may be present in the ileum, cecum and colon. Mongolian gerbils are particularly susceptible to infection, rendering them excellent sentinels for Tyzzer's in research settings. Tyzzer's disease in gerbils may also manifest as diffuse suppurative encephalitis. Rabbits may have subclinical infections, with clinical disease precipitated by stress or corticosteroid administration. Lesions in the rabbit are most common in the intestines, occasionally found in the liver and rarely in the heart. Gross lesions in the heart are usually prominent near the apex of the left ventricle.[4]

Contributor: Department of Population Health and Pathobiology, College of Veterinary Medicine, North Carolina State University, 4700 Hillsborough Street, Raleigh, NC 27606
http://www.cvm.ncsu.edu/dphp/path/anatomicpath.html

References:

1. Borchers A, Magesian KG, Halland S, Pusterla N, Wilson WD. Successful treatment and polymerase chain reaction (PCR) confirmation of Tyzzer's disease in a foal and clinical and pathologic characteristics of 6 additional foals (1986-2005). *J Vet Intern Med*. 2006;20:1212-1218.
2. Cullen JM. Liver, biliary system, and exocrine pancreas. In: McGavin MD, Zachary JF, eds. *Pathologic Basis of Veterinary Disease*. 4th ed. St. Louis, MO: Elsevier; 2007: 433-434.
3. Langan J, Bemis D, Harbo S, Pollock C, Schumacher J. Tyzzer's disease in a red panda (*Ailuris fulgens fulgens*). *J Zoo Wildl Med*. 2000;31:558-562.
4. Percy DH, Barthold SW. *Pathology of Laboratory Rodents and Rabbits*. 3rd ed. Ames, IA: Blackwell Publishing; 2007:57-58, 138-140. 208, 271-273.
5. Raymond JT, Topham K, Shirota K, Ikeda T, Garner MM. Tyzzer's disease in a neonatal rainbow lorikeet (*Trichoglossus haematodus*). *Vet Pathol*. 2001;38:326-327.
6. Simpson VR, Hargreaves J, Birtles RJ, Marsden H, Williams DL. Tyzzer's disease in a Eurasian otter (*Lutra lutra*) in Scotland. *Vet Rec*. 2008;163:539-543.

CASE III: S394/10 (AFIP 3164881).

Signalment: Two-week-old male budgerigar (*Melopsittacus undulatus*).

History: Budgerigars and cockatiels were housed and bred for non-commercial purposes in an outdoor aviary. Incidentally, ectoparasites were diagnosed and treated in the budgies. All cockatiels presented healthy. One of the oldest budgie nestlings was suddenly found dead and was submitted for necropsy, whereas other nestlings were normal. The referring veterinarian suggested an avian polyomavirus infection.

Gross Pathology: Necropsy revealed a poor body condition. The skin displayed single up to 2 mm long feathers. Liver and kidney showed moderate, acute, diffuse congestion. The intestinal tract contained firm ingesta.

Laboratory Results: PCR of formalin-fixed kidney tissue was positive for Avian Polyomavirus.

Electron microscopy: Ultrastructural investigation was performed on affected areas of detached formalin-fixed and paraffin-embedded skin tissue sections. Epithelial cells of feather follicles displayed margination of chromatin and myriad intranuclear viral particles measuring approximately 35 nm in diameter.

Histopathologic Description: Skin: Epidermal epithelial cells of the skin display randomly distributed, multifocal to coalescing areas with enlarged, clear, sometimes foamy cytoplasm (ballooning degeneration). The number of affected cells varies, ranging from one to approximately 100 cells. Additionally, up to 100% of the follicular epithelial cells in nearly all of the feather follicles show similar changes. Affected epithelial cells are characterized by variable karyomegaly with margination of chromatin and intranuclear, amphophilic to basophilic inclusion bodies, partly with central clearing and measuring up to 15 µm in diameter. Besides karyorrhexis, karyolysis and pyknosis of epithelial cells in the ramogenic and proliferation zone of feather quills[30] (inner root sheath), brightly eosinophilic lamellar and fibrillar material as well as irregular layered and partly pale eosinophilic material (keratin lamellae) have accumulated within the collar. No regular feather has passed the skin surface (keratin retention, feather dysplasia). The epidermis displays a slightly increased thickness of the fully keratinized stratum corneum (orthokeratotic hyperkeratosis). All described lesions are without infiltration of inflammatory cells. Multifocally, cutaneous blood vessels show moderate hyperemia.

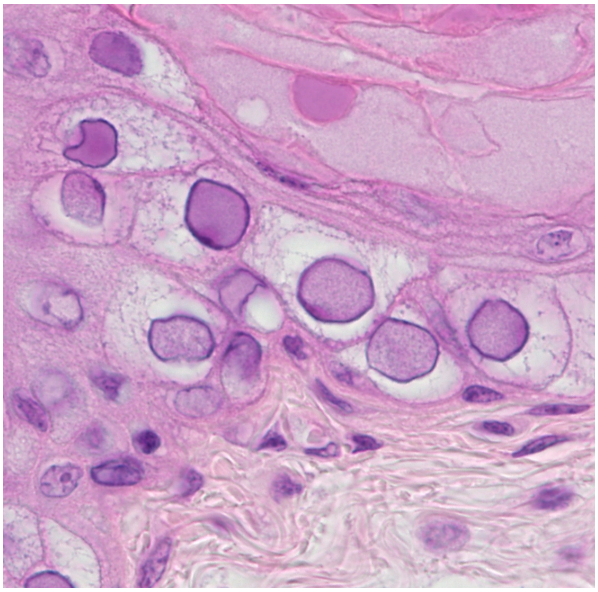

3-1. Feathered skin, epidermis, budgerigar: Numerous epidermal epithelial cells contain randomly distributed, multifocal to coalescing areas with enlarged, vacuolated cytoplasm (ballooning degeneration). Affected epithelial cells contain amphophilic to basophilic intranuclear inclusions which marginate the chromatin. Photograph courtesy of Department of Pathology, University of Veterinary Medicine, Hannover, Bunteweg 17, D-30559, Germany, peter.wohlsein@tiho-hannover.de

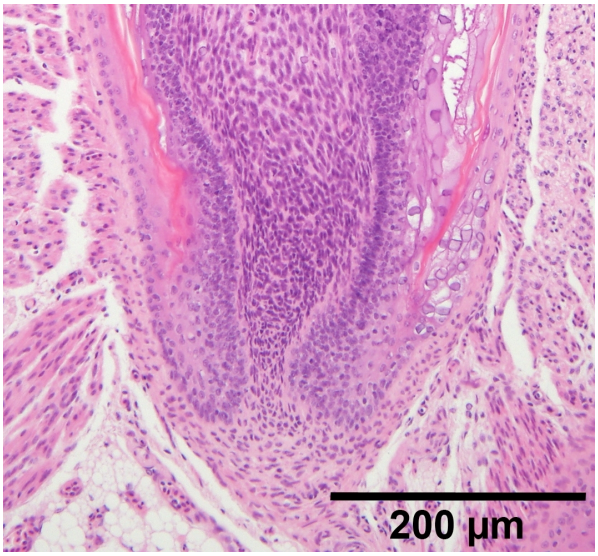

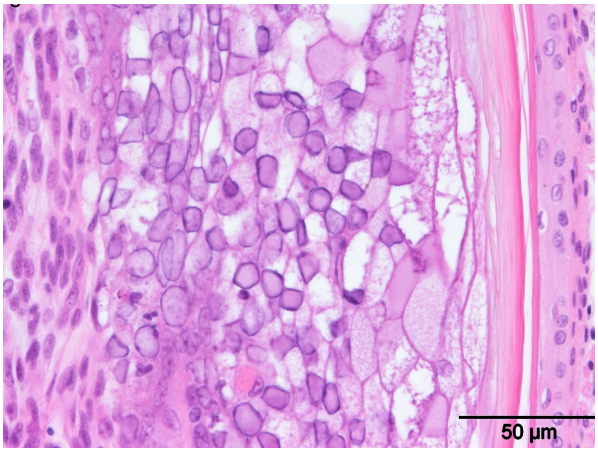

3-2, 3-3. Feathered skin, feather follicle, budgerigar: Similar histologic changes occur in the follicular epithelium as found in the epidermis. Photographs courtesy of Department of Pathology, University of Veterinary Medicine, Hannover, Bunteweg 17, D-30559, Germany, peter.wohlsein@tiho-hannover.de

Contributor's Morphologic Diagnosis: Skin 1. Feather dysplasia and retention, hyperkeratosis, severe, diffuse.
2. Ballooning degeneration of epidermal and follicular epithelial cells, moderate to severe, multifocal to coalescing associated with karyomegaly and intranuclear, amphophilic to basophilic inclusion bodies consistent with avian polyomavirus.
3. Hyperkeratosis, orthokeratotic, slight, diffuse.

Contributor's Comment: Avian polyomavirus, the agent of *Budgerigar fledgling disease*, belongs to the family Polyomaviridae and is characterized by a double-stranded DNA genome without an RNA stage. The etiologic agent of *Budgerigar fledgling disease* was termed by The International Committee on Taxonomy of Viruses[13] *Budgerigar fledgling disease* virus, but nowadays the virus is generally designated as Avian polyomavirus due to its wide avian host range.[15] Additionally, a taxonomy-PubMed search resulted in Budgerigar fledgling disease viruses -1, -4 and -5, lacking the term Avian Polyomavirus (APV). The disease was originally described by Bemier et al. in Quebec, Canada and Bozeman et al. in Georgia and Texas in 1981.[1,3] They reported a multisystemic disease with intranuclear inclusion bodies in multiple organs and were able to identify virus particles of 42 to 55 nm in diameter of affected budgies. In 1986, molecular characterization of the etiologic agent of *Budgerigar fledgling disease* identified initially the first non-mammalian polyomavirus.[21] Mammalian polyomaviruses

Table 1. Summary of pathomorphological changes in juvenile budgerigars due to Avian Polyomaviruses (APV).[27]

Organ/tissue	Histological findings in budgerigars[1]	Clinical/gross changes
Cerebellum	Purkinje cells: ICB*	Intention tremors
Feathers	Nearly all epithelial cells of feather follicles: ICB*; hemorrhage, feather dysplasia	absent feathers, thick sheaths
Skin	Epidermal cells: varying degree of ICB* with ballooning degeneration	"Skin discoloration"
Myocardium (rarely pericardium)	Cardiomyocytes: ICB*, necrosis; lymphoplasmacytic inflammation, hemorrhage	Plaques, adhesions, flocculent fluid
Bursa of Fabricius	Rarely ICB* in lymphocytes; Hemorrhage, depletion, necrosis of lymphocytes in medulla	Swelling, hemorrhage
Oral cavity	ICB* of epithelial cells	Hemorrhage, necrosis
Pancreas	Acinar cells: ICB*; variable inflammation, necrosis, hemorrhage	Hemorrhage, necrosis
Liver	Hepatocytes and Kupffer cells: ICB*, coagulative necrosis	Necrosis, hemorrhage
Spleen	Macrophages of splenic periarteriolar sheaths: abundant ICB*; Necrosis of perivascular histiocytes, lymphoid depletion	Splenomegaly, hemorrhage
Kidney	Tubular- and mesangial cells: ICB*, mesangial cell necrosis; Swollen glomeruli, secondary glomerulopathy: aggregation of immune complexes, Type III hypersensitivity; PAS positive reaction of glomeruli	Nonspecific enlargement
Trachea	ICB* of epithelial cells, mucosal proliferation	
Skeletal muscle	ICB* of myocytes; necrosis, lymphoplasmacytic inflammation	Pallor, hemorrhage

[1]Other species show similar, but somehow different lesions.

*ICB abbreviates karyomegaly with margination of chromatin and intranuclear, amphophilic to basophilic inclusion bodies with a clearing of the center measuring up to 15 µm in diameter.

occur in mice, monkeys, humans, rabbits, and hamsters displaying a narrow host range associated with the ability to induce tumors in mammals.[4] In hamsters, Hamster polyomavirus can cause transmissible lymphomas, keratinizing skin tumors of hair follicles or subclinical infections.[24] Polyomaviruses of rabbits are named "rabbit kidney vacuolating virus" and in mice polyomaviruses are well characterized due to their use in experimental studies.[24]

Clinically, one hallmark of the disease in young budgies is the absence of contour, down feathers and/or filoplume which results in the commonly used names "runners," "creepers," "crawlers" or "bullets" of affected, naked nestlings. While a chronic APV infection is rarely seen in adult birds, primarily budgie nestlings younger than 14 (10-28) days-of-age have an acutely fatal outcome. Animals exhibit typical stunted growth, abnormal feathers, liver necrosis, effusion in the body cavity and sudden death. The mortality rate in budgie fledglings is described as approximately 100%.[16] Interestingly, APV infections often occur in large (commercial) aviaries with hand feeding; concurrent infection with the circovirus of Psittacine Beak and Feather disease (PBFDV) is frequently seen. As a cause PBFD-induced immunosuppression is suggested.[27] French Moult, a syndrome of feather maturation problems in budgies and other psittacine birds, is one manifestation of APV infection, but is suggested to have a milder, more protracted course of disease.[18]

In general, APV has a wide geographical distribution and the presence of APV in Canada and USA[1,3] has already been mentioned. Furthermore, cases of APV infections have been described in Japan,[12] Australia,[23] Germany,[28] Slovakia[22] and Taiwan.[14] APV affects a broad range of other birds, even though the onset of the disease in other species is predominantly later in life (up to one year) and the severity of clinical as well as histopathological changes varies. Other species include conures, parrots, cockatoos, cockatiels, lorries, macaws, splendid parakeets, Gouldian finches, and lovebirds.[17] In 2004, Avian polyomavirus DNA was detected in 0.79% (seven out of 877 animals) of psittacine birds in Italy;[2] the authors stated that due to the extremely low detection rate of the virus the disease seems not to play a role in Italian breeding centers. Psittacine Beak and Feather Disease Virus, which is able to mimic APV infections clinically, was detected in 8.05% (122 out of 1516 animals) of tested animals in Italy,[2] in contrast to a German survey with 39.2% (58 out of 146 animals) of positive PCR results in captive psittacine birds.[25] Usually, virus transmission occurs via inhalation of droppings, oral secretions and/or feather or skin danders, because these materials contain a high load of virus particles. A vertical mode of transmission is suggested but not proven until now.[27] APV infection is a multisystemic disease, and the virus does not show a particular cell tropism. Affected cell types include mesenchymal and epithelial cells. As a consequence nearly all organs/tissues are affected and show histopathologically characteristic intranuclear amphophilic to basophilic inclusion bodies with a clear center, associated with karyomegaly as well as margination of chromatin. Depending on the organ/tissue, inflammation or tissue destruction (necrosis/apoptosis) appears as a corollary of the infection. Table 1 gives an overview upon the organ/tissue-specific morphological findings of APV infections in budgies. During a chronic APV-infection in budgies, glomerulopathy occurs most likely due to immune complex deposition, which is interpreted as type III hypersensitivity. Interestingly, after a multisystemical spread of APV, cellular damage by apoptosis[15] in skin and feather epithelial cells is induced and this apoptosis causes efficient virus release from infected cells without inflammation.

In the present case, typical inclusion bodies as well as karyomegaly and chromatin margination with a pale center were detectable in the epidermis, feather follicles, renal tubular epithelial cells, glomeruli, epithelial cells of the lung, oesophagus, peri-oesophageal connective tissue, small intestinal epithelium, Purkinje cells and preen gland epithelial cells as well as hematopoietic cells in bone marrow. Very few inclusion bodies were detectable in spinal cord neurons and pancreas. Additionally, multifocal, moderate, necrotizing pancreatitis with moderate, acute hemorrhage was detected. Myocytes display inclusion bodies and minimal, lymphoplasmacytic infiltrations, and marked, multifocal necrosis. In the bursa cloacalis, a moderate, central follicular necrosis of lymphocytes was detected without inclusions. Hepatocytes and periportal connective tissue contained a moderate number of inclusions. In addition, moderate, multifocal, lymphoplasmacytic hepatitis with few areas of coagulative necrosis was observed. Remarkably, as an example of a mesenchymal tissue, gizzard muscle cells displayed a very high number of inclusion bodies without cellular reaction. PAS-reaction in the present case does not confirm a glomerulopathy as it is described in APV infections. Clinical, histological, and electron microscopic findings as well as the detection of viral DNA using PCR favors the etiology of Avian polyomavirus. An important differential represents the Avian Adenovirus, which accumulates 75-80 nm large virus particles in the nucleus.

Other avian polyomaviruses include Goose Hemorrhagic Polyomavius,[11] which causes Hemorrhagic Nephritis Enteritis of Geese (HNEG). It represents a fatal disease in European geese. Since the late 1960s several outbreaks in goose flocks have been documented and finally in 2000 it was possible to characterize the etiological agent.[11] Typical clinical signs include high morbidity and mortality in up to 10-week-old geese. The virus shows a tropism for endothelial and lymphoid cells. It is a systemic virus infection with immunosuppressive properties.[19]

Other virus infections in budgies, with or without inclusion bodies, have to be considered and excluded as differentials including Adenovirus, Psittacine Herpesvirus (Pacheco´s disease), Psittacine Beak and Feather disease, Avian

Table 2. Virus-induced inclusions in birds with special emphasis on skin pathology.[27]

Virus (disease)	Histopathology	Macroscopic
Avian Poxvirus	Epidermal hyperplasia, intraepidermal vesicles, ballooning degeneration, *Bollinger bodies* = **abundant, large, eosinophilic, intracytoplasmic ICB***	Proliferative, necrotizing dermatitis, pustules, papules, nodules
Circovirus of Psittacine Beak and Feather Disease (PBFD)	Acute: epidermal hyperplasia, hyperkeratosis, degeneration of germinal cells, ballooning and patchy degeneration of cells in epidermal collar with **ICB*** Chronic: granulomas, giant cells, confluent lymphoplasmacytic infiltrates; macrophages contain **large, globular, basophilic, cytoplasmic ICB***	Dystrophic feathers, necrosis/ hemorrhage of feather shafts; beak necrosis, keratin loss
Avian Adenovirus	Mild, mononuclear, interstitial nephritis, conjunctivitis, encephalitis, CNS vessels: necrosis with endothelial ICB*; multisystemic; karyomegaly, **intranuclear, dark eosinophilic to basophilic ICB***	Among others, renal enlargement
Psittacine Herpesvirus (Pacheco´s disease)	Multisystemic; skin, epidermal hyperplasia, acanthosis, **large, intranuclear ICB* with a clear halo**	Proliferative dermatitis, skin roughening, plaques, depigmentation
Papillomavirus	Hyperplasia of epidermis associated with vascular stroma; enlarged nuclei of epidermal cells are suggestive of ICB*	Proliferative dermatitis
Avian Polyomavirus (Budgerigar Fledgling Disease - BFD)	Multisystemic, skin, karyomegaly with margination of chromatin and **intranuclear, amphophilic to basophilic ICB* with a clearing of the center** measuring up to 15 µm in diameter	Dystrophic feathers, feather loss, "runner"

* ICB abbreviates inclusion bodies

Papillomaviruses and Avian Poxvirus. Table 2 gives an overview of the differentials of avian virus infections with inclusion bodies as a characteristic histopathological feature. In the present case, clinical findings, histopathological changes, ultrastructural detection of virus particles, and the presence of polyomaviral DNA[9] are characteristic for APV in budgies. Other diagnostic possibilities to confirm the diagnosis include immunohistochemistry,[7] *in situ*-hybridisation with DNA probes,[26] virus isolation in chicken embryo fibroblasts,[6] and direct fluorescent antibody tests.[10]

AFIP Diagnosis: Feathered skin: Epidermal and follicular epithelial degeneration and intracellular edema, multifocal, moderate, with follicular dysplasia, feather retention, orthokeratotic hyperkeratosis, karyomegaly, and amphophilic intranuclear epithelial inclusions.

Conference Comment: The contributor provides a thoroughly exquisite review of avian polyomavirus infection and a comprehensive differential diagnosis list for viral diseases of the skin among avian species.

Some of the conference discussion centered on the most appropriate terminology to characterize the histologic changes found in the follicular and epidermal epithelium, including the use of the terms 'ballooning degeneration,' 'vacuolar degeneration,' and 'hydropic degeneration.' According to the authors of *Jubb, Kennedy and Palmer's Pathology of Domestic Animals*, cytoplasmic clearing or clear space within cells of the epidermis can be classified as hydropic degeneration, ballooning degeneration or vacuolar degeneration.[8] 'Hydropic degeneration' refers specifically to intracellular edema of the basal layer and occasionally the basal cells of hair follicle outer root sheath. 'Vacuolar degeneration' is used to denote intracellular edema in cells above and below the basement membrane zone. 'Ballooning degeneration' is used to denote intracellular edema in the epidermis and is considered to be a characteristic feature of viral infection in the skin; historically, the term has been reserved for poxviral and herpesviral infections. In contrast, *Robbins and Cotran Pathologic Basis of Disease* uses the term 'ballooning degeneration' to characterize the acute cell swelling in human acute hepatitis,[5] and the text further defines hydropic (ballooning) swelling in the skin as "intracellular edema of keratinocytes, often seen in viral infections".[20] Finally, to add further complexity to the terminology, avian pathologists describe the histologic changes in the skin caused by polyomaviral infection as cytoplasmic vacuolar (ballooning) degeneration, with karyomegaly and intranuclear inclusions.[29] Despite the differences in terminology among the various references, the histologic changes reflect intracellular edema, cell swelling, and degeneration of epithelial cells of the skin, and hence the histomorphologic diagnosis indicated above.

Contributor: Department of Pathology, University of Veterinary Medicine Hannover, Bünteweg 17, D-30559 Hannover, Germany
http://www.tiho-hannover.de/einricht/patho/index.htm

References:

1. Bernier G, Morin M, Marsolais G. A generalized inclusion body disease in the budgerigar (*Melopsittacus undulatus*) caused by a papovavirus-like agent. *Avian Dis.* 1981;25(4): 1083-1092.
2. Bert E, Tomassone L, Peccati C, et al. Detection of beak and feather disease virus (BFDV) and avian polyomavirus (APV) DNA in psittacine birds in Italy. *J Vet Med B Infect Dis Vet Public Health.* 2005;52(2):64-68.
3. Bozeman LH, Davis RB, Gaudry D, et al. Characterization of a papovavirus isolated from fledgling budgerigars. *Avian Dis.* 1981;25(4):972-980.
4. Cole C, Conzen SD. *Polyomaviridae:* The Viruses and Their Replication. In: Fields B, Knipe DM, Howley PM, et al., eds. *Fields Virology.* 3rd ed. Baltimore, MD: Lippincott Williams & Wilkins; 1996: 2141-2174.
5. Crawford JM, Liu C. Liver and biliary tract. In: Kumar V, Abbas AK, Fausto N, Aster JC, eds. *Robbins and Cotran Pathologic Basis of Disease.* 8th ed. Philadelphia, PA: Elsevier Saunders; 2009:851.
6. Dykstra MJ, Bozeman LH. A light and electron microscopic examination of budgerigar fledgling disease virus in tissue and in cell culture. *Avian Pathol.* 1982;11(1): 11-28.
7. Fitzgerald SD, Reed WM, Fulton RM. Development and application of an immunohistochemical staining technique to detect avian polyomaviral antigen in tissue sections. *J Vet Diagn Invest.* 1995;7(4):444-450.
8. Ginn PE, Mansell JEKL, Rakich PM. Skin and appendages. In: Maxie MG, ed. *Jubb, Kennedy and Palmer's Pathology of Domestic Animals.* Vol.1, 5th ed. Philadelphia, PA: Elsevier Ltd; 2007:563, 567.
9. Gough JF. Outbreaks of budgerigar fledgling disease in three aviaries in Ontario. *Can Vet J.* 1989;30(8):672-674.
10. Graham DL, Calnek BW. Papovavirus infection in hand-fed parrots: Virus isolation and pathology. *Avian Dis.* 1987;31(2):398-410.
11. Guerin JL, Gelfi J, Dubois L, et al. A novel polyomavirus (goose hemorrhagic polyomavirus) is the agent of hemorrhagic nephritis enteritis of geese. *J Virol.* 2000;74(10): 4523-4529.
12. Hirai K, Nonaka H, Fukushi H, et al. Isolation of a papovavirus-like agent from young budgerigars with feather abnormalities. *Nippon Juigaku Zasshi.* 1984;46(4):577-582.
13. Hou J, Jens PJ, Major EO, et al. Polyomaviridae. *Virus taxonomy. Eighth Report of the ICTV.* 2005;231-238, http://www.ictvonline.org/index.asp.
14. Hsu CM, Ko CY, Tsaia HJ. Detection and sequence analysis of avian polyomavirus and psittacine beak and feather disease virus from psittacine birds in Taiwan. *Avian Dis.* 2006;50(3):348-353.
15. Johne R, Muller H. Polyomaviruses of birds: Etiologic agents of inflammatory diseases in a tumor virus family. *J Virol.* 2007;81(21):11554-11559.
16. Kaleta EF, Herbst W, Kaup FJ, et al. Viral etiology of a disease accompanied by hepatitis and feather disorders in budgerigar fledgelings (*Melopsittacus undulatus*). *Zentralbl Veterinarmed B.* 1984;31(3):219-224.
17. Kingston RS. Budgerigar fledgling disease (papovavirus) in pet birds. *J Vet Diagn Invest.* 1992;4(4):455-458.
18. Krautwald ME, Muller H, Kaleta EF. Polyomavirus infection in budgerigars (*Melopsittacus undulatus*): Clinical and aetiological studies. *Zentralbl Veterinarmed B.* 1989;36(6):459-467.
19. Lacroux C, Andreoletti O, Payre B, et al. Pathology of spontaneous and experimental infections by Goose haemorrhagic polyomavirus. *Avian Pathol.* 2004;33(3): 351-358.
20. Lazar AJF, Murphy GF. The skin. In: Kumar V, Abbas AK, Fausto N, Aster JC, eds. *Robbins and Cotran Pathologic Basis of Disease.* 8th ed. Philadelphia, PA: Elsevier Saunders; 2009:1168.
21. Lehn H, Muller H. Cloning and characterization of budgerigar fledgling disease virus, an avian polyomavirus. *Virology.* 1986;151(2):362-370.
22. Literak I, Smid B, Dubska L, et al. An outbreak of the polyomavirus infection in budgerigars and cockatiels in Slovakia, including a genome analysis of an avian polyomavirus isolate. *Avian Dis.* 2006;50(1):120-123.
23. Pass DA. A papova-like virus infection of lovebirds (*Agapornis* sp). *Aust Vet J.* 1985;62(9):318-319.
24. Percy DH, Barthold SW. *Pathology of Laboratory Rodents and Rabbits.* 3rd ed. Ames, IA: Blackwell Publishing; 2007:256.
25. Rahaus M, Wolff MH. Psittacine beak and feather disease: A first survey of the distribution of beak and feather disease virus inside the population of captive psittacine birds in Germany. *J Vet Med B Infect Dis Vet Public Health.* 2003;50(8):368-371.
26. Ramis A, Latimer KS, Niagro FD, et al. Diagnosis of psittacine beak and feather disease (PBFD) viral infection, avian polyomavirus infection, adenovirus infection and herpesvirus infection in psittacine tissues using DNA in situ hybridization. *Avian Pathol.* 1994;23(4):643-657.
27. Schmidt R, Reavill DR, Phalen DN. *Pathology of Pet and Aviary Birds.* Ames, IA: Iowa State Press, Blackwell Publishing Company; 2003.
28. Stoll R, Luo D, Kouwenhoven B, et al. Molecular and biological characteristics of avian polyomaviruses: Isolates from different species of birds indicate that avian polyomaviruses form a distinct subgenus within the polyomavirus genus. *J Gen Virol.* 1993;74(Pt 2)229-237.
29. Tahseen AA, Barnes HJ, Fletcher OJ, Shivaprasd HL, Swayne DE, Williams S. Integumentary system. In: *Avian Histopathology.* 3rd ed. Jacksonville, FL: American Association of Avian Pathologists; 2008:398.
30. Yu M, Wu P, Widelitz RB, et al. The morphogenesis of feathers. *Nature.* 2002;420:308-312.

CASE IV: WCS2009101801 (AFIP 3167494).

Signalment: Adult bay pipefish (*Syngnathus griseolineatus*).

History: This bay pipefish was part of a recently acquired group of pipefish that arrived and was undergoing quarantine. Most animals in the shipment arrived in thin body condition with few to multiple pinpoint coalescent areas of skin ulceration and scale loss. Cytology of the skin scrapes revealed numerous ciliates, bacteria, and fungal hyphae.

Gross Pathology: On presentation to necropsy, this pipefish was in thin body condition and had few visible pinpoint to 0.3 cm patchy areas of skin reddening that extended along the dorsal body wall as well as ventrally around and within the pouch.

Histopathologic Description: Two transverse sections through the body of a bay pipefish (*Syngnathus griseolineatus*) at the level of the pouch are examined. Included in these sections are vertebral body, spinal cord, skeletal muscle, dorsal fin and pouch. Bilaterally, the skeletal muscle bundles that run parallel to the vertebral column are expanded by clear, confluent spaces (edema) and localized hemorrhage. Regionally myofibers display various stages of fragmentation, degeneration and lysis. Associated with this lesion are moderate numbers of round to ovoid, ciliated protozoal organisms which measure approximately 30-50 µm x 20-30 µm, have a large (7-10 µm) basophilic macronucleus and basophilic floccular to granular cytoplasm. Occasionally within the cytoplasm of these organisms there are numerous eosinophilic homogenous droplets (phagocytosed erythrocytes, presumptive). These organisms are often associated with individually affected myofibers and/or are located within the interstitium. In several microscopic fields, organisms can be identified within the lumen of vascular channels. The ventral surface of the skin, particularly in the region of the pouch, is segmentally eroded and hyperplastic. The underlying dermal collagen fibers are markedly loosened and separated by clear space (edema) and exhibit a mild to moderate inflammatory infiltrate composed primarily of lymphocytes, macrophages and plasma cells. Ciliated protozoal organisms morphologically similar to those previously described are scattered throughout the dermis and subdermal connective tissues. Adhered to the eroded sections of epidermis are small aggregates of bacterial cocci.

Contributor's Morphologic Diagnosis: 1. Skeletal muscle: Myofiber degeneration and necrosis, subacute, multifocal, severe with lymphoplasmacytic and histiocytic inflammation, hemorrhage and many intralesional ciliated protozoal organisms.
2. Scaled skin, pouch: Dermatitis, lymphoplasmacytic and histiocytic, chronic-active, regional, moderate with edema; segmental epidermal erosion and hyperplasia; and intralesional ciliated protozoal organisms.

Contributor's Comment: Bay pipefish belong to the family Syngnathidae which include both sea horses and sea dragons. The species are most commonly found in shallow, coastal waters and are characterized by their elongated snouts, fused jaws, the absence of pelvic fins, and by thick plates of bony armor covering the body. Female fish of this family deposit eggs into the ventral pouch or onto a sticky brood patch of the males who are responsible for carrying the eggs until they hatch.

Scuticociliates are facultative parasites of marine fish. Disease associated with these organisms has been described in numerous marine species including lobster,[7] sea dragons,[6,8] tuna[2] and olive flounder.[1] Infection is frequently confined to the dermis with death in these cases thought to be associated with sloughing of the epidermis and subsequent disruption of osmoregulation rather than direct organ damage.[8] However, deaths associated with disseminated disease have been reported, particularly in farmed fish, causing significant economic loss in this industry.[2,3] Histopathology in cases of disseminated disease is similar to that described for this pipefish, with edema, mononuclear inflammation and hemorrhage associated with the presence of organisms.[1-3] Erythrocytes within cytoplasmic 'food vacuoles' are a consistent feature of these organisms on histology making them easy to identify.[3]

AFIP Diagnosis: 1. Scaled skin and brood pouch: Dermatitis, erosive and ulcerative, histiocytic and granulocytic, subacute, multifocally extensive, moderate, with intralesional ciliated protozoa.
2. Skeletal muscle fascia: Myositis and fasciitis, histiocytic and granulocytic, subacute, multifocally extensive, moderate, with myocyte degeneration and necrosis, edema, and many ciliated protozoa.

Conference Comment: In discussing and characterizing the inflammatory cells associated with the lesion, participants reviewed the components of teleost blood. They are remarkably similar to higher order vertebrates with the exception of nucleated erythrocytes and thrombocytes. Their neutrophils are quite similar to mammalian neutrophils, both in structure and function, and are frequently found at sites of inflammation. Monocytes circulate as they do in other vertebrates; they are able to take up residence in tissues, though their phagocytic ability is not quite as robust as it is in mammals. In addition, teleosts have lymphocytes; the presence of eosinophils, basophils and mast cells is questionable in some species.[4]

Responsive epidermal changes in fishes consist of an inflammatory response or hyperplasia. The inflammatory response typically begins with spongiosis and progresses to necrosis; chronic inflammation of the dermis may also result in spongiosis, though not as severe as with epidermal

inflammation, and a lymphocytic infiltrate.[5] Epidermal hyperplasia due to toxins, hormones, or infectious agents is more generalized and occurs more frequently at lower temperatures.[5]

The dermal and hypodermal changes consist of an inflammatory response, ulceration and wound healing. As with mammals, the inflammatory response consists of vascular, exudative and cellular phases; the amount of time for the inflammatory response to occur is correlated with environmental temperature. Rapid colonization of ulcers often masks the inciting cause. Collagen fibers become "water-logged" resulting in the histologic appearance of a bluish sheen on the open surface of the ulcer. The rate of wound healing, as with the dermal inflammatory response, depends on water temperature. In contrast, epidermal wound covering occurs rapidly independent of water temperature in order to prevent secondary infections and to restore the osmotic barrier.[5]

The moderator commented that with this particular parasite, death often occurs so rapidly as to preclude a significant inflammatory response. In some cases, only skin lesions may be present; this often provides a route of secondary bacterial infection resulting in sepsis and death. In this particular case, the moderator and participants agreed that the inflammatory response was not proportional to the myriad amoebae present.

Contributor: Wildlife Conservation Society, Global Health Program – Pathology, 2300 Southern Boulevard, Bronx, NY 10460
http://www.wcs.org

References:

1. Jung S, Kitamura S, Song J, Oh M. *Miamiensis avidus* (Cilophora: Scuticociliatida) causes systemic infection of olive flounder *Paralichthys olivaceus* and is a senior synonym of *Philasterides dicentrarchi*. *Dis Aquat Org*. 2007;73(3):227-234.
2. Munday BL, Donoghue PJ, Watts M, Rough K, Hawkesford T. Fatal encephalitis due to the scuticociliate *Uronema nigricans* in sea-caged, southern bluefin tuna *Thunnus maccoyii*. *Dis Aquat Org*. 1997;30(1):17-25.
3. Puig L, Traveset R, Palenzuela O, Padros F. Histopathology of experimental scuticociliatosis in turbot *Scophthalamus maximus*. *Dis Aquat Org*. 2007;76(2): 131-140.
4. Roberts RJ, Ellis AE. The anatomy and physiology of teleosts. In: Roberts RJ, ed. *Fish Pathology*. 3rd ed. Philadelphia, PA: W.B. Saunders; 2007:25-30.
5. Roberts RJ, Rodger HD. The pathophysiology and systematic pathology of teleosts. In: Roberts RJ, ed. *Fish Pathology*. 3rd ed. Philadelphia, PA: W.B. Saunders; 2007:62-65.
6. Rossteuscher S, Wenker C, Jermann T, Wahli T, Oldenberg E, Schmidt-Posthaus H. Severe Scuticociliate (*Philasterides dicentrarchi*) infection in a population of sea dragons (*Phycodurus eques* and *Phyllopteryx taeniolatus*). *Vet Pathol*. 2008;45(4):546-550.
7. Small HJ, Neil DM, Taylor AC, Bateman K, Coombs GH. A parasitic scuticociliate infection in the Norway lobster (*Nephrops norvegicus*). *J Invertebr Pathol*. 2005;90(2): 108-117.
8. Umehara A, Kosuga Y, Hirose H. Scuticociliata infection in the weedy sea dragon *Phyllopteryx taeniolatus*. *Parasitol Int*. 2003;52(2):165-168.

The Armed Forces Institute of Pathology
Department of Veterinary Pathology

Conference Coordinator
Matthew Wegner, DVM

WEDNESDAY SLIDE CONFERENCE 2010-2011

Conference 13

8 December 2010

Conference Moderator:
Tim Walsh, DVM, Diplomate ACVP

CASE I: 10-4242 / 10-6076 (AFIP 3170327).

Signalment: 30 Sydney rock oysters, QX resistant broodstock, (*Saccostrea glomerata*).

History: 100% of oysters were at risk with 25% sick and 75% mortality.

Gross Pathology: The oysters varied in size (53.6 ± 8.9 mm shell height). They were in poor condition with minimal gonadal development (1.6 ± 0.9 on a 1-5 scale) and pale digestive glands (1.9 ± 0.9 on a 1-3 scale). On close examination several of the oysters appeared to be dead.

Laboratory Results: Of the 30 oysters examined by PCR, 24 (80%) were confirmed positive for *Marteilia sydnei*. Confirmation of a successful DNA extraction from each oyster was done using a second PCR specific for *Saccostrea glomerata* (Sydney rock oyster) DNA. Positive and negative controls were included in each PCR run. Of the oysters positive on PCR, 11 (46%) were positive for *Marteilia sydnei* on cytological examination of digestive gland impression smears (stained with Diff Quik). All oysters positive on cytological examination were also positive on histological examination.

Histopathologic Description: Whole body: Multifocally there is marked disruption of digestive gland architecture with moderate inflammatory cell infiltration of the epithelium and myriad intracellular protozoa. Tubule epithelium is expanded by numerous multicellular protozoa consisting of large, 100-150 µm sporangiosorae containing 8-16 sporonts, each 10-15 µm, tear-shaped and 2-3 spherical, refractile eosinophilic spores. Occasional intraluminal sporangiosorae are noted. There is marked increase in granular enterocytes with diapedesis of haemocytes across tubule epithelium. Surrounding Leydig tissue is diffusely collapsed and infiltrated by low to moderate numbers of haemocytes. Underlying the gill and palp epithelium, moderate infiltrates of haemocytes are noted diffusely in the Leydig tissue.

Contributor's Morphologic Diagnosis: Digestive gland: Adenitis, proliferative, chronic, multifocal, severe, with haemocyte accumulation and myriad intracellular protozoa consistent with *Marteilia sydnei*; Sydney rock oyster (*Saccostrea glomerata*).

Contributor's Comment: Diseases caused by *Marteilia refingens* and *Marteilia sydnei* (QX disease) are referred to as Martiellosis. These organisms are of the phylum Paramyxea and are regarded as major concerns for mollusk aquaculture and are listed by the Office International des Epizooties (OIE 2003).

QX disease has been identified in Sydney rock oysters (*Saccostrea glomerata*) in coastal estuaries of southern Queensland and northern New South Wales. Infected oysters are typically in poor condition, with resorption of the gonad and pale digestive glands. Epizootics occur in summer and autumn and mortality can exceed 90%.[1] The marked increase in prevalence of QX disease and the devastating effect on the local industry has led to the development of a line of QX resistant oysters. Phagocytosis

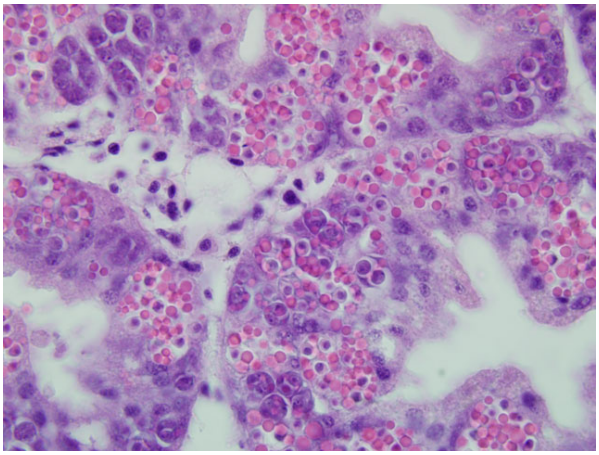

1-1. Digestive gland, Sydney rock oyster, (Saccostrea glomeratus). The glandular architecture is altered by epithelial hypertrophy and hyperplasia, with few inflammatory cells. Epithelial cells are filled with myriad intracytoplasmic protozoa. (HE 400X)

of *M. sydnei* by haemocytes is a key event in clearing the infection.[5] Interbreeding and investigation of the rare QX-infected surviving oyster demonstrated increased haemocyte-localized phenoloxidase concentrations.[7] While oysters selectively bred to be resistant to QX had increased concentrations of phenoloxidase, management of the disease continues to be problematic, in addition to the inadvertent breeding of oysters with reduced phenoloxidase concentrations.[3]

Gross lesions in QX affected oysters are distinctive, with shrinkage of the oyster, poor body condition and a pale, translucent appearance to the oyster and the digestive gland in particular.

The life cycle of *M. sydnei* is well characterized within the oyster and involves an intermediate host, believed to be a polychaete worm.[2] Initial entry of *M. sydnei* occurs at the gills and palps, with localization of initial infective stages in epithelia and systemic spread via the haemolymph and connective tissues to the epithelia of the digestive gland. While epithelial hyperplasia, hypertrophy and fusion of gill filaments are a feature of this stage of infection,[2] they were not noted in this case. As losses had been occurring for several weeks prior to submission, it is possible that systemic spread had occurred. Haemocyte accumulates were noted in the underlying Leydig tissue.

Presporulating stages (sporonts) are found in the digestive gland epithelium and occasionally in the surrounding connective tissues. Development of sporonts is characterized by the production of internal offspring following internal (cell-within-cell) cleavage, without the formation of spores (extrasporogenic proliferation). However, once established in the digestive gland, sporulating forms (sporangiosorae) are formed, containing 8-16 sporonts. Final cleaveage of sporonts results in the formation of 2-3 multinucleated spores delimited by a continuous wall. The subsequent release of spores into the lumen results in destruction of the host digestive gland epithelium. Death of the oyster infected with *M. sydnei* is believed to be due to blockage of the digestive tract with subsequent starvation of the oyster.[2] The unique feature of internal cleavage during sporulation differentiates *Marteilia* spp. from other protista.

The digestive gland is the primary focus of sporulation of *M. sydnei*. It is one of the principle sites of storage of metabolic reserves and of intracellular food digestion. It is a compound tubular organ with primary ducts leaving the stomach, secondary ducts and digestive tubules. Three populations of lining cells can be identified: digestive or secretory-absorptive cells, non-flagellated basiphil cells, and flagellated basiphil cells. Digestive cells are distinctive for their macrovesicles which contain various enzymes (acid phosphatase, non-specific esterases) and have a distinctive eosinophilic appearance in H&E.[4] In a healthy actively-feeding oyster, the lumina of the digestive gland have an "X" or "Y" appearance in cross section. Conversely, in unhealthy, stressed or non-feeding oysters, the digestive glands are dilated with a low cuboidal epithelium. Diapedesis of a small number of haemocytes is regarded as normal and represents movement of haemolymph across mucosal surfaces.[4]

AFIP Diagnosis: 1. Digestive gland: Adenitis, proliferative, diffuse, marked, with epithelial hypertrophy, mild haemocytic inflammation and myriad intracellular epithelial protozoa.
2. Gill: Branchitis, haemocytic, multifocal, mild with epithelial degeneration, necrosis, and sloughing.

Conference Comment: The moderator and participants discussed several considerations when approaching aquaculture disease from a diagnostic perspective. First and foremost, one must understand this is a population health issue which impacts the approach to the types and numbers of samples obtained. In general, one should collect fresh, frozen and fixed diagnostic samples to facilitate multiple diagnostic modalities. Aquaculture fixatives consist of Davidson's or saltwater-formalin to maintain osmotic balance.

As noted by the contributor, digestive cells have distinct eosinophilic macrovesicles. Participants were unsure of the exact nature of this unique feature. A brief discussion of the possibilities for a round eosinophilic body included apoptotic bodies, granules/vacuoles, viral inclusions and protein droplets. An example of protein droplets is the hyaline droplet nephropathy in rats with histiocytic sarcoma. The participants agreed that the feature is consistent with a vacuole.

In addition to the histologic lesions in the digestive gland, several conference participants observed multifocal haemocytic infiltrates in the gill along with degeneration, necrosis, and sloughing of the epithelial cells. The cause of

the lesions in the gills is uncertain, but a few participants speculated on the possibility of opportunistic infection in the terminal stages of martiellosis, such as that caused by ciliated protozoa. Rare ciliated protozoa with a large basophilic macronucleus are observed in a few sections on the surface of the gill epithelium.

The contributor provides a detailed discussion of the epidemiology and pathology associated with martiellosis as well as the histologic features of the mollusk digestive tract. The following mollusk diseases also are listed as current OIE reportable entities: *Bonamia ostreae, B. exitosa, Marteilia refringens, Perkinsus marinus, P. olseni, Xenohaliotis californiensis*, and abalone herpes-like virus. Of these organisms, *B. ostreae, P. marinus*, and *X. californiensis* have affected mollusks native to the United States.[6]

Contributor: State Veterinary Laboratory, EMAI, Narellan, NSW, Australia
www.dpi.nsw.gov.au

References:

1. Adlard RD, Ernst I. Extended range of the oyster pathogen *Mautiella sydnei*. *Bull Eur Assoc Fish Pathol*. 1995;15(4): 119.
2. Berthe FCJ, Le Roux F, Adlard RD, Figueras A. Marteiliosis in mollusks: A review. *Aquat Living Resour*. 2004;17:433-488.
3. Bezemer B, Butt D, Nell J, Adlard R, Raftos D. Breeding for QX disease resistance negatively selects one form of the defensive enzyme, phenoloxidase, in Sydney rock oysters. *Fish Shellfish Immunol*. 2006;20:627-636.
4. Kennedy VS, Newell RIE, Eble OF, eds. In: *The Eastern Oyster* Crassostrea virginica. College Park, MD: Maryland Sea Grant College; 1996:39-51.
5. Kuchel RP, Aladaileh S, Birch D, Vella N, Raftos DA. Phagocytosis of the protozoan parasite *Marteilia sydnei* by Sydney rock oyster (*Saccostrea glomerata*) hemocytes. *J Invert Pathol*. 2010;104(2):97-104.
6. Arzul I, Burreson EM, Friedman C. Diseases of mollusks, sections 2.4.2-2.4.7. In: *Manual of Diagnostic Tests for Aquatic Animals 2010*. OIE; http://www.oie.int/eng/normes/fmanual/A_summry.htm. Accessed online10 January 2011.
7. Peters R, Raftos DA. The role of phenoloxidase suppression in QX disease outbreaks among Sydney rock oysters (*Saccostrea glomerata*). *Aquaculture*. 2003;223:29-39.

CASE II: 06V3449 (AFIP 3170675).

Signalment: 2-year-old mixed gender greenlip abalone (*Haliotis laevigata*).

History: An abrupt onset of high mortality affecting 1 to 4-year-old juveniles and brood stock occurred on three abalone farms in southern Australia. Prior to the onset of these mortalities, abalone had been collected from the wild and there was transfer of stock between the farms. High mortality was observed in affected tanks with many tanks having mortalities of greater than 50%. Abalone died within 1-3 days after onset of clinical signs. Clinical signs included reduced pedal adhesion to the tank surface, loss of the righting reflex, and swollen mouths, sometimes prolapsed, with eversion of the radula.

Laboratory Results: Hemolymph samples collected from the pedal sinus were plated onto Horse Blood Agar, TCBS, and McConkey's Agar and incubated at 20°C for 2 days. No significant pathogens were isolated.

Gross Pathology: Apart from the swollen mouths and prolapsed radula, no significant gross lesions were present.

Histopathologic Description: The lesions are confined to nervous tissue and centered on the cerebral, pleuropedal and buccal ganglia, the cerebral commissure and the peripheral nerves arising from these structures. The lesions are an increased cellularity and individual cell necrosis in the affected nerves. Multifocally, the cell necrosis and edema cause a ragged and disheveled appearance in the neuropil. Occasional neurons have marginated chromatin and central pallor, but no Cowdry type A inclusions are present. The lesions are often strikingly well demarcated, with musculature directly adjacent to affected large nerves and ganglia having no lesions. Those abalone with swollen mouths have dilated sinuses and ruptured connective tissue leading to poorly delineated spaces, some of which are filled with hemolymph fluid and haemocytes.

Contributor's Morphologic Diagnosis: Severe multifocal necrotizing ganglioneuritis.

Contributor's Comment: Abalone viral ganglioneuritis is a recently defined contagious viral disease of abalone caused by infection with abalone herpes-like virus (AbHV).[2] The disease was first reported in Taiwan[1] and more recently in Australia.[2] The relationship between the Australian viral isolate(s) and other herpes-like viral isolates has not, as yet, been elucidated, but it is suggested that this virus is the second member of the Malacoherpesviridae along with Ostreid Herpesvirus-1.[3]

The outbreaks occurred almost simultaneously in three farms following abalone movements from the wild and between farms. An opportunistic bacterial infection was quickly ruled out because several features differed from previous outbreaks of bacterial infection. These included the clinical signs, the pattern of spread of the outbreak on the initial farm, the very high rates of morbidity and mortality in some tanks during the first and subsequent weeks of the outbreak, and the links between movement of stock and subsequent disease outbreaks. The level of both wild broodstock collection and inter-farm exchange was greater this year than previous years due to efforts to increase and share genetic diversity in farms involved with an industry breeding program. Issues of translocation were considered following the national abalone disease survey.[3] Few significant translocation risks were identified in this process; those recognized, such as *Perkinsus olseni*, were taken into account and abalone were collected from areas outside their known distribution.

The lesions centered on neural tissue innervating the mouth parts of the abalone resulting in the clinical signs of swelling and prolapse of the mouth and eversion of the radula. The

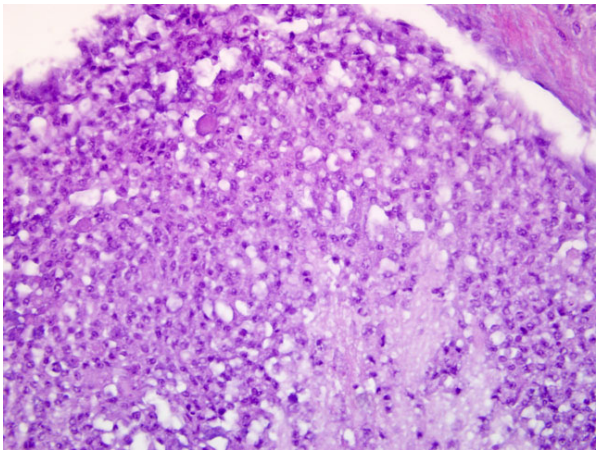

2-1. Cerebral commissure, abalone, (Haliotis laevigata). The neuropil is infiltrated and replaced by many haemocytes, with degeneration, necrosis, and vacuolation. (HE 400X)

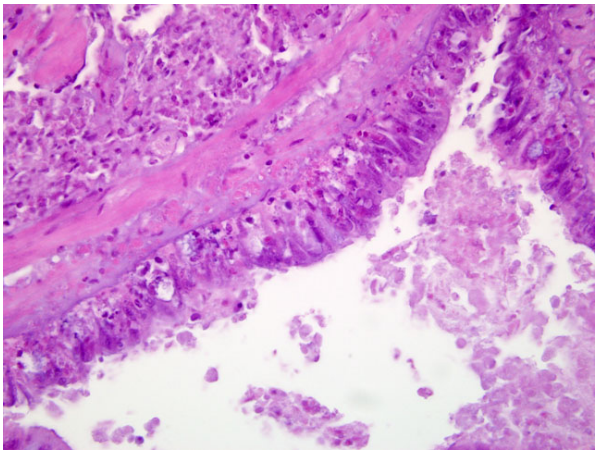

2-2. Radula, abalone, (Haliotis laevigata). Multifocally there is degeneration and necrosis of the epithelium with infiltration of low numbers of haemocytes. (HE 400X)

pleuropedal ganglion and pedal nerves were also commonly affected, leading to paralysis of the foot muscle and loss of adhesion to the tank surface.

The very high mortality, unusual clinical observations in moribund abalone, on-farm and between-farm pattern the outbreak, and the history of abalone movements linking farms were all highly suggestive of a new virulent infectious agent. As new animal and aquatic species become farmed commercially, health surveillance of these species will need to be developed and veterinarians and veterinary laboratories are key players.

AFIP Diagnosis: 1. Neural tissue, cerebral commissure, ganglia, and peripheral nerves: Ganglioneuritis, necrotizing, multifocally extensive, marked with haemocytic inflammation and rare intranuclear inclusion bodies.
2. Radula: Epithelial degeneration and necrosis, multifocal, moderate, with mild haemocytic inflammation.

Conference Comment: Species of abalone reportedly susceptible to herpesvirus infection include the greenlip abalone (*Haliotis laevigata*), the blacklip abalone (*H. rubra*) and *H. diversicolor supertexta* in Chinese Taipai. The initial outbreak in Australia occurred in the summer. Once established in wild abalone populations, morbidity and mortality can be seen throughout the year and appears not to be influenced by seasonality. The moderator commented that this particular entity is spreading and could reach the United States in the near future.[2] Diagnosis of abalone herpes-like virus can be accomplished by histopathology, *in-situ* hybridization, and electron microscopy where viral particles display ultrastructural characteristics of herpesrviridae.[2]

In addition to the histologic lesions in the cerebral commissure and ganglia, several conference participants observed multifocal epithelial degeneration and necrosis in the radula. The cause of the epithelial lesions in the radula is uncertain, but most participants considered the change likely due to the sequela of herpesviral infection, and possibly an acute terminal lesion associated with paralysis of the mouth parts described clinically by the contributor.

Contributor: Gribbles Veterinary Pathology, 1868 Dandenong Rd Clayton, Melbourne, Victoria, Australia, 3168

References:
1. Chang P, Kuo S, Lai S, et al. Herpes-like virus infection causing mortality of cultured abalone *Haliotis diversicolor supertexta* in Taiwan. *Dis Aquat Org*. 2005;65:23-27.
2. Crane M, Corbeil S. Infection with abalone herpes-like virus. In: *Manual of Diagnostic Tests for Aquatic Animals 2010*. OIE; www.oie.int/eng/normes/fmanual/2.4.01_INF_ABALONE.pdf. Accessed online 10 January 2011.
3. Handlinger J, Bastianello S, Callinan R, et al. Abalone aquaculture subprogram: A national survey of diseases of commercially exploited abalone species to support trade and translocation issues and the development of health surveillance programs. Canberra, Australia: Fisheries Research and Development Corporation; FRDC Project No 2002/20:2006.
4. Hooper C, Hardy-Smith P, Handlinger J. Ganglioneuritis causing high mortalities in farmed Australian abalone (*Haliotis laevigata* and *Haliotis rubra*). *Aust Vet J*. 2007;85:188-193.

CASE III: WNo3/1247/22G (AFIP 2890835).

Signalment: Juvenile (3-4 month-old) male and female giant tiger shrimp (*Penaus monodon*).

History: *Penaus monodon* ponds on farms in eastern Australia are typically 1 hectare in area and carry approximately 40 shrimp per square meter during the 5-6 month grow-out period. These moribund, lethargic shrimp were collected when excessive numbers (typically > 20 moribund or dead shrimp per day) were observed at pond edges during the second half of the grow-out period.

Gross Pathology: Affected shrimp were typically reddish in color, with mild to moderate epibiotic fouling and one or more partially amputated appendages.

Histopathologic Description: Whole body: In peripheral nerves, particularly antennal nerves, there is mild to severe, focal to diffuse degeneration and necrosis of axons and their sheaths, together with associated glial cell apoptosis. There is mild to severe, acute retinitis associated with degeneration and necrosis of retinular cells and their axons in the fasciculated zone of the photoreceptor region of the eye. In the lymphoid organ (located cranial to the hepatopancreas) there is moderate to marked increase in numbers of spheroids (aggregates of haemocytes). In the vas deferens of male shrimp, there is moderate to severe focal to locally extensive epithelial necrosis.

In the putative glial cells in the antennal nerve and in the fasciculated zone of the photoreceptor region of the eye, moderate to large numbers of intracytoplasmic rod-shaped, helical nucleocapsids and enveloped virions, morphologically consistent with a yellow head-like virus (Order Nidovirales), were demonstrated by transmission electron microscopy.

By immunohistochemical examination using monoclonal antibodies against yellow head-related viruses, tissues containing lesions (but not histologically normal tissues in the affected shrimp) consistently stained positively.

Contributor's Morphologic Diagnosis: 1. Peripheral neuropathy, necrotizing, acute, segmental, severe.
2. Retinopathy, necrotizing, acute, multifocal, severe (peripheral neuropathy and retinopathy disease).

Contributor's Comment: Since 1994 significant mortalities during the second half of the grow-out period on eastern Australian *P. monodon* farms have often been attributed by farmers to a condition designated as "midcrop mortality syndrome" (MCMS). It is likely that "peripheral neuropathy and retinopathy" (PNR), the emerging disease diagnosed in the current cases, is a component of disease within the MCMS complex.[1,2] PNR has been recorded only in farmed *P. monodon* from eastern Australia.

Outbreak studies strongly suggest that a virus morphologically and immunologically similar to viruses in the yellow head group is the causative infectious agent of PNR. Gill-associated virus (GAV) is the only such virus so far described from eastern Australia, where it is widely endemic in wild and farmed *P. monodon* populations. Evidence suggests GAV is transmitted both vertically in shrimp hatcheries and horizontally via cannibalism in ponds.[2,3]

Production losses are usually minimal if ponds experiencing PNR outbreaks are harvested within three weeks of outbreak recognition. Severe losses (up to 50% mortality) may occur when harvest is delayed for longer periods.[2]

AFIP Diagnosis: 1. Peripheral nerve: Radiculoneuritis, haemocytic and necrotizing, multifocal, moderate.
2. Eye, retina: Retinular cell degeneration and necrosis, multifocal, moderate with axonal degeneration.

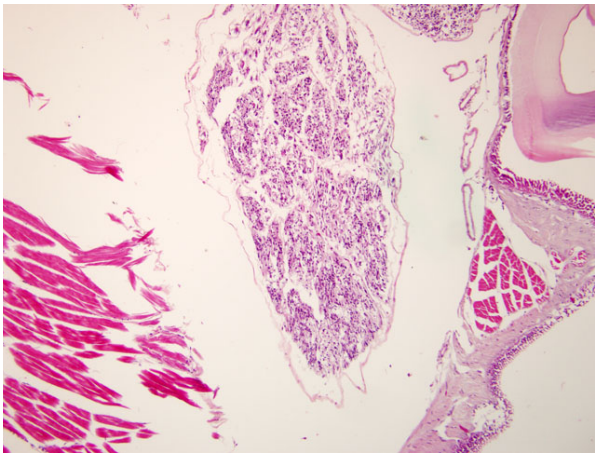

3-1. Peripheral nerve, giant tiger shrimp (Peneus monodon). Peripheral nerves are infiltrated and expanded by moderate numbers of haemocytes. (HE 100X)

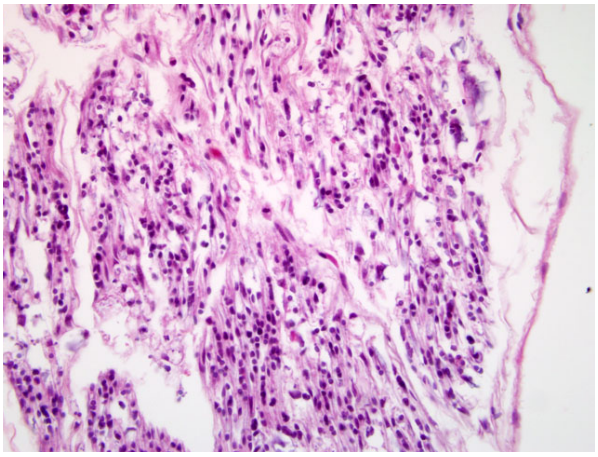

3-2. Peripheral nerve, giant tiger shrimp (Peneus monodon). Peripheral nerves are infiltrated by moderate numbers of haemocytes, and there is associated axonal degeneration, vacuolation, and loss. (HE 400X)

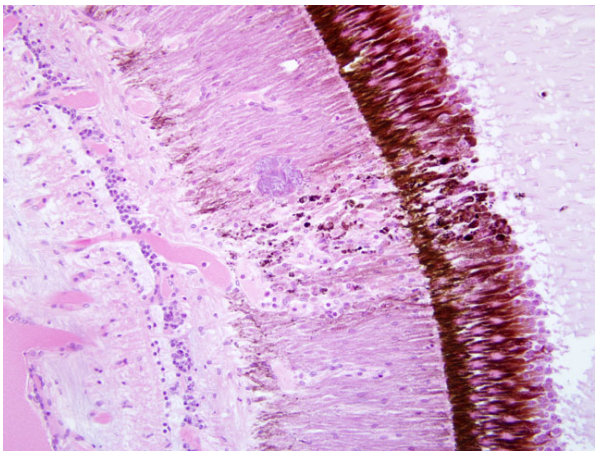

3-3. Eye, retina, giant tiger shrimp (Peneus monodon). Retinular cells are degenerate and necrotic, with infiltration by low numbers of haemocytes. (400X)

Conference Comment: Gill-associated virus (GAV), the type species for the genus *Okavirus*, is one of six genotypes; it is designated as genotype 2 and, along with genotypes 3-6, commonly infects *Penaeus monodon* without causing disease. Yellow head virus (YHV) is designated as genotype 1 and tends to be more virulent than the other five genotypes. Viruses in this group are enveloped with positive-sense, single-stranded RNA. Ultrastructurally, the *Okaviruses* are rod-shaped, enveloped with peplomeres, contain a helical nucleocapsid, and measure 40-60 nm x 150-200 nm. The virus targets ectodermal and mesodermal tissues, notably lymphoid organs, hemocytes, hematopoietic tissues, gill lamellae and nervous tissue. Initial pond infection with YHV and GAV can produce up to 100% and 80% mortality, respectively. Outbreaks are often associated with physiologic stress such as pH or oxygen saturation change.[3]

Diagnosis is suspected by clinicopathologic presentation and confirmed by a variety of ancillary laboratory methods. Affected animals cease feeding and congregate at the pond edges and surface. Macroscopically, animals have a bleached appearance with yellowing of the cephalothorax and pink to yellow discoloration of the gills. Histologically, detection of deeply basophilic, round, intracytoplasmic viral inclusions, particularly in the lymphoid organ, stomach subcuticulum, and gills is often diagnostic. Electron microscopy, wet mounts, fixed hemolymph smears, rt-PCR, *in-situ* hybridization and bioassays are other confirmatory diagnostic tools.[3]

Contributor: NSW Agriculture, Wollongbar Agricultural Institute, Regional Veterinary Laboratory, Wollongbar, NSW, Australia.

References:

1. Callinan RB, Jiang L, Smith PT, Soowannayan C. Fatal, virus-associated peripheral neuropathy and retinopathy in farmed *Penaeus monodon* in eastern Australia: I. Pathology. *Dis Aquat Org*. 2003;53:181-193.

2. Callinan RB, Jiang L. Fatal, virus-associated peripheral neuropathy and retinopathy in farmed *Penaeus monodon* in eastern Australia: II. Outbreak descriptions. *Dis Aquat Org*. 2003;53:195-202.

3. Walker P. Yellow Head Disease. In: *Manual of Diagnostic Tests for Aquatic Animals 2010*. OIE; http://www.oie.int/eng/normes/fmanual/2.2.07_YHD.pdf. Accessed online 10 January 2011.

4. Walker PJ, Cowley JA, Spann K, Hodgson RA, Hall M, Withyachumnarnkul B. Yellow head complex viruses: Transmission cycles and topographical distribution in the Asia-Pacific region. In: Browdy CL, Jory DE, eds. *The New Wave*. Proceedings of the Special Session on Sustainable Shrimp Culture, Aquaculture 2001. The World Aquaculture Society, Baton Rouge, LA, USA.

CASE IV: 07F37 (AFIP 3065923).

Signalment: Adult red swamp crayfish (*Procambarus clarkii*).

History: This spring, a crayfish pond in southern Louisiana has been experiencing high mortality, especially evident in the larger specimens. Affected crayfish are lethargic.

Laboratory Results: In situ hybridization for white spot syndrome virus (WSSV), DNA on embedded tissue sections showed positive staining in affected nuclei. PCR testing (NVSL in Ames, IA) for WSSV in tissues was positive.

Gross Pathology: In some cases, crayfish exhibit marked gill fouling (accumulation of pond detritus on the gills and exoskeleton).

Histopathologic Description: Sections are composed of a transverse abdominal cross section (some slides contain gill tissue as well). There are large numbers of intranuclear inclusions in the cuticular epithelium, hindgut mucosa, and gill epithelium. Within the hindgut, luminal epithelium contains many inclusions with lesser numbers in the acinar gland epithelium and connective tissues. Occasional inclusions are present in the glial cells of the ventral nerve cord. Within the gill, many flange cells contain inclusions. Inclusions are eosinophilic to basophilic and occasionally have a clear halo (Cowdry type A). Affected cells have enlarged nuclei with marginated chromatin. Multifocally, along the abdominal dorsum, there is cuticular epithelial loss and necrosis with cuticular separation and suffusion of proteinaceous fluid (hemolymph) into the intervening space. Multifocally, muscle tissues contain 100-250 micron long by 40-60 micron wide, sagittally acicular to ovoid, transversely polyhedral (4-6 sided) organisms with eosinophilic, birefringent, thick shell plates and a basophilic medial shell membrane (sporocyst). In cases where sporocyst internal tissues are preserved, there is a fine, lightly eosinophilic inner membrane encasing one to several, 10-15 micron wide, lightly eosinophilic amoeboid bodies (spores). Multifocally, myocyte bundles exhibit fine basophilic granularity (mineralization) with varying degrees of sarcoplasmal degeneration and necrosis.

Contributor's Morphologic Diagnosis: Multiple eosinophilic to basophilic intranuclear inclusions and karyomegaly in ectodermal and mesodermal tissues; moderate, multifocal, cuticular epithelial necrosis with cuticle separation; multiple intramuscular parasitic sporocysts (*Psorospermium* sp.); mild, multifocal myocyte necrosis (white spot syndrome virus, p sorospermiasis).

Contributor's Comment: White spot disease (WSD) is caused by the etiologic agent white spot syndrome virus (WSSV). The disease is so named due to the development of white, circular to coalescing spots in the cuticles of afflicted penaeid shrimp which are formed by the deposition of $CaCO_3$, cell debris, chitin, protein, and tegumental gland products as a result of cuticular pore canal destruction.[12,14] It is, unfortunately, a nonspecific alias since the formation of cuticular white spots may also be caused by bacterial infection or elevated water pH.[12] Since the first reported occurrence in 1992, WSD has had a profoundly detrimental impact on the cultured shrimp industries in Asia, Latin America, and the United States of America.[3,5] The beginning of an outbreak is heralded by anorexia; then the appearance within days of moribund shrimp at the water surface; and the development of white spots in some individuals.[1] Outbreaks often have high daily mortality rates with total mortality reaching 100% within 3 to 10 days.[6] All decapod crustaceans are considered susceptible, inclusive of marine, brackish, and freshwater species, as well as all life stages from egg to brood stock. Transmission may occur vertically (trans-ovum) or horizontally through ingestion of infected tissue and waterborne routes. Morbidity and mortality are highly variable between species.[8] In crayfish, WSSV infection clinically causes lethargy and grossly produces mottling or slight discoloration of the cuticle. Mortality rates both experimentally and in outbreaks have been high.[9,11]

The white spot syndrome virus is a double stranded, non-occluded, enveloped, DNA virus currently in the family *Nimaviridae*, genus *Whispovirus*, but had historically been assigned to the *Baculoviridae* family.[1] Virions are large and elliptical to rod shaped, measuring 70-150 nm by 250-380 nm.[6] Infected cells exhibit nuclear hypertrophy, chromatin margination, and eosinophilic to basophilic inclusions. The central aspect of inclusions is composed of unformed virogenic material admixed with formed virions, while mature virions tend to aggregate at nuclear margins in ordered arrays. Progressive infection leads to nuclear dissociation and cell death.[3,14] The WSSV infects tissues of ectodermal and mesodermal origin, namely the foregut, hindgut, gills, antennal gland, integument, gonads, muscle, heart, hemocytes, nervous tissue, and hematopoietic tissue. Considerable debate still exists, however, as to the site of entry, primary replication, and method of spread of WSSV *in vivo*.[5] Histologically, prominent eosinophilic to basophilic intranuclear inclusions are present most commonly in the cuticular epithelium, connective tissues, gills, foregut, and hindgut.[6,7] The presence of Cowdry type A inclusions is considered indicative of early inclusion body development. Likewise, the progression of inclusions from eosinophilia to basophilia is considered a hallmark of advanced infection. Furthermore, these features are used by some to distinguish WSSV from other viral infections.[6,15] Caution is warranted, however, as assessment of inclusions is often based on sections stained by a specific published protocol by T. Bell and Don Lightner. Transmission electron microscopy (TEM), in-situ hybridization, or various PCR methods are necessary for confirmation.[8]

Psorospermium belongs to the class *Mesomycetozoea*, a protistan clade located near the animal-fungal taxonomic divergence.[10] Very little is known about the life cycles and feeding habits of the members of this class. The pathogenicity of this organism in crayfish is uncertain due to the variance in reported host reaction.[4] Originally described in 1857, "the enigmatic parasite of freshwater crayfish" was finally determined to be part of the DRIP clade (*Dermocystidium*, rosette agent, *Ichthyophonus*, and *Psorospermium*) in 1997, which has subsequently been placed in *Mesomycetozoea*. *Psorospermium haeckeli* is the only confirmed species, although others have been described but remain to be accepted.[10] *Psorospermium* spp. has been documented in 15 crayfish species in Europe, North America, and Australia.[13] In astacid crayfish this organism is found most often in connective and epidermal tissues under the carapace. In cambarid crayfish (*P. clarkii*, among others), it is most often present in abdominal muscles.[4]

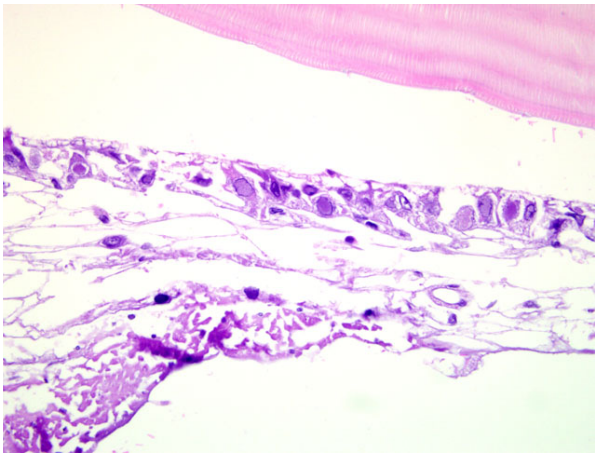

4-1. Subcuticle, crayfish, (Procambarus clarkia). Intranuclear viral inclusions are present in many degenerate and necrotic subcuticular epithelial cells. (HE 400X)

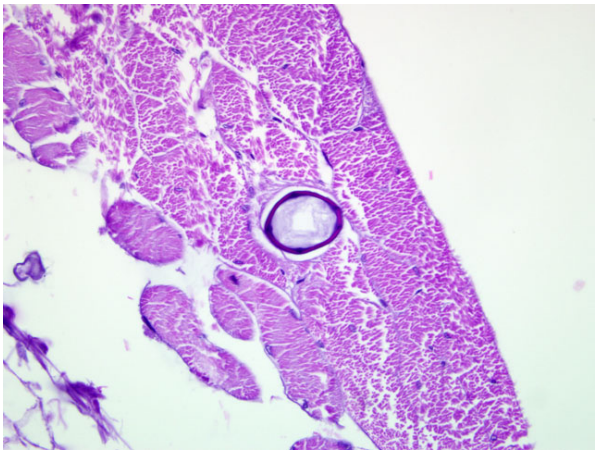

4-2. Skeletal muscle, crayfish, (Procambarus clarkia). Parasitic sporocysts with an eosinophilic, birefringent, thick shell plate and a basophilic medial shell membrane are present within skeletal muscle. (HE 400X)

AFIP Diagnosis: 1. Cuticle and subcuticle: Epithelial degeneration and necrosis, multifocally extensive, moderate with subcuticular separation, edema, karyomegaly and intranuclear inclusion bodies.
2. Skeletal muscle: Intramyocytic basophilic cysts.
3. Alimentary tract, epithelium and subepithelial connective tissue: Karyomegaly, with amphophilic intranuclear inclusion bodies.

Conference Comment: Scientific knowledge of this economically important infectious disease is relatively sparse. As the contributor notes, there are still several unknown factors in the epidemiology and pathogenesis of white spot disease. For instance, the virus can be transmitted both horizontally and vertically; infection can also occur between outwardly healthy, apparently disease-free animals and susceptible animals. The triggers for individual disease development are unknown, with some infections being subclinical while outbreaks have been associated with changes in environmental factors. Lifelong infection of carriers is also common.[2]

In addition to the diagnostic modalities listed by the contributor, there are several, often less labor-intensive, diagnostic techniques available. Clinically, hemolymph from infected shrimp often has delayed or absent clotting reaction. Stained or unstained wet mounts of the gills and cuticular epithelium may readily demonstrate karyomegaly. Dark-field microscopy of unstained hemolymph will show viral aggregates as 0.5 µm reflective spots. White spot syndrome virus has a unique ultrastructural appearance; it is described as bacilliform, being ~300 nm in length by ~150 nm in width. Negatively stained electron micrographic studies may reveal the presence of a tail-like appendage extending from one end of the virion.[2]

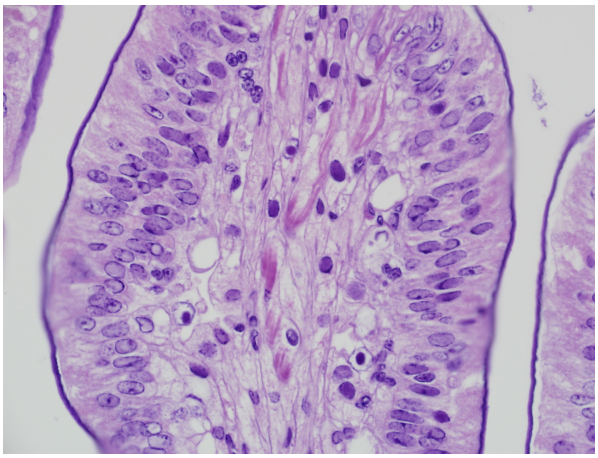

4-3. Hindgut, crayfish, (Procambarus clarkia). Mucosal epithelial cells contain basophilic intranuclear viral inclusion bodies. Photograph courtesy of Louisiana State University School of Veterinary Medicine, Department of Pathobiological Sciences, http://www.vetmed.lsu.edu/pbs/

Contributor: Louisiana State University School of Veterinary Medicine, Department of Pathobiological Sciences, Skip Bertman Drive, LSU, Baton Rouge LA, 70803
http://www.vetmed.lsu.edu/pbs/

References:

1. Anonymous. White spot disease. In: *OIE Manual of Diagnostic Tests for Aquatic Animals 2003*. 4th ed. Paris, France: OIE; 2003:285-297.
2. Chu-Fang Lo G. White spot disease. In: *Manual of Diagnostic Tests for Aquatic Animals 2010*. OIE; http://www.oie.int/eng/normes/fmanual/2.2.05_WSD.pdf. Accessed online 11 January 2011.
3. Durand S, Lightner DV, Redman RM, Bonami JR. Ultrastructure and morphogenesis of white spot syndrome baculovirus (WSBV). *Dis Aquat Org*. 1997;29:205-211.
4. Edgerton BF, Evans LH, Stephens FJ, Overstreet RM. Review article: Synopsis of freshwater crayfish diseases and commensal organisms. *Aquaculture*. 2002;206:57-135.
5. Escobedo-Bonilla CM, Wille M, Alday Sanz V, Sorgeloos P, Pensaert MB, Nauwynck HJ. Pathogenesis of a Thai strain of white spot syndrome virus (WSSV) in juvenile, specific pathogen-free *Litopenaeus vannamei*. *Dis Aquat Org*. 2007;74:85-94.
6. Lightner DV. *A Handbook of Pathology and Diagnostic Procedures for Diseases of Penaeid Shrimp*. Baton Rouge, LA: World Aquaculture Society;1996.
7. Lo CF, Ho CH, Chen CH, et al. Detection and tissue tropism of white spot syndrome baculovirus (WSBV) in captured brooders of *Penaeus monodon* with a special emphasis on reproductive organs. *Dis Aquat Org*. 199730:53-72.
8. Lo G. Chapter 2.3.2 White spot disease. In: Commission OAAHS, eds. *OIE Manual of Diagnostic Tests for Aquatic Animals* (online). Paris, France: OIE;2006.
9. Maeda M, Itami T, Mizuki E, et al. Red swamp crawfish (*Procambarus clarkii*): An alternative experimental host in the study of white spot syndrome virus. *Acta Virol*. 2000;44:371-374.
10. Mendoza L, Taylor JW, Ajello L. The class Mesomycetozoea: A heterogeneous group of microorganisms at the animal-fungal boundary. *Annu Rev Microbiol*. 2002;56:315-344.
11. Richman LK, Montali RJ, Nichols DK, Lightner DV. A newly recognized fatal baculovirus infection in freshwater crayfish. In: *Proceedings of the American Association of Zoo Veterinarians*. 1997;262-264.
12. Sahoo AK, Patil P, Shankar KM. White spots? A loaded question for shrimp farmers. *Curr Sci*. 2005;88:1914-1917.
13. Vogt G, Rug M. Life stages and tentative life cycle of *Psorospermium haeckeli*, a species of the novel DRIPs clade from the animal-fungal dichotomy. *J Exp Zool*. 1999;283:31-42.
14. Wang YG, Hassan MD, Shariff M, Zamri SM, Chen X. Histopathology and cytopathology of white spot syndrome virus (WSSV) in cultured *Penaeus monodon* from peninsular Malaysia with emphasis on pathogenesis and the mechanism of white spot formation. *Dis Aquat Org*. 1999;39:1-11.
15. Wongteerasupaya C, Vickers JE, Sriurairatana S, et al. A non-occluded, systemic baculovirus that occurs in cells of ectodermal and mesodermal origin and causes high mortality in the black tiger prawn *Penaeus monodon*. *Dis Aquat Org*. 1995;21:69-77.

The Armed Forces Institute of Pathology
Department of Veterinary Pathology

Conference Coordinator
Matthew Wegner, DVM

WEDNESDAY SLIDE CONFERENCE 2010-2011

Conference 14

15 December 2010

Conference Moderator:
Dr. Fabio Del Piero, DVM, PhD, Diplomate ACVP

CASE I: 24087-09 (AFIP 3163065).

Signalment: 1-year-old female brown and white Boer goat, caprine (*Capra hircus*).

History: The animal was presented by the food animal clinic with a history of icterus, abdominal pain and pigmenturia.

Gross Pathology: This juvenile brown and white female caprine weighed 49.5 kg and was well fleshed. The fascia and body fat had a pronounced yellow hue. Transparent red fluid was present in the thorax and abdomen and the spleen was diffusely enlarged, with a soft dark red appearance of the incised surface. The liver had a uniform yellow-tan color, and the gallbladder was distended. The kidneys were soft and dark red in color, bulging when incised. The inner renal medulla especially had a red granular character.

Laboratory Results: Elevated AST, GGT and CK were present in antemortem serum samples. Serum copper was elevated. Liver copper was 310 ppm on a wet-weight basis (normal 25-150 ppm), and renal copper was 67 ppm (normal <12 ppm).

Histopathologic Description: Liver: Hepatic cords are poorly defined, containing dissociated cells, particularly in centrilobular and midzonal locations. Individualized cells at these and other sites have eosinophilic cytoplasm and pyknotic or absent nuclei. Some contain brown-gray cytoplasmic granules that are positive for copper by rhodanine staining. Occasional canaliculi are outlined by bile pigment. Small numbers of well-defined unstained cytoplasmic vacuoles, interpreted as lipid, also occur in hepatocytes. In most instances, areas of degeneration and necrosis are devoid of inflammation, although clusters of eosinophils and other leukocytes occasionally occur.

Kidney: Some cortical renal tubules contain flocculent to eosinophilic granular casts, often with granules possessing a more pronounced red color, while others contain degenerating cells. Renal tubular epithelial cells are attenuated, coagulated and pyknotic, or absent. Similar casts occur in the medulla with less tubular damage. Thrombi occur in small, thin-walled interstitial blood vessels.

Special stains revealed bile retention in hepatic canaliculi and granules positive for copper by rhodanine were found in the liver but not the kidney. Iron stains were positive for sloughed cells in renal tubules, but the liver contained little iron pigment.

Contributor's Morphologic Diagnosis: 1. Liver: Hepatocellular degeneration and necrosis, acute, predominantly centrilobular, with cytoplasmic granularity, mild lipidosis and mild bile stasis.
2. Kidney: Acute renal tubular degeneration and necrosis, severe, with hemoglobinuric casts and interstitial thrombosis.

Contributor's Comment: Copper intoxication is somewhat divisible into an acute form, which is generally associated with gastrointestinal disturbance, or a chronic form, which is more often associated with a precipitous hemolytic crisis, although both diseases are characterized by

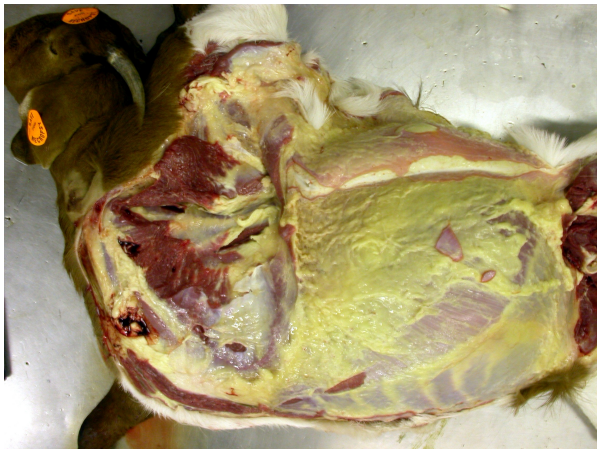

1-1. Subcutis and muscle fascia, goat. Subcutaneous tissue and fascia are bright yellow (icterus). Photograph courtesy of University of Missouri, Veterinary Medical Diagnostic Laboratory, and Department of Veterinary Pathobiology, http://www.cvm.missouri.edu/vpbio/index.html

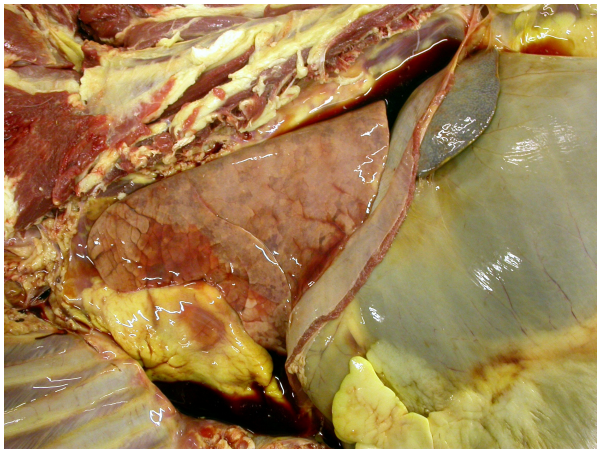

1-2. Thoracic and abdominal cavities, goat. The body cavities contain a serosanguineous effusion. Photograph courtesy of University of Missouri, Veterinary Medical Diagnostic Laboratory, and Department of Veterinary Pathobiology, http://www.cvm.missouri.edu/vpbio/index.html

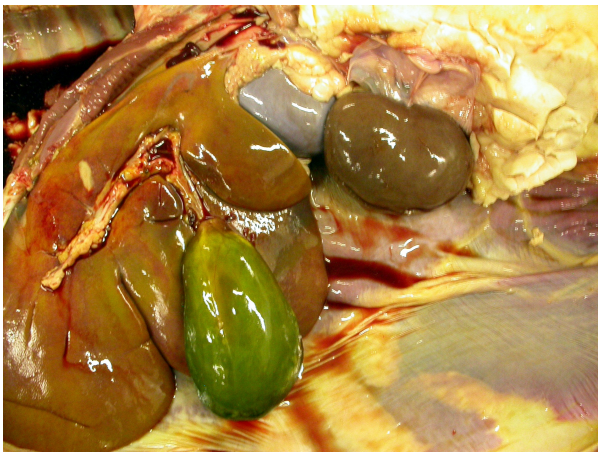

1-3. Liver and gallbladder, goat. The liver is uniformly yellow-tan and the gallbladder is distended. Photograph courtesy of University of Missouri, Veterinary Medical Diagnostic Laboratory, and Department of Veterinary Pathobiology, http://www.cvm.missouri.edu/vpbio/index.html

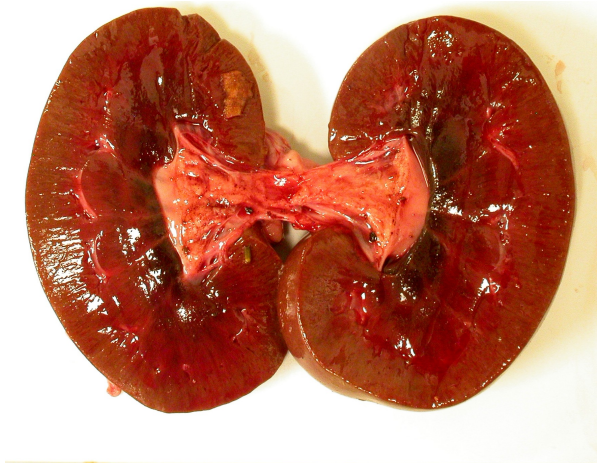

1-4. Kidney, goat. The kidney is soft, red, and bulges on cut surface, with a granular appearance to the medulla. Photograph courtesy of University of Missouri, Veterinary Medical Diagnostic Laboratory, and Department of Veterinary Pathobiology, http://www.cvm.missouri.edu/vpbio/index.html

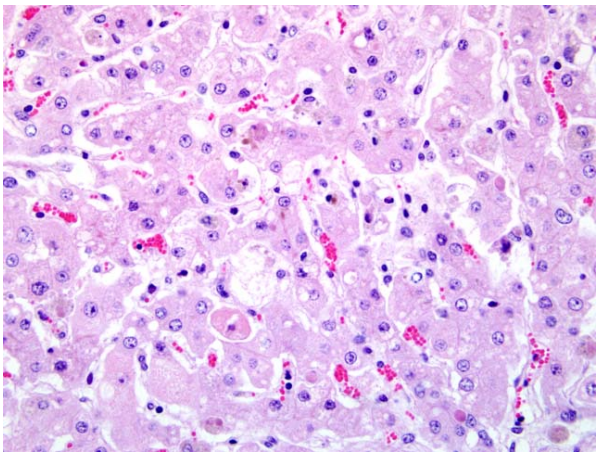

1-5. Liver, goat. Hepatic cords are poorly defined and hepatocytes are often hypereosinophilic with pyknosis (necrosis) or are vacuolated and contain yellow bile or brown-gray hemosiderin pigment. (HE 400X)

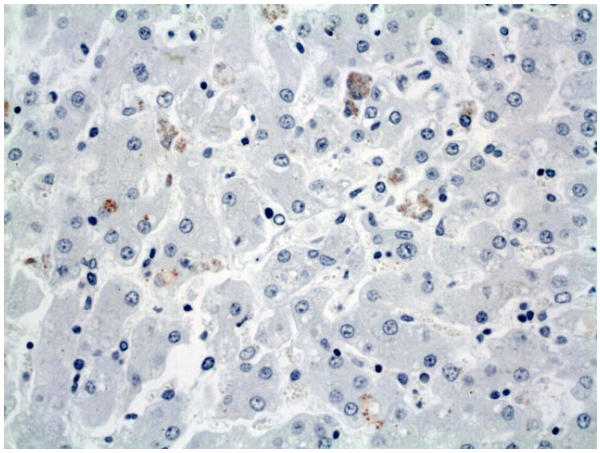

1-6. Liver, goat. The rhodanine stain demonstrates intracytoplasmic copper within hepatocytes and Kupffer cells. Photograph courtesy of University of Missouri, Veterinary Medical Diagnostic Laboratory, and Department of Veterinary Pathobiology, http://www.cvm.missouri.edu/vpbio/index.html (Rhodanine stain)

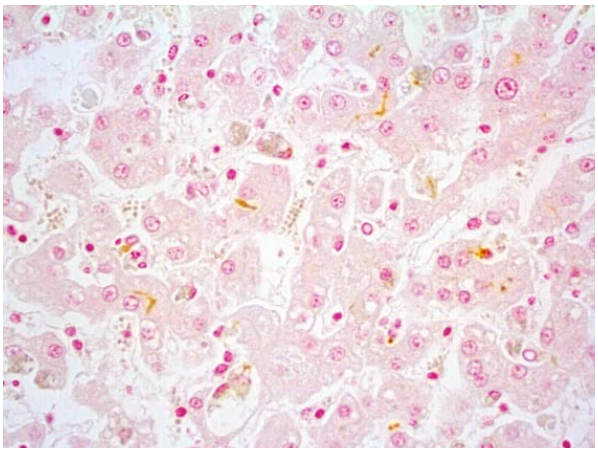

1-7. Liver, goat. Hall's stain demonstrates caniliculi distended with bile. Photograph courtesy of University of Missouri, Veterinary Medical Diagnostic Laboratory, and Department of Veterinary Pathobiology, http://www.cvm.missouri.edu/vpbio/index.html. (Hall's stain)

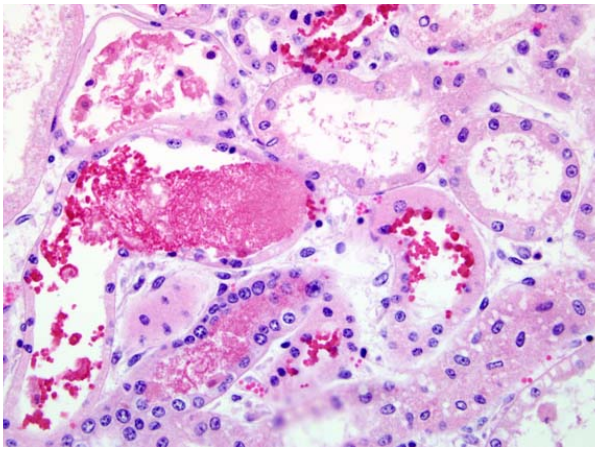

1-8. Kidney, goat. Renal tubules are dilated by eosinophilic or red granular casts (hemoglobin) and are lined by attenuated degenerate or necrotic epithelium, with occasional intraluminal sloughed epithelial cells. (HE 400X)

a precipitous onset of clinical signs. Chronic copper intoxication is most frequently seen in sheep, in which chronic consumption of feed designed for use in other species is a principal cause, although exacerbating factors such as low dietary molybdenum or sulfur, exogenous copper from other sources (including swine or poultry litter) or pre-existing liver damage (often due to exposure to hepatotoxic plants) may be involved. Although they are less susceptible than sheep, acute hemolytic crises have occurred in adult Boer goats associated with increased levels of tissue copper.[1] Hepatic accumulation of copper due to defects in metabolism or excretion occurs during the preclinical hepatopathy, with abrupt acute hepatocellular degeneration that is often precipitated by stress. Massive release of copper, thought to result from degeneration of copper-rich lysosomes, precipitates hemolysis. In sheep, copper loading is characterized proteomically by a reaction to oxidative challenge, with evidence of oxidative stress injury occurring even prior to the hemolytic crisis.[8]

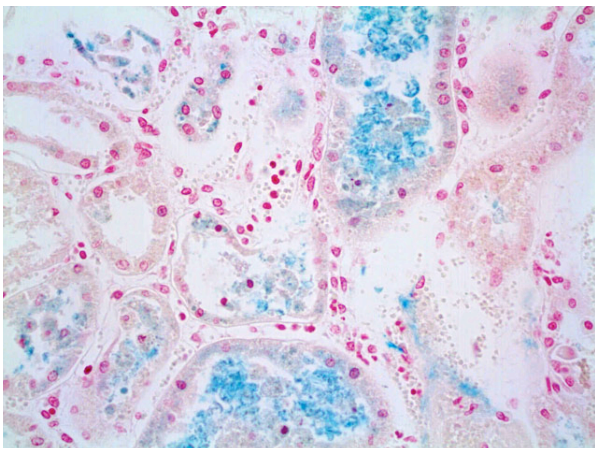

1-9. Kidney, goat. Iron is present within renal tubules and tubular epithelium. Photograph courtesy of University of Missouri, Veterinary Medical Diagnostic Laboratory, and Department of Veterinary Pathobiology, http://www.cvm.missouri.edu/vpbio/index.html. (Prussian blue)

Hemolytic crisis has been reported to follow acute exposure of pre-ruminant kid goats exposed to milk replacer intended for calves,[6] but an outbreak of copper intoxication in lactating dairy goats was characterized by hepatopathy without hemolytic crisis.[2] However, copper intoxication with hemolysis is becoming more recognized in adult and juvenile Boer goats. In this particular animal, the lesions are consistent with a post-hemolytic phase of disease in which renal damage associated with hemoglobinuria is evident.

Liver damage in copper intoxication is thought to result from a combination of hepatocyte apoptosis resulting from exhaustion of intracellular copper-binding proteins and anoxia secondary to anemia. Renal damage may likewise have hemoglobinuria and anemia as cofactors affecting the lesion development. Ultrastructurally, the preclinical phase is morphometrically associated with hepatocyte and Kupffer cell swelling at the expense of the sinusoids and space of Disse, with pronounced lysosomal proliferation. At the time of crisis, lysosomes become even more enlarged and contain many residual bodies.[3]

Copper concentrations should not be above 230 mg/kg in liver, 12 mg/kg in kidney or 1.2 mg/kg in blood as measured by flame atomic absorption spectrometry. A variety of copper storage diseases occur in humans, rodents and companion animals.[4] In Wilson's disease of humans, the rate of ceruloplasmin binding of copper is reduced, as is excretion, due to mutation of the ATP7B gene. The specific genetic defect resulting in variable breed susceptibility in other species is not known.

AFIP Diagnosis: 1. Liver: Hepatocellular degeneration and necrosis, centrilobular to midzonal, diffuse, moderate, with bile stasis, and intracytoplasmic amphophilic granular material (copper).
2. Kidney: Tubular degeneration and necrosis, diffuse, severe, with multifocal tubular regeneration, tubular protein,

granular and hemoglobin casts, and occasional fibrin thrombi.

Conference Comment: Many participants were impressed by the extent of tubulorrhexis present in the kidney. In contrast, fibrin thrombi are not evident in all sections and hence the characterization as "occasional fibrin thrombi."

Participants discussed the histomorphologic features of tubular regeneration. Approximately one week after the initial injury, regeneration is evident. Tubules are lined by attenuated epithelium with hyperchromatic nuclei, and occasional mitotic figures may be seen. As regeneration continues, cells appear smaller with increased cytoplasmic basophilia, and may be closely packed with the appearance of piling up. The moderator offered additional guidelines to aid in the interpretation of tubular regeneration, such as uneven nuclear size (anisokaryosis) and variable distance between nuclei due to cells in different stages of growth and re-epithelialization.[7]

Cases of hemoglobinuric nephrosis often have characteristic "port wine-colored" urine. There are three possible causes of such urine color: hematuria, hemoglobinuria and myoglobinuria. Identifying the cause of discoloration often provides insight as to the underlying disease process; therefore, one must be able to differentiate the three causes in the laboratory. Hematuria is easily diagnosed by centrifugation of the urine specimen; erythrocytes will be present in the urine sediment. Hemoglobinuria and myoglobinuria both lack erythrocytes in the sediment and the urine remains discolored after centrifugation. Addition of saturated ammonium sulfate will cause hemoglobin to precipitate out of the urine sample, resulting in a clear sample; myoglobin does not precipitate, and the urine remains discolored. If a blood sample is also available, centrifugation of a hemoglobinemic sample will result in pink serum, while in a myoglobinemic sample the plasma will remain clear.[4]

Contributor: University of Missouri, Veterinary Medical Diagnostic Laboratory, and Department of Veterinary Pathobiology, 1600 East Rollins Street, Columbia MO 65211.
http://www.cvm.missouri.edu/vpbio/index.html

References:

1. Bozynski CC, Evans TJ, Kim DY, et al. Copper toxicosis with hemolysis and hemoglobinuric nephrosis in three adult Boer goats. *J Vet Diagn Invest*. 2009;21:395-400.
2. Cornich J, Angelos J, Puschner B, Miller G, George L. Copper toxicosis in a dairy goat herd. *J Am Vet Med Assoc*. 2007;231:586-589.
3. Gooneratne SR, Howell JM, Cook RD. An ultrastructural and morphometric study of the liver in normal and copper-poisoned sheep. *Am J Pathol*.1980;99:429-480.
4. Gregory CR. Urinary system. In: Latimer KS, Mahaffey EA, Prasse KW, eds. *Duncan and Prasse's Veterinary Laboratory Medicine: Clinical Pathology*. 4th ed. Ames, IA: Blackwell Publishing; 2003:240-241.
5. Hoffman G. Copper-associated liver diseases. *Vet Clin North Am Small Anim Pract*. 2009;39:489-511.
6. Humphries WR, Morrice PC, Mitchell AN. Copper poisoning in Angora goats. *Vet Rec*. 1987;121:231.
7. Maxie MG, Newman SJ. Urinary system. In: Maxie MG, ed. *Jubb, Kennedy and Palmer's Pathology of Domestic Animals*. Vol. 2, 5th ed. Philadelphia, PA: Elsevier Ltd; 2007:467.
8. Simpson DM, Beynon RJ, Robertson DHL, Loughran MJ, Haywood S. Copper-associated liver disease: A proteomics study of copper challenge in a sheep model. *Proteomics*. 2004;4:524-536.

CASE II: G8199 (AFIP 3168020).

Signalment: 8-month-old Shetland pony, equine (*Equus caballus*).

History: The lethargic pony was referred to the equine veterinarian in a poor body condition, showing moderate pallor of mucous membranes, severe dyspnea and diarrhea. Thoracic radiography revealed diffuse clouding shadows of lung parenchyma with a distinct vascular pattern. The pony died two days after admittance to the clinic.

Gross Pathology: The main findings during necropsy included severe pulmonary edema with multifocal hemorrhage and multifocal thrombosis, moderate to severe disseminated granulomatous pneumonia in all lobes as well as granulomatous lymphadenitis of tracheobronchial lymph nodes. Moreover, moderate chronic verminous endoarteritis of the cranial mesenteric artery with intravascular presence of numerous nematodes consistent with *Strongylus vulgaris* was present. The ileum and large intestine contained numerous nematodes consistent with *Strongylidae* spp. and multifocally revealed moderate chronic ulcerative ileitis and typhlocolitis with multiple firm transmural ulcers of 2-3 cm in diameter, partly constricting the lumen, with hemorrhagic margins as well as multifocal subserosal hemorrhagic plaques (consistent with *hemomelasma ilei*). Most mesenteric lymph nodes were moderately enlarged and firm with an irregular surface (granulomatous lymphadenitis). Liver and kidneys were diffusely moderately swollen, pale and soft, with sporadic small firm white granulomatous foci.

Histopathologic Description: Lung: Expanding and replacing approximately 45% of the normal lung architecture are multiple discrete up to 6 mm in diameter foci with marked central karyorrhectic debris (necrosis), which are sometimes accompanied by intense eosinophilic material (Splendore-Hoeppli phenomenon) and surrounded by numerous degenerate neutrophils, macrophages and fewer lymphocytes and plasma cells. Often within necrotic centers few to large numbers of fungal hyphae of 3-6 µm width are present and are characterized by regular septation, thin, parallel walls and dichotomous, progressive acute angle branching.

Multifocal to coalescing alveolar lumina are expanded by homogeneous eosinophilic material (edema), fibrillar eosinophilic material (fibrin) or abundant extravasated erythrocytes (hemorrhage) in varying composition, discontinued by multifocal areas of alveolar distention and ruptured alveolar septa (emphysema). Overall, alveolar septa are slightly thickened due to multifocal to coalescing moderate engorgement of erythrocytes (conjestion) and/or mild mixed inflammatory cell infiltrates with dominance of neutrophils accompanied by multifocal hyperplasia of type II pneumocytes and a moderate increase of alveolar macrophages (alveolar histiocytosis).

Several small, medium-sized or large arterial and venous blood vessels contain thrombi of different size and extension composed of homogeneous (serous) to fibrillar (fibrinous) eosinophilic material, erythrocytes, necrotic debris, degenerate neutrophils, occasionally admixed with the fungal hyphae described above, accompanied by moderate to marked infiltration of vessel walls by fibrinous to necrotic debris, degenerate neutrophils and sporadically by fungal hyphae. Multifocally, but not present in all slides, there is segmental to circumferential necrosis of bronchial/ bronchiolar walls with sloughed epithelial cells, mixed inflammatory cells, erythrocytes, fibrin and necrotic debris within the lumina in varying composition and sometimes admixed with the fungal hyphae described above. Subpleural, interlobar, perivascular, as well as peribronchial/ peribronchiolar interstitial connective tissue is moderately separated by clear space or homogeneous eosinophilic material (edema) with few mixed inflammatory cell infiltrates.

Contributor's Morphologic Diagnosis: 1. Lung: Pneumonia, severe, multifocally extensive, acute to subacute, necrosuppurative to pyogranulomatous with intralesional hyphae consistent with *Aspergillus* spp. and bronchitis/ bronchiolitis (not present in all slides), moderate to severe, multifocal, acute, necrosuppurative.
2. Lung: Vasculitis, severe, multifocal, acute, fibrino-necrotizing with intramural hyphae consistent with *Aspergillus* spp., thrombosis, alveolar and interstitial edema as well as pulmonary hemorrhage.

Contributor's Comment: The genus *Aspergillus* encompasses more than 200 species of which only approximately 19 cause disease in humans.[1] Aspergilli reproduce asexually by forming conidia-bearing multicellular structures ('conidiophores') which release millions of uninucleate cells 'conidia' into the air that are easily dispersed by the wind and have a diameter small enough (2.5 to 3.5 µm) to reach peripheral airways.[1,25] *Aspergillus* conidia occur in soil, air, water and greatest numbers are found in hay and straw enriched with leaf and grass compost. They are considered to be the main vehicle for infective transmission, and when they get the chance to germinate inside the body producing branched septate hyphae that invade tissues, different forms of aspergillosis can develop.[1,25]

Aspergillosis refers to a variety of diseases caused by several species of *Aspergillus*, which are relatively uncommon in humans and mammals but represent a major cause of mortality in birds. The diseases vary in severity and clinical cause, depending on the species and organs affected as well as the immunocompetence of the host. Members of the *A. fumigatus* group cause most cases of aspergillosis.[9,23] However, several other *Aspergillus* species, particularly *A. flavus*, *A. terreus*, *A. nidulans* and *A. niger* have also been described as causative agents.[7,9,17,26]

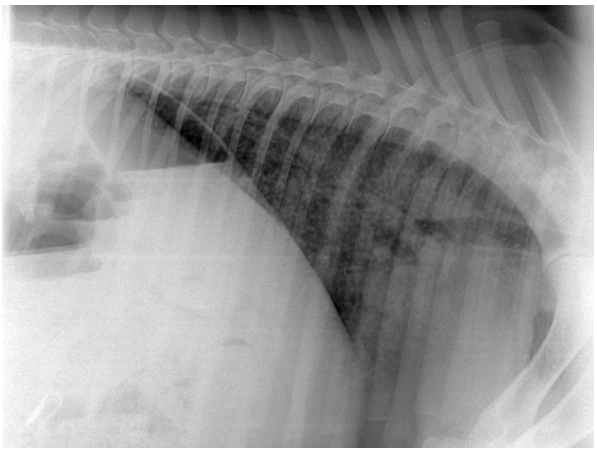

2-1 .Lung, horse. Thoracic radiographs reveal diffuse clouding shadows of lung parenchyma with a distinct vascular pattern. Photograph courtesy of German Primate Center, www.dpz.eu.

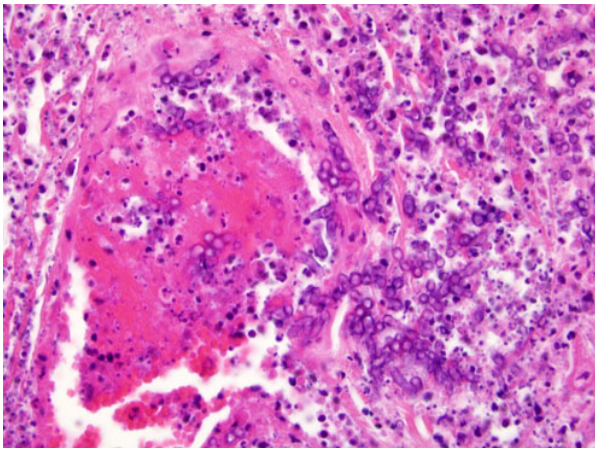

2-2. Lung, horse. Multifocally there is necrotizing vasculitis with many angiocentric fungal hyphae. (HE 400X)

In horses, equine guttural pouch mycosis is the predominant form of aspergillosis and is considered a rare, life-threatening opportunistic infection, with *A. fumigatus* being most frequently isolated. There is no breed or gender predisposition and the pathogenesis remains nearly unknown. However, predisposing factors might be soft tissue trauma and environmental conditions, such as poor ventilation, high humidity and warm temperatures that encourage conidial germination. In the majority of cases, the dorsomedial aspect of the guttural pouch is affected, showing necro-hemorrhagic to fibrinous inflammation accompanied by angioinvasion, erosion of cranial nerves and tissue necrosis as common sequelae.[17,23]

Pulmonary or invasive aspergillosis is very uncommon in horses and usually comprises hematogenous spread of fungal hyphae. Typical lesions are multifocal embolic pneumonia, often centered on pulmonary vessels, and include neutrophilic and fibrinous exudate in alveoli, hemorrhage, necrosis, and leukocytoclastic vasculitis with resultant thrombosis and infarction,[8] all of which is also seen in this

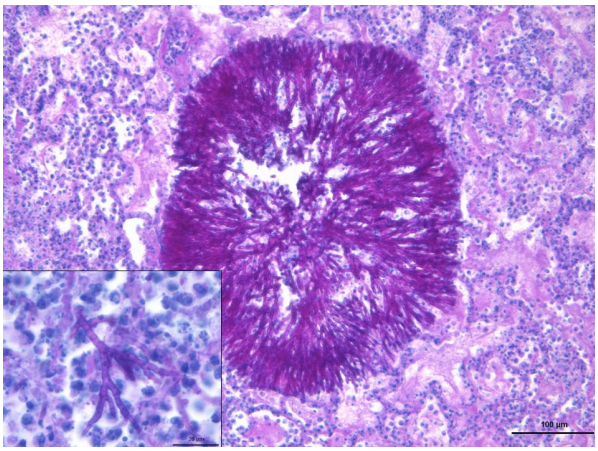

2-3. Lung, equine. Many fungal hyphae are present with regular septation, thin, parallel walls and dichotomous, progressive acute angle branching. Photograph courtesy of German Primate Center, www.dpz.eu.

case. More chronic lesions can appear as classic granulomas with central necrotic cores. Although hyphae are often present within the lesions, and may be readily seen with hematoxylin and eosin, special stains, such as periodic acid-Schiff (PAS) reaction or Gomori-methenamine silver (GMS) stain, are helpful to visualize their characteristic morphology. In this case we used the PAS reaction to show the characteristic frequent dichotomous branching and hyphal morphology, which is described in Table 1.

Important predisposing factors for the development of invasive aspergillosis in horses seem to be prolonged antibiotic, glucocorticoid or NSAID administration;[13,18,22] immunosuppression associated with leukaemia;[5] neutropenia;[4] pituitary adenoma;[6] heavy exposure to conidia from mouldy environmental material;[7,13] or prolonged and intense periods of stress.[14,24] In addition, a compromised intestinal mucosa serving as the site of entry, which also has been found in this case in the form of an ulcerative enterocolitis, is considered to be an important predisposing condition for hematogeneous spread of fungi resulting in invasive, systemic aspergillosis, often with predominant pulmonary manifestation.[4,8,13,18,22,24,26] Furthermore, mixed invasive fungal infections, such as concomitant aspergillosis and mucormycosis, have been reported in horses[7,24] and calves.[10]

Besides horses, dogs, cows and dolphins are also particularly susceptible to certain forms of aspergillosis. In dogs, canine sinonasal aspergillosis predominantly affects mesocephalic or dolichocephalic breeds, where *A. fumigatus* is most commonly isolated; *A. terreus* predominates in cases involving German shepherd dogs. Predisposing factors are unknown, and pathology is concentrated on the nasal cavity and paranasal sinuses. Sometimes the cribriform plate is invaded and CNS infection may be established.[23] Bovine mycotic abortion due to *Aspergillus* infection occurs worldwide and sporadically. Typically second or third trimester abortion is observed, with highest incidence during winter when gravid cows are indoors and fed with heavily

Table 1: Morphological characteristics, pathogenicity factors and manifestations of common mycotic diseases caused by mycelial fungi

Species	Hyphal Morphology	Septae/ Branching	Pathogenicity Factors/ Toxins	Manifestation
Aspergillus spp.[1,3,9]	hyphae width 3-6 µm; thin parallel walls (conidia not seen in tissue)	regularly septate; dichotomous progressive 45º branching	adhesins, antioxidants (e.g. melanin), various proteases; mycotoxins (e.g. gliotoxin, aflatoxin, ochratoxin)	sinonasal, placental, pulmonary, angioinvasion, systemic
Fusarium spp.[9]	hyaline hyphae width 3-7 µm (similar to *Aspergillus* spp.)	septate, frequent characteristic 90º branching (sometimes 45º)	mainly plant pathogenic; mycotoxins (e.g. fumonisin B_1, fusaric acid)	rare mycosis; pulmonary, angioinvasion, dermatitis, keratitis
Candida spp.[9,21]	round or oval hyaline budding blastospores 3-5 µm; hyaline hyphae and pseudohyphae (excl. *C. glabrata*)	septate, irregular branching	adhesins, formation of biofilm (oxylipin farnesol), different aspartate proteinases, "phenotypic switching"; no toxins described	mucocutaneous (e.g. vaginal, oral), cutaneous, GIT, systemic (e.g. pulmonary, renal), rarely angioinvasion
Zygomycetes *(Mucor* spp. *Rhizopus* spp. *Basidiobolus* spp. *Mortierella* spp.*)*[9,16]	broad hyphae (up to 25 µm width and 200 µm length), non-parallel, thin walls (often folded, collapsed or twisted); slightly visualized by PAS and GMS stain	infrequently septate; non-dichotomous, irregular branching; frequently bizarre forms, focal bulbous dilatations	free iron & acidosis play central role; adherins (subendothelial matrix), possibly secreted toxins or proteases; endo-symbiotic endotoxin producing bacteria (Genus *Burkholderia*)	cutaneous, subcutaneous, angioinvasion, systemic (with or without pulmonary focus, rhinocerebral
Pseudallescheria boydii[12,20]	narrow hyphae, parallel walls (similar to *Aspergillus* spp.)	septate, highly branching at less acute angles, intertwined	Glucan, proteases, metalloproteases, superoxide dismutases (phosphatases)	cutaneous, subcutaneous, respiratory tract/ pulmonary, angioinvasion

contaminated hay or silage. *Aspergillus fumigatus* accounts for the majority of cases and suggested routes of infection are ingestion or inhalation. The pathological hallmark is placentitis with leathery appearance of the placenta (almost pathognomonic), intercotyledonary thickening and hypertrophy of cotyledons.[23] Cetacean mycotic pneumonia is the predominant form of aspergillosis in free ranging dolphins and is considered to be a regional disease. Predisposing factors are suspected to be a combination of viral and environmental factors.[23]

In contrast to the rather low incidence of aspergillosis in mammals, avian aspergillosis is a major cause of morbidity and mortality in birds and affects animals of all ages, whether immunocompetent or immunosuppressed in captive or free-ranging environments; captive penguins seem particularly susceptible.[2] In approximately 95% of the cases *A. fumigatus* is isolated, and *A. flavus* occurs second most frequently. Inhalation is the route of infection, with initial colonization in the lower respiratory tract. Susceptibility may be attributed to differences in innate and acquired immunity compared to mammals, as well as predisposing anatomic characteristics, such as lack of an epiglottis and diaphragm (inability to produce strong cough), limited distribution of pseudostratified ciliated respiratory epithelium, lack of surface macrophages, and different heterophilic killing mechanisms (using cationic proteins, hydrolases and lysosymes rather than myeloperoxidases and oxidative mechanisms). A unique feature of avian aspergillosis is the presence of reproductive phases in tissue.[23]

The most common forms of human aspergillosis is pulmonic and may be divided into (1) non-pathogenic saprophytic colonization, including noninvasive pulmonary aspergillomas/mycetomas or invasion of necrotic tissue; (2) hypersensitivity-induced aspergillosis, including *Aspergillus*-asthma, allergic bronchopulmonary aspergillosis, hypersensitivity pneumonitis (or extrinsic allergic alveolitis), bronchocentric granulomatosis and chronic eosinophilic pneumonia; and (3) invasive disease, including pseudomembranous tracheobronchitis, acute bronchopneumonia, angioinvasive aspergillosis, chronic necrotizing aspergillosis and invasive pleural disease.[1,25]

In general, human patients with pre-existing structural lung disease, atopy, occupational exposure or impaired immunity are susceptible.[1] Therefore, saprophytic colonization is increased in patients with advanced stages of chronic obstructive pulmonary disease (COPD), chronic asthma requiring long-term steroid therapy, primary ciliary dyskinesia syndrome and cystic fibrosis.[25] *Aspergillus* spp. also have a significant potential to act as powerful allergens; thus, hypersensitivity-induced *Aspergillus*-asthma in lower airways is caused by Type I anaphylactic reaction in atopic individuals upon exposure to *Aspergillus* conidia or hyphae. Allergic bronchopulmonary aspergillosis (ABPA) is caused by hypersensitivity to colonized *Aspergillus* spp., resembling a complication of asthma, and is immunologically characterized by Type I, Type III and Type IV hypersensitivity reactions. Hypersensitivity pneumonitis (or extrinsic allergic alveolitis) occurs primarily in non-atopic individuals. It is an inflammatory interstitial lung disease possibly resulting from Type III and Type IV hypersensitivity reactions following persistent or intense exposure to *Aspergillus* conidia with acute lung injury via complement-dependent neutrophils (due to Type III reaction) or chronic stages such as granuloma formation, interstitial lung fibrosis and distal bronchiolitis obliterans (due to Type IV reaction).[25]

In human patients with altered local or systemic immune defense mechanisms the most severe and life-threatening invasive disease may develop.[1,25] Invasive pulmonary aspergillosis ranks second to candidiasis in causing systemic fungal infections in immunocompromised human patients, and in most cases lung manifestation occurs with common hematogenous spread to other organs, especially the CNS. Hence, immunosuppression is considered to be the major condition with prolonged neutropenia as the leading cause.[25]

In healthy, immunocompetent individuals, various elements of the pulmonary innate immune system are involved in recognition and elimination of inhaled *Aspergillus* conidia, thereby preventing colonization of the respiratory system. Ciliated and mucus secreting epithelial cells perform effective mucociliary clearance that is important for entrapment and elimination of inhaled conidia. Surfactant, mainly produced by Type II pneumocytes and Clara cells, has been implicated in antimicrobial activity, with surfactant proteins A and D serving as collectins. Alveolar macrophages represent first line phagocytic defense by intracellular killing of swollen spores and prevention from germination. Recruited neutrophils play an essential role by extracellular (degranulation) as well as intracellular (phagocytosis) elimination of Aspergilli. Dectin-1, expressed by macrophages, neutrophils and dendritic cells, is an important receptor of innate antifungal defense, being essential for spore recognition and phagocytosis as well as production of oxygenated free radicals (fungicidal activity). Additionally, certain Toll-like receptors (TLR) have been found to play a predominant role in the recognition of *A. fumigatus* (TLR2: recognition of spores; TLR4: recognition of spores and hyphae).[3]

On the other hand, several pathogenicity factors were found in different *Aspergillus* spp. to overcome certain host defense mechanisms, such as endotoxins that inhibit epithelial ciliary activity, as well as a variety of proteases (including elastase, collagenase and trypsin) that damage epithelial cells and thus impair effective mucociliary clearance.[1,3] Further, *A. fumigatus* produces a phospholipid capable of decreasing the binding of complement factor C3b to its surface, resulting in disturbed complement activation.[3] Also other fungal proteins of *A. fumigatus* are probably related to virulence by promoting mycelial growth into lung parenchyma or structural alterations of conidia that are resistant to host defense mechanisms.[1]

Moreover, it is likely that *Aspergillus* mycotoxins can work as virulence factors due to direct cytotoxic effects. In vitro studies revealed that aflatoxin (produced by *A. fumigatus*) suppresses the function of macrophages, and ochratoxin (produced by *A. ochraceus*) is cytotoxic to lymphocytes and suppresses lymphocytic, monocytic and granulocytic activity. Other possible immunosuppressive mycotoxins, gliotoxin, fumagillin, fumigacin, fumitremorgin A and Asp-hemolysin are discussed, while different mycotoxins together may have synergistic effects. However, further *in vivo* studies are needed for confirmation of direct relation to *Aspergillus* pathogenesis.[15]

Beyond that, melanin pigment, mannitol, catalases and superoxide dismutases are suggested as antioxidant defenses produced by *Aspergillus*.[11,27] Although it seems that certain antioxidant molecules produced by *A. fumigatus* do not directly inhibit the oxidizing activity of phagocytes, inhibition of reactive oxygen species production by macrophages (e.g. during corticosteroid treatment) abolishes their ability to kill the spores while phagocytosis continues so that conidia can germinate and proliferate intracellularly.[3] However, since pulmonary macrophages and neutrophils constitute a crucial part of first line innate host defense, neutropenia and long-term corticosteroid treatment are generally regarded as major risk factors for the pathogenesis of invasive aspergillosis.[1,3,11,19]

AFIP Diagnosis: Lung: Pneumonia, necrohemorrhagic, multifocal to coalescing, severe, with necrotizing vasculitis; intra-alveolar edema and fibrin, and myriad angiocentric fungal hyphae, etiology consistent with *Aspergillus* spp.

Conference Comment: The contributor provides an excellent summary of the comparative pathology and pathogenesis of aspergillosis. Like the contributor, participants noted the close association of fungal hyphae with blood vessels and the presence of angioinvasion, and thus favored the use of the term "angiocentric" in the histomorphologic diagnosis.

Readers are encouraged to review WSC 2010-2011 Conference 5, Case 1 for a review of *Seedosporium apiospermum* (*Pseudallescheria boydii*) keratitis in a flock of chickens.

Contributor: German Primate Center, Kellnerweg 4, 37077 Göttingen, Germany.
www.dpz.eu

References:

1. Al-Alawi A, Ryan CF, Flint JD, Müller NL. *Aspergillus*-related lung disease. *Can Respir J*. 2005;12:377-387.
2. Alvarez-Perez S, Mateos A, Dominguez L, Martinez-Nevado E, Blanco JL, Garcia ME. Polyclonal *Aspergillus fumigatus* infection in captive penguins. *Vet Microbiol.* 2010;144(3-4):444-449.
3. Balloy V, Chignard M. The innate immune response to *Aspergillus fumigatus*. *Microb Infect*. 2009;11:919-927.
4. Breshears MA, Holbrook TC, Haak CE, York PA. Pulmonary aspergillosis and ischemic distal limb necrosis associated with enteric salmonellosis in a foal. *Vet Pathol*. 2007;44:215-217.
5. Buechner-Maxwell V, Zhang C, Robertson J, et al. Intravascular leukostasis and systemic aspergillosis in a horse with subleukaemic acute myelomonocytic leukemia. *J Vet Int Med*. 1994;8:258-263.
6. Carrasco L, Mendez A, Jensen HE. Chronic bronchopulmonary aspergillosis in a horse with cushing's syndrome. *Mycoses*. 1996;39:443-447.
7. Carrasco L, Tarrades MC, Gòmez-Villamandos JC, Luque I, Arenas A, Méndez A. Equine pulmonary mycosis due to *Aspergillus niger* and *Rhizopus stolonifer*. *J Comp Pathol*. 1997;117:191-199.
8. Caswell JL, Williams KJ. The respiratory system. In: McGavin MD, Zachary JF, eds. *Pathologic Basis of Veterinary Disease*. Vol 2, 4th ed. St. Louis, MO: Elsevier; 2007:634-635.
9. Chandler FW, Kaplan W, Ajello L. In: Carruthers GB, ed. *A Colour Atlas and Textbook of the Histopathology of Mycotic Diseases*. London, England: Wolfe Medical Publications; 1980:34-38, 42-46, 101-115, 122-127.
10. Chihaya Y, Furusawa Y, Okada H, Matsukawa K, Matsui Y. Pathological studies on systemic mycoses in calves. *J Vet Med Sci*. 1991;53:1051-1058.
11. Dagenais TRT, Keller NP. Pathogenesis of *Aspergillus fumigatus* in invasive aspergillosis. *Clin Microbiol Rev*. 2009;22:447-465.
12. Davis PR, Meyer GA, Hanson RR, Stringfellow JS. *Pseudallescheria boydii* infection of the nasal cavity of a horse. *J Am Vet Med Assoc*. 2000;217:707-709.
13. Guillot J, Collobert C, Jensen HE, Huerre M, Chermette R. Two cases of equine mucormycosis caused by *Absidia corymbifera*. *Equine Vet J*. 2000;32:453-456.
14. Johnson PJ, Moore LA, Mrad DR, Turk JR, Wilson DA. Sudden death of two horses associated with pulmonary aspergillosis. *Vet Rec*. 1999;145:16-20.
15. Kamei K, Watanabe A. *Aspergillus* mycotoxins and their effect on the host. *Med Mycol*. 2005;43(Suppl):95-99.
16. Kontoyiannis DP, Lewis RE. Invasive zygomycosis: Update on pathogenesis, clinical manifestations, and management. *Infect Dis Clin North Am*. 2006;20:581-607.
17. Ludwig A, Gatineau S, Reynaud MC, Cadoré JL, Bourdoiseau G. Fungal isolation and identification in 21 cases of guttural pouch mycosis in horses (1998 – 2002). *Vet J*. 2005;169:457-461.
18. Pace LW, Wirth NR, Foss RR, Fales WH. Endocarditis and pulmonary aspergillosis in a horse. *J Vet Diagn Invest.* 1994;6:504-506.
19. Park SJ, Mehrad, B. Innate immunity to *Aspergillus* species. *Clin Microbiol Rev*. 2009;22:535-551.
20. Santos AL, Bittencourt VC, Pinto MR, Silva BA, Barreto-Bergter E. Biochemical characterization of potential virulence markers in the human fungal pathogen *Pseudallescheria boydii*. *Med Mycol*. 2009;47:375-386.

21. Schulze J, Sonnenborn U. Yeasts in the gut: From commensals to infectious agents. *Dtsch Arztebl Int*. 2009;106:837-842.
22. Slocombe RF, Slauson DO. Invasive pulmonary aspergillosis of horses: An association with acute enteritis. *Vet Pathol*. 1988;25:277-281.
23. Tell LA. Aspergillosis in mammals and birds: Impact on veterinary medicine. *Med Mycol*. 2005;43(Suppl):71-73.
24. Thirion-Delalande C, Guillot J, Jensen HE, Crespeau FL, Bernex F. Disseminated acute concomitant aspergillosis and mucormycosis in a pony. *J Vet Med*. 2005;52:121-124.
25. Tomee JFC, Van der Werf TS. Pulmonary aspergillosis. *Neth J Med*. 2001;59:244-258.
26. Tunev SS, Ehrhart EJ, Jensen HE, Foreman JH, Richter RA, Messick JB. Necrotizing mycotic vasculitis with cerebral infarction caused by *Aspergillus niger* in a horse with acute typhlocolitis. *Vet Pathol*. 1999;36:347-351.
27. Willger S, Grahl N, Cramer JRR. *Aspergillus fumigatus* metabolism: Clues to mechanisms of *in vivo* fungal growth and virulence. *Med Mycol*. 2009;47(Suppl):72-79.

CASE III: D09-30400 (AFIP 3166595).

Signalment: Adult female warmblood equine (*Equus caballus*).

History: This mare presented to the referring veterinarian for increased respiratory noise. On physical examination a mass was noted in the area of the left arytenoid cartilage. This mass was surgically removed and sent for histopathologic examination. This mare had been imported to Canada from Argentina in apparently good health several years prior to examination for this problem.

Gross Pathology: The received surgical biopsy is a 2.5 cm x 1.5 cm wide, white with brown-black areas, cerebriform mass with a small elliptical base.

Laboratory Results: Polymerase chain reaction (PCR) for the 18S rRNA gene sequence of *Rhinosporidium seeberi* was performed using the formalin fixed, paraffin embedded biopsy material. The resulting amplified DNA was sequenced and the nucleotide sequence was confirmed to be identical to samples of *Rhinosporidium seeberi* present within GENBANK.

Histopathologic Description: Larynx (per contributor): From a cartilaginous base numerous papillary projections of markedly hyperplastic epithelium extend with dramatic down growths into a fibrovascular stalk. Variably sized clusters of glandular tissue are noted within focal regions at the periphery of the biopsy, occasionally exhibiting dilation with small amounts of basophilic granular material within the lumen. Multifocally throughout the submucosa are numerous variably sized, often exceeding 100 μm in diameter, spherical structures (sporangia) with a variably prominent cuticle-like lining and filled with abundant variably sized and colored endospores. Few of the sporangia are ruptured and associated with a marked neutrophilic inflammatory response. Within the fibrous tissue and dissecting between sporangia there is a marked inflammatory infiltrate composed of plasma cells, lymphocytes and fewer macrophages. Although few, sporangia are noted within 1 mm of the lateral margins. No sporangia are within the cartilage of the deep margin.

Contributor's Morphologic Diagnosis: Larynx: Laryngitis, lymphoplasmacytic, histiocytic, severe, multifocal to coalescing, chronic, with marked epithelial hyperplasia, and intralesional sporangia consistent with *Rhinosporidium seeberi.*

Contributor's Comment: Once thought to be a fungus, *Rhinosporidium seeberi* is an unusual organism now included in the class *Mesomycetozoea*, where it is the only member known to cause disease in mammals and birds.[7] Other members of this class are known to cause disease in aquatic animals, primarily fish.[7] Most commonly reported as a pathogen in tropical regions of the world, particularly India, Sri Lanka and Argentina, it has been sporadically reported in numerous locations, including Europe and North America.[6] Typically, these cases are thought to have been acquired in endemic areas and the animals then brought to non-endemic countries, as exemplified in a group of four polo ponies in the United Kingdom thought to have been infected in their native Argentina and not diagnosed until sometime after arrival into the United Kingdom.[5] However, both human and canine cases apparently acquired within Canada have been reported.[2,5]

Most lesions appear as pale to white, single or multiple, polypoid masses; these are most typically found in the nasal cavity.[2] Cases of laryngeal rhinosporidiosis are seemingly

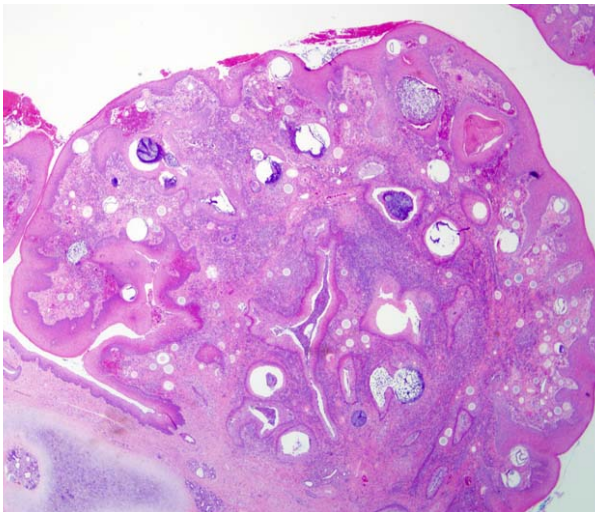

3-1. Larynx, equine. Polypoid masses project into the laryngeal lumen composed of hyperplastic mucosal epithelium, fibrovascular stroma, inflammatory cells, and many sporangia. (HE 20X)

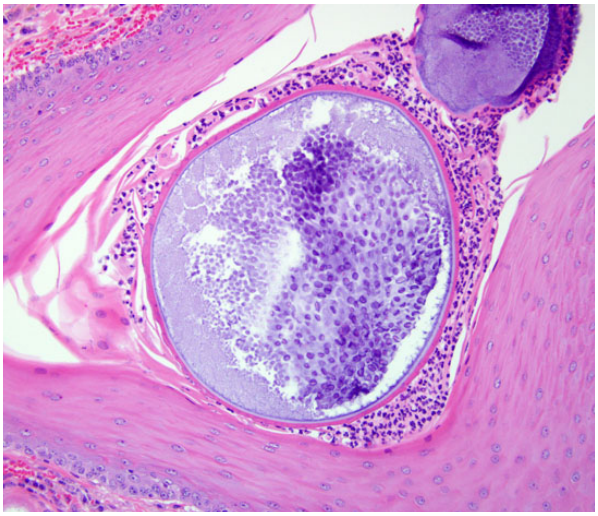

3-2. Larynx, equine. Variably-sized sporangia have a prominent eosinophilic wall lined by a basophilic inner membrane and are filled with numerous endospores; sporangia are occasionally surrounded by inflammatory cells. (HE 200X)

extremely rare, although one case has been reported in a Belgian Warmblood.[8] Affected horses may present with epistaxis due to bleeding of traumatized nasal polyps, increased respiratory noise, or they may be asymptomatic.

It is presumed that the infection is most commonly acquired through exposure to contaminated water. The organism is thought to enter the body through preexisting damage to the normal mucosal barriers. Once in the body, endospores are released from the sporangia where they enlarge and mature to become juvenile, intermediate and finally mature sporangia filled with new endospores which are then available to repeat the cycle.[7]

AFIP Diagnosis: Squamous mucosa with supporting cartilage, larynx (per contributor): Laryngitis, lymphoplasmacytic and neutrophilic, proliferative and polypoid, multifocal, moderate, with fibrosis and numerous intralesional sporangia and endospores, etiology consistent with *Rhinsporidium seeberi*.

Conference Comment: As noted by the contributor, conference participants identified neutrophilic inflammation primarily in association with ruptured sporangia. The aspect of this case that makes it somewhat challenging is tissue identification; and most participants identified the specimen as nasal mucosa. Given the histomorphologic features of the tissue and lesion, and combined with the fact that nasal rhinosporidiosis is much more common and reports of laryngeal infection are exceedingly rare, nasal cavity is a reasonable conclusion as the source of the affected tissue.

Based on the histomorphology of the organism, the etiologic differential diagnosis includes *Coccidioides immitis* and *Emmonsia parva* or *E.crescens* (formerly *Chrysosporium* spp.). The organisms of *C. immitis* are typically smaller, with spherules ranging from 20-200 μm in diameter, and endospores measuring 2-5 μm and more uniform in size and shape throughout the spherule. *Emmonsia* spp. form adiaspores in tissue that are characterized as large, spherical, uninucleate conidia that measure 10-20 μm in diameter for *E. parva* and up to 300 μm for *E. crescens*. *Emmonsia* spp. have a thick wall which is PAS-positive and helps distinguish them from *C. immitis*.[1]

Contributor: Department of Veterinary Pathology, Western College of Veterinary Medicine, 52 Campus Dr., Saskatoon, Saskatchewan, Canada, S7N 5B4

References:

1. Caswell JL, Williams KJ. Respiratory system. In: Maxie MG, ed. *Jubb, Kennedy and Palmer's Pathology of Domestic Animals*. Vol. 2, 5th ed. Philadelphia, PA: Elsevier Ltd; 2007:641, 644-645.
2. Harissi-Dagher M, Robillard N, Corriveau C, Mabon M, Allaire GS. Histopathologically confirmed ocular rhinosporidiosis in two Canadians. *Can J Ophthalmol*. 2006;41:226-229.
3. Hill SA, Sharkey LC, Hardy RM, Wilke VL, Smith MA, Anderson GM. Nasal rhinosporidiosis in two dogs native to the upper Mississippi river valley region. *J Am Anim Hosp Assoc*. 2010;46:127-131.
4. Hoff B, Hall DA. Rhinosporidiosis in a dog. *Can Vet J*. 1986;27:231-232.
5. Leeming G, Smith KC, Bestbier ME, Barrelet A, Kipar A. Equine rhinosporidiosis in United Kingdom. *Emerg Infect Dis*. 2007;13:1377-1379.
6. Lupi O, Tyring SK, McGinnis MR. Tropical dermatology: Fungal tropical diseases. *J Am Acad Dermatol*. 2005;53:931-951, quiz.
7. Mendoza L, Taylor JW, Ajello L. The class mesomycetozoea: A heterogeneous group of microorganisms at the animal-fungal boundary. *Annu Rev Microbiol*. 2002;56:315-344.
8. Nollet H, Vercauteren G, Martens A, et al. Laryngeal rhinosporidiosis in a Belgian warmblood horse. *Zoonoses Public Health*. 2008;55:274-278.

CASE IV: S1001225 (AFIP 3167243).

Signalment: 7-day old female Quarter horse, equine (*Equus caballus*).

History: Acute onset of diarrhea, colic and death in less than 24 hours from the beginning of the clinical signs.

Gross Pathology: The carcass was in a very good state of postmortem preservation and the tail and perineal region were soiled with abundant yellow, dried feces. Diffusely, the jejunum and ileum were thickened (~3-4 mm) and had dark red, edematous mucosa with multifocal pseudomembrane formation, which was more predominant in the ileum and terminal jejunum. The serosa of the jejunum and ileum had multifocal petechiation and a few, focal, larger (up to 1 cm in diameter) subserosal ecchymoses.

The small intestinal content was composed of scant, red to brown fluid. The large colon had a focally extensive area (~50 cm long and involving the left ventral portion, the pelvic flexure and left dorsal portion of the colon) with multifocal to coalescing areas of necrosis and pseudomembrane formation. The cecum had a focal, small (~3 cm in diameter) area of dark red mucosa with mural edema adjacent to the ileocecal valve. The colonic and cecal content was composed of a moderate amount of light brown fluid.

Laboratory Results: The small intestine and colon contents were positive by the ELISA method for *Clostridium perfringens* toxins alpha and beta and *Clostridium difficile* toxins A/B. *Clostridium perfringens* type C (CPE and beta 2 negative) was isolated from the small intestine and colon and *C. difficile* was isolated only from the colon. *Salmonella* PCR and cultures were negative from small intestine.

Histopathologic Description: Jejunum, ileum and colon: There is diffuse, marked, coagulative necrosis of the mucosa, characterized by severe disruption of the architecture with diffuse mucosal hypereosinophilia, loss of the mucosal epithelial lining, attenuation or collapse of the intestinal villi and crypts, and occasional multifocal loss of the mucosa/ submucosal boundaries. On the mucosal surface, admixed with superficial necrotic debris and within the pseudomembrane, there are numerous clusters of bacteria, predominantly thick and short rods. Within the lamina propria and in the submucosa, there is moderate to marked hyperemia and hemorrhage, abundant fibrin and cellular and necrotic debris with very rare neutrophils. There is multifocal vascular thrombosis of small to mid-size caliber blood vessels in the mucosa and submucosa and the submucosal lymphatics are markedly dilated. Within the muscular layer, in one section, there are a few multifocal hemorrhages. The serosa is moderately expanded by clear spaces (edema) and there is mild hemorrhage.

Contributor's Morphologic Diagnosis: Enterocolitis, necrohemorrhagic, acute, diffuse, severe, with pseudomembrane formation, mucosal/submucosal vascular thrombosis, edema and massive numbers of *Clostridia*-like bacilli attached to the mucosal surface.

Contributor's Comment: Equine enteritis and enterocolitis, manifested with diarrhea and colic, are important causes of morbidity and mortality of foals and adult horses. These syndromes have been associated with a variety of etiologies, including *Clostridium* spp., *Salmonella* spp., *Neorickettsia risticii*, *Aeromonas* spp., *Lawsonia intracellularis*, cantharidin toxicity, and larval cyathostomiasis.[15] Although the first reports associating clostridia with enteritis in the foal were published in the 1930's,[13] only in the past few decades have *Clostridium perfringens* (*C. perfringens*) and *Clostridium difficile* (*C. difficile*) been increasingly reported as relevant pathogens involved in cases of enteritis and enterocolitis in horses.[2,3,4,8,12,15,16] *C. perfringens* is classified into five types (A, B, C, D, and E) based on the production of one or more of four so-called

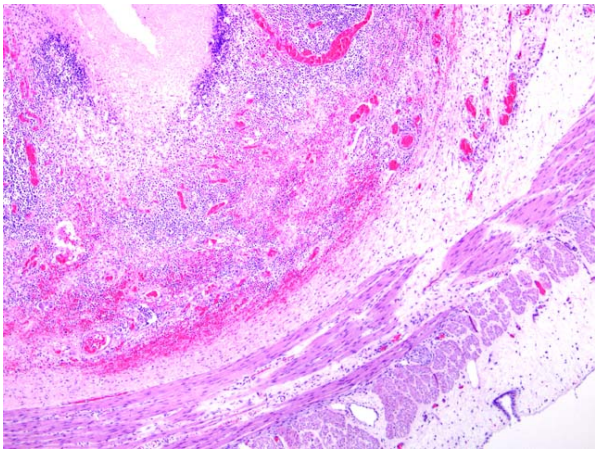

4-1. Ileum, foal, equine. The mucosal epithelium is diffusely necrotic, with hemorrhage and edema in the submucosa, muscularis, and serosa. (HE 40X)

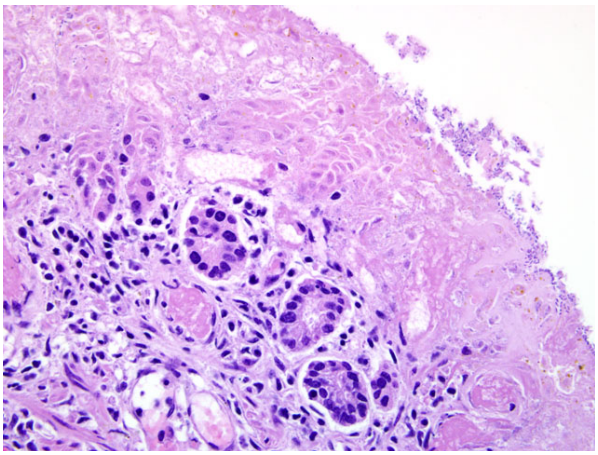

4-2. Ileum, foal, equine. There is coagulative necrosis of the mucosal epithelium, with myriad bacilli lining the surface of necrotic villi. Fibrin thrombi expand some mucosal vessels. (HE 400X; 1000X)

major toxins, namely alpha (CPA), beta (CPB), epsilon (ETX) and iota. Two other major toxins, namely enterotoxin (CPE) and Beta 2 (CPB2), can also be produced by all types of *C. perfringens*, but they are not used in the classification of this microorganism. *C. perfringens* type B and C have been associated with severe necrotizing, hemorrhagic enterocolitis in foals, although type C is considered the most commonly reported clostridial enteric pathogen in foals in North America.[6]

Clostridium perfringens type C produces two major toxins, CPA and CPB. The CPA toxin is a lecithinase, which is considered the main virulence factor in *C. perfringens* type A gas gangrene of humans and animals. However, the contribution of CPA to the virulence of type C isolates is negligible.

The CPB toxin, on the other hand, is a necrotizing toxin that forms pores in the membrane of susceptible cells. This toxin is considered to be responsible for the intestinal necrosis and systemic alterations seen in type C infections of several animal species, including horses. Lethal disease caused by *C. perfringens* type C in many mammalian animal species and humans originates when type C strains proliferate and produce toxins in the intestine.[14] Because CPB is highly susceptible to the action of trypsin, neonatal animals are considered to be particularly susceptible to type C infections due to the low level of intestinal trypsin during the first days of life. Although *C. perfringens* type C causes severe intestinal damage, death in affected animals is thought to primarily result from toxemia following absorption of toxins from the intestine into the circulation.[10,11] Therefore, type C infections are considered to be true enterotoxemias, i.e. diseases produced by toxins generated in the intestine, but that are absorbed into the general circulation and act on organs distant from the gastrointestinal tract. A presumptive diagnosis of *C. perfringens* type C enterotoxemia can be established based on clinical history, i.e. acute onset of diarrhea, colic or sudden death, and gross and microscopic lesions. This presumptive diagnosis can be reinforced by isolation of large numbers of *C. perfringens* type C from the small and/or large intestine, because this microorganism is rarely isolated from the gut of normal horses, as opposed to *C. perfringens* type A which is frequently isolated from clinically normal horses (contributor's unpublished observations). However, failure to isolate *C. perfringens* type C from the gut does not preclude a diagnosis of type C enterotoxemia because confirmation of a diagnosis of type C infection should be based on detection of CPB in intestinal contents.[11] Demonstration of CPB in the gut content can be achieved by *in vivo* assays in mouse and guinea pig (less common nowadays) or *in vitro* methods based on enzyme immunoassays, such as ELISA.

To date, the only published reports of enterotoxemia by *C. perfringens* type C in horses confirmed by toxin detection are limited to sporadic cases.[3,5,7,8,9] On the other hand, a few reports have been published that describe a larger number of animals in which a diagnosis was based on pathology and isolation of *C. perfringens* type C but without toxin detection.[4,16] To our best knowledge, there is no published information of the pathological findings of *C. perfringens* type C enterotoxemia based on a large number of cases with a diagnosis confirmed by CPB detection in intestinal contents.

Currently, we are working on a manuscript to be submitted for publication in which the lesions of the intestinal tract in

	Clostridium perfringens				
	Type A	Type B	Type C	Type D	Type E
Piglet	White scours		Hemorrhagic enteritis		
Cow/calf	Acute intravascular hemolysis (calf); Hemorrhagic bowel syndrome (dairy cattle)	Calf: similar to lamb	Struck-like syndrome in feedlot cattle; Hemorrhagic enteritis (calf)	Enterotoxemia (calf)	Hemorrhagic enteritis (calf)
Sheep/lamb	Acute intravascular hemolysis (lamb)	Lamb dysentery	Struck (adults); Hemorrhagic enteritis (lamb)	Enterotoxemia (pulpy kidney, overeating disease)	
Horse/foal	Necrotizing enteritis (foal)		Hemorrhagic necrotizing enteritis (foal)		
Dog	Hemorrhagic canine gastroenteritis				

several horses with *Clostridium perfringens* type C enterotoxemia confirmed by the detection of the beta toxin in the intestinal contents are characterized. We believe that the lesions present in the submitted slides are very characteristic of, but not diagnostic for, equine type C enterotoxemia.

AFIP Diagnosis: Small intestine; and colon (per contributor): Enterocolitis, fibrinonecrotic, diffuse, severe, with transmural edema, hemorrhage, fibrin thrombi, and myriad surface bacilli.

Conference Comment: As mentioned by the contributor, *Clostridium perfringens* types A-E are distinguished from one another based on their exotoxin profiles. A summary of the toxins produced by each type follows:[1]

- *C. perfringens* type A: α
- *C. perfringens* type B: α, β, ε
- *C. perfringens* type C: α, β
- *C. perfringens* type D: α, ε
- *C. perfringens* type E: α, ι

Each type produces different syndromes based on the species of animal affected.[1]

Contributor: CAHFS, 105 W. Central Ave, San Bernardino, CA 92408.
http://www.cahfs.ucdavis.edu/

References:

1. Brown CC, Baker DC, Barker IK. Alimentary system. In: Maxie MG, ed. *Jubb, Kennedy and Palmer's Pathology of Domestic Animals*. Vol. 2, 5th ed. Philadelphia, PA: Elsevier Ltd; 2007:213-221.
2. Bueschel D, Walker R, Woods L, et al. Enterotoxigenic *Clostridium perfringens* type A necrotic enteritis in a foal. *J Am Vet Med Assoc*. 1998;213(9):1305-1307.
3. Drolet R, Higgins R, Cécyre A. Necrohemorrhagic enterocolitis caused by *Clostridium perfringens* type C in a foal. *Can Vet J*. 1990;31:449-450.
4. East L, Savage C, Traub-Dargatz J, et al. Enterocolitis associated with *Clostridium perfringens* infection in neonatal foals: 54 cases (1988-1997). *J Am Vet Med Assoc*. 1998;212(11):1751-1756.
5. Howard-Martin M, Morton R, Qualls Jr., C, et al. *Clostridium perfringens* type C enterotoxemia in a newborn foal. *J Am Vet Med Assoc*. 1986;189(5):564-565.
6. Jones R. Clostridial enterocolitis. *Vet Clin of North Amer:Eq Prac*. 2000;16(3):471-485.
7. Niilo L, Chalmers GA. Hemorrhagic enterotoxemia caused by *Clostridium perfringens* type C in a foal. *Can Vet J*. 1982;23:299-301.
8. Pearson E, Hedstrom O, Sonn R, et al. Hemorrhagic enteritis caused by *Clostridium perfringens* type C in a foal. *J Am Vet Med Assoc*. 1986;188(11):1309-1310.
9. Sims L, Tzipori S, Hazard G, et al. Haemorrhagic necrotizing enteritis in foals associated with *Clostridium perfringens*. *Aus Vet J*. 1985;62(6):194-198.
10. Songer JG. Clostridial enteric diseases of domestic animals. *Clin Micro Rev*. 1996;9(2):216-234.
11. Songer J, Uzal F. Clostridial enteric infections in pigs. *J Vet Diag Invest*. 2005;17:528-536.
12. Stubbings D. *Clostridium perfringens* enterotoxemia in two young horses. *Vet Rec*. 1990;127:431.
13. Traub-Dargatz J, Jones R. Clostridia-associated enterocolitis in adult horses and foals. *Vet Clin North Amer:Eq Prac*. 1993;9(2):411-421.
14. Uzal F, Songer J. Diagnosis of *Clostridium perfringens* intestinal infections in sheep and goats. *J Vet Diag Invest*. 2008;20:253-265.
15. Weese J, Staempfli H, Prescott J. Clostridial colitis in adult horses and foals: A prospective study. *AAEP Proceedings*. 2001;47:400-402.
16. Wernery U, Nothelfer H, Böhnel H, et al. Equine intestinal clostridiosis in a group of polo ponies in Dubai, U.A.E. *Berl Münch Tier Wscgr*. 1995;109:10-13.

The Armed Forces Institute of Pathology
Department of Veterinary Pathology

Conference Coordinator
Matthew Wegner, DVM

WEDNESDAY SLIDE CONFERENCE 2010-2011

Conference 15

5 January 2011

Conference Moderator:
Gary D. Coleman, DVM, PhD, Diplomate ACVP, Diplomate ACVPM

CASE I: 09A731 (AFIP 3165087).

Signalment: 5.65-year-old female Indian Rhesus macaque (*Macaca mulatta*).

History: Found dead in an outside breeding corral without history of previous illness.

Gross Pathology: The animal was dehydrated with evidence of fecal soiling around the anus. Small intestine and colon were distended with fluid and gas. Contents were blood-tinged and foul smelling. Mesenteric lymph nodes were severely enlarged.

Laboratory Results: Colonic swab cultures contained *Yersinia pseudotuberculosis* and *Campylobacter coli.*

Histopathologic Description: Small intestine: Small intestinal mucosa contains multiple to confluent areas of necrosis and hemorrhage that in some areas extend to the muscularis mucosa. Necrotic foci are filled with neutrophils forming microabscesses with dense microcolonies of extracellular bacteria. Scattered hyalinized eosinophilic deposits around crypts and vessels in the lamina propria demonstrate apple green birefringence when stained with Congo red and observed with polarized light.

Contributor's Morphologic Diagnosis: 1. Enteritis, necrohemorrhagic, suppurative, multifocal, severe, with intra-lesion bacterial colonies. Etiology: *Yersinia pseudotuberculosis.*

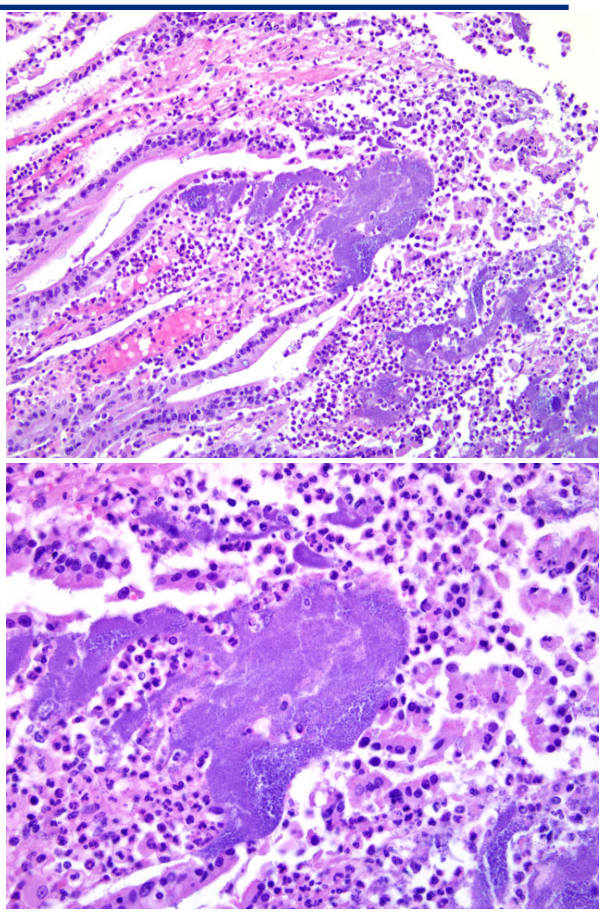

1-1, 1-2. Small intestine, Rhesus macaque, (Macaca mulatta). The mucosal epithelium is necrotic, with multifocal microabscesses and large colonies of extracellular coccobacilli. (HE 200X and 400X)

2. Amyloidosis, secondary, small intestine and mesenteric lymph node (not submitted).

Contributor's Comment: *Yersinia pseudotuberculosis* is a pathogen primarily of rodents and birds but has been reported in rabbits, deer, dogs, cats, swine, sheep, goats, chinchillas, horses, non-human primates, man and exotic mammals. In cases where multiple pathogens are isolated, it may be difficult to associate lesions with a specific pathogen. However, necrotizing lesions in the small intestine, obvious bacterial colonization, and severe neutrophilic response are hallmarks of yersiniosis.[1]

Three species of *Yersinia* are pathogenic for humans and non-human primates: *Y. pestis*, *Y. enterocolitica*, and *Y. pseudotuberculosis*. *Yersinia pestis* is transmitted by flea bite, while *Y. enterocolitica* and *Y. pseudotuberculosis* are typically self-limiting enteric infections transmitted by ingestion of contaminated food and water. All three organisms contain a virulence plasmid P (approximately 70 kb) that codes for a set of proteins called YOPS (for Yersinia outer membrane proteins) that are actually secreted virulence factors necessary for replication in host cells.[2] Additional plasmids pMT1 and pPCP1 in *Y. pestis* impart increased virulence.

Yersinia enterocolitica and *Y. pseudotuberculosis* pass through intestinal M cells, replicate in Peyers patches and, in rodents, frequently disseminate to mesenteric lymph nodes, spleen, liver, and lungs. Septicemia is rare in humans and non-human primates. Some literature suggests *Yersinia* resist phagocytosis by neutrophils and induce apoptosis of macrophages.[4] Recent work suggests that *Yersinia* can alter antibacterial functions, survive within macrophages, and replicate.[4] Two genes in *Y. enterocolitica*, ompR and gsrA, controlling response to altered osmolarity and heat shock, are associated with survival in macrophages.[5] *Yersinia pseudotuberculosis* and *Y. pestis* may inhibit phagosome acidification,[5] can infect naïve macrophages, and continue to replicate when exposed to interferon gamma. The latter ability may be conferred by a Pgm (102 kb) segment of the bacterial genome that reduces production of nitric oxide (NO) in infected macrophages.[5]

AFIP Diagnosis: Small intestine: Enteritis, necrotizing and suppurative, acute, diffuse, marked, with multifocal hemorrhage, microabscesses, amyloidosis, and colonies of coccobacilli.

Conference Comment: Some participants noted the presence of fibrin thrombi within the submucosal and mesenteric vasculature; this histologic finding is not present on all slides due to section variability.

Each of the three species of *Yersinia* mentioned by the contributor (*Y. pestis, Y. pseudotuberculosis,* and *Y. enterocolitica*) produces a distinct syndrome in various species of animals. *Yersinia pestis* may infect cats in the southwestern United States following consumption of infected rodents. The disease syndrome in cats, like humans, can be bubonic, septicemic and pneumonic; the bubonic form is associated with the lowest mortality rate. In cats the bubonic form occurs most frequently, and affected animals are febrile, dehydrated, have lymphadenomegaly and hyperesthesia. Suppuration of lymph nodes may result in draining fistulous tracts. Delay or failure to treat infected animals increases the risk of developing the septicemic form via lymphatic or hematogenous spread. Histologically, there is marked suppurative and necrotizing lymphadenitis with hemorrhage.[3] The septicemic form results in involvement of nearly all organs and clinical signs of septicemic shock and disseminated intravascular coagulation (DIC); death typically occurs in 1-2 days. The pneumonic form occurs as a primary infection through direct inhalation, or can occur secondary to either the bubonic or septicemic forms. Of the three forms, the pneumonic form carries the worst prognosis, with nearly a 100% fatality rate.[3]

Yersinia pseudotuberculosis produces caseonecrotic foci in mesenteric lymph nodes, spleen and liver of susceptible animals, of which there are many. There is marked necrosis, parenchymal collapse and vasculitis in the liver in addition to multiple pyogenic granulomas visible grossly as variably sized white foci. The spleen and lymph nodes have similar foci, and these organs are enlarged by lymphoid and histiocytic hyperplasia.[7] The organism is also linked to abortions in cattle, sheep and goats; the bacteria localize in the caruncle with passage to the chorioallantois and fetus. The lesions are typically that of placentitis of the cotyledons observed histologically as villar necrosis with granulocytic and histiocytic infiltration of the chorioallantois, and fibrinoid necrosis of the media in placental vessels with mononuclear and neutrophilic infiltrates. Septal vessels in the caruncles are thrombosed, resulting in necrosis and hemorrhage with marked neutrophilic and mononuclear infiltrates. The fetus is often delivered in a good state of preservation, with thoracic and abdominal effusion and foci of hepatic necrosis admixed with granulocytic and mononuclear infiltrates. The myocardium, lymph nodes and conjunctiva may have similar inflammatory infiltrates.[6]

Yersinia enterocolitica is known to cause disease in sheep, cattle, goats, deer and pigs in addition to humans and non-human primates. Gross lesions vary with the severity of infection, with fluid intestinal contents and congestion in mild cases, and edema to hemorrhage, ulceration and fibrin exudation in more severe cases. Histologic lesions include large colonies of coccobacilli in the lamina propria and villi in the distal small intestine and marked neutrophilic infiltration with microabscessation, ulceration, hemorrhage, and occasional pyogranulomas. In addition to enteritis, *Y. enterocolitica* is also associated with caseous mesenteric lymphadenitis.[1]

Contributor: Department of Comparative Pathology, Tulane National Primate Research Center, 18703 Three Rivers Rd, Covington, LA 70433
www.tpc.tulane.edu

References:

1. Brown CC, Baker DC, Barker IK. The alimentary system. In: Maxie MG, ed. *Jubb, Kennedy and Palmer's Pathology of Domestic Animals*. 5th ed., Vol. 2. Philadelphia, PA: Elsevier Ltd;2007:204-206.
2. Cornelis GR, Boland A, Boyd AP, et al. The virulence plasmid of *Yersinia*, an antihost genome. *Microbiol Molec Bio Rev*. 1998;62(4):1315-1352.
3. Macy D. Plague. In Greene CE, ed. *Infectious Diseases of the Dog and Cat*. Saint Louis, MO: Saunders Elsevier; 2006:439-445.
4. Monack DM, Mecsas J, Bouley D, Falkow S. *Yersinia*-induced macrophage apoptosis in vivo aids in the establishment of systemic infection in mice. *J Exp Med*. 1998;188(11):2127-2137.
5. Pujol C, Bliska JB. Turning *Yersinia* pathogenesis models inside out: Subversion of macrophage function by intracellular yersiniae. *Clin Immunol*. 2005;114:216-226.
6. Schlafer DH, Miller RB. Female genital system. In: Maxie MG, ed. *Jubb, Kennedy and Palmer's Pathology of Domestic Animals*. 5th ed., Vol. 3. Philadelphia, PA: Elsevier Ltd;2007:500.
7. Valli VEO. Hematopoietic system. In: Maxie MG, ed. *Jubb, Kennedy and Palmer's Pathology of Domestic Animals*. 5th ed., Vol. 3. Philadelphia, PA: Elsevier Ltd; 2007:298-299.

CASE II: WCS20097531 (AFIP 3167495).

Signalment: Juvenile male black howler monkey (*Alouatta caraya*).

History: This animal was part of a group of wild howler monkeys from two species, brown (*Alouatta guariba clamitans*) and black (*Aloutatta caraya*), and was found dead between November 2007-February 2009 in northeastern Argentina. In total, 65 animals were found dead. This particular animal was found dead by people living in the area and was left at a local human health office.

Gross Pathology: The only necropsy finding reported in the animals that were suitable for postmortem examination was mild to moderate yellow discoloration of the mucous membranes, skin and sclera (icterus).

Laboratory Results: Serum, liver and splenic samples from multiple animals examined during the outbreak were positive for Yellow Fever virus by virus isolation, direct immunofluorescence, RT-PCR and genome sequencing.

Histopathologic Description: Liver: Slides contain one sample of liver. Throughout the section there is disruption of the normal liver architecture with diffuse dissociation of the hepatic cords. There is necrosis of most midzonal to centrilobular hepatocytes characterized by rounding of cellular margins, hypereosinophilia of the hepatocyte cytoplasm and deep basophilic staining of the nucleus and loss of cellular detail. Throughout the zones of necrosis there is marked hepatocellular loss, collapse of hepatic cords and the remaining space is filled with erythrocytes. All remaining hepatocytes are swollen with numerous, well demarcated, variably sized, round, clear cytoplasmic vacuoles (microvesicular fatty change). Many hepatocytes contain variably sized hypereosinophilic foci within the cytoplasm (eosinophilic degeneration). Sinusoids adjacent to zones of necrosis contain many shrunken, rounded hypereosinophilic bodies occasionally with an associated small, basophilic, condensed nucleus (Councilman bodies). Some Kupffer cells contain cytoplasmic erythrocytes (erythrophagocytosis) and a small amount of cytoplasmic golden brown, granular pigment (hemosiderin). Occasional portal areas and central veins contain small numbers of lymphocytes, plasma cells and fewer neutrophils. In the background of many sections there are scattered black to brown amorphous microcrystalline granules consistent with acid hematin. These granules are an artifact of tissue fixation that we see in samples collected in the field in unbuffered formalin or paraformaldehyde.

Contributor's Morphologic Diagnosis: Necrosis, acute, midzonal to centrilobular, severe, with parenchymal collapse, hepatic cord dissociation, eosinophilic degeneration and Councilman body formation and diffuse microvesicular hepatocellular fatty change.

Contributor's Comment: This animal is one of a large group of wild howler monkeys of two species that died during a yellow fever outbreak in northeastern Argentina. Serum, liver and splenic samples from numerous animals were positive for yellow fever virus by virus isolation and direct immunofluorescence, followed by RT-PCR for generic flaviviruses and genome sequencing. Limited tissues were available for histologic examination, but in all cases the liver demonstrated the classic features of yellow fever virus infection including:

1. Midzonal acute hepatocellular necrosis
2. Eosinophilic degeneration of hepatocytes/Kupffer cells and Councilman body formation
3. Hepatocellular microvesicular fatty change

Additional findings in other organs examined from these cases, but not provided as part of this submission, included acute renal tubular necrosis with evidence of regeneration and hemoglobin casts and marked lymphocytolysis throughout the splenic white pulp and within multiple lymph nodes.

Yellow fever virus is an arbovirus of the genus *Flavivirus*, family *Flaviviridae* and is the cause of severe hemorrhagic disease in both humans and non-human primates.[2] The flaviviruses are RNA-viruses and include yellow fever virus, dengue virus, West Nile virus, Japanese encephalitis virus and tick-borne encephalitis virus.[2] Mosquitoes are the primary vector of yellow fever virus and include *Aedes aegypti* in urban areas, *Aedes albopictus* in suburban areas and tree-hole-breeding mosquitoes (*Haemagogus* spp.) in forests.[3] *Aedes aegypti* are found throughout most tropical to subtropical regions of the world, including much of the United States. *Haemagogus* spp. are found primarily in the forests of central and South America.[2,8] Currently, yellow fever virus distribution is limited to sub-Saharan Africa and Central and South America. Maintenance of the yellow fever virus can occur in a sylvatic cycle between non-human

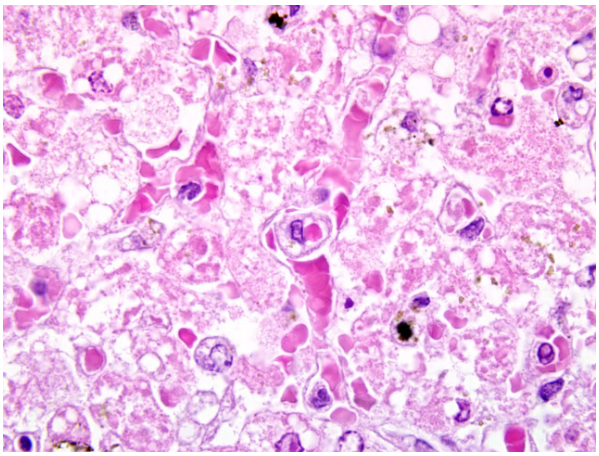

2-1. Liver, howler monkey, (Alouatta caraya). Degenerate vacuolated and necrotic hepatocytes contain brightly eosinophilic cytoplasmic inclusion bodies (Councilman bodies). (HE 1000X)

primates and forest mosquitoes or in an urban cycle between humans and *Aedes aegypti* or *albopictus*. Humans and non-human primates in these situations serve as temporary amplifiers while mosquitoes remain infected for life and serve as the reservoir of infection.[2,8]

While all primates are susceptible to yellow fever virus infection, new world monkeys are most susceptible, likely due to their evolution in the absence of the virus.[3] In particular, spider, wooley and howler monkeys are extremely sensitive and infection is almost always fatal. In yellow fever endemic areas, mortality in highly susceptible howler monkeys can act as an early warning signal for the presence of the virus.[3] In this particular mortality event, after the death of the first four howler monkeys, the National Health Authority of Argentina was alerted and a massive human vaccination campaign against yellow fever was carried out in the surrounding areas.

The characteristic midzonal hepatocellular necrosis seen in yellow fever is reflected clinically in humans and non-human primates as severe jaundice.[2,8] It has been suggested that the zonal nature of this lesion is due to hypoxia secondary to terminal shock; however, yellow fever antigen and RNA have been demonstrated in midzonal hepatocytes.[6] Macrophages are the principle site of initial viral replication and support the rapid spread of infection. The innate immune response is thought to contribute significantly to the pathogenesis of yellow fever infection with the release of cytokines from infected macrophages and dendritic cells disrupting normal vascular function and promoting coagulation.[7] Hepatic damage is proposed to be one of the mechanisms of hemorrhage in yellow fever infection due to a reduction in synthesis of coagulation factors in combination with consumptive coagulopathy.[2]

Eosinophilic degeneration and Councilman body formation are consistent histological features of yellow fever virus infection in both humans and non-human primates. They do not represent viral inclusions, but instead are the result of cell injury.[2] Councilman bodies begin as areas of eosinophilic degeneration within hepatocytes or Kupffer cells due to injury to the endoplasmic reticulum. These foci of condensed cytoplasm then detach from the wall of the sinusoid (if they are of Kupffer cell origin) or from the hepatocellular cord (if they are of hepatocyte origin). In some cases the condensed cytoplasmic material carries along a nuclear remnant. Within the sinusoid, the Councilman body either lies free or is phagocytosed by a Kupffer cell.[2] The cytoplasmic eosinophilic degeneration and condensed nuclear chromatin of these Councilman bodies is most consistent with cellular apoptosis. Virally-induced apoptosis is thought to contribute to hepatocellular death.[6] While this mechanism has not been thoroughly investigated for yellow fever virus, West Nile virus has been shown to trigger apoptosis *in vitro* via the intrinsic pathway.[1] Hepatic lesions in yellow fever have a paucity of inflammation and heal in surviving patients with minimal fibrosis, a finding that is argued to support apoptosis over necrosis as a primary mechanism for cell death. Microvesicular lipidosis was consistently seen in remaining hepatocytes in the livers of these monkeys. This is also described as a constant finding in human cases.[2]

In addition to the severe hepatic damage, yellow fever virus can also result in acute renal failure. Acute renal tubular necrosis is reported in severe human cases of yellow fever[2] and was seen in several of the black howler monkeys examined as part of this outbreak. Again, the tubular necrosis is thought to be the result of hypoxic damage compounded by hemoglobinuria; however, viral antigen has also been demonstrated in renal tubular epithelial cells.[5] These renal lesions are also associated with a paucity of inflammation and an apoptotic mechanism has been suggested as a primary mechanism but to date has not been proven.

From a conservation perspective, yellow fever outbreaks can have devastating effects on howler monkey populations. The initial outbreak in this case affected four groups of howler monkeys that had been under study since 2005, all of which are believed to have died. Brown howler monkeys are endangered in Argentina due to habitat loss, fragmentation and hunting pressures. Currently, yellow fever virus is also feared to put these populations at additional risk.[3] An unfortunate added risk to howler monkeys in yellow fever outbreaks is the misconception that they are the cause of human infection, rather than mosquitoes, which has led to campaigns of poisoning during human outbreaks of the disease.

AFIP Diagnosis: Liver: Hepatocellular degeneration and necrosis, centrilobular to midzonal, diffuse, severe, with hepatocellular disassociation, lipid type vacuolar change, and Councilman bodies.

Conference Comment: As noted by the contributor, hemorrhage and massive hepatic damage often result in consumptive coagulopathy, also referred to as disseminated intravascular coagulation (DIC). Clotting is initiated by release of tissue factor (i.e. tissue thromboplastin or factor III) beginning the extrinsic coagulation pathway; or activation of factor XII after contact with collagen, which commences the intrinsic pathway. Both pathways enter the common pathway, converting prothrombin to thrombin which converts fibrinogen to fibrin. As thrombin is carried away from the site of clotting, it binds to endothelial cell thrombomodulin and becomes an anticoagulant. The thrombin-thrombomodulin complex activates protein C, which in turn inhibits procoagulant factors V and VII. Activated coagulation factors are removed from circulation by the liver.[4]

Disseminated intravascular coagulation can be triggered by the release of tissue factor or thromboplastic substances into the circulation and/or by marked endothelial damage.

	ACT	APTT	PT
Measured parameter	Time for fibrin clot to form in fresh whole blood after addition of contact activator	Time for fibrin clot formation in citrated plasma after addition of an activator of the intrinsic pathway	Time for fibrin clot formation in citrated plasma after addition of thromboplastin (factor III) and calcium
Factors/pathways assessed	Intrinsic (PK, HMWK, factors XII, XI, IX, VII) and common pathways (factors X, V, II, fibrinogen)	Intrinsic (factors XII, XI, IX, VII) and common pathways (factors X, V, II, fibrinogen)	Extrinsic (factor VII) and common pathway (factors X, V, II, fibrinogen)
Conditions associated with prolonged times	Thrombocytopenia, factor deficiency <5% normal activity, anticoagulants, coagulation inhibitors (FDPs)	Hemophilia (factor VIII or IX), hereditary factor XII deficiency, hereditary PK deficiency, DIC, vitamin K factor deficiency secondary to rodenticide intoxication, bile stasis and liver failure	Inherited factor VII deficiency, DIC, acquired vitamin K factor deficiency

PK: prekallikrein; HMWK: high molecular weight kininogen; FDP: fibrin degradation products
In DIC, ACT, APTT and PT are all prolonged; additionally, d-dimers are routinely used to diagnose DIC.[9]

Damaged endothelial cells release tumor necrosis factor (TNF), which promotes coagulation via increased tissue factor expression and decreased thrombomodulin expression on endothelial cells and up-regulation of adhesion molecules for leukocytes, which themselves can damage the endothelium. Widespread activation of the coagulation cascade results in fibrin thrombi lodging in the microvasculature, leading to ischemia and erythrocyte fragmentation referred to as microangiopathic hemolytic anemia. Additionally, there is massive consumption of platelets, clotting factors and plasminogen resulting in hemorrhagic diathesis.[4]

Several tests are available and widely used for clinical assessment of coagulation including activated clotting time (ACT), activated partial thromboplastin time (APTT), and prothrombin time (PT). The chart summarizes the key points of each assay.[9]

Contributor: Wildlife Conservation Society, Global Health Program–Pathology, 2300 Southern Boulevard, Bronx, NY 10460
http://www.wcs.org

References:

1. Chu JJH, Ng ML. The mechanism of cell death during West Nile virus infection is dependent on initial infectious dose. *J Gen Virol*. 2003;84: 3305-3314.
2. del Rio C, Meier FA. Yellow fever. In: Nelson AM, Horsburgh CR eds. *Pathology of Emerging Infections*. Washington DC: American Society for Microbiology; 1998:13-41.
3. Holzmann I, Agostini I, Areta JI, Ferreyra H, Beldomenico P, diBitetti MD. Impact of yellow fever outbreaks on two howler monkey species (*Alouatta guariba clamitans* and *A. caraya*) in Misiones, Argentina. *Am J Primatol*. 2010;72:475-480.
4. Kumar V, Abbas AK, Fausto N, Aster JC. Red blood cell and bleeding disorders. In: Kumar V, Abbas AK, Fausto N, Aster JC, eds. *Robbins and Cotran Pathologic Basis of Disease*. 8th ed. Philadelphia, PA: Elsevier Saunders; 2009:673-674.
5. Lima EQ, Nogueira ML. Viral hemorrhagic fever-induced acute kidney injury. *Sem Nephrol*. 2008;28(4) 409-415.
6. Monath TP. Yellow fever: An update. *Lancet Infect Dis*. 2001;1:11-20.
7. Pastorino B, Nougairede A, Wurtz N, Gould E, de Lamballerie X. Role of host cell factors in flavivirus infection: Implications for pathogenesis and development of antiviral drugs. *Antiviral Res*. 2010;doi:10.1016/j.antiviral.2010.04.014.
8. Sallis ESV, Souza de Barros VLR, Garmatz SL, Fighera RA, Graca DL. A case of yellow fever in a brown howler (*Alouatta fusca*) in Southern Brazil. *J Vet Diagn Invest*. 2003;15:574-576.
9. Topper MJ, Welles EG. Hemostasis. In: Latimer KS, Mahaffey EA, Prasse KW, eds. *Duncan and Prasse's Veterinary Laboratory Medicine: Clinical Pathology*. 4th ed. Ames, IA: Blackwell Publishing; 2003:126-133.

CASE III: 10-5392-2 (AFIP 3167230).

Signalment: 10-year-old neutered male domestic short hair, cat (*Felis catus*).

History: A 10-year-old previously healthy male neutered domestic short hair cat from Oregon was examined after it had shown labored breathing of one day's duration. The indoor/outdoor cat had an unknown vaccination status and no previous health problems. Radiographs showed pneumonia with air bronchograms in caudal lung lobes and mixed interstitial alveolar pattern. The cat's breathing difficulty worsened and it repeatedly received oxygen therapy. A second radiograph two days later showed consolidation of the ventral aspect of the cranial lung lobes. The cat died on the subsequent day.

Gross Pathology: Gross examination of the thoracic cavity by the practitioner revealed pneumonia affecting approximately three fourths of the lung field. No other lesions were noted in the thoracic cavity. Nasal secretions and formalin-fixed lung tissue collected from the cat were submitted to the Veterinary Diagnostic Laboratory (VDL) at Oregon State University. All lung samples received at the VDL were diffusely firm, dark and poorly collapsed. One piece had, on cut section, an enhanced peribronchiolar pattern.

Laboratory Results: Nasal secretions tested positive for the influenza A matrix gene and neuraminidase 1 gene of pandemic (H1N1) 2009 influenza virus by rRT-PCR at the VDL at Oregon State University. The results were confirmed by the USDA's National Veterinary Services Laboratory in Ames, Iowa. Common feline respiratory viruses were not isolated from the nasal swab. Fluorescent antibody (FA) of smears generated from scraped cell cultures for feline herpesviral and feline caliciviral antigen was negative.

Histopathologic Description: Lung: Lesions may vary slightly among sections. In most bronchioles, there is complete or segmental epithelial necrosis; multinucleated cells are occasionally observed. Areas lacking epithelium are covered with fibrin. Bronchiolar lumens contain a few macrophages and sloughed epithelial cells and small amounts of cellular debris. Where present, bronchiolar epithelium is attenuated or appears normal on light microscopy. Alveolar lumens are flooded with wispy to dense protein-rich material (occasionally in the form of hyaline membranes) and is admixed with small to moderate numbers of macrophages and desquamated type II pneumocytes, scattered neutrophils, and rare multinucleated giant cells. In approximately half of the sections, some peribronchiolar alveoli have cuboidal epithelial cells (type II pneumocyte hyperplasia) and/or scattered multinucleated cells. There is also multifocal epithelial necrosis or loss, and lumens are occasionally occluded by dense fibrin accumulations. Lesions not present in sections included multifocal, mild, lymphoplasmacytic to histiocytic bronchitis and minimal epithelial degeneration of bronchial mucosal glands; multifocal, perivascular, mild to moderate edema; and mild, multifocal, pleural, mesothelial hypertrophy and hyperplasia.

Immunostaining for influenza virus antigen was performed. A few of the bronchioles with segmental necrosis had individual or small groups of positive, intact, non-ciliated or necrotic epithelial cells adjacent to negative epithelium with normal morphology. Intense staining traced the surface of some non-ciliated bronchiolar epithelial cells. Denuded bronchiolar surfaces showed irregular, linear to clumped staining. In some bronchiolar and alveolar lumens, cellular debris had intensely staining globules. Individual to small groups of positive-reactive cells were observed in peribronchiolar alveoli with type II pneumocyte hyperplasia. In alveoli with acute damage there was intense staining of some pneumocytes and/or luminal macrophages or sloughed pneumocytes.

Contributor's Morphologic Diagnosis: Severe, diffuse, acute to subacute, bronchointerstitial, fibrino-necrotizing pneumonia; some sections also had multifocal, severe type II pneumocyte hyperplasia of peribronchiolar alveoli.

Contributor's Comment: In the past, cats were considered relatively resistant to influenza virus infections.[3] In recent years this notion was changed by reports of respiratory and systemic disease in domestic cats after experimental and natural infections with highly pathogenic avian influenza virus (HPAIV) H5N1.[7,8,15,16] Infection of cats with HPAIV H5N1 can result in bronchointerstitial pneumonia with epithelial necrosis and fibrin exudation in bronchioles and alveoli. The pneumonia in cynomolgus monkeys, BALB/c mice, miniature pigs, and ferrets after experimental and natural infections with pandemic (H1N1) 2009 influenza virus, and in human patients with lethal swine origin influenza virus (SOIV) infections presents similarly,[6,10,12,14] as did the pneumonia in the cat in this report.[9] The main infectious differential etiologies for acute bronchointerstitial pneumonia in cats are feline herpesvirus and calicivirus,[2] which were not isolated from the nasal swab of this cat.[9]

When viral infections and lesions extend to involve alveoli, there is alveolitis with sero-fibrinous to neutrophilic exudate. It has been observed in domestic cats naturally infected with HPAIV H5N1, ferrets, and mice infected with pandemic (H1N1) 2009 influenza virus, and human patients with lethal pneumonia due to pandemic (H1N1) 2009 influenza virus, [6-10,12,14-16] and was also present in this cat.[9]

It is notable that neither necrosis nor viral antigen was observed in bronchial epithelium in the cat, which can be seen in human patients with lethal pandemic (H1N1) 2009 influenza virus-associated pneumonia, and in ferrets experimentally infected with pandemic (H1N1) 2009 influenza virus.[6,10-12,14] The type II pneumocyte hyperplasia in this cat may have been due to damage to the respiratory

epithelium caused by the acute viral infection, rather than a preexisting condition, as time course was prolonged enough.[2] Co-infections with bacteria are surprisingly uncommon in lethal pandemic (H1N1) 2009 influenza virus infections in humans.[1] Unfixed lung tissue was not available for bacterial culture, but a deep bronchial swab taken from this cat during postmortem examination did not yield bacterial growth.[9]

Transmission of pandemic 2009 (H1N1) influenza virus from a family member to the cat is highly likely in the case presented here. The owner of the cat and single household member had severe influenza-like illness (ILI). Pandemic 2009 (H1N1) influenza was confirmed by PCR testing at a hospital. The cat in this report had no known contact with other animals with respiratory disease due to pandemic (H1N1) 2009 influenza virus. Transmission from an owner was recently implicated in pandemic 2009 (H1N1) infection in a cat,[17] and transmission of Hong Kong pandemic influenza (H3N2) virus from a human patient to two domestic cats has been documented in the literature.[13]

AFIP Diagnosis: Lung: Pneumonia, bronchointerstitial, fibrinonecrotizing, acute to subacute, diffuse, severe, with alveolar edema.

Conference Comment: This case was studied in consultation with the AFIP Department of Pulmonary and Mediastinal Pathology, whose pathologists indicated that most of the pathology in the lung of this cat is attributed to viral infection. They also commented that, given the diffuse involvement of alveoli, diffuse alveolar damage (DAD) is an appropriate histologic interpretation in this case, despite the paucity of characteristic hyaline membranes, and indicated that oxygen therapy may have been contributory. During conference, several participants also observed histologic features suspicious for acute alveolar damage, including alveolar septal necrosis, fibrin, and edema, although none observed organized hyaline membranes lining alveolar walls. Upon disclosure of the clinical history, conference participants agreed that oxygen therapy may have exacerbated the alveolar wall lesion induced by viral infection, and concluded this case may represent an example of acute lung injury (ALI), which is a complication of diverse or multiple contributory predisposing conditions manifested histologically as DAD.

Oxygen therapy/toxicity is one of a number of primary or contributory causes of ALI; although the molecular basis by which oxygen causes the pulmonary lesion is not completely understood, the current favored hypothesis is capillary endothelial and type I pneumocyte damage due to reactive oxygen species.[2] Early in the course of ALI, there is up-regulation of IL-8 by pulmonary macrophages; IL-8 then attracts neutrophils to the lung, and also serves as a potent neutrophil activator. Together with IL-1 and TNF, IL-8 activates endothelial cells and neutrophils, and causes neutrophil sequestration in the pulmonary microvasculature.[5] Release of cytotoxins, chemokines and cytokines from neutrophils contributes to and enhances the inflammatory damage to alveoli. As the attack on the endothelium and alveolar epithelium continues, there is increased vascular permeability and loss of surfactant, both of which contribute to the loss of the ability of the alveoli to expand. The exudation of fibrin and edema, admixed with necrotic epithelial and inflammatory cells, contributes to the formation of hyaline membranes.[5]

The histologic appearance of DAD progresses through three phases: acute exudative phase, subacute proliferative phase, and chronic fibrosing phase. Congestion and edema of alveolar septa, with infiltration of neutrophils and macrophages, characterize the acute exudative phase, although hyaline membrane formation is typically considered the hallmark histologic finding. With loss of type I pneumocytes, the type II pneumocytes spread out to cover the denuded areas, and by 2-3 days post-injury type II pneumocyte proliferation is evident; it peaks at six days. The final phase, interstitial fibrosis, occurs via two pathways.

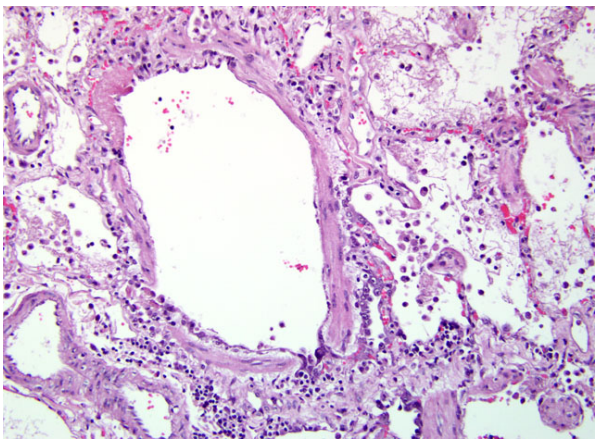

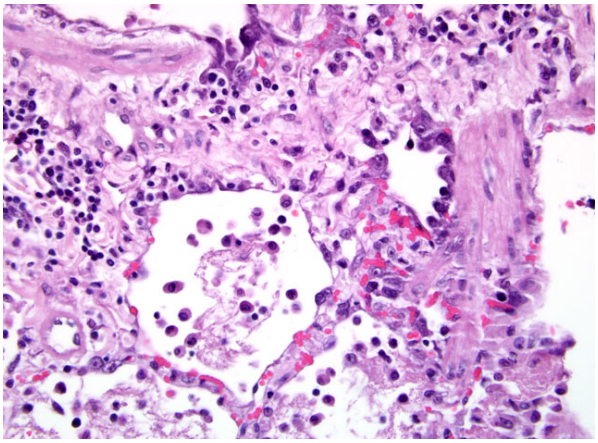

3-1, 3-2. Lung, cat. Bronchiolar epithelial cells are necrotic and sloughed. Alveoli contain fibrin, edema, necrotic cellular debris, and many macrophages. Alveolar septa and the peribronchiolar interstitium are infiltrated by macrophages, lymphocytes, and neutrophils. (HE 200X and 400X)

First, fibroblasts invade affected alveoli and organize into fibrous tissue akin to granulation tissue, which is then incorporated into the alveolar septa and covered by type II pneumocytes. Second, continued damage to endothelial and epithelial cells and inflammation within alveolar septa can recruit fibroblasts via TGF-β, resulting in direct interstitial fibrosis which is often well-organized by day 14.[2]

As noted by the contributor, the immunohistochemical profile included staining not only of bronchiolar epithelium but also of type II pneumocytes and sloughed, necrotic alveolar epithelial cells. Interestingly, Herfst *et al* produced strikingly similar lesions and immunohistochemical staining profiles (i.e. type I and II pneumocytes) in experimentally-infected cynomolgus macaques.[3]

We would like to thank Dr. Russell Harley of the Department of Pulmonary and Mediastinal Pathology, AFIP, for his study and consultation of this case.

Contributor: Veterinary Diagnostic Laboratory, Department of Biomedical Sciences, Oregon State University, Magruder 144, PO Box 0429, Corvallis, OR 97331-0429, USA
http://oregonstate.edu/vetmed/diagnostic

References:

1. Centers for Disease Control and Prevention (CDC). Bacterial coinfections in lung tissue specimens from fatal cases of 2009 pandemic influenza A (H1N1) United States, May-August 2009. *Morb Mortal Wkly Rep.* 2009;58(38): 1071-1074.
2. Caswell JL, Williams KJ. Respiratory System. In: Maxie MG, ed. *Jubb, Kennedy and Palmer's Pathology of Domestic Animals*. Vol. 2, 5th ed. Philadelphia, PA: Elsevier Ltd; 2007:523-653.
3. Herfst S, van den Brand JMA, Schrauwen EJA et al. Pandemic 2009 H1N1 influenza virus causes diffuse alveolar damage in cynomolgus macaques. *Vet Pathol*. 2010;47(6): 1040-1047.
4. Hinshaw VS, Webster RG, Easterday BC, Bean WJ Jr. Replication of avian influenza A viruses in mammals. *Infect Immun*. 1981;34:354-361.
5. Husain AN. The lung. In: Kumar V, Abbas AK, Fausto N, Aster JC, eds. *Robbins and Cotran Pathologic Basis of Disease*. 8th ed. Philadelphia, PA: Elsevier Saunders; 2009:680-682.
6. Itoh Y, Shinya K, Kiso M, et al. In vitro and in vivo characterization of new swine-origin H1N1 influenza viruses. *Nature*. 2009;460:1021-1025.
7. Klopfleisch R, Wolf PU, Uhl W, et al. Distribution of lesions and antigen of highly pathogenic avian influenza virus A/Swan/Germany/R65/06 (H5N1) in domestic cats after presumptive infection by wild birds. *Vet Pathol*. 2007;44:261-268.
8. Kuiken T, Rimmelzwaan G, van Riel D, et al. Avian H5N1 influenza in cats. *Science*. 2004;306:241.
9. Löhr CV, DeBess EE, Baker RJ, et al. Pathology and viral antigen distribution of lethal pneumonia in domestic cats due to pandemic (H1N1) 2009 influenza A virus. *Vet Pathol*. 2010;47:378-386.
10. Mauad T, Hajjar LA, Callegari GD et al. Lung pathology in fatal novel human influenza A (H1N1) infection. *Am J Respir Crit Care Med*. 2010;181:72-79.
11. Memoli MJ, Tumpey TM, Jagger BW, et al. An early 'classical' swine H1N1 influenza virus shows similar pathogenicity to the 1918 pandemic virus in ferrets and mice. *Virology*. 2009;393:338-345.
12. Munster VJ, de Wit E, van den Brand JM, et al. Pathogenesis and transmission of swine-origin 2009 A (H1N1) influenza virus in ferrets. *Science*. 2009;325:481-483.
13. Paniker CKJ, Nair CMG. Infection with A2 Hong Kong influenza virus in domestic cats. *Bull World Health Org*. 1970;43:859-862.
14. Perez-Padilla R, de la Rosa-Zamboni D, Ponce de Leon S, et al. Pneumonia and respiratory failure from swine-origin influenza A (H1N1) in Mexico. *N Engl J Med*. 2009;361:680-689.
15. Rimmelzwaan GF, van Riel D, Baars M, et al. Influenza A virus (H5N1) infection in cats causes systemic disease with potential novel routes of virus spread within and between hosts. *Am J Pathol*. 2006;168:176-183.
16. Songserm T, Amonsin A, Jam-on R, et al. Avian influenza H5N1 in naturally infected domestic cat. *Emerg Infect Dis*. 2006;12:681-683.
17. Sponseller BA, Strait E, Jergens A, et al. Influenza A pandemic (H1N1) 2009 virus infection in domestic cat. *Emerg Infect Dis*. 2010;16:534-537.

CASE IV: BA600/09 (AFIP 3165076).

Signalment: 5-year-old female Thoroughbred cross, equine (*Equus caballus*).

History: On the morning of presentation to the Royal (Dick) School of Veterinary Studies, this mare had been found reluctant to move her limbs. Upon arrival at the school's large animal hospital, she was recumbent with dilated pupils, reduced pupillary light reflex, decreased tongue tone and increased respiratory rate.

Gross Pathology: There was multifocal ecchymotic hemorrhage on the entire surface of the diaphragm, extending into the internal diaphragmatic musculature on cut section. The pelvic musculature also contained multifocal areas of ecchymosis which were particularly obvious in the muscle of the tail head and the gluteal muscles. The pelvic muscles were also slightly paler than normal. The urine was dark brown.

Laboratory Results: AST and CK levels were dramatically elevated and serum required a 1:200 dilution to obtain measurable levels (off the scale in undiluted serum). AST was 16,690U/L and CK was 506,680 U/L (reference ranges 258-554 and 150-385, respectively). The mare was humanely killed due to poor prognosis.

Histopathologic Description: Skeletal muscle, hind limb: One longitudinal section is examined. There is marked multifocal and segmental myofiber necrosis, characterized by myofiber swelling, hypereosinophilia and loss of cross striations. The sarcoplasm is often glassy, consistent with Zenker's-type degeneration, and there are myofibers with contraction bands. Many have fragmented, smudged, granular, flocculent, "moth-eaten" or shredded, ribbon-like sarcoplasm. Very occasionally, small numbers of neutrophils are interspersed within necrotic myofibers.

Kidney: Multiple tubules contain intraluminal deeply eosinophilic, granular material (myoglobin). There are small numbers of lymphocytes and plasma cells in the interstitium. There is moderate autolysis.

Contributor's Morphologic Diagnosis: 1. Moderate to severe multifocal acute myofiber necrosis with mild neutrophilic inflammation – skeletal muscle, hind limb equine.
2. Moderate multifocal intratubular myoglobin pigment (myoglobinuric nephrosis) – kidney – equine.

Contributor's Comment: The gross and histological findings, together with the signalment and clinical history, were considered to be consistent with equine atypical myopathy with secondary myoglobinuric nephrosis.

Equine atypical myopathy (AM) is an acute, frequently fatal rhabdomyolysis that is not associated with exertion or abnormal polysaccharide storage, and is characterixed clinically by weakness, stiffness, and recumbency. Atypical myopathy (previously known as atypical myoglobinuria) has been recognized since the mid-twentieth century; however, recently the number of reported cases has increased and it is now recognized as an emerging disease.[1,4,12] Cases have been reported in many European countries and reports of a seasonal pasture myopathy in the USA bear many similarities to AM.[3,12]

Cases of AM most commonly occur during autumn, with fewer cases in spring. Although the disease is not contagious, several horses on the same pasture may be affected, indicating the tendency for pasture-related factors to predispose to disease. Affected horses are usually young (<3 years old), in normal to poor body condition, and grazing poor quality or bare pasture.[1,12,13] Management practices and pasture characteristics associated with increased risk of disease include permanent pasture, manure spreading, high humidity, sloping pastures, accumulation of dead leaves, and the presence of a waterway.[12] Some epidemiological factors of AM are shared by equine dysautonomia (equine grass sickness) and cases of horses being affected by both diseases concurrently have been reported.[10]

Clinical signs of AM are largely due to degeneration of postural and respiratory muscles, and include stiffness, muscular weakness, recumbency and dyspnea. The onset of clinical signs is rapid, and animals are frequently found recumbent or dead.[12,15] The most consistent laboratory finding is markedly increased levels of creatine kinase (CK), which may reach >100,000 iu/L.[11] Hypocalcemia and hyperglycemia are commonly present, although other electrolyte imbalances are not usually evident, in contrast to exercise-induced rhabdomyolysis.[12] Myoglobinuria is frequently present, except in those animals that have died early in the course of disease. Affected animals often have a distended bladder and are unable to urinate normally; however, blood urea nitrogen and creatinine values are frequently within normal limits, indicating normal renal function.[4,5,11,13]

At necropsy, areas of pallor are present within the postural and respiratory musculature, in particular the intercostal muscles, diaphragm, neck and shoulder musculature, and to a lesser extent the muscles of the back and hind quarters. Cardiac muscle may also be affected; however, this is not a consistent finding.[12,15] Histologically, there is multifocal, monophasic myodegeneration, consistent with Zenker's degeneration/necrosis. Type I myofibers are predominantly affected.[2,7]

Staining with periodic acid-Schiff has failed to indicate increased or abnormal cytoplasmic glycogen or polysaccharides within affected fibers, whereas staining for lipid has revealed abnormal accumulations of neutral fat within myofibers, and staining for nicotinamide adenine dinucleotide (NADH) reductase and succinate

dehydrogenase (SDH) in myofibers has highlighted a weak oxidative potential in these cells.[2,7] Recently, a study identified multiple deficiencies of several mitochondrial dehydrogenases, including those involved in β-oxidation of fatty acids. It is speculated that such deficiencies may be possible etiological factors in AM.[14] A separate study has identified the lethal toxin of *Clostridium sordellii* as a possible trigger or lethal factor in this disease.[8]

AFIP Diagnosis: 1. Skeletal muscle: Myocyte degeneration and necrosis, acute, multifocal, moderate, with contraction bands.
2. Kidney: Cortical tubular degeneration and necrosis, acute, multifocal, moderate, with cortical and medullary intratubular eosinophilic granular casts (myoglobin).

Conference Comment: Skeletal muscle degeneration and necrosis often involve different portions of the myofiber dependent on the amount of injury involved, and classically there are four ways to classify skeletal muscle necrosis:[9]

- Focal monophasic: isolated, single mechanical injury.
- Multifocal monophasic: single event with widespread involvement with all affected myofibers exhibiting the same change; often due to toxins or metabolic defects.
- Focal polyphasic: isolated lesion with affected myofibers in different stages of alteration due to repeated trauma.
- Focal polyphasic: widespread involvement of myofibers over an extended period of time resulting in different stages of reaction; which can be due to genetic disease or nutritional deficiencies.

In this case, conference participants agreed with the contributor in classifying the lesion as multifocal monophasic degeneration and necrosis based on the extent and relative uniformity of the lesion.

In discussing the renal lesion, participants were impressed with the tubular changes. The changes are consistent with acute tubular necrosis, the cause of which appears to be shock and ischemic necrosis. As noted by the moderator, myoglobin is not directly toxic to the renal tubules; however, during periods of hypotension it contributes to necrosis.[6] Tubulorrhexis is an important finding that implies disruption of the basement membrane, which affects reparative capability as regenerating epithelial cells lack the necessary scaffolding.

Contributor: Veterinary Pathology Unit, Division of Veterinary Clinical Sciences, Roslin Institute and Royal (Dick) School of Veterinary Studies, The University of Edinburgh, Easter Bush Veterinary Centre, Roslin, Midlothian, EH25 9RG, UK

References:

1. Bowen JN, Craig JF. Myoglobinuria in horses. *Vet Rec*. 1942;35:354-355.
2. Cassart D, Baise E, Cherel Y, et al. Morphological alterations in oxidative muscles and mitochondrial structure associated with equine atypical myopathy. *Equine Vet J*. 2007;39:26-32.
3. Finno CJ, Valberg SJ, Wunschmann A, Murphy MJ. Seasonal pasture myopathy in horses in the midwestern United States: 14 cases (1998–2005). *J Am Vet Med Assoc*. 2006;229:1134-1141.
4. Harris P, Whitwell K. Atypical myoglobinuria alert. *Vet Rec*. 1990;127: 603.
5. Hosie BD, Gould PW, Hunter AR, Low JC, Munro R, Wilson HC. Acute myopathy in horses at grass in east and south east Scotland. *Vet Rec*. 1986;119:444-449.
6. Maxie MG, Newmann SJ. Urinary system. In: Maxie MG, ed. *Jubb, Kennedy and Palmer's Pathology of Domestic Animals*. Vol. 2, 5th ed. Philadelphia, PA: Elsevier Ltd; 2007:466-467.
7. Palencia P, Rivero JLL. Atypical myopathy in two grazing horses in northern Spain. *Vet Rec*. 2007;161:346-348.
8. Unger-Torroledo L, Straub R, Lehmann AD, et al. Lethal toxin of *Clostridium sordellii* is associated with fatal equine atypical myopathy. *Vet Microbiol*. 2010;144:487-492.
9. Van Vleet JF, Valentine BA. Muscle and tendon. In: Maxie MG, ed. *Jubb, Kennedy and Palmer's Pathology of Domestic Animals*. Vol. 1, 5th ed. Philadelphia, PA: Elsevier Ltd; 2007:198-199.
10. Vercauteren G, van der Heyden S, Lefère L, Chiers K, Laevens H, Ducatelle R. Concurrent atypical myopathy and equine dysautonomia in two horses. *Equine Vet J*. 2007;39:463-465.
11. Votion DM, Linden A, Saegerman C, et al. History and clinical features of atypical myopathy in horses in Belgium (2000–2005). *J Vet Intern Med*. 2007;21:1380-1391.
12. Votion DM, Serteyn D. Equine atypical myopathy: A review. *Vet J*. 2008178:185-190.
13. Votion DM, Linden A, Delguste C, et al. Atypical myopathy in grazing horses: A first exploratory data analysis. *Vet J*. 2009;180:77-87.
14. Westermann CM, Dorland L, Votion DM, et al. Acquired multiple acyl-CoA dehydrogenase deficiency in 10 horses with atypical myopathy. *Neuromuscul Disord*. 2008;18:355-364.
15. Whitwell KE, Harris P, Farrington PG. Atypical myoglobinuria: An acute myopathy in grazing horses. *Equine Vet J*. 1988;20:357-363.

The Armed Forces Institute of Pathology
Department of Veterinary Pathology

Conference Coordinator
Matthew Wegner, DVM

WEDNESDAY SLIDE CONFERENCE 2010-2011

Conference 16

12 January 2011

Conference Moderator:
Richard J. Montali, DVM, Diplomate ACVP, Diplomate ACZM

CASE I: 06-626 (AFIP 3030784).

Signalment: 3-year-old Shubunkin goldfish (*Carassius auratus*).

History: Three-week history of progressive coelomic distention and exophthalmus. There was bristling of the scales and tachypnea.

Gross Pathology: A small amount of serosanguineous fluid was in the coelomic space and there were numerous adhesions between visceral surfaces. Numerous yellow-white foci, ranging from pinpoint to 2 mm diameter, were randomly distributed throughout the viscera and on both visceral and parietal coelomic surfaces. The swim bladder was distended with air. Cytologic examination of touch preparations of material from the coelomic space documented numerous macrophages and numerous 4 µm diameter, lightly basophilic round organisms (amoeba) with small eccentric to peripheral 1 µm diameter nuclei. Organisms were both free and within macrophages.

Histopathologic Description: Tissue: Multiple caseous granulomas of variable size are within the liver, spleen and

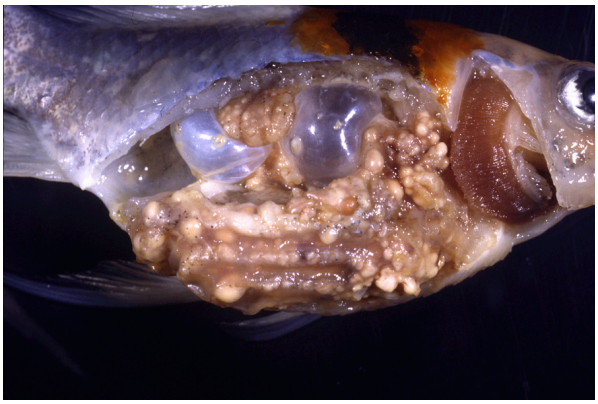

1-1. Coelomic cavity, goldfish. Within the mesentery and viscera are numerous variably sized, tan-white granulomas. Photograph courtesy of College of Veterinary Medicine, Virginia Tech, www.vetmed.vt.edu.

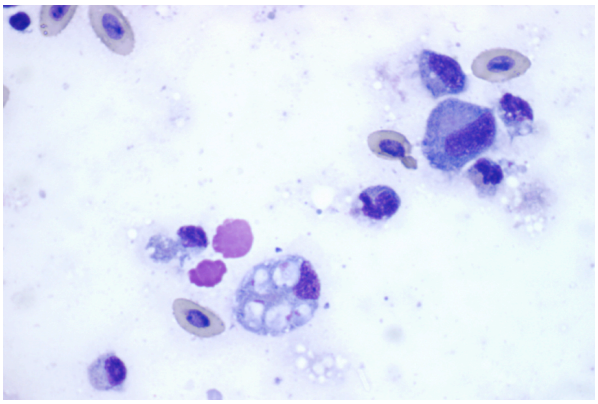

1-2. Coelomic fluid, touch preparation, goldfish. Cytologic examination of material from the coelomic space revealed numerous macrophages with multiple intracytoplasmic lightly basophilic round organisms (amoebae) with small eccentric to peripheral nuclei. Extracellular amoebae were also present. Photograph courtesy of College of Veterinary Medicine, Virginia Tech, www.vetmed.vt.edu.

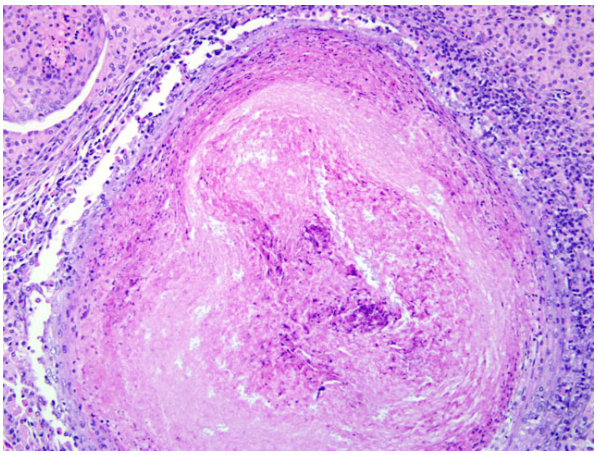

1-3. Liver, goldfish. The liver contains numerous variably-sized centers of necrotic debris surrounded by macrophages, lymphocytes, plasma cells, and neutrophils further bounded by fibroblasts (granulomas). (HE 20X)

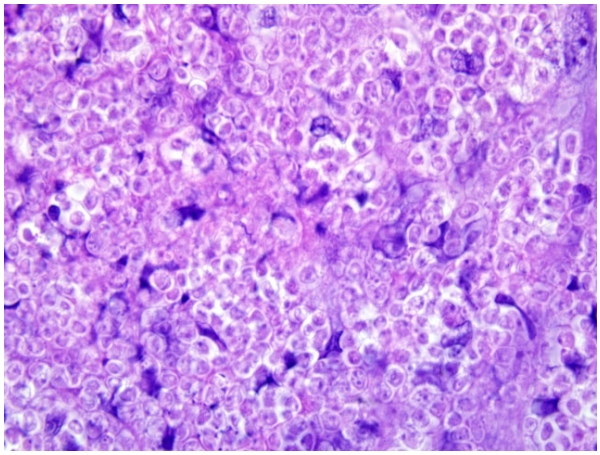

1-4. Coelomic cavity, goldfish. Numerous 4 µm lightly basophilic round amoebae occur vicinity the periphery of necrotic centers within the granulomas. (HE 1000X)

coelomic space. Concentric layers of fibroblasts form a thin capsule around many of the granulomas. A layer of macrophages surrounds the necrotic center and is mixed with lymphocytes, plasma cells and some heterophils. At the interface between the central necrotic debris and the surrounding mantle of macrophages are numerous, round, lightly eosinophilic organisms (amoeba), approximately 4 µm in diameter, with small eccentric nuclei.

Contributor's Morphologic Diagnosis: Multifocal granulomas, liver, spleen, coelom, with intralesional amoebae.

Contributor's Comment: The histopathology of this case is similar to that previously reported.[1] The amoeba was not cultured or classified but is believed to belong to the family Hartmanellidae. Amoebae have been found in many other fresh water aquarium fish species as well.

AFIP Diagnosis: Coelomic viscera: Granulomas, caseating, multifocal to coalescing, with peripheral amoebae.

Conference Comment: Participants and the moderator were impressed by the extent of the granulomas and discussed the possibility of an additional infectious etiology, such as mycobacteriosis. Special stains failed to demonstrate bacteria (acid fast, gram positive or gram negative) or fungal agents. A differential diagnosis list for multiple coelomic granulomas in a goldfish would include granulomatous amoebic disease,[4] miscellaneous amoebic infection,[4] and mycobacteriosis.[3]

Another focus of discussion was the presence of melanomacrophage centers (MMCs). Melanomacrophages are pigment-containing macrophages; most often they contain melanin, but they can have any pigment, such as ceroid or lipofuscin, within their cytoplasm. The pigment is often pink to golden in healthy fish and it becomes darker during periods of illness.[2] Melanomacrophage centers are discrete aggregates of melanomacrophages normally present in the kidney, spleen and liver.[2] They are also seen as part of the host response to foreign bodies and protozoal parasites. It has been found that the quantity, size and histomorphology of MMCs vary with age, season, nutrition status, and exposure to antigens.[2]

Contributor: College of Veterinary Medicine, Virginia Tech, Blacksburg, VA 24061
www.vetmed.vt.edu

References:

1. Dykova I, Lom J, Machackova B, Sawyer TK. Amoebic infections in goldfishes and granulomatous lesions. *Folia Parasitologica*. 1996;43:81-90.
2. Ferguson HW. *Systemic Pathology of Fish: A Text and Atlas of Comparative Tissue Responses in Diseases of Teleosts*. Ames, IA: Iowa State University Press; 1989:7,66,92.
3. Hoole D, Bucke D, Burgess P, Wellby I. *Diseases of Carp and Other Cyprinid Fishes*. Ames, IA: Iowa State University Press; 1989:55-56,67.
4. Noga EJ. *Fish Disease: Diagnosis and Treatment*. Ames, IA: Wiley-Blackwell; 2010:264.

CASE II: N07-584 (AFIP 3109240).

Signalment: 9-year-old female Egyptian fruit bat (*Rousettus aegyptiacus*).

History: Animal from a zoological collection found deceased in its enclosure.

Gross Pathology: The liver was very small and firm with loss of lobular contours, and contained numerous 1-3 mm diameter nodules, consistent with cirrhosis.

Histopathologic Description: Liver: There is cirrhosis, evidenced by streams of fibrous connective tissue dissecting between regenerative nodules of hepatocytes. Numerous small bile ducts and hemosiderophages are present within the fibrous connective tissue. A Prussian blue stain also reveals moderate to large amounts of hemosiderin within Kupffer cells, and a variable amount of hemosiderin within many hepatocytes and biliary epithelial cells. There are multifocal areas of hepatocellular necrosis, sometimes involving entire nodules or several adjacent nodules, and sometimes involving small clusters of hepatocytes within nodules. There are rare individual necrotic hepatocytes near the margin of lobules adjacent to regions of fibrosis and increased hemosiderin deposition. There is moderate to marked, multifocal cholestasis.

Contributor's Morphologic Diagnosis: 1. Hemochromatosis, liver: Marked hemosiderin deposition within macrophages, biliary epithelial cells and hepatocytes, with bridging fibrosis, nodular hyperplasia, and rare individual hepatocyte necrosis, liver.
2. Moderate, multifocal, acute hepatocellular necrosis.
3. Moderate to marked, multifocal cholestasis, liver.

Contributor's Comment: In veterinary cases, hemochromatosis refers to excessive iron deposition with associated tissue damage (fibrosis and/or necrosis), and hemosiderosis refers to increased iron deposition without associated tissue damage. In human cases, the term hemochromatosis is generally reserved for genetic causes of iron overload, and all other cases are referred to as secondary iron overload.

Hemochromatosis has been described in numerous exotic species, including Egyptian fruit bats, hyraxes, mynahs, ramphastids and lemurs.[4] These appear to be diseases of captivity, and thus are believed to be related to husbandry. Some species of animals which are affected consume materials in the wild which are high in tannins, which are iron binders. Wild lemurs consume several plants that are high in tannins.[8] If these animals have adapted to a low level of available iron in their diet, they may absorb iron very efficiently. In a captive situation, with an iron-replete diet which contains no binders, excessive absorption of iron occurs. Iron homeostasis is principally controlled at the level of absorption, as there is no physiologic mechanism for excretion.[5]

Iron is typically bound to transferrin while it is in circulation and ferritin when it is stored. Iron bound to these proteins cannot participate in chemical reactions, as free iron can.[6] In iron overload, however, it is presumed that the storage capacity for iron is overwhelmed, and free iron is then available to participate in the generation of free radicals, either through the Fenton or Haber-Weiss reactions.[7] Free radicals can damage DNA, proteins and lipids. The organs damaged in many humans with iron overload are the liver, pancreatic beta (β) cells and heart, which are organs with high mitochondrial activity.[3] Approximately 1-2% of electrons in the mitochondrial electron transport chain are "leaked" into reactive oxygen species, such as H_2O_2 and O_2^-.[3]

High vitamin C concentrations in the captive diet of these frugivorous bats may also contribute to iron overload and

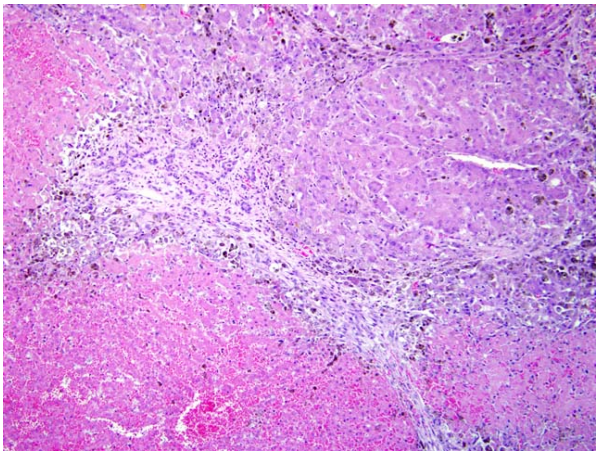

2-1. Liver, Egyptian fruit bat. There are multiple foci of nodular hepatocellular regeneration, interstitial fibrosis, bile duct proliferation (cirrhosis), and many Kupffer cells that contain abundant brown granular intracytoplasmic pigment (hemosiderin). (HE 100X)

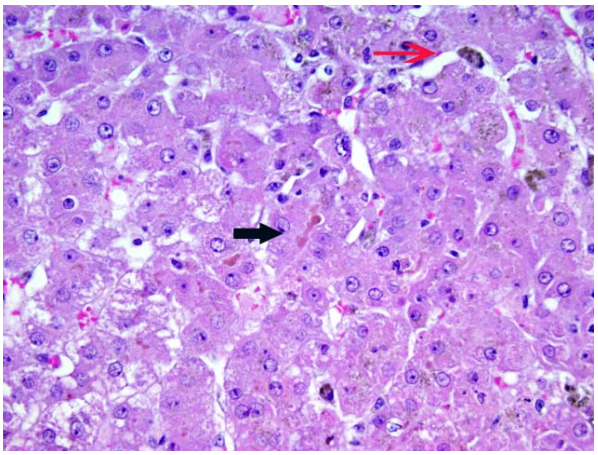

2-2. Liver, Egyptian fruit bat. Bile caniliculi are expanded by linear plugs of gold-brown material (bile, black arrow). Many Kupffer cells and occasional hepatocytes contain brown granular pigment (hemosiderin, red arrow). (HE 400x)

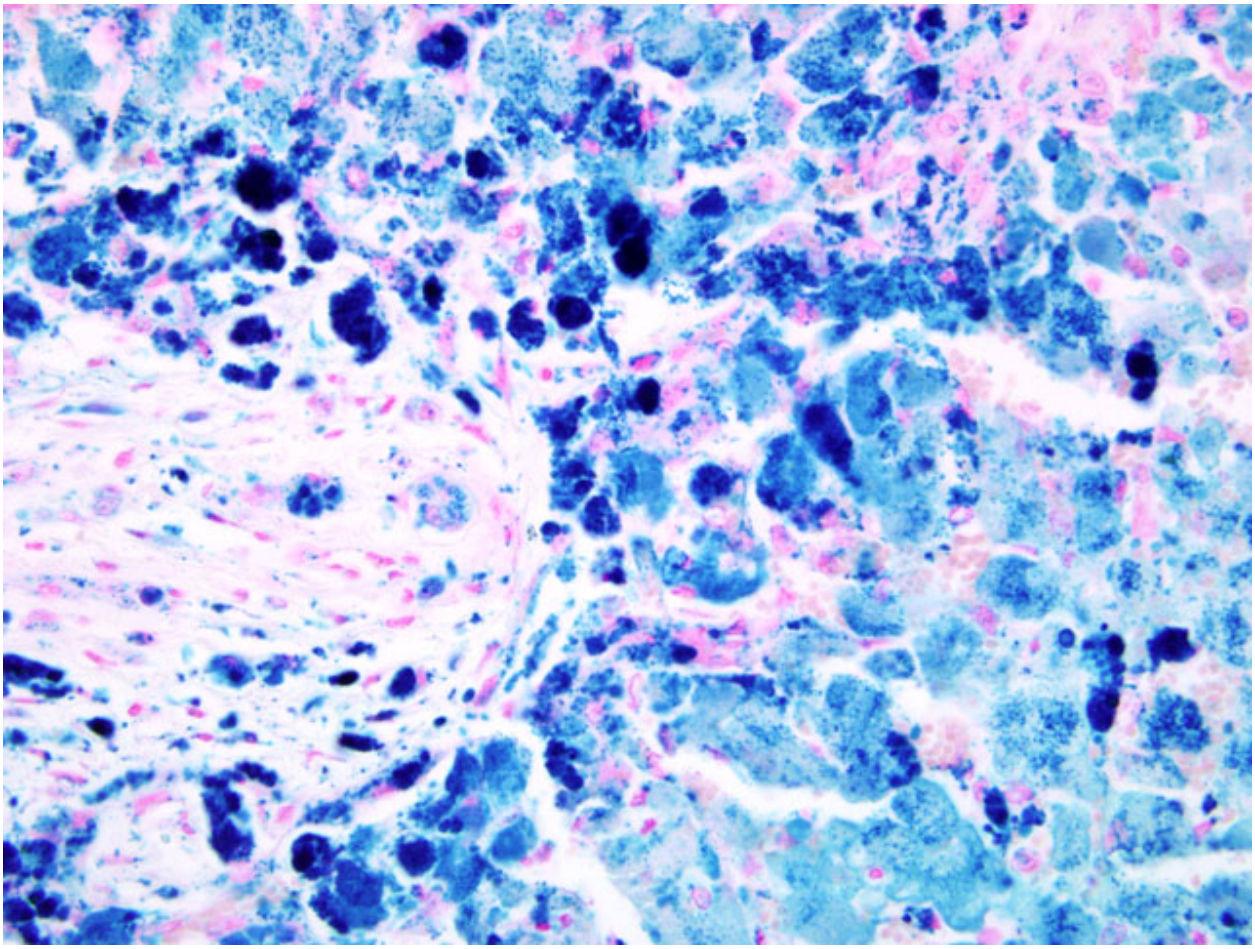

2-3. Liver, Egyptian fruit bat. The Prussian blue stain demonstrates hemosiderin within Kupffer cells, as well as within hepatocytes. (Prussian blue 200X)

associated damage, as vitamin C enhances the absorption of dietary non-heme iron[1] and may exacerbate free radical damage from excess stored iron.[6]

The large areas of necrosis identified in this case are not consistent with hemochromatosis. In cases of hemochromatosis, hepatocyte necrosis is typically limited to individual hepatocytes, often bordering regions of fibrosis and increased iron deposition. A specific cause for the larger areas of necrosis was not identified in this case.

AFIP Diagnosis: Liver: Hepatocellular degeneration, necrosis, loss and nodular regeneration, diffuse, marked, with bridging fibrosis and biliary hyperplasia (cirrhosis), marked bile stasis, and hemosiderosis (hemochromatosis).

Conference Comment: Conference participants were impressed by the level of hepatocellular damage and cirrhotic changes, which precipitated a discussion of whether the hemochromatosis preceded cirrhosis or vice versa. Cirrhosis is considered one of the three primary morphologic changes in hereditary hemochromatosis in humans. The authors of *Robbins and Cotran Pathologic Basis of Disease* note that, in addition to the toxic effects of free radical formation, iron also induces hepatic stellate cell activation with subsequent deposition of collagen.[2] They provide an overview of the pathogenesis of this disease in humans. Briefly, iron accumulation begins in periportal hepatocytes and as the iron load increases, more of the hepatic lobule becomes involved, including biliary epithelium and Kupffer cells. Fibrous septae slowly form, resulting in micronodular patterns of cirrhosis.[2]

The contributor provides a concise, informative overview of hemochromatosis as it pertains to veterinary species.

Contributor: University of Florida, College of Veterinary Medicine, Department of Infectious Diseases and Pathology
http://www.vetmed.ufl.edu/college/departments/patho/

References:

1. Cook JD, Watson SS, Simpson KM, Lipschitz DA, Skikne BS. The effect of high ascorbic acid supplementation on body iron stores. *Blood*. 1984;64:721-726.
2. Crawford JM, Liu C. Liver and biliary tract. In: Kumar V, Abbas AK, Fausto N, Aster JC, eds. *Robbins and Cotran*

Pathologic Basis of Disease. 8th ed. Philadelphia, PA: Elsevier Saunders; 2009:861-863.
3. Eaton JW, Qian M. Molecular bases of cellular iron toxicity. *Free Rad Biol Med*. 2002;32:833-840.
4. Farina LL, Heard DJ, LeBlanc DM, et al. Iron storage disease in captive Egyptian fruit bats (*Rousettus aegyptiacus*): Relationship of blood iron parameters to hepatic iron concentrations and hepatic histopathology. *J Zoo Wildl Med*. 2005;36:212-221.
5. Fleming MD, Andrews NC. The liver and iron. In: Arias IM, ed. *The Liver: Biology and Pathobiology*. 4th ed. Philadelphia, PA: Lippincott, Williams & Wilkins; 2001:345-359.
6. Herbert V, Shaw S, Jayatilleke E. Vitamin C-driven free radical generation from iron. *J Nutr*. 1996;126(Suppl): 1213-1220.
7. Kadiiska MB, Burkitt MJ, Xiang Q, Mason RP. Iron supplementation generates hydroxyl radical in vivo. *J Clin Invest*. 1995;96:1653-1657.
8. Spelman LH, Osborn KG, Anderson MP. Pathogenesis of hemosiderosis in lemurs: Role of dietary iron, tannin and ascorbic acid. *Zoo Biol*. 1989;8:239-251.

CASE III: 2009-051B (AFIP 3167248).

Signalment: 21 years, 9-months-old intact female Japanese macaque (*Macaca fuscata fuscata*).

History: This macaque was born and raised at the Milwaukee County Zoo (Milwaukee, WI, USA). The zoo's Japanese macaque troop was formed in 1981 when 12 animals were brought in to live on Monkey Island at the zoo. Over the next 13 years the troop had about 50 offspring. Members of the troop were relocated to other zoos in the late 1980's and again in the early 1990's. At its most populated, Monkey Island housed approximately 30-40 individuals. All males were vasectomized in the mid 1990's, with the last natural addition to the troop being born in 1995. This species, and this troop, are carriers of cercopithecine herpesvirus 1 (B virus), so the decision was made to prevent additional births but maintain the colony throughout the lives of the remaining animals. There were 16 macaques remaining on the island at the time of this macaque's death.

In early February 2009 the keeper noted that this animal's urine was dark yellow. In March 2009 the animal became icteric. Ultrasound indicated that there was a 4 x 3 cm mass located at the head of the pancreas. The liver had an increased echogenicity and the extrahepatic and intrahepatic bile ducts were dilated and variably tortuous. Obstructive jaundice was diagnosed and euthanasia was elected due to poor prognosis and lack of response to medical management, which included antibiotics and ursodeoxycholic acid administration. The animal maintained her preclinical disease body weight of 8 kg ± 0.2 throughout the final months of her life. Prior to late January 2009 this animal was considered to be in good health with no significant disease(s) reported in the medical history.

Laboratory Results: Urine collected from the floor early in February was positive for bilirubin. Pertinent blood chemistry results from blood collected in early March included elevated blood urea nitrogen (31 mg/dL; International Species Inventory System [ISIS]: 21 ± 6); decreased total calcium (8.0 mg/dL; ISIS: 9.7 ± 6); decreased total protein (6.1 g/dL; ISIS: 7.6 ± 0.8); decreased albumin (2.3 g/dL; ISIS: 4.3 ± 0.4); increased cholesterol (484 g/dL; ISIS: 168 ± 40); increased total bilirubin (6.6 mg/dL; ISIS 0.2 ± 0.1); increased gamma glutamyl transferase (GGT: 443 IU/L; ISIS: 61 ± 25); increased aspartate aminotransferase (AST: 241 IU/L; ISIS: 55 ± 27); increased alanine aminotransferase (ALT: 280 IU/L; ISIS: 46 ± 21); and increased alkaline phosphatase (ALP: 9070 IU/L; ISIS: 348 ± 266).

Gross Pathology: Conjunctival and oral mucous membranes, skin, subcutis, and internal soft tissues including adipose tissue, nerves, and serosal surfaces are discolored yellow (icterus). The abdominal cavity contains 150 mL of yellow-orange, minimally viscous, and moderately cloudy fluid. Approximately 2.5 cm aboral from the pyloric sphincter, a 4.5 x 3 x 2.5 cm, diffusely tan, firm, lobulated mass focally effaces and expands the medial side of the duodenal wall, elevating the ulcerated mucosa and effacing the duodenal papilla. The mass extends into the adjacent head of the pancreas, encompasses and effaces the wall of the common bile duct, and extends into and around distended, bile-filled extrahepatic and intrahepatic bile ducts with mass extension and metastases scattered deep into the hepatic parenchyma. The gallbladder could not be manually expressed. The liver is enlarged based on percent body weight (4% body weight) and has slight rounding of the margins. The capsular surface of the liver is undulated and roughened by pitting. Numerous firm tan, often coalescent, masses are scattered throughout the omentum. The mesentery of the small intestine at the serosal junction is thickened (up to approximately 1 cm), firm, and tan; linear projections of this tan proliferative tissue extend into the mesentery and onto the adjacent serosal surfaces of the small intestine. Few firm tan plaque-like masses are scattered along the parietal peritoneum along the ventral midline of the body wall with varying extension into the adjacent skeletal muscle and focal adherence of the omentum to the mid-ventral body wall at the level of the umbilicus.

Histopathologic Description: The submitted slide contains duodenum, large and ectatic bile and pancreatic ducts (hepatopancreatic duct or ampulla of Vater) and includes adjacent pancreas. The section is taken from the focally expanded region of the duodenum at the major duodenal papilla. Extending from and filling the major pancreatic and common bile ducts at the opening into the major papilla (ampulla of Vater or hepatopancreatic ampulla), regionally and transmurally expanding and/or effacing the duodenum and regionally invading the adjacent pancreas is an epithelial neoplasm. The neoplastic cells form tubules and acini and small islands that are supported by and embedded within both pre-existing stroma and small to massive amounts of newly formed fibrous connective tissue of low to moderate vascularity and cellularity (desmoplasia). Neoplastic epithelial cells are polygonal to cuboidal to columnar with variably distinct cell margins and contain small to moderate amount of amorphous, eosinophilic to amphophilic cytoplasm and 1 to occasionally 2 plump oval nuclei. Nuclei contain finely to coarsely stippled chromatin and 1 to 5 variably distinct and irregular-shaped nucleoli. Mitoses vary from region to region from being rare (0-2/10HPF) to occasionally 3-4 per HPF. There is individual cell necrosis and tubular structures often contain necrotic cellular debris. Multifocally within the neoplasm are few to moderate aggregated to loosely scattered lymphocytes and plasma cells and fewer neutrophils and histiocytes/macrophages.

Not present in the submitted slide: The described epithelial neoplasm extends into the liver multifocally along portal tracts. The neoplasm is also seen within the mesentery and the visceral and parietal peritoneum of the intestine and body wall where it multifocally invades subtending smooth and skeletal muscle, respectively. Throughout examined

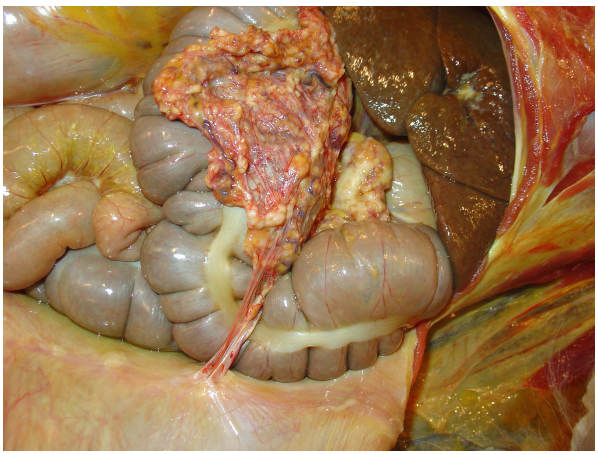

3-1. Omentum, ampullary adenocarcinoma, Japanese macaque. Numerous firm, tan, masses are scattered throughout the omentum and adjacent mesentery, and there is a focal adhesion of the omentum to the ventral body wall at the level of the umbilicus. Photograph courtesy of the Department of Pathobiological Sciences, School of Veterinary Medicine, University of Wisconsin – Madison, www.vetmed.wisc.edu/home.

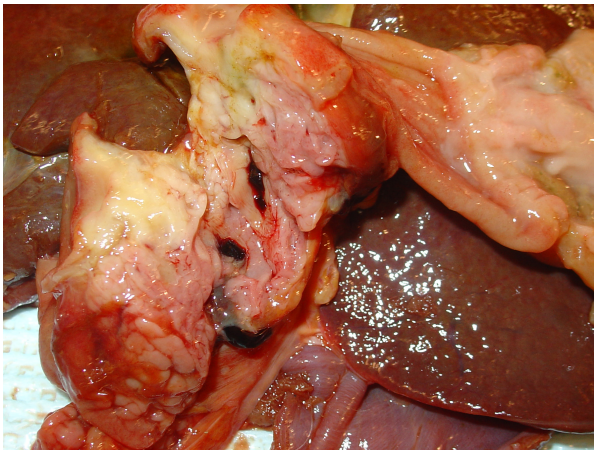

3-2, 3-3. Liver, common bile duct, duodenum, pancreas, ampullary adenocarcinoma, Japanese macaque. Encompassing the common bile duct, head of the pancreas, and expanding and effacing the adjacent pylorus, duodenum and liver is a firm, tan, lobulated mass. Photographs courtesy of the Department of Pathobiological Sciences, School of Veterinary Medicine, University of Wisconsin – Madison, www.vetmed.wisc.edu/home.

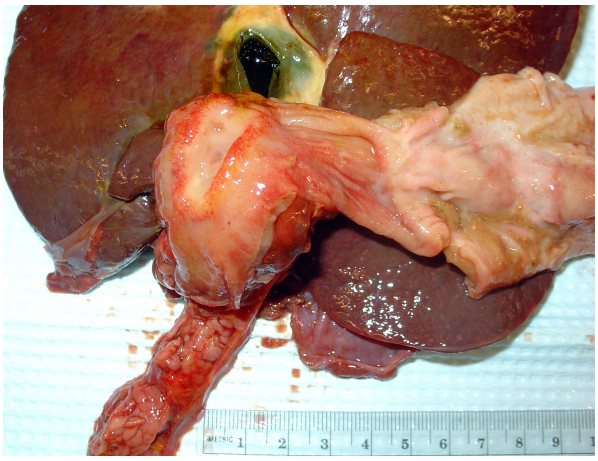

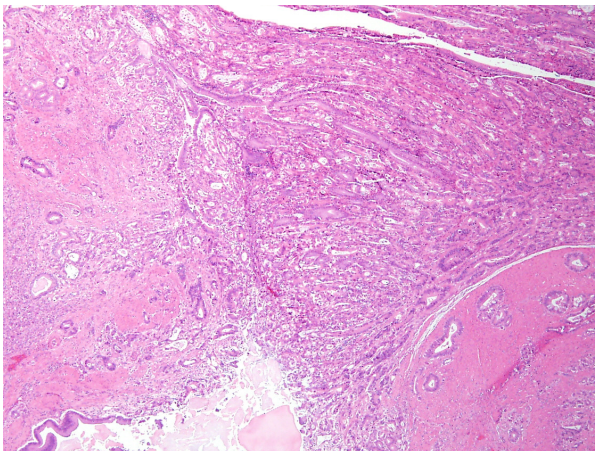

3-4. Pancreas, common bile duct, duodenum, ampullary adenocarcinoma, Japanese macaque. An epithelial neoplasm forming tubules and acini effaces the major pancreatic and common bile ducts at the opening into the major duodenal papilla (ampulla of Vater or hepatopancreatic ampulla), and multifocally extends into the duodenum and pancreas. Photograph courtesy of the Department of Pathobiological Sciences, School of Veterinary Medicine, University of Wisconsin – Madison, www.vetmed.wisc.edu/home.

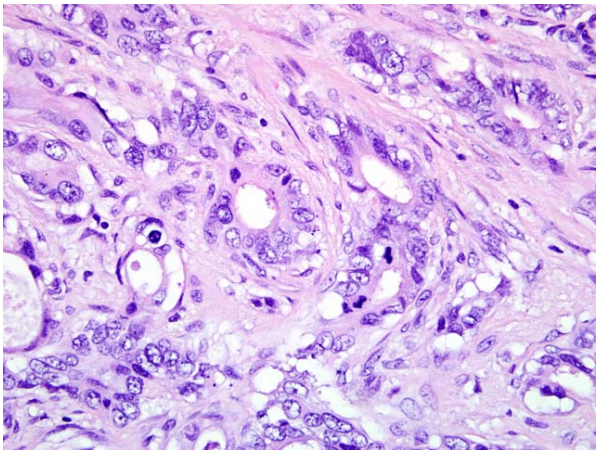

3-5. Duodenum, ampullary adenocarcinoma, Japanese macaque. Neoplastic epithelial cells are arranged in irregular tubules and acini within abundant coarse fibrous stroma with several mitoses evident. (HE, 400X)

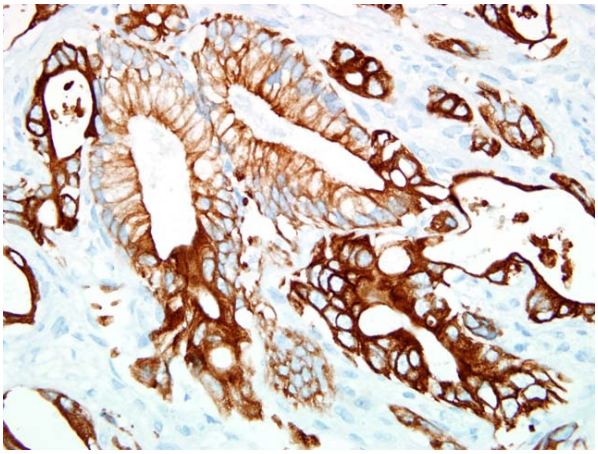

3-6. Duodenum, ampullary adenocarcinoma, Japanese macaque. Neoplastic cells demonstrate strong cytoplasmic immunoreactivity for cytokeratin 7. (CK7, 400X)

sections of liver there is severe portal bridging fibrosis with markedly accentuated lobulation of the liver. Fibrosis occasionally extends tendrils into the periportal to midzonal regions of the lobules. There are moderate numbers of lymphocytes and plasma cells scattered within the portal tracts and bile duct proliferation is marked. Moderate to marked widespread bile stasis and bile duct ectasia is present.

Contributor's Morphologic Diagnosis: 1. Ampulla of Vater (hepatopancreatic ampulla), duodenal papilla, duodenum, pancreas: Ampullary adenocarcinoma with pancreatic metastasis (local invasion).
2. Liver (not provided on submitted slide): Metastatic adenocarcinoma, portal associated and common bile duct obstruction with severe biliary ectasia and bile stasis, widespread bridging portal to portal and periportal fibrosis, bile duct hyperplasia, and portal lymphoplasmacytic hepatitis.

Contributor's Comment: The ampulla of Vater, also referred to as the hepatopancreatic ampulla, is the site of convergence of the common bile duct and pancreatic duct within the major duodenal papilla. Ampullary adenocarcinoma is a recognized entity that is well described in humans and has been reported in a group of aged rhesus macaques (*Macaca mulatta*).[4,5] Adenocarcinoma of the hepatopancreatic ampulla has also been reported in a domestic cat.[3] In humans, adenocarcinoma arising from the ampulla of Vater has been reported in association with familial adenomatous polyposis.[2] The etiology in non-human primates is uncertain.

The Japanese macaque in this report was clinically diagnosed with obstructive jaundice. One month prior to any clinical evidence of jaundice, the animal was diagnosed with bilirubinuria. Bilirubinuria indicates obstruction to bile flow with conjugated bilirubin spilling into the blood. Due to the low renal threshold for conjugated bilirubin, bilirubin can be detected prior to detection of bilirubinemia and prior to clinically recognized jaundice. Increased liver enzymes supported the diagnosis of cholestasis (GGT and ALP) and indicated hepatocellular injury (AST, ALT), which can occur secondary to the damaging effects of bile acids on hepatocytes. The decrease in total protein in this patient was due to decreased albumin which was likely secondary to decreased hepatic production. Since approximately 40% of the body's total calcium is bound to albumin, hypoalbuminemia can result in hypocalcemia as seen in this case.

AFIP Diagnosis: Small intestine; hepatopancreatic ampulla; and pancreas: Ampullary adenocarcinoma, favor pancreatobiliary origin.

Conference Comment: Conference participants discussed the possible origin of this neoplasm, including intestinal, pancreatic, biliary, and pancreatobiliary sites. Based on the histomorphologic features of the neoplasm most participants preferred pancreatobiliary origin. A recent human pathology immunohistochemical reference reports that epithelial tumors of intestinal origin are typically immunopositive for CK20 and CDX2, while pancreatobiliary types are immunopositive for CK7, MUC1 and MUC5a.[1] In this case, immunohistochemical stains performed at the AFIP demonstrated positive immunoreactivity for CK7. In humans, distinguishing between intestinal type and pancreatobiliary type ampullary adenocarcinomas is clinically important, as the latter are more aggressive and are associated with a less favorable prognosis.[1]

This case was also studied in consultation with the AFIP Department of Gastrointestinal Pathology; the subspecialty pathologists from that department also favored the diagnosis of ampullary adenocarcinoma of pancreatobiliary origin based on the mixture of well-formed ductal structures and small infiltrative nests. The gastrointestinal specialty pathologists interpreted the involvement of the duodenal mucosa as local invasion of malignant epithelial cells, although they could not completely exclude the possibility of a primary neoplasm arising in the duodenum.

The comprehensive clinical pathology data and corresponding interpretation from the contributor provide an informative synopsis of the effects of hepatic disease on various clinical chemistry parameters.

We would like to thank the Department of Gastrointestinal Pathology, AFIP, for their review of this case, and specifically Dr. Nancy Dow for her comments.

Contributor: Department of Pathobiological Sciences, School of Veterinary Medicine, University of Wisconsin – Madison
www.vetmed.wisc.edu/home

References:
1. Basturk O, Farris AB III, Adsay NV. Immunohistology of the pancreas, biliary tract, and liver. In: Dabbs DJ, ed. *Diagnostic Immuhistochemistry: Theranostic and Genomic Applications*. Philadelphia, PA: Saunders Elsevier; 2010:563-564.
2. Bjork J, Akerbrant H, Iselius L, et al. Periampullary adenomas and adenocarcinomas in familial adenomatous polyposis: Cumulative risks and *APC* gene mutations. *Gastroenterol*. 2001;121:1127-1135.
3. Haines VL, Brown PR, Hruban RH, et al. Adenocarcinoma of the hepatopancreatic ampulla in a domestic cat. *Vet Pathol*. 1996;33:439-441.
4. Schirmacher P, Buchler MW. Ampullary adenocarcinoma-differentiation matters. *BMC Cancer*. 2008;8:251.
5. Usborne AL, Bolton ID. Ampullary carcinoma in a group of aged Rhesus Macaques (*Macaca mulatta*). *Comp Med*. 2004;54(4):438-442.

CASE IV: A17366 (AFIP 3168008).

Signalment: Young male golden pheasant (*Chrysolophus pictus*).

History: Second young male that died 2 weeks after purchase.

Gross Pathology: The caeca were dilated with multiple small areas of necrosis of the mucosa and thickening of the mucosa.

Laboratory Results: Immunohistochemical staining for smooth muscle actin was positive.

Histopathologic Description: Cecum: The submucosa and the tunica muscularis contain multiple ascarid larvae. They have pronounced cuticles with lateral alae. The coelomyarian muscles are cylinder-shaped and divided in two sections by large lateral chords. Some cross sections contain eosinophilic glands associated with the lateral chords. The intestine consists of large uninucleated columnar cells. Some thick-shelled eggs are present in the lamina propria. Around some parasites, there is a granulomatous inflammation present with necrosis, multinucleated giant cells and heterophils.

Around most of the larvae there is a large unencapsulated, well-demarcated, infiltrative, multilobular, densely cellular mass. The cells are closely packed and growing in bundles and whorls separated by fine fibrovascular stroma. The cells are spindled and large, with a moderate amount of fibrillar eosinophilic cytoplasm which is sometimes vacuolated, and have indistinct borders and central oval nuclei with vesicular chromatin and a prominent nucleolus. The cells and nuclei show moderate variation. Mitoses are 0-1 per HPF.

The epithelium and the crypts show necrosis with infiltration of heterophils. The lamina propria shows a diffuse mixed infiltration of inflammatory cells.

Contributor's Morphologic Diagnosis: 1. Cecum, nodular granulomatous typhlitis and presence of multiple *Heterakis* larvae.
2. Cecum, leiomyoma.

Contributor's Comment: *Heterakis gallinarum* is a widespread parasite with a prevalence up to 90% in pheasants.[1,2] The parasite has a direct life cycle and can cause tissue damage in the ceca of infected birds. The infective eggs can host *Histomonas meleagridis* which causes blackhead disease.

The main lesion in the intestinal wall is the presence of granulomatous nodules in the cecal wall, mostly in the submucosa. Sometimes, the lesions are accompanied by neoplastic nodules in the submucosa or the muscular tunic. The neoplastic nodules can be of variable origin, fibrous hyperplastic tissue, fibrohistiocytic nature and leiomyomas have been described. In this case the nodule was a leiomyoma based on immunohistochemical staining , which is believed to be induced by immature specimens of *Heterakis* spp.[2]

AFIP Diagnosis: Cecum: Typhlitis, transmural, granulomatous, multifocally extensive, marked, with atypical nodular mesenchymal proliferation, and nematode adults, larvae and eggs, etiology consistent with *Heterakis* species.

Conference Comment: Conference participants were equally divided between assigning a morphologic diagnosis of leiomyoma versus a nodular mesenchymal proliferation. All participants agreed with the interpretation of a benign nodular spindle cell proliferation with smooth muscle

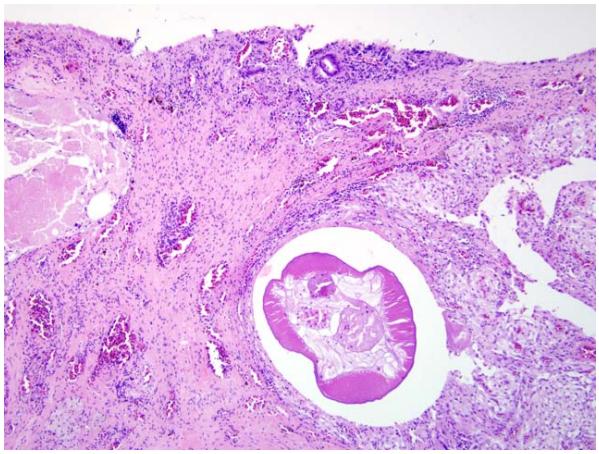

4-1. Cecum, golden pheasant. Within the submucosa, tunica muscularis, and cecal lumen are several adult ascarids surrounded by nodules and whorls of proliferative spindle cells. (HE 40X)

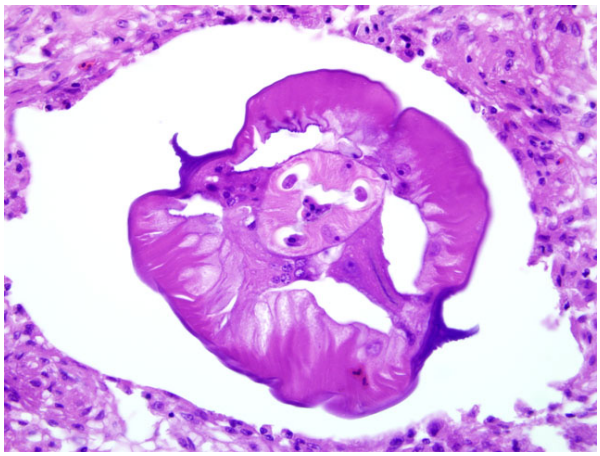

4-2. Cecum, golden pheasant. Adult ascarids have prominent lateral alae, lateral chords, coelomyarian musculature, and an intestine lined by few uninucleate columnar cells. (HE 400X)

features in association with the nematode, but many did not interpret the proliferative lesion as neoplastic, thus the histologic diagnosis of atypical mesenchymal nodular proliferation. A Masson's trichrome stain performed at the AFIP demonstrated the presence of abundant collagen with light staining for muscle within the lesion in the mesenchymal nodules. Additionally, the proliferative spindle cells were negative for smooth muscle by tissue immunohistochemistry in our laboratory. We interpret these findings as more suggestive of a reactive myofibroblastic proliferation vice smooth muscle neoplasia in the case of this pheasant.

Most conference participants favored *Heterakis isoloncheas* the etiology, though all included *H. gallinarum* as a differential diagnosis. In general, *H. gallinarum* more commonly parasitizes domestic poultry and, other than carrying *Histomonas meleagridis*, it is not usually associated with pathologic changes. *Heterakis isoloncheis* a pathogenic parasite of game birds, especially pheasants, and causes typhlitis, nodular proliferations and diarrhea.[3] A presumptive diagnosis of *H. isoloncheca* be made during necropsy by the presence of the parasite within cecal nodules. Definitive differentiation between the two species requires histologic examination and is based on the presence of spicules of either unequal or equal length in *H. gallinarum* and *H. isoloncher*espectively.[3]

Contributor: Laboratory of Veterinary Pathology, Faculty of Veterinary Medicine UGENT, Salisburylaan 133 9820 Merelbeke, Belgium

References:

1. Draycott RAH, Parish DMB, Woodburn MIA, Carroll JP. Spring survey of the parasite *Heterakis gallinarum* in wild-living pheasants in Britain. *Vet Rec*. 2000;147:245-246.
2. Menezes RC, Tortelly R, Gomes DC, Pinto RM. Nodular typhlitis associated with the nematodes *Heterakis gallinarum* and *Heterakis isoloncheis* pheasants: Frequency and pathology with evidence of neoplasia. *Mem Inst Oswaldo Cruz*. 2003;98(8):1011-1016.
3. Urquhart GM, Armour J, Duncan JL, Dunn AM, Jennings FW. Veterinary helminthology. In: *Veterinary Parasitology*. 2nd ed. Cambridge, MA: Blackwell Science, Inc.; 1996:76-77.

The Armed Forces Institute of Pathology
Department of Veterinary Pathology

Conference Coordinator
Matthew Wegner, DVM

WEDNESDAY SLIDE CONFERENCE 2010-2011

Conference 17

19 January 2011

Conference Moderator:
R. Keith Harris, DVM, Diplomate ACVP

Chris H. Gardiner, PhD

CASE I: NIAH2010-1 (AFIP 3164221).

Signalment: Adult, gender undetermined, whooper swan (*Cygnus cygnus*).

History: The whooper swan was found dead around the lake in Ibaraki Prefecture, Japan. The swan was submitted to our laboratory for postmortem examination in March 2006. Whooper swans move to the lakes and ponds of Ibaraki Prefecture from Siberia for their wintering period (October to March).

Gross Pathology: There were no significant gross lesions in the swan.

Laboratory Results: Neither viruses nor significant bacteria were detected by virologic and bacteriologic examination.

Histopathologic Description: Small intestine, multiple sections: Vascular lesions and schistosome infection were seen in the swan. Marked hypertrophy of the venous walls was characterized in the mesentery, serosa, and muscular layer of the intestines (duodenum, small intestine, ceca, and rectum). Venous lesions were also seen in the capsule of spleen, kidney, adrenal gland, and pancreas, as well as in the serosa of air sacs, pleura, and gallbladder; the connective tissue around the aorta; and the capsule and interlobular connective tissue of the liver. Schistosome flukes were detected in the veins but not in the arteries. In mild lesions, nodular proliferation of smooth muscle fibers was observed in the media of mesenteric and serosal veins. In moderate lesions, venous hypertrophy became more marked and the venous lumens were narrowed or occluded by proliferative smooth muscle fibers. The medial smooth muscle fibers of the veins between the muscular layers of the intestines, as well as the mesenteric veins and serosal veins, exhibited nodular or circular hypertrophy. The intestinal muscular layers were depressed and atrophied by hypertrophied veins. In severe lesions, venous hypertrophy increased in severity and distribution. The proliferation of medial smooth muscle fibers under collagen fibers was evident in the medium-sized veins of the livers. There was mild to moderate perivascular lymphocyte infiltration around the hypertrophied veins. The proliferated medial fibers were stained red in azan stain, and positively stained by immunohistochemical staining of alpha smooth muscle actin. Schistosome flukes were detected in the veins. The schistosomes had a tegument, a digestive tract, a sucker, and reproductive organs.

There were oval eggs (about 40 to 70 μm in size) in the liver and lung. The eggs had small projections on one side. Miracidia hatched from some eggs in the liver. There were granulomatous reactions around these eggs in the liver and lung. Bile pigment stained positively using Hall stain within the liver of the eight whooper swans with vascular lesions and schistosomiasis. There was mild to severe deposition of hemosiderin (Berlin blue-positive) in the liver and spleen.

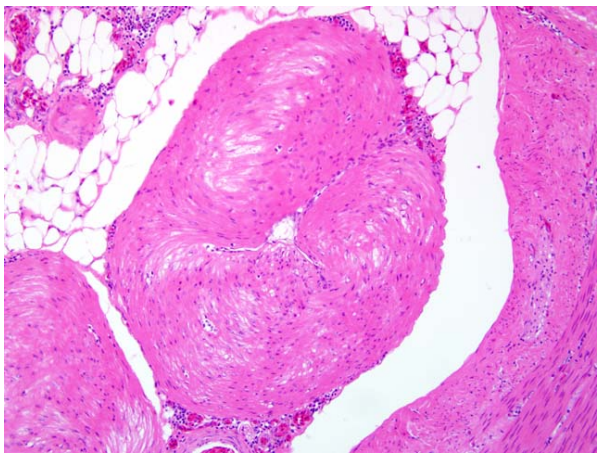

1-1. Small intestine, Whooper swan. Venous walls in the mesentery, serosa, and tunica muscularis have marked medial hypertrophy with occlusion of vessel lumina. (HE 200X)

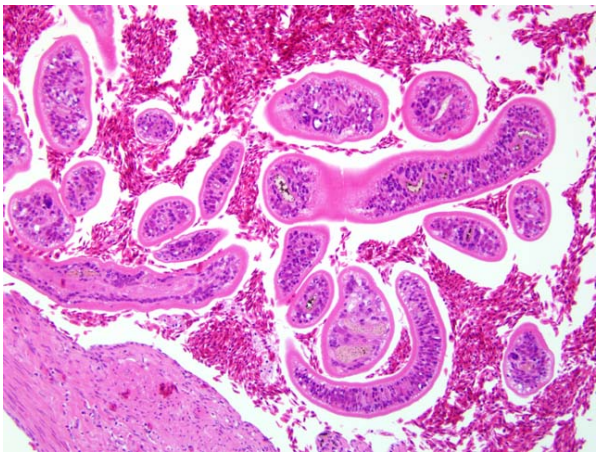

1-2. Mesenteric veins, Whooper swan. Within mesenteric veins are many adult schistosomes characterized by an eosinophilic tegument and spongy parenchyma. (HE 200X)

Contributor's Morphologic Diagnosis: Small intestine: Hypertrophy, medial, venous, severe, with intravenous schistosomes, whooper swans (*Cygnus cygnus*).

Contributor's Comment: Avian schistosomes are a specialized group of trematodes that develop as adults within the circulatory system or nasal tissue of their avian host. They include nine genera: *Allobilharzia, Austrobilharzia, Bilharziella, Dendritobilharzia, Gigantobilharzia, Jilimobilharzia, Macrobilharzia, Ornithobilharzia,* and *Trichobilharzia*.[3] *Trichobilharzia* is the largest genus within the family *Schistosomatidae*, covering roughly 40 species. *Schistosomatidae* is the only group of trematodes that has separate sexes, with most trematodes being hermaphroditic. The blood flukes found in our study appear to be avian schistosomes judging by their morphological characteristics, especially the sucker and gonochorism (separation of the sexes in different individuals).

There is a close relationship between venous hypertrophy and venous parasitism of avian schistosomes. The mechanism of venous hypertrophy is not well known. Two hypotheses for the pathogenesis are put forward.[1] In one it is due to direct irritation of the schistosomes on the venous walls, and in the other it is due to an immunological (allergic) reaction against the schistosomes. The pathological condition of veins referred to as "obliterative endophlebitis"[3] is similar to the lesions observed in the present case. The venous media consists of smooth muscle fibers, but the venous intima of veins has no smooth muscle fibers. This suggests that the pathological condition may not be "endophlebitis" but may in fact be hypertrophy of smooth muscle fibers in the media of veins.

There have been several reports of avian schistosomiasis in whooper swans, mute swans, black swans, Atlantic Brant geese, green-winged teal, blue-winged teal, and northern pintail. However, vascular lesions characterized by venous medial hypertrophy have never been described in these reports. Obstruction of venous return in the mesenteric, intestinal, and portal veins may have contributed to the emaciation and mortality of the affected whooper swans in the present study.

Deposition of hemosiderin and bile pigment with copper was present in the livers of the whooper swans in the present case. Bile pigment was observed in six of the eight whooper swans infected with avian schistosomes, and adult flukes and/or their eggs were detected in the livers. Therefore, cholestatic jaundice may be caused by avian schistosomiasis.

AFIP Diagnosis: Small intestine, tunica muscularis, serosa, and mesentery, blood vessels: Vasculitis, proliferative and lymphoplasmacytic, multifocal, severe, with intravenous adult schistosomes.

Conference Comment: Much of the conference discussion centered on whether the proliferative vascular lesions were smooth muscle or myofibroblastic in origin. The Masson's trichrome stain demonstrated intense red staining of the vascular walls consistent with smooth muscle proliferation. This finding is similar to the vascular changes seen in humans with hepatic schistosomiasis.

Conference participants also discussed the possibility that the observed lesions might be age-related, as the age of the swans is not known. Severe hepatic infections in humans with *Schistosoma mansoni* or *S. japonicum* typically result in multiple granulomas, marked fibrosis and enlargement of portal areas resulting in the lesion colloquially known as "pipe-stem fibrosis."[2,4] Portal veins are frequently obliterated in such cases, and portal arteries often show muscular hypertrophy and intimal sclerosis. Schistosome eggs may travel to the lungs, producing granulomatous pulmonary arteritis, intimal hyperplasia, and progressive arterial obstruction. Histologic lesions in the arteries include granulomatous and fibrosing disruption of the elastic layer.[4]

Contributor: Research Team for Viral Diseases, National Institute of Animal Health, 3-1-5 Kannondai, Tsukuba, Ibaraki 3050856, Japan
http://niah.naro.affrc.go.jp/index.html

References:

1. Akagami M, Nakamura K, Nishino H, Seki S, Shimizu H, Yamamoto Y. Pathogenesis of venous hypertrophy associated with schistosomiasis in whooper swans (*Cygnus cygnus*) in Japan. *Avian Dis*. 2010;54:146-150.
2. Cheever AW, Neafie RC. Schistosomiasis. In: Meyers WM, Heafie RC, Marty AM, Wear DJ, eds. *Pathology of Infectious Diseases, Volume 1: Helminthiases.* Washington, DC: Armed Forces Institute of Pathology, American Registry of Pathology; 2000:23-47.
3. Huffman JE, Fried B. Schistosomes. In: Atkinson CT, Thomas NJ, Hunter DB, eds. *Parasitic Diseases of Wild Birds*. Hoboken, NJ: Wiley-Blackwell; 2008:246-260.
4. McAdam AJ, Sharpe AH. Infectious diseases. In: Kumar V, Abbas AK, Fausto N, Aster JC, eds. *Robbins and Cotran Pathologic Basis of Disease*. 8th ed. Philadelphia, PA: Elsevier Saunders; 2009:393-394.
5. van Bolhuis GH, Rijks JM, Dorrestein GM, Rudolfova J, van Dijk M, Kuiken T. Obliterative endophlebitis in mute swans (*Cygnus olor*) caused by *Trichobilharzia* sp. (Digenea:*Schistosomatidae)* infection. *Vet Pathol*. 2004;41:658-665.

CASE II: 09-14541 (AFIP 3164906).

Signalment: 3-year-old intact male quarterhorse, equine (*Equus caballus*).

History: The reported history included neurological signs of one week duration. The owner noticed drooling, staggering and reddened eyes. The horse was euthanized at the veterinary teaching hospital.

Gross Pathology: The horse was in good body condition, with well developed musculature and adequate adipose tissue stores. The right cranial and middle lung lobes were dark red, firm and heavy. Moderate amounts of serosanguineous fluid were exuded on the cut surfaces of these lobes. The trachea and major bronchi were filled with large amounts of stable white foam. Mild cerebellar coning was observed, and the leptomeninges were moderately congested.

Histopathologic Description: Brain stem: The brain stem contains multifocal areas of necrosis in the white and grey matter. Many foamy macrophages and lesser numbers of lymphocytes and plasma cells infiltrate affected areas. The cytoplasm of many neurons, astroglial cells and Gitter cells often contain free zoites or protozoal cysts with faint walls (schizonts) approximately 20-30 microns in size and filled with many elongated 2 x 5 µm basophilic merozoites. These each contain a small apically located nucleus. Affected neurons are swollen, hypereosinophilic and often pyknotic, with diffuse chromatolysis. White matter contains randomly scattered dilated axon sheaths and spheroids (Wallerian degeneration). Many degenerate axons are invaded by Gitter cells (digestion chambers). Astrocytes multifocally are increased in numbers and appear swollen, with enlarged amount of cytoplasm (reactive astrocytosis). Glial nodules composed of microglial cells are also present. Blood vessels are severely congested. Perivascular spaces are invaded by many lymphocytes, plasma cells and macrophages forming 5-8 cell layer thick perivascular cuffs. Rare multinucleated giant cells are randomly scattered in the neuropil.

Lung (not included): Alveolar spaces, bronchioles and bronchi are with many degenerate neutrophils mixed with fewer macrophages, lymphocytes and cellular debris, fibrin and extravasated erythrocytes. Interlobular septa and pleura

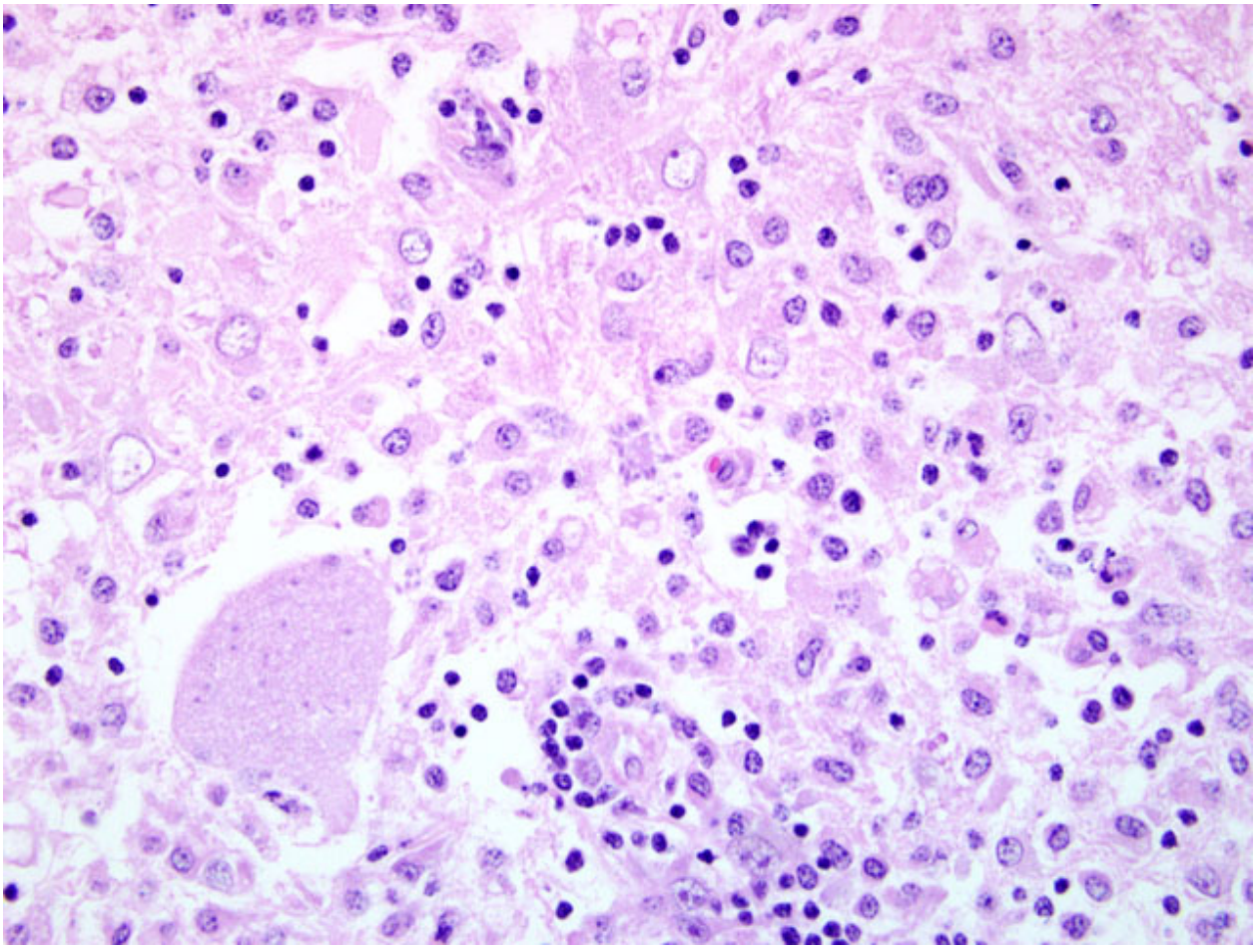

2-1. Brain stem, horse. The white matter is rarefied (necrotic) and replaced by reactive astrocytes, Gitter cells, lymphocytes, and macrophages, with frequent swollen esosinophilic axons (spheroids). (HE 400X)

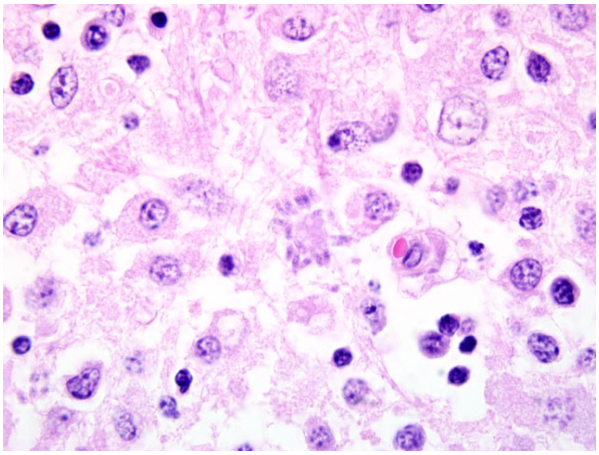

2-2. Brain stem, horse. A ruptured protozoal cyst has released elongated merozoites into the white matter. (HE 1000x)

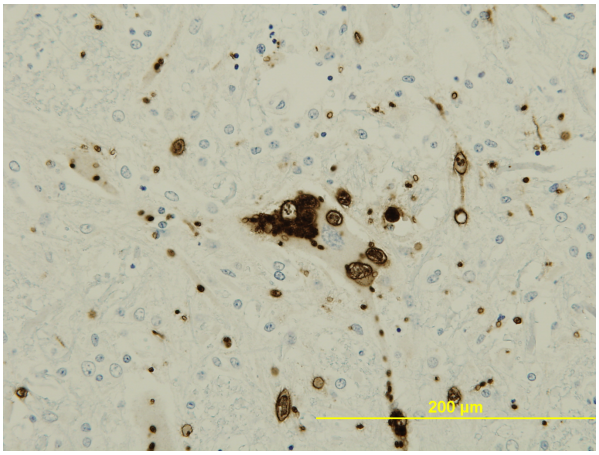

2-3. Brain stem, horse. By immunohistochemistry neurons, astroglial cells, and macrophages are positive for Sarcocystis neurona. Photograph courtesy of Department of Pathobiology, College of Veterinary Medicine, University of Illinois at Urbana-Champaign, http://vetmed.illinois.edu/path

are markedly expanded by clear spaces (edema). Diffusely alveolar spaces are filled with pale proteinaceous fluid material. Blood vessels are moderately congested, and lymphatics are markedly dilated. Coccoid bacterial colonies mixed with small amounts of plant material are scattered randomly in the parenchyma.

Contributor's Morphologic Diagnosis: 1. Brain stem: Encephalitis, necrotizing, granulomatous and lymphoplasmacytic, with gliosis and intralesional protozoal organisms (*Sarcocystis* spp.).
2. Right lung lobes (not submitted): Bronchopneumonia, suppurative, severe, lobar.

Contributor's Comment: Immunohistochemistry for *Sarcocystis neurona* demonstrated positive staining in many neurons, astroglial cells and macrophages within the brain stem. Gomori's methenamine silver stain failed to demonstrate the presence of fungal microflora within sections. *Sarcocystis neurona* is a cause of equine protozoal myeloencephalitis (EPM) in horses; it belongs to cyst-forming coccidia (Apicomplexa: Sarcocystidae). Identical disease is possible due to *Neospora caninum* and *Neospora hughesi*. Horses are considered to be aberrant dead-end hosts of *S. neurona*, whereas armadillos, sea otters, raccoons, skunks and cats are natural intermediate hosts. They become infected when they consume food or water contaminated with protozoal sporocysts. Opossums (*Didelphis* spp.) are believed to be the only definitive host capable of shedding infective sporocysts. Horses of all ages are susceptible to the disease, especially in the summer and fall. Sexual reproduction occurs in the intestinal epithelium of the definitive hosts; infective oocysts, each with two sporocysts, are shed in feces. After ingestion by the intermediate host, sporozoites are released and penetrate intestinal wall and initiate asexual reproduction (schizogony). The forms of asexual reproduction are schizonts and merozoites. The ultimate stage of the asexual reproduction is formation of sarcocysts, usually in the skeletal muscles. Very often, infective sarcocysts (700 µm long and 40 µm wide, with a 1-2 µm thick cyst wall and 5 µm long bradyzoites) can be found in the tongue and other skeletal muscles.

AFIP Diagnosis: Brain stem: Encephalitis, necrotizing, focally extensive, severe, with apicomplexan protozoa.

Conference Comment: Dr. Fabio Del Piero, who attended this conference as a participant, commented that he observes two distinct clinicopathologic presentations of equine sarcocystosis at his diagnostic laboratory. The first syndrome, much like this case, is fulminant and usually occurs in untreated animals in which low numbers of eosinophils are frequently observed in the affected areas of the central nervous system. The second form typically occurs in treated animals, and the histopathologic presentation is usually that of mild lymphocytic encephalitis resembling viral infections. These latter cases, in which definitive etiologic diagnosis is more difficult, are becoming increasingly more common in his experience.

The ultrastructural characteristics of *Sarcocystis* spp. and *Toxoplasma* spp. are distinctive, allowing differentiation between the two organisms. *Sarcocystis* spp. schizonts and merozoites reside within the host cell cytoplasm; no parasitophorous vacuole is present. *Sarcocystis* spp. merozoites have micronemes, a conoid, apical rings and polar rings, but lack rhoptries. *Toxoplasma* spp. tachyzoites reside within an intracellular parasitophorous vacuole and have an inner and outer membrane (pellicle); merozoites possess an anterior apical complex containing a polar ring characterized by a slight thickening continuous with the inner membrane surrounding the anterior opening; an anterior conoid inside the polar ring; rhoptries; and micronemes.

Contributor: Department of Pathobiology, College of Veterinary Medicine, University of Illinois at Urbana-Champaign, 2001 S. Lincoln Ave, Urbana, IL 61802
http://vetmed.illinois.edu/path/

References:

1. Maxie MG, Youssef S. Nervous system. In: Maxie MG, ed. *Jubb, Kennedy, and Palmer's Pathology of Domestic Animals*. Vol. 1, 5th ed. Philadelphia, PA: Elsevier Ltd; 2007:435.

2. Zachary JF. Nervous system. In: McGavin MD, Zachary JF, eds. *Pathologic Basis of Veterinary Disease*. 4th ed. St. Louis, MO: Elsevier; 2007:893-896.

3. Dubey JP, Lindsay DS, Saville WJ, Reed SM, Granstrom DE, Speer CA. A review of *Sarcocystis neurona* and equine protozoal myeloencephalitis (EPM). *Vet Parasitol*. 2001;95:89-131.

CASE III: 07-974 (AFIP 3166496).

Signalment: 5-year-old male miniature pinscher, canine (*Canis familiaris*).

History: This dog was presented 1½ weeks prior to necropsy with tetraparesis (worse on left side), non-weight bearing on left forelimb, and decreased withdrawal and hopping reflexes in left forelimb and eventually left hindlimb. Cervical pain was also observed. It was treated with dexamethasone and the condition continued to deteriorate. Horner's syndrome was observed on the left side. The dog was euthanized due to poor prognosis.

Gross Pathology: A complete gross examination, including the spinal nerves, brachial and lumbosacral plexuses and skeletal muscles was done. No significant changes were noted.

Laboratory Results: Immunoperoxidase on spinal cord sections was performed for *Neospora caninum* and *Toxoplasma gondii*.

Histopathologic Description: Spinal cord, cervical (per contributor): The submitted section is a transverse section of the spinal cord at the C4 level (stained with hematoxylin, phloxin, eosin and saffranin). There is a severe chronic necrotizing myelitis affecting mainly the peripheral portion of most funiculi (white matter), with associated non-suppurative leptomeningitis; the gray matter is only mildly and focally involved in most sections. The lesion is asymmetrical, being more extensive on the left side. It is characterized by vacuolization and loss of neuropil, with numerous gitter cells and variable numbers of neutrophils and perivascular lymphocytes and plasma cells. The leptomeningeal inflammation is mainly lymphoplasmacytic. In some areas there is leptomeningeal fibrosis that extends into the subjacent parenchyma (mostly perivascular), with gliosis. In the ventral horns, there is variable inflammation and occasional neurons demonstrate diffuse chromatolysis. The ventral nerve roots have some Wallerian degeneration and mild inflammation. In the affected white matter, there are several to numerous, round to ovoid, protozoal organisms, roughly 5 µm in diameter, that occurs either within thin-walled cysts (bradyzoites) or individual tachyzoites.

Contributor's Morphologic Diagnosis: Severe and extensive chronic necrotizing myelitis with intralesional protozoal organisms.

Contributor's Comment: Immunoperoxidase identified the protozoal organisms as *Neospora caninum*. The spinal lesions extended from C3 to T4; similar lesions were observed in the cerebellar gray matter and medulla. Lesions were not found in other organs examined.

Neospora caninum is a coccidian parasite of worldwide distribution that has a wide host range. It is very similar in structure and life cycle to *Toxoplasma gondii*, and was misdiagnosed as *T. gondii* until 1988, when Dubey *et al.* described and named this new genus and species.[2] Neosporosis was first described in 1984 in a litter of boxer dogs in Norway. It is a polysystemic protozoal disease that has been reported in several mammalian species;[2,3] in domestic animals, it is a cause of abortion mainly in cattle (also in sheep and goats), a serious disease of dogs and one of the causes of equine protozoal encephalomyelitis. Seropositivity has been observed in humans, but has not been associated with clinical disease; the parasite has never been detected in human tissues, and thus no zoonotic potential has been shown so far (in contrast to toxoplasmosis).[2] *Neospora caninum* has three known infectious stages: tachyzoites, bradyzoites (tissue cysts) and oocysts. Animals with neosporosis act as intermediate hosts in which tachyzoites and bradyzoites are formed by asexual reproduction. Only dogs and coyotes are known definitive hosts, i.e. species in which fecal excretion of oocysts occurs.[2]

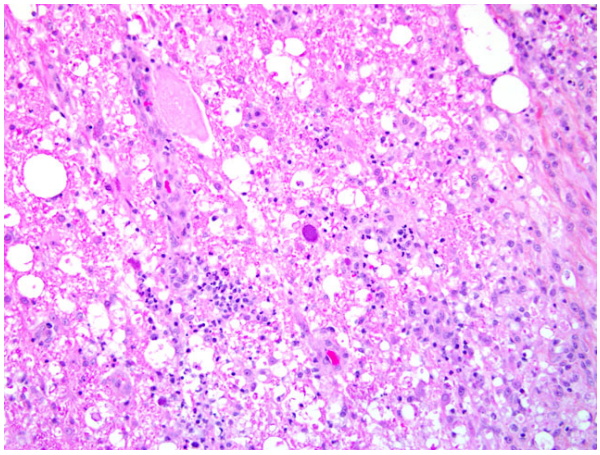

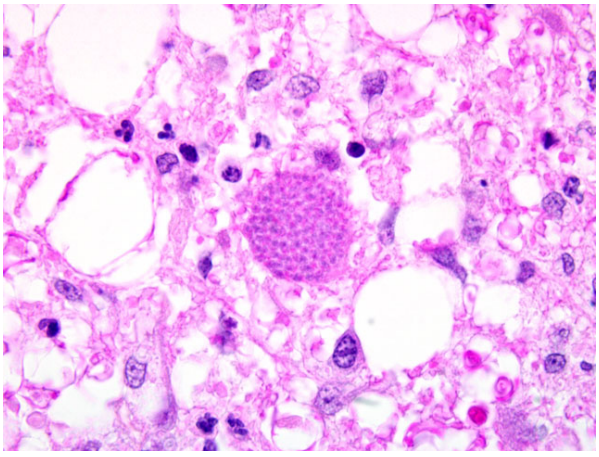

3-1, 3-2. Cervical spinal cord, dog. In the peripheral funiculi there is spongiosis and rarefaction of the neuropil (necrosis) and infiltration by many macrophages, lymphocytes and neutrophils; inflammatory cells are also present in the leptomeninges and ventral nerve roots. Thin-walled protozoal cysts containing bradyzoites are surrounded by inflammatory cells. (HE 200X, 1000X)

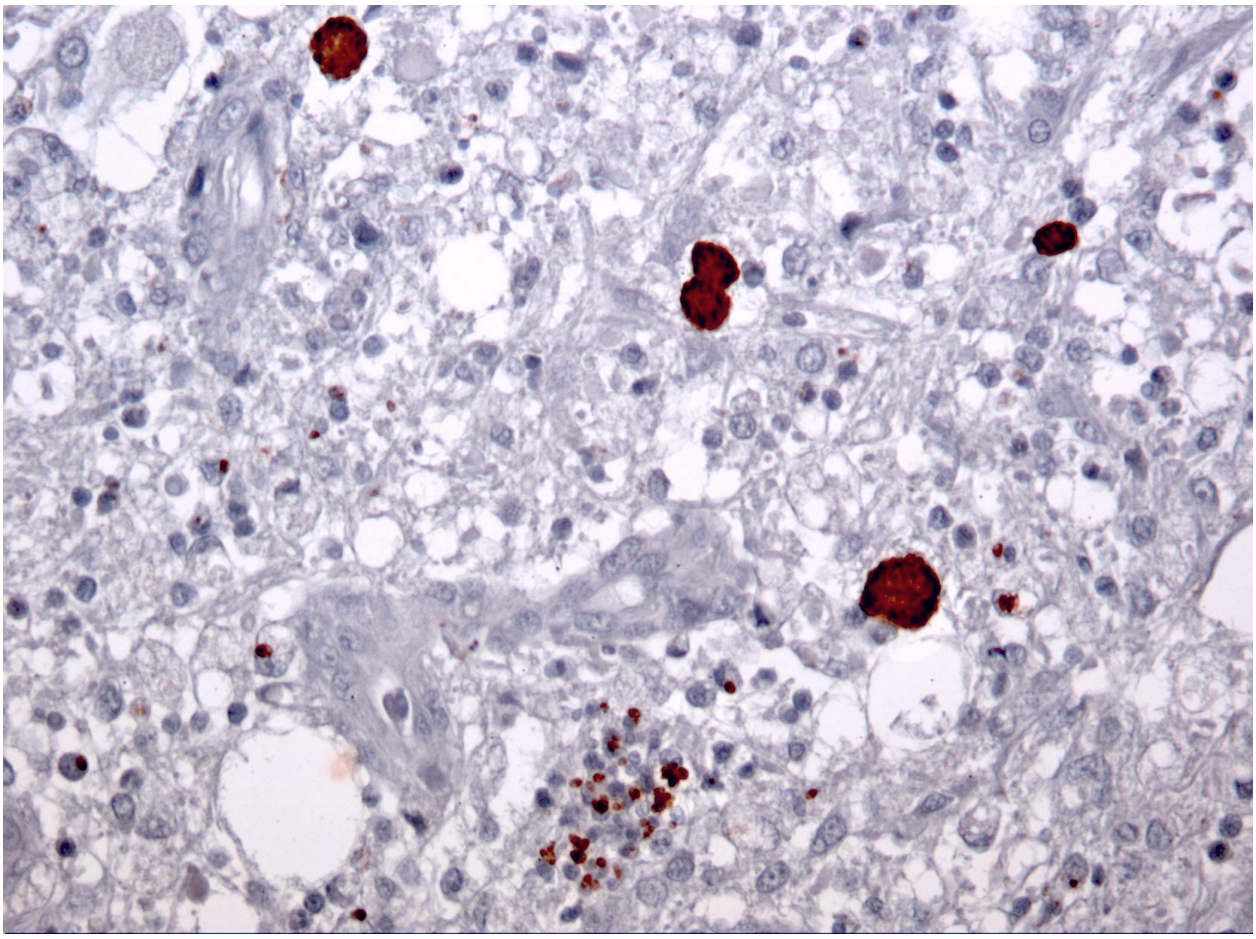

3-3. Cervical spinal cord, dog. By immunohistochemistry protozoal tachyzoites and bradyzoites are positive for Neospora caninum. *Photograph courtesy of the Department of Pathology and Microbiology, Faculty of Veterinary Medicine, University of Montreal, www.medvet.umontreal.ca.*

Horizontal and vertical transmission has been demonstrated. Herbivores are thought to become infected by ingestion of oocysts. Although dogs (and other carnivores) can become infected by ingesting bradyzoite-containing tissues, transplacental infection is believed to be the most common route of transmission.[2,3] Tissue cysts are found mainly in the CNS but also may be found in extraneural tissues, especially skeletal muscles.[2]

Canine neosporosis has been reported in dogs of all ages, but the most severe cases have been reported in dogs less than six months of age. Although lesions have been reported in a variety of organs/tissues, e.g. heart, lung, liver, pancreas and skin, the nervous system and skeletal muscles are most consistently involved.[1,2,3] In puppies, ascending hindlimb paresis/paralysis with muscular atrophy and often arthrogryposis is the most frequent clinical presentation and is mostly due to polyradiculoneuritis and myositis; several littermates can be affected.[1,3] Systemic involvement may be present; myocarditis can cause sudden death. In adults, neurological signs usually reflect widespread CNS involvement, and include paresis/paralysis, ataxia, head tilt and seizures which are associated with a multifocal encephalomyelitis. A recent paper shows that neosporosis is a significant cause of progressive cerebellar ataxia in adult dogs.[3] *Neospora caninum* is considered a primary pathogen, but disease may be exacerbated by corticosteroid therapy.[1] Encephalomyelitis in canine neosporosis is nonsuppurative with varying degrees of necrosis and gliosis; tachyzoites and bradyzoites are seen in neurons and neuropil (intracellular). Although *Neospora* has a thicker cyst wall than *Toxoplasma*, they cannot be reliably differentiated by light microscopy, and immunohistochemistry is required; they can also be differentiated with transmission electron microscopy.

AFIP Diagnosis: Spinal cord and spinal nerve roots: Myelitis and polyradiculoneuritis (radiculitis), necrotizing and neutrophilic, multifocal to coalescing, severe, with nonsuppurative meningitis and many protozoal cysts.

Conference Comment: In addition to the various manifestations in dogs mentioned by the contributor, conference participants also discussed the syndrome of bovine abortion due to *Neospora caninum*. Infection in bovids results from consuming oocysts shed in the feces of canids. Infection does not affect fertilization, and pregnant animals typically abort between the 5th and 6th month of gestation. Interestingly, immunity does not prevent

transplacental infection; therefore, infected cows can abort up to three consecutive pregnancies. Fetuses are expelled in various states of tissue preservation with minimal gross lesions. When present, gross lesions in the fetus consist of random, yellow-tan foci in the brain, heart and skeletal muscle. Grossly, the cotyledons are necrotic with sparing of the intercotyledonary areas. Histologically, in the central nervous system of the fetus there is necrosis of the neuropil with mononuclear inflammatory infiltrates and occasional mineralization; protozoal cysts are more commonly found within the spinal cord rather than in the brain. In addition to localization within brain and spinal cord, intracellular zoites may be found in both cardiomyocytes and Purkinje fibers in the heart.[5]

Rarely dogs, especially immunocompromised adults, can exhibit cutaneous neosporosis which produces either multifocal ulcerative and nodular dermatitis. Dermatitis is often a pyogranulomatous and eosinophilic, or necrotizing and hemorrhagic. Although tissue cysts are absent in the skin in the cutaneous form of the disease, zoites can be found in histiocytes, keratinocytes, neutrophils, endothelial cells and fibroblasts.[4]

Contributor: Department of Pathology and Microbiology, Faculty of Veterinary Medicine, University of Montreal, 3200, Sicotte, C.P.5000, St-Hyacinthe, Quebec, Canada, J2S 7C6
http://www.medvet.umontreal.ca

References:

1. Brown CC, Baker DC, Barker, IK. Alimentary system. In: Maxie MG, ed. *Jubb, Kennedy and Palmer's Pathology of Domestic Animals*. Vol. 2, 5th ed. Philadelphia, PA: Elsevier Ltd; 2007:272-273.
2. Dubey JP, Schares G, Ortega-Mora. Epidemiology and control of neosporosis and *Neospora caninum*. *Clin Microbiol Rev*. 2007;20(2):323-367.
3. Garosi L, Dawson A, Couturier J, et al. Necrotizing cerebellitis and cerebellar atrophy caused by *Neospora caninum* infection: Magnetic resonance imaging and clinicopathopathologic findings in seven dogs. *J Vet Intern Med*. 2010;24:571-578.
4. Ginn PE, Mansell JEKL, Rakich PM. Skin and appendages. In: Maxie MG, ed. *Jubb, Kennedy and Palmer's Pathology of Domestic Animals*. Vol. 1, 5th ed. Philadelphia, PA: Elsevier Ltd; 2007:711.
5. Schlafer DH, Miller RB. Female genital system. In: Maxie MG, ed. *Jubb, Kennedy and Palmer's Pathology of Domestic Animals*. Vol. 3, 5th ed. Philadelphia, PA: Elsevier Ltd; 2007:514-516.

CASE IV: HSRL-425 ZC09-447 (AFIP 3167231).

Signalment: Adult female California sea lion, pinniped (*Zalophus californianus*).

History: Found stranded on the beach, with repeated seizuring episodes. During the rehabilitation, the animal was becoming progressively weaker in spite of treatment and died 7 days later. No seizures were reported during rehabilitation.

Gross Pathology: At postmortem the stomach showed several raised and thick crater-like ulcers containing several nested round pale yellowish (2-5 cm long, 0.1 to 0.2 cm in diameter) worms. There were numerous round worms mixed with digested blood and mucus in the gastric lumen. The gastric and mesenteric lymph nodes were severely enlarged and blackened.

Other findings in the postmortem examination included marked perianal and rear limb edema. The thoracic cavity was filled with 3 - 4 liters of thick, hemorrhagic fluid. The abdominal cavity contained approximately 200 milliliters of serosanguineous fluid.

Laboratory Results: Leukocytosis and anemia.

Histopathologic Description: Stomach, glandular: The gastric mucosa has a locally extensive ulcerated area with extensive necrosis and inflammation. Within the inflammatory process, there are several sections of degenerate cuticular fragments of nematode parasites. The cuticle shows regularly spaced ridges. The parasite is characterized by a body cavity lined by coelomyarian muscles with prominent hypodermis with lateral cords. The inflammatory cells are predominantly degenerative neutrophils (nuclear streaming), macrophages, and occasional eosinophils. Beneath the ulcerative lesion there is a thick layer of granulation tissue with extensive fibrosis and neovascularization that replaces the submucosa and extends to the tunica muscularis. There are multifocal aggregates and clusters of mainly lymphocytes and plasma cells mixed with moderate numbers of macrophages in between the collagen bundles and fibroblasts. The surrounding, less affected mucosa of the glandular stomach is severely congested and contains moderate amounts of superficial hemorrhage. Scattered throughout the mucosa there is a superficial layer of necrotic tissue mixed with fibrillar acellular eosinophilic material (interpreted as fibrin), mixed with a large number of degenerative neutrophils, eosinophils and red blood cells. In some slides submucosal blood vessels show transmural focal areas of mineralization.

(Note: Not all slides have cross sections of the parasite).

Contributor's Morphologic Diagnosis: Stomach: Chronic severe locally extensive ulcerative gastritis with intralesional nematodes and marked granulation tissue.

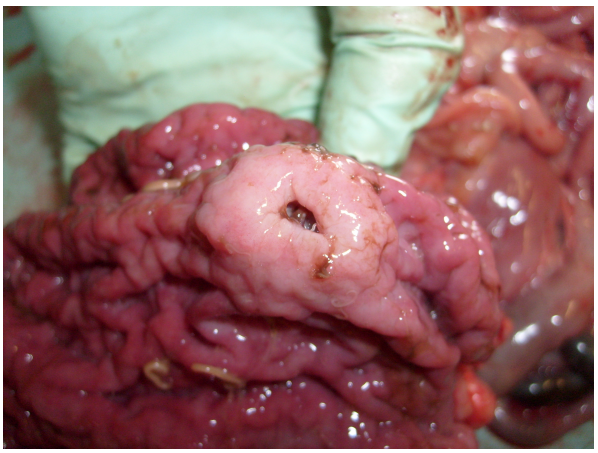

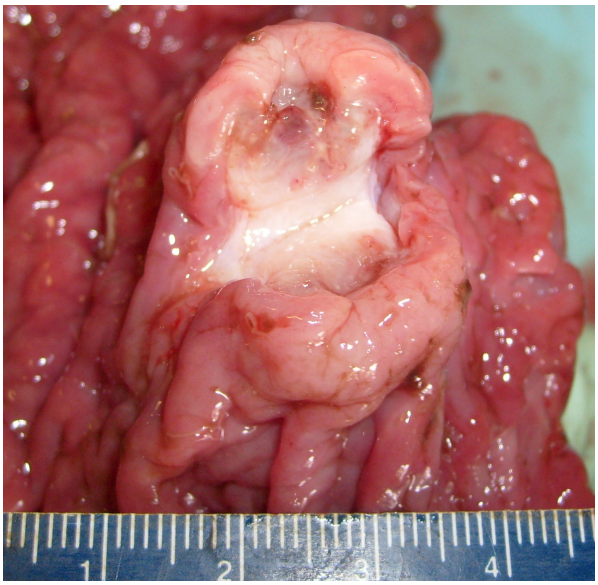

4-1, 4-2. Stomach, California sea lion. Multifocally there are crateriform ulcers within the stomach mucosa. Adult and larval roundworms are present in the mucosa. Photographs courtesy College of Veterinary Medicine, Western University of Health Sciences, Pomona, CA, www.western.edu/xp/edu/veterinary/staff.xml

Contributor's Comment: Gastric ulcers are common necropsy findings in California sea lions (*Zalophus californianus*). The ulcerative lesions are mainly associated with nematodes. The majority of these roundworm infestations are from the family *Anisakidae* (large roundworms). Pinnipeds are typically dead-end hosts for most stomach worms, acquiring them from other aquatic animals (copepods or fish).[3] Animals typically present with severe weight loss, anorexia and dark feces (melena). This case came from a stranded sea lion necropsied at a local marine mammal rehabilitation center and presented with typical gross ulcerative lesions.

Nematodes (roundworms) are the most diverse group of parasites found throughout the gastrointestinal tract of pinnipeds. Common nematode species that cause ulcerative lesions in the stomach of California sea lions include

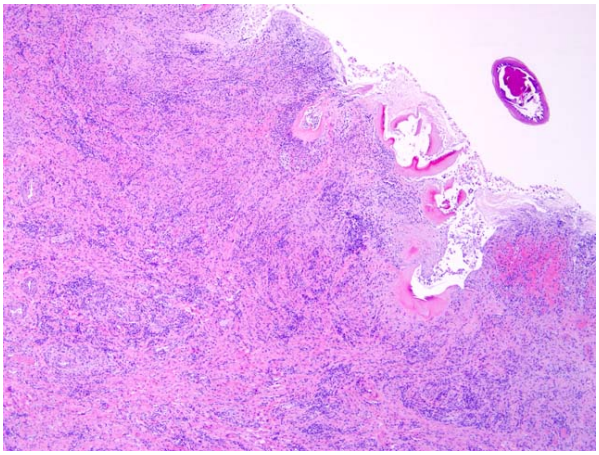

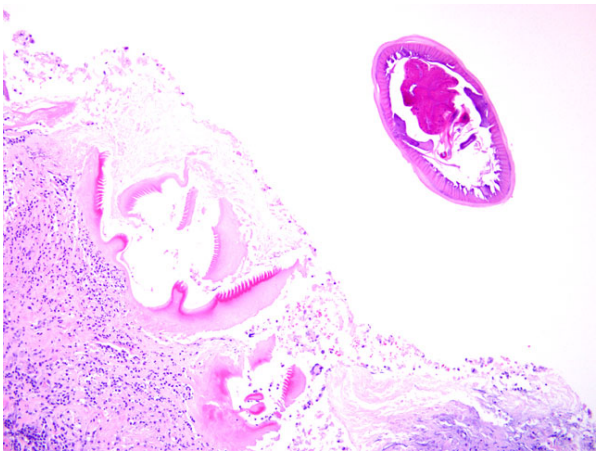

4-3, 4-4. Stomach, California sea lion. The submucosa is expanded by proliferative fibrous connective tissue and the mucosal epithelium is eroded and hyperplastic. Adult anisakid nematodes present in the mucosa and lumen have a cuticle, coelomyarian musculature, lateral cords, and an intestine lined by few uninucleate columnar cells. Hyaline eosinophilic casts of nematode heads (Splendore-Hoeppli material) are embedded within the gastric mucosa. (HE 40X, 100X)

Anisakis spp. (larval stages), *Contracaecum* spp., *Phocascaris* spp. and *Pseudoterranova* spp. (adults).[1,2,5] Large numbers of California sea lions necropsied at the Center exhibit macroscopically ulcerative gastritis that ranges from acute to chronic, moderate to severe, and contain various amounts of edema and hemorrhage.[6] Gross pathological findings in the stomach include well defined single or multiple superficial, transmural to volcanic (crater-like) ulcers in different stages of development that vary in size from 0.5 to 3.5 cm in diameter. Various amounts of digested blood mixed with mucus are found in the lumen. In many cases, the most prominent finding in the stomach is the presence of one to several volcanic ulcers, with variable numbers of adult and larval stages of stomach worms nested and embedded in the center of the lesions. They frequently appear as chronic nodular ulcerative lesions with extensive granulation tissue but no parasites. Microscopic lesions include large areas of necrosis and hemorrhage in the center of the lesion surrounding cross sections of the parasite wall with coelomyarian musculature with prominent hypodermis with lateral cords.[4,6] The inflammatory component is composed of moderate numbers of eosinophils, neutrophils and macrophages, mixed with lymphoplasmacytic infiltrate.

In general, metazoan parasites in large numbers or in immunocompromised marine mammals contribute to the severity of illness or complicate an underlying disease. Secondary bacterial infections are often associated with parasite migration and tissue damage. Starvation, trauma, stress or toxic insults might predispose pinnipeds to the development of gastric ulcers. Stomach worms of *Anisakidae* family seem well adapted to the marine environment and able to colonize the gastric mucosa of different marine mammals as definite hosts.

AFIP Diagnosis: Stomach: Gastritis, necrotizing and ulcerative, multifocal, moderate, with granulation tissue, fibrosis, and adult anisakid nematodes.

Conference Comment: In addition to gastritis, several conference participants also noted the presence of mineralization of the tunica media in the submucosal vessels; the presence of this finding varied between slides.

One of the moderators (Dr. Chris Gardiner) commented that the presence of brightly eosinophilic homogenous material embedded in the gastric mucosa is seen frequently in cases of gastric anisakiasis in sea lions. While many pathologists interpret the material to be the cuticle of the parasite, Dr. Gardiner believes this material is not parasite *per se*; rather, it is a cast of the head of the worm composed of Splendore-Hoeppli material and represents the nematode's attachment site.

Contributor: College of Veterinary Medicine, Western University of Health Sciences, 309 E 2nd Street, Pomona, CA 91766
http://www.westernu.edu/xp/edu/veterinary/staff.xml

References:

1. Dailey MD. Parasitic Diseases. In: Dierauf LA, Gulland FMD, eds.*CRC Handbook of Marine Mammal Medicine*. Boca Raton, FL: CRC Press; 2001:367-372. 2001.
2. Gerber JA, Roletto J, Morgan LE, Smith DM, Gage JG. Findings in pinnipeds stranded along the Central and Northern California coast, 1984-1990. *J Wildl Dis*. 1993;29(3):423-433.
3. Liu S, Edward AG. Gastric ulcers associated with *Contracaecum* spp. (nematode: Ascaroidea) in a Steller sea lion and a white pelican. *J Wildl Dis*. 1971;7:266-271.
4. Migaki G, Van Dyke D, Hubbard RC. Some histopathological lesions caused by helminths in marine mammals. *J Wildl Dis*. 1971;7:281-289.
5. Sweeney JC, Gilmartin WG. Survey of diseases in free-living California sea lions. *J Wildl Dis*. 1974;10;370-376.
6. Tkalcic S. Gastric ulcers in California Sea Lions (*Zalophus californianus*). In: *Proc of the International Scientific Meeting of Anatomy and Physiology Fundamentals of Medicine*. Zagreb, Croatia. 2009:160-162.

The Armed Forces Institute of Pathology
Department of Veterinary Pathology

Conference Coordinator
Matthew Wegner, DVM

WEDNESDAY SLIDE CONFERENCE 2010-2011

Conference 18

9 February 2011

Conference Moderator:
Cathy S. Carlson, DVM, PhD, Diplomate ACVP

CASE I: 10L10D / 10L10C (AFIP 3164833).

Signalment: 9-month-old female Sprague-Dawley rat (*Rattus norvegicus*).

History: This young female rat was part of an institutional breeding colony. She was euthanized due to the presence of a large mandibular mass.

Gross Pathology: The left mandible was surrounded and expanded to approximately 2 cm in width by a highly infiltrative mass. The mass extended beyond the rostral aspect of the mandible and the overlying epithelium was ulcerated. On cut surface, tissue near the oral cavity was tan and friable, while the deeper aspects were hard and gritty. All other organs and tissues were unremarkable.

Histopathologic Description: Mandible, left: Native tissue is extensively effaced by a well-demarcated, non-encapsulated and highly infiltrative mass of neoplastic epithelial cells arranged in islands and anastomosing cords and trabeculae. Peripherally the neoplastic foci have a prominent layer of tightly packed tall-columnar cells with apically-located oval nuclei and prominent basilar cytoplasmic clearing. Centrally, neoplastic foci are comprised of cells that vary from stellate with long

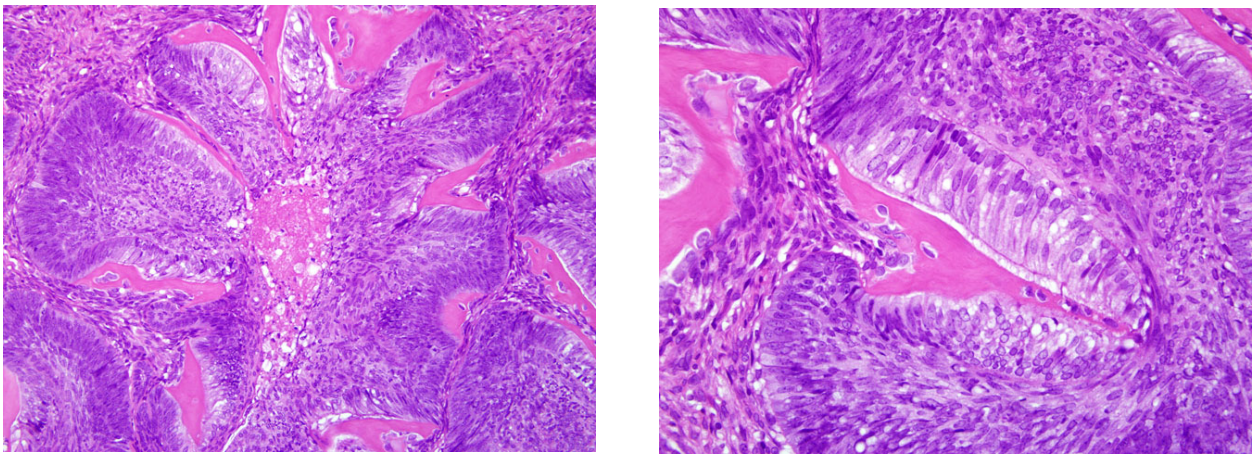

1-1, 1-2. Mandible, ameloblastic odontoma, rat. Islands of epithelial cells have a peripheral palisading layer of tall columnar cells and a central area of stellate cells arranged in whorls with occasional cystic degeneration. Columnar cells (ameloblasts) are multifocally separated from fusiform cells of the interstitium (odontoblasts) by islands and trabeculae of eosinophilic homogenous material (osteodentin). (HE 200X, 400X)

intercellular bridges to fusiform cells that are densely packed with prominent streaming and occasional whorls. The mitotic rate within the palisading layer is high, with 1-5 per high power field, and there are numerous scattered individual apoptotic cells. Along the basilar aspects of the palisading columnar cells are streams of fusiform cells often separated from the epithelial cells by variably thick seams and wedge-shaped foci of homogeneous eosinophilic extracellular matrix material. Matrix material frequently contains individual polygonal to fusiform cells within lacunae and is associated with a shift in appearance of the adjacent mesenchymal cells from fusiform to plump cuboidal or short columnar. There is multifocal ulceration of the oral epithelium and extensive necrosis of the subjacent tissue with loss of cellular detail and replacement by abundant viable and degenerate neutrophils, macrophages and fewer lymphocytes admixed with necrotic bone fragments, cellular and karyorrhectic debris, basophilic granular material (mineral), plant material and myriad colonies of coccoid bacteria.

Contributor's Morphologic Diagnosis: Mandible, left: Odontoameloblastoma.

Contributor's Comment: Odontoameloblastoma is an uncommon oral neoplasm with three distinct features: odontogenic epithelium, odontogenic ectomesenchyme and induction of mineralized dental tissues.[11] Odontogenic epithelium is characterized by peripheral palisading columnar cells with apically located nuclei and basilar cytoplasmic clearing, and central cells connected by long intercellular bridges that resemble the stellate reticulum.[2] Odontoameloblastomas commonly arise in the mandible, are locally aggressive and infiltrative, but do not metastasize.[1]

Much of the odontogenic epithelial component of the neoplasm in the present case is consistent with the follicular variant of ameloblastoma; however, by definition, ameloblastomas are non-inductive neoplasms.[1,8] During odontogenesis, ameloblasts degrade their basement membrane, achieve cell-to-cell contact with odontoblasts, and through their interaction induce the production of dentin.[12] In the neoplasm described in this report, periodic acid-Schiff reaction revealed a locally extensive loss of basement membrane associated with foci of eosinophilic matrix material representative of such induction. The histologic appearance of the eosinophilic matrix material and its presence adjacent to foci of odontogenic epithelium is most consistent with osteodentin, a tertiary form of dentin with few recognizable dentin tubules that is rapidly produced and often entraps odontoblasts giving it a morphologic appearance similar to bone.[6,7] Thus, as in the present case, a predominantly ameloblastic neoplasm with the additional features of odontogenic ectomesenchyme and induction of mineralized dental tissues warrants the diagnosis of odontoameloblastoma.[8,11]

Previous histologic classification schemes for odontogenic neoplasms in domestic animals have referred to lesions with features similar to odontoameloblastoma as ameloblastic odontomas[4,12] and the World Health Organization (WHO) classification of rodent tumors lists the two terms as synonymous;[1] however, the 1992 WHO classification of odontogenic neoplasms[8] does not include ameloblastic odontoma as a recognized tumor classification and thus favors use of the term odontoameloblastoma. In a review of the nomenclature of odontogenic tumors in animals,[3] the author also suggests that the term ameloblastic odontoma no longer be used and that the clinical behavior implied by the terms ameloblastoma (invasive) and odontoma (non-invasive) be considered when incorporating these terms into a diagnosis. Accordingly, the term odontoameloblastoma seems most consistent with the invasive nature of these lesions.

When the inductive component consists of mature tooth structures, the diagnosis of odontoameloblastoma is straightforward; however, the presence of thin seams of atubular dentin or osteodentin should not be overlooked as evidence of induction by odontogenic neoplasms and support the diagnosis of odontoameloblastoma over ameloblastoma.

AFIP Diagnosis: Mandible, left: Ameloblastic odontoma (odontoameloblastoma).

Conference Comment: Conference participants discussed the nomenclature of this tumor. With many neoplasms, the nomenclature varies based on the classification system used. The most recent edition of the WHO *Histological Classification of Tumors of the Alimentary System of Domestic Animals* describes neither odontoameloblastoma nor ameloblastic odontoma.[5] The authors do, however, describe an ameloblastic fibro-odontoma characterized by collagen-poor stroma reminiscent of dental pulp, interconnected cords and sheets of odontogenic epithelium, and advanced dentinal differentiation with deposition of enamel or dentin matrix. This description appears to have the features of an odontoameloblastoma. The Standardized System of Nomenclature and Diagnostic Criteria (SSNDC) Guide for lesions in the rat refers to this tumor as an ameloblastic odontoma (odontoameloblastoma).[10]

Odontogenic tumors are often difficult to describe and diagnose for many veterinary pathologists. They are broadly categorized as epithelial (non-inductive) or epithelial with mesenchyme (inductive). An algorithm is a helpful tool when evaluating odontogenic neoplasms. The included chart summarizes diagnostic criteria for histologically classifying odontogenic neoplasms in several veterinary species.[2,5]

Several participants observed fragments of food and few hair shafts associated with degenerate neutrophils within the gingival sulcus in some histologic sections from this rat. Dialogue surrounding the most likely predisposing factor for this ancillary finding.i,e. the oral neoplasm, and the possible pathologic sequelae led to discussion of a recent publication

Tumor	OE*	Stroma	Mesenchyme	Matrix	Species Affected	Biological Behavior	Misc
Ameloblastoma	Yes	Not essential for diagnosis	None	None	Dog, cat, horse	Progressive; non-metastatic	
Amyloid-producing odontogenic tumor	Yes	Not essential for diagnosis	None	Amyloid	Dog, cat, horse	Progressive; non-metastatic	
Canine acanthomatous ameloblastoma	Yes	Stellate fibroblasts in dense collagen; regularly spaced dilated, empty blood vessels	Periodontal ligament	None	Dog	Locally aggressive; non-metastatic	Interconnected sheets of odontogenic epithelium
Ameloblastic fibroma	Yes	Loose, collagen poor, resembles dental pulp	Dental pulp	None	Young animals, cattle	Locally destructive;non-metastatic	Most common oral neoplasm in cattle
Ameloblastic fibro-odontoma	Yes	Loose, collagen poor, resembles dental pulp	Dental pulp	Dentin or enamel	Young animals, cattle	Locally destructive; non-metastatic	
Complex odontoma	Yes	Well-differentiated dentinal tissue	Dental pulp	Dentin, enamel (may be mineral-ized)	Dog, rodent, primates, horse	Locally destructive; non-metastatic	Horse, rodents produce cementum; "balls of disorganized dental hard substance"
Compound odontoma	Yes	Well-differentiated dentinal tissue; dense collagen and vascular connective tissue	Dental pulp	Dentin, mineralized enamel	Young dogs	Locally destructive; non-metastatic	Multiple tooth-like structures (denticles)

*OE – odontogenic epithelium

concerning the proposed etiopathogenesis of botryomycosis in mice.[9] In the subject paper the author elegantly demonstrates that many mandibulofacial and maxillofacial abscesses likely result from fragmented hair shafts that become embedded in the gingival sulci of barbering animals leading to coagulase-positive *Staphylococcus aureus* infection.

Contributor: Department of Veterinary Pathology, College of Veterinary Medicine, Iowa State University, Ames, IA
http://vetmed.iastate.edu/vpath

References:

1. Deschl U, Ernst H, Frantz J, et al. Digestive system. In: Mohr U, ed. *International Classification of Rodent Tumours.* Part I: The rat, 10. Lyon, France: International Agency for Research on Cancer; 1997:9.
2. Dubielzig RR. Odontogenic tumors and cysts. In: Meuten DJ, ed. *Tumors in Domestic Animals*. 4th ed. Ames, IA: Iowa State University Press; 2002:402-409.
3. Gardner DG. An orderly approach to the study of odontogenic tumours in animals. *J Comp Pathol.* 1992;107:427-438.
4. Gorlin RJ, Chaudhry AP, Pindborg JJ. Odontogenic tumors. Classification, histopathology, and clinical behavior in man and domesticated animals. *Cancer.* 1961;14:73-101.
5. Head KW, Cull JJ, Dubielzig RR, et al. *Histological Classification Tumors of the Alimentary System of Domestic Animals*, *2nd series*. Vol. X. Washington, DC: Armed Forces Institute of Pathology, American Registry of Pathology; 2007:47-52.
6. Holmstedt JO, McClugage SG, Clark JS, Guevara MJ. Osteodentin formation in continuously erupting teeth of guinea pigs. *J Dent Res*. 1977;56:1569-1576.
7. Karim AC, Eddy EL. A light and electron microscopic study of osteodentin formation in the rat incisor after adriamycin administration. *Am J Anat.* 1984;169:207-219.
8. Kramer I, Pindborg J, Shear M. *International Histological Classification of Tumours: Histological Typing of Odontogenic Tumours*. 2nd ed. Heidelberg, Germany: Spinger-Verlag; 1992.
9. Lawson, GW. Etiopathogenesis of mandibulofacial and maxillofacial abscesses in mice. *Comp Med*. 2010;60:200-204.
10. Long PH, Leininger JR, Nold JB, Lieuallen WG. Proliferative lesions of bone, cartilage, tooth and synovium

in rats. In: *Guides for Toxicologic Pathology*. Washington, DC: STP/ARP/AFIP; 1993:6-7.
11. Mosqueda-Taylor A, Carlos-Bregni R, Ramírez-Amador V, Palma-Guzmán JM, Esquivel-Bonilla D, Hernández-Rojase LA. Odontoameloblastoma. Clinico-pathologic study of three cases and critical review of the literature. *Oral Oncol*. 2002;38:800-805.
12. Walsh KM, Denholm LJ, Cooper BJ. Epithelial odontogenic tumours in domestic animals. *J Comp Pathol*. 1987;97:503-521.

CASE II: 10L11 A / J (AFIP 3164879).

Signalment: 12-month-old male C57/Bl6 10ScSn-Dmd mdx/J mouse (*Mus musculus*).

History: A subcutaneous mass was present in the lumbar region. The mouse was euthanized by CO_2.

Gross Pathology: A firm, non-movable subcutaneous mass (1.2 cm x 1.8 cm x 1.5 cm) was present in the lumbar region. The mass was cream-colored on cut section.

Histopathologic Description: Skeletal muscle: Effacing and replacing approximately 80% of the epaxial musculature, and extending from the dorsal muscle surface to the dorsal aspect of the underlying vertebra, is a poorly-demarcated, non-encapsulated, infiltrative neoplastic mass consisting of tightly-packed neoplastic cells arranged in haphazard bundles and streams supported on a fine fibrovascular stroma. Neoplastic cells are polygonal to spindled, with indistinct margins and abundant finely fibrillar basophilic cytoplasm. Nuclei are oval to crimped with coarsely stippled chromatin and 0-1 visible magenta nucleoli. Anisocytosis and anisokaryosis are marked and mitoses are too numerous to count and frequently bizarre. Nuclear rowing is evident, and scattered plump multinucleated neoplastic cells are present. Along the periphery of the primary mass, neoplastic cells dissect between and multifocally surround and separate native myofibers. Adjacent to the mass, multifocal myofibers contain hypereosinophilic and condensed globular sarcoplasm (degeneration), with variable loss of nuclear detail (necrosis). Multifocal myofibers are small in diameter and contain basophilic sarcoplasm and multiple internal nuclei (regenerative), or contain eosinophilic sarcoplasm and central nuclei (post-regeneration). Myofiber diameter is highly variable, and multifocal small-diameter fibers are surrounded by populations of polygonal cells (proliferating myoblasts).

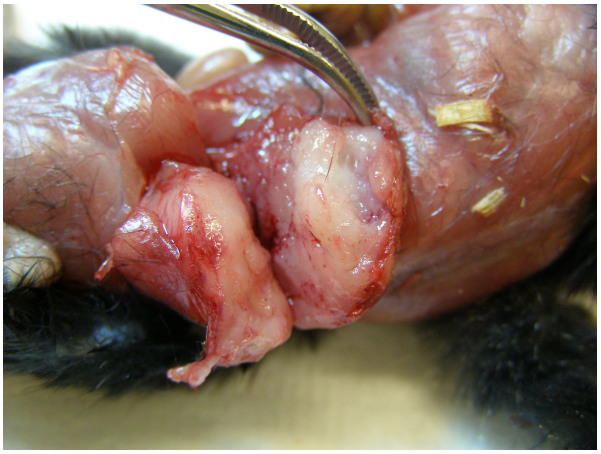

2-1. Skeletal muscle, epaxial region, rhabdomyosarcoma, mouse. A firm, non-moveable subcutaneous mass is present in the lumbar region; the mass is cream colored on cut surface. Photograph courtesy of Department of Veterinary Pathology, College of Veterinary Medicine, Iowa State University, http://vetmed.iastate.edu/vpath.

Contributor's Morphologic Diagnosis: 1. Mass within lumbar epaxial muscle: Rhabdomyosarcoma.
2. Skeletal muscle: Myofiber degeneration, necrosis and regeneration, moderate, diffuse, chronic, with myoblast proliferation.

Contributor's Comment: The heritable, X-linked true muscular dystrophies are the result of defects in the gene encoding the dystrophin protein, and have been described in the dog, cat, mouse, and human.[9] Dystrophin is a cytoplasmic protein expressed in skeletal, cardiac and smooth muscle which as part of the dystrophin-dystroglycan-laminin complex links the myofibrillar actin cytoskeleton to the extracellular matrix and is required for sarcolemmal stability.[10] Absence or defects within the dystrophin protein contribute to contraction-associated myofiber necrosis and regeneration, with progressive muscle weakness and eventual replacement of muscle by fibrotic and adipose tissue in humans. Affected boys usually die early within the second decade of life due to respiratory or cardiac failure.[2,10] The mouse model of Duchenne's muscular dystrophy (mdx)

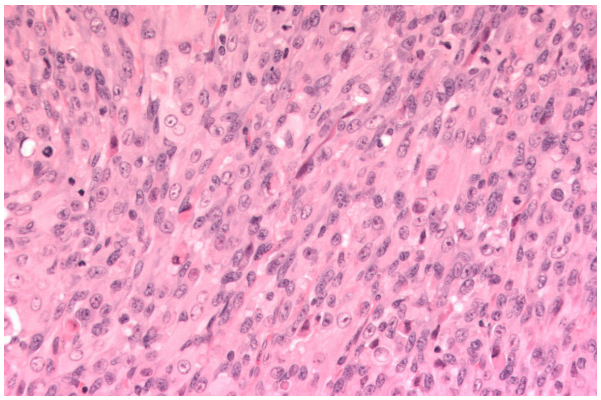

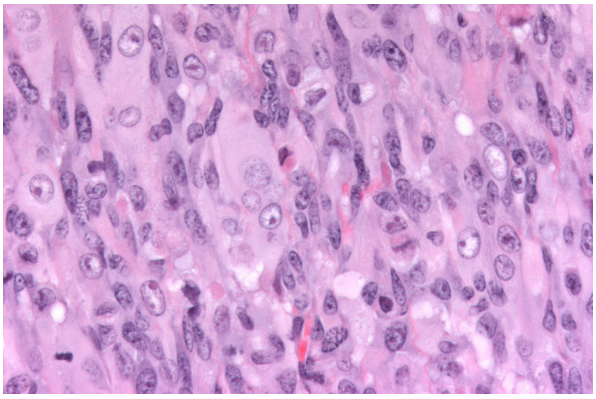

2-2, 2-3. Skeletal muscle, epaxial region, rhabdomyosarcoma, mouse. Skeletal muscle is infiltrated and replaced by pleomorphic neoplastic spindle cells with a high mitotic rate. Photographs courtesy of Department of Veterinary Pathology, College of Veterinary Medicine, Iowa State University, http://vetmed.iastate.edu/vpath.

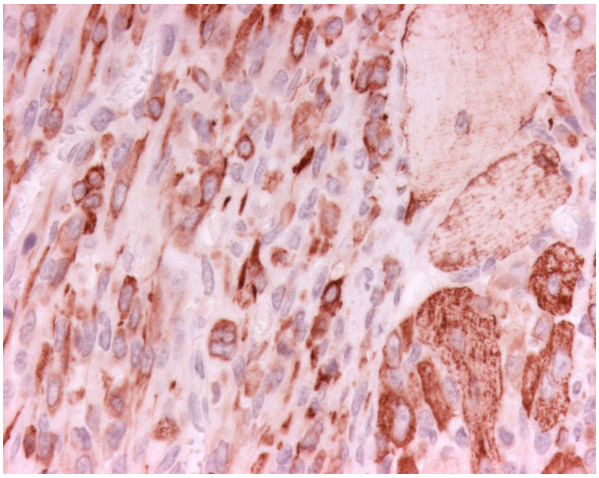

2-4. Skeletal muscle, epaxial region, rhabdomyosarcoma, mouse. Neoplastic cells demonstrate positive cytoplasmic imunnoreactivity for desmin. Photograph courtesy of Department of Veterinary Pathology, College of Veterinary Medicine, Iowa State University, http://vetmed.iastate.edu/vpath.

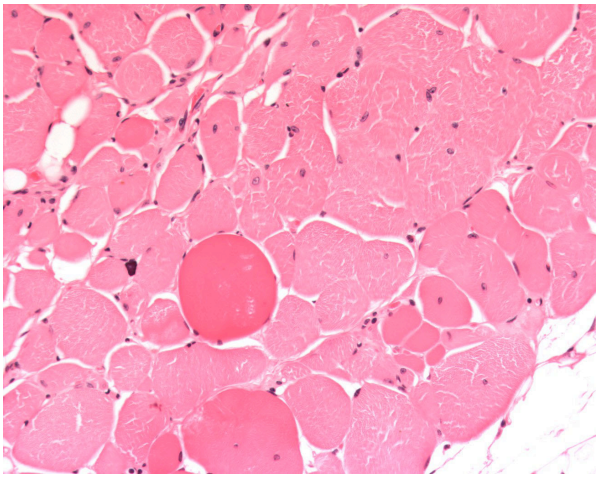

2-5. Skeletal muscle, epaxial region, mouse. Myofibers vary in diameter and often have hypereosinophilic sarcoplasm. Photograph courtesy of Department of Veterinary Pathology, College of Veterinary Medicine, Iowa State University, http://vetmed.iastate.edu/vpath.

arose in 1976 as an X-linked spontaneous dystrophin mutation in a colony of C57/Bl10 mice,[1] and has been extensively utilized in pathogenesis and therapeutic studies. Mice with dystrophin defects experience the onset of myofiber degeneration at 3-5 weeks of age, similar to the juvenile onset of clinical signs in humans; cardiac and diaphragmatic dysfunction likely contribute to a reduced life span compared to wild-type mice. However, unlike the analogous human disease, mdx mice follow a milder clinical course in that limb myofiber regeneration and hypertrophy continue well into adulthood, albeit with a decrease in muscle strength.[2] Histological features of muscular dystrophy include a variation in fiber diameter in that the muscle tissue is comprised of a mosaic of hypertrophied, degenerating and regenerating myofibers. The presence of multinucleated myofibers and fibers with central nuclei are evidence of the regenerative process.

Rhabdomyosarcoma, otherwise rare in other strains of laboratory mice, has been identified as a common spontaneous tumor in aged mice lacking functional dystrophin or alpha-sarcoglycan.[2,4] In a previous longevity study involving 94 mdx mice, six animals developed rhabdomyosarcomas between 16.5 and 24 months of age, whereas no rhabdomyosarcomas were noted in 83 age-matched wild-type background strain (C57BL/10ScSn/J) mice.[2] The mouse in the present case was one of 71 mdx mice housed at the Iowa State University College of Veterinary Medicine, two others of whom developed rhabdomyosarcomas between February 2010 and May 2010. The tumor in the present case was positive for desmin upon immunohistochemical analysis, confirming the diagnosis.[3] The pathogenesis of this entity is unknown, but it is postulated that the continual proliferation of the satellite cell pool, which accompanies the degeneration and regeneration of myofibers, lends itself to random mutations and neoplastic transformation.[2] Early exhaustion of this satellite cell pool in human muscular dystrophy is likely the reason that rhabdomyosarcoma is uncommonly reported in human patients.[2]

Additional changes in this mouse included myocardiocyte loss and replacement by plump fibroblasts and wispy collagen (fibrosis), and the presence of regenerative muscle fibers in the diaphragm.

AFIP Diagnosis: 1. Skeletal muscle, epaxial: Rhabdomyosarcoma.
2. Skeletal muscle: Myocyte degeneration, necrosis, and atrophy, diffuse, moderate, with myocyte regeneration.
3. Bone, vertebrae, ilium, and femur; intervertebral disk; and spinal cord: Essentially normal tissue (not present in all sections).

Conference Comment: Conference participants readily diagnosed the sarcoma as a rhabdomyosarcoma and discussed immunohistochemical stains used to differentiate tumors of muscle origin. Vimentin, desmin, muscle specific actin and myoglobin are commonly used immunomarkers for rhabdomyosarcoma.[11] Many embryonal or primitive muscle tumors may be immunohistochemically negative for myoglobin since it is expressed late in myocyte development.[11] Myogenin and Myo-D1 can be used for primitive skeletal muscle sarcomas and have shown some success in diagnosing rhabdomyosarcomas in dogs.[5,7] These markers are transcription factors in the nuclei of developing myocytes, and therefore exhibit positive nuclear immunoreactivity; however, interpretation of Myo-D1 must be done with care, as there is frequent cytoplasmic staining.[11] There has been recent interest in using Pax7 for diagnosis of primitive rhabdomyosarcoma. The Pax7 protein is a transcription factor expressed in activated and quiescent skeletal muscle satellite cells which acts to regulate their survival and specification.[8] There is intense research in

isolating and characterizing satellite cells, not only to determine their role in neoplasia, but also in treating degenerative diseases of skeletal muscle.[8]

Few participants diagnosed the skeletal muscle degeneration, necrosis and regeneration occurring distant to the neoplasm. Once more clinical information was provided, such as the phenotype of the mouse and its research utilization, they readily identified areas of myocyte change.

Research findings support the role of satellite cells as skeletal muscle stem cells.[8] After skeletal muscle damage, there is active Notch signaling due to upregulation of delta-like ligands on satellite cells causing them to proliferate, which is evident histologically as a round, plump appearance.[6] Inflammatory cells secreting insulin-like growth factor (IGF)-1, platelet-derived growth factor (PDGF) and IL-6 also promote satellite cell and myoblast proliferation and differentiation.[6] Regenerative changes in skeletal muscle are characterized by sarcolemmal basophilia, central alignment of many nuclei (i.e. nuclear rowing) and vesiculate nuclei.[9]

Contributor: Department of Veterinary Pathology, College of Veterinary Medicine, Iowa State University, Ames, IA
http://vetmed.iastate.edu/vpath

References:

1. Bulfield G, Siller WG, Wight PAL, Moore KJ. X chromosome-linked muscular dystrophy (mdx) in the mouse. *Proc Natl Acad Sci.* 1984;81:1189-1192.
2. Chamberlain JS, Metzger J, Reyes M, Townsend D, Faulkner JA. Dystrophin-deficient mdx mice display a reduced life span and are susceptible to spontaneous rhabdomyosarcoma. *FASEB J.* 2007;21:195-204.
3. Cooper BJ, Valentine BA. Tumors of muscle. In: Meuten DJ, ed. *Tumors in Domestic Animals*. 4th ed. Ames, IA: Iowa State Press; 2002:319-363.
4. Fernandez K, Serinagaoglu Y, Hammond S, Martin LT, Martin PT. Mice lacking dystrophin or alpha sarcoglycan spontaneously develop embryonal rhabdomyosarcoma with cancer-associated p53 mutations and alternatively spliced or mutant Mdm2 transcripts. *Am J Pathol*. 2010;176:416-434.
5. Kobayashi M, Sakai H, Hirata A, et al. Expression of myogenic regulating factors, myogenin and MyoD, in two canine botryoid rhabdomyosarcomas. *Vet Pathol*. 2004;41:275-277.
6. Kumar V, Abbas AK, Fausto N, Aster JC . Tissue renewal, regeneration and repair. In: Kumar V, Abbas AK, Fausto N, Aster JC, eds. *Robbins and Cotran Pathologic Basis of Disease*. 8th ed. Philadelphia, PA: Elsevier Saunders; 2009:85-86.
7. Murakami M, Sakai H, Iwatani N, et al. Cytologic, histologic and immunohistochemical features of maxillofacial alveolar rhabdomyosarcoma in a juvenile dog. *Vet Clin Pathol*. 2010;39:113-118.
8. Tedesco FS, Dellvalle A, Diaz-Manera J, Messina G, Cossu G. Repairing skeletal muscle: Regenerative potential of skeletal muscle stem cells. *J Clin Invest*. 2010;120:11-19.
9. VanVleet JF, Valentine BA. Muscle and tendon. In: Maxie MG, ed. *Pathology of Domestic Animals*, 5th ed. Vol. 1. Philadelphia, PA: Elsevier Saunders; 2007:185-280.
10. Watchko JF, O'Day TL, Hoffman EP. Functional characteristics of dystrophic skeletal muscle: Insights from animal models. *J Appl Physiol.* 2002; 93:407-417.
11. Wick MR, Hornick JL. Immunohistopathology of soft tissue and osseous neoplasms. In: Dabbs DJ, ed. *Diagnostic Immuhistochemistry: Theranostic and Genomic Applications*. Philadelphia, PA: Saunders Elsevier; 2010:91-92.

CASE III: 15147-3B-3T (AFIP 3166458).

Signalment: 5 to 6-month-old intact female Landrace large white cross-bred porcine (*Sus domesticus*).

History: A large number of 5 to 6-month-old replacement gilts were transported by truck over a 300-mile distance. The gilts were reported to have walked normally prior to being transported but an "unacceptable" number of them were severely lame after arrival, with the lameness being localized to one or both elbow joints. Humeri from a subset of the affected animals were sent to the Minnesota Veterinary Diagnostic Laboratory for determination of the cause of the lameness. The histologic section is from the distal humerus of one of the affected pigs.

Gross Pathology: The articular cartilage of the trochlea (right) contains a locally extensive, thickened area involving approximately 75% of the articular surface. The axial margin of this thickened area exhibits clefting and flap formation. Most of the thickened area of cartilage remains intact; however, there is an area of loss of articular cartilage (approximately 15% of the total cartilage) in the axial aspect of the trochlea, with exposure of the subchondral bone (ulceration). The cartilage of the sagittal ridge (central area of joint surface) also is focally extensively ulcerated and thickened. Radiographs of the serially sectioned distal humerus (2-3 mm slab sections) demonstrate well-demarcated, locally extensive areas of lucency in the subchondral bone of the trochlea and sagittal ridge. A higher magnification image of one of these slabs demonstrates nearly complete loss of radiodensity in these areas; the trochlea is on the right side of the image.

Histopathologic Description: Bone: The slide contains one coronal section of the distal humeral trochlea. The articular-epiphyseal complex in the abaxial 2/3 of the trochlea is variably thickened, and contains a longitudinal cleft separating the cartilage from the underlying subchondral bone. Subjacent to this cleft is an extensive area of myelofibrosis and loss of bone trabeculae. Focally, in the axial aspect of the trochlea, the cartilage cleft reaches the articular surface. This area of articular cartilage exhibits fibrillation, areas of chondrocyte necrosis, and numerous chondrocyte clones (chondrones). Along the deep surface of the cleft is a variably thin zone of necrotic cartilage characterized by pale, eosinophilic matrix containing low numbers of eosinophilic chondrocytes that contain no discernible nuclei. The viable cartilage immediately adjacent to the zone of necrosis contains numerous chondrocyte clones (chondrones). Subjacent to the cartilage flap is a thick mat of eosinophilic, fibrillar material (fibrin). Underlying this mat of fibrin is well vascularized fibrous connective tissue (granulation tissue), dense fibrous connective tissue (fibrosis), and foci of chondro-osseous tissue and woven bone which replaces the subchondral bone (myelofibrosis). This tissue extends a variable distance into the marrow spaces of the underlying epiphyseal bone. There is localized osteopenia secondary to the decreased overall bone density

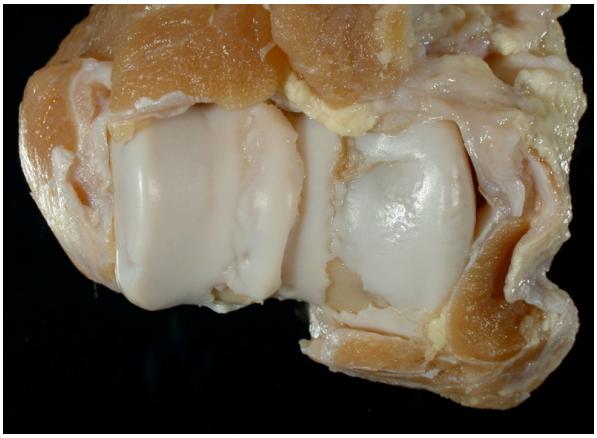

3-1. Humerus, trochlea, articular cartilage, pig. The articular cartilage is extensively ulcerated and thickened with exposure of subchondral bone. Photograph courtesy of University of Minnesota, Department of Veterinary Population Medicine, http://www.cvm.umn.edu/vpm.

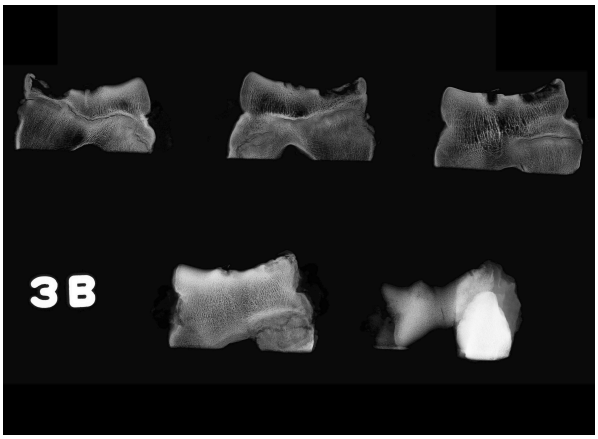

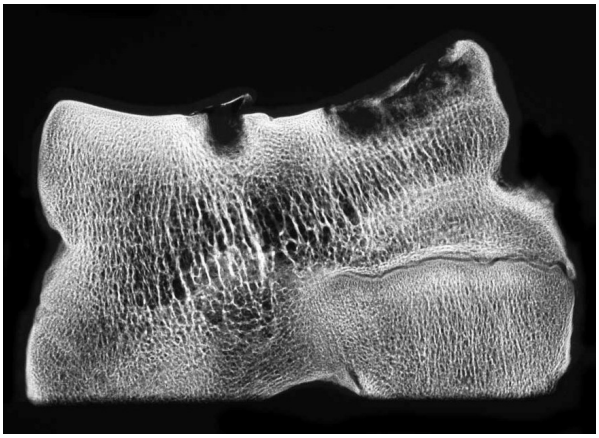

3-2, 3-3. Distal humerus, pig. Radiographs of serially sectioned distal humerus demonstrate well-demarcated, locally extensive areas of lucency in the subchondral bone of the trochlea and sagittal ridge. Photographs courtesy of University of Minnesota, Department of Veterinary Population Medicine, http://www.cvm.umn.edu/vpm.

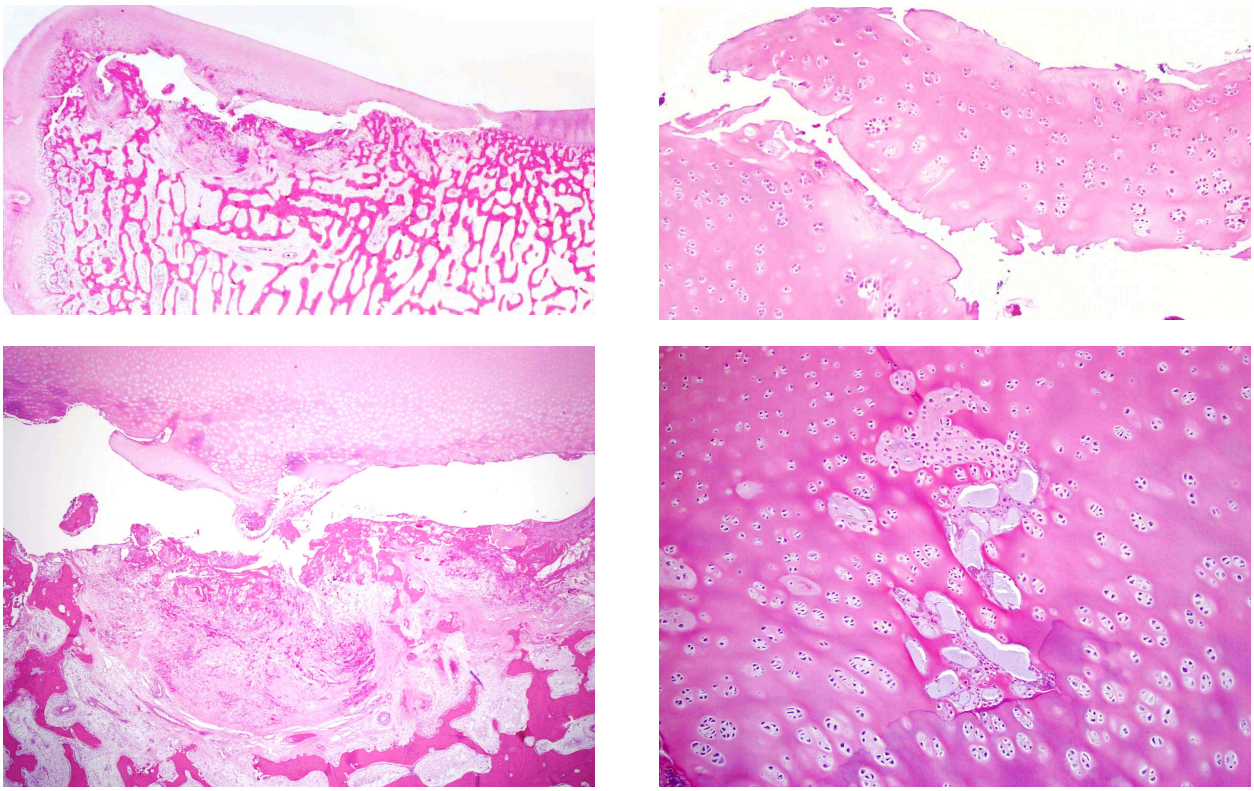

3-4, 3-5, 3-6, 3-7. Humerus, articular-epiphyseal complex, pig. There is a focally extensive longitudinal subchondral cleft (3-4) that reaches the articular surface forming a flap (3-5), with subchondral myelofibrosis and loss of bone trabeculae (3-6). Cartilage at the axial aspect of the joint contains numerous chondrones and foci of neovascularization (3-7). Photographs courtesy of University of Minnesota, Department of Veterinary Population Medicine, http://www.cvm.umn.edu/vpm.

in the affected area that is clearly visible in the associated radiographs. Fragments of bone trabeculae immediately subjacent to the cleft contain margins lined by active osteoblasts and by osteoclasts within erosion lacunae (osteoclastic resorption). The cartilage at the extreme axial aspect of the joint contains moderate numbers of chondrocyte clones (chondrones) and several foci of neovascularization.

Contributor's Morphologic Diagnosis: Articular-epiphyseal cartilage complex: Chronic, locally extensive chondronecrosis with intralesional clefting, failure of endochondral ossification, and myelofibrosis.

Contributor's Name of the Disease: Osteochondrosis dissecans.

Contributor's Comment: Osteochondrosis is a focal or multifocal disturbance of endochondral ossification in which growth cartilage fails to undergo matrix calcification or vascular invasion and is not converted to bone.[3] Osteochondrosis affects multiple animal species, most commonly pigs, horses, and dogs.[2] This condition has a multifactorial etiology, with anatomic conformation and heredity[1,5] being the causes that are supported most commonly by the scientific literature. Studies of the early lesions in horses and swine have reported that failure of blood supply to the growth cartilage leads to cartilage necrosis, resulting in failure of this tissue to undergo matrix calcification or vascular invasion.[1,4]

Osteochondrosis can be classified as *latens* (lesion confined to epiphyseal cartilage), *manifesta* (lesion accompanied by delay in endochondral ossification), and *dissecans* (cleft formation through articular cartilage) to designate the stage of the disease process.[1] In the present case, "trauma" occurring during transportation most likely caused the conversion of *manifesta* lesions to *dissecans* lesions, resulting in clinical lameness in animals that appeared to be sound prior to transportation. In this chronic stage of the disease, necrotic blood vessels within the epiphyseal cartilage are no longer present.

Participants are encouraged to review Wednesday Slide Conference 2008-2009, Conference 21, Case 1 which presents an acute case of osteochondrosis *latens* and *manifesta* in a 6-week-old foal, whereas the present case is an example of chronic lesions of osteochondrosis *dissecans*.

AFIP Diagnosis: Long bone, distal humeral trochlea and articular-epiphyseal complex (per contributor): Chondronecrosis, chronic, focally extensive, with subchondral clefting, osteopenia, myelofibrosis and failure of endochondral ossification.

Conference Comment: As noted by the contributor, there are various classifications of osteochondrosis based on the histomorphologic appearance, which frequently correlates with lesion chronicity. In discussing the progression of osteochondrosis, the moderator commented that the four characteristics of chronic osteochondrosis *dissecans* (OCD) include chondronecrosis, clefting, myelofibrosis and subchondral bone changes. Conference participants commented on the excellent quality of the tissue sections and slide preparation and the classic histopathologic appearance of this lesion.

The predilection sites for development of osteochondrosis *dissecans* vary by species. The clinical information, including the description of the affected joints, is typically more useful for the clinician and radiologist; however, pathologists should be familiar with these sites in order to assess the locations for possible lesions at necropsy:[2]

- Pig: Joint surfaces of medial humeral and femoral condyles; anconeal process; lumbar vertebrae; mediodistal talus; humeral head; glenoid cavity of the scapula; distal ulna; and dorsal acetabulum
- Dog: Caudal aspect of the humeral head (most common); medial aspect of the humeral condyle; lateral and medial femoral condyle(s); and medial trochlear ridge of the tibial tarsal bone
- Horse: Lateral trochlear ridge; medial femoral condyle; patella; dorsal edge of the sagittal ridge of the distal tibia; and various sites in the tarsal and fetlock joints
- Cattle: Lateral trochlear ridge; humeral head; distal radius; elbow joint; and tibial tarsal and occipital condyles

Several conference participants preferred the diagnosis of chondrodysplasia. As noted by the contributor the pathogenesis of osteochondrosis *dissecans* is due to disturbance of endochondral ossification, whereas the underlying pathogenesis of chondrodysplastic diseases is attributed to defects in cartilage formation. The contributor provides an excellent description of the key histologic features of osteochondrosis *dissecans*. In contrast, the histologic lesions of chondrodysplasia are typified by unevenness in the physeal growth plate, nodular hypertrophy of the growth cartilage with multiple small centers of ossification, an increased width of the zones of chondrocyte proliferation and hypertrophy, and failure to form or maintain orderly chondrocyte columns. Clinically, chondrodysplastic lesions typically affect bones which undergo endochondral ossification resulting in various forms of dwarfism. Examples of chondrodysplastic diseases in domestic animals include:[2]

- Cattle: Bulldog type, Telemark lethal, brachycephalic ("snorter) type and long-headed type
- Sheep: Spider lamb syndrome
- Canine: Described in the Alaskan malamute, Norwegian elkhound, English pointer, Great Pyrenees, miniature poodle, beagles, Scottish deerhound and Labrador retrievers.
- Feline: Scottish fold

Contributor: University of Minnesota, Department of Veterinary Population Medicine, 220 Veterinary Diagnostic Lab, 1333 Gortner Avenue, St. Paul, MN
http://www.cvm.umn.edu/vpm/home.html

References:

1. Olstad K, Ytrehus B, Ekman S, Carlson CS, Dolvik NI. Early lesions of osteochondrosis in the distal tibia of foals. *J Orthop Res*. 2007;8:1094-1105.
2. Thompson K. Diseases of bones and joints. In: Maxie MG, ed. *Jubb, Kennedy and Palmer's Pathology of Domestic Animals*. Vol. 1, 5th ed. Philadelphia, PA: Elsevier Ltd; 2007:25-33,136-145.
3. Ytrehus B, Carlson C S, Ekman S. Etiology and pathogenesis of osteochondrosis. *Vet Pathol*. 2007;4:429-448.
4. Ytrehus B, Carlson C S, Lundeheim N, et al. Vascularisation and osteochondrosis of the epiphyseal growth cartilage of the distal femur in pigs-development with age, growth rate, weight and joint shape. *Bone*. 2004;3:454-465.
5. Ytrehus B, Grindflek E, Teige J, et al. The effect of parentage on the prevalence, severity and location of lesions of osteochondrosis in swine. *J Vet Med A Physiol Pathol Clin Med*. 2004;4:188-195.

CASE IV: D09-23400 (AFIP 3166451).

Signalment: 1-day-old female intact Peruvian Paso horse (*Equus caballus*).

History: Since birth, the foal had been unable to rise, had no suckle reflex, and had marked joint laxity. The foal was euthanized at four hours of age.

Laboratory Results: Aerobic cultures of the lung and liver yielded no growth. No *Salmonella* spp. were isolated from tissue pool. Samples of tissue homogenate were negative for equine herpes virus (EHV). A section of liver was submitted for heavy metal and mineral analysis and the results were within normal limits.

Gross Pathology: The entire body of a 32.4 kg intact female foal in good body condition presented for necropsy in an excellent state of postmortem preservation. The foal had a prominent convex nasal bone and marked mandibular brachygnathia inferior (1.5 cm excess over most rostral point on mandible). The placenta weighed 2.7 kg, was complete, and had a normal size, shape, color, and consistency. The thyroid gland lobes were prominent, dark purple, evenly colored, and of normal shape and consistency.

Examination of longitudinal cut sections of femur and humerus revealed triangular-shaped areas of bone extending from the growth plate (base of triangle) into the metaphysis and diaphysis, filling the marrow cavity, and creating an hourglass appearance (also visible radiographically). Bones cut in transverse section had a lamellated appearance. There was excessive laxity of joints in the distal limbs (carpus/tarsus and distal) both ventrodorsally and laterally. The mouth could not be opened fully. All of the right ribs were fractured, except for ribs 1 and 4; at the site of each fracture, there was focal reddening of the adjacent subcutaneous tissues (hemorrhage). The left ribs 4, 5, 6, 7, 8, 10, 11, 14, 15, and 16 were similarly fractured. Many of the long bones were extremely fragile, breaking relatively readily on hand pressure.

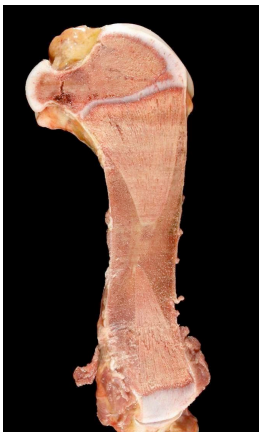

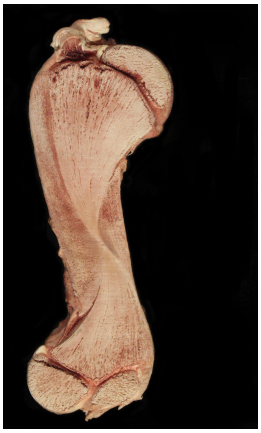

4-1, 4-2. Femur, humerus, Peruvian Paso horse. Gross examination of long bones revealed triangular areas of bone extending from the growth plates into the metaphysis and diaphysis and obliterating the medullary cavity. Photographs courtesy of University of Minnesota, Department of Veterinary Population Medicine, http://www.cvm.umn.edu/vpm.

Postmortem Faxitron radiographs of the skull, humerus, femur, tarsus, and carpus revealed a generalized increase in medullary bone opacity. Specifically, there were parallel linear columns of bone originating from the physeal area and radiating toward the central diaphysis. These columns represented primary spongiosa and obliterated the normal medullary cavity. These medullary opacities formed an hourglass appearance with the central area of the hourglass being the center of the affected bone.

Histopathologic Description: Bone: This is a longitudinal section of long bone metaphysis/diaphysis. The marrow cavity contains a large, wedge-shaped area that occupies approximately 50% of the total tissue area. The tissue in this area is composed of fine trabeculae of bone that exhibit marked retention of calcified cartilage cores (retained primary spongiosa). The outer surfaces of the bony spicules are often scalloped and contain moderate numbers of osteoclasts within erosion lacunae. Osteoblasts appear to be reduced in number and, when identified, are flattened (quiescent). The spaces between bone spicules contain small numbers of erythroid and myeloid precursors admixed with a small amount of loose fibrous connective tissue. The remaining bone trabeculae appear to be composed of woven bone and exhibit a moderate degree of osteoclastic bone resorption. The cortical bone is diffusely trabeculated.

Contributor's Morphologic Diagnosis: Long bone, metaphyseal and diaphyseal osteosclerosis, diffuse, severe, with cortical osteopenia.

Contributor's Comment: Osteopetrosis (or "marble bone disease") is part of a group of rare disorders characterized by defective osteoclastic bone resorption and the accumulation of primary spongiosa in marrow cavities. Osteopetrosis in Peruvian Pasos has been described previously;[1] however, the precise genetic mechanism has not yet been characterized. In humans, juvenile-onset osteopetrosis has an autosomal recessive inheritance pattern, and although the total number of cases is small, evidence to date suggests that the disease in Peruvian Paso horses also is inherited as an autosomal recessive trait.[2] In osteopetrosis, the bone resorptive function of osteoclasts is dysfunctional, leading to loss of normal bone turnover and retention of bone within central medullary cavities. Affected foals suffer many fractures. Since the medullary cavity is filled with retained primary spongiosa, the amount of bone marrow is diminished, leading to anemia and leukopenia. Although affected foals are of normal size at birth and are born alive, they are unable to stand, become lethargic, and are susceptible to infections. These animals are commonly euthanized within the first week of life.

AFIP Diagnosis: Long bone: Osteosclerosis, medullary, diffuse, marked, with retention of primary spongiosa, cortical osteopenia, and lack of marrow hematopoietic elements.

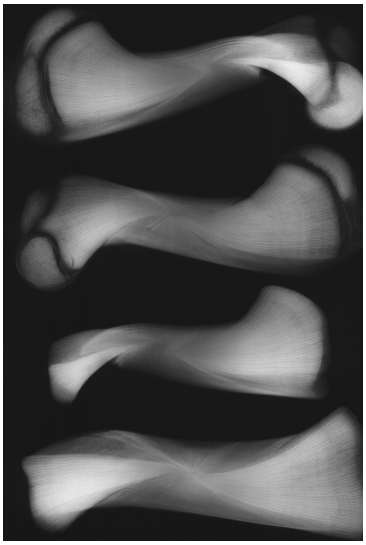

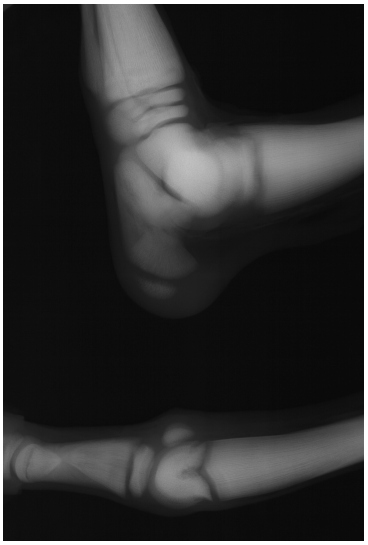

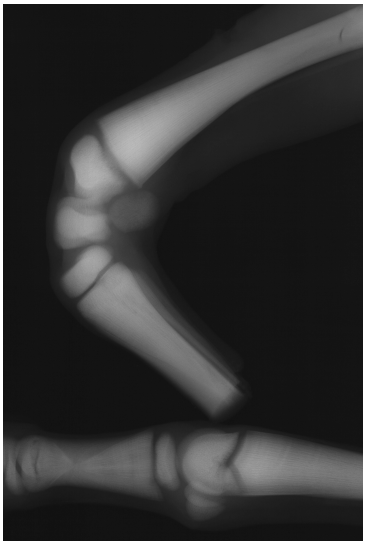

4-3, 4-4, 4-5. Femur, humerus, tarsus, carpus, fetlock, Peruvian Paso horse. Postmortem radiographs demonstrate triangular linear bone densities in the medullary cavity of long bones. Photographs courtesy of University of Minnesota, Department of Veterinary Population Medicine, http://www.cvm.umn.edu/vpm.

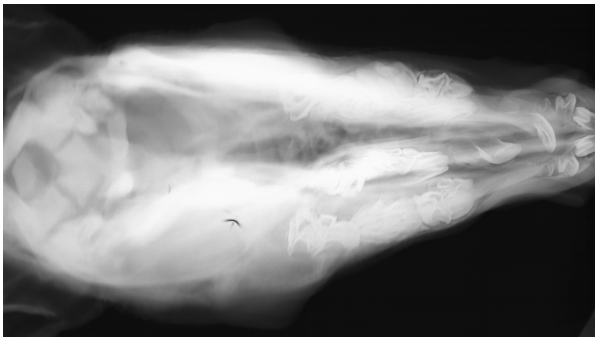

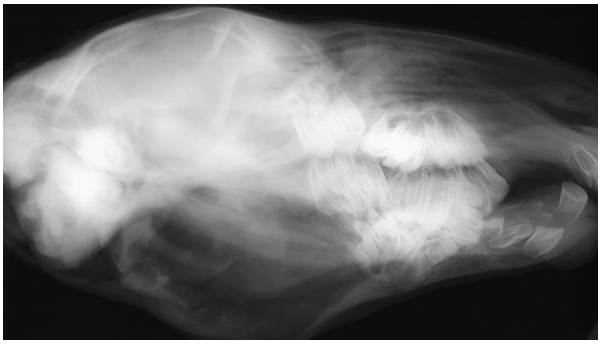

4-6, 4-7. Skull, Peruvian Paso horse. Radiographs showing convex nasal bone and brachygnathia inferior. Photographs courtesy of University of Minnesota, Department of Veterinary Population Medicine, http://www.cvm.umn.edu/vpm.

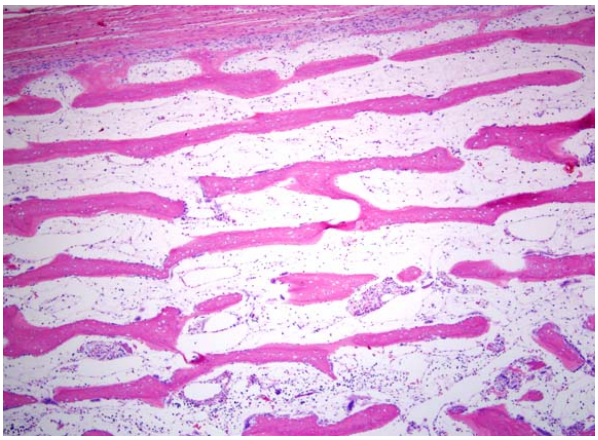

4-8. Long bone, cortex, horse. There is diffuse, prominent cortical osteopenia. (HE 40X)

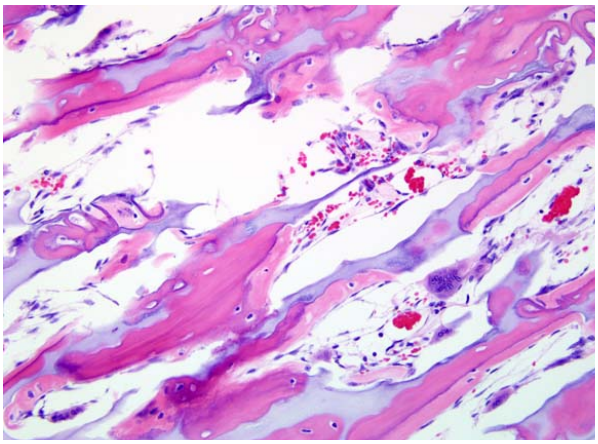

4-9. Long bone, medullary cavity, horse. Primary spongiosa demonstrate an eosinophilic calcified core with an outer amphophilic cartilaginous exterior and a lack of osteoblastic activity. There are several inactive osteoclasts within the frame. (HE 200X)

Conference Comment: Conference participants were intrigued by the cortical osteopenia and failed compaction of cortical bone, and they speculated on the relationship between cortical osteopenia and osteopetrosis. Osteopenia is a common concurrent finding in various forms of human osteopetrosis. A literature search failed to identify any publication explaining a possible pathogenetic mechanism for the simultaneous occurrence of osteopenia in the face of osteopetrosis. In fact, the last sentence of the abstract in a human case report of osteopetrosis stated, "How osteopenia follows [osteopetrosis] is an enigma of human skeletal pathobiology."[3] This situation appears to be seemingly true for veterinary medicine.

The histologic descriptions, interpretations, and diagnoses of bone lesions can be a daunting challenge for veterinary pathologists and training residents alike. The included chart provides a brief summary of some of the more classic bone diseases.[2]

Contributor: University of Minnesota, Department of Veterinary Population Medicine, 220 Veterinary Diagnostic Lab, 1333 Gortner Avenue, St. Paul, MN
http://www.cvm.umn.edu/vpm/home.html

References:

1. Berry C, House J, Poulus P, et al. Radiographic and pathologic features of osteopetrosis in two Peruvian Paso foals. *Can Vet* J. 1994;35:5, 355-361.
2. Thompson K. Diseases of bones and joints. In: Maxie MG, ed. *Jubb, Kennedy and Palmer's Pathology of Domestic Animals*. Vol. 1, 5th ed. Philadelphia, PA: Elsevier Ltd; 2007:25-40, 59, 57-88, 136-145.
3. Whyte MP, Wenkert D, McAlister WH et al. Dysosteosclerosis presents as an "osteoclast-poor" form of osteopetrosis: Comprehensive investigation of a 3-year-old girl and literature review. *J Bone Miner Res*. 2010;25:2527-2539.

Disease	Disease Process	Underlying Abnormality	Gross Features	Key Histologic Features
Chondrodysplasia	Abnormal development of ossification centers	Point mutation in the gene encoding FGFR3	Irregularly thickened physis; Roman-nosed; knock-kneed	Multiple ossification centers in nodules of hypertrophic cartilage; increased width of the proliferative and hypertrophic zones of the physis
Osteogenesis imperfecta	No osteoclastic resorption or realignment of trabeculae	Mutations in COL1A1/COL1A2 genes → defect in type I collagen produced by OB	Brittle bones with normal shape; blue sclera; misshapen, pink teeth	Calcified cartilage spicules lined by thin layer of mineralized matrix & OB; woven, osteopenic cortical bone
Scurvy	Decrease/failure in collagen deposition resulting in failure of EO	Lack L-gulonolactone oxidase for ascorbic acid synthesis	Swollen joints; fractures; periosteal hemorrhages	Naked spicules of calcified cartilage ("scorbutic lattice); sparse OB; infractions; thin physis
Rickets*	Failure of mineralization →defective osteoid mineralization & EO at physis	Decreased vitamin D_3 or phosphorus	Enlarged costochondral junctions ("rachitic rosary"); focal thickening of physeal cartilage; short, thickened diaphysis	Persistent hypertrophic chondrocytes; thick, irregular metaphyseal trabeculae with unmineralized osteoid; infractions
Fibrous Osteodystrophy	Increased bone resorption with replacement by fibrosis	Increased parathormone → functional parathyroid adenoma, 2º renal or 2º nutritional	Bilateral swelling of the skull, especially the mandible and maxilla	Increased OC bone resorption; fibroplasias; OBs producing woven bone; disorganized spicules of woven bone lacking cartilage core
Hypertrophic Osteopathy	Periosteal new bone formation	Chronic inflammation / neoplasia; botryoid rhabdomyosarcoma (dog); ovarian tumors (horse)	Lesions start on the distal limbs and progress proximally	Early → edema, proliferation of vascularized connective tissue in the periosteum; Late → trabeculae of woven bone perpendicular to the cortex
Metaphyseal Osteopathy	Young, growing dogs; long bones but, not distal to carpus	Unknown	Bilaterally symmetrical swelling; sterile suppurative osteomyelitis	Persistence of calcified cartilage lattice of 1º spongiosa; neutrophilic inflammation, necrosis, infractions

The Armed Forces Institute of Pathology
Department of Veterinary Pathology

Conference Coordinator
Matthew Wegner, DVM

WEDNESDAY SLIDE CONFERENCE 2010-2011

Conference 19

2 February 2011

Conference Moderator:
Steven E. Weisbrode, DVM, PhD, Diplomate ACVP

CASE I: 2173 (AFIP 2790938).

Signalment: 3.5-month-old male intact Chow-Rottweiler cross, canine (*Canis familiaris*).

History: This 3.5-month-old male Chow-Rottweiler mixed breed dog was presented to a veterinary clinic with severe neck pain. No cervical vertebral lesions were seen radiographically. The dog responded to symptomatic treatment. A week later the dog again presented with neck pain and sternal recumbency. The nose was swollen, and the submandibular and popliteal lymph nodes were moderately enlarged. The body temperature was normal. A complete blood count (CBC) revealed a marked lymphocytosis (23,800 lymphocytes/uI). Over a 3-4 hour period there was a noticeable increase in the size of all peripheral lymph nodes. Treatment included systemic antibiotics and corticosteroids. The dog became ataxic and developed partial paralysis. The neurologic signs waxed and waned over a period of 7 days, and the lymphadenopathy persisted. The peripheral blood lymphocyte count 5 days after the first CBC was done revealed a lymphocyte count of 6,000 lymphocytes/uI. The

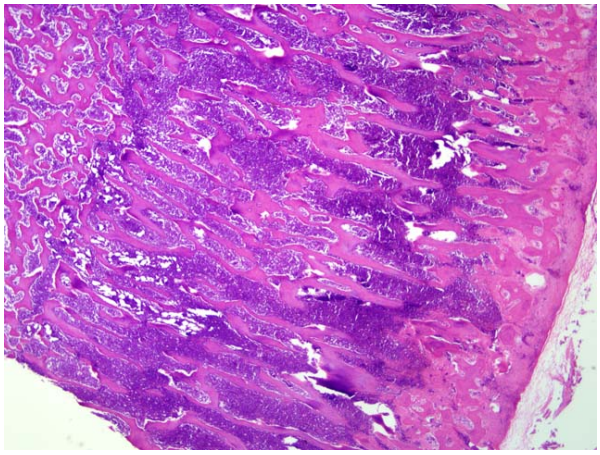

1-1. Bone, cranium, lymphoma, dog.. Trabeculae of periosteal new bone are separated by many neoplastic lymphoid cells. (HE 20X)

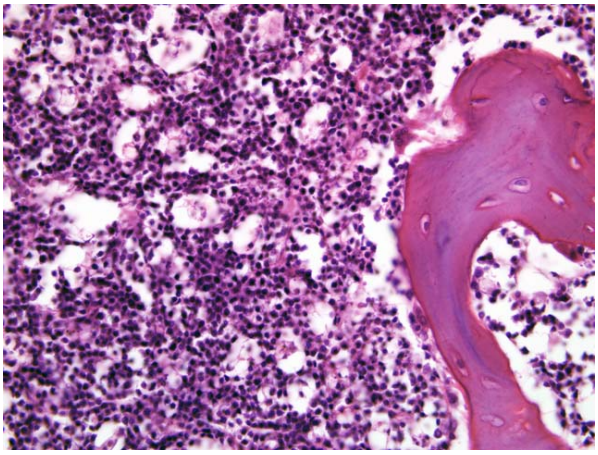

1-2. Bone, cranium, lymphoma, dog. Sheets of neoplastic lymphoid cells replace the medullary cavity and separate trabeculae of new woven bone. (HE 400X)

clinical signs became progressively worse, and the dog was euthanized two weeks after the initial presentation.

Laboratory Results: Immunohistochemical (IHC) staining of bone marrow and lymph node sections revealed that tumor cells were negative for CD3 and CD79α.

Gross Pathology: Marked generalized lymph node enlargement was found. Cut surfaces of the nodes bulged out and had a white homogeneous appearance. The spleen was enlarged and meaty. The thymus was very small. There was marked thickening of the bones of the dorsal cranium (2 cm thick) and moderate thickening of the dorsal lamina of the cervical vertebrae.

Histopathologic Description: Bone, cranium: Histologically, there was a dense infiltrate of a uniform population of medium to large sized lymphocytes in the bone marrow of all sections of bone examined (including femur, sternebrae, and parietal bones). The slides submitted consist of sections of decalcified parietal bone. There was a dense infiltrate of neoplastic lymphocytes in all lymph nodes examined. The infiltrate almost completely obliterated the normal nodal architecture. Neoplastic lymphoid infiltrates were also found in sections of spleen. Microfocal neoplastic lymphoid infiltrates were present in the myocardium and in spinal nerve roots. The thymus was markedly atrophic, and there was lymphoid depletion in Peyer's patches of the small intestine.

Contributor's Morphologic Diagnosis: Lymphoma/ Lymphocytic Leukemia, possible NC cell lymphoma.

Contributor's Comment: This appears to be a case of polyostotic lymphoma with multiple tissue involvement and lymphocytic leukemia. The dog was reportedly initially presented with a pronounced lymphocytosis. There are reports of polyostotic lymphoma in dogs and the affected dogs have been young, most less than 1 year of age. In the one case of polyostotic lymphoma in which staining for T and B lymphocyte markers was performed, the neoplastic lymphocytes did not label positively for any of the marker antibodies tested. In the present case, the affected dog was very young (3.5-months-old) and the neoplastic lymphocytes did not stain with antibodies to T and B cell markers. Immunophenotypic characterization of lymphoma/ lymphocytic leukemia in dogs has revealed that lymphomas are predominantly B-cell origin and lymphocytic leukemias are predominantly T-cell origin. A low percentage of both lymphomas and lymphocytic leukemias of dogs is composed of lymphocytes which do not stain positively for either T-cell or B-cell markers. These "null cell" (NC) lymphocytic neoplasms are thought to be composed of very undifferentiated lymphocytes or natural killer (NK) lymphocytes. It is also possible that these tumors, although composed of cells resembling lymphocytes, are derived from a non-lymphoid hematopoietic cell line.

The neurologic signs in this dog were considered to have been primarily due to the marked thickening of cranial bones and dorsal laminae of cervical vertebrae. Presumably compression of brain, spinal cord, and/or spinal nerves was responsible for the neurologic signs, although no focal degenerative lesions were found in sections of brain or spinal cord. There were microfocal infiltrates of neoplastic lymphocytes in spinal nerve roots, and this infiltrate may have contributed to the neurologic signs. No lymphoid infiltrates were found in the brain or spinal cord.

AFIP Diagnosis: Bone, cranium (per contributor): Malignant lymphoma, with marked cortical osteolysis and periosteal and medullary new woven bone formation.

Conference Comment: Discussion in this case centered on the periosteal components and response to bone injury. The periosteum is composed of an outer fibrous layer and an inner cambium (or osteogenic) layer. The cells of the cambium layer immediately overlying the cortical bone are osteoprogenitor cells that possess the ability to differentiate into osteoblasts.[5,7] The osteoprogenitor cells in the non-reactive periosteum are spindled with flattened nuclei. The periosteum is well supplied with blood vessels, lymphatics and nerve endings.[5]

The typical response of the periosteum to trauma (i.e. fracture) involves differentiation of the osteoprogenitor cells into osteoblasts which rapidly produce new woven bone perpendicular to the cortex.[5,7] In conditions of low oxygen tension there can be an admixture or predominance of cartilage. Though woven bone tends to be the rule, the periosteal osteoblasts can produce lamellar bone when appositional growth is slow.[7] In addition to trauma, any process elevating the perisosteum from the subjacent cortex will result in new bone formation.[5] The new bone is not necessarily static; it can undergo osteoclastic resorption or form lamellar bone.[7] Under certain conditions, the periosteum can become osteoclastic in nature. Most commonly, there is osteoclastic remodeling during long bone growth resulting in diaphyseal narrowing.[7] Additionally, infections of the periosteum can result in osteoclastic bone resorption at the site of inflammation.[7]

In this case, there is expansion of both the fibrous and osteogenic layers. Conference participants speculated on the cause of the periosteal reaction, generating two possible scenarios. First, the tumor could be pushing through the cortex and elevating the periosteum. The second possibility is the mechanical effect of the overlying muscle use causing periosteal tension, separation and subsequent periosteal new bone growth.

Contributor: NMDA – Veterinary Diagnostic Services, P.O. Box 4700, Albuquerque, NM 87196-4700
http://www.nmda.nmsu.edu/animal-and-plant-protection/veterinary-diagnostic-services

References:

1. Ghernati I, Corbin A, Chabanne L, et al. Canine large granular lymphocyte leukemia and its derived cell line products produce infectious retroviral particles. *Vet Pathol*. 2000;37:310-317.
2. Langley-Hobbs SJ, Carmichael S, Lamb CR, Bjornsen AP, Day MJ. Polyostotic lymphoma in a young dog: A case report and literature review. *Small Anim Pract*. 1997;38:412-416.
3. Raskin RE, Krehbiel JD. Histopathology of canine bone marrow in malignant lymphoproliferative disorders. *Vet Pathol*. 1988;25:83-88.
4. Ruslander DA, Gebhard DH, Tompkins MB, Grindem CB, Page RL. Immunophenotypic characterization of canine lymphoproliferative disorders. *In Vivo*. 1997;11:169-172.
5. Thompson K. Diseases of bones and joints. In: Maxie MG, ed. *Jubb, Kennedy and Palmer's Pathology of Domestic Animals*. Vol. 1, 5th ed. Philadelphia, PA: Elsevier Ltd; 2007:13, 15, 21.
6. Vernau W, Moore PF. An immunophenotypic study of canine leukemias and preliminary assessment of clonality by polymerase chain reaction. *Vet Immunol Immunopath*. 1999;64:145-164.
7. Weisbrode SE. Bone and joints. In: McGavin MD, Zachary JF, eds. *Pathologic Basis of Veterinary Disease*. 4th ed. St. Louis, MO: Elsevier; 2007:1052, 1057-1058.

CASE II: R07-114 (AFIP 3103627).

Signalment: Adult male green iguana, reptile (*Iguan iguana*).

History: This iguana was kept indoors in a local zoo. Clinical findings included multiple skin wounds and osteolysis at 3rd to 7th tail vertebra. The animal died of unsuccessful treatment for the tail lesions.

Gross Pathology: The animal had poor overall appearance. The 3rd to 7th tail vertebrae were significantly enlarged where a pale/yellowish lesion measuring 10 cm x 5 cm x 5 cm in diameter with irregular margins was found. Smaller nodules (0.2 cm ~ 0.3 cm in diameter) were scattered throughout the liver, lungs, and epicardium. Both kidneys were pale, moderately to severely enlarged (10 cm x 4 cm x 3 cm) with numerous whitish, pinpoint spots on the capsular surface; the cut surface showed many whitish streaks. Serous atrophy of adipose tissue was observed in the whole body.

Laboratory Results: Microbiological culture: *Serratia marcescens* was isolated from the tail, liver, and lungs.

Histopathologic Description: Tail vertebra with associated skeletal muscle: The tail vertebra has irregular thickening of the periosteum and cortices with multiple irregular areas of necrosis and osteolysis of bone, and the inflammatory process extends outward into the skin. The disrupted bone spicules accompanied with proliferative cartilage and bone tissue of affected areas are characterized by hypereosinophilia or irregular calcification of the matrix. The necrotic foci are roughly nodular and contain variable numbers of epithelioid macrophages and lymphocytes surrounded by fibroblasts. Numerous osteoclast-like cells are present in the affected areas. The periosteum of the vertebra and surrounding skeletal muscle have multifocal to coalescing deposits of necrotic debris surrounded by fibrous connective tissue with inflammatory cells. Numerous colonies of rod-shaped bacteria are present in the center of the affected areas. Immature fibrous connective tissue, similar inflammatory cells and variable amounts of cellular debris have replaced the vertebral bone and surrounding skeletal muscle. The rod bacterial colonies were negative for the B&B stain. Other significant findings in this case are multifocal necrogranulomas randomly scattered throughout the lungs, liver, epicardium and stomach.

Contributor's Morphologic Diagnosis: 1. 3rd to 7th tail vertebrae: Osteomyelitis accompanied with osteolysis, necrogranulomatous, chronic, locally-extensive, severe, with intralesional bacterial colonies of gram-negative rods.
2. Tail, skeletal muscle: Myositis, necrogranulomatous, chronic, locally-extensive, severe.
3. Lungs, liver, heart, stomach: Necrogranulomatous reaction, multifocal, chronic, mild, with intralesional Gram negative rod bacterial colonies (slides not submitted).

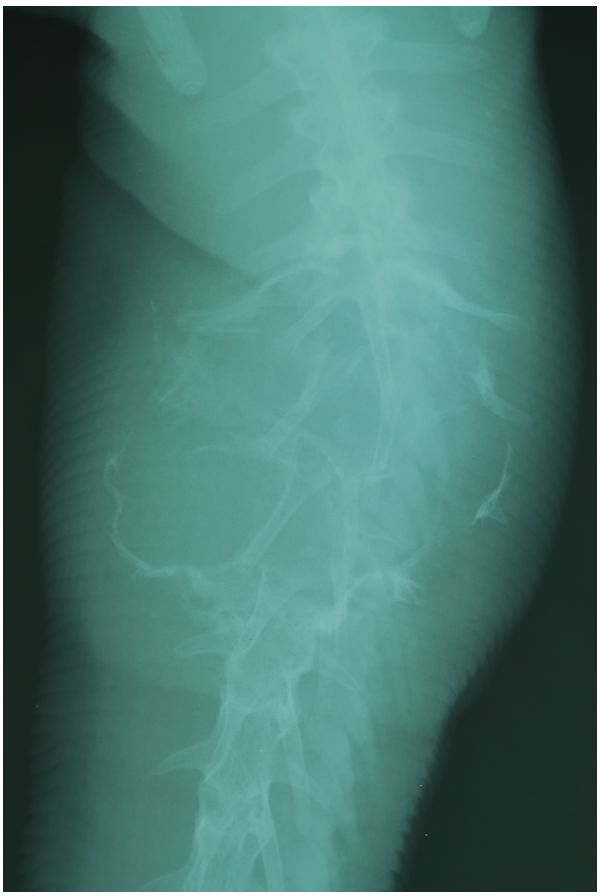

2-1. Vertebral column, tail, green iguana. Radiographically there is severe osteolysis of several adjacent tail vertebrae. Photograph courtesy of Division of Animal Medicine, Animal Technology Institute Taiwan

Contributor's Comment: *Serratia marcescens*, which belongs to *Enterobacteriaceae*, is a motile gram-negative coccobacillus and has been isolated from numerous reptile species. It is a common bacterium in the environment and frequently isolated in soil, water, and food. For human beings, *Serratia marcescens* is mainly an opportunistic pathogen and may cause respiratory, urinary tract, and wound infections. A case of cellulitis of human beings after an iguana bite has been reported. *Serratia* species can acquire resistance against many antimicrobial agents including cephalosporins, macrolides, and many aminoglycosides. Therefore, treatment sometimes is difficult.

This organism appears to be part of the normal oral flora of several reptile species; the bacteria in this case were possibly introduced subcutaneously through a bite wound or other traumatic damage to the integument.

Serratia marcescens has been isolated from subcutaneous granulomas in a green iguana and a northeastern spiny-tailed iguana. However, the pathogenesis of disease in the reptile could be dependent on individual factors, as mice injected

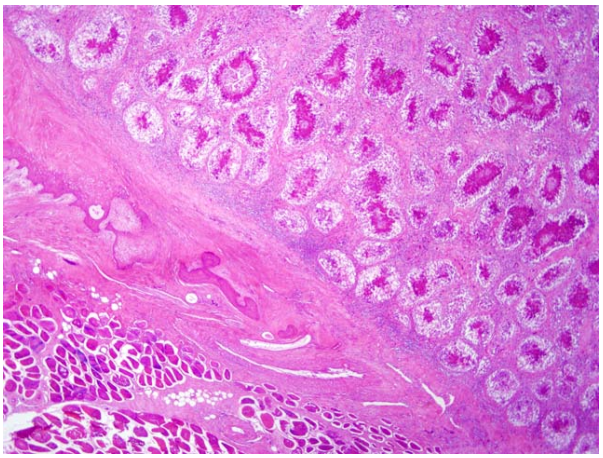

2-2. Vertebrae and skeletal muscle, green iguana. Multifocal to coalescing granulomas replace skeletal muscle and extend into reactive periosteum. There is vertebral osteolysis. (HE 20X)

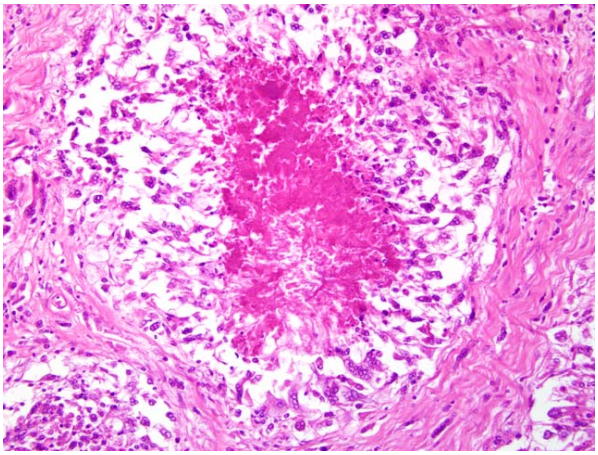

2-3. Skeletal muscle, green iguana. Coalescing granulomas are characterized by a necrotic center surrounded by heterophils and histiocytes bounded by abundant immature fibrous connective tissue. (HE 200X)

intravenously with *Serratia marcescens* eventually clear the infection by the reticuloendothelial system.

AFIP Diagnosis: Bone, vertebra: Heterophilic granulomas, multiple, with periostitis, myositis and fasciitis, bone lysis, and reactive woven bone formation.

Conference Comment: Inflammatory lesions in the bone are classified by the part of the bone affected, and include osteitis (inflammation of the bone), periosteitis, or osteomyelitis (involvement of the marrow cavity). The contributor provides a diagnosis of osteomyelitis.[8] Conference participants did not observe the inflammatory process within the marrow cavity, and thus preferred the histologic diagnosis of periostitis to best characterize the bone involvement in this case. Additionally, participants interpreted the most significant histologic lesions as consistent with multiple heterophilic granulomas, with the skeletal changes being secondary to the primary infection.

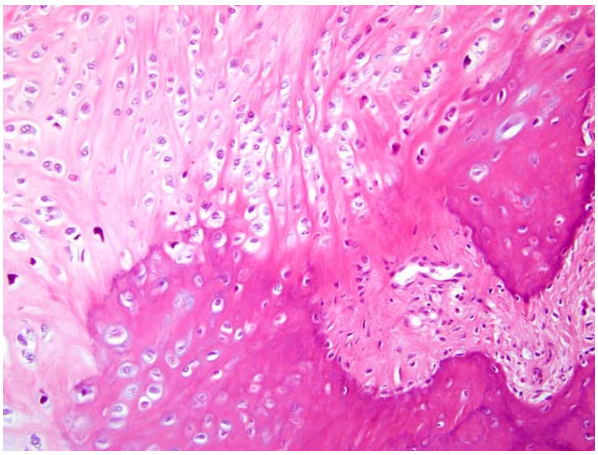

2-4. Vertebra, green iguana. Multifocally Sharpey's fiber-like connective tissue undergoes osseous metaplasia. (HE 200X)

An interesting aspect of this case observed by the conference moderator is the presence of woven, compact periosteal new bone without prominent osteoblasts. The moderator also pointed out examples of metaplasia of fibrous connective tissue to bone in the presence of Sharpey fiber-like insertion. Sharpey's fibers are typically seen embedded in bone matrix at the point of tendon insertion into the bone; they are histologically characterized as dense bands of connective tissue emerging from the tendon or ligament which intermingle with the outermost lamellae.[9] Sharpey's fibers are also present in the periodontal ligament where they anchor the alveolar bone to the cementum of the tooth.[9] A fibromatous epulis of periodontal ligament origin with bone-like matrix will have Sharpey's fibers extending into the surrounding connective tissue.[2]

Unlike this case, most cases of inflammation involving bone are classified as osteomyelitis. There are several anatomic and physiologic factors predisposing animals, particularly young animals, to bacterial osteomyelitis; infection often localizes in sites of active endochondral ossification of the metaphyses and epiphyses of long bones and vertebral bodies. Such factors include:[7]

- Capillaries invading the mineralized cartilage make hairpin turns prior to entering the sinusoidal vessels which communicate with medullary veins.
- Capillaries are fenestrated, allowing bacteria to easily leave the vasculature and enter the marrow cavity.
- Sinusoidal blood flow is sluggish and resident phagocytic cells are relatively inefficient.
- Trauma may alter the metaphyseal environment and enhance bacterial infection.

In addition to host factors, several pathogen factors also favor establishment of infection in the marrow. *Staphylococcus aureus* and other bacteria have receptors for bone surface proteins; bone trauma makes these binding sites more

available to the bacteria. Many bacteria form a thick mucopolysaccharide glycocalyx which surrounds them and functions to allow tighter adherence to the bone surface, protects the organism from the host immune system, and inhibits uptake of antibiotics.

A common finding in osteomyelitis is osteolysis. Cytokines, such as tumor necrosis factor, IL-1, and prostaglandin E_2 when released from inflammatory cells activate osteoclasts.[7] Common causes of bacterial osteomyelitis in select species are as follows:[7]

- Equine: *Escherichia coli* (most common in foals); *Streptococcus* spp.; *Salmonella* spp.; *Klebsiella* spp.; and *Rhodococcus equi*
- Bovine: *Salmonella* spp.; *Arcanobacterium pyogenes*
- Canine: Rare; often in dogs that are neutropenic following infection with canine parvovirus-1
- Feline: *Staphylococcus intermedius*; other *Staphylococcus* spp.; *Streptococci* spp.; *E. coli*; *Proteus* spp.

Contributor: Division of Animal Medicine, Animal Technology Institute Taiwan, P.O. Box 23, Chunan, Miaoli, Taiwan 350

References:

1. Equi RA, Green WR. Endogenous *Serratia marcescens* endophthalmitis with dark hypopyon: A case report and review. *Surv Ophthalmol*. 2001;46:259-268.
2. Head KW, Cullen JM, Dubielzig RR, et al. *Histological Classification Tumors of the Alimentary System of Domestic Animals*, *2nd series*. Vol. X. Washington DC: Armed Forces Institute of Pathology; 2007:53-54.
3. Matsumoto K, Yamamoto T, Kamata R, Maeda H. Pathogenesis of serratial infection: Activation of the Hageman factor-prekallikrein cascade by serratial protease. *J Biochem*. 1984;739-749.
4. Mayer CW, Bangash S, Bocchini JA, Nordberg ML, Bahna SL. *Serratia marcescens* osteomyelitis in an infant. *Allergy Asthma Proc*. 2006;27:544-548.
5. Novak SS, Seigel RA. Gram-negative septicemia in American alligators (*Alligator mississippinesis*). *J Wildl Dis*. 1986;22:484-487.
6. Thomas MJ, Lowes JA, Tabaqchali S. *Serratia marcescens* in mixed aerobic infections of bone: A report of two patients. *J Bone Joint Surg*. 1980;62:389-390.
7. Thompson K. Diseases of bones and joints. In: Maxie MG, ed. *Jubb, Kennedy and Palmer's Pathology of Domestic Animals*. Vol. 1, 5th ed. Philadelphia, PA: Elsevier Ltd; 2007:15, 21, 95-97.
8. Weisbrode SE. Bone and joints. In: McGavin MD, Zachary JF, eds. *Pathologic Basis of Veterinary Disease*. 4th ed. St. Louis, MO: Elsevier; 2007:1076.
9. Young B, Lowe JS, Stevens A, Heath JW. Oral tissues. In: Young B, Lowe JS, Stevens A, Heath JW, eds. *Wheater's Functional Histology: A Text and Colour Atlas*. 5th ed. Philadelphia, PA: Elsevier, Churchill Livingstone; 2006:257.

CASE III: S 688/07 (AFIP 3164801).

Signalment: 11-year-old female Yucatan pig (*Sus scrofa*).

History: The animal had abrupt hind leg paresis. Radiographic and computed tomographic examination revealed osteolysis of thoracic and lumbar vertebrae as well as proximal parts of the second and tenth ribs.

Gross Pathology: All thoracic and lumbar vertebrae had marked osteolysis and replacement of the bone marrow by a soft yellowish to pink mass. The spinal cord was compressed by nodules of the same mass at the second and third lumbar vertebra. The proximal end of the tenth rib had a pathological fracture and a nodule (3 × 1.0 × 0.5 cm) of soft yellowish tissue protruding into the thoracic cavity. Bone marrow of this rib was also replaced by soft yellow to pink tissue.

Laboratory Results: Lymphopenia (3.76 G/L [ref.: 6 – 16.0 G/L]); hypophosphatemia (1.75 mmol/L [ref.: 2.1 – 3.3 mmol/L]).

Histopathologic Description: Rib: The bone marrow is focally infiltrated, effaced and replaced by a non-encapsulated, poorly circumscribed, infiltrative, highly cellular neoplastic mass. Neoplastic cells form solid sheets that are supported by a moderate fibrovascular stroma. Cells are ovoid to polygonal with distinct cell borders, moderate amounts of pale eosinophilic cytoplasm, sometimes with a crescent shaped perinuclear halo. Nuclei are located eccentrically, ovoid, sometimes cleaved, and 2 - 2.5 times the size of erythrocytes in diameter (15-18 µm), with coarsely stippled chromatin and 1 to 3 mostly indistinct nucleoli. There is moderate anisocytosis and marked anisokaryosis. Mitotic rate is 1 to 2 mitoses per high power field with some atypical mitoses. There are multifocal prominent apoptotic neoplastic cells characterized by hypereosinophilia and/or nuclear fragmentation (karyorrhexis). Trabecular and cortical bone is multifocally devoid of osteoblasts and there is mild activation of osteoclasts and resorption of bone. Continuity of the cortical bone is multifocally disrupted by infiltration of neoplastic cells and pathological fractures (not visible in all slides). There is marked periosteal reactive fibroplasia sometimes intermingled with extravasated erythrocytes (hemorrhage) or necrosis. Within the fibrous tissue are multifocal infiltrates of mature lymphocytes. Adjacent to pathological fractures the neoplastic cells multifocally invade the intrathoracic adipose tissue.

Contributor's Morphologic Diagnosis: Rib: Plasma cell myeloma, with pathological fracture, callus formation and medullary cavity fibrosis (not present on all slides), Yucatan pig, porcine.

Contributor's Comment: Plasma cell myelomas (multiple myelomas) are rare neoplasms in animals other than dogs.[4] In the pig they are exceedingly rare.[3,4] Plasma cell myelomas are multicentric neoplastic proliferations of plasma cells originating within the bone marrow and usually secrete large amounts of monoclonal immunoglobulin heavy and/or light chains resulting in monoclonal gammopathy.[1] Most common sites of origin are the vertebrae, ribs, sternum and the skull.[6] An important feature of plasma cell myelomas is invasion of the adjacent bone by activated osteoclasts resulting in skeletal destruction and pathological fractures.[1] Lytic bone lesions within the spongiosa are usually crescent shaped and the corticalis is rarefied.

In humans, diagnostic criteria for plasma cell myelomas are more than 10% clonal plasma cells in the bone marrow, occurrence of monoclonal proteins in the serum and/or urine, and evidence of plasma cell neoplasia associated organ damage. The latter may include hypercalcemia, renal insufficiency, anemia, and lytic bone lesions.[1] Twelve to 15% of cases in people are accompanied by amyloid deposition due to synthesis of immunoglobulin light chains. In this pig, no amyloid deposition was noted. Rare cases of non-secretory multiple myelomas exist in humans,[1] and the present case is apparently also a non-secretory variant. In non-secretory variants, the presence of more than 30% of clonal plasma cells in the bone marrow is a diagnostic criterion.[1]

Clinical signs may include lameness due to bone pain, anemia, renal failure, hyperproteinemia or splenomegaly. Macroscopically, pathological fractures, lytic bone lesions, and nodular, soft, tan masses may be present. Renal failure in plasma cell myelomas is due to hypercalcemia and/or secretion of light chains that are referred to as Bence-Jones protein. The latter may pass the glomeruli and result in tubular damage.

Histologically, plasma cell myelomas consist of uniform cells with moderate to marked amounts of densely stained cytoplasm often with a perinuclear halo and a nuclear diameter of 1.5 to 2 (12-15 µm) times the size of red blood cells. Chromatin is dark staining and 1 to 3 indistinct nucleoli may be visible. Mitotic rate is low, and frequency of mitoses is often below that of normal bone marrow.[6,7]

Immunophenotypic characterization of plasma cell myelomas can be challenging because terminally differentiated B-cells lose their typical markers, such as CD20 and CD79α. If they remain immunopositive, a diagnosis of plasma cell myeloma is supported, while in the opposite case the diagnosis cannot be excluded.[1,8] In this case, some tumor cells expressed CD79α, supporting the diagnosis of plasma cell origin. An important differential diagnosis for the histological lesion is solitary osseous plasmacytoma. This can be excluded by the multifocal distribution of the lesion in the case of this pig. However, solitary osseous plasmacytoma can give rise to plasma cell myeloma.[6] In summary, this is a rare case of porcine plasma cell myeloma (multiple myeloma) with associated characteristic bone lesions.

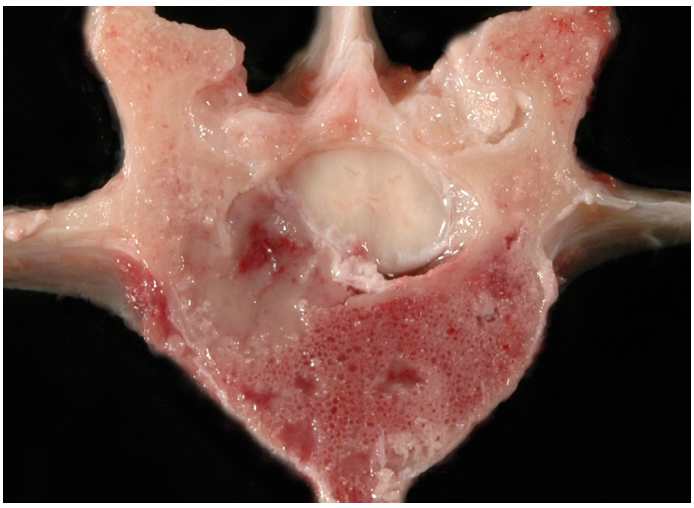

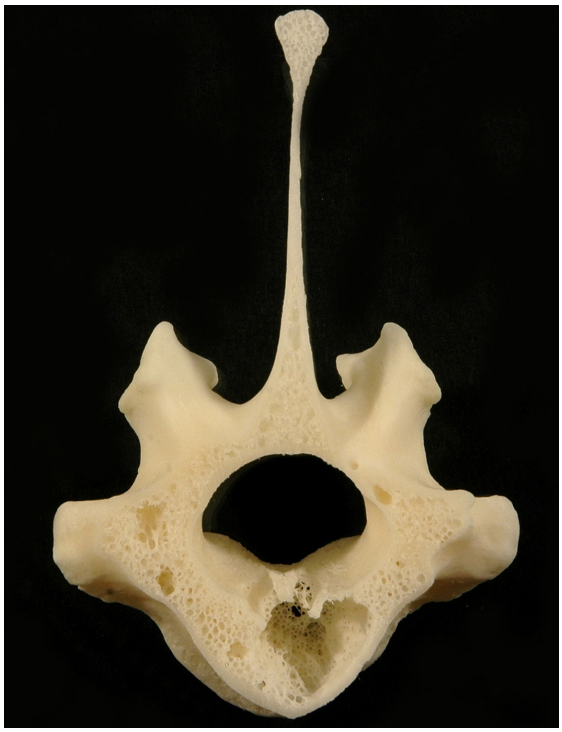

3-1, 3-2. Vertebra (with spinal cord), plasma cell myeloma, Yucatan pig. A soft pink yellowish mass infiltrates and replaces the vertebral body (3-1), and there is a large focus of osteolysis (3-2). Photographs courtesy of Department of Veterinary Pathology, Freie Universitaet Berlin, Germany, http://www.vetmed.fu-berlin.de/einrichtungen/institute.

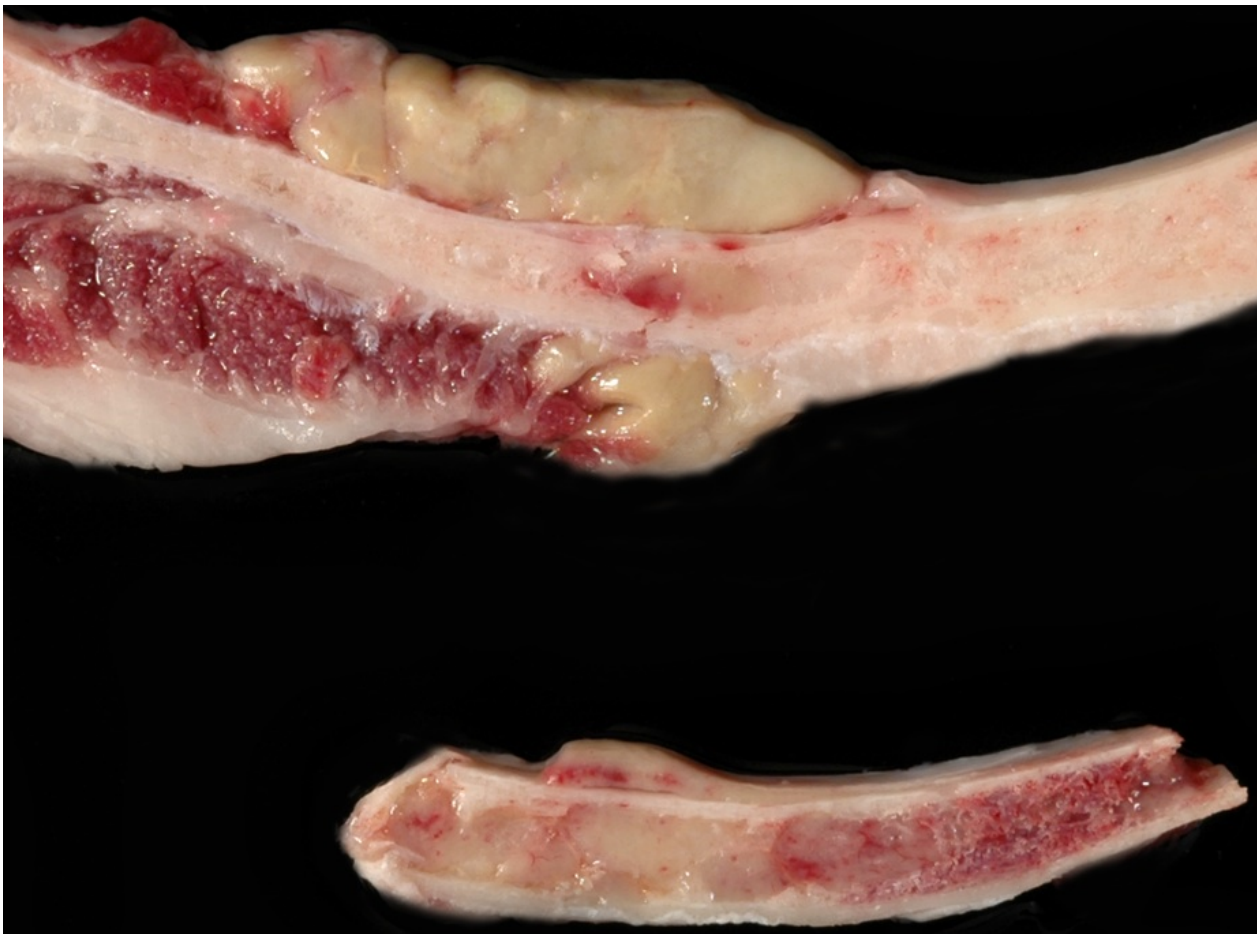

3-3. Rib, plasma cell myeloma, Yucatan pig. A soft yellow mass surrounds the rib and expands the marrow cavity near the site of a pathologic fracture. Photograph courtesy of Department of Veterinary Pathology, Freie Universitaet Berlin, Germany, http://www.vetmed.fu-berlin.de/einrichtungen/institute.

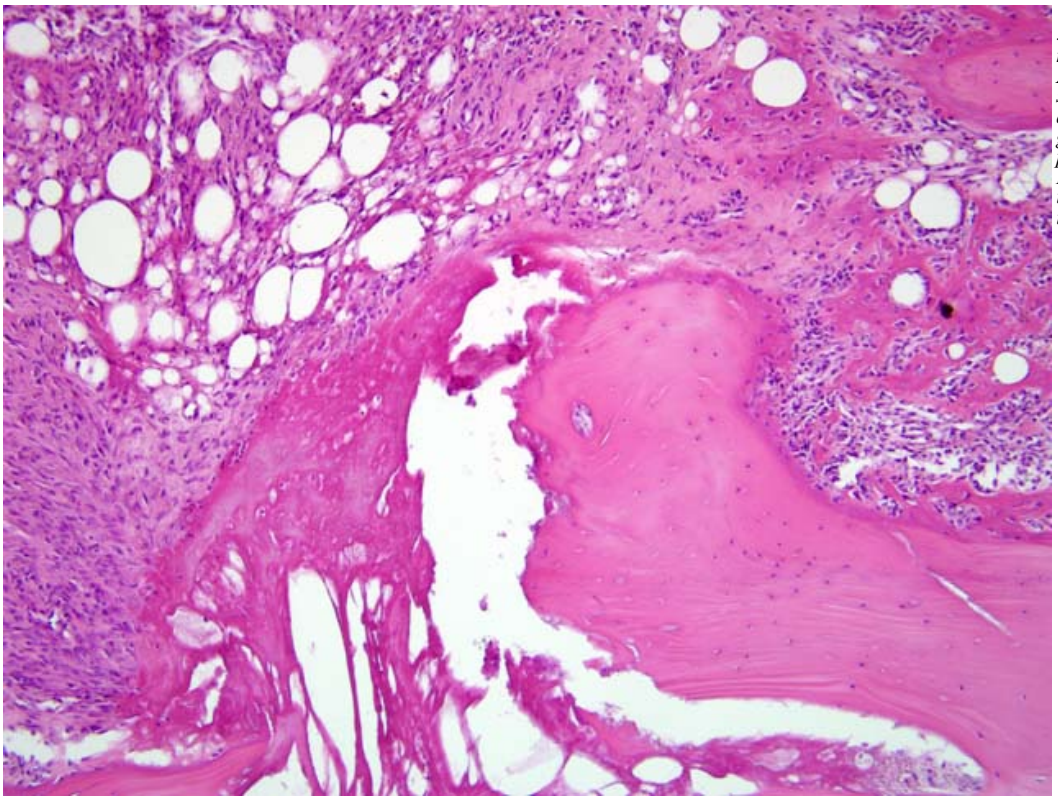

3-4. Rib, plasma cell myeloma, Yucatan pig. An early callous with spindle cell proliferation and periosteal new bone growth surrounds a pathologic fracture. Necrotic bone occurs at the fragmented ends of the fracture. (HE 100X)

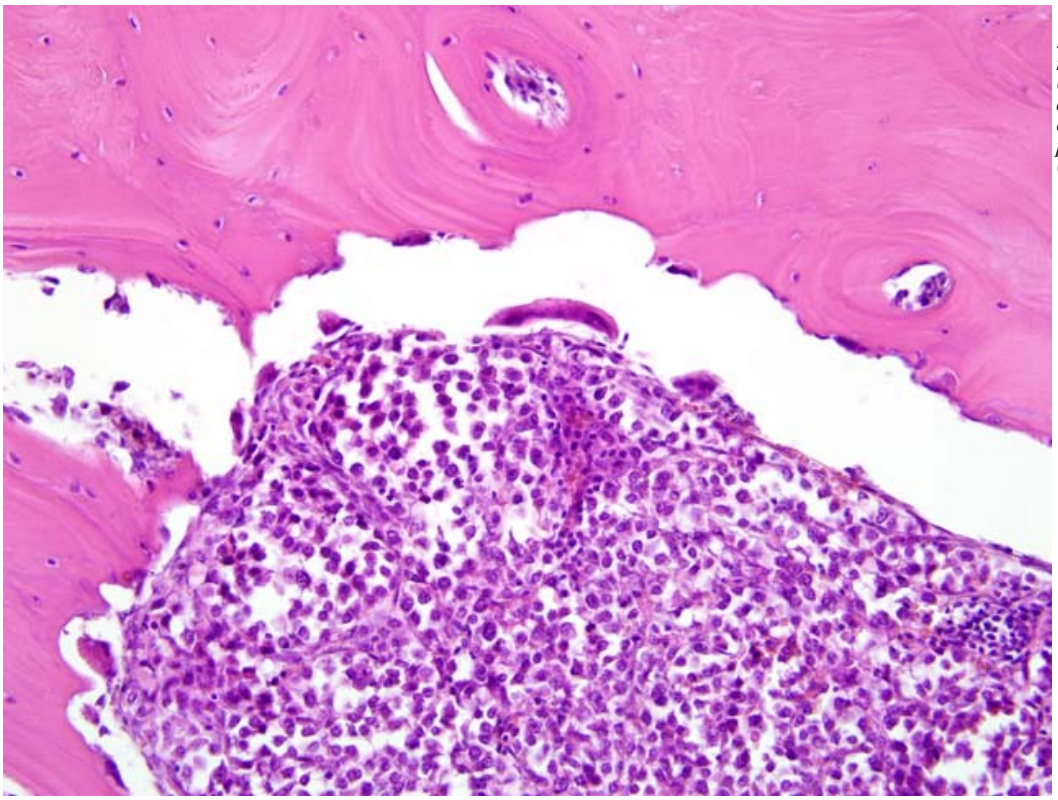

3-5. Rib, plasma cell myeloma, Yucatan pig. Osteoclasts resorb bone at the interface of the endosteal bone and the plasma cell neoplasm. (HE 200X)

AFIP Diagnosis: Bone, rib: Plasma cell myeloma, intramedullary and extracortical, with lysis of cortical bone, pathologic fracture, and early callus formation.

Conference Comment: Though undecided on the underlying neoplastic process, conference participants agreed the disruption in the cortical bone represented a pathologic fracture. Fractures of normal bone due to application of excessive force are referred to as traumatic, while pathologic fractures occur in abnormal bone due to minimal trauma or normal use. During bone fracture, there is damage to the periosteum, cortical bone and soft tissue, resulting in hemorrhage with subsequent hematoma formation. Due to the distance of the fracture ends from the vascular supply, these areas often undergo necrosis characterized histologically as death and loss of osteocytes from their lacunae. Complete disappearance of osteocytes can take as long as to 2 - 4 weeks, and thus the only histologic finding may be osteocyte pyknosis. Macrophages, platelets, proliferating osteogenic tissue and lytic bone release bone morphogenic proteins (BMPs), transforming growth factor-β (TGF-β), and platelet-derived growth factor (PDGF) to regulate callus formation and healing. In the first two days after fracture, there is infiltration by undifferentiated mesenchymal cells from the periosteum, endosteum, and medullary cavity. During this time, the hematoma undergoes neovascularization. As the mesenchymal cells form a loose collagen network, the immature collagen, mesenchymal cells and vasculature begin organizing into granulation tissue. As woven bone is laid down, it forms the primary callus around the fracture to stabilize it and allow time for development of a secondary callus of lamellar bone.[9]

Participants also discussed the pathophysiology of osteolysis seen with myeloma. Neoplastic cells secrete macrophage inflammatory protein-1α (MIP-1α) which upregulates the expression of the receptor activator of nuclear factor-κB (NF-κB) ligand (RANKL).[2] The RANKL binds to its receptor on osteoclast precursor cells, resulting in upregulation of NF-κB, which is required for differentiation and survival of osteoclasts.[5] The differentiation of osteoclasts is tightly regulated to prevent excessive osteolysis that could result in potentially life-threatening hypercalcemia; marrow stromal cells are able to block osteoclast precursor differentiation. Stromal cells secrete WNT protein, which binds to osteoblast receptors LPR5 and LPR6 and triggers the activation of the β-catenin pathway and ultimate production of osteoprotegrin.[5] Osteoprotegrin binds to RANK, essentially preventing RANKL binding and osteoclast differentiation.[5]

Participants commented on the slide variability, with the plasma cell neoplasia or bone fracture occasionally missing from individual slides.

Contributor: Department of Veterinary Pathology, Freie Universitaet Berlin, Germany
http://www.vetmed.fu-berlin.de/einrichtungen/institute/we12/index.html

References:

1. Kyle RA, Child JA, Anderson K. Criteria for the classification of monoclonal gammopathies, multiple myeloma and related disorders: A report of the International Myeloma Working Group. *Br J Haematol*. 2003;121:749-757.
2. Kumar V, Abbas AK, Fausto N, Aster JC. Diseases of white blood cells, lymph nodes, spleen and thymus. In: Kumar V, Abbas AK, Fausto N, Aster JC, eds. *Robbins and Cotran Pathologic Basis of Disease*. 8th ed. Philadelphia, PA: Elsevier Saunders; 2009:609-610.
3. Marcato PS. Swine lymphoid and myeloid neoplasms in Italy. *Vet Res Commun*. 1987;11:325-337.
4. Rintisch U, Munzer B, Klopfleisch R, Lahrmann KH. Multiple myeloma in a Yucatan pig. *Berl Munch Tierarztl Wochenschr*. 2010;123:70-73.
5. Rosenberg AE. Bones, joints and soft-tissue tumors. In: Kumar V, Abbas AK, Fausto N, Aster JC, eds. *Robbins and Cotran Pathologic Basis of Disease*. 8th ed. Philadelphia, PA: Elsevier Saunders; 2009:1206-1209.
6. Valli VE. Hematopoietic system. In: Maxie MG, ed. *Jubb, Kennedy and Palmer's Pathology of Domestic Animals*. Vol. 3, 5th ed. Philadelphia, PA: Elsevier Ltd; 2007:107-324.
7. Valli VE, Jacobs RM, Parodi AL, Vernau W, Moore PF. *Histological Classification of Hematopoietic Tumors of Domestic Animals*. 2nd Series, Vol. VIII. Washington, DC: Armed Forces Institute of Pathology; 2002.
8. Vega F, Chang CC, Medeiros LJ, et al. Plasmablastic lymphomas and plasmablastic plasma cell myelomas have nearly identical immunophenotypic profiles. *Mod Pathol*. 2005;18:806-815.
9. Weisbrode SE. Bone and joints. In: McGavin MD, Zachary JF, eds. *Pathologic Basis of Veterinary Disease*. 4th ed. St. Louis, MO: Elsevier; 2007:1091-1094.

CASE IV: F10/10 (AFIP 3167507).

Signalment: 14-year-old stallion PRE ("Pura Raza Española"), equine (*Equus caballus*).

History: The horse had left hind limb lameness of four months duration leading up to euthanasia. On initial examination, the lameness was localized to the middle phalanx region, and an abscess of the sole was found (radiographs were not taken). The abscess was surgically drained and the horse was treated with an NSAID (Meloxicam) for one month. The lameness improved with treatment, but the horse was still lame. After an additional one month, a cystic lesion in the center of the middle phalanx was found on radiographs. The horse was rested and a continued NSAID treatment was followed. After an additional two months the cystic lesion was still the same size and the horse was euthanized.

Gross Pathology: The left and right hind legs, including proximal, middle and distal phalanges were examined. A cavity within the bone, measuring 3.5 x 4 x 5 cm, in the center of the middle phalanx of the left hind leg was found. The lesion was divided internally by red septa containing streaks of fibrin and soft fibrous tissue, creating multiple cystic spaces of variable sizes. Pronounced soft tissue was present mainly in the proximal part of the lesion. A mild uneven dorsal periosteal border could be palpated. The joints were intact. The right hind leg was normal. Radiographs also show the cystic lesion in the left hind leg middle phalanx.

Histopathologic Description: Tissue from bone, articular cartilage, and subchondral bone of the left proximal middle phalanx: Intact articular cartilage covers a sclerotic subchondral bone of lamellar compact bone structures; focal superficial chondrocyte clusters can be seen in the articular cartilage in some of the sections. The cavity with the bone is characterized by multiple blood-filled spaces of variable sizes. The soft tissue of the lesion in the bone shows large areas of fibrin with adjacent granulation tissue, including neovascularization and fibroblast activity. Also, focal areas of osteoid with reactive trabecular woven bone are present in the loose connective tissue in most of the submitted sections. The border between the lesion and bone shows mild multifocal osteoclast activity and connective tissue with loose strands of fibroblasts and vessels.

Contributor's Morphologic Diagnosis: Bone cyst, unicameral-aneurysmal-like, middle phalanx, left hind leg, equine.

Contributor's Comment: Aneurysmal bone cysts are defined as destructive expansive lesions in bone.[1] It is a rare lesion but has mostly been reported in young individuals, both in humans,[2] dogs,[3] cats,[10] cattle[1] and horses.[6,11,12] However, too few cases are described to define a predilection site or age prevalence. A unicameral cyst of bone is a slow growing expansive lesion also reported in young individuals.[14] These cysts may be solitary or multiple. The content of the unicameral cyst contains connective tissue with multinucleated giant cells and hemosiderin-laden macrophages, with foci of reactive bone. Periosteal bone formation is not a feature of this type of cyst.[14]

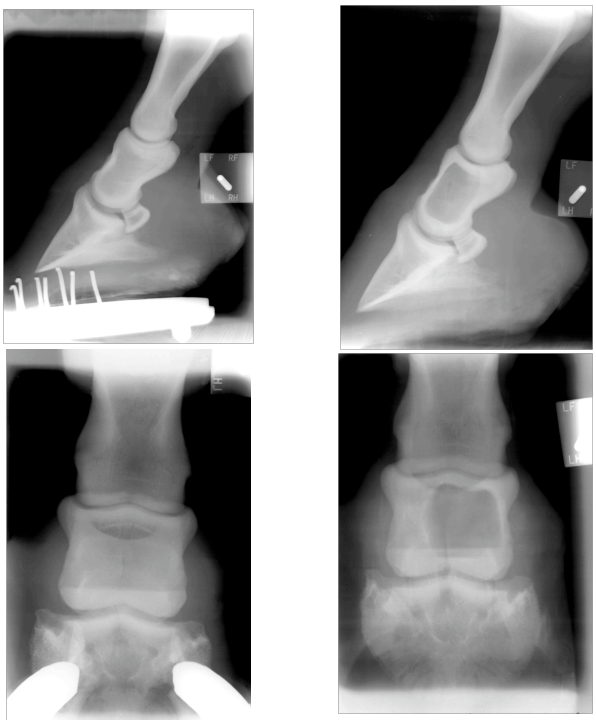

4-1, 4-2, 4-3, 4-4. Phalanges 1,2,3, hind limb, horse. Radiographs comparing the normal right limb (4-1 and 4-3) and the affected left limb (4-2 and 4-4). There is a large radiolucent cyst expanding the medullary cavity of P2 of the left foot (4-2 and 4-4). Photographs courtesy of Department of BVF, Division of Pathology, Uppsala, Sweden, www.slu.se.

The aneurysmal cyst is characterized by blood-filled spaces separated by loose fibrous tissue. The tissue sometimes contains foci of giant cells and hemosiderin-filled macrophages; hence the soft tissue is similar to the unicameral cyst. Osteoid or reactive bone can also be present in the connective tissue. The typical aneurysmal bone cyst arises from the outer surface of the bone close to the periosteum. The periosteum often shows reactive bone proliferation. An underlying preexisting lesion is always discussed, but seldom identifiable, due to the reactive granulation tissue. Fibrous dysplasia and neoplasia have been seen in association with aneurysmal bone cysts. An altered blood flow due to trauma has been suggested as a cause.[14]

In humans, the aneurysmal bone cysts are mostly reported in the metaphyseal or diaphyseal areas of the long bones -- femur, tibia, humerus and in the spine. It is mostly seen in the immature skeleton, but can be found in adults as well.[7,8] Cysts of the phalanges are uncommon, but bone cysts have been reported,[9] including epidermoid bone cysts.[5]

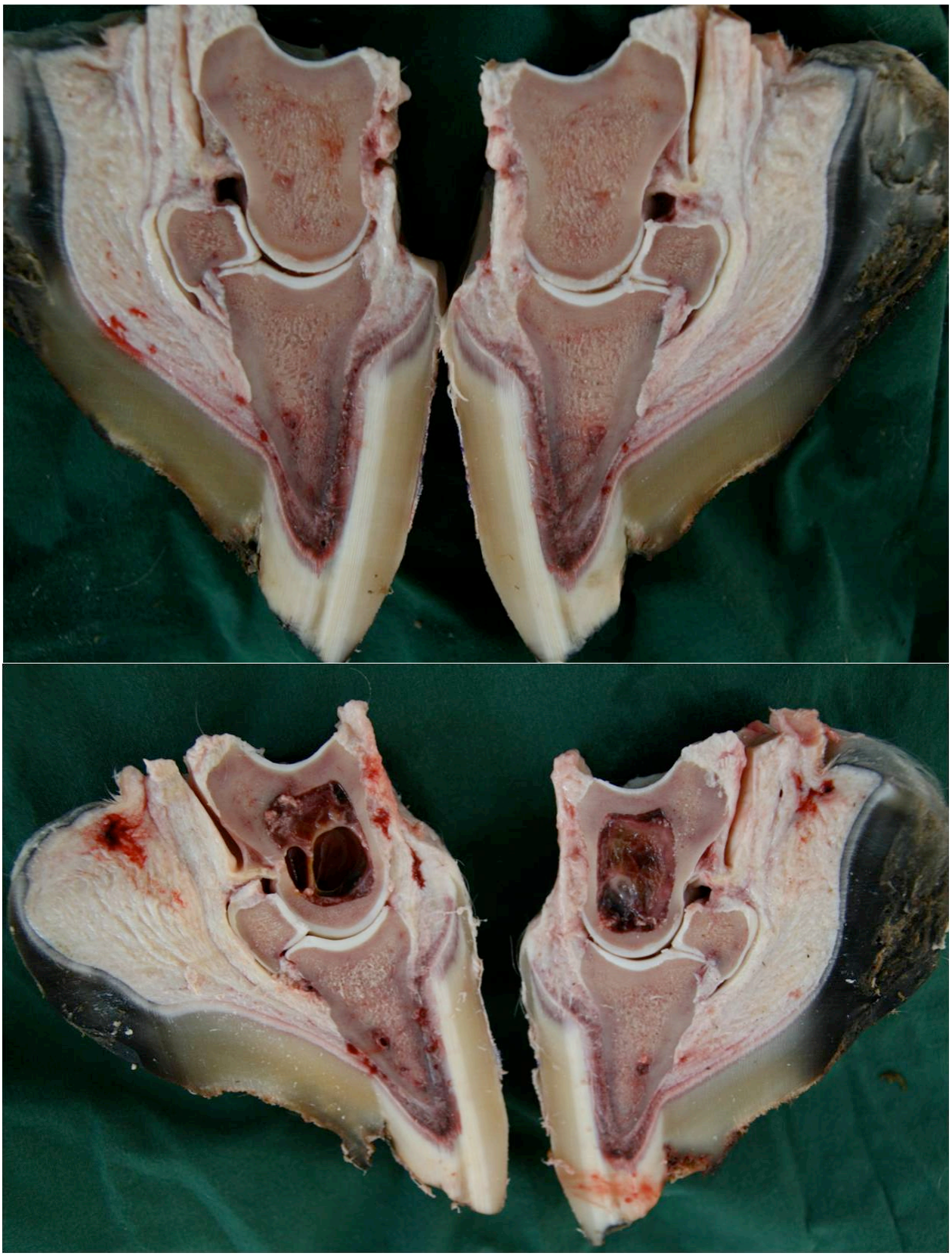

4-5, 4-6. Normal right (4-5) and affected left middle phalanx (4-6), hind foot, horse. A cavity within P2 contains fibrin and soft fibrous tissue and is divided internally by red septa creating multiple cystic spaces. Photographs courtesy of Department of BVF, Division of Pathology, Uppsala, Sweden, www.slu.se.

The present lesion is unusual with reference to the age of the animal and the location as well as the size. The histological appearance is compatible with an aneurysmal cyst as well as a unicameral cyst. The lack of involvement of the periosteum favors a unicameral cyst; however, the multiple blood-filled spaces are more compatible with an aneurysmal cyst. The presented lesion does not show any evidence of fibrous dysplasia, epidermoid cyst or neoplasia. In summary, this is a solitary bone cyst of the middle phalanx with macroscopic appearance of a unicameral cyst. The microscopic features are compatible with a unicameral bone cyst, but also histologically similar to an aneurysmal cyst.

AFIP Diagnosis: Bone, left hind limb, second phalanx (per contributor): Unicameral bone cyst.

Conference Comment: Tissue sectioning and orientation presented some difficulties with histologic interpretation for many conference participants. Based solely on the species information and histopathologic evaluation most participants included myelofibrosis and/or myelonecrosis in the differential diagnosis; in the absence of additional information and the histologic findings of hemorrhage, fibrin, granulation tissue and reactive fibroblasts are not inconsistent with necrosis and fibrosis of the marrow space. With the additional clinical information, radiographs, and gross images subsequently made available during conference, attendees and the conference moderator essentially agreed with the contributor's interpretation and histomorphologic diagnosis.

This case also was studied in consultation with the AFIP Department of Orthopedic Pathology, since this entity is rarely seen histologically in veterinary species; their differential diagnosis included aneurysmal bone cyst (ABC), unicameral bone cyst (UBC), and ganglion cyst. In the opinion of the orthopedic pathology subspecialists, the histologic findings in this horse are most consistent with a ganglion cyst. Additionally, humans with UBC often respond well to corticosteroid therapy; the history from this horse does not indicate that corticosteroid therapy was attempted. Furthermore, a brief literature search did not identify reports of ganglion cysts in veterinary species. The few reports of aneurysmal bone cysts in horses indicate that most animals are euthanized due to lesion recurrence or failure of treatment, which often includes corticosteroids.[6,11,12]

Disease	Histopathogenesis	Gross Appearance	Histologic Appearance
Fibrous dysplasia	Possible developmental defect; replacement of bone by expanding mass of fibro-osseous tissue	• Enlarged external contour • Firm with mineralized foci • Many serosanguineous cysts	• Well-differentiated fibrous tissue with regularly spaced, uniformly sized trabeculae of woven bone • Lack of osteoblasts on trabeculae • Osteoclasis
Subchondral DJD	Fissure/clefting of articular cartilage → undermined by synovial fluid → pressure, cytokines → osteoclast activation → lysis	Subchondral cystic spaces and necrosis	• Cystic spaces lined by synovial cell-like membrane • Serous fluid
Subchondral OCD	Failure of endochondral ossification → necrosis → cavitation of retained growth cartilage	Subchondral cystic spaces and necrosis	• Myxomatous matrix with fibrosis • ± degenerate cartilage
Unicameral bone cyst	Unknown; possibly due to decreased venous drainage in areas of active endochondral ossification	• Cysts with serous-like or serosanguineous fluid • Lined by connective tissue • ± pathological fracture	• Cyst wall: Variably dense connective tissue and woven to lamellar bone • Marginal remodeling • ± multinucleate giant cells and hemosiderophages
Aneurysmal bone cyst	Unknown; possible causes include altered blood flow e.g ischemia, hemorrhage, vascular malformation	• Cysts with blood or serosanguineous fluid • ± pathological fracture	• Hemorrhage and hemosiderosis • Cavernous blood-filled spaces • Spaces separated by fibrous, fibro-ossesous, or undifferentiated mesenchymal cell septa • Osteoclast-like multinucleated giant cells

In contrast, unicameral bone cysts in horses typically respond well to surgical curettage.[13]

The moderator and participants discussed the differential diagnosis and histopathogenesis for radiographic bone cysts, which includes fibrous dysplasia, subchondral degenerative joint disease (DJD), subchondral osteochondrosis (OCD), unicameral bone cyst, and aneurysmal bone cyst; these entities are summarized in the included chart.[13,15]

We thank the Department of Orthopedic Pathology for their review of this case, and specifically Dr. Daniel Strum for his comments.

Contributor: Department of BVF, Division of Pathology, Box 7028, SLU, (Travvägen 12D), 750 07 Uppsala, Sweden www.slu.se

References:

1. Belknap EB, Brodie S, Lawry J, Getzelman R. Aneurysmal bone cyst in a Holstein bull. *J Am Vet Med Assoc*. 1992;201:1413-1415.
2. Biller DS, Johnson GC, Birchard SJ, Fingland RB. Aneurysmal bone cyst in a rib of a cat. *J Am Vet Med Assoc*. 1987;190:1193-1195.
3. Chan G, Arkader A, Kleposki R, Dormans JP. Case report, Primary aneurysmal bone cyst of the epiphysis. *Clin Orthop Relat Res*. 468:1168-1172, 2010.
4. Dabareiner RM. Diseases of bones, joints, and connective tissues. In: Smith BP, ed. *Large Animal Internal Medicine*. 4th ed. St. Louis, MO: Mosby Elsevier; 2009:1190-1192.
5. Eimani MT, Kumar PV. Epidermoid cyst of the terminal phalanx of the right thumb diagnosed by fine needle aspiration cytology. *Acta Cytol*. 1999;43:326-328.
6. Lamb CR, Schelling SH. Congenital aneurysmal bone cyst in the mandible of a foal. *Equine Vet J*. 1989;21:130-132.
7. Leithner A, Windhager R, Lang S, Haag OA, Kainberger F, Kotz R. Aneurysmal bone cyst: A population based epidemiologic study and literature review. *Clin Orthop Relat Res*. 1999;363:176-179.
8. Mankin HJ, Hornicek FJ, Ortiz-Cruez E, Villafuerte J, Gebhardt MC. Aneurysmal bone cyst: A review of 150 patients. *J Clin Oncol*. 2005;23:6756-6762.
9. Ropars M, Kaila R, Briggs T, Cannon S. Aneurysmal bone cysts of the metacarpals and phalanges of the hand. A 6 case series and literature review (in French). *Chir Main*. 2007;26:214-217.
10. Shimada A, Yanagida M, Umemura T, Tsukamoto S, Suganuma TJ. Aneurysmal bone cyst in a dog. *J Vet Med Sci*. 1996;58:1037-1038.
11. Steiner JV, Rendano VT Jr. Aneurysmal bone cyst in the horse. *Cornell Vet*. 1982;72:1193-1195.
12. Thomas HL, Livesey MA, Caswell JL. Multiple aneurysmal bone cysts in a foal. *Can Vet J*. 38:570-573.
13. Thompson K. Diseases of bones and joints. In: Maxie MG, ed. *Jubb, Kennedy and Palmer's Pathology of Domestic Animals*. Vol. 1, 5th ed. Philadelphia, PA: Elsevier Ltd; 2007:112, 129, 143-144.
14. Thompson K. Diseases of bones and joints. In: Maxie MG, ed. *Jubb, Kennedy and Palmer's Pathology of Domestic Animals*. Vol. 1, 5th ed. Philadelphia, PA: Elsevier Ltd; 2007:129-130.
15. Weisbrode SE. Bone and joints. In: McGavin MD, Zachary JF, eds. *Pathologic Basis of Veterinary Disease*. 4th ed. St. Louis, MO: Elsevier; 2007:1085-1086.

The Armed Forces Institute of Pathology
Department of Veterinary Pathology

Conference Coordinator
Matthew Wegner, DVM

WEDNESDAY SLIDE CONFERENCE 2010-2011

Conference 20

16 February 2011

Conference Moderator:
Matthew Starost, DVM, PhD, Diplomate ACVP

CASE I: 09189WFUHS (AFIP 3165085).

Signalment: 24-year-old female cynomolgus macaque (*Macaca fascicularis*).

History: The animal presented with a suspected tooth root abscess in October 2009. Pre-operative blood work was within normal limits and the animal was taken to surgery for extraction of the first right maxillary pre-molar and the second and third molar. This was followed with a post-operative course of clindamycin. Swelling and bleeding persisted in the oral cavity and over the right side of the nose and face after surgery and the extraction sites did not heal. Over the next month bleeding from the oral and right nasal cavity increased. A radiograph revealed osteolysis of the right maxilla and a soft tissue opacity at that site. Euthanasia was elected November 2009.

Of significance in the medical history is an episode of endometriosis in 2007 for which an ovariectomy was performed.

Gross Pathology: The animal was in good body condition and weighed 4.14 kg. Fat stores, muscle mass and hydration status were all adequate. Marked dental tartar was present on all remaining teeth, but most molars had been extracted. A 0.5 cm x 4 cm long oronasal fistula created a communication between the right nasal cavity and the mouth at the site of the most recent surgical extractions. Upon reflection of the facial skin, a 2.5 cm diameter mass of soft grey tissue was present in the right maxillary sinus and the bone of the overlying maxilla was eroded away.

Laboratory Results: CBC and biochemistry panel were within normal limits.

Histopathologic Description: Oronasal tissue: The mass is composed of a dense population of polyhedral to oval neoplastic cells that form nests, packets and cords separated by trabeculae of dense fibrovascular connective tissue. Frequently, within these nests and packets, the cells form small acinar and ductular structures. The cells are approximately 15-20 microns in diameter and contain oval, centrally placed nuclei with dispersed chromatin and rarely apparent nucleoli. Anisocytosis and anisokaryosis are mild

1-1. Nasal cavity, maxilla, adenocarcinoma, cynomolgus macaque. The right maxilla is swollen with deviation of the nasal septum. Photograph courtesy of Wake Forest University of Health Sciences, Animal Resource Program, http://www.wfubmc.edu/Faculty/Kock-Nancy-D.htm.

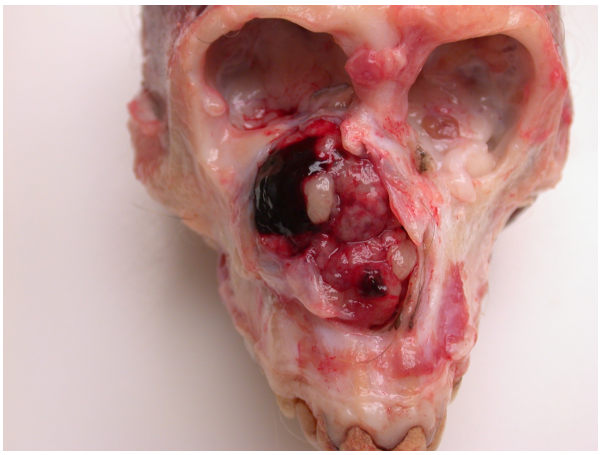

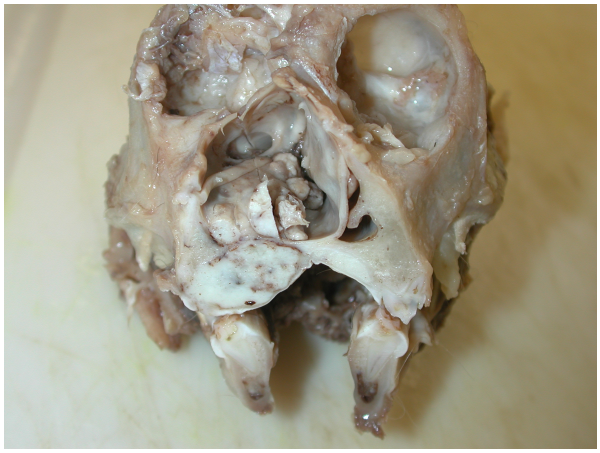

1-2, 1-3. Nasal cavity, adenocarcinoma, cynomolgus macaque. A hemorrhagic, fleshy mass occupies the right nasal cavity and there is severe osteolytic destruction of the maxillofacial bones. A cross section demonstrates destruction of the nasal turbinates and neoplastic tissue extending into the maxilla and hard palate. Photographs courtesy of Wake Forest University of Health Sciences, Animal Resource Program, http://www.wfubmc.edu/Faculty/Kock-Nancy-D.htm.

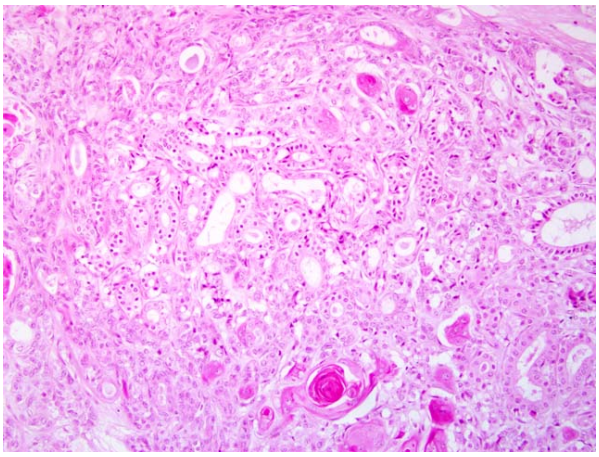

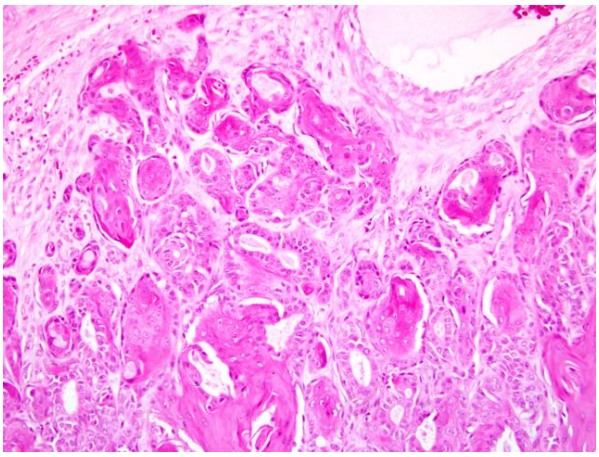

1-4, 1-5. Sinonasal cavity, adenocarcinoma, cynomologous macaque. Neoplastic epithelial cells are arranged in nests, tubules, and acini, with multifocal squamous differentiation. (HE 100X, 200X)

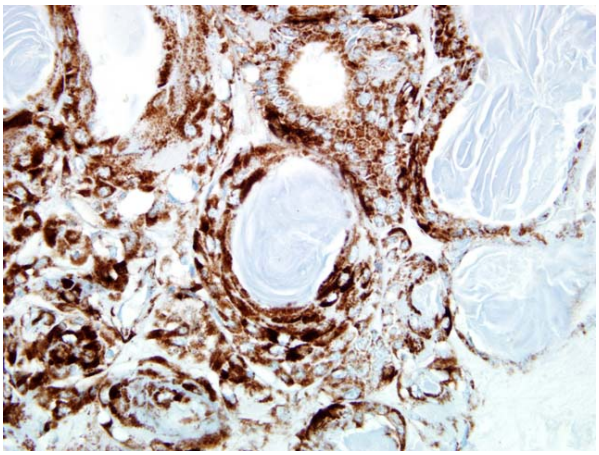

1-6. Sinonasal cavity, adenocarcinoma, cynomologous macaque. Neoplastic myoepithelial cells that transition with areas of squamous differentiation show strong positive cytoplasmic immunoreactivity for smooth muscle actin. (SMA 400X)

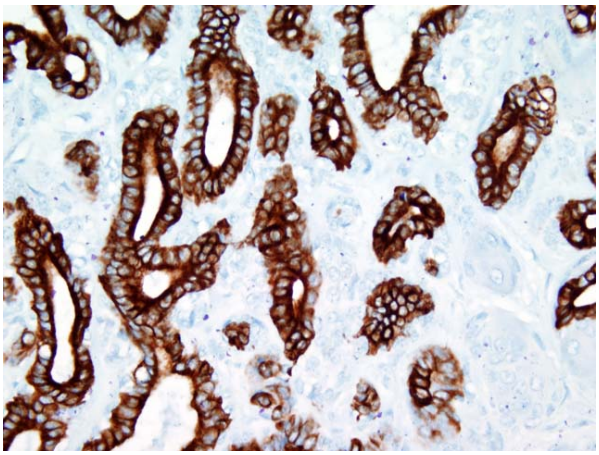

1-7. Sinonasal cavity, adenocarcinoma, cynomologous macaque. Neoplastic epithelial cells show strong cytoplasmic immunoreactivity for cytokeratins 8 and 18. (CK8/18 400X)

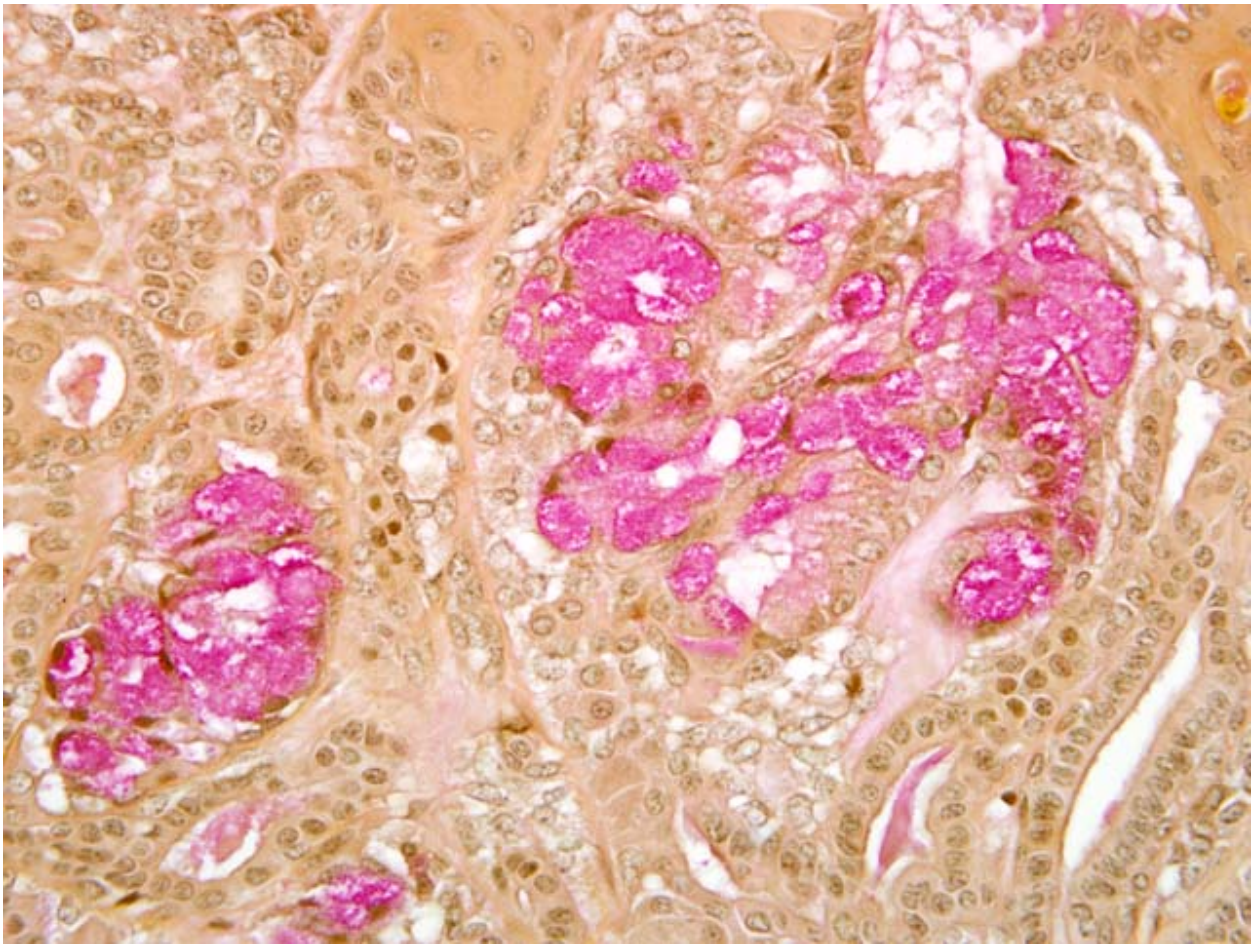

1-8. Sinonasal cavity, adenocarcinoma, cynomologous macaque. Multifocally glandular lumina and the cytoplasm of neoplastic epithelial cells contain intracellular carminophilic material (mucin). (MUCI 400X)

and mitotic figures are rare. The mass is well demarcated and unencapsulated with an invasive border from which tumor cells infiltrate irregularly into the surrounding soft tissue, bone and around blood vessels. Neutrophils and lymphocytes are present at the tumor border. Multifocal aggregates of deeply eosinophilic, polyhedral cells with indistinct borders containing small round nuclei (squamous differentiation) punctuate areas of the mass. In areas where the mass infiltrates bone, there is effacement of the alveolar bone (where the tooth roots of the extracted teeth would have rested). Tumor cells replace all cells in the marrow cavities and invade bone of the maxilla. Focal aggregates of osteoblasts and small groups of 3-5 osteoclasts are noted.

By immunohistochemistry the cell cytoplasm stains positive for pancytokeratin in some areas, particularly the glandular and ductular structures; they are negative for vimentin.

Contributor's Morphologic Diagnosis: Nasal adenocarcinoma with squamous differentiation, right nasal cavity and maxillary sinus

Contributor's Comment: While periodontal disease was present in this animal, the cause for the suspected tooth root abscess was actually an invasive growth of a nasal adenocarcinoma into the maxilla that also invaded and replaced the alveolar bone and tooth roots on the right upper arcade.

Nasal adenocarcinoma is an uncommonly reported tumor of the upper respiratory tract in non-human primates. There are few reports of nasal adenocarcinomas or carcinomas occurring in non-human primates in the literature.[1,7,9] In humans, it has been associated with various occupational exposures to inhaled substances such as the fine particulate matter found in the woodworking and textiles industries and fumes and vapors common to the chemical industry.[6,10] Experimental work in macaques has also shown that ozone may act as a toxic inducing agent when in contact with the nasal mucosal epithelium.[5] Adenocarcinomas are characteristically composed of glandular structures that usually contain some degree of secretory product. The most common forms are tubular, tubulopapillary and acinar. Mixed patterns are frequent. Low-grade tumors have glandular spaces or papillary fronds lined by cuboidal to columnar cells in a single layer with a round to oval nucleus and inconspicuous nucleoli, whereas high-grade tumors have

irregular glandular spaces, more solid sheets of cells and a high mitotic rate with cellular pleomorphism and nuclear atypia. Mucus is the most common secretion in adenocarcinomas and often there is retention, creating cystic spaces. In addition to tubular, tubulopapillary and acinar classifications, adenocarcinomas may be further classed as mucinous or adenocarcinomas with marked desmoplasia (fibrous response). Adenocarcinoma with squamous metaplasia or differentiation is reserved to describe tumors with minor portions containing regular squamous differentiation, as in this case. Adenosquamous carcinoma refers to tumors that are typically highly invasive and have prominent intermixing of adenocarcinomatous and malignant squamous cell components.[11]

AFIP Diagnosis: Sinonasal tissue: Adenocarcinoma, salivary gland-type, with extensive squamous differentiation.

Conference Comment: Most conference participants favored a diagnosis of adenosquamous carcinoma, primarily mucoepidermoid type. This generated discussion of a differential diagnosis list for this lesion which, in addition to the contributor's diagnosis of adenocarcinoma with squamous differentiation, would also include adenosquamous carcinoma, undifferentiated carcinoma and carcinosarcoma. Adenosquamous carcinomas are characterized by a mixture of squamous cell carcinoma (SCC) and adenocarcinoma with frequent intracellular carminophilic mucin.[2] Adenosquamous carcinomas of the lung are histologically identical to those in the sinonasal region.[2] Undifferentiated sarcomas of the head and neck are composed of a population of undifferentiated, uniformly chromatic cells with a prominent lymphoplasmacytic infiltrate and absence of squamous or glandular differentiation.[2] Carcinosarcomas have a dominant spindle cell population, sarcoma-like stroma and a minor component of SCC or in situ carcinoma; the neoplastic spindle cells can produce collagen, osteoid and cartilaginous matrix.[2]

This case was also studied in consultation with the AFIP's Department of Oral and Maxillofacial Pathology, whose pathologists agreed with the contributor's diagnosis of a sinonasal adenocarcinoma; they further classified the tumor as salivary gland-type. In addition to the extensive squamous differentiation, the subspecialty pathologists also commented on the presence of a prominent myoepithelial component as indicated by immunopositivity for smooth muscle actin.

In humans, glandular malignant neoplasms of the sinonasal tract are classified as salivary and non-salivary types; non-salivary sinonasal adenocarcinoma (ACA) is further subdivided into intestinal-type and non-intestinal-types as outlined below.[3,4]

1. Non-salivary type
    a. Intestinal-type adenocarcinoma
        i. Papillary-type
        ii. Colonic-type
        iii. Solid-type
        iv. Mucinous-type
        v. Mixed
    b. Non-intestinal-type
        i. Low-grade
        ii. High-grade
2. Salivary gland-type
    a. Adenoid cystic carcinoma
    b. Acinic cell carcinoma
    c. Mucoepidermoid carcinoma
    d. Epithelial-myoepithelial carcinoma
    e. Clear cell carcinoma
    f. Other (rarely reported)
        i. Malignant myoepithelioma
        ii. Carcinoma ex pleomorphic adenoma
        iii. Polymorphous low-grade adenocarcinoma
        iv. High grade adenocarcinoma

The intestinal type is histologically similar to intestinal ACA; well-differentiated sinonasal intestinal-type ACAs can have Paneth cells, enteroendocrine cells, and goblet cells and may form villi with a muscularis mucosae.[2,4] Non-intestinal-type sinonasal ACAs are classified as low-grade or high-grade. The histologic appearance can vary between and within tumors, with papillary, oncocytic and clear cell patterns; the high-grade form tends to be more solidly cellular.[2,4]

Salivary gland-type ACAs of the sinonasal tract account for between 5-10% of all sinonasal ACAs in humans.[8] Though histologically similar to salivary gland ACAs, they are a distinct entity in that they arise from seromucus glands and surface epithelium of the nasal cavity and paranasal sinuses.[8] The salivary gland-type tumors are composed of glandular epithelium surrounded by myoepithelial cells.[2] Neoplastic epithelial cells frequently contain intracellular and extracellular mucin which stains with mucicarmine and Alcian blue.[8] Mucin frequently accumulates in small cystic spaces. In contrast to many glandular neoplasms in which neoplastic epithelial cells undergo squamous or ductal differentiation, the squamous component of salivary gland-type ACA arises from myoepithelial cells.[8]

This type of neoplasia in humans can initially present as swelling of the palate and face and loosening of the teeth, which were the presenting clinical signs in this case.[3] These tumors often invade adjacent bone, causing osteolysis. Though considered a malignant neoplasm, these tumors rarely metastasize, though most patients succumb to the effects of locally aggressive invasion.[3]

We would like to thank the Department of Oral and Maxillofacial Pathology for their review of this case, and specifically CAPT Robert Foss, DDS, for his enlightening comments.

Contributor: Wake Forest University Health Sciences, Animal Resources Program, Medical Center Boulevard, Winston-Salem, NC 27157
http://www.wfubmc.edu/schoolOfMedicine/schoolOfMedicine_default.aspx?id=26651

References:

1. Brown RJ, Cole WC, Berg HS, Chiang HS, Chang CP, Nanknieder AR. Nasal adenocarcinoma in a Taiwan macaque. *Vet Pathol.* 1977;14:294.
2. Ellis SE, Gaffey MJ, Frierson Jr. HF. Squamous cell carcinoma: Diagnostically problematic variants. In: *Atlas of Tumor Pathology: Tumors of the Upper Aerodigestive Tract and Ear*. 3rd series, Fascicle 26. Washington, D.C.: Armed Forces Institute of Pathology; 1997;71-106.
3. Everson JW. Nasal cavity and paranasal sinuses: Salivary gland-type adenocarcinoma. In: Barnes L, Everson JW, Reichart P, Sidransky D, eds. *World Health Organization Classification of Tumors: Pathology and Genetics of Head and Neck Tumors*. Lyon, France: IARC Press; 2005:24-25.
4. Franchi A, Santucci M, Wenig BM. Nasal cavity and paranasal sinuses: Adenocarcinoma. In: Barnes L, Everson JW, Reichart P, Sidransky D, eds. *World Health Organization Classification of Tumors: Pathology and Genetics of Head and Neck Tumors*. Lyon, France: IARC Press; 2005:20-23.
5. Harkema JR, Plopper CG, Hyde DM, St. George JA, Wilson DW, Dungworth DL. Response of the macaque nasal epithelium to ambient levels of ozone. *Am J Pathol.* 1987;128(1):29-44.
6. Hildesheim A, Dosemeci M, Chan C-C, et al. Occupational exposure to wood, formaldehyde, and solvents and risk of nasopharyngeal carcinoma. *Can Epidem Biom Prev.* 2001;10:1145–1153.
7. Kaspareit J, Friderichs-Gromoll S, Buse E, Habermann G. Spontaneous neoplasms observed in cynomolgus macaques (*Macaca fascicularis*) over a 15-year period. *Exp Tox Path.* 2007;59:163-169.
8. Leivo I. Update on sinonasal adenocarcinoma: Classification and advances in immunophenotype and molecular genetic make-up. *Head Neck Pathol*. 2007;1:38-43.
9. Neubauer R, Rabin H, Arnstein P, et al. Characterization of a spontaneous undifferentiated carcinoma from an African green monkey (*Cercopithecus aethiops*). *In Vitro Cell Dev Biol.* 1976;12(7):533-539.
10. Pesch B, Pierl CB, Gebel M, et al. Occupational risks for adenocarcinoma of the nasal cavity and paranasal sinuses in the German wood industry. *Occup Environ Med*. 2008;65:191-196.
11. Wilson DW, Dungworth DL. Tumors of the respiratory tract. In: Meuten DJ, ed. *Tumors of Domestic Animals.* 4th ed. Ames, IA: Iowa State Press; 2002:380-392.

CASE II: YN08-445 (AFIP 3166455).

Signalment: 13-year, 7-month-old male sooty mangabey (*Cercocebus atys*).

History: This adult male sooty mangabey was born at the Field Station of the Yerkes National Primate Research Center. He was diagnosed as being diabetic. Severe preputial edema was noted and due to poor prognosis, he was sacrificed two days later.

Gross Pathology: The animal weighed 13.36 kilograms at necropsy. There was a large amount of turbid, milky white fluid intermixed with adhesions between the gastrointestinal serosa and the mesentery in the abdominal cavity. Multiple, white, firm, ovoid, well-encapsulated structures measuring approximately 0.25-1.5 cm in diameter were present on the diaphragm, peritoneum, mesentery and serosa of the urinary bladder. The mesenteric lymph nodes were enlarged, pale white and firm on sectioning. The prepuce had severe subcutaneous edema.

Laboratory Results: Diabetic. Serology: SIV positive and HTLV1 negative. Microbiology: no significant pathogens were isolated from blood, liver or colon.

Histopathologic Description: Lymph node: The nodules in the abdominal cavity are well-circumscribed by fibroblasts. Severe extensive aggregates of neutrophils, multinucleate giant cells and few eosinophils intermixed with aseptate, branching, fungal hyphae (consistent with a zygomycotic agent) are present at the center of these nodules. The enlarged mesenteric lymph nodes have severe pyogranulomatous infiltrates intermixed with intralesional fungal organisms. Staining with Gomori methenamine silver stain confirmed the presence of a zygomycete.

Contributor's Morphologic Diagnosis: Severe multifocal granulomatous peritonitis with intralesional fungi (zygomycete).

Contributor's Comment: Zygomycosis is a relatively new term that refers to a group of uncommon but frequently fatal mycoses caused by fungi of the class *Zygomycetes*.[2] This mycosis is characterized by subcutaneous, systemic, or rhinocerebral infections.[1] The common diagnostic feature of *zygomycetes* is that the organisms form infrequently septate hyphae which are significantly broader than other fungi with filamentous tissue forms, e.g. *Aspergillus*. The hyphae are unpigmented and range from 6-25 µm in diameter. The class Zygomycetes has two orders: Mucorales (genera: *Rhizopus, Mucor, Absidia, Mortierella, Rhizomucor* among others), members of which cause mucormycosis; and *Entomophthorales* (genera: *Basidiobolus* and *Conidiobolus*), which cause entomophthoromycosis.[1] Zygomycetes are widespread in nature, occurring as soil saprophytes, components of normal skin and hair flora or as common laboratory contaminants. They may enter the host through cutaneous, gastrointestinal or respiratory routes.[1]

The members of the order *Mucorales* cause most human disease, characterized by a rapidly evolving course, disseminated disease, tissue destruction, and invasion of blood vessels.[1] This disease is associated with preexisting conditions which lead to immunosuppression, such as diabetes, nutritional deficiencies, severe burns, hematologic or oncologic diseases, transplant recipients, and high-risk neonates.[2,4] Zygomycosis is a rare disease of animals, including dogs, cats, horses, llamas, sheep, pigs and several nonhuman primate species.[4,5] Both Old World and New World primates are susceptible to the infection, which is rare in prosimians.[4] Ulceration and necrosis of the alimentary tract mucosa are the most frequently described gross lesions.[5]

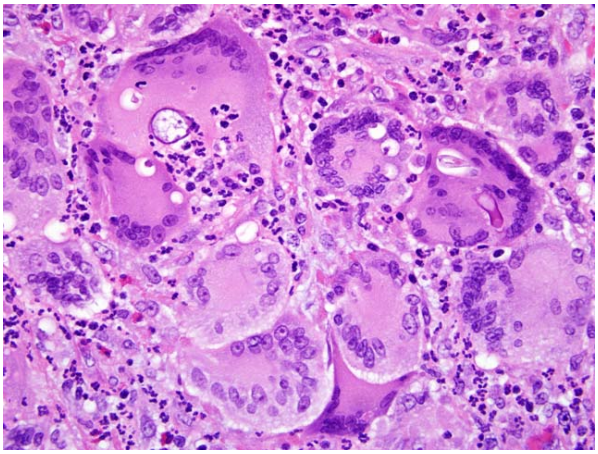

2-1. Mesentery, sooty mangabey. Areas of pyogranulomatous and eosinophilic inflammation have numerous multinucleate giant cells that often contain fragments of fungal hyphae. (HE 400X)

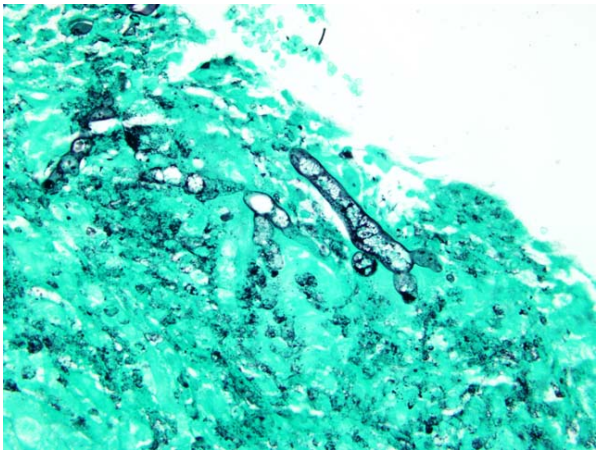

2-2. Mesentery, sooty mangabey. Gomori methenamine silver stain demonstrates aseptate, branching fungal hyphae. (GMS 400X)

Culture or immunofluorescence studies, or both, are necessary for species-specific identification of the fungi.[4] In the current case, samples suitable for culture or molecular identification were unavailable. The organisms can be more easily seen and better characterized when stained with periodic acid–Schiff (PAS) or Gomori methenamine silver (GMS) techniques.[4] GMS revealed the presence of aseptate hyphae with broad, irregular, branching often at perpendicular angles (consistent with a Zygomycete) in these granulomas. A negative acid fast bacilli stain precluded the presence of *Mycobacterium* in these lesions.

AFIP Diagnosis: Mesentery: Peritonitis and steatitis, pyogranulomatous and eosinophilic, focally extensive, severe, with fibrosis, many multinucleate macrophage giant cells, and few aseptate fungal hyphae, etiology consistent with zygomycetes.

Conference Comment: Conference participants agreed that the etiologic agent was most likely a zygomycete; few ventured beyond that in an attempt to further classify it as a member of either the *Mucorales* or the *Entomophthorales* family.

This case was also studied in consultation with the AFIP's Department of Infectious Disease Pathology, whose subspecialty pathologists favored a member of the *Entomophthorales* as the etiologic agent because of the marked eosinophilic infiltrate. Infection with *Entomophthorales* is histologically characterized by multiple pyogranulomas, marked eosinophilic infiltration, foreign body giant cells, and rare fungal hypae.[1] Though not evident in this specimen and, in contrast to *Mucorales*, Splendore-Hoeppli material often surrounds fungal hyphae, forming an "eosinophilic sleeve" highlighting the hyphae.[3] Members of *Entomophthorales* may exhibit lateral and deep spreading; invasion of the blood vessels is uncommon.[1]

Entomophthorales is a cause of cutaneous zygomycosis in the horse and, rarely, the dog and cat. Dogs and cats are typically infected with *Conidiobolus* spp. Gross lesions in the dog consist of poorly circumscribed dermal nodules which spread to form "satellite nodules" followed by necrosis, ulceration, and fistulation with purulent or serosanguineous exudate.[3]

Horses are most commonly infected with *Basidiobolus haptosporus* and *Conidiobolus coronatus*, which produce round, ulcerated, and usually solitary swellings most often involving the chest, trunk, head and neck. The lesions are pruritic and contain gritty, yellow-white granules referred to as "kunkers" or "leeches." On cut surface, the granulomas appear as a wavy swath of yellow-white material sharply demarcating the granulomas from the superficial hemorrhage and edema.[1]

Infection of sheep with *C. incongruus* produces rhinitis with asymmetrical facial swelling. Infected animals typically die within 7-10 days after showing clinical signs.[1]

Contributor: Yerkes National Primate Research Center, Emory University, 954 Gatewood Road, Atlanta, GA, 30329 http://www.yerkes.emory.edu/

References:

1. Ginn PE, Mansell JEKL, Rakich PM. Skin and appendages. In: Maxie MG, ed. *Jubb, Kennedy and Palmer's Pathology of Domestic Animals*. Vol. 1, 5th ed. Philadelphia, PA: Elsevier Ltd; 2007:707-708.
2. Gonzalez CE, Rinaldi MG, Sugar AM. Zygomycosis. *Clin Infect Dis North Am* 2002;16:895-914.
3. Gross TL, Ihrke P, Walder EJ, Affolter VK. Lichenoid diseases of the dermis. In: *Skin Diseases of the Dog and Cat: Clinical and Histopathologic Diagnosis*. 2nd ed. Ames, Iowa: Blackwell Publishing Ltd.; 2005:303-309.
4. Migaki G, Schmidt RE, Toft JD 2nd, Kaufmann AF. Mycotic infections of the alimentary tract of nonhuman primates: a review. *Vet Pathol*. 1982;19(Suppl 7):93-103.
5. Torres-Urbano CJ, Rose RE, Walters SL. Disseminated zygomycosis in a cynomolgus monkey (*Macaca fascicularis*). *J Am Assoc Lab Anim Sci*. 2010;49:75-78.

CASE III: CSUGP131 (AFIP 3166606).

Signalment: 12-week-old intact female Dunkin-Hartley guinea pig (*Cavia porcellus*).

History: This guinea pig was infected with 500 colony forming units (CFU) of *Burkholderia pseudomallei* by intranasal inoculation. The animal was euthanized 12 days post-inoculation because of deteriorating clinical condition, including pyrexia, lethargy and dyspnea.

Gross Pathology: Disseminated throughout the parenchyma of all lung lobes and present rarely within the liver and spleen parenchyma are multifocal, discrete, raised white nodules that measure 1 – 3 mm in diameter. On cut surface, larger nodules are surrounded by a circumferential pale tan rim of tissue with centralized, white to tan, friable debris (abscesses).

Histopathologic Description: Lung: Multifocal, discrete, and often coalescing inflammatory foci effacing approximately 80% of the pulmonary parenchyma are often centered on bronchi and bronchioles and are composed of centralized accumulations of degenerate heterophils surrounded by a periphery of epithelioid histiocytes and admixed fibroblasts. Larger inflammatory foci have abundant central necrosis. The lumen of airways is often filled with degenerate heterophils that multifocally infiltrate through and obscure the bronchiolar and bronchial wall. There is segmental loss and effacement of airway epithelium. Adjacent alveolar septa are expanded up to two times normal by fibrin, edema, heterophils and other mononuclear inflammatory cells. Alveolar spaces contain abundant eosinophilic edema fluid and fibrin strands admixed with alveolar macrophages with foamy cytoplasm. Multifocally, there are rows of enlarged cuboidal pneumocytes lining alveolar septa containing large nuclei with open chromatin (type 2 pneumocyte hyperplasia). Multifocally, peribronchiolar and perivascular connective tissue is expanded by clear edema fluid. Perivascular inflammatory infiltrates are present consisting of macrophages, lymphocytes and heterophils that multifocally infiltrate and obscure the vessel wall. Associated with the inflammation, vessel walls have segmental hyalinization (fibrinoid necrosis) or expansion of the adventitia and segmental obliteration of the wall by fibrous connective tissue that occasionally extends to fill the vascular lumen (not present in all slides). Multifocally, inflammatory infiltrates extend into the pleural connective tissue and are admixed with fibroblasts and mucinous matrix.

Contributor's Morphologic Diagnosis: Lung: Multifocal and coalescing, necrotizing heterophilic and histiocytic bronchopneumonia with fibrosis, pleuritis, and leukocytoclastic to fibrosing and obliterative vasculitis, chronic, severe.

Etiology: *Burkholderia pseudomallei*

Contributor's Comment: The gram-negative, aerobic, motile bacillus *Burkholderia pseudomallei* is the causative agent of melioidosis and is endemic to the tropical climates of Southeast Asia and Northern Australia. The bacterium is recognized as an important emerging pathogen, accounting for a significant proportion of septicemic mortality in endemic areas and is classified as a select agent. *Burkholderia pseudomallei* is a saprophytic, facultative intracellular bacterium with primary reservoirs being rice paddies, stagnant water, and moist tropical soils. *Burkholderia pseudomallei* can persist for up to 10 years in low-nutrient conditions, but is not a spore-forming bacterium. Additionally, the bacterium is resilient in adverse conditions including exposure to detergents, acidic pH, and dehydration.[1,3] There is a strong association between occurrence of melioidosis cases in humans and monsoons, presumably due to dislodging the organism from its environmental niche and aerosolization. *Burkholderia pseudomallei* is capable of infecting and surviving within *Acanthamoeba* trophozoites, and it is presumed that factors allowing for intra-protozoal survival are reflected as virulence factors upon invasion of human and animal macrophages.[1,3]

Burkholderia pseudomallei has an extremely wide host range and is a recognized pathogen of human and animal species, most commonly infecting sheep, goats and pigs. However, sporadic cases and small epizootics have been reported in a variety of animal species including non-human primates, kangaroo, wallaby, deer, buffalo, cow, camel, llama, zebra, koala, dog, cat, horse, mule, parrot, rat, hamster, ground squirrels, seal, dolphin and crocodile. Cases in bovids, birds and reptiles are rare, and these species are considered to be relatively resistant to *B. pseudomallei*.[5] A wide spectrum of clinical manifestations may arise from infection with *B. pseudomallei* ranging from acute, rapidly progressive, and often fatal septicemia to chronic multi-organ disease with abscess formation. Accepted routes of transmission are via either percutaneous inoculation or inhalation.[3] Disease manifestations in animals include pneumonia, arthritis, orchitis, mastitis, abortion, meningoencephalitis, dermatitis, and lymphangitis. Acute disease may manifest in the majority of affected species, and most often occurs in younger animals. Chronic manifestations of the disease appear to be more common.[5] Pneumonia is the most common manifestation of disease in humans and is present in approximately 50% of cases. Differences in human clinical manifestations depending on geographic location are recognized, with a high incidence of prostatic abscesses occurring in Australian males, while up to 40% of Thai children present with suppurative parotitis. Skin and soft-tissue infections are also common manifestations and may be the source for hematogenous spread of the organism.[3] *Burkholderia pseudomallei* is intrinsically resistant to multiple groups of antibiotics, including 3rd generation cephalosporins, penicillins, aminoglycosides, quinolones and macrolides. This limits therapeutic options and accounts for the high rate of

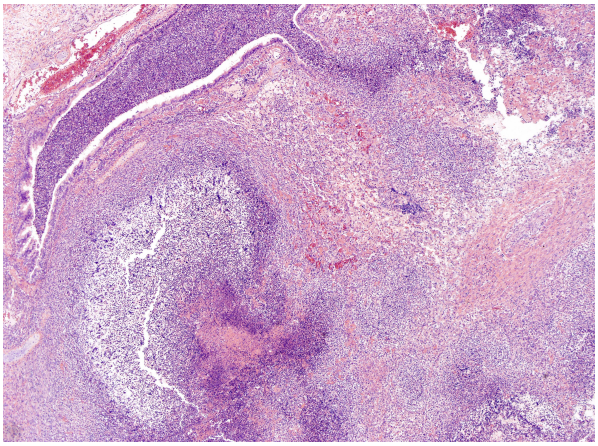

3-1. Lung, Dunkin-Hartley guinea pig. Multifocal areas of necrotizing heterophilic inflammation are surrounded by fibrosis and histiocytes. Heterophils fill airways. Photograph courtesy of Colorado State University, College of Veterinary Medicine and Biomedical Sciences

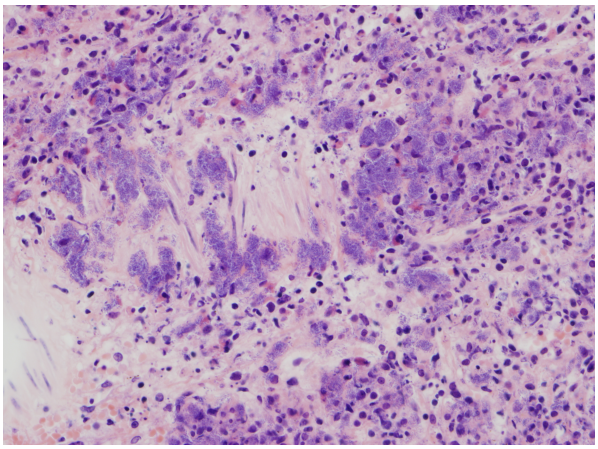

3-2. Lung, Dunkin-Hartley guinea pig. H&E from a guinea pig in this study with more acute disease manifestations demonstrates numerous small intahistiocytic bacilli. Photograph courtesy of Colorado State University, College of Veterinary Medicine and Biomedical Sciences

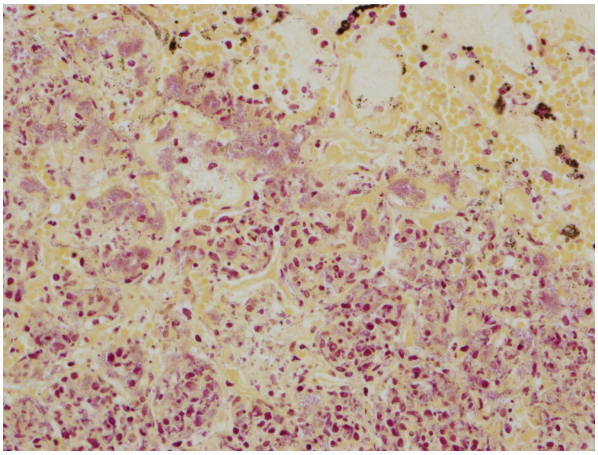

3-3. Lung, Dunkin-Hartley guinea pig. Gram staining demonstrates gram-negative bacilli. Photograph courtesy of Colorado State University, College of Veterinary Medicine and Biomedical Sciences.

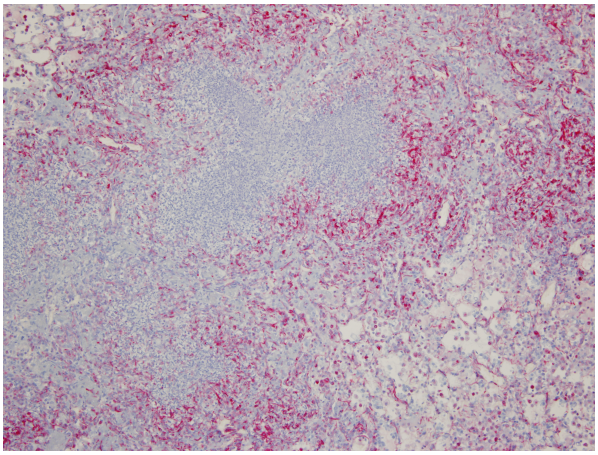

3-4. Lung, Dunkin-Hartley guinea pig. Vimentin immunohistochemistry demonstrates circumferential mesenchyal cells surrounding foci of necrotizing inflammation. Photograph courtesy of Colorado State University, College of Veterinary Medicine and Biomedical Sciences.

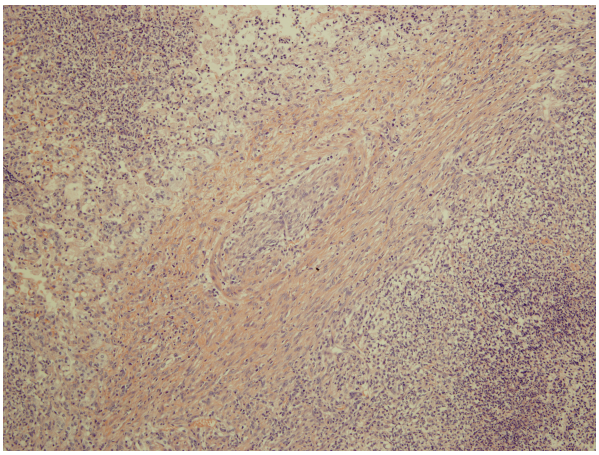

3-5. Lung, Dunkin-Hartley guinea pig. An arteriolar wall is segmentally replaced and surrounded by fibrous connective tissue and fibrosis partially occludes the lumen. (Masson's stain) Photograph courtesy of Colorado State University, College of Veterinary Medicine and Biomedical Sciences.

therapeutic failure. Ceftazidime and amoxicillin-clavulanate are the current antibiotics of choice in treatment of melioidosis.[3]

The pathogenesis and virulence factors of *B. pseudomallei* are heavily researched and are well described in a recent review.[1] Initial infection occurs via attachment to epithelial cells at the site of inoculation by an unknown molecule presumably associated with the exterior polysaccharide capsule of the bacterium. The organism is capable of invading non-phagocytic and phagocytic cell types. *Burkholderia pseudomallei* employs a type 3 secretion system (T3SS), a system seen in many other virulent bacteria which utilizes effector molecules to manipulate host cell function. Actin cytoskeletal rearrangement in the host cell induced by T3SS may account for cellular invasion. Subsequently, the bacterium is able to escape the initial phagocytic vacuole by way of T3SS effectors and replicate in the cytoplasm. *Burkholderia pseudomallei* can also

modulate production of reactive oxygen intermediates in professional phagocytes as an important mechanism of pathogenesis and evade intracellular killing mechanisms. Upon reaching a critical threshold of replication based on quorum sensing, the organism lyses the cell by inducing caspase 1-dependent lysis or apoptosis. This allows for secondary hematogenous dissemination.

The histopathologic features of human melioidosis are described as acute, necrotizing to chronic neutrophilic and granulomatous inflammation. Multinucleated giant cells are a common feature, and in some cases intracellular bacteria within macrophages are so numerous as to resemble globi, a term describing aggregates of bacteria in lepromatous leprosy. Small abscesses may be identified in numerous organs including lung, liver and spleen.[7] Bacterial organisms may be more indistinct with chronic manifestations of melioidosis, as indicated in the provided slides. However, more acute manifestations of the disease in this infection model did display large numbers of intrahistiocytic and extracellular bacilli. Animal models of melioidosis have been developed in several species and may be further expanded given the wide host range of *B. pseudomallei*. However, significant differences in the pathogenesis of disease are recognized in different models and it is thus difficult to assess which model best reflects human disease.[6]

AFIP Diagnosis: Lung: Bronchopneumonia, suppurative and necrotizing, diffuse, marked, with alveolar edema, pleuritis, multifocal fibrosis, and rare vasculitis.

Conference Comment: Conference participants agreed on a diagnosis of necrotizing and suppurative bronchopneumonia. The etiologic differential diagnosis considered by participants included adenovirus, *Streptococcus zooepidemicus*, *Streptococcus pneumoniae*, *Klebsiella pneumoniae*, and *Bordetella bronchiseptica*. Gross findings in adenoviral pneumonia of guinea pigs typically include consolidation of the cranial and hilar lung lobes; histologic findings include non-suppurative, necrotizing bronchitis and bronchiolitis. Nuclei of infected cells frequently contain characteristic large, basophilic intranuclear viral inclusion bodies.[4]

Of the bacterial etiologies considered by participants, *K. pneumonia* and *B. bronchiseptica* are Gram-negative; histologic findings are typically necrotizing and suppurative owing to the lipopolysaccharide of their cell walls, which damages the endothelium and is a potent activator of leukocytes. The streptococcal organisms usually elicit a fibrinopurulent pneumonia, pleuritis and serositis. The strain of *S. pneumoniae* most often infecting guinea pigs is capsular polysaccharide type 19, though type 4 is occasionally isolated.[4]

Repair of the airways and lungs frequently involves local stem cells. Within the trachea, Clara-like cells and cells within the submucosal glands appear to act as stem cells; basal cells of the trachea and bronchi also appear to have stem cell properties, allowing them to replace injured epithelium. Bronchiolar Clara cells have bipotential properties, allowing them to differentiate into ciliated epithelial cells or produce additional Clara cells. Bone marrow-derived stem cells may also play a role in pulmonary repair through differentiation into epithelial and mesenchymal cells.[2]

For a review of the primary defense mechanisms of the lung, the reader is encouraged to review Wednesday Slide Conference 15, Case II, 2009-2010.

Contributor: Colorado State University, College of Veterinary Medicine and Biomedical Sciences

References:

1. Adler NR, Govan B, Cullinane M, Harper M, Adler B, Boyce JD. The molecular and cellular basis of pathogenesis in melioidosis: How does *Burkholderia pseudomallei* cause disease? *FEMS Microbiol Rev.* 2009;33:1079-1099.
2. Caswell JL, Williams KJ. Respiratory system. In: Maxie MG, ed. *Jubb, Kennedy and Palmer's Pathology of Domestic Animals*. Vol. 2, 5th ed. Philadelphia, PA: Elsevier Ltd; 2007:529.
3. Cheng AC, Currie BJ. Melioidosis: Epidemiology, pathophysiology, and management. *Clin Microbiol Rev*. 2005;18:383-416.
4. Percy DH, Barthold SW. *Pathology of Laboratory Rodents and Rabbits*. 3rd ed. Ames, IA: Blackwell Publishing; 2007:221-232.
5. Sprague LD, Neubauer H. Melioidosis in animals: A review on epizootiology, diagnosis and clinical presentation. *J Vet Med B Infect Dis Vet Public Health.* 2004;51:305-320.
6. Titball RW, Russell P, Cuccui J, et al. *Burkholderia pseudomallei*: Animal models of infection. *Trans R Soc Trop Med Hyg.* 2008;102(Suppl 1):111-116.
7. Wong KT, Puthucheary SD, Vadivelu J. The histopathology of human melioidosis. *Histopathol*. 1995;26:51-55.

CASE IV: YALE 174-CASE-1 (AFIP 3169856).

Signalment: 6-8-week-old female C3H/HeJ mouse (*Mus musculus*).

History: There were unexpected deaths in mice used for feeding *Borrelia burgdorferi*-infected ticks.

Gross Pathology: At necropsy there was marked bilateral submandibular lymphadenopathy, mild splenomegaly, and marked paucity of abdominal adipose tissue.

Laboratory Results: Serology was negative for corona virus, EDIM, LCMV, Ectromelia, MPV, Sendai virus, TMEV, PVM, and *Mycoplasma pulmonis*. Warthin-Starry stain of brain tissue was negative, but cardiac tissue was positive for spirochetes.

Histopathologic Description: Heart: There is a mild to moderate focally extensive inflammatory infiltrate admixed with fibroblast proliferation and necrotic cellular debris centered on the connective tissue surrounding the great vessels at the base of the heart. The inflammatory infiltrate extends multifocally into the wall of the aorta and multifocally into the superficial surrounding myocardium. The inflammatory infiltrate consists of a mixture of macrophages and neutrophils with fewer numbers of lymphocytes and plasma cells. Infrequent spirochetes are observed on Warthin-Starry-stained sections of heart.

Contributor's Morphologic Diagnosis: Carditis, myocarditis, and vasculitis, mild to moderate, chronic-active, focally extensive with intralesional spirochete bacteria consistent with *Borrelia burgdorferi*.

Contributor's Comment: Lyme disease is a globally occurring, usually nonfatal multisystemic disorder caused by the gram-negative spirochete *Borrelia burgdorferi*.[2,11,13] In the United States, it is the most commonly reported vector-borne disease, most often transmitted by *Borrelia*-infected nymphal ticks of the genus *Ixodes*. Lyme disease has been reported in 49 states and the District of Columbia. Ninety-two percent of the cases occurred in 10 states, mainly in the northeast.[13] Elsewhere in the world, infection has occurred in Russia, China, Japan, and Europe.[13] *Borrelia* is capable of infecting both humans and animals, including mice, rats, hamsters, rabbits, dogs, cattle, and horses.[1,3,4,12]

In humans, Lyme disease is characterized by a target-shaped skin rash, neurological symptoms, and various inflammatory processes including arthritis and carditis. Within 2-3 weeks of infection, clinical manifestations in the joints and heart peak, then begin to regress. While 60% of patients in the United States develop arthritis, an estimated 4 to 10% with untreated infections develop cardiac manifestations of the disease.[2,10,13] Arthritis often recurs, but carditis is transient and usually present for a few days to several weeks.[2,10,11] Common clinical complaints in patients with Lyme carditis include light-headedness, syncope, dyspnea, and heart palpitations. Electrocardiographic abnormalities, such as prolonged P-R intervals and heart block, are often identified, though some patients are asymptomatic. In patients with EKG abnormalities, alternating tachycardia and bradycardia are not uncommon.[13]

Several laboratory animal species are susceptible to experimental Lyme disease.[3,11,12] Because of the relative ease by which their genome can be manipulated, mice are currently the most valuable animal model for studying *Borrelia* infection.[5,10] Severity of disease varies by strain, with C57BL/6, SJL, and BALB/c being most resistant, and C3H/He being most severely affected.[2,3] Investigations utilizing transgenic and knockout mice have proven useful for studying the immune system response and pathology associated with *B. burgdorferi* infection.[5,10,14]

In the rodent model, carditis and arthritis are consistent pathologic findings.[3,5,11-13] Neurologic disease and skin lesions, though common in humans, are uncommon manifestations of borreliosis in animal models.[3,4] Histopathologic cardiovascular lesions in human and animal patients with Lyme disease may occur in any layer of the heart.[2] In some cases, *B. burgdorferi* spirochetes may be demonstrated in cardiac tissue by indirect immunofluorescence or silver staining.[2,11,14] Organisms typically reside in the connective tissue at the AV junction, epicardium and, occasionally, in the myocardium.[14] In addition, vasculitis in small and large intramyocardial vessels is observed. Macrophages tend to be the predominant inflammatory cell type, evident by immunohistochemistry at 7 days post-infection, followed by plasma cells and neutrophils.[2,3,10,14] This is in contrast to joint lesions, in which neutrophils are the predominant inflammatory cell type.[10] Polyarthritis after infection with *B. burgdorferi* occurs in mice of all strains, but the severity, frequency, and extent of arthritis is strain and age-dependent. Swelling of the joints, especially the tibiotarsal joints, is often noted.[3,11]

In the case presented, 12 C3H/HeJ mice were used as feeders for *Ixodes scapularis* nymphal ticks infected with *B. burgdorferi*. The clone of *Borrelia* usually used is cN40, a low passage isolate with proven infectivity for laboratory mice.[2] Eight nymphs are placed on the mouse, allowed to feed for 72 hours, then removed. This procedure is not normally associated with mortality in the feeder mice. Cardiac lesions, with or without joint lesions, are common with this clone. Brain lesions are not typically observed. However, in this case, a new batch of ticks infected with *B. burgdorferi* 206 was used and 8 of 12 mice were found dead between days 11 and 13 post-feeding. The ticks tested negative for other pathogenic agents, including *Ehrlichia, Babesia,* and *Anaplasma*. One mouse was submitted for necropsy to rule out other infectious causes for the acute deaths observed in these mice. The lack of any other significant pathologic lesions and the presence of the lesions noted within the brain and heart, along with the presence of

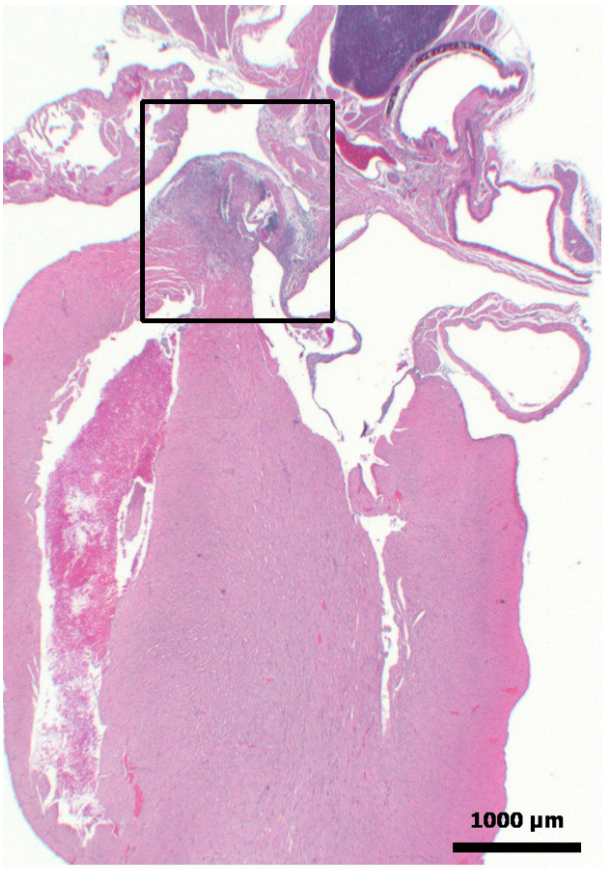

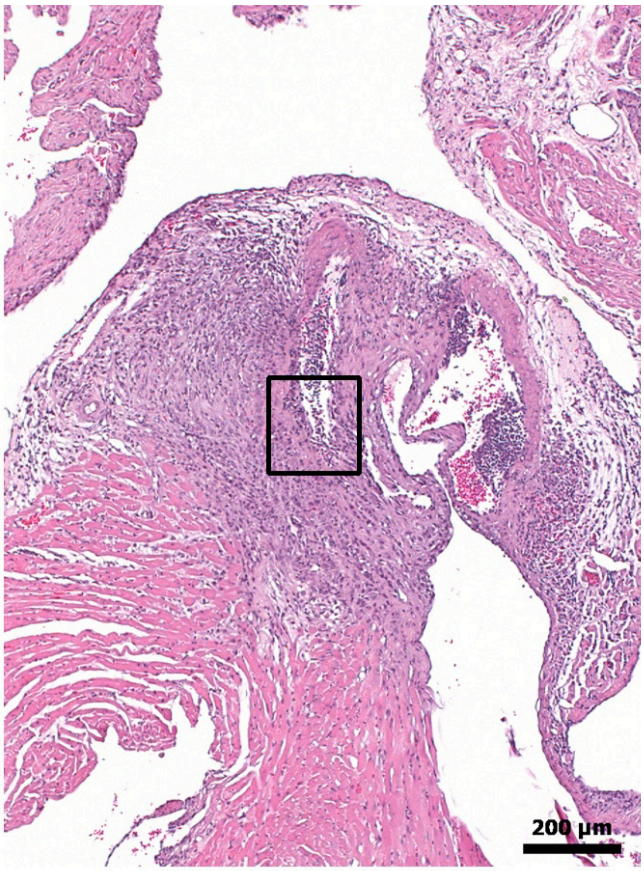

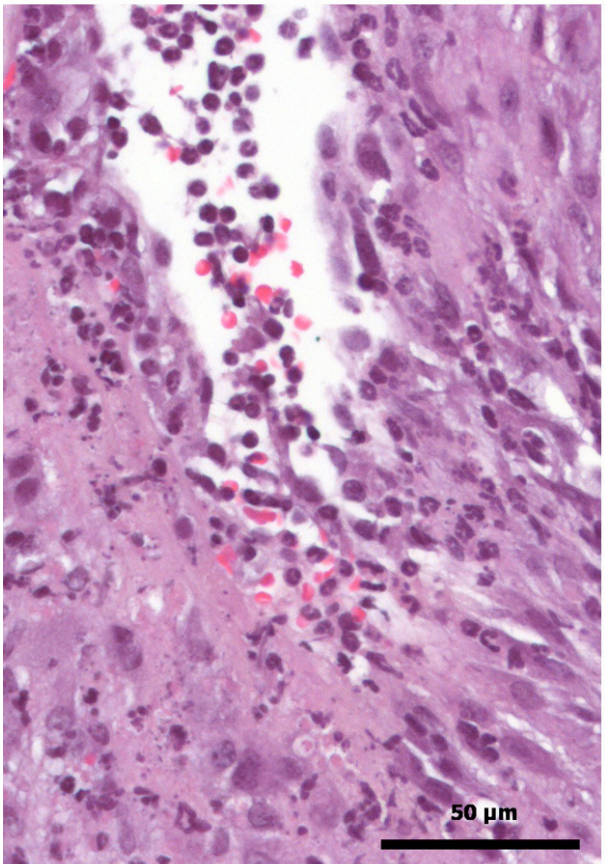

4-1. Heart, mouse. There is mild to moderate focally extensive inflammation admixed with fibroblast proliferation and necrotic cellular debris in the connective tissue surrounding the great vessels at the base of the heart. The inflammatory infiltrate extends multifocally into the wall of the aorta and multifocally into the superficial surrounding myocardium. The inflammatory infiltrate consists of a mixture of macrophages and neutrophils with fewer numbers of lymphocytes and plasma cells. Photographs courtesy of Section of Comparative Medicine, Yale University School of Medicine.

Organism	Tick Vector	Susceptible host(s)
Ehrlichia canis	*Rhipicephalus sanguineous, Dermacentor variabilis*	Dog, ± cat
Ehrlichia ruminantium	*Amblyomma hebraeum*	Cow, sheep, goat, dog
Ehrlichia equi	*Ixodes pacificus*	Horse, dog, man
Anaplasma marginale, A. centrale	*Dermacentor* spp.	Cow
Anaplasma phagocytophilum	*Ixodes scapularis*	Dog, cat, horse, man
Rickettsia rickettsii	*Dermacentor* spp., *Rhipicephalus* spp., *Amblyomma* spp.	Dog, cat, man
Francisella tularensis	*Dermacentor andersoni, D. variabilis, D. occidentalis, Amblyomma americanum*	Many
Babesia canis vogeli	*Rhipicephalus sanguineous*	Dog
Babesia canis canis	*Dermacentor reticulatus*	Dog
Babesia gibsoni	*Rhipicephalus sanguineous*	Dog
Babesia microti	*Ixodes scapularis, I. ricinus*	Man

References: 6-9,15

spirochetes in the heart by Warthin-Starry stain, suggest the mice died secondary to cardiac complications of *B. burgdorferi*. The investigator euthanized the remainder of the mice and eliminated all the ticks from this batch. The HE stained slides submitted for this conference came from mice experimentally infected with *B. burgdorferi* from other studies, where all have the classic carditis seen in this experimental model and were known positive for *B. burgdorferi.*

AFIP Diagnosis: Heart: Endomyocarditis, valvular and atrial, lymphohistiocytic and neutrophilic, multifocal, mild to moderate, with focal epicarditis.

Conference Comment: The contributor provides an excellent overview of borreliosis in laboratory rodents.

Conference participants commented on slide variability; some sections had lymph nodes that exhibited diffuse hyperplasia. Additionally, focal epicarditis was present in some sections.

Participants reviewed various non-viral tick-borne diseases of veterinary importance with respect to the pathogen and its associated vector. The included chart provides a brief summary.

Lyme borreliosis in the dog can clinically manifest as a systemic illness, arthritis, renal disease and meningitis. Polyarthritis and shifting leg lameness are common manifestations, with the limbs closest to the tick attachment site affected first.[8] Apparent resolution of the lameness in untreated dogs does not necessarily equate to a halt in joint pathology, as progressive, non-erosive arthritis is commonly detected.[8] Renal disease in infected dogs is clinically evident as azotemia, uremia, proteinuria, peripheral edema and body cavity effusions; these findings are consistent with acute renal failure. Meningitis may manifest later in the disease process in humans, and lesions have been experimentally reproduced in dogs, though clinical signs were not evident.[8]

For a review of the pathogenesis and microscopic changes in the kidney, the reader is encouraged to review Wednesday Slide Conference, Conference 25, Case IV, 2009-2010.

Contributor: Section of Comparative Medicine, Yale University School of Medicine, 375 Congress Ave., New Haven, CT 06519-1404

References:

1. Appel MJ, Allan S, Jacobson RH, et. al. Experimental Lyme disease in dogs produces arthritis and persistent infection. *J Infect Dis.* 1993;167:651-664.
2. Armstrong AL, Barthold SW, Persing DH, Beck DS. Carditis in Lyme disease susceptible and resistant strains of laboratory mice infected with *Borrelia burgdorferi. Am J Trop Med Hyg.* 1992;47:249-258.
3. Barthold SW, Beck DS, Hansen GM, Terwilliger GA, Moody KD. Lyme borreliosis in selected strains and ages of laboratory mice. *J Infect Dis*. 1990;162:133-138.

4. Barthold SW, Moody KD, Terwilliger GA, Jacoby RO, Steere AC. An animal model for Lyme arthritis. *Ann NY Acad Sci*. 1988;539:264-273.
5. Bockenstedt LK, Kang I, Chang C, Persing D, Hayday A, Barthold SW. CD4+ T helper 1 cells facilitate regression of murine Lyme carditis. *Infect Immun*. 2001;69:5264-5269.
6. Greene CE, Breitschwerdt EB. Rocky Mountain spotted fever, murine typhuslike disease, rickettsialpox, typhus, and Q fever. In: Greene CE, ed. *Infectious Diseases of the Dog and Cat*. 3rd ed. St. Louis, MO: Saunders Elsevier; 2006:234.
7. Greene CE, DeBey BM. Tularemia. In: Greene CE, ed. *Infectious Diseases of the Dog and Cat.* 3rd ed. St. Louis, MO: Saunders Elsevier; 2006:446.
8. Greene CE, Straubinger RK. Borreliosis. In: Greene CE, ed. *Infectious Diseases of the Dog and Cat.* 3rd ed. St. Louis, MO: Saunders Elsevier; 2006:417-435.
9. Greig B, Armstrong PJ. Ehrlichiosis, neorickettsiosis, anaplasmosis, and *Wolbachia* infection: Canine granulocytotropic anaplasmosis (*A. phagocytophilum* infection). In: Greene CE, ed. *Infectious Diseases of the Dog and Cat*. 3rd ed. St. Louis, MO: Saunders Elsevier; 2006:219-223.
10. Montgomery RR, Booth CJ, Wang X, Blaho VA, Malawista SE, Brown CR. Recruitment of macrophages and polymorphonuclear leukocytes in Lyme carditis. *Infect Immun*. 2007;75:613-620.
11. Moody KD, Barthold SW, Terwilliger GA, Beck DS, Hansen GM, Jacoby RO. Experimental chronic Lyme borreliosis in Lewis rats. *Am J Trop Med Hyg*. 1990;42:165-174.
12. Moody KD, Terwilliger GA, Hansen GM, Barthold SW. Experimental *Borrelia burgdorferi* infection in *Peromyscus leucopus*. *J Wildl Dis*. 1994;30:155-161.
13. Pinto DS. Cardiac manifestations of Lyme disease. *Med Clin North Am*. 2002;86:285-296.
14. Ruderman EM, Kerr JS, Telford SR,3rd, Spielman A, Glimcher LH, Gravallese EM. Early murine Lyme carditis has a macrophage predominance and is independent of major histocompatibility complex class II-CD4+ T cell interactions. *J Infect Dis*. 1995;171:362-370.
15. Taboada J, Lobetti R. Babesiosis. In: Greene CE, ed. *Infectious Diseases of the Dog and Cat.* 3rd ed. St. Louis, MO: Saunders Elsevier; 2006:723-724.

The Armed Forces Institute of Pathology
Department of Veterinary Pathology

Conference Coordinator
Matthew Wegner, DVM

WEDNESDAY SLIDE CONFERENCE 2010-2011

Conference 21

23 February 2011

Conference Moderator:
Thomas J. Van Winkle, VMD, Diplomate ACVP

CASE I: 04-0556-7 (AFIP 2936145).

Signalment: Two-year-old male Rottweiler dog, canine (*Canis familiaris*).

History: This dog was presented with a two month clinical history of slowly progressive and relentless ataxia, hypermetria and proprioceptive loss of forelimbs with final paresis. Cranial nerve function and spinal reflexes appeared normal. No pathological nystagmus or tremors were observed. The dog was euthanized. Parents of this dog were apparently normal.

Gross Pathology: At necropsy no organic gross lesions were observed other than a white, more or less bilateral, opaque discoloration of the dorsolateral funiculus of spinal cord.

Laboratory Results: Myelography of cervical spinal cord revealed no compression lesion. Magnetic resonance imaging (MRI) of the cervical spinal cord and brain was normal. Cerebrospinal fluid (CSF) cytology revealed a normal protein content of 0.30 g/L (normal=0-0.45 g/L) and no pleocytosis.

Histopathologic Description: Cervical spinal cord: Microscopically, the lesions are characterized by a loss of myelin visible on HE-stained sections where the normally intense eosinophilia of the white matter is lost and the neuropil has a fine fibrillar meshwork pattern dotted with numerous oligodendrocyte nuclei. With the Luxol fast blue stain, the deep blue color of the white matter is replaced by a light blue staining. A narrow rim of normal white matter is usually present between the edge of the lesion and the glia limitans, a characteristic sharp line of demarcation between the normal white matter and the lesion. The demyelination is associated with edema, swelling and splitting of myelin sheaths with gitter cells and a marked reactive astrocytosis. Only mild axonal changes (Wallerian degeneration) are seen, attesting to axonal preservation. The vessels permeating the lesion are prominent and cuffed by mononuclear phagocytes.

Contributor's Morphologic Diagnosis: Cervical spinal cord: Bilateral and often symmetrical demyelination in the dorsolateral funiculus, astrocytic hypertrophy and proliferation (astrocytosis, astrogliosis).

Disease name: Leukoencephalomyelopathy of the Rottweiler dog.

Contributor's Comment: Leukoencephalomyelopathy is a rare condition of the Rottweiler clinically beginning between 1.5 and 3.5-years-old, and characterized by a slow progressive ataxia, hypermetria and paresis of all four limbs, often beginning in the forelimbs, and late severe proprioceptive loss.[2,7] Generally no signs other than locomotor disturbances are observed.[7]

The main site of the lesion is the cervical spinal cord, which, on gross inspection, has a dull white, opaque discoloration of the lateral (especially dorsal parts) and dorsal funiculi.[1,2] Lesions are bilateral with a more or less characteristic symmetric distribution. Histologic examination reveals lesions to be present also in the deep cerebellar white matter,

1-1. Spinal cord, Rottweiller, dog. Bilaterally, there is an opaque, white discoloration of the dorsolateral funiculi. Photograph courtesy of Ecole Nationale Veterinaire d'Alfort, Pathology Department, 7 avenue du General de Gaulle, 94704 Maisons-Alfort Cedex, France.

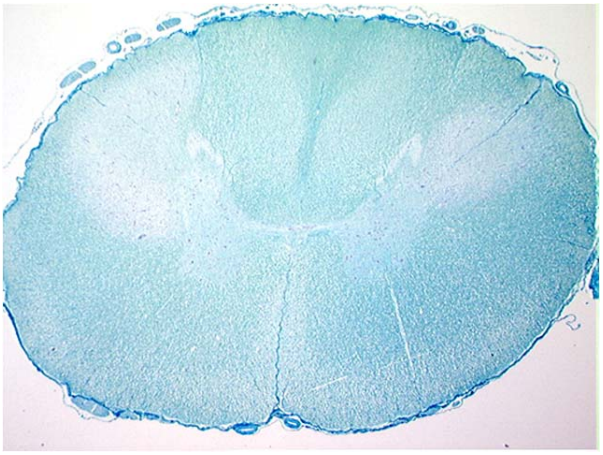

1-2. Cervical spinal cord, Rottweiller, dog. The loss of normal deep blue staining with the Luxol fast blue stain demonstrates demyelination of axons. Photograph courtesy of Ecole Nationale Veterinaire d'Alfort, Pathology Department, 7 avenue du General de Gaulle, 94704 Maisons-Alfort Cedex, France.

brain stem, optic tracts and in other regions of the spinal cord.[7]

Transmission electron microscopic examination reveals irregular myelin splitting, thinning of myelin sheaths and naked axons, paucity of axonal organelles, absence of axonal swelling and neurofilament aggregates.[4]

The clinical differential diagnosis includes:

1. Neuroaxonal dystrophy: Progressive sensory ataxia in adult dogs characterized by head bobbing and positional nystagmus, with lesions of axonal spheroids, axonal degeneration and loss.
2. Canine distemper myelitis, characterized by high protein content and pleocytosis at CSF analysis.
3. Cervical spinal cord compression (wobbler syndrome): Myelography is required to exclude this possibility.

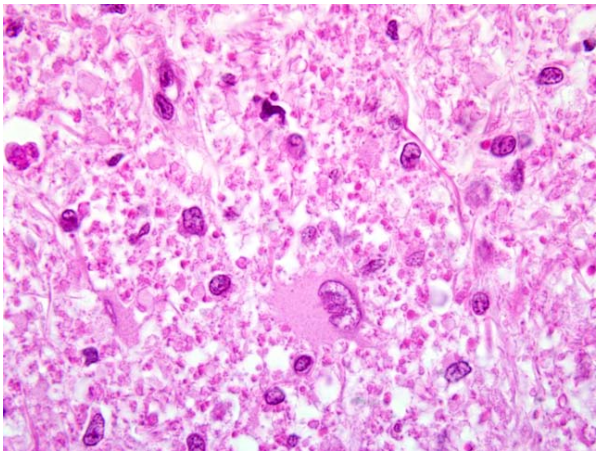

1-3. Cervical spinal cord, Rottweiller, dog. In the dorsolateral funiculi myelin is lost and replaced by a fine fibrillar eosinophilic meshwork. There are numerous oligodendrocytes, gemistocytic astrocytes, and microglial cells. (HE 1000X)

AFIP Diagnosis: Spinal cord, dorsal lateral funiculus: Demyelination, bilaterally symmetrical, diffuse, marked with gliosis (leukomyelopathy).

Conference Comment: The moderator offered guidelines for histologic differentiation of oligodendroglial cells, astrocytes and microglial cells. Oligodendroglial cells typically have a small, dense nucleus; astrocytes have a large nucleus with a nucleolus; and microglial cells have an elongate nucleus that often appears twisted.

Demyelination can be primary or secondary in nature. Primary demyelination results from direct damage to the myelin sheath with sparing of the axon. Secondary demyelination, the more common of the two types, occurs following axonal injury and loss.[8] Primary demyelinating diseases are rare animals; examples include canine distemper virus infection, caprine arthritis-encephalitis virus infection, hepatic encephalopathy and globoid cell leukodystrophy.[5] The process of demyelination begins with direct damage to oligodendroglia and/or the myelin sheath followed by release of lipids and myelin components into the extracellular space, activation of microglia and macrophage accumulation.[8]

Secondary demyelination frequently results from Wallerian degeneration. After damage to the nerve, degeneration and fragmentation of the axon and myelin occur at 24 and 48 hours, respectively. The proximal segment degenerates back to the first viable node of Ranvier while the distal segment dies. The cellular and myelin debris are phagocytosed by Schwann cells and macrophages. If the axon endoneurium has not been disrupted, regeneration ensues with the sprouting nerves entering the neural tube followed by remyelination by Schwann cells. Growth occurs at a rate of 1-4 mm per day.[8]

Unlike the peripheral nervous system, there is little regenerative potential within the central nervous system

(CNS) due to a combination of the complex oligodendrocyte/axon relationship, the poor regenerative capacity of oligodendroglia, the absence of a basal lamina scaffold, and the inhibitory effect of myelin and lipid on axonal sprouting. Thus, demyelination in the CNS often results in the formation of an astroglial scar.[3]

Contributor: Ecole Nationale Veterinaire d'Alfort**,** Pathology Department, 7 avenue du General de Gaulle, 94704 Maisons-Alfort Cedex, France

References:

1. Gamble DA, Chrisman CL. A leukoencephalomyelopathy of rottweiler dogs. *Vet Pathol*. 1984;21(3):274-80.
2. Jubb KVF, Huxtable CR. The nervous system. In: Jubb KVF, Kennedy PC, Palmer N, eds. *Pathology of Domestic Animals*. Vol. 1, 4th ed. San Diego, CA: Academic Press; 1993:373-374.
3. Maxie MG, Youssef S. Nervous system. In: Maxie MG, ed. *Jubb, Kennedy and Palmer's Pathology of Domestic Animals*. Vol. 1, 5th ed. Philadelphia, PA: Elsevier Ltd; 2007:287-289.
4. Slocombe RF, Mitten R, Mason TA. Leucoencephalomyelopathy in Australian Rottweiler dogs. *Aust Vet J*. 1989;66(5):147-150.
5. Summers B, Cummings J, de Lahunta A. Principles of neuropathology. In: *Veterinary Neuropathology*. St. Louis, MO: Mosby; 1995:16-17.
6. Summers B, Cummings J, de Lahunta A. Degenerative diseases of the central nervous system. *Veterinary Neuropathology*. St. Louis, MO: Mosby; 1995:285-286.
7. Wouda W, van Nes JJ. Progressive ataxia due to central demyelination in Rottweiler dogs. *Vet Q*. 1986;8(2):89-97.
8. Zachary JF. Nervous system. In: McGavin MD, Zachary JF, eds. *Pathologic Basis of Veterinary Disease*. 4th ed. St. Louis, MO: Elsevier; 2007:853-856,933.

CASE II: N2006-751 (AFIP 3073348).

Signalment: 9-year-old female white-fronted (parma) wallaby, marsupial (*Macropus parma*).

History: This wallaby had a several month history of progressive neurologic deficits, including ataxia and circling to the right, accompanied by weakness, muscle loss, and anorexia. She also had a history of lumbar vertebral spondylosis and dental abscess.

Laboratory Results: West Nile Virus, Wallaby retrovirus and *Toxoplasma* titers were negative. Radiographs, complete blood count and serum chemistries were non-diagnostic.

Gross Pathology: Near the right temporomandibular joint is an approximately 1.5 cm diameter abscess which extends from the medial aspect of the mandibular ramus into the maxillary bone through the calvarium and into the brain parenchyma. The abscess has a variably thick wall and the contents are pasty and grey-green with numerous small, firm, white-yellow flecks. Viewed from the ventral surface, the brain is asymmetrical with moderate expansion of the right caudal composite gyrus and pyriform lobe by an abscess that is contiguous with the abscess adjacent to the temporomandibular joint.

Histopathologic Description: Brain, cerebrum: Transverse section of the brain at the level of the interthalamic adhesion. Extending from the meningeal surface of the right ventrolateral cerebrum into the parenchyma is a large, 1.0 cm diameter, discrete focus of severe inflammation and necrosis creating a mass effect with thalamic midline shift to the left and herniation of the right cingulate gyrus under the falx cerebri (not visible in histologic sections; see submitted image). The mass is composed of dozens of irregularly shaped, large bacterial colonies surrounded by abundant degenerate neutrophils, fewer epithelioid and large foamy histiocytic cells, and peripherally by lymphocytes and plasma cells. The bacterial colonies are tangled mats of branched, filamentous to beaded bacteria surrounded by peripherally radiating homogeneous, acellular, brightly eosinophilic clubbed material (Splendore-Hoeppli reaction). The bacterial colonies are separated from each other by confluent areas of liquefactive necrosis. The adjacent brain parenchyma is rarefied, with numerous gitter cells. Blood vessels in the vicinity are variably surrounded by cuffs of lymphocytes and plasma cells 1-10 cells thick.

Special Stains:

- Gram stain (Brown and Brenn): Bacteria are gram- positive
- Kinyoun Acid-Fast: Bacteria are not acid-fast

Note: While all slides clearly demonstrate the agent and inflammatory response described, the amount of brain parenchyma in the submitted slides is variable.

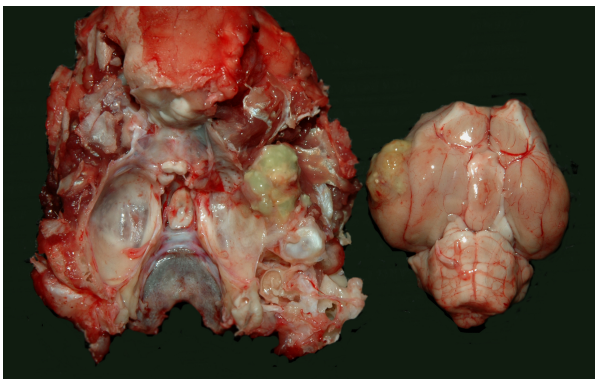

2-1. Brain, skull and oropharynx, white-fronted wallaby. Viewed from the ventral surface the brain is asymmetrical, with moderate expansion of the right caudal composite gyrus and pyriform lobe by an abscess that is contiguous with the abscess adjacent to the temporomandibular joint (left). Photograph courtesy of Wildlife Conservation Society, Pathology Dept. – WHC, Bronx, NY 10460, www.wcs.org.

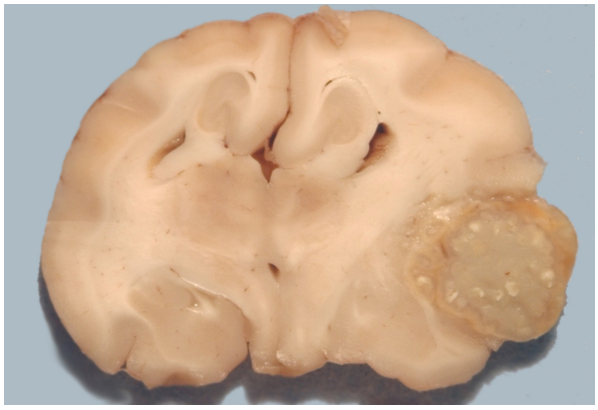

2-2. Brain, white-fronted wallaby. Extending from the meningeal surface of the right ventrolateral cerebrum into the parenchyma is a large, 1.0 cm diameter, discrete focus of inflammation and necrosis. Photograph courtesy of Wildlife Conservation Society, Pathology Dept. – WHC, Bronx, NY 10460, www.wcs.org.

Unfortunately, some slides contain processing artifacts as the tissue fragmented easily when cut.

Contributor's Morphologic Diagnosis: Brain: Pyogranulomatous meningoencephalitis, chronic, locally extensive, severe, with intralesional large filamentous, branching gram positive and non-acid-fast bacterial colonies surrounded by Splendore-Hoeppli reaction, consistent with *Actinomyces* spp.

Contributor's Comment: Lumpy jaw, or chronic alveolar osteomyelitis, is a common disease of marsupials belonging to the family Macropodidae (macropods), especially kangaroos and wallabies.[2,4,5,7] Unlike cattle, where the disease known as lumpy jaw is rather exclusively associated with *Actinomyces bovis*, in macropods the term is more inclusive and in the literature includes two general presentations,[2] one associated with *Fusobacterium necrophorum* and the other with *Actinomyces* spp. Typically, lesions associated with *Fusobacterium necrophorum* (necrobacillosis) are necrotizing and/or

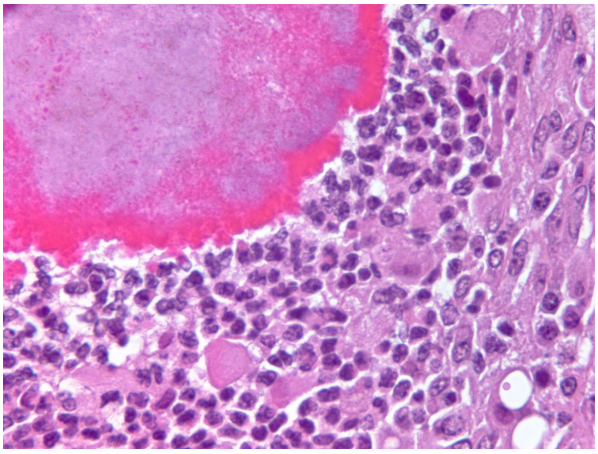

2-3. Brain, white-fronted wallaby. The cerebrum is expanded by many bacterial colonies surrounded by peripherally radiating homogeneous, acellular, brightly eosinophilic clubbed material (Splendore-Hoeppli reaction) and further surrounded by many degenerate neutrophils, histiocytic cells, and peripherally by lymphocytes and plasma cells. Photograph courtesy of Wildlife Conservation Society, Pathology Dept.–WHC, Bronx, NY 10460, www.wcs.org.

purulent with acute inflammation of soft tissues, severe necrosis and lysis of the affected bone, fetid odor, and little periosteal new bone formation; this presentation is commonly reported in Australia.[2] By contrast, infection with *Actinomyces* spp. (actinomycosis) is a chronic infection characterized by excessive periosteal new bone formation, disfigurement of face, formation of draining tracts, and lacks the fetid odor and necrosis of *Fusobacterium* infections; this presentation is reported in zoos in the Northern Hemisphere.[2] Both presentations can lead to significant mortality via starvation secondary to tooth loss, or septicemia/toxemia from bacterial infection. Lumpy jaw is more common in captive macropods than in free-ranging animals, but is not exclusively a disease of captivity.[5] In both captive and free living animals stress and crowding appear to be predisposing factors.[7] This discussion focuses mainly on actinomycosis.

Actinomyces spp. are commensal organisms of the mammalian oral cavity, found on mucus membranes and tooth surfaces.[1] Infection with this opportunistic pathogen begins with a traumatic break in the oral mucosa, potentially from tooth eruption, rough browse or other plant material. Infection becomes established in the alveolar or paralveolar tissues where bacterial colonies form and trigger a suppurative response in the immediate vicinity and mononuclear inflammation and fibrosis at the periphery. This process extends into the adjacent bone forming multiple small abscesses surrounded by granulation tissue and fibrosis, with lysis of bony trabeculae and excessive periosteal bone formation. This creates an expanded, yet porous bone that can best be seen on macerated specimens. Early lesions are very difficult to recognize without a thorough oral examination including dental radiographs. Histologic evaluation of early lesions demonstrates colonies of *Actinomyces*-like bacteria in the periodontal space, associated with alveolar bone res orption.[7]

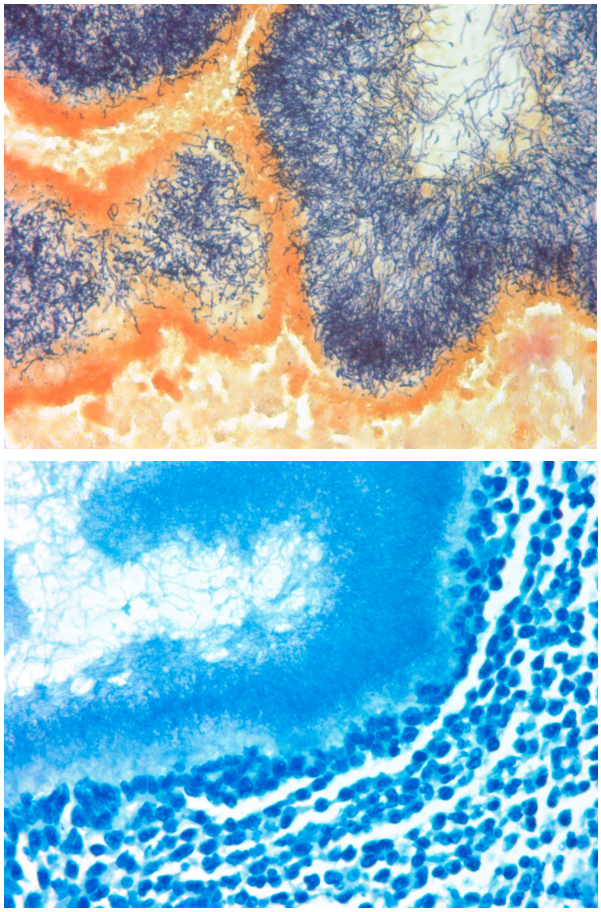

2-4, 2-5. Brain, white-fronted wallaby. Bacteria are gram positive by the Brown-Brenn staining method (2-4) and are non-acid-fast by the Kinyoun method stain (2-5). Photographs courtesy of Wildlife Conservation Society, Pathology Dept. – WHC, Bronx, NY 10460, www.wcs.org.

The hallmark feature of *Actinomyces* infection is presence of "sulfur granules" scattered within the suppurative exudate.[1,8] Grossly, sulfur granules are yellow/white particles, varying in firmness, that are up to several millimeters in diameter. Histologically they are composed of characteristic 'club colonies' with brightly eosinophilic Splendore-Hoeppli reaction arranged as palisading clubs at the periphery of the bacterial colonies.[1,8] Splendore-Hoeppli material is proposed to be aggregates of antigen-antibody complexes, and although it is not exclusive to a particular agent (it can be seen in some bacterial, fungal and parasitic infections as well as occasionally with foreign bodies) its presence is diagnostically helpful. Bacterial pathogens that commonly elicit this tissue response are few, and in animals these include *Actinobacillus lignieresii* (wooden tongue), *Staphylococcus aureus* (botryomycosis), and *Nocardia* spp. Bacterial morphology and special stains are then useful in distinguishing between these agents. Of these bacteria, only two are branching filamentous bacteria (as seen in this case): *Actinomyces* and *Nocardia*. Both *Actinomyces* and *Nocardia* are gram-positive, but only *Nocardia* is weakly acid-fast.[1] In this case, *Actinomyces* was not cultured from the jaw abscess; however, the characteristic histomorphology

(mats of branching filamentous bacteria) and staining patterns of the bacterial colonies (Gram positive and non-acid fast) was highly suggestive of *Actinomyces* spp. Most often, the lesions of "lumpy jaw" contain mixed bacterial populations due to overgrowth or invasion of other commensal oral flora. The best chance of isolating *Actinomyces* is with submission of sulfur granules for bacterial culture.[4] *Actinomyces bovis* and *A. viscosus* have been isolated from macropods with lumpy jaw.[7]

Alveolar actinomycosis is a chronic, disfiguring disease that is difficult, if not impossible, to cure. The causative agent, a gram-positive bacterium, is susceptible to penicillin antibiotics; however, tissue penetration is problematic given the degree of fibrosis and potential persistence of bacteria within dentin tubules of affected teeth.[3] Other treatments reported include draining and flushing the lesion with sodium iodide,[2] hydrogen peroxide or sodium hypochlorite,[4] and removal of the apex of the tooth root with endodontic filling.[4]

The peculiar susceptibility of macropods to chronic alveolar osteomyelitis may be related to a process known as molar progression, and the propensity for accumulation of calcified deposits on the molar and premolar teeth.[7] Molar progression is a feature of many, but not all, macropods and is thought to optimize the processing of plant material in the dental mill. It is the mesial (forward and medial) movement of molariform teeth along the jaw with age. In tammar and parma wallabies, molar progression is primarily due to the growth and resultant forward movement of the bones bearing the teeth ("mesial shift") rather than the forward movement of the teeth relative to the supportive bone ("mesial drift").[6] The result is the formation of 'post functional' molariform teeth that no longer contribute to mastication of food and are subsequently shed. Before being shed, these teeth often manifest alveolar bone loss and food impaction. Macropods are also prone to development of abundant dental calculus on their teeth. This is likely due to the high phosphate content of their saliva, pH of 6-8, and large numbers of *Bacterionema matruchottii*,[7] which promote plaque formation and bone resorption. Both of these processes can create defects in the oral mucous barrier integrity and an environment favorable to colonization by the causative bacteria of both presentations of lumpy jaw in macropods - *Actinomyces* and *Fusobacterium necrophorum*. In macropods, the mandible and maxilla appear equally affected by alveolar osteomyelitis, whereas the lesion in cattle is predominantly mandibular with the maxilla rarely involved.[2,8]

Secondary lesions of chronic alveolar osteomyelitis in macropods include tooth loss, deformation of the affected bone, and local extension into the palatine bones and nasal cavities,[2,7] but the local extension through the calvarium and into the brain, as seen in this case, is a rare occurrence. The involvement of the right rostral thalamus in the resultant brain lesion correlates well with the clinical signs of propulsive circling to the right ("adversive syndrome").[3] Other routes of infection were considered in this case; however, there was no evidence of external skull or facial trauma or puncture wounds to suggest traumatic inoculation of bacteria, and no evidence of otitis to suggest local extension from the ear. Histologic examination of the right maxilla revealed multiple foci of chronic alveolar osteomyelitis with *Actinomyces*-like bacteria (identical to the colonies seen in the brain lesion) in the area of the periodontal ligament near the apex of the tooth root and within the maxillary bone, supporting the proposed origin of the brain abscess as local extension of maxillary alveolar osteomyelitis.

AFIP Diagnosis: Brain: Meningoencephalitis, pyogranulomatous, focally extensive, severe with mild multifocal perivascular meningitis, large colonies of filamentous bacilli, and Splendore-Heoppli material (sulfur granules).

Conference Comment: As noted by the contributor, there is slide variation in the amount of tissue present for evaluation and frequent tissue artifact. The contributor provides an excellent review of actinomycosis in macropods, with particular emphasis on the clinical signs, disease course and pathogenesis.

Contributor: Wildlife Conservation Society, Pathology Dept. – WHC, 2300 Southern Boulevard, Bronx, NY 10460 www.wcs.org

References:

1. Bilberstein EL, Hirsh DC. Filamentous bacteria: Actinomyces, nocardia, dermatophilus, and streptobacillus. In: Hirsh DC, MacLachlan NJ, Walker RL, eds. *Veterinary Microbiology*. 2nd ed. Ames, IA: Blackwell Publishing; 2004:215-222.
2. Butler R. Montremes and Marsupials (Monotremata and Marsupialia), bacterial diseases. In: Fowler ME, ed. *Zoo and Wild Animal Medicine*. 2nd ed. Philadelphia, PA: WB Saunders Company; 1986:572-576.
3. De Lahunta A. Diencephalon. In: De Lahunta A, ed. *Veterinary Neuroanatomy and Clinical Neurology*. 2nd ed. Philadelphia, PA: WB Saunders Company; 1983:344-355.
4. Fagan DA, Oosterhuis JE, Benirschke K. "Lumpy jaw" in exotic hoofstock: A histopathologic interpretation with treatment proposal. *J Zoo Wildl Med*. 2005;36(1):36-43.
5. Griner, LA. Marsupialia. In: Griner LA, ed. *Pathology of Zoo Animals*. San Diego, CA: Zoological Society of San Diego; 1983:301-309.
6. Lentle RG, Hume ID, Stafford KJ, Kennedy M, Haslett S, Springett BP. Molar progression and tooth wear in tammar (*Macropus eugenii*) and parma (*Macropus parma*) wallabies. *Australian Journal of Zoology*. 2003;51:137-151.
7. Miller WA, Beighton D, Butler R. Histological and osteological observations on the early stages of lumpy jaw. In: Montali RJ, Migaki, G, eds. *The Comparative Pathology of Zoo Animals, Proceedings from the Symposia at the National Zoological Park, 1978*. Washington, DC:

Smithsonian Institution Press; 1980:231-239.
8. Palmer N. Bones and joints. In: Jubb KVF, Kennedy PC, Palmer N, eds. *Pathology of Domestic Animals*. 4th ed. Vol 1. San Diego, CA: Academic Press; 1993:106-108.

CASE III: 09-7191 (AFIP 3164121).

Signalment: Eleven-year-old castrated male Scottish terrier, canine (*Canis familiaris*).

History: The dog had bouts of vomiting with elevated liver enzymes and atypical Cushing's disease of 3 weeks duration. There was a 3-day history of vestibular/cerebellar disease and fever. A cerebrospinal fluid analysis had 20 cells (mostly eosinophils). The MRI was normal. The disease progressed to the point of the patient becoming non-ambulatory. The dog did not improve with corticosteroid and cyclosporine treatment and was euthanized.

Gross Pathology: There were no gross lesions reported by the submitting veterinarian.

Histopathologic Description: Brain: In sections of cerebral cortex, basal ganglia, midbrain, cerebellum and medulla there are multifocal areas of malacia containing aggregates of foamy macrophages in areas of disrupted neuropil. Blood vessels are cuffed by inflammatory cells including many eosinophils mixed with lymphocytes, plasma cells and macrophages. Perivascular cuffs of similar composition are present in the overlying meninges. Cross sections of nematode parasites with a cuticle, prominent lateral alae, paired triangular-shaped excretory columns and a digestive tract occur in areas with inflammation and without.

Contributor's Morphologic Diagnosis: Encephalitis, granulomatous and eosinophilic, subacute, multifocal, severe with intralesional nematodes. (Etiology: *Baylisascaris* spp.)

Contributor's Comment: *Baylisascaris procyonis,* the raccoon ascarid roundworm, causes central nervous system (CNS) disease in over 45 species of animals including dogs and humans.[4] Reported cases in dogs have all been puppies exposed to fecal material of raccoons that were housed in close proximity.[4,5]

The raccoon sheds eggs of the parasite in the feces. The eggs are resistant and can survive for years in the environment. They require two to four weeks to mature to the infective stage. Dogs, a susceptible aberrant host, are infected by consuming eggs from a contaminated environment followed by visceral migration of the larvae, some of which enter the brain and cause damage and clinical disease.[4]

The parasite causes a severe inflammatory reaction and physical damage because of its large size and aggressive migration.[1] A rapid clinical course, peripheral eosinophilia, and eosinophlic pleocytosis of the cerebrospinal fluid are highly suggestive of *Baylisascaris* larval migration in the central nervous system (CNS).[4] Treatment with anthelmenthics is not usually effective and the prognosis is guarded in all cases. Corticosteroids are administered in an attempt to decrease the inflammatory process associated with parasite migration and may result in some clinical improvement.

AFIP Diagnosis: Brain, cerebrum: Meningoencephalitis, eosinophilic and lymphohistiocytic, multifocal, mild to moderate with necrosis, gliosis, gitter cells, and rare larval nematodes.

Conference Comment: Participants commented on the slide variation, with some sections having prominent nematode larvae and others almost devoid of parasites. The moderator pointed out that eosinophilic and lymphohistiocytic inflammation, gitter cells, and random, "punched-out" holes of necrosis strongly suggest aberrant parasitic migration, regardless of the lack of parasites in tissue sections. Most participants favored *Baylisascaris procyonis* as the etiologic agent; the moderator likewise favored *B. procyonis* based on the size of the nematode and the frequency of occurrence in the CNS of the dog. This generated discussion of other parasites which undergo aberrant migration through the CNS of animals. The included chart summarizes the entities discussed.[2,3]

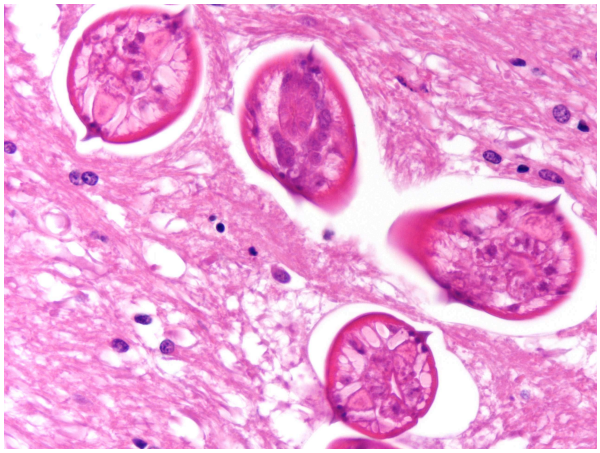

3-1. Brain, dog. Cross sections of Baylisascaris nematodes have prominent lateral alae, an intestine, external cuticle and triangular shaped excretory columns. Photograph courtesy of Arizona Veterinary Diagnostic Laboratory, 2831 N. Freeway, Tucson, Arizona 85602.

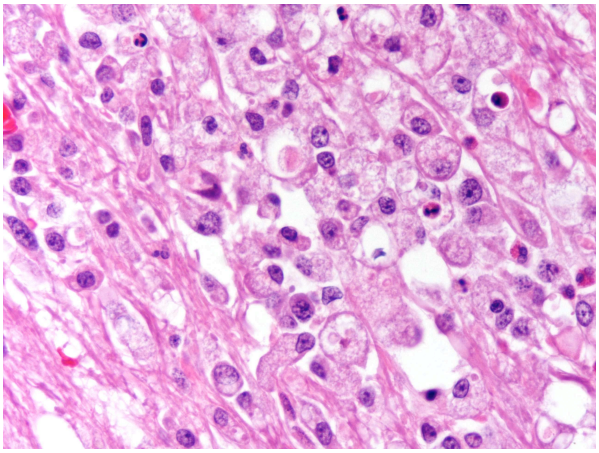

3-2. Brain, dog. An area of malacia caused by parasitic migration contains many foamy macrophages and few eosinophils. Photograph courtesy of Arizona Veterinary Diagnostic Laboratory, 2831 N. Freeway, Tucson, Arizona 85602.

Parasite	Natural Host	Aberrant Host
Coenurus cerebralis (larval stage of *Taenia multiceps*)	Dog, wild carnivores	Sheep, horse, other herbivores, man
Cysticercus cellulosae (larval stage of *Taenia solium*)	Humans	Pig, dog
Parastrongylus (*Angiostrongylus*) *cantonensis*	Rat	Dog, man
Parelaphostrongylus tenuis	White-tailed deer	Sheep, red deer, elk, moose
Elaephora schneideri	Mule deer, black-tailed deer	Sheep, goat, elk, moose, sika deer, white-tailed deer
Setaria digitata	Cow, buffalo	Horse, camel, sheep, goat
Halicephalobus gingivalis	Free-living	Horse
Angiostrongylus vasorum	Dog	Dog
Stephanurus dentatus	Pig	Pig
Strongylus spp.	Horse	Horse
Dirofilaria immitis	Dog	Dog, cat
Cuterebra cerebralis	Rodent, rabbit	Cat, dog

Contributor: Arizona Veterinary Diagnostic Laboratory, 2831 N. Freeway, Tucson, Arizona 85602

References:

1. Kazacos KR, Boyce WM. *Baylisascaris* larva migrans. *J Am Vet Med Assoc*. 1989;195:894-903.
2. Maxie MG, Robinson WF. Cardiovascular system. In: Maxie MG, ed. *Jubb, Kennedy and Palmer's Pathology of Domestic Animals*. Vol. 3, 5th ed. Philadelphia, PA: Elsevier Ltd; 2007:92.
3. Maxie MG, Youssef S. Nervous system. In: Maxie MG, ed. *Jubb, Kennedy and Palmer's Pathology of Domestic Animals*. Vol. 1, 5th ed. Philadelphia, PA: Elsevier Ltd; 2007:438-439.
4. Rudman DG, Kazacos KR, Storandt ST, Harris DL, Janovitz EB. *Baylisascaris procyonis* larva migrans in a puppy: A case report and update for the veterinarian. *J Am Anim Hosp Assoc*. 1996;32:73-76.
5. Thomas JS. Encephalomyelitis in a dog caused by *Baylisascaris* infection. *Vet Pathol*. 1988;25:94-95.

CASE IV: 10-8794103 (AFIP 3176070).

Signalment: 12-week-old intact male Kelpie puppy, canine (*Canis familiaris*).

History: The puppy presented with acute onset of ataxia and tremors; signs only became apparent in the past few days. The owner has 5 of the 10 puppies of this litter: 2 males and 3 females. All 3 females and this male were showing clinical signs; the male was the worst affected. The other 5 pups owned by someone else were apparently all fine.

Gross Pathology: No gross abnormalities were seen in the brain of this puppy.

Laboratory Results: Cerebrospinal fluid analysis:

Appearance	Colorless and clear
Microscopy	
Erythrocytes	1500 x 10^6/L
Leucocytes	7 x 10^6/L
Gram stain	No bacteria or protozoal organisms seen
Chemistry	
Protein	0.30 g/L (0.10-0.33)
Cytology	Cytospin: few mononuclear cells & rare neutrophils Insufficient cells for differential count. Minimal hemorrhage

Interpretation: No significant abnormalities

Histopathologic Description: Brain, cerebellum: Multifocally and segmentally, there is degeneration and loss of Purkinje cells, with rare discrete clear spaces in the Purkinje cell layer (empty baskets). In some of the folia, there is almost complete absence of the Purkinje cell layer. Multifocally, remaining Purkinje cells are shrunken, angular and hypereosinophilic with karyolysis or pyknosis (necrosis), or swollen and finely vacuolated with dispersal of Nissl substance (chromatolysis). More severely affected regions have mild spongiotic change affecting the inner aspect of molecular layer neuropil associated with proliferation of Bergmann's astrocytes (gliosis). Multifocally, there is thinning of the inner granular cell layer, with patchy hypocellularity and scattered individual granular neurons with pyknotic nuclei. Rarely, swollen Purkinje cell dendrites extend into the molecular layer (torpedoes). Multifocally within the white matter of the cerebellar folia, there is mild Wallerian-type degeneration, with scattered discrete round clear vacuoles containing individual phagocytes (Gitter cells) and occasional slightly swollen, hypereosinophilic axons (spheroids).

Contributor's Morphologic Diagnosis: Brain, cerebellum: Purkinje cell degeneration, necrosis and loss, multifocal to segmental, moderate, with secondary granular cell loss and mild white matter Wallerian degeneration

Contributor's Comment: Abiotrophy refers to a premature or accelerated degeneration of formed elements; this differs from hypoplasia, in which an organ fails to form completely during development.[4,18] Case develops as overt cell loss within localized or multiple brain compartments; other cases may have more subtle changes in neuronal cell body, processes, or myelin sheath, leading to neuronal circuit dysfunction.[8] The term abiotrophy describes the pathological process of neuronal degeneration, but does not provide a clue to the underlying mechanism.[4,12,18] In most instances, the specific cellular defect is unknown; however, postulated theories include glutamate receptor excitotoxicity, channelopathies and autoantibody-mediated disorders.[1,4,6-8,11]

One of the most common of the domestic animal neuronal abiotrophies is that which affects the cerebellar cortex. Most of these are limited to the Purkinje neurons, which appear to be excessively susceptible to such intrinsic disturbances of their metabolic apparatus.[4,7] Where sufficient numbers of affected animals have been studied, autosomal recessive inheritance has been proven or implicated in most cases; however, X-linked cerebellar ataxia has been reported in the English pointer, and an unusual case of cerebellar Purkinje cell degeneration associated with coat color dilution in Rhodesian ridgebacks was also reported.[3,4,8] Moreover, in a few cases of late (adult) onset cerebellar degeneration, extrinsic factors have also been considered as a possible underlying cause.[4,6,10] Indeed, some authors have made the distinction between cerebellar abiotrophy and cerebellar cortical degeneration (CCD) with abiotrophy defined as a proven inherited disease.[1,2,4,18]

Cerebellar abiotrophy has been reported in various domestic specie,s including dogs, cats, sheep, cattle, pigs, and horses.[4] The condition occurs in numerous dog breeds, including, but not limited to Beagle, Samoyed, Old English Sheepdog, Gordon Setter, Border Collie, Rough-coated Collie, Finnish Terrier, Scottish Terrier, Brittany Spaniel, Labrador Retriever, Airedale, Lagotto Romagnolo, Rhodesian Ridgeback, American Staffordshire Terrier, and Miniature Schnauzer.[1-4,6,7,10,11,14-17,19] Each breed appears to possess a different phenotype with respect to the range of signs shown, age of onset, and rate of progression, suggesting differing genetic etiologies in different breeds.[17]

Animals with cerebellar abiotrophy may show signs of dysfunction at birth or during early ambulation (neonatal abiotrophy), but it is more usual to be born with normal neurologic function followed by delayed onset of clinical signs ranging from a few weeks to several years of age, corresponding to the onset of neuronal degeneration (postnatal abiotrophy).[8] At one end of the scale, such as in Labrador Retrievers and Border Collies, signs are seen at an early age (6 to 12 weeks), with rapid progression (few weeks). In contrast, Gordon Setters do not usually present

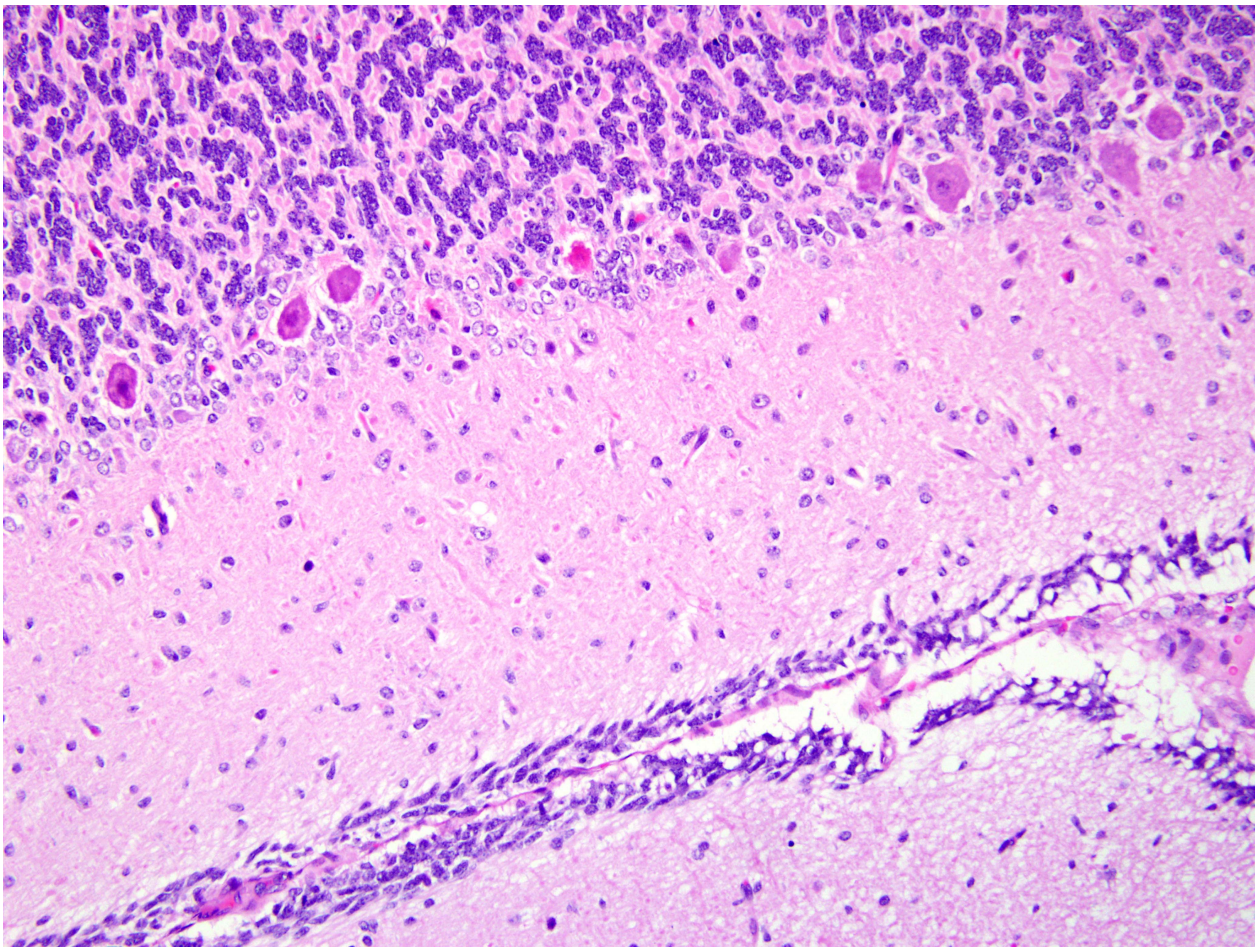

4-1. Brain, cerebellum, Kelpie, dog. Purkinje cells are shrunken, angular, hypereosinophilic, and pyknotic (necrosis) or are lost leaving empty baskets. There is retention of the external granular cell layer, mild gliosis in the molecular layer, and thinning of the granular cell layer. (HE 200X)

with signs until 6 months to 2 years of age, and progression is slow (months to years); and most affected American Staffordshire Terriers are recognized between 4 to 6 years of age.[8] Brittany Spaniels have the latest onset of cerebellar signs (average age of 10 years) with similar slow progression.[1,8]

Clinical signs (ataxia, intention tremor, hypermetria/ spasticity, proprioceptive deficits, wide-based stance, stumbling/falling) reflect the loss of function of inhibitory cerebellar cortical neurons, resulting in abnormal range, rate and force of voluntary movements.[7] Other clinical findings may include loss of menace reflex and nystagmus.[1-3,7,10] The disease and clinical signs are usually progressive, although in some cases affected animals reach a stage at which clinical signs will plateau. Moreover, there is suggestion that affected animals may learn over time to partially compensate for their deficit. In some breeds, e.g. Brittany Spaniel, severity of cerebellar signs does not seem to correlate with the often minimal degree of histopathologic abnormality.[8]

In most cases, definitive diagnosis can only be made at necropsy by histopathological examination, although MRI has been used a diagnostic tool to demonstrate cerebellar atrophy.[5,6,10,17,18] Grossly, the cerebellum of affected animals may exhibit no overt abnormality, or may be smaller than normal, sometimes with slight flattening or narrowing of the folia.[2,19] For example, a normal dog's cerebellum accounts for approximately 10 to 12 per cent of the brain's mass, versus 5 to 7% in some studies.[6,7,10]

The most significant histopathological finding in cerebellar cortical abiotrophy usually is depletion of Purkinje cells.[6,10,18] These neurons complete their migration and differentiation during gestation, whereas granule cell development is not complete until approximately 10 weeks postnatally in the dog and cat.[8,19] Because the integrity of the granule cell neuron is dependent on its synaptic relationship with the dendritic zone of the Purkinje cell, loss of the latter neuron usually results in a secondary depletion of granule cell neurons.[4,7,11,19] There may also be atrophy of the molecular layer. The histological picture has been similar for dogs of the same breed, often with specific regional distribution and severity.[2,6,19] For example, in the Scottish Terrier changes are most pronounced within the dorsal cerebellum and less severe ventrally, with relative sparing of the nodulus and uvula.[17]

Other regions of the brain are often normal; however, multisystem neuronal abiotrophies involving degeneration of extrapyramidal nuclei and other motor systems have been reported.[8] In Kerry Blue Terriers, Purkinje and granule cell degeneration is followed by degeneration of olivary nuclei, then the caudate nucleus and substantia nigra, possibly reflecting a form of transsynaptic degeneration.[4,8] In some cases, granule cell degeneration appears to occur first, followed by Purkinje cell loss, e.g. Rough-coated Collie, or with sparing of the Purkinje cells, e.g. Lagotto Romagnolo, Brittany Spaniel and Border Collie.[6,15]

Cerebellar abiotrophy was first reported in the Australian Kelpie in 1989 by Thomas & Robertson.[16] A prospective breeding trial was conducted after a dog breeder reported several pups with signs of cerebellar disease. Affected pups have normal mental alertness and exhibit clinical symptoms from 5-6 weeks of age, including mild, non-progressive to severe ataxia, hypermetria, proprioceptive deficits and head tremor without accompanying weakness.[16] Fitting has been observed in some dogs.[13] Although the onset of degeneration appears to be prior to 6 weeks of age, there is variation in clinical signs and mildly affected dogs may not be identified until several months of age.[16] Histological lesions are confined to the cerebellum, most commonly and severely within the anterior lobules of the vermis and characterized by regional loss of Purkinje cells, marked reduction in granular cell density, and mild spongiosis and Wallerian degeneration in the white matter tracts of affected folia.[16]

All affected animals can be traced back to a small number of related common ancestors within eight generations. These dogs featured prominently in sheep dog trials and thus had been widely used for breeding, increasing the likelihood of increased disease incidence.[16] The disease is thought to be due to a single mutation amplified by using a popular sire in a small gene pool and inbreeding. Affected dogs should be homozygous, identical-by-descent, and close to the mutation.[13] Three candidate genes (SETX2, ATCAY3 and SYNE14) that are known to cause cerebellar abiotrophy in humans were tested and subsequently excluded as the candidate gene in Kelpies by homozygosity analysis.[13]

Dr. Allan Wilton of the University of New South Wales, in collaboration with the Working Kelpie Council of Australia, is working toward developing a genetic test for the cerebellar abiotrophy mutation in Kelpies (also referred to as 'ataxia'). Blood spot collection kits (sampling from dogs' ears) have been developed and distributed to dog breeders for subsequent DNA analysis utilizing microarray technology.

AFIP Diagnosis: Brain, cerebellum: Purkinje cell degeneration, necrosis and loss, multifocal and segmental, moderate, with granular cell loss, Purkinje and granular layer gliosis, and retention of external granular cell layer.

Conference Comment: The contributor provides a detailed review of cerebellar abiotrophy in the dog, with particular attention paid to the Australian Kelpie. Conference participants also commented on the presence of an external granular cell layer in the cerebellum of this case; most were of the opinion that this is not a typical histologic finding for a normal 12-week-old-dog. The external granular cell layer arises from germinal cells which migrate to the surface of the cerebellar folia. Here, the cells proliferate, differentiate into various microneurons e.g., basket cells, stellate cells, and granule cells, and migrate to their final location. This process begins in late gestation and continues for a couple of weeks after birth.[9] Failure of the microneurons to establish orderly synaptic connections results in cellular disorganization of the cerebellum.[9] Whether the presence of an external granular cell layer is associated with the disease process in the case of this Kelpie puppy is unknown; the feature is not described in the literature. Retention of the external granular granule cell layer in this puppy may reflect the disease variability inherent in cases of cerebellar abiotrophy.

Contributor: Gribbles Veterinary Pathology 1868 Dandenong Rd Clayton, Melbourne, Victoria, Australia, 3168

References:

1. Berry ML, Blas-Machado U. Cerebellar abiotrophy in a miniature schnauzer. *Can Vet J*. 2003;44(8):657–659.
2. Bildfell RJ, Mitchell SK, de Lahunta A. Cerebellar cortical degeneration in a Labrador retriever. *Can Vet J*. 1995;36(9): 570-572.
3. Chieffo C, Stalis IH, Winkle TJ, Haskins ME, Patterson DF. Cerebellar Purkinje cell degeneration and coat color dilution in a family of Rhodesian Ridgeback dogs. *J Vet Intern Med*. 1994;8(2):112-116.
4. de Lahunta A. Abiotrophy in domestic animals: A review. *Can J Vet Res*. 1990;54(1):65-76.
5. Henke D, Böttcher P, Doherr MG, Oechtering G, Flegel T. Computer-assisted magnetic resonance imaging brain morphometry in American Staffordshire terriers with cerebellar cortical degeneration. *J Vet Intern Med*. 2008;22(4):969-975.
6. Jokinen TS, Rusbridge C, Steffen F, et al. Cerebellar cortical abiotrophy in Lagotto Romagnolo dogs. *J Small Anim Prac*. 2007;48(8):470-473.
7. Kent M, Glass E, deLahunta A. Cerebellar cortical abiotrophy in a beagle. *J Small Anim Prac*. 2000;41(7): 321-323.
8. March PA. Degenerative brain disease. *Vet Clin North Am Small Anim Pract*. 1996;26(4):945-971.
9. Maxie MG, Youssef S. Nervous system. In: Maxie MG, ed. *Jubb, Kennedy and Palmer's Pathology of Domestic Animals*. Vol. 1, 5th ed. Philadelphia, PA: Elsevier Ltd; 2007:310-312.
10. Olby N, Blot S, Thibaud JL, et al. Cerebellar cortical degeneration in adult American Staffordshire terriers. *J Vet Intern Med*. 2004;18(2):201-208.

11. Sandy JR, Slocombe RF, Mitten RW, Jedwab D. Cerebellar abiotrophy in a family of border collie dogs. *Vet Pathol*. 2002;39(6):736-738.
12. Shamir M, Perl S, Sharon L. Late onset of cerebellar abiotrophy in a Siamese cat. *J Small Anim Prac.* 1999;40(7): 343-345.
13. Shearman JR, Lau VM, Wilton AN. Elimination of SETX, SYNE1 and ATCAY as the cause of cerebellar abiotrophy in Australian Kelpies. *Anim Genet*. 2008;39(5): 573.
14. Steinberg S, Van Winkle T, Bell JS, de Lahunta A. Cerebellar degeneration in Old English Sheepdogs. *J Am Vet Med Assoc*. 2000;217(8):1162-1165.
15. Tatalick LM, Marks SL, Baszler TV. Cerebellar abiotrophy characterized by granular cell loss in a Brittany. *Vet Pathol*. 1993;30(4):385-388.
16. Thomas JB, Robertson D. Hereditary cerebellar abiotrophy in Australian Kelpie dogs. *Aust Vet J.* 1989;66(9): 301-302.
17. Urkasemsin G, Linder KE, Bell JS, de Lahunta A, Olby NJ. Hereditary cerebellar degeneration in Scottish terriers. *J Vet Intern Med*. 2010;24(3):565-570.
18. Van der Merwe LL, Lane E. Diagnosis of cerebellar cortical degeneration in a Scottish terrier using magnetic resonance imaging. *J Small Anim Prac*. 2001;42(8):409-412.
19. Yasuba M, Okimoto K, Iida M, Itakura C. Cerebellar cortical degeneration in beagle dogs. *Vet Pathol*. 1988;25(4): 315-317.

The Armed Forces Institute of Pathology
Department of Veterinary Pathology

Conference Coordinator
Matthew Wegner, DVM

WEDNESDAY SLIDE CONFERENCE 2010-2011

Conference 22

2 March 2011

Conference Moderator:
Donald Nichols, DVM, Diplomate ACVP

CASE I: S597-04 (AFIP 2937487).

Signalment: 18-month-old male roan antelope of west African origin, caprine (*Hippotragus equines koba*).

History: This animal was part of a juvenile bachelor herd (12 animals) on a 6,000 hectare game ranch in the South African lowveld, south of Kruger National Park. The herd was captured in Benin (West Africa) and translocated to this area in South Africa two months prior to release after a one month adaptation period under boma conditions. Approximately 16 days after release from the boma into the natural Acacia bushveld, this animal was noticed to exhibit depression. It was found dead the following day before therapeutic and clinical diagnostic procedures could be instituted.

Gross Pathology: At necropsy, external examination revealed excellent body condition. The tick load (mainly *Rhipicephalus evertsi* and *R. appendiculatus*) was considered moderate but acceptable, keeping in mind that a certain number of ticks would have detached from the carcass at death. The mucous membranes were severely icteric, and low viscosity (watery) of the blood on blood vessel incision was indicative of anemia. Generalized cortical lymphoid hyperplasia in all lymph nodes was noted. Upon evisceration, serosal petechiae and ecchymoses (almost suggilations in certain areas) were observed, especially on the rumen. Hemorrhages were also multifocally present in the paler renal cortices. The renal medulla showed marked bilirubin and hemoglobin staining and the urine was reddish (hemoglobinuria). Dipstick analysis revealed 2+ protein, 3+ bilirubin, 2+ hemoglobin/blood, and pH 6.5. The cut surface of the adrenal glands showed multiple cortical ecchymoses, without recognizable stress-induced cortical hypertrophy. The liver was dark purple-brown, had rounded edges, and there was a globally accentuated centrilobular/periportal pattern on cut surface. The gallbladder wall was severely thickened due to edema and extensive hemorrhage, with mild gallbladder distention. The content of the gallbladder was normal. The spleen was markedly enlarged (4-5 times normal size) and bulged on cut surface revealing a turgid pulpy consistency of the expanded red pulp. There were multiple petechiae and ecchymoses on the epicardial and endocardial surfaces. Yellow-white foam filled the tracheal lumen and extended for the whole of its length (pulmonary edema, severe). Macroscopic findings and blood smear results (see below) confirmed an etiological diagnosis of theileriasis.

Laboratory Results: Blood smear: Numerous (4+) blast-transformed lymphocytes with many, but not all, containing numerous intracytoplasmic theilerial macroschizonts (Koch's blue bodies); many active (vacuolated) monocytes with some containing phagocytosed parasitized erythrocytes; about 25% of the erythrocytes contained 1-4 theilerial merozoites (piroplasms); mild reticulocytosis; and severe thrombocytopenia.

Impression smears of the liver, spleen and lymph nodes revealed parasitized blast-transformed lymphocytes, similar to those found in the blood.

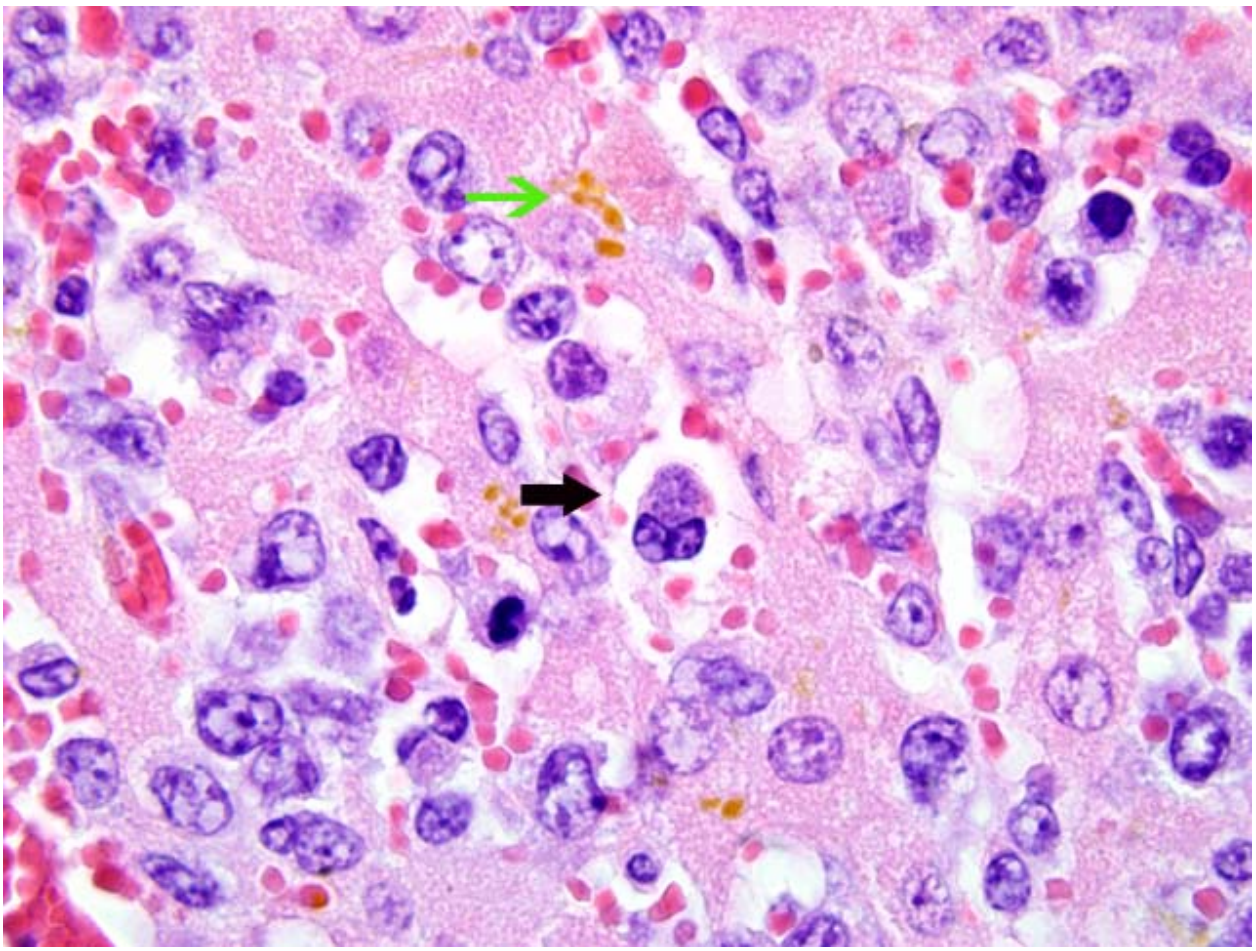

1-1. Liver, roan antelope. Hepatic sinusoids are filled by many lymphoblastic round cells. Lymphoid cells are sometimes binucleate, and occasionally contain intracellular protozoal schizonts (black arrow). Bile caniliculi are occasionally expanded by linear plugs of gold-brown material (bilirubin, green arrow). (HE 1000X)

PCR for identification of Theileria species: Specimens from this case were evaluated by means of the reverse line blot (RLB) method and compared to all known *Theileria* and *Babesia* spp. Only a *Babesia/Theileria* catch-all signal was found. Sequencing of the protozoal DNA recovered from this case revealed a novel theilerial species which closely matched the protozoal DNA recovered from a sable calf that died of theileriosis in 1992 in South Africa.[7] This parasite has not been formally named, but *Theileria hippotragi* is the manuscript name.

Histopathologic Description: Liver: The most striking microscopic change in the liver is the accumulation of pleomorphic, lymphoblast-like round cells in the lumen of the sinusoids. These cells tend to occur as poorly-defined foci, especially in the vicinity of the portal triads. The hepatic cords are distorted and there is variable (pressure) atrophy of the hepatocytes. The larger round cells, many of which are bi- or multinucleate, often contain schizonts or large numbers of merozoites in their cytoplasm. Sinusoidal congestion is apparent, especially around the central veins; this is accompanied by cholestasis, evidenced by markedly distended bile canaliculi.

Contributor's Morphologic Diagnosis: Liver, lymphoblastic sinusoidal infiltration, with architectural disruption, congestion, cholestasis, roan antelope.

Contributor's Comment: Theileriasis in African wildlife, previously known as cytauxzoonosis, has been reported in eland (*Taurotragus oryx*), common duiker (*Sylvicapra grimmia*), greater kudu (*Tragelaphus strepticeos*), giraffe (*Girrafa camelopodis*), roan antelope (*Hippotragus equinus*), sable antelope (*Hippotragus niger*), and tsessebe (*Damaliscus lunatus*). The morphological pathology is only reasonably well-documented in eland,[2] grey duiker,[5] giraffe,[4] and tsessebe.[3] Both the schizont and piroplasms stages appear to be pathogenic. Schizogony occurs in lymphocytes and/or monocytes/macrophages (the identity of the host cell type is still contentious). Parasite-transformed host cells tend to accumulate in capillary and sinusoidal beds, especially those of the liver, spleen, lymph nodes, lungs and kidneys (particularly the glomeruli). Microscopic foci of necrosis and petechial hemorrhages in these organs (not a marked feature in the liver presented here) are most likely a consequence of circulatory disturbances in these vascular beds. Piroplasms inhabit red blood cells, where they

multiply by binary fission. Presumed piroplasm-induced injury to red blood cells varies in severity, both within and between affected wildlife species. In some cases, severe anemia and icterus are apparent.

In South Africa, theileriasis of wildlife appears to have a significant impact on free-living populations of roan, sable, and tsesssebe. In certain habitats and circumstances, the disease is responsible for high morbidity and mortality rates in juveniles; this results in low recruitment rates and extirpation of metapopulations. Research into control strategies for the disease in these three valuable antelope species is currently being conducted.

Theileria-like piroplasms and/or schizonts have been found in both asymptomatic and sick Afrotropical wildlife species belonging to a number of different orders and many families. The systematic and taxonomy of this, probably large, clade of protozoal organisms is in its infancy, but the use of nucleotide-sequencing techniques will certainly provide much needed impetus for the required research.

AFIP Diagnosis: Liver: Hepatitis, lymphoblastic, diffuse, marked, with bile stasis, multifocal vasculitis, hepatocellular degeneration and necrosis, multifocal hemorrhage, and many lymphoid intracytoplasmic protozoal schizonts.

Conference Comment: There was intensive discussion as to the most appropriate classification of the liver lesion among conference attendees; some participants favored hepatitis, while others favored the diagnosis of lymphocytosis. In the opinion of the moderator, when the hepatic parenchyma and/or sinusoids are infiltrated by inflammatory cells the most appropriate morphologic diagnosis is hepatitis. In contrast, others favored the diagnosis of lymphocytosis/lymphoblastosis based on the pathogenesis described in the literature, and preferred to classify the remaining hepatic changes as secondary. Two reference texts define acute hepatitis as having morphologic characteristics of a combination of inflammation and hepatocellular apoptosis and necrosis; regeneration may or may not be present.[1,8] A third text defines hepatitis as being either focal or diffuse infectious processes or leukocyte inflammatory infiltrate regardless of cause.[9] Based on either set of criteria, there is sufficient hepatocellular necrosis and leukocytic (lymphoblastic-lymphocytic) infiltration to characterized the lesion as hepatitis.

The life cycle of theilerial organisms was reviewed. Briefly, the organism is transmitted through the bite of *Rhipicephalus* and *Hyalomma* species ticks. Once inside the host, the sporozoites infect lymphocytes and induce transformation to lymphoblasts. Macroschizonts, found in the cytoplasm of lymphoblasts, are referred to as Koch's blue bodies. The macroschizonts proceed to the microschizont stage, causing cell lysis and release of merozoites which subsequently infect erythrocytes. Once inside the erythrocytes, they enter the final stage forming piroplasms.[9]

The clinical signs associated with theileriosis begin with high fever and diffuse lymphadenopathy around two weeks post-infection. Dyspnea, progressive anemia, and lymphocytolysis contribute to the acute form of the disease and subsequent death of the animal. Gross findings include diffuse enlargement of lymphoid tissues; serous effusions, ulcerative abomasitis, an enlarged spleen early in disease which later becomes shrunken; mottled gray-white patches in the liver and kidney; and congested, edematous lungs. Histologically, there is variation in the lesions based on the progression of the disease process. Initially there is diffuse lymphoid hyperplasia, lymphocytolysis of small lymphocytes with replacement by lymphoblastic lymphocytes, interstitial infiltration of the kidney, and lymphocyte infiltration of pulmonary interstitium resulting in alveolitis. Later in the disease process, lymphoid tissues are shrunken with hemorrhage and fibrin throughout the parenchyma and the bone marrow is hypocellular.[9]

Finally, conference participants briefly discussed the difference between theileriosis and cytauxzoonosis; while theilerial protozoa infect lymphocytes, cytauxzoons infect macrophages.[9]

Contributor: Private Bag X04, Ondersteoort 0100, Republic of South Africa
http://www.up.ac.za/academic/veterinary

References:

1. Cullen JM. Liver, biliary system, and exocrine pancreas. In: McGavin MD, Zachary JF, eds. *Pathologic Basis of Veterinary Disease*. 4th ed. St. Louis, MO: Elsevier; 2007:409.
2. Grootenhuis JG, Morrison WI, Karstad L, et al. Fatal theileriosis in eland (*Taurotragus oryx*): Pathology of natural and experimental cases. *Res Vet Sci*. 1980;29:219-229.
3. Jardine JE. The pathology of cytauxzoonosis in a tsessebe (*Damaliscus lunatus*). *J S Afr Vet Assoc*. 1992;63:48-51.
4. McCully RM, Keep ME, Basson PA. Cytauxzoonosis in a giraffe [*Giraffa camelopardalis* (Linnaeus, 1758)] in Zululand. *Onderstepoort J Vet Res*. 1970;37:7-10.
5. Neitz WO, Thomas AD. *Cytauxzoon sylvicaprae* gen. nov., spec. nov., a prozoon responsible for a hitherto undescribed disease in the duiker [*Sylvicapra grimmia* (Linné)]. *Onderstepoort J Vet Sci Anim Ind*. 1948;23:63-76.
6. Stalker MJ, Hayes MA. Liver and biliary system. In: Maxie MG, ed. *Jubb, Kennedy and Palmer's Pathology of Domestic Animals*. Vol. 2, 5th ed. Philadelphia, PA: Elsevier Ltd; 2007:337-338.
7. Stoltsz WH, Duntersville MT. In vitro establishment and cultivation of a *Cytauxzoon* sp. (*Theileria* sp.) froma sable antelope (*Hippotragus niger*, Harris 1838). *J S Afr Vet Assoc*. 1992;63:182.
8. van den Ingh TSGAM, Van Winkle T, Cullen JM, Charles JA, Desmet VJ. Morphological classification of parenchymal disorders of the canine and feline liver: 2 Hepatocellular death, hepatitis and cirrhosis. In: *WSAVA Standards for Clinical and Histological Diagnosis of Canine*

and Feline Liver Disease. St. Louis, MO: Elsevier; 2006:90-91.
9. Valli VEO. Hematopoietic system. In: Maxie MG, ed. *Jubb, Kennedy and Palmer's Pathology of Domestic Animals*. Vol. 3, 5th ed. Philadelphia, PA: Elsevier Ltd; 2007:304-308.

CASE II: AR05-406 (AFIP 3026271).

Signalment: Adult, gender unknown, northern leopard frog, amphibian (*Rana pipiens*).

History: The animal was found dead after a clinical history of progressive abdominal distention of several weeks' duration.

Gross Pathology: The coelomic cavity was distended by 2-3 mL of serosanguineous, clear fluid. The kidneys were unable to be identified grossly, having been distorted and replaced by a 0.5 x 0.5 cm white, nodular, firm mass.

Histopathologic Description: Kidney: Remnants of normal renal architecture consisting of rare glomeruli and tubules are found within an invasive multilobular, non-encapsulated mass of epithelial cells which form irregular glandular structures separated by collagenous stroma. The epithelial cells are cuboidal to columnar with moderate amounts of eosinophilic cytoplasm and centrally located 8-10 micron diameter nuclei with dispersed, coarsely stippled chromatin. Rare mitoses are noted. The lumina of the glandular structures often contain cell debris and eosinophilic homogenous material (protein).

Contributor's Morphologic Diagnosis: Renal adenocarcinoma.

Contributor's Comment: Lucké's renal adenocarcinoma is an invasive and malignant tumor spontaneously affecting the northern leopard frog (*Rana pipiens*) and caused by Ranid herpesvirus-1, a currently unclassified herpesvirus. Viral morphology is icosahedral, with virions measuring 95-110 nm in diameter. Infected leopard frogs are mainly found in the northeastern and north central United States. Affected frogs may not show signs until advanced tumor growth, with emaciation, lethargy, ascites and sudden death occurring most commonly. Tumor growth can affect one or both kidneys, and grossly the tumors are pale tan and multilobulated. Histologically papillary adenocarcinomas are the most common morphology.[9]

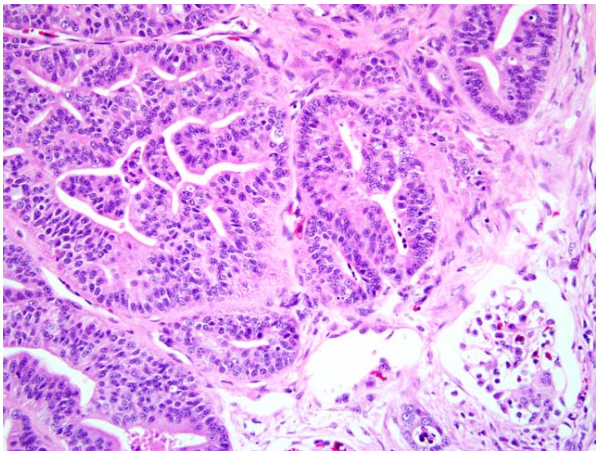

2-1. Kidney, papillary adenocarcinoma, Northern leopard frog, (Rana pipiens). The kidney is replaced by a malignant epithelial neoplasm arranged in long tubuloglandular structures supported by a moderate fibrovascular stroma. Few remnant glomeruli are present at lower right. (HE 200X)

Embryos and larvae are susceptible to viral infection but tumor growth is not recognized until young adulthood.[10] There is a seasonal change in tumor prevalence, with tumors being most common in early spring when frogs emerge from hibernation. The virus replicates during cooler winter temperatures and eosinophilic intranuclear inclusions and virions can be detected during this replication period. Virions are not detected in tumors maintained at warm temperatures;[11,12] however, during this latent period the RHV-1 genome is present.[1] Increased tumor invasiveness and metastasis has also been shown to be temperature-dependent. Tumor metastasis occurs frequently in warm temperatures (77%) and is not recognized in cold temperatures. Temperature-dependent tumor collagenase activity has been demonstrated and is believed to contribute to the differential tumor growth

Table 1

Virus Family/Genus	Virus	Tumor Type Induced
Herpesviridae / Alphaherpesvirinae / Mardivirus	Marek's disease virus (Gallid herpesvirus-2)	T-cell lymphosarcoma in chickens
Herpesviridae / Gammaherpesvirinae / Rhadinovirus	Ateline herpesvirus-2 and saimirine herpesvirus-2	Lymphoma and leukemia in aberrant hosts
Herpesviridae / Gammaherpesvirinae / Lymphocryptovirus	Epstein-Barr virus	Burkitt's lymphoma, nasopharyngeal carcinoma and B-cell lymphomas in humans and non-human primates
	Baboon herpesvirus (Papiine herpesvirus-1)	Lymphoma in baboons
Herpesviridae / Gammaherpesvirinae / Rhadinovirus	Cottontail rabbit herpesvirus	Lymphoma in rabbits
Alloherpesviridae / Ranid herpesvirus	Lucké frog herpesvirus (Ranid herpesvirus-1)	Renal adenocarcinoma in frogs
Herpesviridae / Gammaherpesvirinae	Otarine herpesvirus-1	Urogenital carcinoma in California sea lions
Herpesviridae / Alphaherpesvirinae	Psittacid herpesvirus-1	Cloacal and crop papillomas in parrots (Internal papillomatosis of parrots); associated with pancreatic duct carcinoma in a macaw

and metastasis.[6,8]

AFIP Diagnosis: Kidney: Renal adenocarcinoma, papillary.

Conference Comment: Conference participants discussed other oncogenic herpesviruses. In humans, Epstein-Barr virus is associated with Burkitt's lymphosarcoma in Africa, and human herpesvirus-8 causes Kaposi's sarcoma, most commonly in AIDS patients. The included chart, adapted from *Fenner's Veterinary Virology*, outlines some of the oncogenic herpesviruses of interest to veterinary species.[3,4,5,7]

Since the submission of this case, Ranid herpesvirus-1 has been classified as a member of the *Alloherpesviridae* family, *Batrachovirus* in the International Committee on Virus Taxonomy's most recent release.[2]

Contributor: Wake Forest University Health Sciences, Animal Resources Program, Medical Center Boulevard, Winston-Salem, NC 27157
http://www.wfubmc.edu/schoolOfMedicine/schoolOfMedicine_default.aspx?id=26651

References:

1. Carlson DL, Sauerbier W, Rollins-Smith LA, McKinnell RG. The presence of DNA sequences of Lucké herpesvirus in normal and neoplastic kidney tissue of *Rana pipiens*. *J Comp Pathol*. 1994;110:349-355.
2. International Committee on Taxonomy of Viruses. http://www.ictvonline.org/index.asp?bhcp=1. Accessed 4 April 2011.
3. Johne R, Konrath A, Krautwald-Junghanns ME, Kaleta EF, Gerlach H, Muller H. Herpesviral, but no papovaviral sequences, are detected in cloacal papillomas of parrots. *Arch Virol*. 2002;147:1869-1880.
4. King DP, Hure MC, Goldstein T, et al. Otarine herpesvirus-1: A novel gammaherpesvirus associated with urogenital carcinoma in California sea lions (*Zalophus californianus*). *Vet Microbiol*. 2002;86:131-137.
5. MacLachlan NJ, Dubovi. Pathogenesis of viral infections and diseases. In: MacLachlan NJ, Dubovi EJ, eds. *Fenner's Veterinary Virology*. 4th ed. San Diego, CA: Elsevier; 2011:71-72.
6. McKinnell RG, Carlson DL. Lucké renal adenocarcinoma, an anuran neoplasm: Studies at the interface of pathology, virology, and differentiation competence. *J Cell Physiol*. 1997;173:115-118.
7. Mundhenk L, Müller K, Lierz M, et al. Psittacid herpesvirus DNA in a pancreatic duct carcinoma in a macaw. *Vet Rec*. 2009;164:306-308.
8. Ogilvie DJ, McKinnell RG, Tarin D. Temperature-dependent elaboration of collagenase by the renal adenocarcinoma of the leopard frog, *Rana pipiens*. *Cancer Res*. 1984;44:3438-3441.
9. O'Rourke DP, Schultz TW. Biology and diseases of amphibians. In: Fox JG, Anderson LC, Loew FM, Quimby FW, eds. *Laboratory Animal Medicine*. 2nd ed. Academic Press; 2002:817-818.
10. Tweedell KS. Induced oncogenesis in developing frog kidney cells. *Cancer Res*. 1697;27:2042-2052.
11. Zambernard J, McKinnell. Virus-free renal tumors obtained from pre-hibernating leopard frogs of known geographic origin. *Cancer Res*. 1969;29:653-655.
12. Zambernard J, Vatter AE, McKinnell. The fine structure of nuclear and cytoplasmic inclusions in primary renal tumors of mutant leopard frogs. *Cancer Res*. 1966;26:1688-1700.

CASE III: BERNE 2/10 (AFIP 3164904).

Signalment: Adult female Chagoi Koi carp, piscine (*Cyprinus carpio*).

History: The affected animal originated out of a group of koi carp of different age classes and strains kept in a garden pond. About 10 animals, Kigoi and Chagoi, were affected showing singular to several small, up to 1 cm in diameter, nodules on various locations on the skin.

Gross Pathology: Affected skin tissue was submitted for histopathological examination (surgical biopsy). Small nodular swellings up to 1 cm diameter were recorded.

Histopathologic Description: Skin: The dermis is markedly expanded by severe edema, small amounts of macrophages often with vacuolation of the cytoplasm (foamy macrophages), lymphocytes, plasma cells and scattered neutrophils and eosinophilic granular cells and by multiple numerous, round to elongated, different sized (50 µm to 200 µm) cystic-like structures comprising a thick-wall (approximately 10µm) hyaline capsule filled with basophilic round structures of varying size (3 µm to 10 µm), interpreted as dermocystidium spores. The spores contain a large amount of eosinophilic cytoplasm with a central hyaline refractile body and a peripheral small dark nucleus. In several cysts the organisms are degenerated. There is moderate edema within the epidermis (spongiosis).

Contributor's Morphologic Diagnosis: Dermatitis, lymphohistiocytic, moderate, diffuse, chronic with severe edema and intralesional *Dermocystidium* cysts.

Contributor's Comment: The genus *Dermocystidium* are unicellular parasites of an uncertain taxonomic classification[3] that has been reported as a yet-unnamed clade of eukaryotic protistan organisms in aquatic animals like fish (*Dermocystidium*, *Ichthyophonus*, rosette agents), amphibians (*Dermocystidium*), and crustaceans (*Psorospermium*).[6] More than 20 species of *Dermocystidium* were found as cysts in skin or gill, or as systemic infections in carp, goldfish, salmonids, eels, newts and frogs.[1] *Dermocystidium percae* infection in perch (*Perca fluviatilis*) has a high prevalence in polluted environments which can act as an important stress factor.[5] *Dermocystidium koi* produces nodular swellings up to 1 cm in diameter in the skin of koi (*Cyprinus caprio*). Minimal local inflammation and edema is observed at the edge of the swellings. The fungal nature of *D. koi* suggests hyphae and spore development which microscopically have been described as aseptate hyphae.[4,8] There is little information about the epidemiology and life cycle of *D. koi*, but it is presumed to occur worldwide. *Dermocystidium salmonis* is a more significant pathogen, resulting in extensive gill pathology and high mortality.[3]

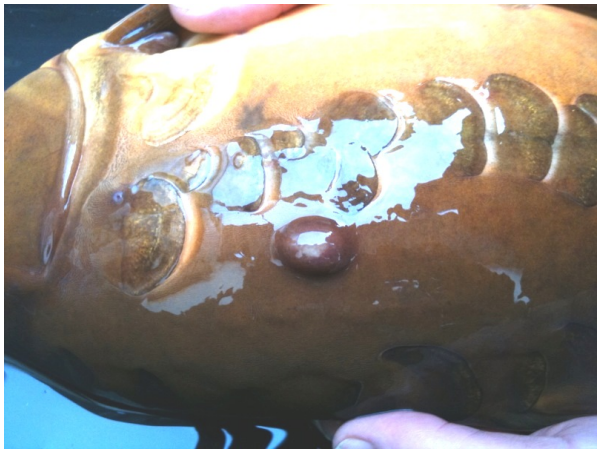

3-1. Scaled skin, Chagoi Koi carp. Affected fish have singular to several small, up to 1 cm in diameter, nodules at various locations on the skin. Photograph courtesy of Centre for Fish and Wildlife Health, Institute of Animal Pathology, Vetsuisse Faculty, Berne, Switzerland, http://www.itpa.vetsuisse.unibe.ch/html.

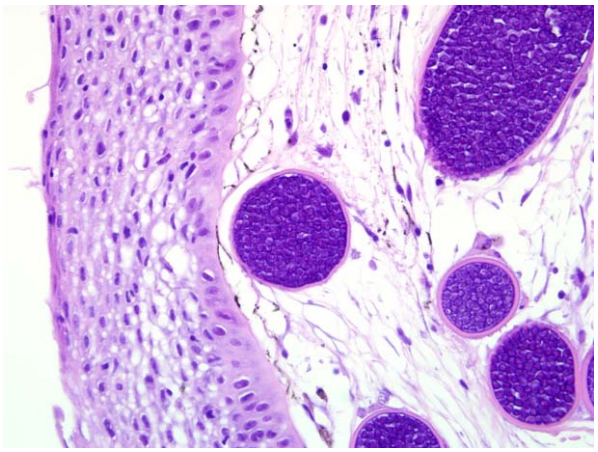

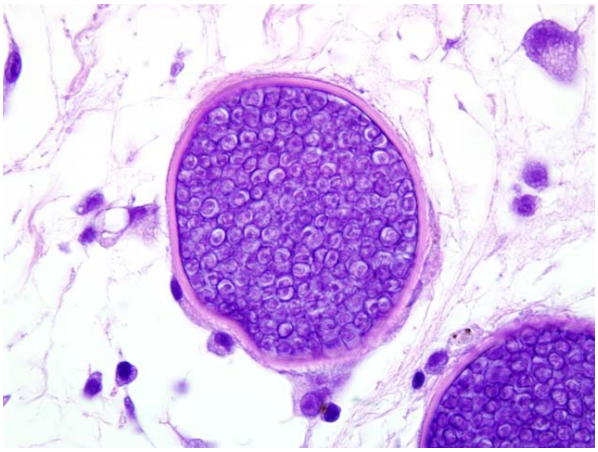

3-2, 3-3. Scaled skin, Chagoi Koi carp. The dermis is markedly expanded by edema and few inflammatory cells; there are many cyst-like structures containing numerous fungal spores with central basophilic nuclei. (HE 400X, 1000X)

AFIP Diagnosis: Skin: Dermatitis, lymphohistiocytic and granulocytic, diffuse, mild with moderate edema and many parasitic cysts.

Conference Comment: Conference participants commented on slide variation, with some sections having epidermal parasitic cysts. Occasionally, these epidermal cysts showed evidence of rupture and exfoliation of parasitic spores.

In the opinion of the moderator the dermal edema is the most striking histologic lesion in this case. Conference participants speculated on the pathogenesis for the edema, and three theories were briefly discussed: disruption of the epidermis resulting in loss of osmoregulation; primary cutaneous vasculitis; or secondary, bystander damage to blood vessels by the dermal inflammatory infiltrates.

As the contributor notes, *Dermocystidium* spp. often cause gill lesions in addition to dermal lesions. The disease in fry is particularly devastating, resulting in death due to anoxia from massive gill infection which physically prevents the operculum from closing.[7] In addition to the cutaneous lesions seen in this case, other histologic findings with *Dermocystidium* spp. infection include granulomatous inflammation of gills with apoptosis and hyperplasia of the lamellar epithelium, and splenic congestion and fibrosis surrounding cysts.[7] The gross lesions of *Dermocystidium* spp. infection in the skin are striking, presenting as numerous 1 mm linear white streaks that closely resemble infection with *Epitheliocystis* spp. The differential diagnosis for protozoal skin and gill lesions in fishes includes amoebae, coccidia, microsporidia, myxosproidia (*Myxobolus* spp.), *Ichthyophonus* spp., trichodinids, *Chilodonella* spp., and *Ichthyobodo* spp.[2]

Contributor: Centre for Fish and Wildlife Health, Institute of Animal Pathology, Vetsuisse Faculty, Berne, Switzerland
http://www.itpa.vetsuisse.unibe.ch/html

References:

1. Ferguson HW. Gills and pseudobranchs. In: *Systemic Pathology of Fish: A Text and Atlas of Comparative Tissue Responses in Diseases of Teleosts*. Ames, IA: Iowa State University Press; 1989:33.
2. Feist SW, Longshaw M, Hurell RH, Mander B. Observations of *Dermocystidium* sp. infections in bullheads, *Cottus gobio L*., from a river in southern England. *J Fish Dis*. 2004;27:225-231.
3. Höglund J, Alfjorden A, Nikkilä T. Infection of juvenile salmon *Salmo salar* with a Dermocystidium-like organism in Sweden. *Dis Aquat Org*. 1997;30:171-176.
4. Lehmann J, Schafer W, Mock D. Zystische Veränderungen der Haut durch Dermocystidium koi beim Koi-Karpfen. *Tierärztl Prax*. 1994;22:185-186.
5. Morley NJ, Campbell C, Lewis JW. The occurrence and distribution of *Dermocystidium percae* (Mesomycetozoea) in perch (*Perca fluviatilis*) in the lower Thames Valley, UK. *J. Appl Ichthyol*. 2008;24:629-631.
6. Ragan MA, Goggin CL, Cawthorn RJ, et al. A novel clade of protistan parasites near the animal-fungal divergence. *Proc Natl Acad Sci USA 93*. 1996;11907-11912.
7. Roberts RJ. The mycology of teleosts. In: Roberts RJ, ed. *Fish Pathology*. 3rd ed. Philadelphia, PA: W.B. Saunders; 2007:339-340.
8. Wildgoose WH. *Dermocystidium koi* found in skin lesions in koi carp (*Cyprinus carpio*). *Vet Rec*. 1995;23:317-318.

CASE IV: 53079 (AFIP 3164991).

Signalment: 20-year-old male shingleback skink, reptile (*Tiliqua rugosus*).

History: This skink presented for slowly progressive weight loss. A mass was seen in the oral cavity during clinical examination. Examination of cytology and biopsy specimens revealed narrow-based budding yeasts consistent with *Cryptococcus* sp. *Cryptococcus neoformans* type A/D was cultured from the mass. The skink was treated long term with anitifungal medications, and at a follow-up examination two months later the oral lesion had resolved. However, despite ongoing antifungal treatments, the skink never recovered completely and periodically needed assisted feeding to maintain weight. Nine months after initial presentation the skink's condition declined and it died.

Gross Pathology: The animal was 496 g and in good body condition with adequate adipose stores. Disseminated throughout the lungs, but more concentrated cranially, were approximately 10-20, multifocal to coalescing, soft, pale tan nodules ranging from 0.3 to 0.6 cm in diameter. The nodules bulged into both the coelomic and luminal aspects of the lung and were homogeneously pale tan and gelatinous on section.

Laboratory Results: *Cryptococcus neoformans* type A/D was cultured from an oral cavity mass 9 months prior to death.

Histopathologic Description: Lung: Expanding the parenchyma are multiple nodules composed of sheets of foamy macrophages that sometimes occlude faveolar openings. Large numbers of yeasts are present in these areas predominantly within macrophages and occasionally extracellularly in small sheets and clusters. The yeasts are characterized by a central round, pale-staining, refractile, amphophilic to basophilic, 4-12 µm diameter yeast body surrounded by a 2-6 µm clear space (capsule). The yeasts frequently exhibit narrow-based budding. Small numbers of lymphocytes, plasma cells and multinucleated giant cells are also present. Adjacent faveoli are frequently dilated and filled with wispy to hyaline eosinophilic material mixed with variable numbers of similar yeasts and a small amount of necrotic cellular and mineralized debris (some variation between slides).

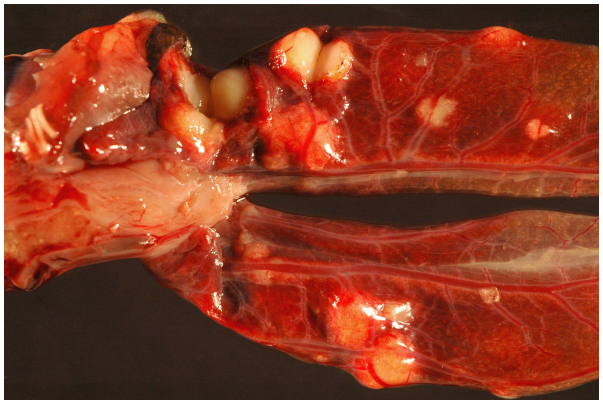

4-1. Lungs, shingleback skink. Within both lungs there are approximately 10 to 20, multifocal to coalescing, soft, pale tan nodules ranging from 0.3 to 0.6 cm in diameter. Photograph courtesy of Wildlife Disease Laboratories, San Diego Zoo's Institute for Conservation Research, http://www.sandiegozoo.org/conservation/.

Brain, cerebrum: Throughout the section, the meninges are markedly expanded by large numbers of foamy macrophages and similar yeasts that compress and multifocally extend into the neuroparenchyma along blood vessels (some variation between slides). Small numbers of lymphocytes, plasma cells, and multinucleated giant cells are also present.

Contributor's Morphologic Diagnosis: 1. Lung: moderate chronic multifocal histiocytic pneumonia with intralesional yeasts (etiology: *Cryptococcus neoformans*).

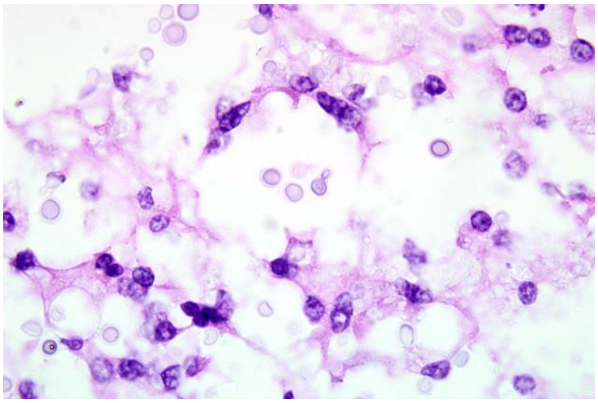

4-2. Brain, meninges, shingleback skink. The meninges are diffusely expanded by numerous foamy macrophages and fungal yeasts surrounded by a clear capsule; some exhibit narrow-based budding. (1000X)

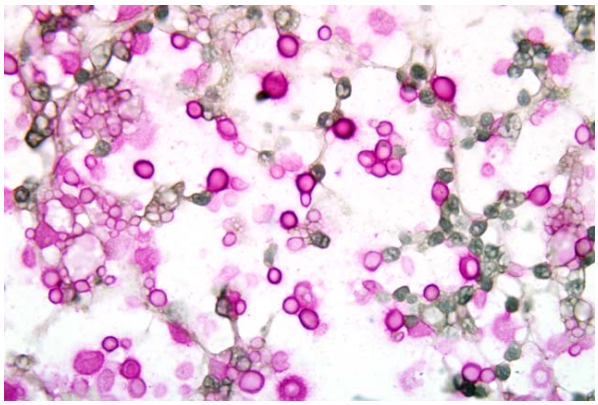

4-3. Brain, meninges, shingleback skink. Carminophilic yeast exhibit narrow-based budding. (MUCI 1000X)

2. Brain: severe chronic diffuse histiocytic meningoencephalitis with intralesional yeasts (etiology: *Cryptococcus neoformans*).
3. Oral cavity (not submitted): moderate focal histiocytic stomatitis with intralesional yeasts (etiology: *Cryptococcus neoformans*).

Contributor's Comment: *Cryptococcus neoformans* is a basidiomycete yeast-like fungus with a global distribution. It can cause disease in a variety of species and is the most common cause of systemic fungal disease in domestic cats.[2] There are 2 varieties of *C. neoformans*: *neoformans* and *gattii*, with four major serotypes, A B C D. Isolates of *C. neoformans* (formerly *C. neoformans* var. *neoformans*) have capsular serotypes A or D or both (AD), and isolates of *C. gattii* (formerly *C. neoformans* var. *gattii*) have serotypes B and C.[2,7] *Cryptococcus neoformans* is found in soil, bird feces, and decaying organic matter. *Cryptococcus gattii* has been found in association with eucalyptus trees, bat guano and decaying wood.[2,9]

Grossly, lesions may be gelatinous or solid masses, or ulcerated nodules. In histologic sections, the organisms are easily identified by their characteristic size (2-20 microns), narrow-based budding and thick capsule that can be highlighted with a mucicarmine stain.[3] At low magnification, the lesions have a vacuolated or bubbly appearance due to the thick yeast capsule. Typically, inflammatory cells are present in low numbers and are primarily epithelioid macrophages and fewer lymphocytes and plasma cells.[2]

Cryptococcosis is only rarely seen in reptiles and amphibians. It has been reported in a common anaconda (*Eunectes murinus*),[6] an eastern water skink (*Eulamprus quoyii*),[4] and a toad.[8] Recently *C. gattii* has been in the news as an emerging pathogen of animals and humans in the northwestern United States and Vancouver, Canada.[1,9]

This is the first instance of cryptococcosis in a reptile at our institution. The lesions in this skink have a similar appearance and distribution as those reported for other species. The inflammation in the oral cavity was not grossly visible, and in histologic sections the inflammation did not extend above the mucosal surface. We have been unable to determine whether the oral cavity mass noted nine months prior to death was the initial site of infection, with later spread to lung and brain, or whether systemic infection was already present at that time. There was no evidence that this skink had a compromised immune system.

AFIP Diagnosis: 1. Lung: Pneumonia, histiocytic, nodular, multifocal, marked, with many narrow-based budding encapsulated yeasts, etiology consistent with *Cryptococcus* spp.
2. Brain: Meningitis, histiocytic, diffuse, marked with many narrow-based budding encapsulated yeasts, etiology consistent with *Cryptococcus* spp.

Conference Comment: Several conference participants classified the lesions as granulomatous; for a review of the distinction between histiocytic and granulomatous inflammation, please see WSC 2010 Conference 3, Case II.

Conference participants also discussed the various virulence factors of *Cryptococcus neoformans,* which include a polysaccharide capsule, melanin production and several enzymes. The polysaccharide capsule not only prevents phagocytosis by host immune cells, it also inhibits inflammatory cell migration and recruitment; activates complement; and suppresses T-cell response.[2,5] The capsule also undergoes phenotype switching, changing the capsule structure and size and allowing it to further elude the immune system.[5] Melanin production is believed to contribute to virulence by acting as an antioxidant to counteract reactive oxygen and nitrogen species produced by the host. Finally, the yeast secretes several enzymes, one of which is serine proteinase, which cleaves fibronectin and basement membrane proteins to allow tissue invasion; other secreted factors modulate the host immune response.[5] Participants also discussed the differences between *C. neoformans* and *C. gattii*; while the former typically affects immunocompromised individuals, the latter is able to cause disease in healthy, immunocompetent individuals.

Immunity to *C. neoformans* depends on delayed-type hypersensitivity reaction. Briefly, interferon-gamma (IFN-γ) and other cytokines recruit and activate macrophages, and possibly neutrophils, resulting in production of reactive oxygen and nitrogen species. Additionally, cytotoxic T-cell response may limit infection through direct response to the yeast.[2]

Contributor: Wildlife Disease Laboratories, San Diego Zoo's Institute for Conservation Research, San Diego Zoo PO Box 120551, San Diego, CA 92112-0551
http://www.sandiegozoo.org/conservation/

References:
1. Byrnes EJ III, Bildfell RJ, Dearing PL, et al. *Cryptococcus gattii* with bimorphic colony types in a dog in western Oregon: Additional evidence for expansion of the Vancouver Island outbreak. *J Vet Diagn Invest*. 2009;21:133-136.
2. Caswell JL, Williams KJ. Respiratory System. In: Maxie MG, ed. *Jubb, Kennedy and Palmer's Pathology of Domestic Animals*. Vol. 2, 5th ed. Philadelphia, PA: Elsevier Ltd; 2007:642-644.
3. Chandler FW, Kaplan W, Ajello L. *Color Atlas and Text of the Histopathology of Mycotic Diseases*. Chicago, IL: Year Book Medical Publishers, Inc.;1980:54-58.
4. Hough I. Cryptococcosis in an eastern water skink. *Aust Vet J*. 1998;76:471-472.
5. Kumar V, Abbas AK, Fausto N, Aster JC. Infectious diseases. In: Kumar V, Abbas AK, Fausto N, Aster JC, eds. *Robbins and Cotran Pathologic Basis of Disease*. 8th ed. Philadelphia, PA: Elsevier Saunders; 2009:384.

6. McNamara TS, Cook RA, Behler JL, Ajello L, Padhye AA. Cryptococcosis in a common anaconda (*Eunectes murinus*). *J Zoo Wildl Med*. 1994;25:128-132.
7. Mitchell TG, Perfect JR. Cryptococcosis in the era of AIDS - 100 years after the discovery of *Cryptococcus neoformans*. *Clin Micro Rev*. 1995;8:515-548.
8. Seixas F, da Luz Martins M, de Lurdes Pinto M,Travassos PJ, Miranda M, dos Anjos Pires M. A case of pulmonary cryptococcosis in a free-living toad (*Bufo bufo*). *J Wildl Dis* 2008;44:460-463.
9. Sorrell TC. *Cryptococcus neoformans* variety *gatii*. *Med Mycol*. 39:155-168, 2001.

The Armed Forces Institute of Pathology
Department of Veterinary Pathology

Conference Coordinator
Matthew Wegner, DVM

WEDNESDAY SLIDE CONFERENCE 2010-2011

Conference 23

9 March 2011

Conference Moderator:
Dr. Donald H. Schlafer DVM, MS, PhD, Diplomate ACVP, Diplomate ACVM, Diplomate ACT

CASE I: 19274/1A (AFIP 3167216).

Signalment: 8-year-old female exotic shorthair cat (*Felis catus*).

History: The cat, previously used for breeding, was presented to the clinician in poor body condition. At clinical examination an abdominal mass, initially interpreted as an enlarged mesenteric lymph node, and multiple mammary cysts were noted. After one week a laparotomy was performed in order to localize and remove the abdominal lesion. The cat was not pregnant.

Gross Pathology: At surgery a right uterine horn mass was seen together with multiple, firm, infiltrative, omental and visceral abdominal wall nodules. Ovariohysterectomy was performed and the uterine mass and sampled omental nodules were submitted for histology. After about 20 days the cat was euthanized because of worsening of clinical signs and presence of anorexia.

Laboratory Results: Routine pre-surgical hematology and biochemistry were in normal range.

Histopathologic Description: Uterus: Effacing the uterine wall and filling the uterine lumen is an irregularly nodular mass (not completely present in all slides submitted) composed of an atypical, pleomorphic, densely cellular, infiltrative, transmural, mixed, epithelial population arranged in 1 to 5-cell-thick irregular tubules or occasional papillae in moderate fibrous stroma and showing focal continuity with adjacent normal endometrium. There are two distinct cellular populations: one population is composed of cubic to cylindrical cells (20-35 micron) with moderate slightly eosinophilic finely granular cytoplasm with defined borders. The nucleus is round to oval (7-20 micron), basally to centrally located, with granular chromatin and one evident eosinophilic nucleolus. Anisocytosis and anisokaryosis are moderate, and there are 0-1 mitotic figures per HPF. The second population is prevalent with occasional transitional areas with the previous one and, focally, with the adjacent endometrium. Cells are highly pleomorphic with frequent areas of anaplasia, and round to polygonal with irregular shape and moderate to scant homogeneous intensely eosinophilic cytoplasm (up to 60 microns). Nuclei are irregularly round often pleomorphic (up to 40 microns) with hyperchromatic granular or clumped chromatin and multiple eosinophilic nucleoli with frequent anisonucleosis. Anisocytosis and anisokaryosis are severe, and mitotic figures are frequent and atypical. Both populations show anaplastic syncytial multinucleated giant cells, frequently located on tubular lumina or surface of papillae, with up to 40 nuclei and are occasionally severely pleomorphic. There are multifocal areas of necrosis, with the presence of cholesterol clefts, hemorrhage, and vascular and peritoneal invasion. Hypercellular stromal areas with irregularly arranged or grouped, minimally atypical, spindle cells are occasionally evident. Peripherally is a section of ovary (not completely present in all slides submitted) with ovulatory follicles and multiple corpora lutea, along with a section of ampulla. Separated from the uterus is a section with omental vessels and a neoplastic focus, probably consistent with a peritoneal neoplastic implant. A neoplastic population arranged in irregular tubules and immersed in abundant

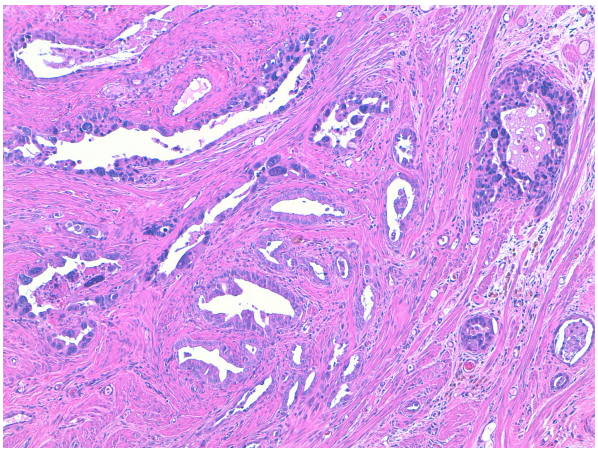

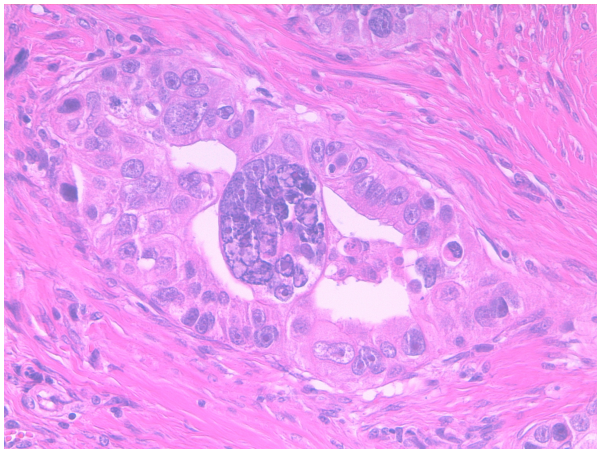

1-1, 1-2. Uterus, endometrial adenocarcinoma, cat. A neoplastic epithelial cell population ranging from moderately atypical columnar to severely anaplastic polygonal cells is arranged in irregular tubules on an abundant fibrous stroma. There are occasional multinucleate neoplastic cells (1-2). Photographs courtesy of Dipartimento di Sanità Pubblica, Patologia Comparata ed Igiene Veterinaria, Facoltà di Medicina Veterinaria, Università degli Studi di Padova, http://www.sanitaveterinaria.unipd.it/.

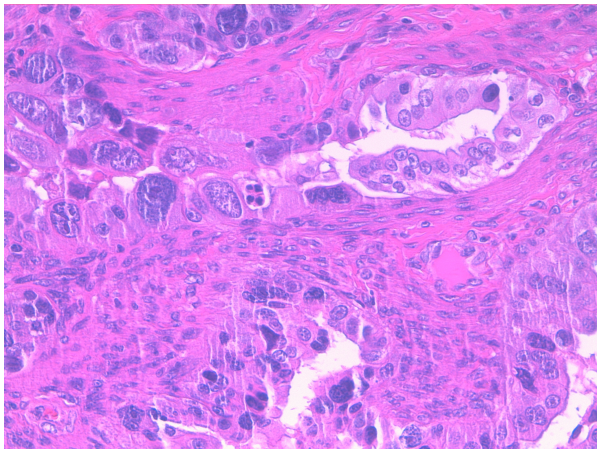

1-3. Uterus, endometrial adenocarcinoma, cat. There is transition from moderately atypical columnar cells to a pleomorphic cell population. Photograph courtesy of Dipartimento di Sanità Pubblica, Patologia Comparata ed Igiene Veterinaria, Facoltà di Medicina Veterinaria, Università degli Studi di Padova, http://www.sanitaveterinaria.unipd.it/.

stroma characterized by cytologic features similar to what previously described was diffusely found in all omental nodules examined (not submitted in the present specimen).

Contributor's Morphologic Diagnosis: Uterus: adenocarcinoma, tubular and papillary, infiltrative, with anaplasia, syncytial giant cell formation, and vascular and peritoneal invasion, cat, feline.

Contributor's Comment: In contrast to women, carcinoma of the endometrium and cervix is rare in domestic animals other than cattle and rabbits, and doesn't show a hormone-conditioned development as reported in women.[7,10] In cattle, the tumor manifests as single or multiple uterine wall nodules with serosal umbilication, scirrhous reaction, and invasion of veins and lymphatics. Metastases develop in the internal iliac lymph nodes and lung.[6]

Recently in uterine adenocarcinomas of the rabbit, the expression of sex steroid hormone receptors, estrogen-alpha (ER-alpha) and progesterone (PR) didn't correlate with prognosis, but was associated with histopathologic pattern. Papillary adenocarcinoma lost the expression of both ER-alpha and PR and was characterized by expansile growth, myometrial attenuation and late invasion; in contrast tubulo-solid adenocarcinoma maintained the sex steroid hormone expression with early myometrial infiltration and without myometrial attenuation.[2]

A 9.6-year period survey confirmed that uterine tumors are uncommon in the cat, representing only 0.29% of all feline neoplasms examined during the study (more than 4000 cases). A higher proportion of pure-bred cats, possibly because they reached advanced age and were sexually intact, was noted. The most common uterine tumor was adenocarcinoma. Previous studies reported leiomyoma to be prevalent, and in a 20-year survey, no cases of adenocarcinomas were recorded. Moreover, there have been additional case reports of endometrial adenocarcinoma, squamous cell carcinoma, mixed Mullerian tumor, leiomyosarcoma, endothelioma (or hemangioma), fibroadenoma, cystadenoma, and submucosal fibroma.[8]

A recent immunohistochemical study of feline endometrial adenocarcinomas hypothesized an association, as in women, between neoplastic endometrial transformation and alteration in cyclo-oxygenase-2 (COX-2) expression. The study showed diffuse membranous and cytoplasmic labeling compared to normal uteri where the COX-2 expression is confined to apical cell membrane. Besides synthesis of COX-2, reduced progesterone expression is reported to be involved in development of malignancy, whereas no clear evidence of epithelial-mesenchymal transition or altered E-cadherin or beta-catenin were found.[4]

In women, epithelial tumors of Muellerian type consist of endometrioid adenocarcinoma, adenosquamous carcinoma, serous papillary carcinoma, clear cell adenocarcinoma, mucinous adenocarcinoma, squamous cell carcinoma, small cell carcinoma, giant cell carcinoma and undifferentiated carcinoma. Histologic variants of endometrioid adenocarcinoma in women are endometrioid adenocarcinoma with squamous metaplasia, papillary variant, secretory variant, ciliated cell variant, Sertoliform variant and adenoid cystic variant.[3]

The most frequent form of endometrial neoplasia in post-menopausal women, that usually occurs after menopause, is adenocarcinoma, a proportion of which, and particularly the endometrioid type, is related to a prolonged exogenous (administration of estrogens) or endogenous (presence of ovarian granulosa-cell tumor) estrogenic stimulation and can evolve from an atypical endometrial hyperplasia.[3]

Besides choriocarcinoma, both well-differentiated endometrioid adenocarcinomas and undifferentiated carcinoma show, respectively, focal trophoblastic (choriocarcinomatous) differentiation and the presence of syncytiotrophoblast-like multinucleated cells.[3] Moreover few case reports of non-gestational and non-teratomatous uterine choriocarcinomas are associated with endometrioid carcinoma, serous carcinoma and carcinosarcoma. Foci of trophoblastic differentiation and choriocarcinoma are also found in ovarian, gastric and mammary neoplasia. The hypothesis concerning these findings regards aberrant differentiation of somatic uterine epithelial adenocarcinomatous cells or of entrapped trophoblasts or germ cells.[8]

Endometrioid adenocarcinoma with choriocarcinomatous differentiation is a very rare form of non-gestational tumors with trophoblastic differentiation characterized by a more aggressive clinical course in women. A recent case report regarding this entity discussed the differential diagnosis for the presence of pleomorphic giant cells in gynaecologic tumors as choriocarcinomatous differentiation, giant cell carcinoma, carcinosarcoma and undifferentiated carcinoma with giant cells. Demonstration of immunohistochemical reactivity for human chorionic gonadotropin (hCG) in tumor cells is needed for a definitive diagnosis.[1] A recent case of spontaneous metastatic uterine choriocarcinoma in a rabbit also revealed positivity for hCG in neoplastic syncytiotrophoblasts.[5]

In the submitted case, an admixture of conventional adenocarcinoma with markedly anaplastic neoplastic cells is observed. These cells show severe anisocytosis and anisokaryosis, multifocal anisonucleosis and presence of severely pleomorphic giant cells and formation of neoplastic syncytial giant cells. This is an unusual finding, as endometrial adenocarcinomas in the cat are mainly composed of tubulopapillary or solid proliferation of neoplastic cells with variable nuclear atypia, especially in estrogen-negative tumors. The presence of multinucleation, severe anaplasia or mixed population is not reported in the cat or rabbit.[2,8] This finding is compatible with a form of choriocarcinomatous differentiation of uterine adenocarcinoma, carcinosarcoma, or with the presence of syncytiotrophoblast-like multinucleated cells in undifferentiated carcinoma. Moreover, pleomorphic giant cells are found in giant cell carcinoma, carcinosarcoma and undifferentiated carcinoma with giant cells. Since the stromal component in this case doesn't show significant or diffuse atypia, carcinosarcoma is excluded as the arrangement of neoplastic population in tubules and papillae is not indicative of an undifferentiated carcinoma. Conversely, giant cell carcinoma can have areas of conventional adenocarcinoma.[3] To verify the possible presence of a choriocarcinomatous differentiation, an immunohistochemical staining for hCG should be performed in order to identify the multinucleated anaplastic component as trophoblastic in origin (syncytiotrophoblasts).

AFIP Diagnosis: Uterus: Endometrial adenocarcinoma, tubular and papillary.

Conference Comment: The conference moderator stressed the importance of knowing the stage of estrus and the pregnancy status of the animal at the time of tissue sampling in order to appropriately interpret the histologic findings in the uterus. Glandular hyperplasia with evidence of inflammation, necrosis, and piling of the epithelium is present in the uterus of normal, intact, cycling animals and in pregnant animals with a placenta; the histologic changes in

Stage of Estrous Cycle	Uterine Histomorphology	Endometrial Gland Activity / Species Differences
Proestrus	• Hypertrophy of mucosal epithelium • Infiltration by neutrophils • Increased vascularity of propria-submucosa with congestion and edema	Glands are relatively straight with some increase in length
Estrus	• Thickening of mucosal epithelium with mononuclear leukocytes • Maximal vascularization of propria-submucosa with congestion, edema and hemorrhage	Cow: Glands continue to elongate; increased edema with mast cell infiltration; microscopic hemorrhage with metrorrhagia
Metestrus	Decreasing congestion and edema	Glandular growth results in coiling
Diestrus	Continued decrease in the level of congestion and edema	Zenith of glandular development with branching and coiling of glands
Anestrus	• Thin mucosa and propria-submucosa • Epithelium becomes cuboidal	Glandular regression with scattered simple tubules and adenomeres

the uterus associated with a normal response to physiologic hormonal stimuli, such as pregnancy, can look remarkably similar to neoplasia. To demonstrate this point, the moderator showed part of a histologic slide of uterus from a normally cycling queen; participants were unable to determine if the changes were neoplastic or physiologic until the moderator revealed the entire specimen.

The included chart, adapted from Samuelson's *Textbook of Veterinary Histology*, briefly summarizes uterine changes throughout the estrous cycle.[9]

The contributor provides a detailed review of uterine adenocarcinomas in the cat and humans.

Contributor: Dipartimento di Sanità Pubblica, Patologia Comparata ed Igiene Veterinaria, Facoltà di Medicina Veterinaria, Università degli Studi di Padova.
http://www.sanitaveterinaria.unipd.it/

References:

1. Akbulut M, Tosun H, Soysal ME, Oztekin O. Endometrioid carcinoma of endometrium with choriocarcinomatous differentiation: A case report and review of the literature. *Arch Gynecol Obstet*. 2008;278:79-84.
2. Asakawa MG, Goldschmidt MH, Une Y, Nomura Y. The immunohistochemical evaluation of estrogen receptor-alpha and progesterone receptors of normal, hyperplastic, and neoplastic endometrium in 88 pet rabbits. *Vet Pathol*. 2008;45:217-225.
3. Fox H, Buckley CH, Wells M. Tumors of the female genital tract. In: Fletcher CDM, ed. *Diagnostic Histopathology of Tumors*. Edinburgh, UK: Churchill Livingstone; 1996:423-519.
4. Gil da Costa RM, Santos M, Amorim I, Lopes C, Dias Pereira P, Faustino AM. An immunohistochemical study of feline endometrial adenocarcinoma. *J Comp Path*. 2009;140:254-259.
5. Kaufmann-Bart M, Fischer I. Choriocarcinoma with metastasis in a rabbit (Oryctolagus cuniculi). *Vet Pathol*. 2008;45:77-79.
6. Kennedy PC, Cullen JM, Edwards JF, et al. Tumors of the uterus. In: Schulman FY, ed. *Histological Classification of Tumors of the Genital System of Domestic Animals*. 2nd series. Vol IV. Washington, D.C.: The Armed Forces Institute of Pathology, American Registry of Pathology; 1998;31-33.
7. MacLachlan NJ, Kennedy PC. Tumors of the genital systems. In: Meuten DJ, ed. *Tumors in Domestic Animals*. 4th ed. Ames, IA: Iowa State Press; 2002:547-573.
8. Miller MA, Ramos-Vara JA, Dickerson MF et al. Uterine neoplasia in 13 cats. *J Vet Diagn Invest*. 2003;15:515-522.
9. Samuelson DA. Female reproductive system. *Textbook of Veterinary Histology*. St. Louis, MO: Saunders Elsevier; 2007:463.
10. Schlafer DH, Miller RB. Female genital system. In: Maxie MG, ed. *Jubb, Kennedy, and Palmer's Pathology of Domestic Animals*. 5th ed. Vol. 3. St. Louis, MO: Elsevier Saunders; 2007:545-550.

CASE II: S418/08 (AFIP 3167245).

Signalment: Adult female crossbred domestic swine (*Sus scrofa domestica).*

History: During the last 2 years, an increased abortion rate was observed in several holdings with free-range pigs in Mecklenburg-Western-Pomerania, as in this case.

Gross Pathology: Randomly distributed within the endometrium, slightly elevating the edematous mucosa, numerous small, sharply demarcated grey-yellow nodules were present. The nodules were firm and gritty when cut. Few of these granulomas gleamed through the uterus wall and were also visible in the perimetrium.

Laboratory Results: Microbiology revealed a moderate growth of small colonies suspicious for *Brucella* spp. By PCR of endometrial tissue samples, DNA specific for *Brucella suis*, biovar 2 was amplified.

Histopathologic Description: Uterus: Multifocally within the severely edematous endometrium and submucosa there are large, up to 3 mm diameter, sharply demarcated areas of caseous necrosis surrounded by numerous histiocytes, epithelioid macrophages, large numbers of lymphocytes and few neutrophils. A pronounced infiltration with lymphocytes is observed in the subjacent and perivascular connective tissue, predominantly surrounding endometrial glands. Myriad coccobacilli are occasionally present within the necrotic centers of the granulomas (not visible in all sections).

Contributor's Morphologic Diagnosis: Uterus: Endometritis, mild to moderate, granulomatous and necrotizing, domestic swine, *Sus scrofa domestica,* etiologic diagnosis consistent with "miliary brucellosis."

Contributor's Comment: Brucellosis is a zoonotic disease which is caused by gram-negative, strictly aerobic, nonmotile coccobaccilli. These are facultative intracellular microbes taxonomically categorized in the class alpha-proteobacteria, family *Brucellaceae*.[4] Nine different Brucella species are known, but only seven of them infect terrestrial animals, namely *B. melitensis, B. abortuts, B. suis, B. canis, B. ovis, B. neotomae, and B. microti.* In contrast, *B. ceti* and *B. pinnipedialis* are confined to marine mammals. Each *Brucella* species can further be classified in several biovars.[3] Brucellosis is endemic in Mediterranean countries, Africa, India, Asia, the Middle East and Central and South America.[4] The only known focus of *Brucella abortus* infection left in the United States is in bison and elk in the Greater Yellowstone Area, including Yellowstone National Park.

Five biovars have been described for *B. suis*, the cause of porcine brucellosis. Swine are mainly affected by biovars 1, 2 and 3. Hares are the important natural reservoir of biovar 2. Furthermore, pigs are susceptible to infection with *B. melitensis* as well as *B. abortus*.[1] Besides pigs, several species can be affected by different biovars of *B. suis* including reindeer, caribou and rarely, cattle and dogs. Additionally, all biovars of *B. suis* can induce serious infections in man,[4] in particular biovars 1 and 3.

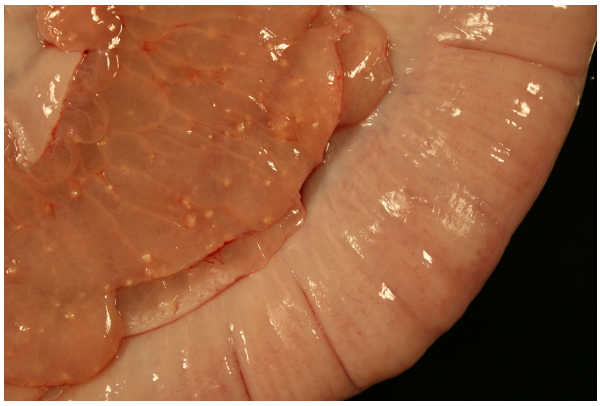

2-1. Uterus, domestic swine. Randomly distributed within the endometrium and slightly elevating the edematous mucosa are numerous small, sharply demarcated grey-yellow nodules. Photograph courtesy of Friedrich-Loeffler-Institut, Federal Research Institute for Animal Health, 17493 Greifswald-Insel Riems, Germany, www.fli.bund.de.

Brucella suis affects pigs of all ages and breeds. Infection occurs through inhalation or ingestion of organisms. High numbers of bacteria are shed in urine, vaginal discharges, semen and the products of birth.[4] Venereal transmission is also possible.[1] The infectious agents invade the mucosa and gain entry into regional lymph nodes. The incubation period ranges from 2 weeks up to 7 months. Subsequently most animals develop bacteremia that results in dissemination to the spleen, liver, and bone marrow, as well as mammary glands and reproductive organs. However, a self-limiting infection which is restricted to lymph nodes only may also occur in piglets.[4]

Signs of disease in sows include infertility, abortion between weeks 4 and 12 of gestation, stillbirths, mummification, or birth of weak piglets. Abortions due to *Brucella* spp. are typically associated with placentitis. The gross examination of the placenta may reveal red, yellow, normal or necrotic areas. A leathery, wet appearance of the intercotyledonary region with focal thickening is typical in cattle as well as sheep and goat.[5] In boars, the most prominent clinical sign is unilateral orchitis. Other signs are infertility, lameness and paralysis.[4]

A characteristic image is seen in hares infected with *B. suis* biovar 2. While the hare's body condition may be unaltered, a widespread distribution of nodular suppurative inflammation can be seen. In particular, the reproductive organs, but also the spleen, liver and lung are affected.

Brucellosis can be diagnosed by culture, serology or molecular-based techniques. In most cases, serological tests are applied, although they are not completely specific. In this

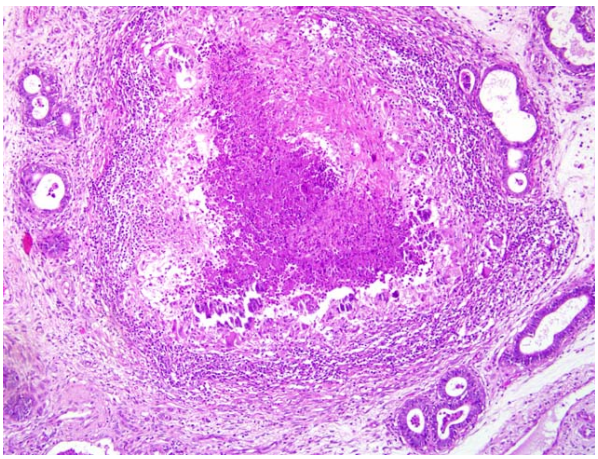

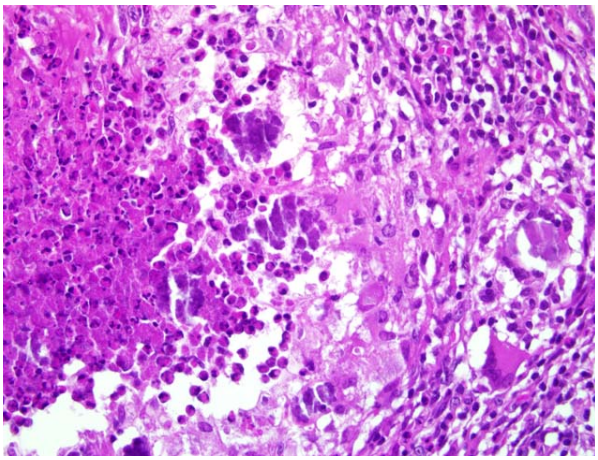

2-2, 2-3. Uterus, domestic swine. The endometrium is expanded by edema and numerous pyogranulomas containing colonies of basophilic coccobacill that replace endometrial glands. (HE 100X, 400X)

regard. it has to be emphasized that a reaction due to *B. melitensis* cannot be distinguished from cross-reactions to other bacteria, in particular *Yersinia enterocolitica* O:9 (USDA). Further techniques which are available for most species include immunostaining of tissue samples as well the polymerase chain reaction (PCR).

In 2008, five outbreaks of brucellosis were reported in Mecklenburg-Western-Pomerania, a Federal State in the northeast of Germany. Three of these outbreaks were caused by *B. suis* biovar 2. Like the situation in other European countries, *B. suis* is hypothesized to be locally endemic in wild boars, and this seems to be the source of transmission of *B. suis* biovar 2 introduction to free-range pig holdings.

AFIP Diagnosis: Uterus: Endometritis, lymphoplasmacytic, diffuse, severe with marked edema, multiple pyogranulomas, and epithelial hyperplasia, degeneration and necrosis.

Conference Comment: When histologically assessing the endometrium, the moderator commented there are 7 structures to evaluate.

1. Lumen: Examine for the presence of exudate; the lack of observation of an exudate histologically does not mean there is an absence of exudates, as the material can be lost during fixation and processing
2. Epithelium: There should be a single layer of mucosal epithelium
3. Stratum compactum
4. Endometrial glands: Glands will be hyperplastic and hypertrophied during estrous. The glandular lumina contain sloughed epithelial cells often mistaken for neutrophils
5. Endometrial stroma: Edema indicates inflammation or estrous and is often referred to as the stratum spongiosum
6. Blood vessels: Medium sized arterioles may have hyalinized walls. Animals with multiple pregnancies may have prominent vessels in the endometrium
7. Lymphatics

Several participants commented on the presence of endometrial glands within the muscular wall of the uterus; discussion of whether or not to diagnose this as adenomyosis followed. Adenomyosis is used when there are endometrial glands and stroma between the smooth muscle bundles.[2] Adenomyosis is occasionally due to congenital malformations within the uterus. Additionally, adenomyosis may result from hyperplastic overgrowth of the endometrium.[2] The moderator commented that in this case adenomyosis is not present, as the lesion most likely resulted from smooth muscle contraction in response the inflammatory milieu of cytokines which then physically forced the endometrial glands into the superficial muscular layer.

Conference participants spent some time reviewing the differential diagnosis for intracytoplasmic microbes within trophoblasts in different veterinary species.[2] The following brief list generated by participants is not intended to be all-inclusive.

- Horse: *Streptococcus* spp., *Candida* spp., *Encephalitozoon cuniculi*
- Sheep: *Coxiella burnetii*, *Chlamydophila abortus*, *Toxoplasma gondii*
- Pigs: *Toxoplasma gondii*
- Cow: *Candida* spp., *Brucella abortus*, *Neospora caninum*
- Dog: *Brucella canis*

The contributor provides an excellent review of porcine brucellosis.

Contributor: Friedrich-Loeffler-Institut, Federal Research Institute for Animal Health, 17493 Greifswald-Insel Riems, Germany
www.fli.bund.de

References:

1. Anonymous. Porcine Brucellosis. In*: OIE Terrestrial Manual*. World Health Organization, 2009;1-7.
2. Schlafer DH, Miller RB. Female genital system. In: Maxie MG, ed. *Jubb, Kennedy, and Palmer's Pathology of Domestic Animals*. 5th ed. Vol. 3. St. Louis, MO: Elsevier Saunders; 2007:464-465,484-518.
3. Seleem MN, Boyle SM, Sriranganathan N. Brucellosis: A re-emerging zoonosis. *Vet Microbiol*. 2010;140:392-398.
4. Songer JG, Post KW. The genus brucella. In: Songer JG, Post KW, eds. *Veterinary Microbiology, Bacterial and Fungal Agents of Animal Disease*. St. Louis, MO: Saunders; 2004:200-207.
5. Spickler AR, Roth JA. Brucellosis. In: *Emerging and Exotic Diseases of Animals Textbook*. Ames, IA: Iowa State Press; 2006:141-143. http://www.cfsph.iastate.edu/Factsheets/pdfs/brucellosis.pdf.

CASE III: X9402 (AFIP 3164120).

Signalment: 11-year-old female La Plata three-banded armadillo (*Tolypeutes maticus*).

History: This animal was presented to the hospital twice in one month for lethargy and decreased appetite. During the most recent episode, the lethargy was severe and the animal was minimally responsive. A 3cm uterine mass was documented on abdominal ultrasound and the hematocrit had dropped from 35.5% to 25% in one week. Hemorrhage from the tumor was suspected as a cause of the lethargic episodes, and exploratory laparotomy was pursued to remove the uterine mass.

Gross Pathology: The body of the uterus was diffusely enlarged to approximately 20 x 20 x 25 mm with short uterine horns and attached ovaries. On section, the endometrium was markedly thickened, filling the lumen of the organ. An even band of myometrium was evident around the periphery.

Histopathologic Description: Uterus: Diffusely, the mucosa is hyperplastic with vacuolated epithelium that is thrown into extensive papillary projections. Some vessels within the projections are dilated and contain increased numbers of neutrophils. Occasional glandular lumina contain neutrophils, wispy eosinophilic material and/or sloughed epithelial cells, and there are few clusters of neutrophils in the endometrial interstitium. Diffusely, and to a visually defined depth, well-formed but irregular glands extend into the myometrium. In these deeper areas, there are irregular cysts that are up to 4 x 2 mm and lined by cuboidal epithelium. There is multifocal hemorrhage at the luminal surface and within glands.

Contributor's Morphologic Diagnosis: 1. Uterus: adenomyosis.
2. Uterus: endometritis, suppurative, acute, multifocal, mild.

Contributor's Comment: Adenomyosis is the presence of endometrial glands in the uterine stroma. It is most common in menstruating mammals, such as primates, but is rarely reported in dogs, cats and cattle[3], and there is one case report of focal adenomyosis in an African hedgehog.[2] In the National Zoo pathology database, adenomyosis has been diagnosed at necropsy in four cervids; two each bovids, felids, rodents, and viverrids; one bat; and one primate. The condition was diagnosed via ante-mortem hysterectomy in five primates, two felids, and one each rodent, canid, and edentate, the case described here. Like humans, armadillos have discoid, hemochorial and trabecular placentation, but they do not menstruate.

Development of adenomyosis is described by three theories.[1] First and most probable, endometrial glands invaginate and grow between muscle bundles of the myometrium. The second theory outlines endometrial growth via the myometrial lymphatic system. Thirdly, endometrial glands may form from myometrial tissue via metaplastic change.

In primates, clinical signs associated with adenomyosis include heavy or prolonged menstruation, painful menstruation, and irregular cycles.[1] Approximately 90% of human cases occur in multiparous women. This armadillo had never been pregnant to our knowledge, but heat cycles had been noted by keepers and veterinarians.

AFIP Diagnoses: 1. Uterus: Adenomyosis, multifocal, moderate.
2. Uterus: Endometrial hyperplasia, cystic and papillary, diffuse, moderate with multifocal mild neutrophilic endometritis.

Conference Comment: Most conference participants readily identified both adenomyosis and endometrial hyperplasia in the uterus. The moderator and participants commented on the section quality, observing that it is

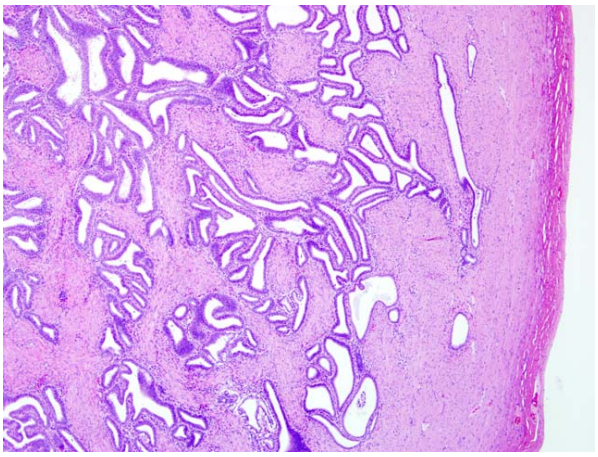

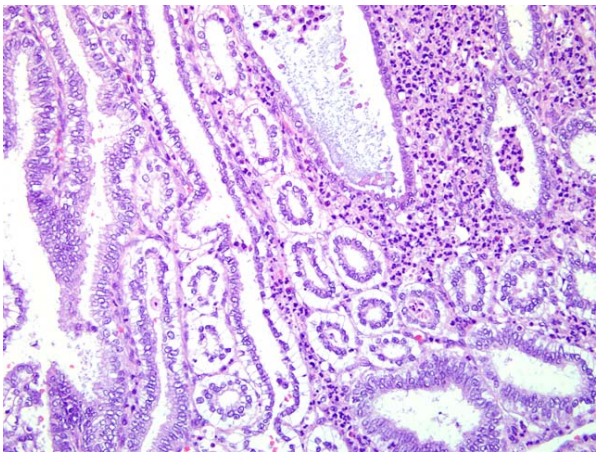

3-1, 3-2. Uterus, La Plata three-banded armadillo. Well formed, dilated and often irregular endometrial glands extend into the myometrium and closely approach the subserosa (3-1). Hyperplastic and dilated endometrial glands form papillary folds lined by epithelial cells that pile up several layers thick; the interstitium and dilated glands occasionally contain neutrophils (3-2). (40X, 200X)

difficult to fully evaluate the uterus and the lesion because only a small segment of uterus is present.

Participants discussed the pathophysiology of endometrial hyperplasia and subsequent endometritis. The first requirement for development of the proliferative endometrial lesion is estrogen priming, which increases expression of intracellular progesterone receptors. Next, there is prolonged progestational stimulation of the endometrium, resulting in conversion of the epithelium to its secretory mode, thereby producing lesions of cystic endometrial hyperplasia. Subsequent colonization by bacteria such as *Escherichia coli*, *Proteus* spp., *Staphylococcus* spp., or *Streptococcus* spp., results in ensuing endometritis. Recently, it has been shown that stimulation of the progesterone-primed endometrium by trauma, bacterial infection, or a foreign body can produce both cystic endometrial hyperplasia and endometritis.[4]

Species	Endometrial Hyperplasia	Pyometra
Bitch[4]	• Common • Continued progesterone secretion following estrogen-priming of the endometrium	• Common • Appropriate stimulation of progesterone-primed endometrium • *E. coli* most common • Also *Proteus* spp., *Staphylococcus* spp., or *Streptococcus* spp
Cow[4]	• Not as common as the dog, but more frequent than equids • Often associated with ovarian follicular cysts or granulosa-cell tumors • Prolonged estrogenism	• Associated with corpus luteum activity → elevated progesterone • Common early post-partum following dystocia, retained fetal membranes, or metritis • Also common after breeding when venereal infection results in early embryonic death • Progesterone effects: ○ Increased susceptibility to infection ○ Maintains closure of cervix ○ Inhibits myometrial contraction • Streptococci, staphylococci, coliforms, *Arcanobacterium pyogenes*, *Pseudomonas spp.*
Mare[4]	• Rare	• Continue cycling • Cervix is often open • Rarely results in systemic illness • Severity of endometrial change is related to the length of the estrous cycle • *Streptococcus zooepidemicus* is most common • *E. coli*, *Actinomyces* spp., *Pasteurella* spp., *Pseudomonas* spp.

Contributor: Department of Pathology, National Zoological Park, P.O. Box 37012 MRC 5501, Washington, DC 20008
http://nationalzoo.si.edu/

References:

1. Bergeron C, Amant F, Ferenczy A. Pathology and physiopathology of adenomyosis. *Best Prac Res Clin. Obst Gynecol*. 2006;20(4):511-521.
2. Done LB, Deem SL, Fiorello CV. Surgical and medical management of a uterine spindle cell tumor in an African hedgehog (*Atelerix albiventris*). *J Zoo Wildl Med.* 2007;38(4):601-3.
3. Foster RA. Female reproductive system. In: McGavin MD, Zachary JF, eds. *Pathologic Basis of Veterinary Disease*. 4th ed. St. Louis, MO: Mosby; 2007:1288.
4. Schlafer DH, Miller RB. Female genital system. In: Maxie MG, ed. *Jubb, Kennedy, and Palmer's Pathology of Domestic Animals*. 5th ed. Vol. 3. St. Louis, MO: Elsevier Saunders; 2007:466-473.

CASE IV: P314-10 (AFIP 3166498).

Signalment: 7-month-old male domestic shorthair cat (*Felis catus*).

History: A seven-month-old, apparently healthy male, domestic cat was presented to a veterinary clinic for elective neutering. Bloodwork performed prior to surgery revealed marginally elevated total serum protein. During surgery, the referring veterinarian noticed multifocal "thickenings" on the surface of both testes and epididymides. Both testes with epididymides were submitted for histopathology.

Gross Pathology: As described by the referring veterinarian, a few slightly raised whitish plaques, 1-2 mm in diameter, were present on the surface of both testes and epididymides (tunica vaginalis).

Laboratory Results: Immunoperoxidase for feline coronavirus was performed (Animal Health Laboratory; University of Guelph); results are provided in the contributor's comment.

Histopathologic Description: Testicle: Two different slides are submitted, but the basic lesion is present in both. Multifocally expanding the tunica vaginalis, there is a moderate multifocal to coalescing mixed inflammatory infiltrate consisting of variable proportions of neutrophils, macrophages, plasma cells, and lymphocytes. Depending on the focus examined, the infiltrate ranges from lymphoplasmacytic to granulomatous/pyogranulomatous with focal fibrin deposition. Pyogranulomatous foci are characterized by mostly degenerate neutrophils with variable numbers of macrophages, admixed with cellular debris. In some sections, mostly granulomatous inflammation extends into the epididymis. There is also multifocal edema. Diffusely, seminiferous tubules are devoid of spermatozoa with sloughed degenerate and occasionally multinucleated germ cells in the tubular lumen (immaturity and degeneration). Special stains did not reveal any microorganisms.

Contributor's Morphologic Diagnosis: 1. Moderate, multifocal, pyogranulomatous vaginalitis.
2. Moderate, multifocal, granulomatous epididymitis (in some sections).

Contributor's Comment: The nature and location of the lesions suggests feline infectious peritonitis. Immunohistochemistry confirmed the diagnosis, as feline coronavirus antigen was demonstrated within the histiocytic cells of the pyogranulomatous foci. A few months later, the cat is still clinically normal.

Feline infectious peritonitis (FIP) is caused by Feline infectious peritonitis virus (FIPV), an enveloped, single stranded, positive sense RNA virus in the family *Coronaviridae* that infects domestic and wild felids. FIPV appears to have evolved by a deletion mutation from feline enteric coronavirus (FECV), a coronavirus that has tropism for villous enterocytes and causes mostly inapparent infections or mild diarrhea in cats, predominantly kittens. The mutated coronavirus (FIPV) has tropism for and the ability to replicate in macrophages, which allows widespread dissemination of the virus in the host and development of a systemic, generally fatal disease in susceptible individuals (usually less than 2 years); most animals infected with FIPV do not, however, develop clinical disease. The pathogenesis of FIP is complex and still not fully understood. Cell-mediated immunity is responsible for FIPV clearance. The degree of humoral immunity is also important, and in part determines the evolution of the disease. Viral strain differences, breed and likely other factors are also involved. FIP is characterized by the deposition of immune complexes mainly in venules and arterioles of many serosal surfaces and organs (e.g. kidney, spleen, lungs) leading to the development of vasculitis (Arthus type III reaction) which is, with pyogranulomatous inflammation, the microscopic hallmark of the disease. This vascular lesion is variably

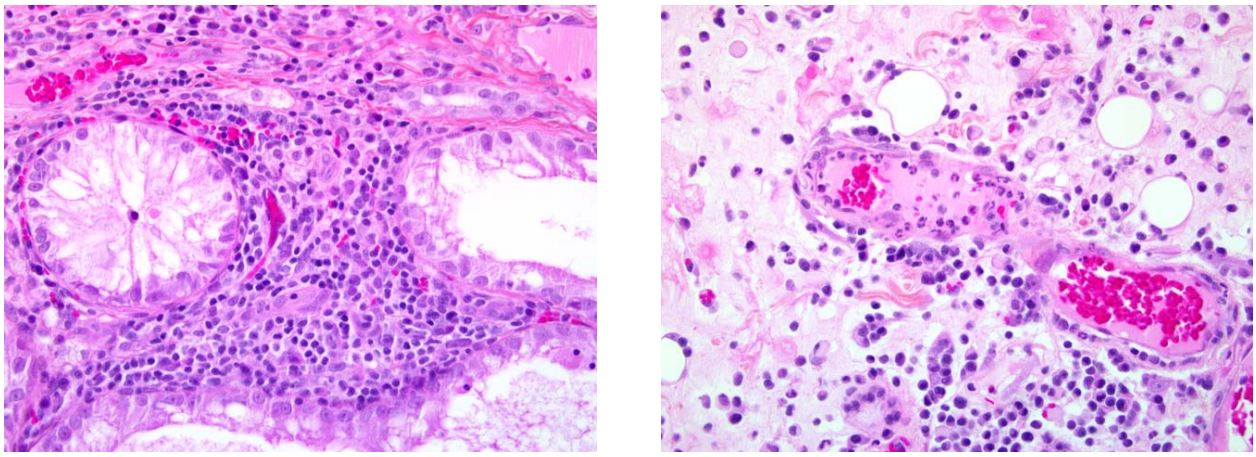

4-1, 4-2. Testis, domestic cat. Pyogranulomatous foci are composed of viable and degenerate neutrophils with variable numbers of macrophages, lymphocytes, and plasma cells admixed with cellular debris. There is atrophy of seminiferous tubules (4-1). Multifocally vessels are infiltrated and disrupted by similar inflammatory cells and the endothelium is hypertrophied and reactive (4-2). (HE 400X)

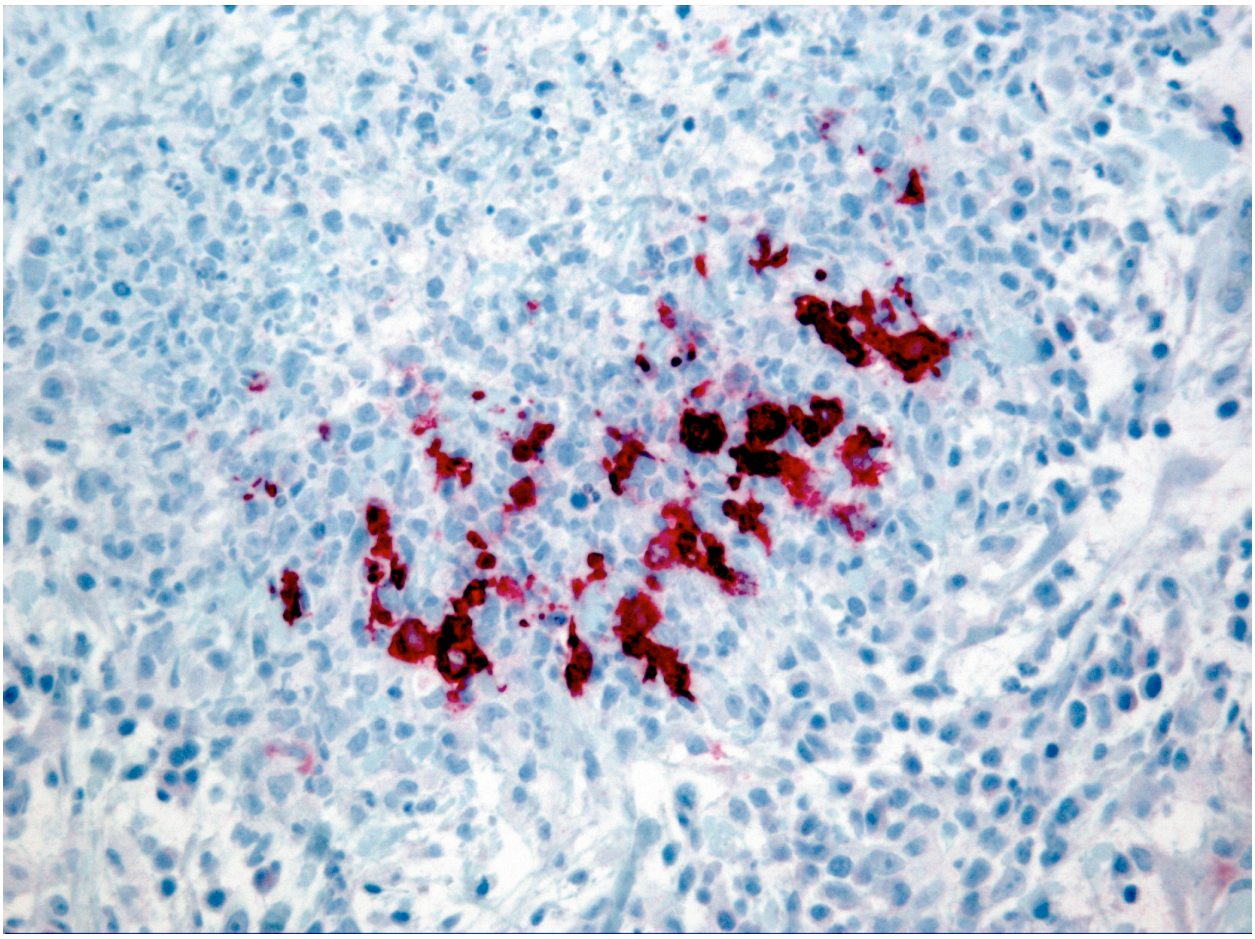

4-3. Testis, domestic cat. Histiocytic cells within pyogranulomatous foci are positive for feline coronavirus antigen. Photograph courtesy of Department of Pathology and Microbiology, Faculty of Veterinary Medicine, University of Montreal, http://www.medvet.umontreal.ca.

associated with edema, fibrin exudation, necrosis, and/or hemorrhage. The vasculitis is the basis of the effusion grossly observed in most FIP cases. If the cat survives, then macrophages accumulate in affected tissues, as they cannot eliminate the virus. Three forms of the disease are recognized: the "effusive" (or "wet") form; the "noneffusive" (or "dry") form; and a mixed form. Although described as separate entities, the wet and dry forms are actually both ends of a spectrum.[1,2]

Orchitis and periorchitis (vaginalitis) are uncommon FIP-related lesions. These lesions are believed to develop by extension of the peritonitis along the tunica vaginalis. Pathologists and clinicians should keep this uncommon presentation of FIP in mind when presented with a cat with testicular lesions.[3,5]

AFIP Diagnosis: Testis: Orchitis, periorchitis, and serositis, pyogranulomatous, perivascular, multifocal, moderate with phlebitis, testicular atrophy and germ cell degeneration.

Conference Comment: Conference participants discussed some of the key histologic features of testicular degeneration. Death of Sertoli cells and spermatogonia results in sloughing into the seminiferous tubular lumina. The moderator noted that Sertoli cells will occasionally phagocytize necrotic/apoptotic spermatids, forming spermatid giant cells which are frequent in the submitted specimens. As the cellular loss proceeds, there is stromal collapse resulting in increased interstitial tissue and a thickened, wavy PAS-positive basement membrane around seminiferous tubules. When evaluating tubules to assess spermatogenesis, the moderator stated that, on average, one out of every six to eight seminiferous tubules should have mature spermatids.

The moderator stressed the importance of examining all four germinal layers in the testis; Samuelson's *Textbook of Veterinary Histology* provides an excellent description of the germinal layers. The population of spermatogonium cells is the first germinal layer and gives rise to the remaining cell types. There are three histologically distinct populations of spermatogonia. Reserve cells, also referred to as dark type A spermatogonia, are relatively senescent with heterochromic nuclei and scant cytoplasm. The few reserve cells that enter the spermiogenic cycle are transformed to one of two cell types. The first type is light type A spermatogonia, sharing many histomorphological features with their dark type predecessor but have nuclei which are lighter in color or

euchromatic. The second type is type B spermatogonia; these cells resemble light type A cells, but the former have a round nucleus as opposed to the oval nucleus of the latter. The second germinal layer is composed of primary spermatocytes, the largest cells in spermiogenesis; these cells are round with large, round, vesiculate nuclei. The primary spermatocytes give rise to the third layer, the secondary spermatocytes, often inapparent on routine histologic examination. Finally, spermatids are formed, characterized by development of a flagellum, an acrosome and condensed, elongate nuclear material.[5]

Participants noted slide variation with some slides having epididymis with granulomatous inflammation.

Contributor: Department of Pathology and Microbiology, Faculty of Veterinary Medicine, University of Montreal
http://www.medvet.umontreal.ca

References:

1. Brown CC, Baker DC, Barker IK. Alimentary system. In: Maxie MG, ed. *Jubb, Kennedy and Palmer's Pathology of Domestic Animals*. 5th ed., Vol. 2. Philadelphia, PA: Saunders Elsevier; 2007:174, 290-293.
2. Hartmann K. Feline infectious peritonitis. *Vet Clin North Am Small Anim Pract*. 2005;35(1):39-79.
3. Foster RA, Caswell JL, Rinkardt N. Chronic fibrinous and necrotic orchitis in a cat. *Can Vet J*. 1996;37(11):681-682.
4. Sigurdardóttir OG, Kolbjørnsen O, Lutz H. Orchitis in a cat associated with coronavirus infection. *J Comp Pathol*. 2001;124(2-3):219-222.
5. Samuelson DA. Male reproductive system. *Textbook of Veterinary Histology*. St. Louis, MO: Saunders Elsevier; 2007:421-427.

The Armed Forces Institute of Pathology
Department of Veterinary Pathology

Conference Coordinator
Matthew Wegner, DVM

WEDNESDAY SLIDE CONFERENCE 2010-2011

Conference 24

16 March 2011

Conference Moderator:
Michael Goldschmidt, BVMS, MSc, Diplomate ACVP

CASE I: AP08-2649 (AFIP 3142086).

Signalment: 9-year-old spayed female mixed-breed canine (*Canis familiaris*).

History: This dog presented to the North Carolina State University, College of Veterinary Medicine Emergency Service for evaluation of cyanotic mucous membranes and tachypnea. Additional findings included diffuse pitting edema in the right hind limb. Right hind limb edema was first noted 4 years ago and was initially localized to the paw region. At the time of initiation, the dog held its leg up, but there was no associated traumatic event. Hind limb edema occurred intermittently over the next four years, but progressively worsened. Treatment with doxycycline and carprofen initially relieved the swelling and was administered for three recurrent episodes; however, after treatment for an episode in 2008, approximately three weeks prior to presentation to the veterinary school, she experienced vomiting and diarrhea. Carprofen was discontinued and treatment with prednisolone, ranitidine, and sucralfate was initiated. The leg continued to swell up to 5 times the normal size at which point all medications were discontinued. Labored breathing was first noted approximately one week prior to presentation along with trembling and shivering. Limited response to oxygen therapy and supportive care following admission, combined with a poor prognosis, resulted in the owner's decision to humanely euthanize the dog.

Gross Pathology: At necropsy, subcutaneous tissues of the right hind limb were diffusely thickened by gelatinous edema fluid and multifocal hemorrhages. Lesions were most severe surrounding the metatarsus. Several sections through the leg did not reveal a mass.

The lungs were mottled pink-red, semi-firm, and markedly congested and edematous. Numerous (>20) pink-tan nodules ranging from 3 mm to 1 cm in diameter were distributed throughout the lungs. The liver was enlarged (5.4% total body weight), had rounded edges, and contained numerous tan, soft to firm, raised nodules that ranged from 1 mm to 4 cm in diameter. On cut surface, hepatic nodules were tan to mottled tan-brown. Larger nodules contained necrotic centers that oozed thick, dark brown exudate. The entire gastrointestinal tract was transmurally thickened. The pancreas was moderately enlarged, firm, and tan.

Laboratory Results: Immunohistochemistry - Endothelial cells lining the abnormal lymphatic channels had the following intracytoplasmic labeling:

- Greater than 90% of the cells had strong, nearly diffuse labeling with Factor VIII-related antigen (von Willebrand's factor).
- 100% of the cells had strong, diffuse labeling with vimentin (mesenchymal marker).
- Approximately 60-70% of the cells had weak to strong, multifocal labeling with LYVE-1 (lymphatic vessel endothelial receptor 1).

Histopathologic Description: Skin, right hind limb (submitted tissue): Numerous anastamosing lymphatic channels dissect between deep dermal collagen bundles and extend into the subcutis and superficial dermis. The channels

are lined by single layers of attenuated to mildly plump endothelial cells that separate variably sized islands of collagen and adipocytes. Individual cells are fusiform to spindled, contain elongate to irregular hyperchromatic nuclei, and have scant, pale basophilic cytoplasm. Cell borders are variably distinct, and anisocytosis and anisokaryosis are minimal. Mitotic figures are not observed. Mild numbers of lymphocytes and plasma cells often form small discrete aggregates around blood vessels with mild, multifocal infiltration into the surrounding dermis and panniculus. The dermis and subcutis are moderately expanded by clear edema fluid.

Lung, liver, pancreas, gastrointestinal tract (tissues not included on the submitted slide): The lung, liver, pancreas, and gastrointestinal tract contained multiple masses composed of neoplastic epithelial cells consistent with metastatic cholangiocarcinoma.

Contributor's Morphologic Diagnosis: Right hind limb: Subcutaneous lymphangiomatosis with marked edema and multifocal, mild, lymphoplasmacytic dermatitis and panniculitis.

Contributor's Comment: The cause of progressive respiratory distress that was unresponsive to therapy is attributed to pulmonary metastasis of a cholangiocarcinoma. Sections of cholangiocarcinoma were not included in this submission.

Tissue submitted was from the skin and subcutis of the right hind limb. Histologic lesions in this tissue were consistent with lymphangiomatosis. Lymphangiomatosis is a rare disorder characterized by increased numbers of lymphatic endothelial cells forming irregular, anastomosing, vascular clefts and empty channels.[6] This condition is reported in both cats and dogs, and is grossly characterized by a poorly circumscribed mass or regionally extensive swelling.[6] Tumors of lymphatic origin typically occur in the skin and subcutis with the caudal ventral abdomen and inguinal regions predisposed.[5] Additional reported locations include the head, neck, cranial trunk, axilla, bone, and extremities.[3] Lesions present as intermittent, fluctuant swellings with a variably protracted clinical course and have reportedly affected an entire limb. Lesions often form ulcers and draining tracts with leakage of fluid resulting in cutaneous vesiculation.[6] Smaller discrete lesions should be referred to as lymphangioma, whereas lymphangiomatosis has been described as lymphangioma affecting soft tissues and/or parenchymal organs in a diffuse or multifocal manner.[2,6] Lymphangioma, lymphangiomatosis, and lymphangiosarcoma tend to occur in younger animals; however, lymphangiosarcoma has been reported in dogs ranging from 8 weeks to 13 years of age.[3] A single case of lymphangiosarcoma has been described in a cow and two cases have been described in horses.[8,11,12] Immunohistochemistry may be used to confirm endothelial origin of proliferative lymphatic conditions using factor VIII-related antigen, CD31, vimentin, and LYVE-1.[1,2,6] For this case, the abnormal endothelial cells had strong, nearly diffuse intracytoplasmic immunoreactivity for factor VIII-related antigen and vimentin, and moderate, multifocal immunoreactivity for LYVE-1.

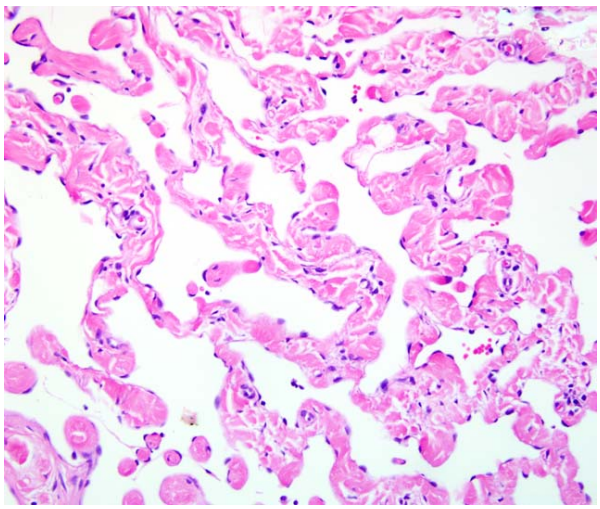

1-1. Haired skin, deep dermis and subcutis, lymphangioma (lymphangiomatosis), dog. Numerous anastamosing empty lymphatic channels dissect deep dermal collagen bundles and are lined by a single layer of flattened endothelium. (HE 200X)

If metastatic disease is not present, distinguishing lymphangiosarcoma from lymphangiomatosis based on clinical and histological features may be difficult.[6] It has been suggested that some of the previously described cases of non-metastatic lymphangiosarcomas with well-differentiated endothelial cells may have represented lymphangiomastosis, particularly when these lesions were found in young dogs.[4,13] Lymphangiomatosis, although histologically benign, is often recurrent and progressive.[6] Surgical resection, chemotherapy, and radiotherapy have been used to treat both lymphangiomatosis and lymphangiosarcoma.[6,8]

AFIP Diagnosis: Haired skin and subcutis, right hind limb (per contributor): Lymphangioma (lymphangiomatosis).

Conference Comment: Extensive discussion occurred among conference participants and the moderator regarding the best nomenclature for this interesting lesion, i.e. lymphangiomatosis and lymphangioma. In the absence of clinical information, all participants agreed the histologic findings represent a poorly demarcated proliferation of lymphatic endothelial cells that dissect dermal and subcutaneous collagen, with minimal cellular and nuclear atypia. The moderator favored the diagnosis of lymphangioma based on the biologic behavior of these lesions and the lack of a consensus in veterinary medicine as to the precise definition for lymphangiomatosis. This was case also studied in consultation with the subspecialty physician pathologists from the AFIP Department of Soft Tissue Pathology; they favored the diagnosis of

lymphangiomatosis based on the diffuse, extensive infiltrative process with poor tumor demarcation. In human pathology, the diagnosis of lymphangioma is reserved for well-defined masses.

In humans, there is a form of lymphangioma referred to as progressive lymphangioma which occurs in adults, most commonly on the limbs, and is characterized grossly as a red cutaneous macule that enlarges with age.[10] Histologically, there is a proliferation of thin-walled lymphatic channels that dissects between dermal collagen bundles and forms horizontal clefts; lesions may extend into the subcutis. Cutaneous lymphangiomatosis occurs as a diffuse, benign lymphatic proliferation affecting multiple tissue planes over a large area, most commonly in young children;[10] interestingly, the lesion tends to regress when the child stops growing. Lymphangiomatosis is characterized histologically as many variably dilated lymphatic channels which dissect between all normal structures, resulting in islands of normal tissue that appear to be "hanging in the air." A distinguishing feature between these two entities is the presence of cutaneous vesicles in lymphangiomatosis, a feature which is lacking in lymphangiomas.[10]

A review of veterinary pathology reference texts[5,6,7,14] reveals discordance over the preferred nomenclature for this proliferative lymphatic lesion. Based on descriptions in humans, there are features of both lymphangioma and lymphangiomatosis in the case of this dog. The most recent WHO fascicle only describes lymphangioma, which occurs most commonly in young animals and is believed to represent congenital malformation.[7] The moderator commented that in the cases he has evaluated, the lesions are difficult to fully resect owing to the lack of a "mass effect" making palpation of the edges of the lesion difficult, resulting in incomplete surgical resection. The lesions are progressive, a feature also described in the reference texts, exhibit characteristic pitting edema, and occur most commonly on the abdomen, ventral neck, inguinal area and prepuce. The moderator further commented that in his experience, lymphangiomatosis involves many parts of the body, is histologically characterized by multiple dilated lymphatics, and contains a myxoid stroma.

In the case of this dog, the signalment and clinical history (e.g. older animal with a lesion is located on the limb) and the histologic findings of thin-walled lymphatic channels that dissect dermal collagen with formation of horizontal clefts with extension into the subcutis support a diagnosis of lymphangioma. However, the findings of diffuse lymphatic proliferation affecting multiple tissue planes over a large area and islands of tissue "hanging in the air" are more consistent with the classification of lymphangiomatosis, demonstrating the complexity of this lesion. One important fact for which the references agree is the progressive nature of both lymphangioma and lymphangiomatosis, a clinical feature that may be more relevant than the histologic classification from a prognostic standpoint.[5,6,7,14]

Contributors: Comparative Molecular Pathology Unit, Laboratory of Cancer Biology and Genetics, Center for Cancer Research, National Cancer Institute, National Institutes of Health, 37 Convent Drive, Bldg. 37, Room 2002 Bethesda, MD 20892
http://ccr.ncifcrf.gov/resources/molecular_pathology/

North Carolina State University, College of Veterinary Medicine, Department of Population Health and Pathobiology, 4700 Hillsborough Street, Raleigh North Carolina 27606
http://www.cvm.ncsu.edu/dphp/phpdeptdiv.html

References:

1. Barnes JC, Taylor SM, Clark EG, Haines DM, Broughton SJ. Disseminated lymphangiosarcoma in a dog. *Can Vet J.* 1997;38:42-44.
2. Berry WL, Nesbit JW, Pearson J. Lymphangiomatosis of the pelvic limb in a Maltese dog. *J Sm Anim Prac.* 1996;37:340-343.
3. Diessler ME, Castellano MC, Massone AR, Portiansky EL, Allende MG, Idiart JR. Cutaneous lymphangiosarcoma in a young dog: Clinical anatomopathological and lectinhistochemical description. *J Vet Med A Physiol Pathol Clin Med.* 2003;50:452-456.
4. Fossum TW, Miller MW, Mackie JT. Lymphangiosarcoma in a dog presenting with massive head and neck swelling. *J Am Anim Hosp Assoc.* 1998;34:301-304.
5. Ginn PE, Mansell JEKL, Rakich PM. Skin and appendages. In: Maxie MG, ed. *Jubb, Kennedy and Palmer's Pathology of Domestic Animals*. Vol. 1, 5th ed. Philadelphia, PA: Elsevier Ltd; 2007:768.
6. Gross TL, Ihrke PJ, Walder EJ. Vascular tumors. In: *Skin Diseases of the Dog and Cat.* 2nd ed. Ames, IA: Blackwell Science; 2005:748-755.
7. Hendrick MJ, Mahaffery EA, Moore FM, Vos JH, Walder EJ. *Histological Classification of Mesenchymal Tumors of Skin and Soft Tissues of Domestic Animals*. 2nd Series. Vol. 2. Washington D.C.: Armed Forces Institute of Pathology, American Registry of Pathology; 1998:22-25.
8. Ijzer J, van den Ingh TSGAM. Lymphangiosarcoma in a horse. *J Comp Path.* 2000;122:312-316.
9. Itoh T, Mikawa K, Mikawa M, Nibe K, Uchida K. Lymphangiosarcoma in a dog treated with surgery and chemotherapy. *J Vet Med Sci*. 2004;66(2):197-199.
10. Kempson RL, Fletcher CDM, Evans HL, Hendrickson MR, Sibley RK. Vascular tumors. In: *Atlas of Tumor Pathology: Tumors of the Soft Tissues.* 3rd Series, Fascicle 30. Washington D.C.: Armed Forces Institute of Pathology/ American Registry of Pathology; 1998:360-363.
11. Ruggles AJ, Irby NL, Saik JE, Orsini PG. Ocular lymphangiosarcoma in a cow. *J Am Vet Med Assoc*. 1992;200(12):1987-1988.
12. Sanchez B, Nieto A, Ruiz DE Leon MA, Rodriguez J, Flores J. Metastatic lymphangiosarcoma in a horse. *Vet Pathol*. 2002;39:266-268.

13. Shiga A, Shirota K, Une Y, Nomura Y. Lymphangiosarcoma in a dog. *J Vet Med Sci*. 1994;56(6): 1199-1202.
14. Van Vleet JF, Ferrans VJ. Cardiovascular system. In: McGavin MD, Zachary JF, eds. *Pathologic Basis of Veterinary Disease*. 4th ed. St. Louis, MO: Elsevier; 2007:611.

CASE II: 10-05194 (AFIP 3164900).

Signalment: 12-year 10-month-old castrated male Cocker Spaniel, canine (*Canis familiaris*).

History: This was a mass on the left front digit present for four months. The mass had not changed since first noticed. The left prescapular lymph node was enlarged and there were multiple other pedunculated skin masses. A mass was removed from the right front paw one year prior but not biopsied. The dog had chronic severe dental disease, severe chronic bilateral ear infections, keratoconjunctivitis sicca bilaterally, and hyperpigmentation and lichenification of the groin. The dog had been on long-term metronidazole, rimadyl, tacrolimis, and clindamycin.

Gross Pathology: The mass markedly enlarged the digit but did not grossly invade the bone.

Histopathologic Description: Haired skin, left front foot (per contributor): The deep dermis contains an unencapsulated, poorly demarcated, highly cellular, invasive neoplastic mass which effaces and surrounds the adnexal structures. The mass is composed of cuboidal epithelial cells arranged in tubules and acini that are often palisading and are supported by a small to large amount of collagenous stroma (desmoplasia) that multifocally contains many plasma cells and lymphocytes. The epithelial cells have a small amount of pale eosinophilic cytoplasm with distinct cell borders. The central or basally located nuclei are large and round, with finely stippled chromatin and 1 small nucleolus. Anisocytosis and anisokaryosis are marked. Mitotic figures range from 0-15 per 400x field, with an average of 5 per 400x field. Multifocally the neoplastic cells demonstrate piling upon one another, with occasional protrusion and blebbing into the acinar or tubular lumina, some of which also contain few sloughed or necrotic cells, proteinaceous material, or mild hemorrhage. Many follicles and glands are surrounded by numerous lymphocytes and plasma cells, fewer macrophages, and rare mast cells. Multiple follicles are mildly dilated, filled with laminated keratin, and contain 0-12 cross and/or tangential sections of arthropods that are up to 50 microns in diameter and 300 microns long. The arthropods have a thin eosinophilic chitinous exoskeleton, blunt jointed appendages, skeletal muscle, and digestive and/or reproductive tracts. The overlying epidermis is minimally hyperplastic with orthokeratotic hyperkeratosis. There is moderate pigmentary incontinence as well as scattered macrophages that contain a pale grey-tan pigment consistent with lipofuscin.

Contributor's Morphologic Diagnosis: 1. Adenocarcinoma, apocrine or eccrine origin, left front paw. 2. Intrafollicular mites (*Demodex* spp.)

Contributor's Comment: Sweat glands are divided into two types: apocrine and merocrine (eccrine).[11] Apocrine gland secretion consists of release of a large secretory granule that is surrounded by a small amount of cytoplasm and cell membrane, and is microscopically apparent as apical blebbing.[3] In merocrine secretion, the contents of the secretory granules is released by fusion of the granule with the cell membrane.[3] Apocrine glands are the most abundant in domestic animals, and consists of saccular tubular glands with a coiled secretory portion and a straight duct that is lined by two layers of epithelium and typically opens into the hair follicle.[11] Merocrine glands are limited to the non-haired areas of the footpad of dogs and cats, the frog of ungulates, planum rostrale and the carpal glands of pigs, and the planum nasolabiale of cows.[11] Myoepithelial cells are specialized smooth muscle cells that aid in emptying both apocrine and merocrine glands of secretion.[3,11]

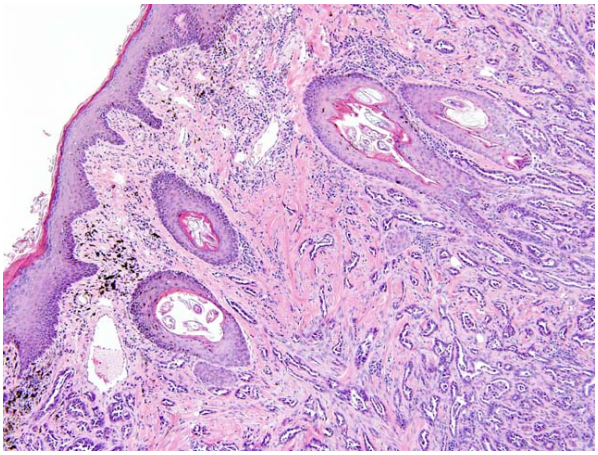

2-1. Haired skin, left front foot, apocrine adenocarcinoma, canine. An invasive neoplasm composed of cuboidal epithelial cells arranged in tubules and acini effaces the dermis, surrounds adnexal structures, and occasionally extends into the epidermis. Ectatic follicles contain cross sections of Demodex mites. Photograph courtesy of University of Illinois at Champaign-Urbana, Department of Pathobiology.

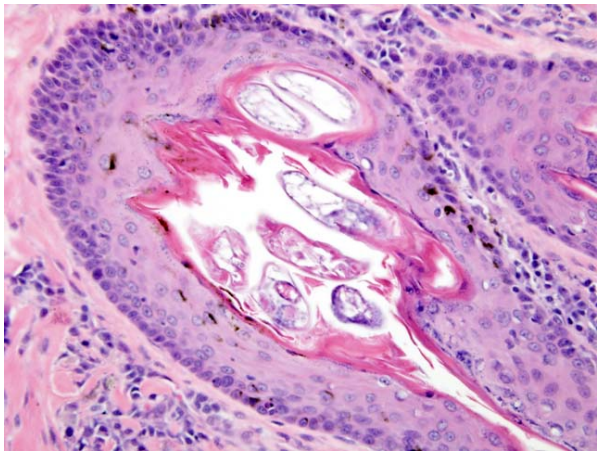

2-2. Haired skin, left front foot, apocrine adenocarcinoma, canine. Multiple follicles are ectatic and contain sections of arthropods with a exoskeleton, blunt jointed appendages, skeletal muscle, and digestive and/or reproductive tracts. Photograph courtesy of University of Illinois at Champaign-Urbana, Department of Pathobiology.

Apocrine gland carcinomas include solid, cystic, and tubular types.[5,6,7] The tubular type is the most common and typically has marked desmoplasia.[5,7] Apocrine carcinomas are locally aggressive, extending through the dermis, subcutis, and underlying skeletal muscle. Lymphatic invasion and spread to the regional lymph nodes and lungs is common.[5,6] Apocrine carcinomas also occur as ductal, compound, and mixed types, similar to mammary gland tumors.[5,7]

Tumors of eccrine glands are extremely rare but do occur as adenomas or carcinomas of the footpad of dogs and cats.[5,6,8,10] Eccrine carcinomas are morphologically similar to apocrine gland carcinomas and are very difficult to differentiate by light microscopy.[5,10] There are no reliable immunohistochemical antibodies that can separate eccrine carcinoma from apocrine carcinoma.[10] Differentiation is based on proving that the tumor arises from the footpad, rather than the adjacent haired skin,[6,10] or by observing the apical blebbing that occurs when apocrine glands are in their secretory state.[3,6] Both tumors types stain positively with antibody to carcinoembryonic antigen, which can help differentiate them from other tumor types.[5,8]

Demodex mites are obligate parasites that are normal inhabitants of the hair follicles and sebaceous glands of dogs and most other domestic animals and humans. The exception is *Demodex cati*, which is found in the superficial stratum corneum.[4] Disruption of the host-parasite equilibrium can result in overgrowth of the mites and lesions of demodicosis. *Demodex* has been found in association with several dermatologic conditions in humans[1] and animals.[4,9]

Juvenile-onset demodicosis is often familial, and is thought to be due to a genetic cell-mediated immunity disorder.[4,9] In adult-onset demodecosis, the overgrowth of the mites is often associated with hyperadrenocorticism, corticosteroid administration, hypothyroidism, chemotherapy, or other serious diseases.[4] *Demodex* is not typically associated with tumors in animals, but a significant increase in the prevalence and density of *Demodex* has been found in eyelid basal cell carcinomas in people, and is postulated to be a triggering factor for carcinogenesis due to chronic irritation.[2] Demodicosis lesions in dogs are often generalized but are more severe on the face and paws, and in some may be confined to the paws.[4,9] In this case, the patient had congestive heart failure, chronic severely infected gums, hypothyroidism, and had indications of pituitary-dependent hyperadrenocorticism in addition to a locally aggressive neoplasm in the area of mite overgrowth. The dog had hyperpigmentation and lichenification, which can be found in chronic cases of both generalized demodicosis[9] and hyperadrenocorticism.

Histologically, demodicosis can range from early lesions of lymphocytic mural interface dermatitis, perifollicular pigmentary incontinence, and follicular hyperkeratosis, to suppurative folliculitis and pyogranulomatous furunculosis due to development of secondary bacterial infections.[4] Rupture of the follicles results in release of mites into the dermis, and fragments of mites have occasionally been found in the draining lymph nodes.[4]

AFIP Diagnosis: 1. Haired skin and subcutis: Apocrine adenocarcinoma.
2. Haired skin: Follicular ectasia, hyperkeratosis and hyperplasia, focally extensive, mild with histiocytic and lymphoplasmacytic dermatitis, pigmentary incontinence, and intrafollicular arthropod parasites, etiology consistent with Demodex species
3. Haired skin, subcutis, vessels: Smooth muscle hypertrophy and hyperplasia, multifocal, with occasional luminal occlusion.

Conference Comment: Participants agreed with the diagnosis of adenocarcinoma, with most favoring apocrine origin based on the observation of occasional decapitation-type secretion (apical blebbing), location of the tumor in haired skin, and the extreme rarity of eccrine carcinoma in veterinary species. Another unique feature of apocrine adenocarcinomas noted by the moderator, and not found with eccrine carcinoma, is extension of neoplastic cells into the overlying epidermis with associated epidermal ulceration.

Participants also discussed the various histologic variants of apocrine adenocarcinoma mentioned above by the contributor. Several raised the possibility of apocrine ductal carcinoma; the moderator pointed out that there should be foci of squamous differentiation in addition to a double-layer of neoplastic epithelial cells, both of which are lacking in this specimen. In dogs and cats, eccrine carcinomas occur in the footpads, whereas apocrine adenocarcinomas and apocrine ductal carcinomas generally arise on the legs of dogs and on the head, legs and abdomen of cats.

Participants discussed the significance of finding *Demodex* spp. in this, as well as other, biopsy specimens. The finding of demodicosis must be communicated to the submitting clinician, regardless of the severity or apparent insignificance since treatment with steroids will worsen the condition. The moderator commented that follicular epithelial hyperplasia, melanin within basal cells, and perivascular lymphoplasmacytic dermatitis is highly suggestive of demodicosis and should prompt the reviewing pathologist to thoroughly search hair follicles for the presence of *Demodex* spp.

Contributor: University of Illinois at Champaign-Urbana, Department of Pathobiology, 2840 Veterinary Medicine Basic Sciences Building, MC-002, 2001 South Lincoln Avenue, Urbana, Illinois 61802

References:
1. Dhingra KK, Saroha V, Gupta P, Khurana N. Demodex-associated dermatologic conditions-A coincidence or an

etiological correlate. Review with a report of a rare case of sebaceous adenoma. *Pathol Res Pract*. 2009;205:423-426.
2. Erbagci Z, Erbagci I, Erkilic S. High incidence of demodicidosis in eyelid basal cell carcinomas. *Int J Dermatol*. 2003;42:567-571.
3. Frappier BL. Epithelium. In: Dellman HD, Eurell J, eds. *Textbook of Veterinary Histology*. 5th ed. Baltimore, MD: Lippincott Williams & Wilkins; 1998:31.
4. Ginn PE, Mansell JEKL, Rakich PM. Skin and appendages. In: Maxie MG, ed. *Jubb, Kennedy and Palmer's Pathology of Domestic Animals*. Vol. 1, 5th ed. Philadelphia, PA: Elsevier Ltd; 2007:724-726.
5. Ginn PE, Mansell JEKL, Rakich PM. Skin and appendages. In: Maxie MG, ed. *Jubb, Kennedy and Palmer's Pathology of Domestic Animals*. Vol. 1, 5th ed. Philadelphia, PA: Elsevier Ltd; 2007:758.
6. Goldschmidt MH, Dunstan RW, Stannard AA, von Tscharner C, Walder EJ, Yager JA. *Histological Classification of Epithelial and Melanocytic Tumors of the Skin of Domestic Animals*. 2nd Series. Vol III. Washington, D.C.: The Armed Forces Institute of Pathology, American Registry of Pathology; 1998:29-32.
7. Goldschmidt MH, Hendrick MJ. Tumors of the skin and soft tissues. In: Meuten DJ, ed. *Tumors in Domestic Animals*. 4th ed. Ames, IA: Iowa State Press; 2002:72-73.
8. Goldschmidt MH, Hendrick MJ. Tumors of the skin and soft tissues. In: Meuten DJ, ed. *Tumors in Domestic Animals*. 4th ed. Ames, IA: Iowa State Press; 2002:76.
9. Gross TL, Ihrke PJ, Walder EJ, Affolter VK. Pustular and nodular diseases with adnexal destruction. In: *Skin Diseases of the Dog and Cat*. 2nd ed. Ames, IA: Blackwell Science Ltd; 2005:442-446.
10. Gross TL, Ihrke PJ, Walder EJ, Affolter VK. Sweat gland tumors. In: *Skin Diseases of the Dog and Cat*. 2nd ed. Ames, IA: Blackwell Science Ltd; 2005:677-691.
11. Monteiro-Riviere NA. Integument. In: Dellman HD, Eurell J, eds. *Textbook of Veterinary Histology*. 5th ed. Baltimore, MD: Lippincott Williams & Wilkins; 1998:316-318.

CASE III: 4096-10 (AFIP 3165075).

Signalment: 8-year-old Rhodesian Ridgeback, canine (*Canis familiaris*).

History: Five skin punch biopsies were submitted from the nasal planum and lips. The clinician reported a one-month duration of crusting, scaling and depigmentation of the affected areas with some vesicles.

Gross Pathology: None.

Histopathologic Description: Haired skin: The epidermis is thickened (acanthotic) and there is a broad zone of plasma cells with some lymphocytes in the superficial dermis and occasionally infiltrating into the basal layer of the epidermis (interface lichenoid inflammation). Many scattered dermal macrophages contain somewhat coarsely granular melanin pigment (pigmentary incontinence). Scattered individual eosinophilic, shrunken, basal cells (apoptotic cells) are present and suggestive of an autoimmune condition.

Contributor's Morphologic Diagnosis: Discoid lupus erythematosus (DLE).

Contributor's Comment: This is probably the most common autoimmune disease we see in our submissions and is most common in Collies and Shetland sheepdogs.[3] Typically, it involves the nose, lips, and periorbital skin but may involve the trunk, distal limbs, footpads, genitals and perianal area.[1,3,4] Systemic lupus (SLE) is similar or identical microscopically but is usually more widespread and may have more apoptotic basal cells but less of the lichenoid inflammation than DLE.[4] SLE should have a positive anti-nuclear-antibody serology as well and it may be associated with systemic illness. Vogt-Koyangi-Harada-like syndrome of melanin autoimmunity has more dermal macrophages with finer melanin clumps in them and it is most common in Akitas, Siberian Huskies, Alaskan Malamutes, Chow Chows, and their mixes; it is also limited to the face, but with uveitis. Mucocutaneous pyoderma of the lips also has heavy lichenoid plasma cell dermatitis with pigmentary incontinence; it may have neutrophils as well, and the apoptotic cells are more superficial keratinocytes rather than basal cells.

The dog was treated with short term prednisolone and doxycycline and long-term niacinamide (all 3 are presumed immunosuppressors used to treat DLE and SLE)[5] and the dog was normal in about one month.

AFIP Diagnosis: Haired skin: Dermatitis, lichenoid, interface, lymphoplasmacytic, neutrophilic and histiocytic, diffuse, marked with epidermal acanthosis, spongiosis, parakeratosis, and rare apoptotic basal cells.

Conference Comment: Participants and the moderator were hesitant to assign the specific diagnosis of discoid lupus erythematosus (DLE) in this case due to the variation in specimen quality and the presence of only rare basal cell apoptosis. Many conference participants experienced difficulty in separating tissue processing artifact from pathological changes. Participants agreed with the contributor that several histologic features are suggestive for DLE, although the basal cell apoptosis is not as conspicuous in this dog as would be expected for most animals with the condition. The additional history of clinical response to immunomodulatory treatment supports an underlying autoimmune process, such as DLE.

The moderator commented that the differential diagnosis for superficial lymphoplasmacytic dermatitis with neutrophilic inflammation includes lupus (systemic lupus erythematosus or discoid lupus erythematosus) and mucocutaneous pyoderma (MP). A retrospective study by Weimelt et. al.[8] demonstrated the difficulty in differentiating these two conditions, as the histopathological features of both frequently overlap making treatment modality and clinical response difficult to determine and predict. Whereas mucocutaneous pyoderma responds well to antibiotics, treatment of lupus involves immunomodulatory drugs.

Since DLE and SLE are nearly indistinguishable histologically, it is worthwhile to briefly review the pathogenesis of SLE. Lymphopenia and an overall decrease in the numbers of T-lymphocytes occurs, and there is an imbalance in the ratio of CD4+:CD8+ T-lymphocytes, with an increase up to 6 to 1 (in healthy dogs the ratio is 2.3 to 1); this favors B-cell stimulation and antibody production.[2] In addition to the imbalance in T-cell populations, there is loss of self-tolerance in both B-cells and T-cells.[2,6] After massive cell death due to exogenous (e.g. ultraviolet light, environmental) insults or endogenous (metabolic, hormonal, genetic) triggers, there is defective clearance of cellular debris, resulting in increased amounts of nuclear antigen.[6] The altered B-cells are stimulated by the released nuclear antigens to produce anti-nuclear antibodies. The anti-nuclear antibodies then bind additional antigen, and the resulting

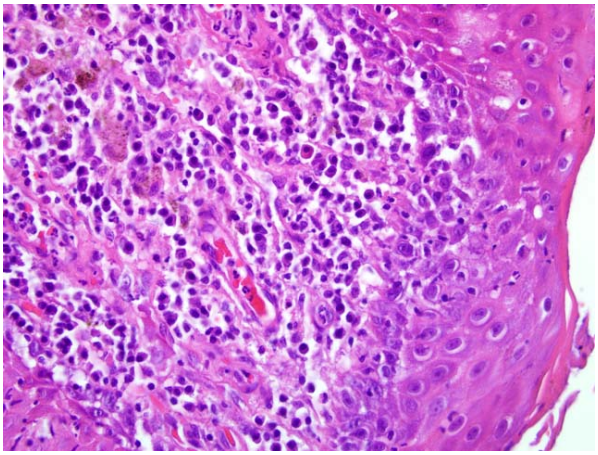

3-1. Haired skin, canine. Multifocally there is mild lymphoplasmacytic lichenoid interface inflammation and epidermal acanthosis and spongiosis. (HE 400X)

antigen-antibody complexes then bind to Fc receptors on B-cells and antigen-presenting cells (APC). The stimulated APCs secrete type 1 interferon, which is autostimulatory (including for other B-cells).[6]

Antinuclear antibodies have been shown to bind to one of four nuclear components: DNA, histones, non-histone proteins bound to RNA, and nuclear antigens.[6] Generalized tissue damage ensues as part of a Type III hypersensitivity reaction whereby antigen-antibody complexes deposit in the kidney, skin, blood vessels etc.[2,6] The antibody-antigen complexes lodge beneath the basement membrane of the epidermis.[2]

As part of the continuous review and study of the complex pathology of DLE, some authors recommend referring to the lesion as photosensitive nasal dermatitis, suggesting the nomenclature of this entity should change as the pathogenesis is further elucidated.[2] In the skin, DLE and SLE are both photoresponsive, and ultraviolet (UV) light aggravates the autoimmune condition by causing translocation of intracellular antigens (frequently nuclear antigens) to the keratinocyte cell membrane. Autoantibodies then bind the translocated cell membrane antigens, and the keratinocytes are subsequently killed by T-cells or monocytes (antibody dependent cellular cytotoxicity).[2] Injured and necrotic keratinocytes release cytokines (IL-1, IL-2, IL-6, and TNF-β), which then recruit and activate B-cells and histiocytes to the sites of injury.[2]

The use of mouse models for human SLE has been recently reviewed and readers are encouraged to consult the article for a thorough discussion of the pathogenesis of SLE.[7]

Contributor: Arkansas Livestock and Poultry Commission Lab
www.arlpc.org

References:

1. Gerhauser I, Strothmann-Lüerssen I, Baumgärtner W. A case of perianal dermatitis in a dog: Is this an unusual manifestation of lupus erythematosus? *Vet Pathol*. 2006;43:761-764.
2. Ginn PE, Mansell JEKL, Rakich PM. Skin and appendages. In: Maxie MG, ed. *Jubb, Kennedy and Palmer's Pathology of Domestic Animals*. Vol. 1, 5th ed. Philadelphia, PA: Elsevier Ltd; 2007:652-654.
3. Goo M-J, Park J-K, Hong I-H, et al. Discoid lupus erythematosus (DLE) in a Spitz dog. *J Vet Med Sci*. 2008;70:633-635.
4. Gross TL, Ihrke P, Walder EJ, Affolter VK. *Skin Diseases of the Dog and Cat*. 2nd ed. Ames, IA: Blackwell Publishing; 2005:52-55, 263-265.
5. Kahn CM, ed. *The Merck Veterinary Manual*. 9th ed. Westhouse Station, NJ: Merck & Co; 2005:2012-2013.
6. Kumar V, Abbas AK, Fausto N, Aster JC. Diseases of the immune system. In: Kumar V, Abbas AK, Fausto N, Aster JC, eds. *Robbins and Cotran Pathologic Basis of Disease*. 8th ed. Philadelphia, PA: Elsevier Saunders; 2009:213-217.
7. Rottman JB, Willis CR. Mouse models of systemic lupus erythematosus reveal a complex pathogenesis. *Vet Pathol*. 2010;47:664-676.
8. Wiemlet SP, Goldschmidt MH, Greek JS, Jeffers JG, Wiemelt AP, Mauldin EA. A retrospective study comparing the histopathological features and response to treatment in two canine nasal dermatoses, DLE and MCP. *Vet Dermatol*. 2004;15:341-348.

CASE IV: 109087E (AFIP 3167325).

Signalment: 7-year-old female Thoroughbred, equine (*Equus caballus*).

History: The horse was referred with a two-month history of multiple papules, round elevated cutaneous lesions with central crusts on the trunk and limbs, and associated scaling and crusting on the head and neck. The lesions were secondarily pruritic. The animal also had reluctance to move associated with distal limb edema. No parasite, bacteria or fungus was identified on skin scrapings, and cytology of the crust revealed the presence of many acantholytic cells and numerous filamentous bacteria consistent with *Dermatophilus congolensis*. The cutaneous lesion quickly spread to the whole body and the animal was euthanized due to progressive loss of body condition and hindlimb pain.

Gross Pathology: The mare had generalized chronic severe crusting, scaling and exfoliative dermatitis, except in the pasterns, associated with emaciation and pitting edema of the hindlimbs.

Histopathologic Description: Haired skin: Sections of skin are characterized by multiple foci within the superficial epidermis, especially the granular layer, consisting of detachment of keratinocytes with loss of cellular bridges, round and well-defined cell borders, and abundant deeply eosinophilic cytoplasm with a viable nucleus characteristic of acantholytic cells. In advanced foci, the acantholysis leads to formation of large subcorneal and intraepidermal clefts of about 300 µm filled with many acantholytic cells admixed with well-preserved neutrophils (acantholytic pustules and vesicles). Acantholytic pustules are also observed in the outer follicular sheaths. Ruptured pustules form numerous thick laminated crusts at the surface of the epidermis where acantholytic cells and non-suppurative neutrophils predominate. The superficial dermis is diffusely thickened by a mild perivascular infiltrate composed of neutrophils and few plasma cells and lymphocytes, associated with moderate capillary congestion and mild superficial edema.

Contributor's Morphologic Diagnosis: Skin : Subcorneal acantholytic vesiculo-pustular dermatitis, chronic severe, characteristic of pemphigus foliaceus in a horse, *Equus caballus*.

Contributor's Comment: Pemphigus foliaceus (PF) is the most common autoimmune skin disease in horses, first described in this species in 1981. Pemphigus foliaceus has also been reported in the dog, cat and goat. There is a lack of breed or sex predilection in horses, even if one case study suggested Appaloosas to be predisposed.[3,4] The disease can occur at any age from few months-old foals to aging horses up to 25 years old. A higher risk in winter and fall has been observed in one case study, but this seasonal pattern was not confirmed in a second one.[3,4] Lesions are generalized crusting, scaling and alopecia first affecting the face, neck, trunk and extremities but often spreading in a few months to involve the whole body. Equine PF can be painful and pruritic. The lower extremities and ventral abdomen often develop edema; the exact pathogenesis of this remains unknown. Systemic signs, such as weight loss, anorexia, fever, anemia, neutrophilia and hypoalbuminemia, have been reported.[2,4] The primary lesion consists of fragile and transient intraepidermal and follicular vesicles evolving into crusting so that the lack of intact pustules in some cases can be a diagnostic challenge.

Diagnosis of PF in horses is based on histologic features and by ruling out differential diagnoses, such as dermatophytosis in the horse. Fungal infection caused by *Trichophyton* spp. has been reported to cause generalized pustular and crusting exfoliative dermatitis with the presence of many acantholytic cells. Acantholysis is thought to be mediated by fungal proteolytic enzymes. A PAS stain can help to exclude such infection from cases of pemphigus foliaceus lacking characteristic subcorneal pustules. Deposition of IgG at epidermal intercellular bridges can be demonstrated by immunofluorescence (IF) or immunohistochemistry (IHC) but is not specific of PF.[2]

"Pemphigus" encompasses a group of blistering skin diseases caused by a type II hypersensitivity response involving production of circulating autoantibodies directed against cellular adhesion proteins of desmosomes. Different forms of pemphigus are recognized based on the level at which the acantholysis occurs within the epidermis according to the location of target antigen (*cf.* Table I). In human beings, PF autoantibodies target the desmosomal protein desmoglein 1 (Dsg1) which is expressed more intensely in the upper layer, explaining the formation of superficial epidermal cleft. Autoantibodies against desmoglein 1 have been reported only in few cases of canine PF where others antibodies are involved.[1] In domestic

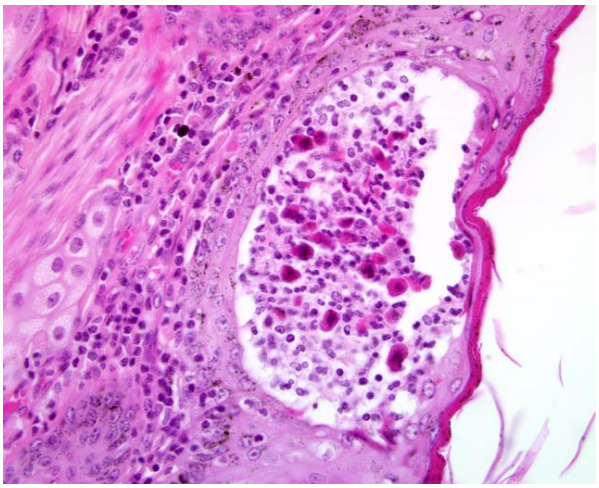

4-1. Haired skin, equine. Intraepidermal pustules are filled with many acantholytic keratinocytes admixed with non-degenerate neutrophils. There is mild lymphoplasmacytic and histiocytic inflammation in the superficial dermis. (HE 400X)

Table I: Autoimmune acantholytic dermatoses in animals

Disease	Species	Distribution	Target	Location of Vesicles
Pemphigus foliaceus (PF)	Dog, Cat, Horse, Goat	Skin	Dsg 1 in human and dog (<10%)	Subcorneal
Pemphigus vulgaris	Dog, Cat, Horse, Goat, Llama, Monkey	Oral mucosa, skin	Dsg 3	Suprabasal
Paraneoplasic pemphigus	Dog	Oral mucosa, skin and non stratified squamous epithelia	Dsg 3 and plakins	Suprabasal
Pemphigus erythematous (variant of PF)	Dog, Cat	Skin (face and feet)		Subcorneal, lichenoid infiltrate
Panepidermal Pustular Pemphigus (PF subtype)	Dog	Oral mucosa, skin		All epidermal layers
Pemphigus vegetans	Dog (one case)	Skin, oral mucosa	Dsg 1	Suprabasal, exophytic hyperplasia

animals PF seems to be an immunologically heteregenous disease.

Acantholysis can result from mechanisms other than autoimmunity;[1] mutations involving genes encoding desmosomal adhesion proteins (genetic acantholytic dermatoses) or infectious proteases produced by some strains of fungus or bacteria can cleave desmosomes (proteolytic acantholytic dermatoses). The following acantholytic dermatoses are described in various species: dermatophytosis caused by *Trichophyton* spp; some staphylococcal infections of dog and swine (such as exfoliative epidermitis caused by *Staphylococcus hyicus* in swine); and bullous impetigo in the dog caused by *Staphylococcus pseudointermedius*. This bacterium (which produces a circulating exfoliative toxin specific for desmoglein-1) induces blisters locally and at sites distant from primary infection. In human beings, a third group of acantholytic dermatoses is recognized as genetic diseases involving mutations in genes encoding desmosomal adhesion proteins. Such genetic acantholysis has rarely been described in the dog and cattle.

AFIP Diagnosis: Haired skin: Dermatitis, superficial, histiocytic and lymphoplasmacytic, diffuse, mild with intra-epidermal pustules, acantholytic keratinocytes, acanthosis, parakeratosis, and pigmentary incontinence.

Conference Comment: The moderator and participants commented on the excellent quality of the specimen. The moderator noted that it is rare to observe such well-developed pustules as seen in this case. Additionally, the large size of the biopsy specimen reduces the chances of tissue loss during processing. The contributor provides an excellent review of the pemphigus complex of diseases in veterinary species, with due attention to pathogenesis as well as the disease manifestation in horses.

Contributor: Department of Pathology, Nantes-Atlantic National College of Veterinary Medicine, Food Science and Engineering - ONIRIS, 44 307 Nantes Cedex 03, France
www.oniris-nantes.fr

References:

1. Olivry T, Linder KE. Dermatoses affecting desmosomes in animals: A mechanistic review of acantholytic blistering skin diseases. *Vet Dermatol*. 2009;20:313-326.
2. Olivry T. A review of autoimmune skin diseases in domestic animals: I – Superficial pemphigus. V*et Dermatol*. 2006;17:291-305.
3. Vandenabeele SI, White SD, Affolter VK, Kass PH, Ihrke PJ. Pemphigus foliaceus in the horse: A retrospective study of 20 cases. *Vet Dermatol*. 2004;15:381-388.
4. Zabel S, Mueller RS, Fieseler KV, Bettenay SV, Littlewood JD, Wagner R. Review of 15 cases of pemphigus foliaceus in horses and a survey of the literature. *Vet Rec*. 2005;157:505-509.

The Armed Forces Institute of Pathology
Department of Veterinary Pathology

Conference Coordinator
Matthew Wegner, DVM

WEDNESDAY SLIDE CONFERENCE 2010-2011

Conference 25

23 March 2011

Conference Moderator:
JoLynne Raymond, DVM, Diplomate ACVP

CASE I: 03N2865 (AFIP 2936141).

Signalment: 10-month-old female Siamese, feline (*Felis catus*).

History: Previous history includes persistently thin body condition despite a voracious appetite. This young cat presented to the VMTH Emergency Service after being found obtunded and seizuring by the owners. On physical examination, the cat exhibited generalized seizures and was soaked in urine. The cat was hypothermic (84.5ºF), dehydrated (10%), and had weak femoral pulses. Initial diagnostic procedures revealed metabolic and respiratory acidosis with elevated blood lactate. Urine specific gravity was 1.010. Seizures were controlled with IV phenobarbital; however, the cat went into respiratory and cardiovascular arrest three hours after presentation and resuscitation was unsuccessful.

Gross Pathology: On post-mortem examination, there was severe, segmental, nodular thickening of medium-sized blood vessels throughout the mesentery. Intercostal vessels and the coronary arteries along the coronary and interventricular groove were similarly affected. Multiple triangular depressions were noted bilaterally in the renal cortices that extended to a point at the corticomedullary junction. On cut section of the kidneys, the arcuate blood vessels were prominent and the vessel walls were markedly thickened. Lymphoid hyperplasia was noted in the mesenteric lymph nodes and duodenal mucosal lymphoid patches.

Laboratory Results:
Body Temp: 96.0º F.
pH: 7.015.
CO_2 total: 18.1.
Glucose: 60 mg/dL
Aerobic and anaerobic culture of the lung yielded no significant growth.

Histopathologic Description: Kidney: In the examined sections of kidney, there is a severe proliferative and inflammatory process affecting medium and small arteries, primarily at the corticomedullary junction and hilus. In affected vessels the tunica media and intima are markedly

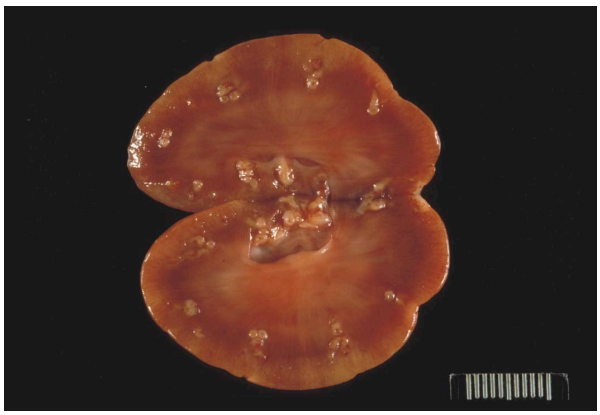

1-1. Kidney, cat. On cut surface the arcuate blood vessels are prominent and the vessel walls are markedly thickened. Photograph courtesy of Veterinary Medical Teaching Hospital (VMTH), Anatomic Pathology, University of California, Davis.

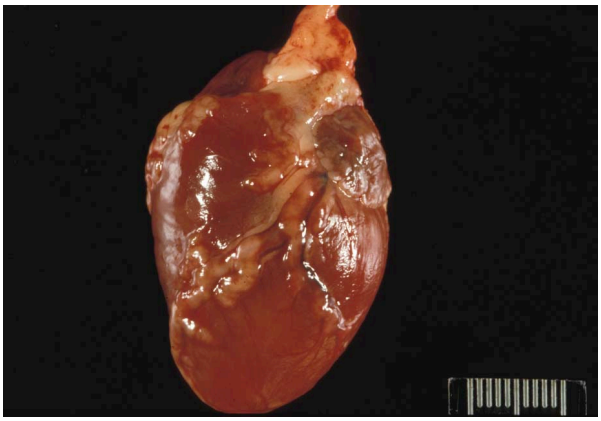

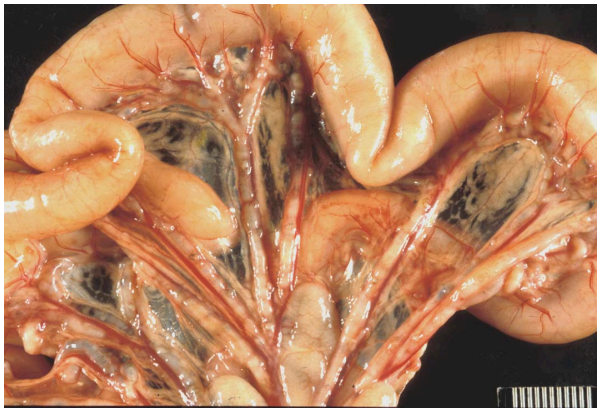

1-2, 1-3. Heart and small intestine, cat. Coronary (1-2) and mesenteric (1-3) arteries demonstrate severe, segmental, nodular thickening. Photographs courtesy of Veterinary Medical Teaching Hospital (VMTH), Anatomic Pathology, University of California, Davis.

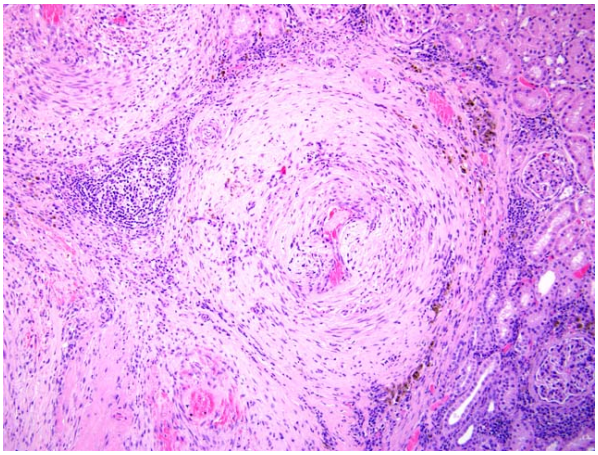

1-4. Kidney, arteries, cat. The tunica media and intima are markedly expanded by hypertrophied and hyperplastic spindle cells (smooth muscle and fibroblasts) which greatly restrict the lumen. There are adjacent periarterial and periglomerular lymphoid infiltrates. (HE 100X)

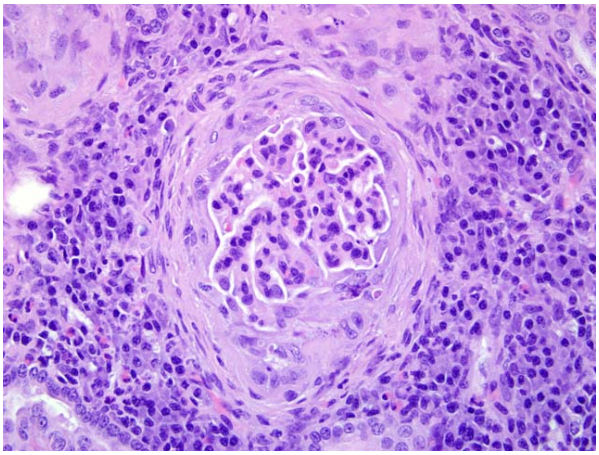

1-5. Kidney, cortex, cat. There are glomerular synechiae and periglomerular fibrosis, and the adjacent cortical interstitium contains lymphoplasmacytic inflammation. (HE 400X)

expanded by increased numbers of plump spindle cells (smooth muscle cells and fibroblasts), greatly reducing or obstructing the vessel lumen. The connective tissue and smooth muscle in the vessel walls are hyalinized and separated by wispy basophilic material, hemorrhage, brightly eosinophilic fibrillar material (fibrin/fibrinoid necrosis), and occasional globular, amorphous eosinophilic deposits (amyloid via Congo red staining). The internal elastic lamina is often irregular or split, endothelial cells are plump and reactive, and there are profiles of small arterioles in the tunica media of severely affected vessels. There is a variable inflammatory infiltrate within and surrounding affected vessels characterized by moderate numbers of plasma cells and lymphocytes, with fewer neutrophils, eosinophils and mast cells. Clusters of hemosiderin-laden macrophages are within and surrounding many affected vessels. There are several wedge-shaped regions of intense interstitial inflammation and fibrosis extending from the corticomedullary junction. In these areas the inflammation is comprised of lymphocytes, plasma cells, and fewer eosinophils and dense bands of fibrous connective tissue surround remaining tubules and variably sclerotic glomeruli. Prominent lymphoid follicles with central necrosis surround blood vessels throughout the sections.

Contributor's Morphologic Diagnosis: 1. Kidney, small and medium arteries: Severe, segmental, chronic-ongoing, necrotizing and proliferative arteritis.
2. Kidneys: Multifocal subacute infarction and multifocal severe lymphoplasmacytic interstitial nephritis.
3. Kidneys Marked perivascular lymphoid hyperplasia with lympholysis.

Contributor's Comment: The number of tissues affected by the vasculopathy in this cat was extensive and included the arcuate arteries in the kidney, the coronary arteries, the mesenteric and serosal arteries, the cervical arteries adjacent to the thyroid gland, and the intercostal arteries. In all affected tissues, the arteriopathy was characterized by extensive intimal and medial smooth muscle hyperplasia and fibrosis, segmental fibrinoid necrosis, variable non-suppurative arteritis and segmental amyloidosis. As small arteries in the brain were similarly affected, the seizures and

eventual death in this cat were attributed to vascular compromise and hypoxia in the brain and heart. Amyloid deposition was noted in many tissues, including the spleen, thyroid gland, liver, stomach and intestinal mucosa and affected vasculature. The amyloid was confirmed to be type AA, or reactive amyloid, via potassium permanganate staining and was attributed to long-standing vascular inflammation. Marked lymphoid hyperplasia, with lymphoid necrosis and lympholysis, was also a prominent finding in many lymphoid and parenchymal organs, including the kidneys. These changes are reminiscent of lymphoid tissue response in viral infections, such as Type D retroviral infection in non-human primates[7] and feline immunodeficiency virus (FIV) in cats.[11]

The severe vascular lesions in this cat resemble those found in polyarteritis nodosa in humans and other animal species.[5,13] Classic polyarteritis nodosa is characterized by segmental, transmural, necrotizing inflammation of medium and small muscular arteries. The most commonly affected blood vessels are in the kidneys, heart, liver, and gastrointestinal tract, sparing the pulmonary circulation, similar to the distribution of lesions in this cat. Affected vessels are in varying stages of necrosis, and in chronic stages there is marked fibrous thickening of the vessel walls creating a nodular appearance to affected vasculature. In humans, segmental erosion and weakening of arterial walls can lead to aneurysmal dilatation and rupture. It is hypothesized that an inflammatory stimulus (autoimmune disease, viral, bacterial, fungal or protozoal infection) incites the vascular lesions; however, no one etiology has been implicated as a definitive cause of the disease in either humans or animal species. In humans, polyarteritis nodosa is associated with hepatitis B virus in approximately 30% of cases, and is rarely associated with anti-neutrophil cytoplasmic antibodies (ANCA).[13] There are several older reports of proliferative vascular lesions in cats; however, in all of these reports an underlying etiology for the vasculopathy was not determined.[1,4] A proliferative arteriopathy has also been described in cows affected by malignant catarrhal fever[10] and in non-human primates with simian immunodeficiency virus (SIV) infection.[3] Polyarteritis nodosa has also been reported in beagle dogs[14] and laboratory rats;[12] however, the etiology remains unknown.

Numerous histochemical stains (Giemsa, PAS, acid fast, Brown and Benn, and GMS) were completed on affected tissues in this cat in an attempt to identify possible infectious agents; however, all stains were negative. Immunohistochemical stains were also completed on affected tissue using antibodies against *Sarcocysis neurona*, *Neospora* spp., *Toxoplasma gondii*, feline enteric coronavirus (FIP), feline leukemia virus (FeLV), and bacillus of Calmette-Guerin (BCG). Antibodies against IgG (1:2000 dilution) were not immunoreactive in these sections. Other antibodies against other immunoglobulins were not available. In sections of the thymus, spleen, and bone marrow, a few lymphoid cells expressed FeLV antigen. As the number of positive staining cells was minimal and the FeLV status is unknown for this cat, it is not possible to definitively determine whether the positive staining is indicative of viral infection. All other stains were negative. A section of kidney submitted for PCR analysis for FeLV, feline immunodeficiency virus (FIV), and feline herpesvirus-1 was negative. Serum was not available for diagnostic procedures.

AFIP Diagnosis: 1. Kidney, medium and small arteries: Arteritis, proliferative and necrotizing, multifocal, marked with periarterial lymphoid hyperplasia.
2. Kidney: Nephritis, cortical, interstitial, lymphoplasmacytic, multifocal to coalescing, moderate with synechiae, senescent glomeruli, and periglomerular fibrosis.

Conference Comment: Participants engaged in discussion of the pathogenesis of immune-mediated arteritis. The authors of *Robbins and Cotran Pathologic Basis of Disease* describe three phases in type III hypersensitivity.[6] The first phase involves generation of antigen-antibody complexes around one week after antigen exposure. Secreted antibody binds to antigen present in the systemic circulation. Antigen-antibody complexes are deposited in a variety of tissues during the second phase. The final phase involves immune-mediated damage to the affected tissues via immune complex binding and complement fixation; these complexes are recognized by neutrophil Fc and complement C3b receptors. Release of neutrophil contents results in local tissue damage, necrosis and subsequent inflammation. As the vascular inflammatory process progresses, neutrophils are replaced by mononuclear leukocytes. In many cases, antigen complexes are rapidly cleared from the lesion, and therefore are not detected during testing for the presence of IgG and/or IgM; thus, failure to detect immunoglobulin does not exclude an immune-mediated process.[6]

In response to the immune-mediated inflammation and damage, the vasculature must begin the reparative process. The two cell types involved in vascular repair are the endothelial cells and vascular smooth muscle cells of which the smooth muscle cells are most prominent. Regulation of smooth muscle proliferation is accomplished through a balance of promoters and inhibitors of proliferation. Platelet-derived growth factor, thrombin, fibroblast growth factor, IFN-γ, and IL-1 promote proliferation, while heparin sulfate, nitric oxide, and TGF-β are inhibitory.[9] Vascular injury with endothelial damage or loss stimulates smooth muscle cell proliferation. The increase in smooth muscle cells results from recruitment from the tunica media; recruitment and differentiation of smooth muscle precursor cells; and proliferation of local smooth muscle cells through mitosis.[9] In addition to proliferation, smooth muscle cells also produce extracellular matrix, much the same as occurs in wound healing, resulting in a "scar" of fibrous connective tissue and smooth muscle cells.[8]

Conference participants reviewed some of the diseases resulting in proliferative arteritis in veterinary species.[8]

- Ox: Malignant catarrhal fever (ovine herpesvirus 2)
- Rat: Polyarteritis nodosa
- Non-human primates: Associated with Simian immunodeficiency virus in macaques
- Dog: Beagle pain syndrome
- Mink: Aleutian disease of mink

Contributor: Veterinary Medical Teaching Hospital (VMTH), Anatomic Pathology, University of California, Davis

References:

1. Altera KP, Bonasch H. Periarteritis nodosa in a cat. *J Am Vet Med Assoc*. 1966;149:1307-1311.
2. Campbell LH, Fox JG, Drake DF. Ocular and other manifestations of periarteritis nodosa in a cat. *J Am Vet Med Assoc*. 1972;161:1122-1126.
3. Chalifoux LV, Simon MA, Pauley DR, MacKey JJ, Wyand MS, Ringler DJ. Arteriopathy in macaques infected with simian immunodeficiency virus. *Lab Invest*. 1992;67:338-349.
4. Curtis R, Laing PW. Polyarteritis in a cat. *Vet Rec*. 1979;105:354.
5. Jubb KVF, Kennedy PC, Palmer N. Cardiovascular system. In: *Pathology of Domestic Animals*. 4th ed. Vol. 3. San Diego, CA: Academic Press Inc; 1993:67-68.
6. Kumar V, Abbas AK, Fausto N, Aster JC. Diseases of the immune system. In: Kumar V, Abbas AK, Fausto N, Aster JC, eds. *Robbins and Cotran Pathologic Basis of Disease*. 8th ed. Philadelphia, PA: Elsevier Saunders; 2009:204-205
7. Lowenstin LJ. Type D retroviral infection, macaques. In: Jones TC, Mohr U, Hunt RD, eds. *Nonhuman primates I*, Berlin, Germany: Springer-Verlag; 1993:20-32.
8. Maxie MG, Robinson WF. Cardiovascular system. In: Maxie MG, ed. *Jubb, Kennedy and Palmer's Pathology of Domestic Animals*. Vol. 1, 5th ed. Philadelphia, PA: Elsevier Ltd; 2007:69-71.
9. Mitchell RN, Schoen FJ. Blood vessels. In: Kumar V, Abbas AK, Fausto N, Aster JC, eds. *Robbins and Cotran Pathologic Basis of Disease*. 8th ed. Philadelphia, PA: Elsevier Saunders; 2009:490-492.
10. O'Toole D, Li H, Roberts S, et al. Chronic generalized obliterative arteriopathy in cattle: A sequel to sheep-associated malignant catarrhal fever. *J Vet Diagn Invest*. 1995;7:108-121.
11. Parodi AL, Femenia F, Morillon A, Crespeau F and Fontaine JJ. Histopathological changes in lymph nodes of cats experimentally infected with the feline immunodeficiency virus. *J Comp Pathol*. 1994;111(2): 165-174.
12. Percy DH, Barthold SW. *Pathology of Laboratory Rodents and Rabbits*. 2nd ed. Ames, IA: Iowa State University Press; 2001:153-154.
13. Schoen FJ, Cotran RS. Blood vessels. In: Cotran R S, Kumar V, Collins T, eds. *Robbins Pathologic Basis of Disease*. 6th ed. Philadelphia, PA: W.B. Saunders; 1999:515-521.
14. Synder PW, Kazacos EA, Scott-Moncrieff JC, et al. Pathologic features of naturally occurring juvenile polyarteritis in beagle dogs. *Vet Pathol*. 1995;32:337-345.

CASE II: 09-093 (AFIP 3162471).

Signalment: 5-month-old male New Zealand white rabbit (*Oryctolagus cuniculi*).

History: This animal had not been used for any experimental purposes. On a Saturday, the animal was noted to have bilateral mucopurulent nasal discharge, lethargy, dehydration, and an unkempt coat with fecal and urine staining. A culture of the nasal exudate was taken, and the animal was empirically started on parenteral enrofloxacin. On Monday, the animal was anesthetized with intramuscular ketamine and xylazine and euthanatized with intravenous pentobarbital.

Gross Pathology: The forepaws and muzzle area were stained with a moderate amount of dried yellow purulent exudate apparently originating from the nares. Nares were crusted over with mucopurulent discharge. Bilaterally, the nasal cavities contained approximately 0.5 mL viscous creamy suppurative exudate each, with mild atrophy of the nasal turbinates. Neither tympanic bulla contained any exudate or evidence of inflammation.

In the thoracic cavity, the cranioventral lung lobes, particularly the left cranial and middle lobes, were affected by multifocal to coalescing areas of necrosuppurative inflammation with extension to the pleura. No exudate was noted within the trachea. A culture was taken from the lung parenchyma. The caudodorsal lung lobes were noted to be slightly enlarged and firm with rib impressions. There was no evidence of infection or inflammation in the brain or meninges.

Laboratory Results:

1. Nasal culture: 4+ *Bordetella bronchiseptica*; 3+ *Pasteurella* spp. (not *P. multocida*); 3+ coagulase-negative *Staphylococcus*; 2+ non-hemolytic *Streptococcus*; 2+ microaerophilic *Streptococcus*; 1+ *Actinobacter* species.
2. Lung culture: No growth.
3. Serology was negative for *Pasteurella multocida.*

Histopathologic Description: Lung: There are two discrete pathologic processes present in the lung, with variable proportions on different slides. Filling the lumina of bronchi, bronchioles, and alveoli, and occasionally effacing normal alveolar architecture, are large numbers of predominantly degenerate heterophils admixed with necrotic cellular debris and variable amounts of fibrillar eosinophilic proteinaceous material (fibrin). In some sections, there is focally extensive coagulative necrosis of the lung parenchyma with preservation of tissue architecture and hypereosinophilic ghost cells (infarction) as well as overt abscessation. The Brown and Hopps tissue Gram stain shows low to moderate numbers of intralesional gram-negative rods.

Multifocally to diffusely, alveolar spaces are filled with flocculent eosinophilic proteinaceous material with low to moderate numbers of intra-alveolar macrophages, often with abundant foamy cytoplasm. Alveoli are lined by plump cuboidal epithelial cells, creating an adenomatous appearance (type II pneumocyte hyperplasia). Scattered sloughed necrotic pneumocytes with hypereosinophilic cytoplasm and pyknotic, karyorrhectic or karyolytic nuclei are present in alveoli. Within the clear spaces of the intra-alveolar proteinaceous material there are 1-2 µm faintly basophilic coccoid organisms. These organisms are visualized with Wright-Giemsa, toluidine blue, and Gomori methenamine silver stains.

Low numbers of heterophils and eosinophils can be seen in the adventitia and intima of scattered small and medium pulmonary arteries. This is a commonly observed change in rabbits, and has been associated with the use of ketamine/ xylazine anesthetic.[4]

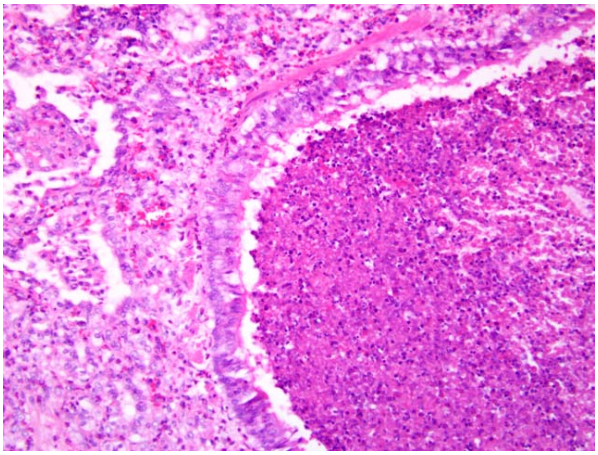

2-1. Lung, rabbit. Filling the lumina of bronchi, bronchioles, and alveoli, and occasionally replacing alveolar architecture, are many degenerate neutrophils admixed with abundant necrotic cellular debris. (HE 200X)

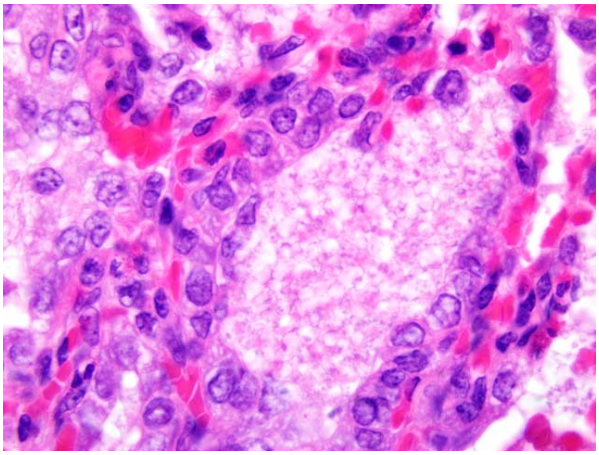

2-2. Lung, rabbit. Alveolar septa are thickened and lined by hypertrophied type II pneumocytes and alveoli are filled with flocculent eosinophilic proteinaceous material containing many fungal trophic forms surrounded by a clear halo. (HE 1000X)

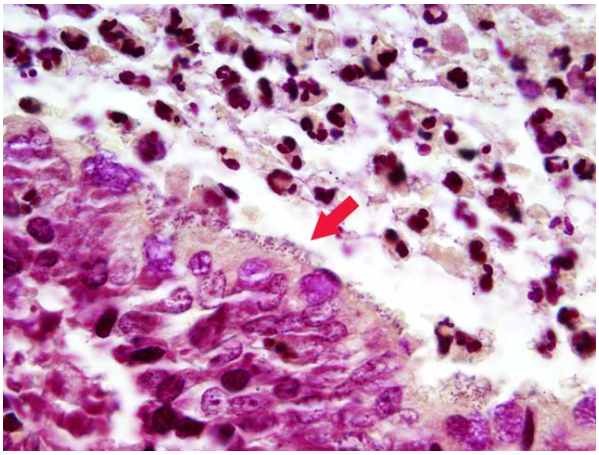

2-3. Lung, rabbit. The Brown-Hopps method tissue gram stain demonstrates Gram negative ciliotropic bacilli along the respiratory epithelium (arrow) and within the lumen. (1000X)

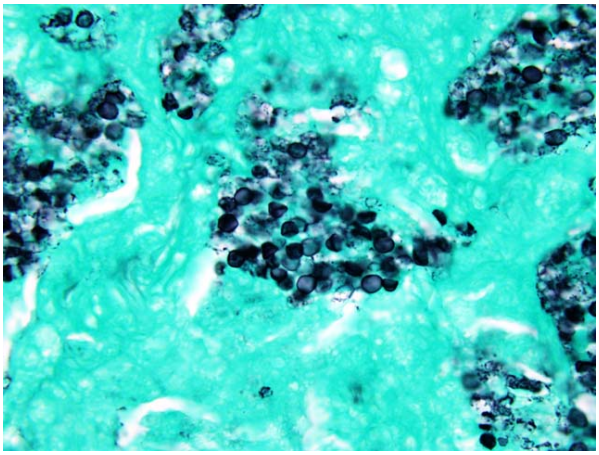

2-4. Lung, rabbit. Many Pneumocystis species trophic forms are demonstrated in alveoli by the Gomori methenamine silver stain. (GMS 1000X)

Contributor's Morphologic Diagnosis: 1. Lung, bronchopneumonia, necrosuppurative, subacute, multifocal, severe.
2. Lung, alveolitis, histiocytic, chronic, multifocal to coalescing, severe, with type II pneumocyte hyperplasia, eosinophilic intra-alveolar flocculent exudate and intra-lesional fungal trophic forms.

Contributor's Comment: Clinically, grossly, and histologically, this animal presented with the classic lesions of pasteurellosis (snuffles).[6] However, *Pasteurella multocida* was not isolated from the nasal culture, nor have routine deep nasal cultures of diagnostic rabbit necropsies at this institution yielded any animals positive for *P. multocida*. Additionally, this animal had negative titers for *P. multocida* in serum obtained before necropsy. *Bordetella bronchiseptica* was isolated in a mixed culture from the nasal exudate. This agent typically causes a less severe and more indolent disease in rabbits, characterized by a more purulent and less necrotizing pneumonic process.[6] It is suspected that the same factors allowing the overgrowth of *Pneumocystis oryctolagi* resulted in the more aggressive clinical course of *B. bronchiseptica* in this animal.

Pneumocystosis was an unexpected finding in this animal, as there were no experimental manipulations or known reasons for immunosuppression. *Pneumocystis oryctolagi* (formerly *P. carinii* f.sp. *oryctolagi*) specifically colonizes the type I alveolar epithelial cells (pneumocytes) of Old World rabbits, and Dei-Cas *et al.* provide an excellent review of this[4] and other *Pneumocystis* species.[1] *Pneumocystis* species are highly host adapted, and display genetic co-phylogeny/co-speciation with their hosts.[1] No significant cross-species colonizations have been reported to occur, even in SCID mice and nude rats. The trophic forms of *Pneumocystis* organisms have filopodia that penetrate host epithelial cell cytoplasm without disruption of the cell membrane or apparent alteration of host cell structure or function.[4] The ultrastructural characteristics of these filopodia are species-specific.

Rabbits have a characteristic and consistent age-dependent pattern of colonization with *P. oryctolagi*.[4,8] Although initial experiments in rabbits dating back to the 1950s used corticosteroids to visualize pneumocystosis, it was later observed that spontaneous subclinical pneumocystosis was histologically evident at the time of weaning (approximately 4-6 weeks of age). Transplacental infections may occur.[7] Colonization results in diffuse lung histology changes as well as serum biochemical abnormalities, but these changes spontaneously resolve within 3-4 weeks, such that very few organisms are detectable in 60 to 90 day old rabbits. This pattern of colonization is hypothesized to be due to the decline of maternal antibodies (passive immunity) prior to the acquisition of active immunity.[8] Spontaneous pneumocystosis in weanling rabbits typically presents a unique and characteristic histologic pattern wherein individual widely spaced organisms line the alveolar epithelium, in contrast to the typical appearance of pneumocystosis in mice, rats, non-human primates and man (as well as this case), where crowded organisms fill the alveolar lumen.[3] Additionally, the flocculent eosinophilic (honeycomb) proteinaceous exudate typical of pneumocystosis in other species is rarely seen in weanling rabbits. It should be noted that the age of this rabbit (5 months) is well beyond that of weaning.

Pneumocystis organisms have two distinct forms in tissue sections: the trophic form (formerly trophozoite); and the cystic form. Trophic forms are irregular in size and shape, 2-8 µm, with a well stained nucleus. Cystic forms are 4-7 µm with a thick cell wall. This cell wall remains unstained with Wright-Giemsa and H&E stains, creating a halo effect around the organism. The number of nuclei present varies from 1-8, depending upon maturity (8 in mature cysts, fewer in sporocyte stages).

Other described species of *Pneumocystis* include *P. murina* in mice, *P. carinii* and *P. wakefieldiae* in rats, and *P. jirovecii* in man. *Pneumocystis* has also been identified in non-human primates, ferrets, horses, pigs, shrews, and dogs.[1,2]

AFIP Diagnosis: 1. Lung: Pneumonia, necrosuppurative, multifocal, moderate.
2. Lung: Pneumonia, interstitial, histiocytic, multifocal to coalescing, marked with type II pneumocyte hyperplasia and myriad intralesional fungal trophic forms, etiology consistent with *Pneumocystis* species.

Conference Comment: All conference participants readily diagnosed and agreed with necrosuppurative pneumonia; participants commented on section variability, with some slides having evidence of bronchopneumonia. Few participants recognized the additional histiocytic interstitial pneumonia associated with *Pneumocystis oryctolagi*. The moderator commented that the findings of eosinophilic flocculent material within alveoli and type II pneumocyte hyperplasia are highly suggestive of pneumocystosis, regardless of the host species. The moderator commented that rabbits are unique as an animal model of pneumocystosis because they can develop spontaneous disease without the administration of glucocorticoids, which is required in models utilizing mice, rats and ferrets. The contributor provides an excellent review of pneumocystosis in the rabbit, as well as a brief review of the disease in other veterinary species.

Bordetella bronchiseptica has several virulence factors which contribute to the development of disease. Upon colonization of the host, a group of genes regulated by the *Bordetella* virulence group (*bvg*) operon is expressed, particularly adhesion proteins such as filamentous hemagglutinin (FHA), pertactin, and fimbriae. Expression of virulence factors regulated by the *bvg* operon depends on environmental conditions; activation of virulence factors occurs at 37ºC, whereas a temperature of 25ºC or the presence of sulfate or nicotinic acid is inhibitory. The expression of adhesion proteins allows bacterial attachment to the ciliated epithelium of the respiratory tract, which is followed by another round of expression of *bvg*-regulated genes. These proteins are involved in motility, iron scavenging, and the activity of various enzymes like urease and phosphatases.[2]

Several exotoxins also are involved in the pathogenesis of primary *B. bronchiseptica* infection. One of the most important and destructive toxins is a hemolysin, adenylate cyclase, which is an RTX toxin with similar activity to the RTX toxin produced in bovine mannheimiosis and the Apx toxin of porcine pleuropneumonia. The toxin forms pores in host leukocytes which allows the functional part of the adenylate cyclase to enter the host cell. This results in increased production of cyclic adenosine monophasphate and suppresses phagocytosis and the oxidative burst necessary for clearing the infection. There is also production of peptidoglycan-derived tracheal toxin which stimulates host cell nitric oxide production; nitric oxide is ciliostatic and induces apoptosis of respiratory epithelium. Bacterial FHA also binds to histiocyte complement receptors, resulting in uptake of the bacteria which subsequently survive by inhibiting the oxidative burst. *Bordetella bronchiseptica* bacteria also have the ability to secrete adenylate cyclase while in histiocytes, resulting in apoptosis.[2]

Participants reviewed causes of necrosuppurative pneumonia in other veterinary species.

- Pig: *Actinobacillus pleuropneumoniae*
- Ox, sheep: *Mannheimia haemolytica*
- Guinea pigs: *Bordetella bronchiseptica*
- Rat: CAR bacillus; *Corynebacterium kutscheri*
- Non-human primate: *Streptococcus pneumoniae*; *Klebsiella pneumoniae*

Contributor: Department of Comparative Medicine, H054, Penn State Milton S. Hershey Medical Center, Penn State College of Medicine, 500 University Dr, Hershey, PA, 17033-0850
http://www.hmc.psu.edu/comparativemedicine/

References:
1. Aliouat-Denis CM, Chabe M, Demanche C, et al. *Pneumocystis* species, co-evolution and pathogenic power. *Infect Genet Evol.* 2008;8:708-726.
2. Caswell JL, Thompson KJ. Respiratory system. In: Maxie MG, ed. *Jubb, Kennedy and Palmer's Pathology of Domestic Animals*. Vol. 2, 5th ed. Philadelphia, PA: Elsevier Ltd; 2007:638-639.
3. Dei-Cas E, Brun-Pascaud M, Bille-Hansen V, Allaert A, Aliouat EM. Animal models of pneumocystosis. *FEMS Immunol Med Microbiol.* 1998;22:163-168.
4. Dei-Cas E, Chabe M, Moukhlis R, et al. *Pneumocystis oryctolagi* sp. nov., an uncultured fungus causing pneumonia in rabbits at weaning: Review of current knowledge, and description of a new taxon on genotypic, phylogenetic and phenotypic bases. *FEMS Microbiol Rev.* 2006;30:853-871.
5. Marini RP, Li X, Harpster NK, Dangler C. Cardiovascular pathology possibly associated with ketamine/xylazine anesthesia in Dutch belted rabbits. *Lab Anim Sci.* 1999;49:153-160.
6. Percy D, Barthold, SW. *Pathology of Laboratory Rodents and Rabbits*. 3rd ed. Ames, IA: Blackwell Publishing; 2007:65-67,143-146.
7. Sanchez CA, Chabe M, Aliouat el M, et al. Exploring transplacental transmission of *Pneumocystis oryctolagi* in first-time pregnant and multiparous rabbit does. *Med Mycol.* 2007;45:701-707.
8. Tamburrini E, Ortona E, Visconti E, et al. *Pneumocystis carinii* infection in young non-immunosuppressed rabbits. Kinetics of infection and of the primary specific immune response. *Med Microbiol Immunol.* 1999;188:1-7.

CASE III: RB040-2959 (AFIP 3164422).

Signalment: 3.5-year-old male New Zealand white (NZW) rabbit (*Oryctolagus cuniculus*).

History: A 3.5-year-old intact male NZW apo-AI and LCAT (apolipoprotein and lecithin:cholesterol acyltransferase) double transgenic rabbit initially presented with a discrete raised 0.5 x 1.0 x 1.0 cm mass on the face approximately one centimeter rostral to the medial canthus of the left eye. The facial mass was surgically removed as an excisonal biopsy. Within three months, the mass had recurred and was raised and ulcerated, measuring 4.0 x 2.0 x 1.5 cm. A second surgery was performed to resect the tumor with wider margins. Over the next three weeks, the rabbit's condition declined and the rabbit developed respiratory distress and died acutely.

Gross Pathology: At necropsy, there was a healed incision at the site of the excisional biopsy. One facial mass was 1.5 x 2.5 x 3.5 cm white, resilient, somewhat lobulated and a similar, 1.0 x 1.0 x 1.5 cm mass was present caudal to the first mass. Two subcutaneous masses were present between the rami of the mandible. Within all lung lobes there were multifocal to coalescing, firm, grayish-white variably sized masses which measured up to 7 mm in diameter. The masses extended into the parietal pleura and multifocally within the diaphragm. Lesions were not observed in any other major organs.

Histopathologic Description: Haired skin: Histological examination of the original excised skin biopsy revealed a raised mass that invaded into the dermis which was partially ulcerated, non-encapsulated and well-delineated composed of tightly packed polygonal to spindle cells with a fine fibrovascular stroma. The cells were moderately anisocytotic and anisokaryotic with moderate, lightly eosinophilic finely granular cytoplasm with indistinct cell borders. Nuclei were round to oval, with finely stippled chromatin and 1-4 nucleoli; mitoses were frequent at 5 to 7/hpf. Vascular invasion was evident, with tumor cells present within multiple venules and lymphatic vessels in multiple tissues. Within the skin, neoplastic cells were seen fingering into the adjacent dermis and extended to the cut border of the facial mass. Similar neoplastic foci with a packeting of cells were present in the submandibular lymph nodes, lungs, parietal pleura, and liver. Tumor cell morphology in these metastatic sites resembled the morphology of the tumor from the excisional biopsies.

The masses from the biopsies and necropsy were stained for Fontana-Masson method (melanin stain); results were negative. Immunohistochemistry (IHC) demonstrated positive cytoplasmic staining for vimentin in both polygonal and spindle cells. There was positive cytoplasmic staining for Mart-1 and S-100 protein in the polygonal cells, but negative staining in the spindle cells. Staining with actin, HHF35, AE1/AE3, HMB-45, SMA and tyrosinase were negative.

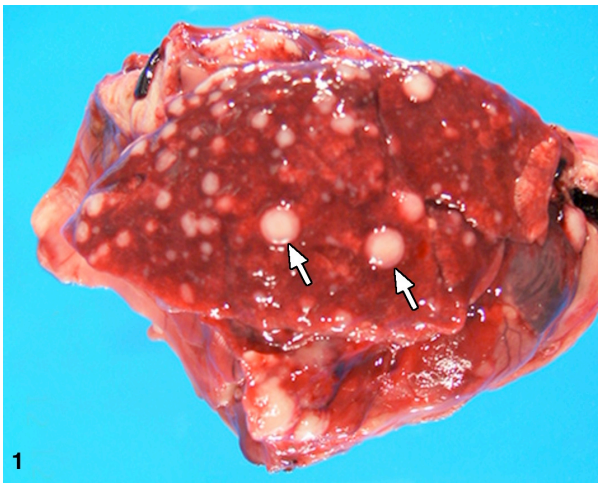

3-1. Lung, amelanotic melanoma, rabbit. Within all lung lobes there are multifocal to coalescing firm grayish-white variably sized masses measuring up to 7 mm in diameter. Photograph courtesy of National Institutes of Health, Division of Veterinary Resources.

Transmission electron microscopy (TEM) of the neoplastic cells revealed small numbers of clustered stage II melanosomes with a size range of 100-900 nm with myelin-like membranes in sheets.

Contributor's Morphologic Diagnosis: Skin, Melanoma, amelanotic.

Contributor's Comment: This case of an amelanotic melanoma in an albino rabbit is rare. Albinism is an autosomal recessive disorder in which there are an adequate number of normally distributed melanocytes, but the melanin is not synthesized in a great enough quantity due to a point mutation in the gene for tyrosinase. Amelanotic melanomas have been reported in human albinos and experimentally induced in albino guinea pigs.[18,22] Human amelanotic melanomas are rare, only accounting for 5% of all melanoma cases.[22] While melanomas are most commonly found in skin, any tissue that has melanin can be a site of tumor development.[11]

Melanomas are uncommon in rabbits.[2,3,4,9,10,21] Amelanotic melanomas are extremely rare, with only one report in the literature.[10] The first case of melanoma in a rabbit was reported over 80 years ago.[20] Melanomas have been reported in pet and laboratory rabbits, with the NZW strain being over-represented.[10] In a retrospective study at the School of Veterinary Medicine at the University of Pennsylvania of 179 pet rabbits with a total of 190 tumors, eight were diagnosed as malignant melanoma by H&E and IHC.[3] These melanomas were located on the skin of the pinna, eyelid, head, limb and scrotum. These melanomas had the typical appearance of aggressively growing tumors with high cellular pleomorphism and high numbers of mitotic figures. All tumors contained abundant melanin.[3]

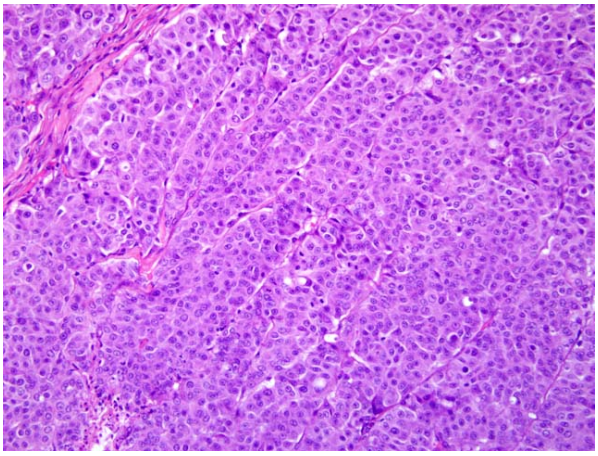

3-2. Haired skin, amelanotic melanoma, rabbit. The dermis is effaced by a densely cellular neoplasm composed of polygonal to spindle cells arranged in vague packets and supported by a scant fibrous stroma. (HE 200X)

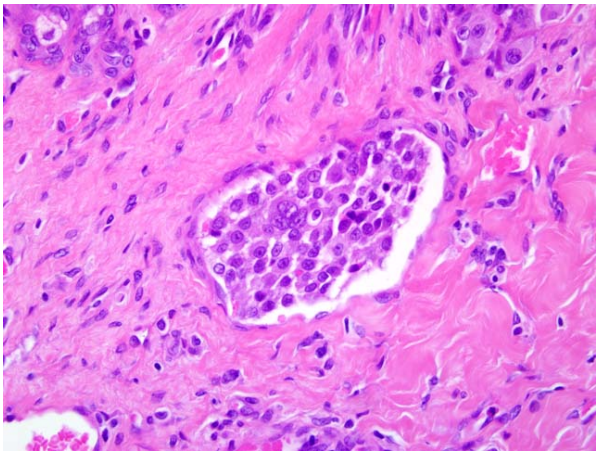

3-3. Haired skin, melanoma, rabbit. Multifocally neoplastic cells are within the lumen of vessels. (HE 400X)

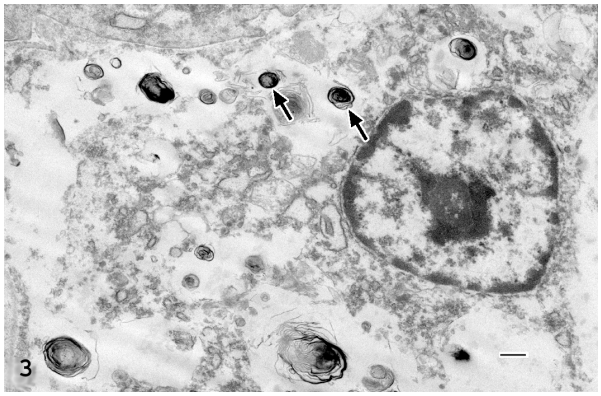

3-4. Melanoma, rabbit. Transmission electron microscopy of neoplastic cells reveals small numbers of clustered stage II melanosomes with a size range of 100-900 nm with myelin-like membranes in sheets (arrows). Photograph courtesy of National Institutes of Health, Division of Veterinary Resources.

Melanomas have been reported in other species, including the cat,[15] opossum,[15] monkey,[19] rat,[14] dog,[11] ferret[24] and horse.[16] Melanomas account for 7% of all malignant tumors in dogs, and are most often found in the oral cavity with metastases commonly occurring in the lung and lymph nodes. Metastases also can be found in the brain, heart and spleen and, in rare cases, the bone marrow.[13] Melanomas are very rare in cats, with only 4 diagnosed out of 3145 cats or 0.1% necropsied at the Animal Medical Center in New York. The most common site was intraocular with metastasis in 63% of the cases. Tumors thicker than two millimeters in human cases often metastasize to lymph nodes, skin, subcutaneous tissue, lung, liver, small intestine, pancreas, heart, brain, and spleen.[11]

The ability for melanomas to express a wide range of antigens complicates the diagnosis. Antibodies key to differentiating melanomas include S-100, HMB-45, Mart-1 and MiTF.[23] Many times IHC is necessary for a definitive diagnosis of melanomas due to their ability to be the "great pretender". In the present case, the neoplasm was undifferentiated and contained both spindle and polygonal cells. The initial biopsy closely mimicked a basal cell carcinoma; however, the pan-cytokeratin stain was negative. To rule out melanoma, a Fontana-Masson stain was performed and was negative for melanin. Next, a panel of antibodies was used, revealing the mass to be diffusely vimentin positive; yet, only Mart-1 and S-100 were positive in the polygonal cells. The inconclusiveness of negative spindloid staining warranted TEM.

Transmission electron microscopy can be utilized to show melanin granules that may be few in number and small in size.[5] The melanosomes generally are granular, myelin-like with shapes including oval, round, spindle-shaped, rod-like, or irregular, and are found singular not in groups. The present case demonstrated features of type II melanosomes.

AFIP Diagnosis: Haired skin and subcutis: Malignant melanoma, amelanotic.

Conference Comment: Participants reviewed common spontaneous cutaneous neoplasms in the rabbit, including those induced by viruses. The recent publication cited by the contributor provides a comprehensive review of the more common cutaneous neoplasms in rabbits. Briefly, trichoblastomas are most common, followed by Shope fibroma, lipoma, myxosarcoma, malignant peripheral nerve sheath tumor, and fibrosarcoma. Of those tumors, Shope fibroma is induced by viral infection with rabbit fibromavirus. Shope papillomas, another viral-induced skin tumor, is caused by a papovavirus. The included chart summarizes key points of these two important viral-induced neoplasms in rabbit species.[20]

In addition, participants reviewed the features of melanocytic neoplasia in several domestic and laboratory animal species.[1,6,7,8]

- Dog: Cutaneous, digit, oral cavity, and eye; melanocytic neoplasms of the conjunctiva tend to be malignant,

while those involving the anterior uvea are typically benign.
- Cat: Rare, other than the eye; in the eye, found particularly frequent in the iris.
- Cow: Uncommon; can occur as benign congenital tumors, as well as at any age.
- Horse: Old gray horses; perineum, genitalia, tail head, distal limbs.
- Pig: Most common in Durocs and Hormel crosses; congenital tumors in the Sinclair miniature pig.
- Angora goat: dorsal ear, face, perineum.
- Fish: Most common in platyfish and swordfish.

Disease name	Rabbit (Shope) papillomatosis	Rabbit (Shope) fibromatosis
Species affected	Cottontail rabbits (*Sylvilagus*); domestic rabbits (*Oryctolagus*)	Cottontail rabbits; European domestic rabbits
Virus*	Cottontail rabbit papillomavirus	Rabbit fibroma virus (leporipoxvirus)
Gross findings	Pedunculated, cornified mass(es) on the eyelids and ears	Firm, flat, circumscribed tumors of the feet and legs ± muzzle, periorbital, perineal
Histologic findings	Consistent with squamous papilloma	Fibroblast proliferation with mixed inflammatory infiltrate, may be myxoid, large intracytoplasmic eosinophilic inclusion bodies in proliferative cells
Progression/ Regression	May progress to SCC[#]	Benign, self-limiting infection

* Virus nomenclature is based on the most recent International Committee on Taxonomy of Viruses taxonomy list.[12]
[#] Squamous cell carcinoma

Contributor: National Institutes of Health, Division of Veterinary Resources, Office of Research Services, 9000 Rockville Pike, Building 28A, Room 106, Bethesda, Maryland, 20892

References:

1. Baumann PC, Okihiro MS. Cancer. In: Ostrander GK, ed. *The Laboratory Fish*. San Diego, CA: Academic Press; 2000:604.
2. Beniashvili DS. Spontaneous rabbit melanoblastoma. *Voprosy Onkologii.* 1972;18:84-85.
3. Bomhard W, Goldschmidt MH, Shofer FS, Perl L, Rosenthal KL, Mauldin EA. Cutaneous neoplasms in pet rabbits: A retrospective study. *Vet Pathol*. 2007;44:579-588.
4. Brown WH, Pearce L. Melanoma (sarcoma) of the eye in a syphilitic rabbit. *J. Exp Med.* 1926;43:807-813.
5. Eyden B, Moss J, Shore I, Banerjee SS. Metastatic small cell malignant melanoma: A case requiring immunoelectronmicroscopy for the demonstration of lattice-deficient melanosomes. *Ultrastruct Pathol.* 2005;29:71-78.
6. Ginn PE, Mansell JEKL, Rakich PM. Skin and appendages. In: Maxie MG, ed. *Jubb, Kennedy and Palmer's Pathology of Domestic Animals*. Vol. 1, 5th ed. Philadelphia, PA: Elsevier Ltd; 2007:759-760.
7. Goldschmidt MH, Hendrick MJ. Tumors of the skin and soft tissues. In: Meuten DJ, ed. *Tumors In Domestic Animals*. 4th ed. Ames, IA: Blackwell Publishing; 2002:78-83.
8. Hargis AM, Ginn PE. The integument. In: McGavin MD, Zachary JF, eds. *Pathologic Basis of Veterinary Disease*. 4th ed. St. Louis, MO: Elsevier; 2007:1255.
9. Holz K, Heutgens W. Multiple Melanombildungen bein einem Kaninchen. *Stsch Tierarztl Wochenschr.* 1955;62:146-148.
10. Hotchkiss CE, Norden H, Collins BR, Ginn PE. Malignant melanoma in two rabbits. *Lab Anim Sci.* 1994;44:377-79.
11. Hussein MR. Extracutaneous malignant melanomas. *Cancer Investigation*. 2008;26:516-534.
12. International Committee on Taxonomy of Viruses. http://www.ictvonline.org/index.asp?bhcp=1. Accessed 13 April 2011.
13. Kim DY, Royal AB, Villamil JA. Disseminated melanoma in a dog with involvement of leptomeninges and bone marrow. *Vet Pathol*. 2009;46:80-83.
14. Kurotaki T, Tomonari Y, Kanno T, Wako Y, Tsuchitani M. Malignant amelanotic melanoma behind the left eye in a female Crj:CD(SD)IGS rat: A case report. *Vet Pathol*. 2008;45:681-84.
15. Kusewitt DF, Applegate LA, Bucana CD Ley RD. Naturally occurring malignant melanoma in the South American opossum (*Monodelphis domestican*). *Vet Pathol*. 1990;27:66-68.
16. Murphy J, Young S. Intraocular melanoma in a horse. *Vet Pathol*. 1979;16:539-42.
17. Patnaik AK, Mooney S. Feline melanoma: A comparative study of ocular, oral, and dermal neoplasms. *Vet Pathol*. 1988;25:105-112.
18. Pawlowski A, Heaberman HF, Menon A. Skin melanoma induced by 7, 12-dimethylbenzanthracene in albino guinea pigs and its similarities to skin melanoma of humans. *Cancer Res.* 1980;40:3652-3660.
19. Pellegrini, G, Bienvenu JG, Meehan JT, et al. Cutaneous melanoma with metastasis in a cynomolgus monkey (*Macaca fascicularis*). *J Med Primatol.* 2009;38:444-47.
20. Percy DH, Barthold. *Pathology of Laboratory Rodents and Rabbits*. 3rd ed. Ames, IA: Blackwell Publishing; 2007:255,258.
21. Sustmann. Multiple melanombildungen bein kaminchen. *Dtsch Tierarztl Wochenschr.* 1922;30:402.
22. Terenziani M, Spreafico F, Serra A, Podda M, Cereda S. Amelanotic melanoma in a child with oculocutaneous albinism. *Med Petiatr Oncol*. 2003;41:179-80.
23. Tong LCB, Kamil ZS, Habeeb A Al, Ghazarian D. Non-melanocytic mimics of melanoma, part II: Intradermal and intraepidermal mimics. *J Clin Pathol*. 2008;62:290-307.
24. Tunev SS, Wells MG. Cutaneous melanoma in a ferret (*Mustela putorius furo*). *Vet Pathol.* 2002;39:141-43.

CASE IV: B10-10951 (AFIP 3167236).

Signalment: 3-month-old male beagle dog (*Canis familiaris*).

History: The dog had two episodes of vomiting and diarrhea and presented with weight loss, depression, and dehydration. A fecal antigen test for parvovirus was reported to be negative and CBC and chemistry results were unremarkable. The dog was treated with subcutaneous fluid, vitamin B, clavamox, and sulfadine. It is unknown whether the dog was euthanized or succumbed to a natural death. Samples of jejunum, duodenum, and mesenteric lymph node were submitted for histological evaluation.

Gross Pathology: An approximately 2 inch portion of the jejunum was dark red and the mesenteric lymph nodes were enlarged.

Histopathologic Description: Small intestine: There is multifocal loss of crypts with collapse of the overlying mucosa. Villi are multifocally blunted, fused, eroded or ulcerated and lining epithelial cells are cuboidal, attenuated, or dysplastic. The lamina propria is edematous, congested, and infiltrated by neutrophils, lymphocytes, and macrophages. Crypts are occasionally ectatic, lined by attenuated epithelial cells, and multifocally contain mucin admixed with necrotic cellular debris. There is extensive crypt regeneration characterized by cytoplasmic basophilia, an increased nuclear to cytoplasmic ratio, a prominent nucleolus, and frequent mitoses. Scattered crypt epithelial cells contain 4 x 6 µm polygonal eosinophilic to amphophilic intranuclear inclusions that peripheralize the chromatin. Within Peyer's patches, there is marked germinal center lymphoid depletion and necrosis with infiltration by neutrophils and macrophages. In several slides, clusters of basophilic short bacilli (gram-negative) are adhered to the apical surface of superficial villus epithelial cells. The mesenteric lymph node (not submitted) is edematous and the subcapsular and medullary sinuses are expanded by draining neutrophils, macrophages, and red blood cells.

Contributor's Morphologic Diagnosis: Small intestine: severe acute to subacute necrotizing enteritis with crypt loss and regeneration, villus collapse, Peyer's patch lymphoid depletion and necrosis, epithelial intranuclear inclusions (canine parvovirus-2) and superficial bacteria.

Contributor's Comment: Parvoviruses are small, nonenveloped, single-stranded DNA viruses that are extremely resistant to environmental inactivation.[1,6] Capsid proteins, such as viral protein 1 (VP-1) and VP-2, play a critical role in determining host range, tissue tropism, and antigenicity of specific parvoviruses.[2,6] These viruses require the host cell machinery to replicate, but cannot induce mitosis. Therefore, they often infect rapidly dividing cells, such as intestinal crypt cells; hematopoietic and lymphoid tissues; and developing tissues in the fetus.[1,2] The canine parvovirus type 2 (CPV-2) originated in 1978 either from feline parvovirus (FPV) or a wild carnivore strain, and has quickly evolved to develop new strains (2a, 2b, 2c). The feline panleukopenia virus (FPV) and canine parvovirus 1 (canine minute virus) have remained fairly stable; however, mutations in CPV-2 occur relatively frequently and have enabled the virus to spread to other species, including the domestic cat.[2,3,6] The CPV-2c variant, containing a Glu-426 mutation in the capsid protein, is currently the most prevalent form of CPV-2.[6]

Canine parvovirus 2 (CPV-2) exposure occurs oronasally. The virus initially infects the epithelium over tonsils and Peyer's patches, then replicates in local lymphoid tissues before disseminating throughout the body via infected lymphoblasts. Approximately 3-4 days post infection, lymphocytolysis leads to release of the virus and cell free viremia. Neutralizing antibodies appear by 5-7 days post

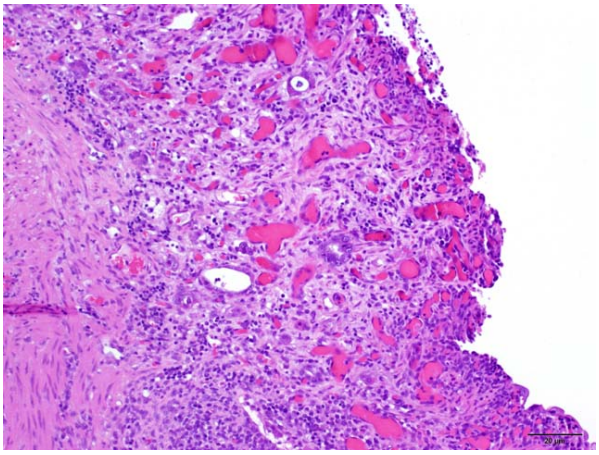

4-1. Small intestine, dog. There is multifocal loss of crypts and collapse of the overlying mucosa. Photograph courtesy of Department of Pathobiology, University of Pennsylvania, School of Veterinary Medicine, www.vet.upenn.edu

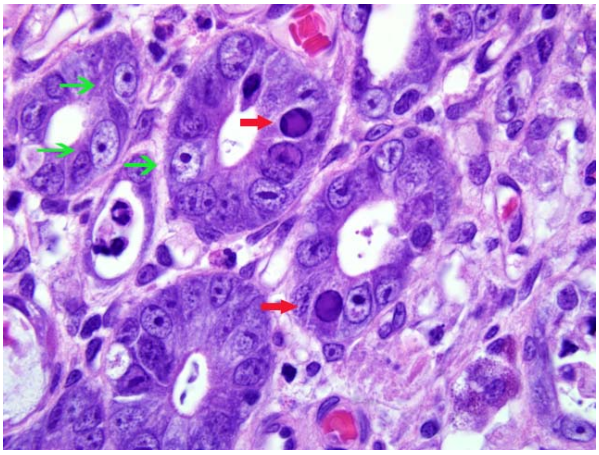

4-2. Small intestine, dog. Scattered crypt epithelial cells contain 4 x 6 µm polygonal eosinophilic to amphophilic intranuclear inclusions (red arrows) that peripheralize the chromatin. Many reactive nucleoli are visible (green arrows). (HE 1000X)

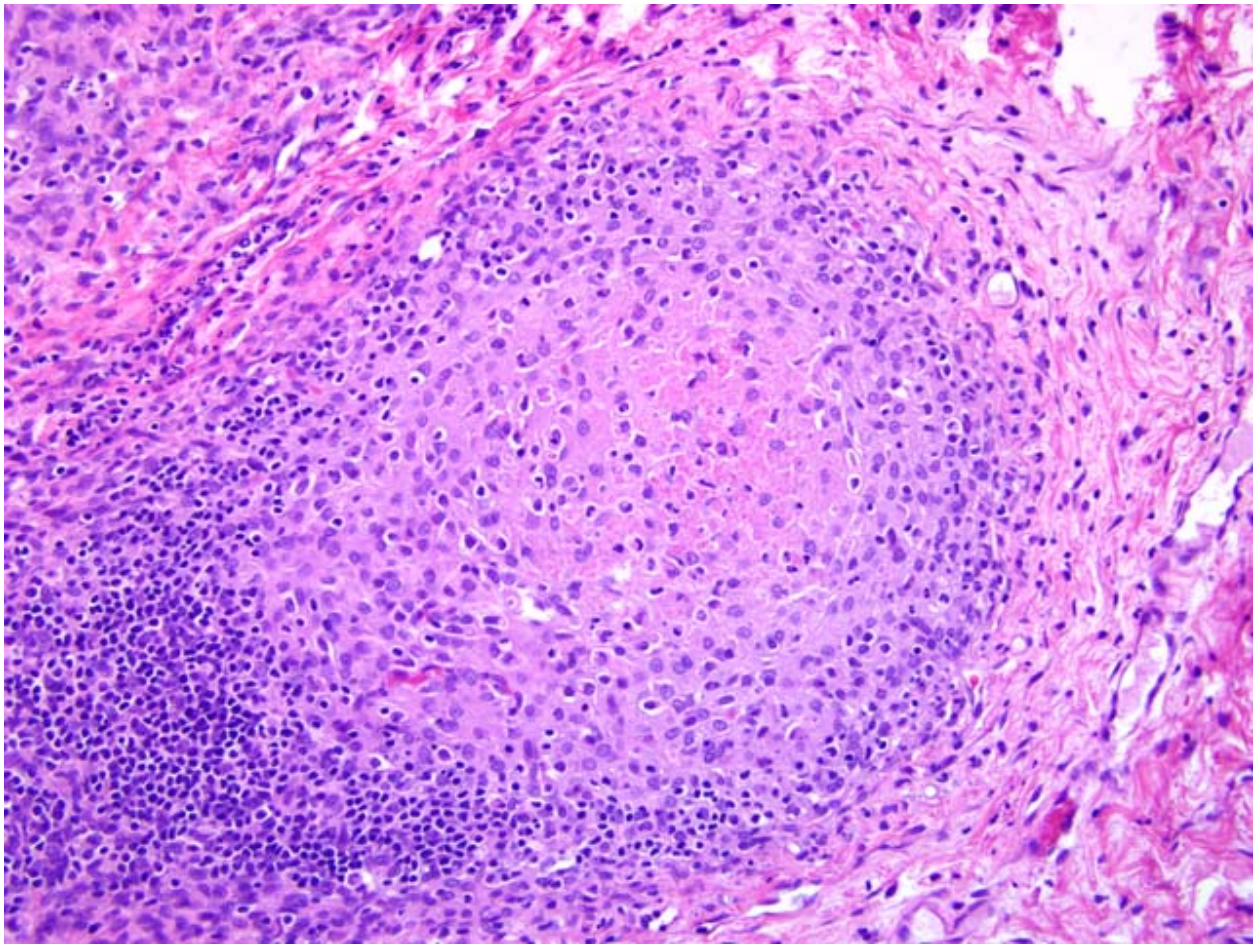

4-3. Small intestine, dog. There is lymphoid depletion and necrosis in Peyer's patches. (HE 200X)

infection and correlates with termination of viremia.[1] Parvovirus infection most commonly occurs in 4-12-week-old puppies, when maternal antibodies decline, but can affect older dogs.[6] A myocardial form of the disease characterized by necrosis and intranuclear inclusions in cardiomyocytes occurs in neonates, most commonly born to naïve bitches.[1]

Infection of crypt epithelial cells occurs secondary to virus dissemination and viremia and is most common in areas over or close to Peyer's patches. Maximum infection of intestinal crypt cells occurs during days 5-9 post-infection. The most important factors dictating the severity of the intestinal disease include the availability of the virus, determined by the rate of lymphocyte proliferation, as well as the rate of proliferation of progenitors in the crypts.[1] Bone marrow cells are also often infected, leading to depletion of myeloid and erythroid lineages. Transient neutropenia due to increased consumption along with damaged bone marrow precursors occurs commonly in cats with FPV, but is less frequent in dogs. Megakaryocytes are less sensitive, but can also be decreased. Lymphopenia due to viral lymphocytolysis is common.[1]

Peyer's patches are often grossly evident from the serosal and/or mucosal surfaces as dark red oval depressions with CPV-2 infection. Other gross findings in the intestine may include mucoid to fluid contents that can contain blood, patchy fibrinous exudate, segmental to widespread mucosal congestion and mural hemorrhage, and fibrin deposition on the serosa. Similar changes can be observed less commonly in the colon. There is often thymic atrophy and enlargement of mesenteric lymph nodes.[1] Intestinal histologic features of CPV-2 infection include necrosis and depletion of Peyer's patches; crypt necrosis, loss, and regeneration; collapse and blunting of mucosal villi; mild to moderate proprial inflammation; epithelial intranuclear inclusions; and possibly secondary infectious agents. Similar lymphoid involution and crypt necrosis can be observed with canine distemper virus infection.[1]

The predominant lesions and presence of inclusions can vary significantly, depending on the stage and severity of disease and the presence of concurrent or secondary infections. Furthermore, a negative rapid fecal parvovirus test result, as was reported in this case, cannot reliably rule out parvovirus infection in cases with typical clinical signs.[9] A culture was

not performed in this case; however, the gram negative bacteria adhered to the apical surface of superficial enterocytes resemble attaching and effacing *Escherichia coli*.[4]

AFIP Diagnosis: Small intestine: Enteritis, necrohemorrhagic, diffuse, severe with villar blunting and fusion, crypt necrosis and regeneration, Peyer's patch necrosis, and crypt epithelial intranuclear amphophilic viral inclusions.

Conference Comment: As noted by the contributor, parvoviruses require actively dividing cells for viral replication. The virus hijacks the host cell DNA polymerases during the S-phase of the cell cycle.[7] Participants discussed the phases and checkpoints in the cell cycle. Cells not in a senescent state (G_0) are in one of four phases of the cell cycle:[5]

- G_1: Pre-synthetic phase
- S: Synthesis of DNA phase
- G_2: Pre-mitotic phase
- M: Mitotic phase

In order to detect and respond to DNA damage, there are checkpoints between the G_1/S transition to check for DNA integrity and a G_2/M transition to check replicated DNA for errors.[5] The G_1/S transition is the rate-limiting step in the cell cycle and is the "point of no return" for the cell, as once the cell enters the S-phase it is committed to completing replication. The G_1/S transition is tightly controlled by cyclins and cyclin-dependent kinases (CDK) which in turn act on retinoblastoma susceptibility protein (RB) and transcription factor E2F.[5] In the normal, non-cycling state, RB is tightly bound to E2F rendering E2F inactive. When RB is phosphorylated by activated CDK, it releases E2F, which then stimulates transcription of genes necessary for cell cycling.[5] The cyclin-CDK complexes responsible for regulating the cell cycle are listed in the included chart along with their respective CDK inhibitors.[10]

Conference participants briefly discussed parvoviruses relevant to other veterinary species.[7,8]

- Feline panleukopenia virus: Generalized disease in kittens manifested as panleukopenia and enteritis; cerebellar hypoplasia
- Porcine parvovirus: Stillborn; mummification; embryonic death; infertility (SMEDI); abortion
- Mink enteritis virus: Leukopenia; enteritis
- Aleutian mink disease virus: Chronic immune complex disease; encephalopathy; neonatal interstitial pneumonia
- Goose parvovirus: Hepatitis; myocarditis; myositis
- Duck parvovirus: Hepatitis; myocarditis; myositis
- Mice minute virus and mouse parvovirus 1: Subclinical infection; congenital malformations
- Kilham's rat virus (RV), H-1 virus, and rat parvovirus (RPV): Scrotal and testicular hemorrhage (RV); congenital malformations; hemorrhagic syndrome
- Hamster parvovirus: Enamel hypoplasia of incisor teeth; cerebral mineralization; testicular atrophy; and high mortality

Cyclin-CDK Complex	Cell Cycle Phase Regulated	CDK Inhibitors
Cyclin D-CDK4	G_1/S transition	p15, p16, p18, p19; p21, p27, p57
Cyclin D-CDK6	G_1/S transition	p15, p16, p18, p19; p21, p27, p57
Cyclin E-CDK2	G_1/S transition	p21, p27, p57
Cyclin A-CDK2	S-phase	p21, p27, p57
Cyclin A-CDK1	S-phase	p21, p27, p57
Cyclin B-CDK1	G_2/M transition	p21, p27, p57

Contributor: Department of Pathobiology, University of Pennsylvania, School of Veterinary Medicine, Suite 4005 MJR-VHUP, 3800 Spruce Street, Philadelphia, PA 19104
http://www.vet.upenn.edu/FacultyandDepartments/Pathobiology/PathologyandToxicology/tabid/412/Default.aspx

References:

1. Brown CC, Baker DC, Barker IK. Alimentary system. In: Maxie MG, ed. *Jubb, Kennedy, and Palmer's Pathology of Domestic Animals*. 5th ed. Vol. 2. Philadelphia, PA: Saunders Elsevier: 2007:177-182.
2. Hoelzer K, Parrish CR. The emergence of parvoviruses of carnivores. *Vet Res*. 2010;41:39.
3. Ikeda Y, Nakamura K, Miyazawa T, Tohya Y, Takahashi E, Masami. Feline host range of canine parvovirus: Recent emergence of new antigenic types in cats. *Emerg Infect Dis*. 2002;8:341-846.
4. Janke B, Francis DH, Collins JE, Libal MC, Zeman DH, Johnson DD. Attaching and effacing *Escherichia coli* infections in calves, pigs, lambs, and dogs. *J Vet Diagn Invest*. 1989;1:6-11.
5. Kumar V, Abbas AK, Fausto N, Aster JC. Tissue renewal, repair, and regeneration. In: Kumar V, Abbas AK, Fausto N, Aster JC, eds. *Robbins and Cotran Pathologic Basis of Disease*. 8th ed. Philadelphia, PA: Elsevier Saunders; 2009:86-87.
6. Lamm CG, Reebok GB. Parvovirus infection in domestic companion animals. *Vet Clin North Am Small Anim Pract*. 2008;38:837-850.

7. Parrish CR. Parvoviridae. In: In: MacLachlan NJ, Dubovi, eds. *Fenner's Veterinary Virology*. 4th ed. San Diego, CA: Elsevier; 2011:225-228.
8. Percy DH, Barthold. *Pathology of Laboratory Rodents and Rabbits*. 3rd ed. Ames, IA: Blackwell Publishing; 2007:24-25,127-128, 181.
9. Schmitz S, Coenen C, Konig M, Thiel H, Neiger, R. Comparison of three rapid commercial canine parvovirus antigen detection tests with electron microscopy and polymerase chain reaction. *J Vet Diagn Invest*. 2009;21:344-345.
10. Stricker TP. Kumar V. Neoplasia. In: Kumar V, Abbas AK, Fausto N, Aster JC, eds. *Robbins and Cotran Pathologic Basis of Disease*. 8th ed. Philadelphia, PA: Elsevier Saunders; 2009:284-286.